

**LOCAL AND SYSTEMIC PROFILES OF INFLAMMATION,
ADAPTATION AND REGULATION AT THE INTERFACE
BETWEEN TISSUE AND IMMUNITY**

**Juvenile dermatomyositis
and beyond**

Judith Wienke

**Local and systemic profiles of inflammation,
adaptation and regulation at the interface
between tissue and immunity**

– Juvenile dermatomyositis and beyond

Judith Wienke

**Local and systemic profiles of inflammation, adaptation and regulation
at the interface between tissue and immunity**

– Juvenile dermatomyositis and beyond

Author: Judith Wienke
ISBN: 978-94-6380-574-2
Cover: MaaHoo Studio
Lay-out and printing: Proefschriftmaken.nl

© Judith Wienke, 2019

All rights reserved. No part of this thesis may be reproduced or transmitted in any form or by any means, electronic or mechanical, including photocopy, or stored in any information storage or retrieval system, without prior permission in writing of the author.

Printing of this thesis was kindly financially supported by the Prinses Beatrix Spierfonds and Infection & Immunity Utrecht.

Local and systemic profiles of inflammation, adaptation and regulation at the interface between tissue and immunity

– Juvenile dermatomyositis and beyond

Lokale en systemische profielen van inflammatie, adaptatie en regulatie op het grensvlak tussen weefsels en immuniteit

– Juvenile dermatomyositis en meer
(met een samenvatting in het Nederlands)

PROEFSCHRIFT

ter verkrijging van de graad van doctor
aan de Universiteit Utrecht
op gezag van de rector magnificus,
prof. dr. H.R.B.M. Kummeling,
ingevolge het besluit van het college voor promoties
in het openbaar te verdedigen
op donderdag 14 november 2019 des middags te 2.30 uur

door

Judith Wienke

geboren op 17 januari 1988 te Jena, Duitsland

Promotor: Prof. dr. A.B.J. Prakken

Copromotoren: Dr. F. van Wijk
Dr. A. van Royen-Kerkhof

The research described in this thesis was supported by grants from the Prinses Beatrix Spierfonds and Innovatiefonds Zorgverzekeraars. The work in this thesis was additionally supported by De Bas Stichting and CureJM.

Table of contents

Chapter 1	General introduction	7
Chapter 2	Systemic and Tissue Inflammation in Juvenile Dermatomyositis: From Pathogenesis to the Quest for Monitoring Tools	27
Chapter 3	Galectin-9 and CXCL10 as Biomarkers for Disease Activity in Juvenile Dermatomyositis: A Longitudinal Cohort Study and Multicohort Validation	69
Chapter 4	Endothelial and inflammatory biomarker profiling at diagnosis reflects clinical heterogeneity of juvenile dermatomyositis and is prognostic for response to treatment	111
Chapter 5	Distinctive biomarker profiles of endothelial activation and dysfunction in treatment-naive rare systemic autoimmune diseases: implications for cardiovascular risk	143
Chapter 6	Human placental bed transcriptomic profiling reveals inflammatory activation of endothelial cells in preeclampsia	191
Chapter 7	Human regulatory T cells at the maternal-fetal interface show functional site-specific adaptation with tumor-infiltrating-like features	225
Chapter 8	T cell interaction with activated endothelial cells induces sustained CD69 expression independent of T cell activation: priming for tissue-residency?	297
Chapter 9	General discussion	325
Addendum		355
	Nederlandse samenvatting	357
	Dankwoord	365
	Curriculum Vitae	373
	List of publications	375

1

General introduction

THE INTERFACE BETWEEN TISSUE AND IMMUNITY

Systemic inflammation as well as tissue-specific inflammation are hallmarks of systemic autoimmune diseases, including Juvenile Dermatomyositis. This thesis explores local and systemic profiles of inflammation, adaptation and regulation at the interface between tissue and immunity. Figure 1 shows how the chapters in this thesis are connected. In autoimmune diseases, tissue inflammation is caused by infiltration of autoreactive immune cells, among which T cells, into affected tissues, which leads to damage and impaired function of the tissue/organ. However, T cells are not only found in tissues during autoimmune diseases. They have been found to have crucial physiological roles in the maintenance of immune homeostasis in tissues. Moreover, functional adaptation and specialization of T cell subsets to specific tissue sites is key for immune regulation in these tissues, to prevent erroneous T cell activation. One important example of a physiological situation in which T cell adaptation and regulation is required, is pregnancy. During pregnancy, the maternal immune system, which has evolved to recognize foreign antigens, has to tolerate a semi-allogeneic fetus. Next to adaptation and regulation of immune cells, endothelial cells play an important role in tissue immune homeostasis. Endothelial cells make up the interface between tissues and circulating immune cells as they line blood vessels and control the passage of immune cells from blood into tissues. Like T cells, endothelial cells are very responsive to their (tissue) microenvironments and adapt their function and phenotype accordingly. During autoimmune inflammation, endothelial cells become actively engaged and mediate the passage of autoreactive T cells into tissues, thereby contributing to the disease pathogenesis. However, endothelial cells can also become damaged by the chronic inflammatory process, resulting in endothelial dysfunction which is observed in many systemic autoimmune diseases, including juvenile dermatomyositis. Endothelial dysfunction is also a hallmark of the pregnancy disorder preeclampsia. Signs of systemic inflammation, tissue inflammation and endothelial dysfunction can be picked up in the circulation as cytokines, chemokines and other mediators that are produced by activated immune and non-immune cells. (The combination of) these molecules reflect the site, magnitude and type of inflammation or endothelial dysfunction and can serve as biomarkers for specific diseases, disease processes or clinical outcomes and may thereby have potential for clinical application which can contribute to the improvement of patient care.

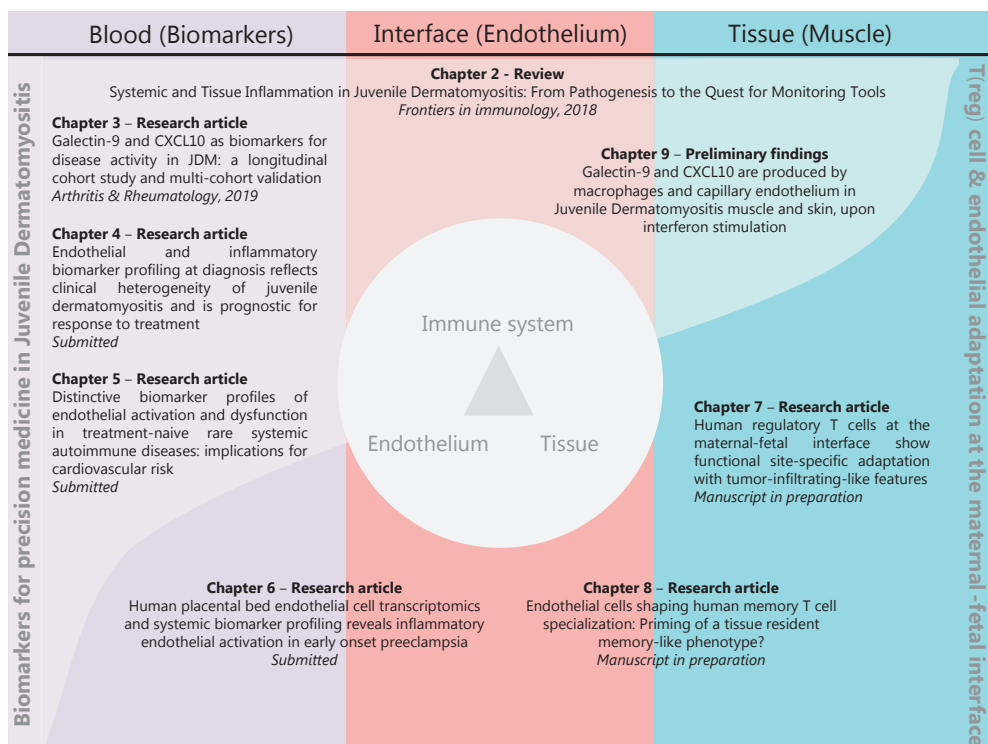


Figure 1. Interrelation of chapters in this thesis

The immune system

The immune system has evolved to defend its host against invasion by pathogens such as bacteria, viruses and fungi. It recognizes and responds to foreign antigens as an interactive network of cells, humoral factors, lymphoid organs and non-lymphoid tissues. The immune system can be divided into two main parts: the innate and adaptive system. The innate system mounts rapid but aspecific responses against pathogens, to control expansion and prevent overgrowth in an early phase. The advantage of the innate response is that it is rapid and broadly effective. However, it is aspecific and not capable of building up memory for a previously encountered antigen. The adaptive immune system, on the other hand, is highly specific and capable of building up memory, but takes several days to weeks to mount an effective response. It can be subdivided into a cellular and humoral branch. The cellular branch consists of B cells and T cells. The specificity of T cells and B cells is mediated by their receptor, which recognizes only selective antigens. To prevent erroneous specificity for antigens expressed by host cells (i.e. auto-antigens), young T cells and B cells undergo a strict selection process during their development before being released into the circulation. B cells produce antibodies which recognize their antigens. These antibodies make up the humoral part of the adaptive immune system. T cells directly recognize their

target through the T cell receptor. T cells can be subdivided into different subsets. The most important distinction is made between cytotoxic T cells (CD8⁺ T cells) and T helper (Th) cells (CD4⁺ T cells). CD8⁺ T cells can directly kill bacteria or virus-infected cells by releasing toxic components or employing membrane-bound ‘death signals’. CD4⁺ T cells comprise Th1 cells, providing help to CD8⁺ T cells, Th2 cells facilitating B cell responses, and Th17 cells, which are pathogenic cells especially involved in immune responses against fungi. After a pathogen has been successfully eliminated, a long-lived pool of memory T cells is left behind which is capable of a more rapid response during a future encounter with the same pathogen. Next to defending the body against external pathogens, the adaptive immune system also has an important role in the recognition and eradication of unhealthy or even cancerous cells, thereby contributing to tissue homeostasis. An effective immune system is therefore also important for the prevention of tumor development.¹ Interferons, which are soluble proteins that can effectively control viral replication, are an important example of innate immune mediators. Next to being crucial for defense against viruses, interferons have been identified as important players in the immunopathogenesis of autoimmune diseases. Interferons are divided into type 1 (interferon α and β) and type 2 (interferon γ). Transcriptional responses of immune and non-immune cells to interferons, the “interferon signature”, can be used as a readout for the interferon activity of the immune system and is therefore relevant as an activity measure of interferon-driven autoimmune diseases.

T cells in tissues

Since pathogens are most often encountered in the external environment, barrier tissues such as the skin, lung, and intestines, are equipped with a special population of T cells residing in and surveilling these tissues. These tissue-resident memory T cells (TRM, both CD8⁺ and CD4⁺) are characterized by a special phenotypic and transcriptional profile, poised to mount a rapid and effective response against any pathogen that attempts invasion. CD69, a surface molecule which was previously only known as an early activation marker on T cells, is now recognized as one of the key molecules distinguishing resident T cells from transiently-bypassing T cells in tissues.^{2,3} Increasing evidence suggests that TRM are not only present in barrier tissues, but also reside in other (human) tissues.^{4,5} From studies in mice, which have paved the way into this research area in the past decade, it has become evident that TRM adapt their functional profiles to their specific tissue microenvironments.^{2,5} Human studies on TRM are still scarce due to the challenge of acquiring human tissue samples, but essential differences between murine and human TRM programs have already been identified.^{6,7} This highlights that results from murine studies on TRM may not be entirely translatable to the human situation, and that investigation of human TRM will be crucial to understand human immune regulation in non-lymphoid tissues. One of the key questions that has been only partly addressed so far, is which events or signals induce the

specific phenotype and functional profile of tissue-resident memory cells that enables them to reside 'silently' in tissues for a prolonged period, but to respond rapidly and effectively when necessary.

Control of the immune response by regulatory T cells

As the most important function of the immune response is to kill pathogens, it is equipped with many agents that are directly toxic to cells. These agents may not only be detrimental to the targeted pathogens, but can also cause collateral damage to surrounding healthy cells – especially in densely 'populated' tissues. It is therefore of utmost importance that immune responses are tightly regulated, and that effective eradication of a pathogen is balanced with as little as possible collateral damage. One of the mechanisms limiting collateral damage, is a physiological resolution of the immune response once a pathogen has been successfully eliminated. The immune system subsequently goes back into a resting – but surveilling – state. Many different mechanisms are at play to effect this control of the immune response. T cell responses, which are especially damaging as they have evolved to directly and efficiently kill bacteria or virus-infected cells, are controlled by a specialized subset of CD4⁺ T cells called regulatory T cells (Tregs). Tregs are identified by the specific transcription factor forkhead box P3 (FOXP3) and employ multiple suppressive mechanisms to regulate T cell responses, including inhibitory receptors and soluble mediators.⁸ Tregs are also important in the prevention of unwanted immune responses. An important example is pregnancy, in which the semi-allogeneic fetus has to be tolerated by the maternal immune system, instead of being recognized and treated as foreign.^{9,10}

Breaching the immunologic balance: from immunodeficiency to autoimmunity

When the tight immune balance is disturbed, two possible scenarios can ensue.¹¹ A weak immune system renders the host in an immunocompromised (or in severe cases, immunodeficient) state, which puts the host at risk for a severe or even lethal infection. Immunodeficiency can be caused by a genetic condition or can be acquired, e.g. by infection with the human immunodeficiency virus. A mild, transient immunocompromised state due to tight regulation of the immune response is also present during pregnancy to prevent an immune response against the fetus.¹² Moreover, immunodeficiency increases the risk for cancer growth due to reduced immune surveillance. On the other end of the spectrum is an immune system mounting too strong, too long or erroneous immune responses. When an immune response is not effectively controlled after a pathogen is eliminated, it can

become chronic, causing collateral damage to healthy tissues. Chronic inflammation plays an important role in the pathogenesis of autoimmune diseases.

Autoimmune diseases: systemic and local inflammation

Autoimmune reactions occur when an immune response is erroneously directed at antigens displayed by cells of the host itself (auto-antigens), which leads to specific immune responses against healthy tissues. To date, it is still elusive which triggers are responsible for the development of such misdirected immune reactions, but both genetic predisposition and environmental factors are thought to play a role. Chronic autoimmune reactions are called autoimmune diseases. Autoimmune diseases can be either localized (i.e. immune system targeting only one cell type, tissue or organ) or systemic (targeting multiple cell types, organs and/or tissues). An example of a localized autoimmune disease is localized scleroderma, which causes inflammation and scarring of the skin, but rarely causes signs of systemic inflammation.¹³ Examples of systemic autoimmune diseases, with a clear systemic inflammatory component, are eosinophilic fasciitis (affecting the fascia and skin) and dermatomyositis (affecting predominantly muscles and skin). These autoimmune diseases are characterized by infiltration of activated immune cells (among which T cells) into affected tissues, causing inflammation and subsequent tissue damage, which leads to loss of function of the affected tissue or organ.^{13,14} To date, the interplay between the systemic and local (tissue) components of autoimmune diseases is still not well understood. Autoimmune diseases are treated with immunosuppressive medication, such as prednisone, methotrexate and/or disease-modifying anti-rheumatic drugs (DMARDs) or biologicals, to restore the immunological balance. However, these drugs are not curative, as they do not cure the (still unknown) cause of autoimmune diseases, but rather suppress excessive inflammation. Immunosuppressive medication is therefore often required for prolonged periods of time, as inflammation may flare up again when immunosuppression is tapered down or stopped. Although some of the tissue damage inflicted by inflammation can be reversed upon effective treatment and physiological recovery, scarring (fibrosis) occurring due to prolonged inflammation may not always be reversible. Accumulating tissue damage in combination with medication side effects may therefore affect long-term functional outcomes of patients.

Juvenile dermatomyositis – An autoimmune disease with local and systemic inflammation

Juvenile dermatomyositis (JDM) is a rare autoimmune disease occurring in children, with an incidence of 2-4/million/year.¹⁵ JDM is characterized by inflammation of skeletal muscles and

skin, leading to muscle weakness and a typical skin rash. Dermatomyositis is not unique to children and can also occur in adults. Other types of myositis, such as non-specific myositis or myositis in the context of another systemic immune disease have also been described in children and adults. JDM is a heterogeneous disease and patients can present with, or develop a spectrum of symptoms, also including involvement of vital organs such as the lungs, heart, brain and intestines.^{16–18} Although the pathogenesis is still largely unknown, environmental and genetic factors may predispose to the disease.^{15,19–22} The autoimmune process is characterized by a type I interferon signature and by infiltration of immune cells such as CD4⁺ T cells and macrophages into skin and muscle tissue.^{23–26} The resulting inflammation and scarring negatively affects muscle function in the short and long term.^{14,27} Clinical disease activity is currently defined by a combination of clinical scores for muscle weakness and skin symptoms, and laboratory measurement of muscle enzymes.¹⁹ The clinical heterogeneity of JDM has been linked to the presence of myositis-specific autoantibodies, which may distinguish distinct clinical phenotypes and are prognostic for the disease course and need for second-line therapy.^{28,29} Current treatment guidelines recommend immunosuppression for at least two years, tapering steroids over the first year and withdrawing treatment if a patient has been off steroids and in remission on methotrexate (or alternative DMARD) for a minimum of 1 year.³⁰ However, for some patients this standardized regimen may not be optimal. Approximately 50% of patients do not respond to initial treatment or present with disease flares during follow-up, resulting in additional tissue damage and impaired physical recovery.^{31–33} In the other half of patients, some could likely benefit from shorter treatment duration, taking into account that overtreatment with steroids can result in serious side effects in children, such as Cushing's syndrome, osteoporosis and growth delay.^{34–36} As opposed to standardized treatment regimens, personalized treatment strategies aim at aligning the medication choice and dosing with the specific needs of a patient, and therefore represent a promising alternative to the conventional treatment strategy. However, two major clinical challenges in the care for patients with JDM have so far hampered the development of personalized treatment strategies: 1) the identification of patient subgroups in need of more intensive therapy or specific drug choices at diagnosis, and 2) objective assessment of disease activity during clinical follow-up. Moreover, although patients with autoimmune diseases are regularly monitored during clinical follow-up, disease flares are difficult to predict. This unpredictability represents a major burden for patients.³⁷ Prediction of disease flares is therefore a third window of opportunity to personalize treatments in JDM. In **chapter 2**, an extensive review on these challenges is provided, in which the quest for biomarkers as potential tools to monitor disease activity and disease severity in JDM is discussed.

The quest for biomarkers in (systemic) autoimmune diseases

Due to the generalized nature of systemic autoimmune diseases, signs of inflammation can often be picked up in the circulation. Active immune cells in the blood and/or tissues generate a large amount of soluble mediators (either directly toxic, or needed for communication with other cells), which can be measured in the circulation as a readout of the immune responses. Such mediators can be reflective of the type, location (i.e. tissue) and/or magnitude of the immune response, and some can thereby serve as biomarkers for specific immune processes or clinical outcomes. The use of circulating biomarkers measured in serum or plasma has a high potential for clinical application because of the minimally-invasive and time-efficient procedure, especially compared to some of the alternative diagnostic methods such as imaging methods or sampling of tissue biopsies. As in different autoimmune diseases different types of inflammation play a role, and different tissues can be affected, diseases may have their own disease-specific biomarker signatures, which can be used for diagnostic purposes. Autoimmune diseases are currently classified based on their clinical symptom profiles, but the discovery of new biomarkers, and especially disease-specific biomarker profiles, may provide new insights that could lead to novel molecular classification strategies rather than clinical classification of autoimmune diseases. For example, the wide spectrum of interferon-associated autoimmune diseases may harbour molecular disease subsets beyond the currently recognized disease entities, each with their own molecular profile. Biomarkers can also be predictive of a certain outcome, e.g. response to treatment or disease flare (prognostic biomarkers). These can aid in the stratification of patients for specific treatment strategies and preventive treatment. Lastly, biomarkers may represent the disease activity at a specific point in time by reflecting inflammatory processes in the circulation and/or tissues. Even low levels or (subclinical) inflammation could potentially be reflected in biomarker levels. This may be relevant since unrecognized, local inflammation leading to tissue damage and subsequent organ dysfunction may have serious consequences for short-term and long-term outcomes. In conclusion, specific biomarkers may have the potential of facilitating personalized treatment strategies, as they can serve as minimally-invasive monitoring tools for patient stratification and during clinical follow-up.

Endothelial function in homeostasis and (autoimmune) inflammation

The lining of blood vessels is composed of endothelial cells. The layer of endothelial cells forms the interface between blood and tissues and connects the two immune compartments. Since endothelial cells are in direct contact with blood on the one side and tissues on the other side, they are capable of receiving (and responding to) signals from both.³⁸ Endothelial

cells act as gatekeepers between the vessel lumen and surrounding tissue, controlling the passage of macromolecules and the transit of leukocytes into and out of the bloodstream. Under homeostatic conditions, the endothelial lining undergoes constant remodeling, which is dynamically modulated by a balance between pro-angiogenic and anti-angiogenic (angiostatic) signals.³⁹ Vascular remodeling is also a crucial process during pregnancy. To ensure sufficient blood supply to the growing and developing fetus, early during pregnancy arteries in the uterine wall located at the placental bed undergo extensive remodeling into 'spiral arteries'. These tightly coiled arteries show a 5-10 fold dilation, allowing for high volume blood flow to the placenta c.q. fetus.⁴⁰

During inflammation due to an infection, endothelial cells become actively engaged by the soluble mediators that activated immune on non-immune cells produce. In response to these cytokines and chemokines, endothelial cells start to produce additional cytokines and chemokines that can serve as chemoattracts for lymphocytes. Moreover, they start to express surface molecules that facilitate binding of lymphocytes and their migration into tissues to eliminate the invading pathogen. During this physiological inflammatory response, endothelial cells thus act as facilitators of immune responses in tissues to eliminate invading pathogens.⁴¹ However, during chronic inflammation as seen in autoimmune diseases, endothelial activation may enforce a detrimental positive feedback loop of tissue inflammation due to their role in lymphocyte chemoattraction and production of pro-inflammatory mediators.⁴¹ Thus far, it is only partly understood whether and how endothelial cells actively influence the phenotype and/or function of lymphocytes transmigrating from blood into the tissues.

Endothelial dysfunction in autoimmune diseases and preeclampsia

Endothelial cells are not only actively engaged during inflammation, but can also become collaterally (or even targeted) damaged. In many systemic autoimmune diseases including dermatomyositis, a loss of capillaries and/or endothelial dysfunction is observed in the affected tissues.⁴²⁻⁴⁷ This vasculopathy is thought to result from deposition of complement, immune complexes and anti-endothelial antibodies, but a disturbed balance between angiostatic and angiogenic factors may also play a role.^{43,44,48-55} The degree of vasculopathy correlates with the expression of interferon-inducible angiostatic chemokines,⁵⁵ indicating that vascular injury may be related to the interferon signature.¹⁴ In JDM, the severity of vasculopathy in the muscle is even directly linked to a more severe clinical presentation and outcome of patients.⁵⁶ This suggests that local vasculopathic changes can reflect systemic vasculopathy and the resulting clinical symptoms.

A classic example of a condition with disrupted endothelial homeostasis with severe consequences, is preeclampsia.⁵⁷ Preeclampsia is a hypertensive disorder occurring during pregnancy which poses a severe health threat to both mother and child. The

pathophysiologic hallmark of preeclampsia is impaired spiral artery remodeling at the placental bed, which leads to a chain of events resulting in hypertension, proteinuria and end-organ dysfunction in the mother, and in many cases restricted growth of the fetus. Although the exact pathogenesis is still elusive, a profound dysbalance of circulating angiostatic and angiogenic molecules has been found in these patients.⁵⁷ Lastly, endothelial dysfunction has an important implication for long-term outcome: it is associated with an increased risk of cardiovascular disease in patients with preeclampsia or systemic autoimmune diseases, as also specifically demonstrated in (juvenile) dermatomyositis.^{58–61} In conclusion, endothelial cells are crucial players in the pathogenesis and morbidity of systemic autoimmune diseases and preeclampsia. Monitoring of endothelial (dys)function with validated biomarkers may therefore be a novel but clinically relevant strategy to improve long-term clinical outcome of patients with autoimmune diseases or preeclampsia.

Taken together, this thesis explores the interplay between endothelial cells and (T-cell mediated) chronic inflammation, to identify and validate biomarkers with a potential for clinical application in juvenile dermatomyositis, and create novel insights into T cell regulation at the maternal-fetal interface.

SCOPE AND OUTLINE OF THE THESIS

The scope of this thesis is to connect the human immune compartments in the circulation and tissues with their interface, the endothelium, in chronic inflammation and pregnancy, with the aim of providing novel insights that may be translated into a clinical application.

Part I focuses on the identification and validation of biomarkers facilitating precision medicine in Juvenile Dermatomyositis. In **Chapter 2** the state-of-the-art on biomarker-guided monitoring of disease activity in JDM is reviewed, and challenges and opportunities for personalized treatment strategies are discussed. In **Chapter 3** two previously identified biomarkers for disease activity in JDM⁶² are validated in two large, international cross-sectional cohorts and their potential for prediction of flares is investigated in a prospective cohort. In addition, a technical innovation with biomarker measurements in dried blood spots is explored. In **Chapter 4** biomarkers associated with endothelial dysfunction and inflammation are examined for their potential to predict response to treatment in patients with JDM in two independent cohorts of treatment-naïve patients. In **Chapter 5** autoimmune disease-specific profiles of biomarkers for endothelial dysfunction and inflammation are investigated and their implications for cardiovascular risk are discussed.

Part II focuses on the adaptation of immune cells and endothelial cells to their microenvironments, with the maternal-fetal interface as central tissue site. In **Chapter 6**

endothelial activation and dysfunction in preeclampsia is investigated by systemic biomarker profiling and transcriptomic profiling of endothelial cells from the maternal-fetal interface. In **Chapter 7** the specialized function and site-specific tissue adaptation of human tissue-resident regulatory T cells to the maternal-fetal interface is assessed by transcriptomic profiling. In **Chapter 8** the role of endothelial cells in initiating the functional program of tissue-resident TRM cells is investigated.

REFERENCES

1. Parkin J, Cohen B. An Overview of the Immune System. *Lancet (London, England)* **2001**, 357 (9270), 1777–1789.
2. Kumar B V, Ma W, Miron M, et al. Human Tissue-Resident Memory T Cells Are Defined by Core Transcriptional and Functional Signatures in Lymphoid and Mucosal Sites. *Cell Rep.* **2017**, 20 (12), 2921–2934.
3. Szabo PA, Miron M, Farber DL. Location, Location, Location: Tissue Resident Memory T Cells in Mice and Humans. *Sci. Immunol.* **2019**, 4 (34).
4. Smolders J, Heutink KM, Franssen NL, et al. Tissue-Resident Memory T Cells Populate the Human Brain. *Nat. Commun.* **2018**, 9 (1), 4593.
5. Stelma F, de Niet A, Sinnige MJ, et al. Human Intrahepatic CD69 + CD8+ T Cells Have a Tissue Resident Memory T Cell Phenotype with Reduced Cytolytic Capacity. *Sci. Rep.* **2017**, 7 (1), 6172.
6. Mackay LK, Minnich M, Kragten NAM, et al. Hobit and Blimp1 Instruct a Universal Transcriptional Program of Tissue Residency in Lymphocytes. *Science* **2016**, 352 (6284), 459–463.
7. Vieira Braga FA, Hertoghs KML, Kragten NAM, et al. Blimp-1 Homolog Hobit Identifies Effector-Type Lymphocytes in Humans. *Eur. J. Immunol.* **2015**, 45 (10), 2945–2958.
8. Sakaguchi S, Miyara M, Costantino CM, et al. FOXP3+ Regulatory T Cells in the Human Immune System. *Nat. Rev. Immunol.* **2010**, 10 (7), 490–500.
9. Erlebacher A. Mechanisms of T Cell Tolerance towards the Allogeneic Fetus. *Nat. Rev. Immunol.* **2013**, 13 (1), 23–33.
10. Mor G, Aldo P, Alvero AB. The Unique Immunological and Microbial Aspects of Pregnancy. *Nat. Rev. Immunol.* **2017**, 17 (8), 469–482.
11. van der Vlist M, Kuball J, Radstake TRD, et al. Immune Checkpoints and Rheumatic Diseases: What Can Cancer Immunotherapy Teach Us? *Nat. Rev. Rheumatol.* **2016**, 12 (10), 593–604.
12. Svensson-Arvelund J, Ernerudh J, Buse E, et al. The Placenta in Toxicology. Part II: Systemic and Local Immune Adaptations in Pregnancy. *Toxicol. Pathol.* **2014**, 42 (2), 327–338.
13. Mertens JS, Seyger MMB, Thurlings RM, et al. Morphea and Eosinophilic Fasciitis: An Update. *Am. J. Clin. Dermatol.* **2017**, 18 (4), 491–512.
14. Wienke J, Deakin CT, Wedderburn LR, et al. Systemic and Tissue Inflammation in Juvenile Dermatomyositis: From Pathogenesis to the Quest for Monitoring Tools. *Front. Immunol.* **2018**, 9, 2951.
15. Meyer A, Meyer N, Schaeffer M, et al. Incidence and Prevalence of Inflammatory Myopathies: A Systematic Review. *Rheumatology (Oxford)*. **2015**, 54 (1), 50–63.
16. Pachman LM, Hayford JR, Chung A, et al. Juvenile Dermatomyositis at Diagnosis: Clinical Characteristics of 79 Children. *J. Rheumatol.* **1998**, 25 (6), 1198–1204.
17. Shah M, Mamyrova G, Targoff IN, et al. The Clinical Phenotypes of the Juvenile Idiopathic Inflammatory Myopathies. *Medicine (Baltimore)*. **2013**, 92 (1), 25–41.
18. Rider LG. The Heterogeneity of Juvenile Myositis. *Autoimmun. Rev.* **2007**, 6 (4), 241–247.
19. Feldman BM, Rider LG, Reed AM, et al. Juvenile Dermatomyositis and Other Idiopathic Inflammatory Myopathies of Childhood. *Lancet (London, England)* **2008**, 371 (9631), 2201–2212.

20. Pachman LM, Lipton R, Ramsey-Goldman R, et al. History of Infection before the Onset of Juvenile Dermatomyositis: Results from the National Institute of Arthritis and Musculoskeletal and Skin Diseases Research Registry. *Arthritis Rheum.* **2005**, 53 (2), 166–172.
21. Shah M, Targoff IN, Rice MM, et al. Brief Report: Ultraviolet Radiation Exposure Is Associated with Clinical and Autoantibody Phenotypes in Juvenile Myositis. *Arthritis Rheum.* **2013**, 65 (7), 1934–1941.
22. Vegosen LJ, Weinberg CR, O'Hanlon TP, et al. Seasonal Birth Patterns in Myositis Subgroups Suggest an Etiologic Role of Early Environmental Exposures. *Arthritis Rheum.* **2007**, 56 (8), 2719–2728.
23. Lopez De Padilla CM, Vallejo AN, Lacomis D, et al. Extranodal Lymphoid Microstructures in Inflamed Muscle and Disease Severity of New-Onset Juvenile Dermatomyositis. *Arthritis Rheum.* **2009**, 60 (4), 1160–1172.
24. Wedderburn LR, Varsani H, Li CKC, et al. International Consensus on a Proposed Score System for Muscle Biopsy Evaluation in Patients with Juvenile Dermatomyositis: A Tool for Potential Use in Clinical Trials. *Arthritis Rheum.* **2007**, 57 (7), 1192–1201.
25. Vercoulen Y, Bellutti Enders F, Meerding J, et al. Increased Presence of FOXP3+ Regulatory T Cells in Inflamed Muscle of Patients with Active Juvenile Dermatomyositis Compared to Peripheral Blood. *PLoS One* **2014**, 9 (8), e105353.
26. Shrestha S, Wershil B, Sarwark JF, et al. Lesional and Nonlesional Skin from Patients with Untreated Juvenile Dermatomyositis Displays Increased Numbers of Mast Cells and Mature Plasmacytoid Dendritic Cells. *Arthritis Rheum.* **2010**, 62 (9), 2813–2822.
27. Blom KJ, Takken T, Huijgen BCH, et al. Trajectories of Cardiorespiratory Fitness in Patients with Juvenile Dermatomyositis. *Rheumatology (Oxford).* **2017**, 56 (12), 2204–2211.
28. Rider LG, Nistala K. The Juvenile Idiopathic Inflammatory Myopathies: Pathogenesis, Clinical and Autoantibody Phenotypes, and Outcomes. *J. Intern. Med.* **2016**, 280 (1), 24–38.
29. Tansley SL, Simou S, Shaddick G, et al. Autoantibodies in Juvenile-Onset Myositis: Their Diagnostic Value and Associated Clinical Phenotype in a Large UK Cohort. *J. Autoimmun.* **2017**, 84, 55–64.
30. Enders FB, Bader-Meunier B, Baildam E, et al. Consensus-Based Recommendations for the Management of Juvenile Dermatomyositis. *Ann. Rheum. Dis.* **2017**, 76 (2), 329–340.
31. Huber AM, Lang B, LeBlanc CM, et al. Medium- and Long-Term Functional Outcomes in a Multicenter Cohort of Children with Juvenile Dermatomyositis. *Arthritis Rheum.* **2000**, 43 (3), 541–549.
32. Gowdie PJ, Allen RC, Kornberg AJ, et al. Clinical Features and Disease Course of Patients with Juvenile Dermatomyositis. *Int. J. Rheum. Dis.* **2013**, 16 (5), 561–567.
33. Ravelli A, Trail L, Ferrari C, et al. Long-Term Outcome and Prognostic Factors of Juvenile Dermatomyositis: A Multinational, Multicenter Study of 490 Patients. *Arthritis Care Res. (Hoboken).* **2010**, 62 (1), 63–72.
34. Ravelli A, Lattanzi B, Consolaro A, et al. Glucocorticoids in Paediatric Rheumatology. *Clin. Exp. Rheumatol.* **2011**, 29 (5 Suppl 68), S148-52.
35. Santiago RA, Silva CAA, Caparbo VF, et al. Bone Mineral Apparent Density in Juvenile Dermatomyositis: The Role of Lean Body Mass and Glucocorticoid Use. *Scand. J. Rheumatol.* **2008**, 37 (1), 40–47.

36. Shiff NJ, Brant R, Guzman J, et al. Glucocorticoid-Related Changes in Body Mass Index among Children and Adolescents with Rheumatic Diseases. *Arthritis Care Res. (Hoboken)*. **2013**, 65 (1), 113–121.
37. Dave (Cure JM Foundation) M. Patient Perspectives on Juvenile Myositis Research Priorities http://www.curejm.org/medical_professionals/pdfs/2017-05-04_JM-Research-Priorities.pdf (accessed May 31, 2018).
38. Carman C V, Martinelli R. T Lymphocyte-Endothelial Interactions: Emerging Understanding of Trafficking and Antigen-Specific Immunity. *Front. Immunol.* **2015**, 6, 603.
39. Dejana E, Hirschi KK, Simons M. The Molecular Basis of Endothelial Cell Plasticity. *Nat. Commun.* **2017**, 8, 14361.
40. Brosens JJ, Pijnenborg R, Brosens IA. The Myometrial Junctional Zone Spiral Arteries in Normal and Abnormal Pregnancies: A Review of the Literature. *Am. J. Obstet. Gynecol.* **2002**, 187 (5), 1416–1423.
41. Pober JS, Sessa WC. Evolving Functions of Endothelial Cells in Inflammation. *Nat. Rev. Immunol.* **2007**, 7 (10), 803–815.
42. Varsani H, Charman SC, Li CK, et al. Validation of a Score Tool for Measurement of Histological Severity in Juvenile Dermatomyositis and Association with Clinical Severity of Disease. *Ann. Rheum. Dis.* **2015**, 74 (1), 204–210.
43. Crowe WE, Bove KE, Levinson JE, et al. Clinical and Pathogenetic Implications of Histopathology in Childhood Polydermatomyositis. *Arthritis Rheum.* **1982**, 25 (2), 126–139.
44. Emslie-Smith AM, Engel AG. Microvascular Changes in Early and Advanced Dermatomyositis: A Quantitative Study. *Ann. Neurol.* **1990**, 27 (4), 343–356.
45. Baumann M, Gumpold C, Mueller-Felber W, et al. Pattern of Myogenesis and Vascular Repair in Early and Advanced Lesions of Juvenile Dermatomyositis. *Neuromuscul. Disord.* **2018**, 28 (12), 973–958.
46. Sallum AME, Marie SKN, Wakamatsu A, et al. Immunohistochemical Analysis of Adhesion Molecule Expression on Muscle Biopsy Specimens from Patients with Juvenile Dermatomyositis. *J. Rheumatol.* **2004**, 31 (4), 801–807.
47. Kim E, Cook-Mills J, Morgan G, et al. Increased Expression of Vascular Cell Adhesion Molecule 1 in Muscle Biopsy Samples from Juvenile Dermatomyositis Patients with Short Duration of Untreated Disease Is Regulated by miR-126. *Arthritis Rheum.* **2012**, 64 (11), 3809–3817.
48. Goncalves FGP, Chimelli L, Sallum AME, et al. Immunohistological Analysis of CD59 and Membrane Attack Complex of Complement in Muscle in Juvenile Dermatomyositis. *J. Rheumatol.* **2002**, 29 (6), 1301–1307.
49. Yu H-H, Chang H-M, Chiu C-J, et al. Detection of Anti-p155/140, Anti-p140, and Antiendothelial Cells Autoantibodies in Patients with Juvenile Dermatomyositis. *J. Microbiol. Immunol. Infect.* **2016**, 49 (2), 264–270.
50. Karasawa R, Tamaki M, Sato T, et al. Multiple Target Autoantigens on Endothelial Cells Identified in Juvenile Dermatomyositis Using Proteomics. *Rheumatology (Oxford)*. **2018**, 57 (4), 671–676.
51. Whitaker JN, Engel WK. Vascular Deposits of Immunoglobulin and Complement in Idiopathic Inflammatory Myopathy. *N. Engl. J. Med.* **1972**, 286 (7), 333–338.

52. Kissel JT, Mendell JR, Rammohan KW. Microvascular Deposition of Complement Membrane Attack Complex in Dermatomyositis. *N. Engl. J. Med.* **1986**, 314 (6), 329–334.
53. Kissel JT, Halterman RK, Rammohan KW, et al. The Relationship of Complement-Mediated Microvasculopathy to the Histologic Features and Clinical Duration of Disease in Dermatomyositis. *Arch. Neurol.* **1991**, 48 (1), 26–30.
54. Sakuta R, Murakami N, Jin Y, et al. Diagnostic Significance of Membrane Attack Complex and Vitronectin in Childhood Dermatomyositis. *J. Child Neurol.* **2005**, 20 (7), 597–602.
55. Fall N, Bove KE, Stringer K, et al. Association between Lack of Angiogenic Response in Muscle Tissue and High Expression of Angiostatic ELR-Negative CXC Chemokines in Patients with Juvenile Dermatomyositis: Possible Link to Vasculopathy. *Arthritis Rheum.* **2005**, 52 (10), 3175–3180.
56. Gitiaux C, De Antonio M, Aouizerate J, et al. Vasculopathy-Related Clinical and Pathological Features Are Associated with Severe Juvenile Dermatomyositis. *Rheumatology (Oxford)*. **2016**, 55 (3), 470–479.
57. Powe CE, Levine RJ, Karumanchi SA. Preeclampsia, a Disease of the Maternal Endothelium: The Role of Antiangiogenic Factors and Implications for Later Cardiovascular Disease. *Circulation* **2011**, 123 (24), 2856–2869.
58. Silverberg JI, Kwa L, Kwa MC, et al. Cardiovascular and Cerebrovascular Comorbidities of Juvenile Dermatomyositis in US Children: An Analysis of the National Inpatient Sample. *Rheumatology (Oxford)*. **2018**, 57 (4), 694–702.
59. Weng M-Y, Lai EC-C, Kao Yang Y-H. Increased Risk of Coronary Heart Disease among Patients with Idiopathic Inflammatory Myositis: A Nationwide Population Study in Taiwan. *Rheumatology (Oxford)*. **2019**.
60. Bellamy L, Casas J-P, Hingorani AD, et al. Pre-Eclampsia and Risk of Cardiovascular Disease and Cancer in Later Life: Systematic Review and Meta-Analysis. *BMJ* **2007**, 335 (7627), 974.
61. Wu P, Haththotuwa R, Kwok CS, et al. Preeclampsia and Future Cardiovascular Health: A Systematic Review and Meta-Analysis. *Circ. Cardiovasc. Qual. Outcomes* **2017**, 10 (2).
62. Bellutti Enders F, van Wijk F, Scholman R, et al. Correlation of CXCL10, Tumor Necrosis Factor Receptor Type II, and Galectin 9 with Disease Activity in Juvenile Dermatomyositis. *Arthritis Rheumatol. (Hoboken, N.J.)* **2014**, 66 (8), 2281–2289.

PART I



Systemic and Tissue Inflammation in Juvenile Dermatomyositis: From Pathogenesis to the Quest for Monitoring Tools

Judith Wienke, Claire T. Deakin, Lucy R. Wedderburn,
Femke van Wijk* and Annet van Royen-Kerkhof*

*These authors contributed equally

Frontiers in Immunology, 2018 Dec 18;9:2951

ABSTRACT

Juvenile Dermatomyositis (JDM) is a systemic immune-mediated disease of childhood, characterized by muscle weakness, and a typical skin rash. Other organ systems and tissues such as the lungs, heart, and intestines can be involved, but may be under-evaluated. The inflammatory process in JDM is characterized by an interferon signature and infiltration of immune cells such as T cells and plasmacytoid dendritic cells into the affected tissues. Vasculopathy due to loss and dysfunction of endothelial cells as a result of the inflammation is thought to underlie the symptoms in most organs and tissues. JDM is a heterogeneous disease, and several disease phenotypes, each with a varying combination of affected tissues and organs, are linked to the presence of myositis autoantibodies. These autoantibodies have therefore been extensively studied as biomarkers for the disease phenotype and its associated prognosis. Next to identifying the JDM phenotype, monitoring of disease activity and disease-inflicted damage not only in muscle and skin, but also in other organs and tissues, is an important part of clinical follow-up, as these are key determinants for the long-term outcomes of patients. Various monitoring tools are currently available, among which clinical assessment, histopathological investigation of muscle and skin biopsies, and laboratory testing of blood for specific biomarkers. These investigations also give novel insights into the underlying immunological processes that drive inflammation in JDM and suggest a strong link between the interferon signature and vasculopathy. New tools are being developed in the quest for minimally invasive, but sensitive and specific diagnostic methods that correlate well with clinical symptoms or reflect local, low-grade inflammation. In this review we will discuss the types of (extra)muscular tissue inflammation in JDM and their relation to vasculopathic changes, critically assess the available diagnostic methods including myositis autoantibodies and newly identified biomarkers, and reflect on the immunopathogenic implications of identified markers.

INTRODUCTION

Juvenile Dermatomyositis (JDM) is a systemic immune-mediated disease of childhood. It is the most common idiopathic inflammatory myopathy in children, with an incidence of 2–4/million/year.¹ Although the exact etiology is still elusive, both genetic and environmental factors are thought to play a role in the development of the disease.^{2–5} JDM is characterized by inflammation of skeletal muscles and skin, leading to muscle weakness and a typical skin rash of the face and hands (heliotrope rash and Gottron's papules, respectively), which are also used as classification criteria.^{6,7} Next to the muscle and skin, other organs can be affected. Vital organ involvement, especially of the lungs, is still the major cause of death in JDM patients.^{8,9} Although rare, cardiac involvement and microangiopathy of the intestine, brain and kidneys have been described.¹⁰ Thus, rather than being confined to specific tissues, JDM is a truly systemic disease, which can affect multiple organ systems. Before the introduction of corticosteroids as a treatment option, mortality and morbidity among JDM patients were high, and long-term outcomes were not the primary focus. Since then, mortality rates have dropped from over 30% to 2–3%.¹¹ With increasing survival, long-term outcomes become an important concern of patients and physicians, as patients' quality of life and societal participation depend on it. Long-term outcomes are likely dependent on various factors such as disease severity and activity, response to treatment and medication side effects which together determine the cumulative organ and tissue damage.

Especially low-grade inflammation and extramuscular manifestations of the disease are difficult to investigate in routine clinical care and may therefore be overlooked. Unrecognized, local inflammation leading to tissue damage and subsequent organ dysfunction may have serious consequences for short-term and long-term outcomes. So far, reliable assessment of disease activity and the type and extent of tissue involvement has been rather challenging. Current clinical tools for assessment of disease activity require active collaboration of patients, which can be difficult for young, unwell children. Detecting low-grade inflammation or differentiating clinically between various causes of muscle impairment is even more challenging. Hence, there is a great need for minimally invasive, objective and reliable diagnostic tools for the assessment and monitoring of (low-grade) disease activity and related organ involvement. Optimally, such tools could guide clinical decision making, facilitate individually tailored treatment regimens, and reduce the risk of over- and under-treatment.

In this review we will discuss the types of (extra)muscular tissue involvement that have been described in JDM and their relation to vasculopathic changes, critically assess the available diagnostic and monitoring tools and reflect on the immunopathogenic implications of identified markers.

SIGNS OF SYSTEMIC DISEASE ACTIVITY IN JDM BASED ON AFFECTED TISSUES AND ORGANS

JDM patients can present with a spectrum of symptoms. Most, but not all patients, have the classic combination of muscle involvement and typical skin rashes. Approximately 1–5% of JDM patients present with amyopathic JDM, but it was estimated that 26% of these patients will eventually progress to classical JDM, which can occur up to years after onset.¹² This indicates that the phenotype can evolve over the course of the disease, possibly also dependent on treatment. True amyopathic JDM however is very rare and mild muscle involvement may be present but missed.¹³ Amyopathic JDM generally has a relatively mild disease course with fewer systemic manifestations, less required immunosuppressive treatment and a good prognosis.^{12,14,15}

(Sub)Cutaneous and Other Extramuscular Symptoms

Cutaneous symptoms can range from the pathognomonic heliotrope rash and Gottron's papules, to photosensitive rashes such as malar and truncal erythema, and severe complications such as skin ulceration and dystrophic calcinosis. Calcinosis occurs in 12–47% of patients and can occur in the skin and in subcutaneous, myofascial, or muscle tissue. Most often it is a long-term complication and its presence has been associated with delayed diagnosis and more severe disease with poorer functional outcomes. Effective treatment of calcinosis is still challenging, but aggressive high-dose immunosuppression or, in very severe cases, autologous stem cell transplantation have been shown to be able to reverse calcinosis, suggesting that chronic (low-grade) inflammation may be accountable for calcifications.^{16–20} Cutaneous and oral ulceration affects up to 30% of patients and is thought to result from occlusive endarteropathy of the small vessels.^{10,21} Lipodystrophy affects 8–14% of JDM patients and is often associated with hormonal and metabolic changes.^{10,22–24} We suspect that patients with lipodystrophy may therefore have an increased risk of cardiovascular events in the long-term. Limb edema and arthritis are also common, occurring in 11–32 and 23–58% of patients, respectively.¹⁰

Next to the skin and musculoskeletal system, other organ systems can be involved, of which the lung is the most frequently affected. Up to 75% of children with JDM develop respiratory involvement, which may result from a complication of respiratory muscle weakness or immunosuppressive therapy, or from interstitial lung disease (ILD).^{25,26} ILD occurs in 8–19% of juvenile myositis patients and has been described as the major cause of death in JDM.^{27–30} Cardiac involvement may be present subclinically more often than recognized, as even in JDM patients without clinical cardiac dysfunction abnormal ECG and echocardiographic findings are relatively common.^{31–33} Conduction abnormalities and myocarditis have been

reported, and systolic and diastolic dysfunction was found after long-term follow-up.^{34–37} Cardiac complications are thought to result from myocarditis and coronary artery disease as well as involvement of the small vessels of the myocardium.³⁸ Involvement of the gut or neural system are rare complications of JDM and are also thought to result from an underlying small vessel angiopathy or vasculitis.^{39–41} Intestinal consequences of the small vessel angiopathy include ulceration, perforation, hemorrhage, pneumatosis intestinalis and malabsorption.^{42–44}

Vasculopathy

The pathologic changes underlying symptoms and tissue damage in the skin, muscles, and vital organs have a common factor: in all the affected tissues typical vasculopathic changes are observed, which include loss of capillaries (capillary dropout), perivascular inflammation, and (occlusive) small vessel angiopathy.^{21,45} In a recently reported French JDM cohort of 116 patients, vasculopathy-related complications were the main cause of admission to the intensive care unit, illustrating the severity and relevance of vascular involvement in JDM.⁴⁶ These complications include life-threatening disorders like systemic capillary leak syndrome, recently also described in 3 patients with JDM.⁴⁷

Deposition of complement, immune complexes and antiendothelial antibodies is thought to play an important role in endothelial damage and subsequent capillary dropout.^{48–54} Clinically, the severity of vasculopathy and the disease phenotype have also been linked. The presence of prominent vascular injury in muscle biopsies identified a subgroup of patients with more severe clinical presentation and outcomes, including profound muscle weakness, limb edema and gastrointestinal involvement.⁵⁵ This suggests that local vasculopathic changes can reflect systemic vasculopathy and the resulting clinical symptoms. Nailfold capillaroscopy, a commonly and easily used indicator of disease activity in clinical practice, is also based on this principle. The pathologic changes observed in nailfold capillaries, such as capillary dropout, branching and dilatation, likely reflect the systemic blood vessel abnormalities. Loss of end row nailfold capillaries is significantly associated with clinical disease activity scores for muscle and skin and can thus be used as a marker of skin and muscle activity. Nailfold capillaroscopy is especially suited as a non-invasive tool to follow up changes in disease activity over time in patients.^{56–59}

Taken together, JDM is a truly systemic disease in which not only the muscles and skin are affected, but also vital organs can be involved. The presence of typical vasculopathic changes in the various affected tissues points toward a central role for systemic endothelial dysfunction in the pathogenesis of JDM.

MONITORING OF DISEASE ACTIVITY AND TISSUE INVOLVEMENT

During clinical follow-up, monitoring of disease activity is crucial to determine the rate of medication tapering or to assess the requirement for intensification of immunosuppressive therapy. Next to clinical evaluation, various tools have been investigated for monitoring of disease activity, among which autoantibodies and other circulating biomarkers, and histopathologic evaluation of muscle biopsies, as well as several imaging techniques.

Clinical Assessment

The primary and most important evaluation of disease activity involves clinical assessment by experienced clinicians and health care professionals. Over the past years, several scoring tools have been devised for internationally standardized evaluation of disease activity.⁶⁰ The most commonly used tools are now the childhood myositis assessment scale (CMAS), manual muscle testing of 8 muscle groups (MMT-8), physician's and patient's global assessment on a visual analog scale (PGA), cutaneous assessment tool (CAT), cutaneous dermatomyositis disease area and severity index (CDASI), disease activity score (DAS), myositis disease activity assessment tool (MDAAT) and childhood health assessment questionnaire (CHAQ).⁶¹⁻⁶⁹ Combined scoring systems are currently being developed.⁷⁰ The Pediatric Rheumatology International Trials Organization (PRINTO) has composed criteria for defining clinically inactive disease.⁷¹ A recent re-evaluation of these PRINTO criteria showed that skin disease may be underestimated as a factor in the assessment of disease activity.⁷² Clinical measures of disease activity, however, have limited capacity to detect low-grade inflammation in the tissues which does not cause overt symptoms, but may still contribute to tissue damage in the long term. Moreover, it is challenging to differentiate between various underlying causes of symptoms by clinical assessment. For example, muscle weakness may result from an ongoing inflammatory process, from medication side effects (e.g. steroid myopathy), muscle damage or effects of immobility. Biological assessment of the affected tissues and organs can therefore be helpful or even necessary to aid clinical decision-making concerning medication dose and additional interventions.

Biomarkers for Disease Course, Activity, and Tissue Involvement

Laboratory investigation of blood is a minimally invasive and time-efficient procedure, especially compared to muscle biopsy and some of the imaging methods. It is therefore particularly suited as a method for serial sampling during clinical follow-up. Laboratory investigation can be used for measurement of autoantibodies and for biomarkers related to disease activity and specific (extra)muscular symptoms.

Autoantibodies

Antibodies found in myositis include myositis-specific autoantibodies (MSA), relatively specific to myositis, and myositis-associated antibodies (MAA), which are observed both in myositis and other connective tissue diseases.⁶ In the past years, different disease phenotypes have been linked to the presence of autoantibodies and particularly myositis-specific autoantibodies.¹⁶ The frequencies of autoantibodies in juvenile patients differ substantially from adult DM patients.⁷³ Anti-TIF1 (p155/140) and anti-NXP2 (p140 or MJ) are the most commonly identified autoantibodies in Caucasian JDM patients (20–35 and 16–23%, respectively).^{28,73–76} Anti-TIF1 is associated with skin ulceration, photosensitive skin rashes, lipodystrophy, and edema,^{24,75–78} whereas anti-NXP2 is associated with a severe disease course with more profound muscle involvement, calcinosis, gastrointestinal ulceration, joint contractures, and dysphonia.^{75,77,79,80} A recently identified myositis specific autoantibody which is especially frequent in the Asian JDM population, is anti-MDA5 (CADM-140).⁸¹ It is found in 33% of Asian JDM patients, compared to 7% of Caucasian patients.^{8,82} Patients with anti-MDA5 have a higher risk of developing ILD than patients without these antibodies. This anti-MDA5 conferred risk is seen in both Asian and Caucasian JDM cohorts, although the risk difference appears to be more pronounced in Asian cohorts.^{8,83} Common symptoms in Caucasian patients with anti-MDA5 antibodies include oral and cutaneous ulceration, arthritis, and milder muscle disease with fewer histologic abnormalities and a higher remission rate off medication after 2 years of follow-up.^{76,82,84,85} Less frequently identified autoantibodies in the juvenile population include anti-Mi2 (4–10%) and anti-aminoacyl-tRNA synthetase antibodies such as anti-Jo-1 (1–3%) and anti-SAE (<1%). Anti-SRP and anti-HMG-CoA-reductase (Anti-HMGCR) autoantibodies, both accounting for <3% of juvenile myositis patients, are associated with a necrotizing type of myopathy with severe muscle weakness.^{73,76,86,87}

It remains unclear whether each MSA reflects a distinct pathologic process, influencing the type and severity of disease phenotype and tissue involvement. Notably, autoantibodies against Jo-1, TIF1, SRP, and Mi-2 are not only informative at disease onset, but their levels have been found to correlate with disease activity during follow-up in the context of rituximab treatment.⁸⁸ This highlights that perhaps autoantibodies should be measured during or soon after the first clinic visit as their levels may decline and become undetectable in remission.

A last and different (not myositis-specific) category of autoantibodies identified in JDM comprises autoantibodies against components of endothelial cells, which are thought to contribute to capillary loss. These anti-endothelial cell autoantibodies (AECA) were detected in 76% of JDM patients, as opposed to 30% of control patients.⁴⁹ Twenty-two candidate target autoantigens for AECA were identified in JDM plasma, 17 of which were proteins associated with antigen processing and protein trafficking.⁵⁰ Identification of autoantibody targets may provide novel insights into the auto-immune process and self-antigens involved in JDM.

Biomarkers for Systemic Inflammation and Muscle Disease Activity

Reliable assessment of disease activity during follow-up can be aided by laboratory markers that represent systemic and/or local inflammation. Especially for detection of low-grade inflammation and for differentiation between various causes of muscle weakness, laboratory investigation can be a helpful or even necessary tool.

So far, reliable and validated laboratory markers for disease activity and tissue involvement in JDM are still lacking. A large number of proteins in plasma, serum, and urine as well as circulating immune cell subsets have been investigated as potential biomarkers for (tissue-specific) disease activity in patients with JDM (Tables 1 and 2). In theory, every biological parameter that can be measured, could serve as a biomarker. To be suited for use in clinical practice however, a biomarker has to meet additional criteria, such as being reliable, robust, relatively stable and easy to measure. In the following paragraphs we highlight all biological markers that have been associated with disease activity in JDM, regardless of their suitability for use in clinical practice, as some of these identified markers may still contribute to the understanding of the immunopathogenesis of JDM. However, it is important to note that due to the rarity of the disease, many of these studies were carried out in small cohorts of <30 patients (as outlined in Tables 1 and 2). Insights based on such small numbers have limitations in a heterogeneous disease like JDM. Therefore, validation of identified markers in larger cohorts is crucial before implementation into clinical practice.

Currently used laboratory markers

The markers that are currently used in clinical practice, AST, ALT, LDH, aldolase and in particular creatine kinase activity (CK), do not correlate as well with disease activity in JDM as in DM.^{125–127} At diagnosis, any one muscle enzyme was only elevated in 80–86% of patients with JDM and CK was found to be elevated in only 61–64% of patients.^{125,128} In almost 20% of patients the most abnormal measurement of CK was not elevated above normal values.²⁸ Low muscle enzymes at first presentation may be associated with delayed diagnosis.¹²⁹

Table 1. Biomarkers for disease activity in JDM cohorts

Biomarker	Global disease activity	Muscle disease activity	Other activity measures	Patients	Material & technique	Cohort	References
<i>Interferon related biomarkers</i>							
MxA		++++* (DAS, O), +++* (DAS, FU)	NS (skin DAS)	14 act JDM: 7 untreated, 7 treated	PBMC, qRT-PCR	USA	O'Connor ⁸⁹
IFN α activity	##* (DAS, off therapy at 36 months)	NS (DAS)	##* (skin DAS, off therapy at 36 months), ** (vsHC)	39 JDM and 19 ped HC	Serum, Functional reporter assay	USA	Niewold ⁹⁰
IFN gene score	r _p : NS (DAS)	r _p : NS (DAS)		27 JDM		USA	Baechler ⁹¹
IFN chemokine score	r _p : +++* (DAS)	r _p : +++* (DAS)		29 JDM			
Eotaxin	+** (DAS)	NS (DAS)	+** (skin DAS), * (vsHC)	54 JDM			
MCP-1	+* (DAS)	NS (DAS)	NS (skin DAS), ** (vsHC)	54 age+sex matched controls	Serum, Luminex	Norway	Sanner ⁹²
IP-10	NS (DAS)	NS (DAS)	NS (skin DAS), (vsHC)	Median time 16.8 yrs after onset			
IP-10	+++*** (PGA)	####* (CMAS)		2014: 25 JDM (18 act, 19 rem) 14 ped HC, 8 NIMD		NL	Enders ^{93,94}
TNFR2	+++*** (PGA)	NS (CMAS)		2015: 3 refractory JDM (pre and post aSCT)	Plasma and serum, Luminex		
Galectin-9	+++*** (PGA)	##* (CMAS)					
Soluble IL-2R	** (diagnosis vs rem)			7 JDM: 7 at diagnosis, 7 in rem	Serum, ELISA & HPLC	Japan	Kobayashi ⁹⁵
Neopterin	Higher in act than rem						

(Continued)

Table 1. Biomarkers for disease activity in JDM cohorts

Biomarker	Global disease activity	Muscle disease activity	Other activity measures	Patients	Material & technique	Cohort	References
Neopterin		++++ (act), ++++ (FU 3 pts) (both with study-specific DAS)		15 JDM (21 samples: 12 act, 9 rem)	Serum, radioimmunoassay	Italy	De Benedetti ⁹⁶
Urine neopterin	+++ (PGA)	### (MMT), ### (CMAS)	+++ (skin VAS), +++ (CHAQ), +++ (MRI)				
Urine quinolonic acid	+++ (PGA)	### (MMT), #### (CMAS)	+++ (CHAQ), +++ (MRI)	39 JDM, 3 JDM with overlap CTD, 3 JPM	Urine and plasma, ELISA, HPLC, gas chromatographic mass spectrometry	USA	Rider ⁹⁷
Plasma neopterin/quinolonic acid	NS (PGA)	NS (CMAS, MMT)					
<i>Other markers of inflammation</i>							
MRP8/14	++++ (PGA)	### (CMAS)	NS (CHAQ)	56 JDM	Serum, ELISA	UK	Nistala ⁹⁸
CRP			Low during relapse in 4 patients	9 JDM: 4 during relapse and 3 rem	Serum	UK	Haas ⁹⁹
<i>Immune cell subsets</i>							
Changes in %CD19+ cells	+++ (DAS)						
T cell subsets	NS (DAS)						
T cell activation (CD25, HLA-DR)	NS (DAS)						
					PBMC, Flow cytometry	USA	Eisenstein ¹⁰⁰
(Continued)							

Table 1. Biomarkers for disease activity in JDM cohorts

Biomarker	Global disease activity	Muscle disease activity	Other activity measures	Patients	Material & technique	Cohort	References
T cell recognition of human Hsp60	Higher in rem than act			22 JDM: 6 new-onset, 6 act, 10 rem	PBMC, ³ H-thymidine assay	NL	Ei1st ¹⁰¹
Th1 within CXCR5+ CD4 T cells	Higher in rem than act***						
Ratio (Th2+Th17)/Th1 in CXCR5+ CD4 T cells	Higher in act than rem***			45 JDM (52 samples); 26 act, 26 rem, 43 ped HC	PBMC, Flow cytometry	USA	Morita ¹⁰²
% Plasmablasts (CD19+CD20-CD27+CD38++)	Higher in act than rem***						
Change in % CD3+CD69+ T cells	++						
Change in HLA-DR-CD11c+ mDC			++ (extra)	24 JDM	PBMC, Flow cytometry	USA	Ernste ¹⁰³
Change in HLA-DR-CD123+ pDC		##					
% FOXP3+ Tregs		NS (CMAS)					
Defective suppressive function of Tregs	In 4/11 active pts vs 0/9 in remission			48 JDM: 21 act, 27 rem	Muscle biopsies, immunohistochemistry Flow cytometry, ³ H-thymidine incorporation	NL	Vercoulen ¹⁰⁴

(Continued)

Table 1. Biomarkers for disease activity in JDM cohorts

Biomarker	Global disease activity	Muscle disease activity	Other activity measures	Patients	Material & technique	Cohort	References
RORC	*	*	NS (extra)				
IL-17F	NS	*	NS (extra)				
GATA3	NS	*	NS (extra)				
STAT4	***	***	NS (extra)	26 JDM new-onset	Whole blood, qRT-PCR	USA	Lopez de Padilla ¹⁰⁵
Changes in STAT6	NS	NS	* (extra)				
Changes in IL-17D	NS	NS	** (extra)				
Changes in BCL6	NS	NS	** (extra)				
% Immature transitional B cells	+++*** (PGA)			68 JDM (113 samples): 20 pre-treatment, 93 on treatment	PBMC, Flow cytometry	UK	Piper ¹⁰⁶
Absolute number immature transitional B cells	+++*** (PGA)						
<i>Markers related to endothelial activation or dysfunction</i>							
vWF			Sens 0.85; Spec 0.45 (for flare)	16 JDM, prospective	Serum	CA	Guzman ¹⁰⁷
vWF	Sens 0.40 (6/15 act had high vWF)	NS (muscle strength)	NS (skin rash, calcinosis)	15 JDM	Serum	USA	Bloom ¹⁰⁸
C3d	Elevated in 6/7 pts with act			15 JDM: 7 act, 5 mild disease, 3 rem, 15 ped HC	Plasma, radioimmuno assay and rocket immunoelectrophoresis	USA	Scott ¹⁰⁹
Fibrinopeptide A			* (vsHC)				
Factor VIII-related antigen			** (vsHC)				

(Continued)

Table 1. Biomarkers for disease activity in JDM cohorts

Biomarker	Global disease activity	Muscle disease activity	Other activity measures	Patients	Material & technique	Cohort	References
MIRNA-10a	NS (DAS)	NS (DAS)	NS (skin DAS)	15 untreated JDM	Muscle biopsies, RT-PCR	USA	Xu ¹¹⁰
EPC number	NS (DAS)	NS (DAS)	NS (skin DAS)	34 JDM: 6 untreated, 19 act on med, 9 rem	PBMC, Flow cytometry	USA	Xu ¹¹¹
<i>Lipid metabolism</i>							
HDL	NS (PGA)	++ (CMAS), NS (MMT)	NS (Skin, CHAQ)	16 JDM, 1 JPM	Serum	USA	Coyle ¹¹²
LDL	r _p : ++ (DAS)	r _p : ## (CMAS)	r _p : +++ (MYOACT)				
Triglycerides	All r _p : +++ (DAS), +++ (MITAX)	All r _p : ## (CMAS), ## (MMT)	r _p : +++ (MYOACT)	25 JDM	Serum	Brazil	Kozu ¹¹³
IL-6	NS	#	NS (extra)	26 JDM	Whole blood, qRT-PCR	USA	Olazagastl ¹¹⁴
Resistin	++++	++++	+ (extra)				

Spearman correlations (r_s) of biomarkers with global/muscle/skin/extraskeletal VAS are shown unless otherwise specified: +; r_s = 0.2, ++; r_s = 0.4, +++; r_s = 0.6, ++++; r_s = 0.8, #; r_s = -0.2, ##; r_s = -0.4, ###; r_s = -0.6, ####; r_s = -0.8, r_p: Pearson correlation. Statistical significance: *P < 0.05, **P < 0.01, ***P < 0.001, NS, not significant. Sens, sensitivity; Spec, specificity. Abbreviations biomarkers: IFN, interferon; MCP-1, CCL2; IP-10, CXCL10; TNFR2, Tumor necrosis factor receptor 2; IL-2R, Interleukin-2 receptor; MRP8/14, myeloid related protein 8/14 (S100A8/9); CRP, C-reactive protein; Hsp60, heat shock protein 60; Th, T helper; mDC, myeloid dendritic cell; pDC, plasmacytoid dendritic cell; Treg, Regulatory T cell; IL, interleukin; vWF, von Willebrand factor; EPC, endothelial progenitor cell; HDL, high density lipoprotein; 25(OH)D, Vitamin D. Abbreviations disease activity: DAS, disease activity score; VAS, visual analog scale; PGA, physician's global activity VAS; MyoAct, Myositis disease activity assessment visual analog scales; MITAX, myositis intention to treat activity index; MMT, manual muscle testing; CMAS, childhood myositis assessment scale; vsHC, compared to healthy controls; CHAQ, childhood healthy assessment questionnaire; MRI, magnetic resonance imaging; ANA, anti-nuclear antibody; extra, extraskeletal/extramuscular symptoms. Abbreviations patients: JDM, juvenile dermatomyositis; JPM, juvenile polymyositis; HC, healthy control; ped, pediatric; act, active; rem, remission/asymptomatic/inactive disease; yrs, years; NIMD, non-inflammatory muscle disease; aSCT, autologous stem cell transplantation; CTD, connective tissue disease; O, onset of disease; FU, follow-up. Abbreviations material & technique: ELISA, enzyme-linked immuno sorbent assay; HPLC, high-performance liquid chromatography; PBMC, peripheral blood mononuclear cells; qRT-PCR, quantitative real time polymerase chain reaction.

Table 2. Biomarkers for disease activity in mixed cohorts containing patients with JDM

Biomarker	Global disease activity	Muscle disease activity	Other activity measures	Patients (samples)	Material & technique	Cohort	References
<i>Interferon related biomarkers</i>							
Type I IFN signature	NS				Whole blood, microarray		
IP-10	NS						
ITAC	NS			2 JDM, 10 DM, 15 ad HC	Serum, Luminex	USA	Baechler ¹¹⁵
MCP-1	++						
MCP-2	++++						
IFN gene score	++	+++ (VAS), ##** (MMT)	+++ (skin), +* (extra)		Whole blood, qRT-PCR		
IP-10	++++						
I-TAC	+++						
MCP-1	+++						
MCP-2	+++						
MIP-1 α	+++						
IL-6	+++	++ (VAS), ##** (MMT)	+* (skin), +++ (extra)	19 JDM, 37 DM, 20 ad HC		USA	Bligic ¹¹⁶
IL-10	+						
TNF α	+						
TNFR1	+						
MIG, MIP-1 β , IL-8	NS						
Type I IFN chemokine score (Summarization of ITAC, IP-10, MCP-1, and MCP-2)	++ (JDM), +++** (mixed)	++++ (VAS, mixed), ##** (MMT, mixed)	+* (skin), +++ (extra)		Serum, multiplexed sandwich immunoassay		

(Continued)

Table 2. Biomarkers for disease activity in mixed cohorts containing patients with JDM

Biomarker	Global disease activity	Muscle disease activity	Other activity measures	Patients (samples)	Material & technique	Cohort	References
Type I IFN gene score	+	+++	NS (extra)		Whole blood, qRT-PCR		
Type I IFN chemokine score	++***	++***	++++* (extra)				
IP-10	++***	++**	++*** (extra)	21 JDM (each active and remission sample), 30 DM (each active and remission sample)		USA	Reed ¹¹⁷
ITAC	++**	++**	+++ (extra)				
MCP-1	++**	++**	+++ (extra)		Serum, multiplexed sandwich immunoassay		
MCP-2	NS	++***	NS (extra)				
IL-6	++***	++***	+* (extra)				
IL-8	+	+	NS (extra)				
TNFα	++	++***	+* (extra)				
<i>Other markers of inflammation</i>							
IL-1Ra	High in act than rem	++ (CK)	*** (vsHC)	2 JDM, 5 DM, 2 caDM, 4 PM, 2 OM, 12 HC	Serum, ELISA	Switzerland	Gabay ¹¹⁸
sTNFR75 (sTNFR2)		++ (CK)					
BAFF		+++ (CK, mixed)		49 DM (of which ≥1 JDM), 44 PM, 6 IBM, 30 HC	Serum, ELISA	Sweden & Czech Republic	Krystufkova ¹¹⁹
BAFF	+++ (mixed)	+ (mixed)	+++ (extra, mixed)	20 JDM, 45 DM, 26 PM, 7 IBM, 21 HC		USA	Lopez de Padilla ¹²⁰
ΔBAFF (downregulates BAFF activity)	++*** (mixed)	++ (mixed)	++++* (extra, mixed)		PBMC, qRT-PCR		

(Continued)

Table 2. Biomarkers for disease activity in mixed cohorts containing patients with JDM

Biomarker	Global disease activity	Muscle disease activity	Other activity measures	Patients (samples)	Material & technique	Cohort	References
Anti-Jo1	LMM: +++**	LMM: ##*** (MMT), +++** (ME)	LMM: +** (extra), +++** (HAQ)				
Anti-TIF1γ	LMM: +++**	LMM: ##*** (MMT), NS (ME)	LMM: +++** (HAQ), NS (extra)	Refractory pts: 48 JDM, 76 DM, 76 PM (all analyses in mixed cohort)	Serum, ELISA & RNA and protein immunoprecipitation	USA	Aggarwal ⁸⁸
Anti-SRP	LMM: NS	LMM: NS (MMT), +** (ME)	LMM: NS (extra), HAQ				
Anti-Mi2	LMM: +++**	LMM: ##*** (MMT), +++** (ME)	LMM: +* (extra), NS (HAQ)				
<i>Immune cell subsets</i>							
% CD3+ cells	Higher in rem than act* (DM, not JDM)						
% CD8+ cells	Higher in rem than act* (DM, not JDM)			14 JDM, 24 DM, 17 ad HC, 9 ped HC	PBMC, Flow cytometry	Japan	Ishida ¹²¹
% CD20+ cells	Higher in act than rem* (DM, not JDM)						
% CD3+ cells	Higher in rem than act* (DM)						
% CD8+ cells	Higher in rem than act* (DM)						
% IFNγ+ of CD4 T cells	Higher in rem than act** (DM)						
% IFNγ+ of CD8 T cells	Higher in rem than act** (DM)			29 DM act (of which ≥1 JDM), 20 DM rem, 13 PM act, 37 PM rem, 32 ad HC	PBMC, Flow cytometry	Hungary	Aleksza ¹²²
% CD19+ cells	Higher in act than rem* (DM)						
% IL-4+ of CD4	Higher in act than rem* (DM)						

(Continued)

Table 2. Biomarkers for disease activity in mixed cohorts containing patients with JDM

Biomarker	Global disease activity	Muscle disease activity	Other activity measures	Patients (samples)	Material & technique	Cohort	References
<i>Markers related to endothelial activation or dysfunction</i>							
sVCAM-1		NS (CK, mixed)	NS (skin, mixed)	5 JDM, 27 DM, 4 PM, 25 HC	Serum, ELISA	Japan	Kubo ¹²³
sE-selectin		*(CK, mixed)					
sICAM	Higher in act than rem* (mixed)			4 JDM, 2 ped MCTD, 8 ped SLE, 4 ped Vasculitis			
sICAM-3, sVCAM-1, sE-selectin, sE-selectin	NS (mixed)				Serum, ELISA	USA	Bloom ²⁴

Spearman correlations (r_s) of biomarkers with global/muscle/skin/extraskeletal VAS are shown unless otherwise specified. +: $r_s = 0.2$, ++: $r_s = 0.4$, +++: $r_s = 0.6$, ++++: $r_s = 0.8$; #: $r_s = -0.2$, ##: $r_s = -0.4$, ###: $r_s = -0.6$, ####: $r_s = -0.8$. r_p : Pearson correlation, LMM, linear mixed model; Statistical significance: * $P < 0.05$, ** $P < 0.01$, *** $P < 0.001$, **** $P < 0.0001$, NS, not significant. Abbreviations biomarkers: IFN, interferon; MCP-1, CCL2; MCP-2, CCL8; IP-10, CXCL10; ITAC, CXCL11; MIP-1 α , CCL3; IL, interleukin; TNF, Tumor necrosis factor; TNFR1 /2= TNF receptor 1/2, MIG, CXCL9; MIP-1 β , CCL4; IL-1Ra, IL-1 receptor alpha; BAFF, B cell activating factor. Abbreviations disease activity: CK, creatine kinase; ME, muscle enzymes; VAS, visual analog scale; MMT, manual muscle testing; HAQ, health assessment questionnaire; extra, extraskeletal/extramuscular symptoms. Abbreviations patients: JDM, juvenile dermatomyositis; JPM, juvenile polymyositis; DM, adult dermatomyositis; caDM, cancer-associated DM; PM, adult polymyositis; OM, overlap myositis; IBM, inclusion body myositis; SPA, spondylarthritis; SLE, systemic lupus erythematosus; SSC, systemic sclerosis; MCTD, mixed connective tissue disease; HC, healthy control; ped, pediatric; ad, adult; act, active; rem, remission/asymptomatic/inactive disease. Abbreviations material & technique: ELISA, enzyme-linked immunosorbent assay; PBMC, peripheral blood mononuclear cells; qRT-PCR, quantitative real time polymerase chain reaction.

During follow-up, CK may underestimate disease activity due to suppressed release by corticosteroids, circulating inhibitors of CK activity, or loss of muscle mass.^{127,130–132} On the other hand, CK and aldolase can be elevated in steroid myopathy and are therefore not reliable as markers for disease activity requiring more potent immunosuppression.¹³³ However, according to recent consensus guidelines, these muscle enzymes are still regarded as an important monitoring tool.^{134,135}

Markers related to the interferon signature

An important group of investigated biomarkers is related to the type 1 interferon (IFN) signature, which has been demonstrated in the peripheral blood and muscle biopsies of JDM patients.^{136,137} Activated plasmacytoid dendritic cells (pDC) are generally thought to be the main producers of the type 1 IFNs (IFN α and IFN β) in JDM. This notion may be challenged by a recent study measuring circulating IFN α with a highly sensitive assay and investigating the cellular source of IFN α in several systemic inflammatory diseases. JDM patients had higher levels of circulating IFN α than patients with systemic lupus erythematosus (SLE), but lower levels than patients with monogenic interferonopathies. However, neither isolated circulating pDC nor other circulating immune cell subsets from JDM patients expressed more IFN α than cells from healthy controls, suggesting that a non-circulating cellular source may be responsible for IFN α production in JDM.¹³⁸

Due to the lack of available methods to measure circulating IFN α and IFN β until recently, the type 1 IFN signature, consisting of genes upregulated in response to IFN α or IFN β stimulation, was used as a surrogate marker of type 1 IFN levels. The type 1 IFN signature in whole blood of three mixed DM and JDM cohorts correlated weakly to moderately with global disease activity [spearman r (r_s) = 0.33–0.44] and muscle activity (r_s = 0.44–0.47), while single IFN signature related serum chemokines MCP-1, IP-10 (CXCL10) and ITAC (CXCL11) had moderate to strong correlations with global (r_s = 0.42–0.66), muscle (r_s = 0.44–0.50), and extraskelatal disease activity (r_s = 0.42–0.55).^{115–117} MxA expression in PBMC, also used as a surrogate for the IFN signature, had a very strong correlation with muscle disease activity of JDM patients (r_s = 0.80) at disease onset, but not with skin disease activity.⁸⁹ IFN α activity measured by a functional reporter assay was also higher in JDM patients than controls.⁹⁰

Recently, IP-10, TNF receptor 2 (TNFR2) and galectin-9 were found to strongly correlate with global disease activity (r = 0.60–0.75) in two studies by Enders et al.^{93,94} IP-10, together with MCP-1 and eotaxin, was also higher in 54 JDM patients a median of 17 years after disease onset than matched healthy controls.⁹² TNFR2 correlated with CK in a mixed IIM cohort (r_s = 0.55).¹¹⁸ Galectin-9 was recently identified as a biomarker for the IFN signature in SLE and anti-phospholipid syndrome.¹³⁹ IP-10, TNFR2 and galectin-9 are promising biomarkers for disease activity, as they can potentially discriminate between active disease and remission even during treatment.^{93,94} After stem cell transplantation and concomitant eradication of circulating immune cells, their levels stayed high over several months, which suggests that these proteins are not primarily produced by circulating immune cells, but rather by non-

circulating immune or tissue cells, just as IFN α .^{138,94} IP-10 and galectin-9 are currently being validated as biomarkers for disease activity in two large international JDM cohorts. One of the best investigated biomarkers so far in JDM is neopterin, a catabolic product of guanosine triphosphate, which was previously shown to be a marker of immune activation that can be induced by stimulation with IFN γ .¹⁴⁰ In the first study identifying serum neopterin as a biomarker for JDM, neopterin levels correlated strongly with muscle strength impairment in 15 JDM patients ($r_s = 0.68$).⁹⁶ Elevated serum neopterin levels at diagnosis compared to remission were confirmed in an independent cohort.⁹⁵ In a juvenile myositis validation cohort, plasma neopterin ($n = 13$), and quinolonic acid ($n = 24$), however, did not correlate with myositis disease activity measures.⁹⁷ Urine neopterin ($n = 45$) moderately correlated with global ($r_s = 0.42$), muscle ($r_s = 0.50$ – 0.62) and skin activity ($r_s = 0.49$), and edema on MRI ($r_s = 0.55$). Urine quinolonic acid also correlated with global and muscle activity and edema on MRI ($r_s = 0.45$ – 0.61).⁹⁷ Despite these efforts of validation, neopterin has not been widely implemented into clinical practice as a biomarker for disease activity in JDM.

Other inflammatory mediators

Next to type 1 IFN-related markers, other inflammatory mediators have been studied as biomarkers for JDM. The innate TLR4 ligand myeloid related protein 8/14 (MRP8/14 or S100A8/9), originally found to be elevated in patients with systemic-onset juvenile idiopathic arthritis (JIA), correlated moderately to strongly with global and muscle disease activity in a large cohort of 56 JDM patients ($r_s = 0.55$ – 0.65).^{141,98} Another marker adopted from studies in JIA, the soluble IL-2 receptor, was elevated at disease onset compared to remission.^{95,142} Serum/plasma levels of the more conventional proinflammatory cytokines IL-6, IL-8, and TNF α also moderately correlated with global ($r_s = 0.19$ – 0.46) and muscle disease activity ($r_s = 0.35$ – 0.52) in three mixed JDM and DM cohorts.^{116,117} Remarkably, CRP levels did not increase during disease flares.⁹⁹ BAFF and especially its antagonistic non-cleavable form Δ BAFF, both important for survival and maturation of B cells, moderately correlated with global, muscle and extraskelatal VAS ($r_s = 0.27$ – 0.54), and CK ($r_s = 0.37$) in two mixed IIM cohorts.^{120,119}

Markers related to vasculopathy and cardiovascular risk

Due to the vasculopathic component of JDM, markers related to endothelial activation and dysfunction were explored for their association with disease activity. Von Willebrand factor (vWF) was increased during most periods of active disease in a prospective cohort study, but did not reliably predict disease flares in another study.^{107,108} sICAM-1, a marker of endothelial activation, was higher during active disease than remission in a combined cohort of juvenile patients with various systemic autoimmune diseases. VCAM-1, sICAM-3, and L-selectin did not correlate with disease activity, although expression of MiRNA-10a in JDM muscle, which is negatively associated with VCAM-1 expression, showed a correlative trend with muscle and global DAS [Pearson $r (r_p) = -0.45$].^{123,124,110} C3d and fibrinopeptide A, which are related to

vasculopathic changes, were higher in JDM patients with active disease than in remission.¹⁰⁹ Endothelial progenitor cell numbers did not differ between JDM patients and controls and did not correlate with disease activity.¹¹¹

In view of the increased cardiovascular risk in JDM patients, the lipid profile has been investigated in relation to disease activity.⁴¹ Serum HDL negatively correlated with muscle activity ($r_s = -0.54$), but not global or skin activity.¹¹² Triglyceride levels correlated strongly with global disease activity assessed by DAS ($r_s = 0.61$) and LDL was higher in patients with a higher disease activity.¹¹³ Gene expression of the adipokine resistin in PBMC was also upregulated in JDM patients compared to controls and moderately correlated with global and muscle disease activity ($r_s = 0.51$ and $r_s = 0.50$, respectively).¹¹⁴ These results indicate that the cardiovascular risk profile is more pronounced in JDM patients with active disease.

Circulating immune cell subsets as biomarkers for disease activity

Among the circulating immune cell subsets, T cells and B cells have been studied most extensively in relation to disease activity in JDM. In two mixed cohorts of JDM and DM patients, the frequency of T cells, and especially CD8⁺ and IFN γ -producing T cells, was decreased during active disease, while the frequency of B cells and IL-4 producing CD4⁺ T cells was increased compared to remission.^{121,122} This may suggest a shifted balance toward a T helper 2 (Th2) type immune response. In cohorts with only JDM patients, total B cell numbers were also increased compared to controls and changes in B cell frequencies accompanied changes in disease activity ($r_s = 0.47$).^{100,106} Within the B cell compartment, numbers and frequencies of circulating immature transitional B cells correlated strongly with global disease activity ($r_s = 0.69$ – 0.71). Compared to healthy pediatric controls, these specialized B cells were highly proliferative, had a prominent IFN signature and produced less of their regulatory signature cytokine IL-10.¹⁰⁶ Plasmablast frequencies were also increased during active disease compared to remission.¹⁰²

Several T cell subsets have been studied in JDM. In 26 new onset JDM patients the blood gene expression of Th17-related genes, such as RORC and IL-17F, Th1-related genes, including STAT4, and Th2-related genes, including GATA3 and STAT6, was studied in relation to disease activity. RORC, IL-17F, STAT4, and GATA3 positively correlated with muscle activity and RORC and STAT4 correlated with global activity. This would suggest that the immune response is not specifically skewed toward a certain T helper response. However, at baseline, JDM patients had higher gene expression of Th17 related cytokines IL-23, IL-17F, IL-6, and IL-21 than DM patients, indicating that the Th17 pathway may play a more prominent role in the pathogenesis of JDM than DM. Changes in BCL6, a transcription factor for follicular helper T cells, correlated negatively with a change in extramuscular activity.¹⁰⁵ Within CXCR5⁺ follicular helper T cells, the Th1 subset was decreased in active JDM compared to remission and controls, and Th2 and Th17 subsets were increased in JDM compared to controls.¹⁰² Regulatory T cell frequencies in muscle biopsies did not correlate with muscle activity, but suppressive activity of circulating Tregs may be impaired

during active disease.¹⁰⁴ Finally, global disease activity correlated moderately with the activation status of circulating T cells assessed by CD69 expression ($r_s = 0.43$), but not with CD25 and HLA-DR expression.^{100,103} The expansion and functional alteration of particular B cell and CD4⁺ T cell subsets, coinciding with changes in disease activity, hints toward the involvement of these cell subsets in the pathogenesis of JDM.

In conclusion, many circulating, either soluble or cellular, markers have been studied for their relation with muscle and global disease activity. Correlations with disease activity were only moderate for most markers, and some of these molecules are relatively unstable in blood samples or complicated to measure, rendering them unsuited for use in clinical practice. The highest correlations with disease activity were found for markers related to the IFN signature, the lipid profile, for MRP8/14, and immature transitional B cells. However, most of these biomarkers were identified in small patient cohorts and except for neopterin, so far none have been reproduced or thoroughly validated in independent and large JDM cohorts. Neopterin was investigated in a validation cohort, but its correlation with disease activity could only be confirmed in urine, not in plasma. Galectin-9 and IP-10 are currently being validated in two international cohorts and are promising biomarkers for implementation in clinical practice due to their high sensitivity and stability in serum.

Biomarkers for Extramuscular Disease Activity

Next to markers for global and muscle disease activity, biomarkers for involvement of specific tissues and organs have been investigated. Four studies by Kobayashi et al. have focused on biomarkers for ILD, and specifically the rapid progressive (RP-ILD) and chronic ILD type, in a Japanese JDM cohort. Not only the presence, but also the level of anti-MDA5 was a sensitive and specific marker for ILD, with the highest levels found in patients with RP-ILD.^{8,143,144} In addition, BAFF, APRIL, KL-6, and IL-18 levels were higher in patients with RP-ILD compared to chronic ILD and JDM patients without ILD.¹⁴⁵ KL-6 was prognostic for ILD, as it stayed high in patients with persistent damage on HRCT.¹⁴⁴ Biomarkers for cardiac involvement were tested in a Norwegian JDM cohort, a median of 17 years after diagnosis. Eotaxin and MCP-1 were elevated in patients with cardiac dysfunction and correlated moderately to strongly with systolic and diastolic dysfunction especially in patients with persistently active disease ($r_s = 0.45-0.65$).¹⁴⁶ In the same cohort, a reduced heart rate variability, which is an indicator of cardiac disease, correlated moderately with ESR, hsCRP, and also MCP-1 and eotaxin levels ($r_s = 0.29-0.47$).¹⁴⁷ Next to the autoantibody NXP2, which is prognostic for the development of calcinosis, phosphorylated matrix Gla protein was shown to be higher in patients with calcinosis than without calcinosis.^{79,148} Reduced osteocalcin levels were found to be predictive of reduced bone mass, even before start of steroids.¹⁴⁹ The presence of the TNF α -308A allele is associated with a more severe disease in JDM. However, apparent associations with this allele are likely to reflect the association with ancestral haplotype 8.1 due to linkage disequilibrium and should be interpreted with this in

mind.¹⁵⁰ Patients with this genotype are reported to show prolonged symptoms requiring ≥ 36 months of immunosuppressive therapy, a higher incidence of pathologic calcifications, increased production of TNF α by peripheral blood mononuclear cells in vitro and JDM muscle fibers in vivo, a higher IFN α activity and a higher rate of complications arising from occlusion of capillaries. Vascular occlusion has been linked to higher levels of the anti-angiogenic thrombospondin-1.^{90,151–154}

In summary, a number of potential biomarkers for extramuscular disease activity have been identified, and especially for ILD and cardiac dysfunction the biomarkers seem promising. Validation in independent cohorts will have to confirm their potential as biomarkers for these extramuscular symptoms.

Histopathology of Muscle and Skin Biopsies

The diagnostic criteria for JDM by Peter and Bohan encompass histopathological findings consistent with DM: “necrosis of myofibers, phagocytosis, regeneration with basophils, large vesicular sarcolemmal nuclei, and prominent nucleoli, atrophy in a perifascicular distribution, variation in fiber size and an inflammatory exudate, often perivascular.”^{155,156} For a long time, muscle biopsies were therefore taken as part of routine diagnostic workup. However, with evolving diagnostic options and more specialized trained pediatric rheumatologists muscle biopsies are currently not always considered a necessity for diagnosis.¹³⁵

One of the main problems hindering standardized evaluation of muscle biopsies was the lack of an internationally agreed upon scoring tool. An international consensus group of pediatric rheumatologists and pathologists developed such a tool, which encompasses 4 histopathological scoring domains: inflammatory, vascular, muscle fiber and connective tissue changes.¹⁵⁷ The scoring tool has now been validated in an independent cohort consisting of 55 patients and was found to correlate with clinical measures of disease activity, including CMAS, PGA, and MMT-8 ($r_s = 0.40–0.62$).⁴⁵ Muscle biopsy scores may also have prognostic potential: in combination with MSA group, these scores were found to predict the risk of remaining on treatment over time, based on analysis of muscle biopsies from 101 JDM patients.¹⁵⁸

The most common findings in muscle biopsy specimens in JDM compared to healthy individuals or patients with non-inflammatory muscle diseases, are profound upregulation of MHC I expression on muscle fibers, increased expression of integrins and complement and membrane attack complex deposition on capillaries and perimysial large vessels, a type 1 IFN signature and immune cell infiltrates consisting mostly of mature pDC, memory CD4⁺ T cells, and B cells (Figure 1).^{48,52,159–169} The IFN signature, measured by expression of MxA, correlated with muscle disease activity.¹⁶⁶ In skin biopsies similar features are found, with the additional presence of diffuse mast cell infiltration.¹⁶⁴

Several studies have suggested associations between histopathological findings in muscle biopsies and disease duration before the biopsy or disease severity at a later time point. Biopsy specimens taken after a short duration of untreated disease (<2 months), showed higher expression of VCAM-1 (which correlated with higher serum soluble VCAM-1) and expression of genes involved in stress response and protein turnover, whereas biopsies taken after more than 2 months of untreated disease had more pDC infiltration, higher expression of genes involved in the immune response and vascular remodeling and more apoptosis-related markers.^{171–173} Thus, it should be taken into account that histological findings can depend on the disease duration before the biopsy. In addition, these findings may indicate that endothelial activation is an early feature of JDM, which precedes immune cell infiltration and vasculopathy. The degree of vasculopathy and vascular injury (as defined by marked capillary dropout, increased direct immunofluorescent arterial staining and lymphocytic vasculitis, amongst others) was associated with a more severe and chronic disease, with severe or persistent weakness, low remission rates at 12 months requiring additional treatment, subcutaneous edema, and chronic ulcerative disease of the skin and gastrointestinal tract.^{21,55,165} The degree of vasculopathy was also correlated with the expression of angiostatic chemokines MIG, IP-10 and ITAC.¹³⁷ This indicates that the degree of vascular injury may be one of the most important factors determining long-term disease outcomes and that it is related to the IFN signature.

Not only the type of immune cell infiltration, but also the organization of immune cells in the muscle is of significance in JDM. Organization of immune infiltrates in lymphocytic aggregates or lymphoid follicle-like structures with dendritic cells and T cells, as compared to diffuse infiltrates, was associated with a more severe disease course and less response to treatment.¹⁷⁴ MHC I expression, one of the most prominent and early histological features in JDM, did not correlate with clinical features of the disease.^{159,160,175}

The importance of thorough and standardized assessment of tissue involvement is underlined by the fact that even in cases with amyopathic DM, with normal EMG and MRI findings, the muscle biopsy can show focal endomysial lymphocyte and macrophage aggregates and 90% positivity for HLA class I in the sarcolemma.¹⁷⁶ Unrecognized, low-grade muscle inflammation may be undertreated, resulting in a larger risk of long term damage. However, muscle biopsy is not routinely performed for children with JDM in all centers and therefore in future, biomarkers which are measurable in blood and correlate with biopsy features would represent a major advance.

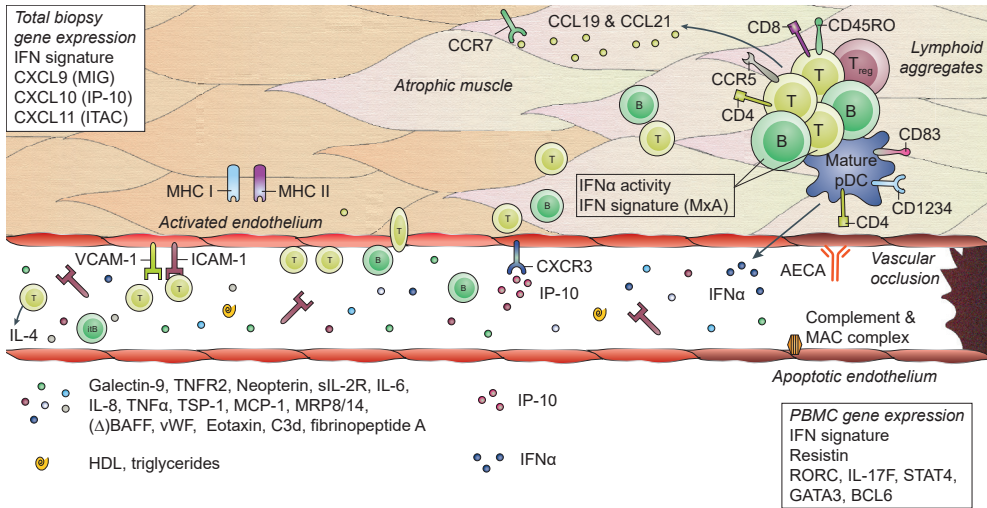


Figure 1. Histopathological features and biomarkers in JDM.

JDM is characterized by vasculopathic changes in the tissues, with loss and dysfunction of endothelial cells, leading to capillary dropout and subsequent atrophy of muscle fibers. The exact chain of events leading to loss of blood vessels and muscle fibers is not known, but it is thought that both overexpression of MHC-I (and MHC-II) on myocytes and endothelial damage are early events in the cascade.^{159,170} They result in the first attraction of immune cells to the tissue, probably by a stress response of the myocytes and endothelial cells, leading to a first production of chemoattractants. The immune cell infiltrates, which can be organized in lymphoid structures, consist mostly of CD4⁺ and CD8⁺ memory T cells, B cells, mature plasmacytoid dendritic cells (pDC) and monocytes. CD4⁺ and CD8⁺ T cells are considered responsible for direct killing of muscle cells. pDC are considered the main producers of type I interferons (IFNs), which explains the IFN-I signature that is found in the muscles of JDM patients. Some typical IFN-inducible chemokines, CXCL9 (MIG), CXCL10 (IP-10), and CXCL11 (ITAC), are known for their angiostatic properties. The receptor for these cytokines, CXCR3, is upregulated on endothelial cells in JDM muscle, which may be one of the factors contributing to endothelial dysfunction.¹³⁷ Other factors include anti-endothelial circulating antibodies (AECA), complement and membrane attack complex (MAC) deposition on endothelial cells. Endothelial cells in muscle also express high levels of ICAM-1 and VCAM-1, which further enables extravasation of immune cells into the tissues and promotes a positive feedback loop resulting in further tissue damage. Not only immune cells in the tissues, but also circulating immune cells show a type I IFN signature and increased IFN α activity. Various circulating markers reflecting immune activation and endothelial activation or distress are increased during active disease in JDM and can potentially be used as biomarkers for disease activity.

IMMUNOPATHOGENIC IMPLICATIONS: INTERFERONS AND VASCULOPATHY

From the biological research conducted in JDM so far, it has become clear that IFNs and their signature play an important role in the immunopathogenesis of JDM (Figure 1). The IFN signature is detectable in muscle fibers, myogenic precursor cells, endothelial cells, skin and several circulating cell subsets of patients with JDM and could point toward a viral etiology.^{89,106,167} Although it has never been demonstrated definitively, several studies suggest that infections may be more common before onset of JDM.¹⁷⁷⁻¹⁸⁰ Not only are IFNs potent drivers of (auto)inflammation, they may also be anti-angiogenic factors that could directly or indirectly contribute to endothelial damage and loss in JDM: directly by inhibiting angiogenesis and disrupting the vascular network organization and indirectly by inducing several other angiostatic factors such as galectin-9, IP-10, and ITAC.^{137,181-186} In addition, type 1 IFNs inhibit the generation of myotubes and induce atrophy-associated genes in differentiated myotubes. Human skeletal muscle cells can also produce large quantities of IP-10 upon stimulation with IFN γ and TNF α .^{186,187}

Rather than being produced by circulating immune cells, IFNs are probably mainly produced within inflamed tissues. Satellite cells, active myogenic cells and endothelial cells in JDM muscle strongly express IFN β .¹⁶⁷ The notion that non-circulating cells within tissues are responsible for IFN production also fits observations by Rodero et al.¹³⁸ In particular within muscle of JDM patients the dysbalance between angiogenic and angiostatic factors can contribute to endothelial loss.^{137,188} Endothelial cells in JDM muscle downregulate genes related to vessel development, cell adhesion and migration, which are essential for angiogenesis.¹⁶⁷ Downregulation of these genes is likely a key event in the development of vasculopathy. Next to being a target of the inflammation, the endothelium may also play an active role in the inflammatory process. In biopsies from JDM patients endothelial cells express inflammatory features, such as high levels of adhesion molecules ICAM-1 and VCAM-1, and produce cytokines and chemokines.¹⁶¹ These can facilitate the attraction and invasion of immune cells into tissues, thereby supporting the inflammatory process and subsequent damage. IP-10 and ITAC were the most highly upregulated genes in endothelial cells from JDM muscle and correlated with the degree of vasculopathy.^{137,167} Endothelium-derived IP-10 can even stabilize the interaction between T cells and endothelial cells, thereby possibly contributing to the chronicity of T cell infiltration.¹⁸⁹ Recently, a new function has been ascribed to endothelial cells as “semi-professional” antigen presenting cells, which act as sentinels for antigens, and possibly self-antigens, in tissues and facilitate T cell trafficking into these tissues.^{190,191} The high expression of MHC molecules on endothelial cells in JDM muscle may support the notion that this process is involved in JDM.^{160,175} Although the exact mechanisms of interaction between immune cells and endothelial cells in JDM are still elusive, they may be more elaborate than so far recognized.

CONCLUSIONS AND FUTURE PERSPECTIVES FOR BIOMARKER RESEARCH

JDM is a multisystem disease. Not only the skin and skeletal muscles are affected, but also other organ systems and tissues such as the lungs, heart and intestines are frequently (subclinically) involved and may be under-evaluated. Vasculopathy due to loss and dysfunction of endothelial cells as a result of the inflammatory process is thought to underlie the symptoms in most of these organs and tissues. Monitoring of disease activity and damage in all of these affected tissues is important during clinical follow-up, as these are key determinants for the long-term outcomes of patients. Tools for monitoring of tissue activity and damage include histopathological investigation of biopsies, and laboratory testing of blood for specific biomarkers as well as several imaging methods. Each of these methods has their strengths and weaknesses and can be of value for specific diagnostic questions at disease onset or during follow-up, as outlined in the consensus-based recommendations for the management of JDM.^{135,192} There is still a need for minimally invasive, but at the same time sensitive and specific diagnostic methods that correlate well with clinical symptoms or reflect low-grade, local inflammation. Tissue-specific biomarkers can therefore be of great value as a monitoring tool.

To be able to identify sensitive, robust and reliable biomarkers or develop monitoring tools, it is of key importance to set up well-defined and large prospective patient cohorts, with a thorough longitudinal collection of a standardized clinical dataset assessing disease activity and organ involvement, paired with collection of patient material.¹⁹³ Such a dataset is required to ensure a strict definition of active and inactive disease [e.g., as proposed by Almeida et al.⁷²]. An important consideration for a successful biomarker study is the timing of data and sample collection: depending on the purpose of the biomarker, time points before start of immunosuppressive treatment, before each adjustment of medication, during flares, at paired time points during active and inactive disease or even at regular intervals of max 3–4 months may be crucial to reliably investigate the potency of a biomarker.

Next to the “classical” statistical approach, comparing patients with active disease and patients in remission (cross-sectionally or in paired samples), new computational approaches providing analysis methods that can integrate longitudinal data from multiple patients and multiple (bio)markers or scoring tools should be considered. These methods take into account the fluctuating nature of a relapsing-remitting disease such as JDM and are therefore better suited to test the reliability of a tool that will be used for longitudinal follow-up in clinical practice.^{194,195}

To achieve implementation of a marker or tool into clinical practice, both clinical and technical validation in independent cohorts is of utmost importance. Only few markers prove to be stable, reliable and easy to measure, which are key features for a marker or tool to be suited for implementation into clinical practice. Also the invasiveness of the method should

be taken into account. Ideally, a period of experimental implementation can demonstrate the added value and feasibility of a marker or tool in clinical practice. To achieve all this in a large group of JDM patients to ensure sufficient statistical power, international networks with well-established collaborations are fundamental.

Eventually, monitoring of disease activity with a reliable tool can be used to guide treatment and thereby facilitate precision medicine, with high dose therapy when indicated but also preventing overtreatment. This may reduce both the duration of active disease and thereby the disease-inflicted damage, and medication side effects, which will benefit the long-term outcomes on various domains, such as muscle weakness, organ damage, cardiopulmonary fitness, and quality of life. Next to facilitating personalized treatment strategies, newly identified biomarkers may also provide insights into the immunopathogenesis of JDM and provide new treatment targets. For instance, new treatment strategies targeting the IFN signature, such as anti-IFN antibodies (sifalimumab) or JAK-inhibition (ruxolitinib) have been shown to reduce the IFN signature in blood and muscle of adult dermatomyositis patients, and may therefore be promising new strategies for patients with JDM.^{186,196,197} Several studies discussed in this review suggest a strong link between the IFN signature and vasculopathy; and vasculopathy has been related to disease severity. Targeting the IFN signature may thus benefit vascularization in JDM and thereby improve outcomes.

REFERENCES

1. Meyer A, Meyer N, Schaeffer M, et al. Incidence and Prevalence of Inflammatory Myopathies: A Systematic Review. *Rheumatology (Oxford)*. **2015**, 54 (1), 50–63.
2. Miller FW, Cooper RG, Vencovsky J, et al. Genome-Wide Association Study of Dermatomyositis Reveals Genetic Overlap with Other Autoimmune Disorders. *Arthritis Rheum*. **2013**, 65 (12), 3239–3247.
3. Miller FW, Chen W, O'Hanlon TP, et al. Genome-Wide Association Study Identifies HLA 8.1 Ancestral Haplotype Alleles as Major Genetic Risk Factors for Myositis Phenotypes. *Genes Immun*. **2015**, 16 (7), 470–480.
4. Rothwell S, Cooper RG, Lundberg IE, et al. Dense Genotyping of Immune-Related Loci in Idiopathic Inflammatory Myopathies Confirms HLA Alleles as the Strongest Genetic Risk Factor and Suggests Different Genetic Background for Major Clinical Subgroups. *Ann. Rheum. Dis*. **2016**, 75 (8), 1558–1566.
5. Wedderburn LR, Rider LG. Juvenile Dermatomyositis: New Developments in Pathogenesis, Assessment and Treatment. *Best Pract. Res. Clin. Rheumatol*. **2009**, 23 (5), 665–678.
6. Lundberg IE, Tjarnlund A, Bottai M, et al. 2017 European League Against Rheumatism/American College of Rheumatology Classification Criteria for Adult and Juvenile Idiopathic Inflammatory Myopathies and Their Major Subgroups. *Ann. Rheum. Dis*. **2017**, 76 (12), 1955–1964.
7. Lundberg IE, Tjarnlund A, Bottai M, et al. 2017 European League Against Rheumatism/American College of Rheumatology Classification Criteria for Adult and Juvenile Idiopathic Inflammatory Myopathies and Their Major Subgroups. *Arthritis Rheumatol. (Hoboken, N.J.)* **2017**, 69 (12), 2271–2282.
8. Kobayashi N, Takezaki S, Kobayashi I, et al. Clinical and Laboratory Features of Fatal Rapidly Progressive Interstitial Lung Disease Associated with Juvenile Dermatomyositis. *Rheumatology (Oxford)*. **2015**, 54 (5), 784–791.
9. Huber AM, Mamyrova G, Lachenbruch PA, et al. Early Illness Features Associated with Mortality in the Juvenile Idiopathic Inflammatory Myopathies. *Arthritis Care Res. (Hoboken)*. **2014**, 66 (5), 732–740.
10. Feldman BM, Rider LG, Reed AM, et al. Juvenile Dermatomyositis and Other Idiopathic Inflammatory Myopathies of Childhood. *Lancet (London, England)* **2008**, 371 (9631), 2201–2212.
11. Huber A, Feldman BM. Long-Term Outcomes in Juvenile Dermatomyositis: How Did We Get Here and Where Are We Going? *Curr. Rheumatol. Rep*. **2005**, 7 (6), 441–446.
12. Gerami P, Walling HW, Lewis J, et al. A Systematic Review of Juvenile-Onset Clinically Amyopathic Dermatomyositis. *Br. J. Dermatol*. **2007**, 157 (4), 637–644.
13. Plamondon S, Dent PB. Juvenile Amyopathic Dermatomyositis: Results of a Case Finding Descriptive Survey. *J. Rheumatol*. **2000**, 27 (8), 2031–2034.
14. Oberle EJ, Bayer ML, Chiu YE, et al. How Often Are Pediatric Patients with Clinically Amyopathic Dermatomyositis Truly Amyopathic? *Pediatr. Dermatol*. **2017**, 34 (1), 50–57.
15. Mamyrova G, Kishi T, Targoff IN, et al. Features Distinguishing Clinically Amyopathic Juvenile Dermatomyositis from Juvenile Dermatomyositis. *Rheumatology (Oxford)*. **2018**, 57 (11), 1956–1963.
16. Rider LG, Nistala K. The Juvenile Idiopathic Inflammatory Myopathies: Pathogenesis, Clinical and Autoantibody Phenotypes, and Outcomes. *J. Intern. Med*. **2016**, 280 (1), 24–38.
17. Rider LG. The Heterogeneity of Juvenile Myositis. *Autoimmun. Rev*. **2007**, 6 (4), 241–247.

18. Huber AM, Lang B, LeBlanc CM, et al. Medium- and Long-Term Functional Outcomes in a Multicenter Cohort of Children with Juvenile Dermatomyositis. *Arthritis Rheum.* **2000**, 43 (3), 541–549.
19. Fisler RE, Liang MG, Fuhlbrigge RC, et al. Aggressive Management of Juvenile Dermatomyositis Results in Improved Outcome and Decreased Incidence of Calcinosis. *J. Am. Acad. Dermatol.* **2002**, 47 (4), 505–511.
20. Holzer U, van Royen-Kerkhof A, van der Torre P, et al. Successful Autologous Stem Cell Transplantation in Two Patients with Juvenile Dermatomyositis. *Scand. J. Rheumatol.* **2010**, 39 (1), 88–92.
21. Crowe WE, Bove KE, Levinson JE, et al. Clinical and Pathogenetic Implications of Histopathology in Childhood Polydermatomyositis. *Arthritis Rheum.* **1982**, 25 (2), 126–139.
22. Huemer C, Kitson H, Malleson PN, et al. Lipodystrophy in Patients with Juvenile Dermatomyositis—Evaluation of Clinical and Metabolic Abnormalities. *J. Rheumatol.* **2001**, 28 (3), 610–615.
23. Verma S, Singh S, Bhalla AK, et al. Study of Subcutaneous Fat in Children with Juvenile Dermatomyositis. *Arthritis Rheum.* **2006**, 55 (4), 564–568.
24. Bingham A, Mamyrova G, Rother KI, et al. Predictors of Acquired Lipodystrophy in Juvenile-Onset Dermatomyositis and a Gradient of Severity. *Medicine (Baltimore).* **2008**, 87 (2), 70–86.
25. Pouessel G, Deschildre A, Le Bourgeois M, et al. The Lung Is Involved in Juvenile Dermatomyositis. *Pediatr. Pulmonol.* **2013**, 48 (10), 1016–1025.
26. Richardson AE, Warriar K, Vyas H. Respiratory Complications of the Rheumatological Diseases in Childhood. *Arch. Dis. Child.* **2016**, 101 (8), 752–758.
27. Kobayashi S, Higuchi K, Tamaki H, et al. Characteristics of Juvenile Dermatomyositis in Japan. *Acta Paediatr. Jpn. Overseas Ed.* **1997**, 39 (2), 257–262.
28. Shah M, Mamyrova G, Targoff IN, et al. The Clinical Phenotypes of the Juvenile Idiopathic Inflammatory Myopathies. *Medicine (Baltimore).* **2013**, 92 (1), 25–41.
29. Sanner H, Aalokken TM, Gran JT, et al. Pulmonary Outcome in Juvenile Dermatomyositis: A Case-Control Study. *Ann. Rheum. Dis.* **2011**, 70 (1), 86–91.
30. Morinishi Y, Oh-Ishi T, Kabuki T, et al. Juvenile Dermatomyositis: Clinical Characteristics and the Relatively High Risk of Interstitial Lung Disease. *Mod. Rheumatol.* **2007**, 17 (5), 413–417.
31. Cantez S, Gross GJ, MacLusky I, et al. Cardiac Findings in Children with Juvenile Dermatomyositis at Disease Presentation. *Pediatr. Rheumatol. Online J.* **2017**, 15 (1), 54.
32. Pachman LM, Cooke N. Juvenile Dermatomyositis: A Clinical and Immunologic Study. *J. Pediatr.* **1980**, 96 (2), 226–234.
33. Na S-J, Kim SM, Sunwoo IN, et al. Clinical Characteristics and Outcomes of Juvenile and Adult Dermatomyositis. *J. Korean Med. Sci.* **2009**, 24 (4), 715–721.
34. Constantin T, Ponyi A, Orban I, et al. National Registry of Patients with Juvenile Idiopathic Inflammatory Myopathies in Hungary—Clinical Characteristics and Disease Course of 44 Patients with Juvenile Dermatomyositis. *Autoimmunity* **2006**, 39 (3), 223–232.
35. Shehata R, al-Mayouf S, al-Dalaan A, et al. Juvenile Dermatomyositis: Clinical Profile and Disease Course in 25 Patients. *Clin. Exp. Rheumatol.* **1999**, 17 (1), 115–118.
36. Schwartz T, Sanner H, Gjesdal O, et al. In Juvenile Dermatomyositis, Cardiac Systolic Dysfunction Is Present after Long-Term Follow-up and Is Predicted by Sustained Early Skin Activity. *Ann. Rheum. Dis.* **2014**, 73 (10), 1805–1810.

37. Schwartz T, Sanner H, Husebye T, et al. Cardiac Dysfunction in Juvenile Dermatomyositis: A Case-Control Study. *Ann. Rheum. Dis.* **2011**, *70* (5), 766–771.
38. Schwartz T, Diederichsen LP, Lundberg IE, et al. Cardiac Involvement in Adult and Juvenile Idiopathic Inflammatory Myopathies. *RMD open* **2016**, *2* (2), e000291.
39. Jimenez C, Rowe PC, Keene D. Cardiac and Central Nervous System Vasculitis in a Child with Dermatomyositis. *J. Child Neurol.* **1994**, *9* (3), 297–300.
40. Ramanan A V, Sawhney S, Murray KJ. Central Nervous System Complications in Two Cases of Juvenile Onset Dermatomyositis. *Rheumatology (Oxford)*. **2001**, *40* (11), 1293–1298.
41. Silverberg JI, Kwa L, Kwa MC, et al. Cardiovascular and Cerebrovascular Comorbidities of Juvenile Dermatomyositis in US Children: An Analysis of the National Inpatient Sample. *Rheumatology (Oxford)*. **2018**, *57* (4), 694–702.
42. Robinson AB, Hoeltzel MF, Wahezi DM, et al. Clinical Characteristics of Children with Juvenile Dermatomyositis: The Childhood Arthritis and Rheumatology Research Alliance Registry. *Arthritis Care Res. (Hoboken)*. **2014**, *66* (3), 404–410.
43. Laskin BL, Choyke P, Keenan GF, et al. Novel Gastrointestinal Tract Manifestations in Juvenile Dermatomyositis. *J. Pediatr.* **1999**, *135* (3), 371–374.
44. Mamyrova G, Kleiner DE, James-Newton L, et al. Late-Onset Gastrointestinal Pain in Juvenile Dermatomyositis as a Manifestation of Ischemic Ulceration from Chronic Endarteropathy. *Arthritis Rheum.* **2007**, *57* (5), 881–884.
45. Varsani H, Charman SC, Li CK, et al. Validation of a Score Tool for Measurement of Histological Severity in Juvenile Dermatomyositis and Association with Clinical Severity of Disease. *Ann. Rheum. Dis.* **2015**, *74* (1), 204–210.
46. Besancon A, Brochard K, Dupic L, et al. Presentations and Outcomes of Juvenile Dermatomyositis Patients Admitted to Intensive Care Units. *Rheumatology (Oxford)*. **2017**, *56* (10), 1814–1816.
47. Meneghel A, Martini G, Birolo C, et al. Life-Threatening Systemic Capillary Leak Syndrome in Juvenile Dermatomyositis. *Rheumatology (Oxford)*. **2017**, *56* (10), 1822–1823.
48. Goncalves FGP, Chimelli L, Sallum AME, et al. Immunohistological Analysis of CD59 and Membrane Attack Complex of Complement in Muscle in Juvenile Dermatomyositis. *J. Rheumatol.* **2002**, *29* (6), 1301–1307.
49. Yu H-H, Chang H-M, Chiu C-J, et al. Detection of Anti-p155/140, Anti-p140, and Antiendothelial Cells Autoantibodies in Patients with Juvenile Dermatomyositis. *J. Microbiol. Immunol. Infect.* **2016**, *49* (2), 264–270.
50. Karasawa R, Tamaki M, Sato T, et al. Multiple Target Autoantigens on Endothelial Cells Identified in Juvenile Dermatomyositis Using Proteomics. *Rheumatology (Oxford)*. **2018**, *57* (4), 671–676.
51. Whitaker JN, Engel WK. Vascular Deposits of Immunoglobulin and Complement in Idiopathic Inflammatory Myopathy. *N. Engl. J. Med.* **1972**, *286* (7), 333–338.
52. Kissel JT, Mendell JR, Rammohan KW. Microvascular Deposition of Complement Membrane Attack Complex in Dermatomyositis. *N. Engl. J. Med.* **1986**, *314* (6), 329–334.

53. Kissel JT, Halterman RK, Rammohan KW, et al. The Relationship of Complement-Mediated Microvasculopathy to the Histologic Features and Clinical Duration of Disease in Dermatomyositis. *Arch. Neurol.* **1991**, 48 (1), 26–30.
54. Emslie-Smith AM, Engel AG. Microvascular Changes in Early and Advanced Dermatomyositis: A Quantitative Study. *Ann. Neurol.* **1990**, 27 (4), 343–356.
55. Gitiaux C, De Antonio M, Aouizerate J, et al. Vasculopathy-Related Clinical and Pathological Features Are Associated with Severe Juvenile Dermatomyositis. *Rheumatology (Oxford)*. **2016**, 55 (3), 470–479.
56. Schmeling H, Stephens S, Goia C, et al. Nailfold Capillary Density Is Importantly Associated over Time with Muscle and Skin Disease Activity in Juvenile Dermatomyositis. *Rheumatology (Oxford)*. **2011**, 50 (5), 885–893.
57. Feldman BM, Rider LG, Dugan L, et al. Nailfold Capillaries as Indicators of Disease Activity in Juvenile Idiopathic Inflammatory Myopathies (JIIM). *Arthritis Rheum.* **1999**, 42, S181.
58. Smith RL, Sundberg J, Shamiyah E, et al. Skin Involvement in Juvenile Dermatomyositis Is Associated with Loss of End Row Nailfold Capillary Loops. *J. Rheumatol.* **2004**, 31 (8), 1644–1649.
59. Bertolazzi C, Cutolo M, Smith V, et al. State of the Art on Nailfold Capillaroscopy in Dermatomyositis and Polymyositis. *Semin. Arthritis Rheum.* **2017**, 47 (3), 432–444.
60. Rider LG, Werth VP, Huber AM, et al. Measures of Adult and Juvenile Dermatomyositis, Polymyositis, and Inclusion Body Myositis: Physician and Patient/Parent Global Activity, Manual Muscle Testing (MMT), Health Assessment Questionnaire (HAQ)/Childhood Health Assessment Questionnaire (C-HAQ),. *Arthritis care (&) Res.* **2011**, 63 Suppl 1, S118-57.
61. Lovell DJ, Lindsley CB, Rennebohm RM, et al. Development of Validated Disease Activity and Damage Indices for the Juvenile Idiopathic Inflammatory Myopathies. II. The Childhood Myositis Assessment Scale (CMAS): A Quantitative Tool for the Evaluation of Muscle Function. The Juvenile Dermatomyositis D. *Arthritis Rheum.* **1999**, 42 (10), 2213–2219.
62. Rider LG, Koziol D, Giannini EH, et al. Validation of Manual Muscle Testing and a Subset of Eight Muscles for Adult and Juvenile Idiopathic Inflammatory Myopathies. *Arthritis Care Res. (Hoboken)*. **2010**, 62 (4), 465–472.
63. Rider LG, Feldman BM, Perez MD, et al. Development of Validated Disease Activity and Damage Indices for the Juvenile Idiopathic Inflammatory Myopathies: I. Physician, Parent, and Patient Global Assessments. Juvenile Dermatomyositis Disease Activity Collaborative Study Group. *Arthritis Rheum.* **1997**, 40 (11), 1976–1983.
64. Huber AM, Dugan EM, Lachenbruch PA, et al. Preliminary Validation and Clinical Meaning of the Cutaneous Assessment Tool in Juvenile Dermatomyositis. *Arthritis Rheum.* **2008**, 59 (2), 214–221.
65. Huber AM, Lachenbruch PA, Dugan EM, et al. Alternative Scoring of the Cutaneous Assessment Tool in Juvenile Dermatomyositis: Results Using Abbreviated Formats. *Arthritis Rheum.* **2008**, 59 (3), 352–356.
66. Bode RK, Klein-Gitelman MS, Miller ML, et al. Disease Activity Score for Children with Juvenile Dermatomyositis: Reliability and Validity Evidence. *Arthritis Rheum.* **2003**, 49 (1), 7–15.
67. Huber AM, Hicks JE, Lachenbruch PA, et al. Validation of the Childhood Health Assessment Questionnaire in the Juvenile Idiopathic Myopathies. Juvenile Dermatomyositis Disease Activity Collaborative Study Group. *J. Rheumatol.* **2001**, 28 (5), 1106–1111.

68. Tiao J, Feng R, Berger EM, et al. Evaluation of the Reliability of the Cutaneous Dermatomyositis Disease Area and Severity Index and the Cutaneous Assessment Tool-Binary Method in Juvenile Dermatomyositis among Paediatric Dermatologists, Rheumatologists and Neurologists. *Br. J. Dermatol.* **2017**, *177* (4), 1086–1092.
69. Sultan SM, Allen E, Cooper RG, et al. Interrater Reliability and Aspects of Validity of the Myositis Damage Index. *Ann. Rheum. Dis.* **2011**, *70* (7), 1272–1276.
70. McCann LJ, Kirkham JJ, Wedderburn LR, et al. Development of an Internationally Agreed Minimal Dataset for Juvenile Dermatomyositis (JDM) for Clinical and Research Use. *Trials* **2015**, *16*, 268.
71. Lazarevic D, Pistorio A, Palmisani E, et al. The PRINTO Criteria for Clinically Inactive Disease in Juvenile Dermatomyositis. *Ann. Rheum. Dis.* **2013**, *72* (5), 686–693.
72. Almeida B, Campanilho-Marques R, Arnold K, et al. Analysis of Published Criteria for Clinically Inactive Disease in a Large Juvenile Dermatomyositis Cohort Shows That Skin Disease Is Underestimated. *Arthritis Rheumatol. (Hoboken, N.J.)* **2015**, *67* (9), 2495–2502.
73. Betteridge ZE, Gunawardena H, McHugh NJ. Novel Autoantibodies and Clinical Phenotypes in Adult and Juvenile Myositis. *Arthritis Res. Ther.* **2011**, *13* (2), 209.
74. Rider LG, Miller FW. Deciphering the Clinical Presentations, Pathogenesis, and Treatment of the Idiopathic Inflammatory Myopathies. *JAMA* **2011**, *305* (2), 183–190.
75. Rider LG, Shah M, Mamyrova G, et al. The Myositis Autoantibody Phenotypes of the Juvenile Idiopathic Inflammatory Myopathies. *Medicine (Baltimore)*. **2013**, *92* (4), 223–243.
76. Tansley SL, Simou S, Shaddick G, et al. Autoantibodies in Juvenile-Onset Myositis: Their Diagnostic Value and Associated Clinical Phenotype in a Large UK Cohort. *J. Autoimmun.* **2017**, *84*, 55–64.
77. Gunawardena H, Wedderburn LR, North J, et al. Clinical Associations of Autoantibodies to a p155/140 kDa Doublet Protein in Juvenile Dermatomyositis. *Rheumatology (Oxford)*. **2008**, *47* (3), 324–328.
78. Habers GEA, Huber AM, Mamyrova G, et al. Brief Report: Association of Myositis Autoantibodies, Clinical Features, and Environmental Exposures at Illness Onset With Disease Course in Juvenile Myositis. *Arthritis Rheumatol. (Hoboken, N.J.)* **2016**, *68* (3), 761–768.
79. Tansley SL, Betteridge ZE, Shaddick G, et al. Calcinosis in Juvenile Dermatomyositis Is Influenced by Both Anti-NXP2 Autoantibody Status and Age at Disease Onset. *Rheumatology (Oxford)*. **2014**, *53* (12), 2204–2208.
80. Gunawardena H, Wedderburn LR, Chinoy H, et al. Autoantibodies to a 140-Kd Protein in Juvenile Dermatomyositis Are Associated with Calcinosis. *Arthritis Rheum.* **2009**, *60* (6), 1807–1814.
81. Sato S, Hirakata M, Kuwana M, et al. Autoantibodies to a 140-Kd Polypeptide, CADM-140, in Japanese Patients with Clinically Amyopathic Dermatomyositis. *Arthritis Rheum.* **2005**, *52* (5), 1571–1576.
82. Tansley SL, Betteridge ZE, Gunawardena H, et al. Anti-MDA5 Autoantibodies in Juvenile Dermatomyositis Identify a Distinct Clinical Phenotype: A Prospective Cohort Study. *Arthritis Res. Ther.* **2014**, *16* (4), R138.
83. Hoshino K, Muro Y, Sugiura K, et al. Anti-MDA5 and Anti-TIF1-Gamma Antibodies Have Clinical Significance for Patients with Dermatomyositis. *Rheumatology (Oxford)*. **2010**, *49* (9), 1726–1733.
84. Hall JC, Casciola-Rosen L, Samedy L-A, et al. Anti-Melanoma Differentiation-Associated Protein 5-Associated Dermatomyositis: Expanding the Clinical Spectrum. *Arthritis Care Res. (Hoboken)*. **2013**, *65* (8), 1307–1315.

85. Fiorentino D, Chung L, Zwerner J, et al. The Mucocutaneous and Systemic Phenotype of Dermatomyositis Patients with Antibodies to MDA5 (CADM-140): A Retrospective Study. *J. Am. Acad. Dermatol.* **2011**, 65 (1), 25–34.
86. Tansley SL, Betteridge ZE, Simou S, et al. Anti-HMGR Autoantibodies in Juvenile Idiopathic Inflammatory Myopathies Identify a Rare but Clinically Important Subset of Patients. *J. Rheumatol.* **2017**.
87. Kishi T, Rider LG, Pak K, et al. Association of Anti-3-Hydroxy-3-Methylglutaryl-Coenzyme A Reductase Autoantibodies With DRB1*07:01 and Severe Myositis in Juvenile Myositis Patients. *Arthritis Care Res. (Hoboken)*. **2017**, 69 (7), 1088–1094.
88. Aggarwal R, Oddis C V, Goudeau D, et al. Autoantibody Levels in Myositis Patients Correlate with Clinical Response during B Cell Depletion with Rituximab. *Rheumatology (Oxford)*. **2016**, 55 (6), 991–999.
89. O'Connor KA, Abbott KA, Sabin B, et al. MxA Gene Expression in Juvenile Dermatomyositis Peripheral Blood Mononuclear Cells: Association with Muscle Involvement. *Clin. Immunol.* **2006**, 120 (3), 319–325.
90. Niewold TB, Kariuki SN, Morgan GA, et al. Elevated Serum Interferon-Alpha Activity in Juvenile Dermatomyositis: Associations with Disease Activity at Diagnosis and after Thirty-Six Months of Therapy. *Arthritis Rheum.* **2009**, 60 (6), 1815–1824.
91. Baechler EC, Bilgic H, Reed AM. Type I Interferon Pathway in Adult and Juvenile Dermatomyositis. *Arthritis Res. Ther.* **2011**, 13 (6), 249.
92. Sanner H, Schwartz T, Flato B, et al. Increased Levels of Eotaxin and MCP-1 in Juvenile Dermatomyositis Median 16.8 Years after Disease Onset; Associations with Disease Activity, Duration and Organ Damage. *PLoS One* **2014**, 9 (3), e92171.
93. Bellutti Enders F, van Wijk F, Scholman R, et al. Correlation of CXCL10, Tumor Necrosis Factor Receptor Type II, and Galectin 9 with Disease Activity in Juvenile Dermatomyositis. *Arthritis Rheumatol. (Hoboken, N.J.)* **2014**, 66 (8), 2281–2289.
94. Enders FB, Delemarre EM, Kuemmerle-Deschner J, et al. Autologous Stem Cell Transplantation Leads to a Change in Proinflammatory Plasma Cytokine Profile of Patients with Juvenile Dermatomyositis Correlating with Disease Activity. *Annals of the rheumatic diseases*. England January 2015, pp 315–317.
95. Kobayashi I, Ono S, Kawamura N, et al. Elevated Serum Levels of Soluble Interleukin-2 Receptor in Juvenile Dermatomyositis. *Pediatr. Int.* **2001**, 43 (1), 109–111.
96. De Benedetti F, De Amici M, Aramini L, et al. Correlation of Serum Neopterin Concentrations with Disease Activity in Juvenile Dermatomyositis. *Arch. Dis. Child.* **1993**, 69 (2), 232–235.
97. Rider LG, Schiffenbauer AS, Zito M, et al. Neopterin and Quinolinic Acid Are Surrogate Measures of Disease Activity in the Juvenile Idiopathic Inflammatory Myopathies. *Clin. Chem.* **2002**, 48 (10), 1681–1688.
98. Nistala K, Varsani H, Wittkowski H, et al. Myeloid Related Protein Induces Muscle Derived Inflammatory Mediators in Juvenile Dermatomyositis. *Arthritis Res. Ther.* **2013**, 15 (5), R131.
99. Haas RH, Dyck RF, Dubowitz V, et al. C-Reactive Protein in Childhood Dermatomyositis. *Ann. Rheum. Dis.* **1982**, 41 (5), 483–485.
100. Eisenstein DM, O'Gorman MR, Pachman LM. Correlations between Change in Disease Activity and Changes in Peripheral Blood Lymphocyte Subsets in Patients with Juvenile Dermatomyositis. *J. Rheumatol.* **1997**, 24 (9), 1830–1832.

101. Elst EF, Klein M, de Jager W, et al. Hsp60 in Inflamed Muscle Tissue Is the Target of Regulatory Autoreactive T Cells in Patients with Juvenile Dermatomyositis. *Arthritis Rheum.* **2008**, *58* (2), 547–555.
102. Morita R, Schmitt N, Bentebibel S-E, et al. Human Blood CXCR5(+)CD4(+) T Cells Are Counterparts of T Follicular Cells and Contain Specific Subsets That Differentially Support Antibody Secretion. *Immunity* **2011**, *34* (1), 108–121.
103. Ernste FC, Crowson CS, de Padilla CL, et al. Longitudinal Peripheral Blood Lymphocyte Subsets Correlate with Decreased Disease Activity in Juvenile Dermatomyositis. *J. Rheumatol.* **2013**, *40* (7), 1200–1211.
104. Vercoulen Y, Bellutti Enders F, Meerding J, et al. Increased Presence of FOXP3+ Regulatory T Cells in Inflamed Muscle of Patients with Active Juvenile Dermatomyositis Compared to Peripheral Blood. *PLoS One* **2014**, *9* (8), e105353.
105. Lopez De Padilla CM, Crowson CS, Hein MS, et al. Gene Expression Profiling in Blood and Affected Muscle Tissues Reveals Differential Activation Pathways in Patients with New-Onset Juvenile and Adult Dermatomyositis. *J. Rheumatol.* **2017**, *44* (1), 117–124.
106. Piper CJM, Wilkinson MGL, Deakin CT, et al. CD19(+)CD24(hi)CD38(hi) B Cells Are Expanded in Juvenile Dermatomyositis and Exhibit a Pro-Inflammatory Phenotype After Activation Through Toll-Like Receptor 7 and Interferon-Alpha. *Front. Immunol.* **2018**, *9*, 1372.
107. Guzman J, Petty RE, Malleson PN. Monitoring Disease Activity in Juvenile Dermatomyositis: The Role of von Willebrand Factor and Muscle Enzymes. *J. Rheumatol.* **1994**, *21* (4), 739–743.
108. Bloom BJ, Tucker LB, Miller LC, et al. Von Willebrand Factor in Juvenile Dermatomyositis. *J. Rheumatol.* **1995**, *22* (2), 320–325.
109. Scott JP, Arroyave C. Activation of Complement and Coagulation in Juvenile Dermatomyositis. *Arthritis Rheum.* **1987**, *30* (5), 572–576.
110. Xu D, Huang C-C, Kachaochana A, et al. MicroRNA-10a Regulation of Proinflammatory Mediators: An Important Component of Untreated Juvenile Dermatomyositis. *J. Rheumatol.* **2016**, *43* (1), 161–168.
111. Xu D, Kacha-Ochana A, Morgan GA, et al. Endothelial Progenitor Cell Number Is Not Decreased in 34 Children with Juvenile Dermatomyositis: A Pilot Study. *Pediatr. Rheumatol. Online J.* **2017**, *15* (1), 42.
112. Coyle K, Rother KI, Weise M, et al. Metabolic Abnormalities and Cardiovascular Risk Factors in Children with Myositis. *J. Pediatr.* **2009**, *155* (6), 882–887.
113. Kozu KT, Silva CA, Bonfa E, et al. Dyslipidaemia in Juvenile Dermatomyositis: The Role of Disease Activity. *Clin. Exp. Rheumatol.* **2013**, *31* (4), 638–644.
114. Olazagasti JM, Hein M, Crowson CS, et al. Adipokine Gene Expression in Peripheral Blood of Adult and Juvenile Dermatomyositis Patients and Their Relation to Clinical Parameters and Disease Activity Measures. *J. Inflamm. (Lond)*. **2015**, *12*, 29.
115. Baechler EC, Bauer JW, Slattery CA, et al. An Interferon Signature in the Peripheral Blood of Dermatomyositis Patients Is Associated with Disease Activity. *Mol. Med.* **2007**, *13* (1–2), 59–68.
116. Bilgic H, Ytterberg SR, Amin S, et al. Interleukin-6 and Type I Interferon-Regulated Genes and Chemokines Mark Disease Activity in Dermatomyositis. *Arthritis Rheum.* **2009**, *60* (11), 3436–3446.
117. Reed AM, Peterson E, Bilgic H, et al. Changes in Novel Biomarkers of Disease Activity in Juvenile and Adult Dermatomyositis Are Sensitive Biomarkers of Disease Course. *Arthritis Rheum.* **2012**, *64* (12), 4078–4086.

118. Gabay C, Gay-Croisier F, Roux-Lombard P, et al. Elevated Serum Levels of Interleukin-1 Receptor Antagonist in Polymyositis/dermatomyositis. A Biologic Marker of Disease Activity with a Possible Role in the Lack of Acute-Phase Protein Response. *Arthritis Rheum.* **1994**, 37 (12), 1744–1751.
119. Krystufkova O, Vallerskog T, Helmers SB, et al. Increased Serum Levels of B Cell Activating Factor (BAFF) in Subsets of Patients with Idiopathic Inflammatory Myopathies. *Ann. Rheum. Dis.* **2009**, 68 (6), 836–843.
120. Lopez De Padilla CM, McNallan KT, Crowson CS, et al. BAFF Expression Correlates with Idiopathic Inflammatory Myopathy Disease Activity Measures and Autoantibodies. *J. Rheumatol.* **2013**, 40 (3), 294–302.
121. Ishida T, Matsumoto Y, Ohashi M, et al. Analysis of Lymphocyte Subpopulations in Peripheral Blood in Adult and Juvenile Cases of Dermatomyositis. *J. Dermatol.* **1993**, 20 (1), 30–34.
122. Aleksza M, Szegedi A, Antal-Szalmas P, et al. Altered Cytokine Expression of Peripheral Blood Lymphocytes in Polymyositis and Dermatomyositis. *Ann. Rheum. Dis.* **2005**, 64 (10), 1485–1489.
123. Kubo M, Ihn H, Yamane K, et al. Increased Serum Levels of Soluble Vascular Cell Adhesion Molecule-1 and Soluble E-Selectin in Patients with Polymyositis/dermatomyositis. *Br. J. Dermatol.* **2000**, 143 (2), 392–398.
124. Bloom BJ, Miller LC, Blier PR. Soluble Adhesion Molecules in Pediatric Rheumatic Diseases. *J. Rheumatol.* **2002**, 29 (4), 832–836.
125. McCann LJ, Juggins AD, Maillard SM, et al. The Juvenile Dermatomyositis National Registry and Repository (UK and Ireland)—Clinical Characteristics of Children Recruited within the First 5 Yr. *Rheumatology (Oxford)*. **2006**, 45 (10), 1255–1260.
126. Pachman LM, Hayford JR, Chung A, et al. Juvenile Dermatomyositis at Diagnosis: Clinical Characteristics of 79 Children. *J. Rheumatol.* **1998**, 25 (6), 1198–1204.
127. Targoff IN. Laboratory Manifestations of Polymyositis/dermatomyositis. *Clin. Dermatol.* **1988**, 6 (2), 76–92.
128. Mathiesen PR, Zak M, Herlin T, et al. Clinical Features and Outcome in a Danish Cohort of Juvenile Dermatomyositis Patients. *Clin. Exp. Rheumatol.* **2010**, 28 (5), 782–789.
129. Ntusi NBA, Heckmann JM. Myopathy with a Normal Creatine Kinase Level in Juvenile Myopathic Dermatomyositis. *S. Afr. Med. J.* **2010**, 100 (1), 24–25.

130. Hinderks GJ, Frolich J. Low Serum Creatine Kinase Values Associated with Administration of Steroids. *Clinical chemistry*. United States December 1979, pp 2050–2051.
131. Kagen LJ, Aram S. Creatine Kinase Activity Inhibitor in Sera from Patients with Muscle Disease. *Arthritis Rheum*. **1987**, *30* (2), 213–217.
132. Rider LG, Miller FW. Laboratory Evaluation of the Inflammatory Myopathies. *Clin. Diagn. Lab. Immunol*. **1995**, *2* (1), 1–9.
133. Naim MY, Reed AM. Enzyme Elevation in Patients with Juvenile Dermatomyositis and Steroid Myopathy. *J. Rheumatol*. **2006**, *33* (7), 1392–1394.
134. Hinze CH, Oommen PT, Dressler F, et al. Development of Practice and Consensus-Based Strategies Including a Treat-to-Target Approach for the Management of Moderate and Severe Juvenile Dermatomyositis in Germany and Austria. *Pediatr. Rheumatol. Online J*. **2018**, *16* (1), 40.
135. Enders FB, Bader-Meunier B, Baildam E, et al. Consensus-Based Recommendations for the Management of Juvenile Dermatomyositis. *Ann. Rheum. Dis*. **2017**, *76* (2), 329–340.
136. Rice GI, Melki I, Fremont M-L, et al. Assessment of Type I Interferon Signaling in Pediatric Inflammatory Disease. *J. Clin. Immunol*. **2017**, *37* (2), 123–132.
137. Fall N, Bove KE, Stringer K, et al. Association between Lack of Angiogenic Response in Muscle Tissue and High Expression of Angiostatic ELR-Negative CXC Chemokines in Patients with Juvenile Dermatomyositis: Possible Link to Vasculopathy. *Arthritis Rheum*. **2005**, *52* (10), 3175–3180.
138. Rodero MP, Decalf J, Bondet V, et al. Detection of Interferon Alpha Protein Reveals Differential Levels and Cellular Sources in Disease. *J. Exp. Med*. **2017**, *214* (5), 1547–1555.
139. van den Hoogen LL, van Roon JAG, Mertens JS, et al. Galectin-9 Is an Easy to Measure Biomarker for the Interferon Signature in Systemic Lupus Erythematosus and Antiphospholipid Syndrome. *Ann. Rheum. Dis*. **2018**.
140. Wachter H, Fuchs D, Hausen A, et al. Neopterin as Marker for Activation of Cellular Immunity: Immunologic Basis and Clinical Application. *Adv. Clin. Chem*. **1989**, *27*, 81–141.
141. Holzinger D, Frosch M, Kastrop A, et al. The Toll-like Receptor 4 Agonist MRP8/14 Protein Complex Is a Sensitive Indicator for Disease Activity and Predicts Relapses in Systemic-Onset Juvenile Idiopathic Arthritis. *Ann. Rheum. Dis*. **2012**, *71* (6), 974–980.
142. Silverman ED, Laxer RM, Nelson DL, et al. Soluble Interleukin-2 Receptor in Juvenile Rheumatoid Arthritis. *J. Rheumatol*. **1991**, *18* (9), 1398–1402.
143. Kobayashi I, Okura Y, Yamada M, et al. Anti-Melanoma Differentiation-Associated Gene 5 Antibody Is a Diagnostic and Predictive Marker for Interstitial Lung Diseases Associated with Juvenile Dermatomyositis. *J. Pediatr*. **2011**, *158* (4), 675–677.
144. Kobayashi I, Ono S, Kawamura N, et al. KL-6 Is a Potential Marker for Interstitial Lung Disease Associated with Juvenile Dermatomyositis. *J. Pediatr*. **2001**, *138* (2), 274–276.
145. Kobayashi N, Kobayashi I, Mori M, et al. Increased Serum B Cell Activating Factor and a Proliferation-Inducing Ligand Are Associated with Interstitial Lung Disease in Patients with Juvenile Dermatomyositis. *J. Rheumatol*. **2015**, *42* (12), 2412–2418.

146. Schwartz T, Sjaastad I, Flato B, et al. In Active Juvenile Dermatomyositis, Elevated Eotaxin and MCP-1 and Cholesterol Levels in the Upper Normal Range Are Associated with Cardiac Dysfunction. *Rheumatology (Oxford)*. **2014**, 53 (12), 2214–2222.
147. Barth Z, Nomeland Witczak B, Schwartz T, et al. In Juvenile Dermatomyositis, Heart Rate Variability Is Reduced, and Associated with Both Cardiac Dysfunction and Markers of Inflammation: A Cross-Sectional Study Median 13.5 Years after Symptom Onset. *Rheumatology (Oxford)*. **2016**, 55 (3), 535–543.
148. van Summeren MJH, Spliet WGM, van Royen-Kerkhof A, et al. Calcinosis in Juvenile Dermatomyositis: A Possible Role for the Vitamin K-Dependent Protein Matrix Gla Protein. *Rheumatology (Oxford)*. **2008**, 47 (3), 267–271.
149. Reed A, Haugen M, Pachman LM, et al. Abnormalities in Serum Osteocalcin Values in Children with Chronic Rheumatic Diseases. *J. Pediatr.* **1990**, 116 (4), 574–580.
150. Chinoy H, Salway F, John S, et al. Tumour Necrosis Factor-Alpha Single Nucleotide Polymorphisms Are Not Independent of HLA Class I in UK Caucasians with Adult Onset Idiopathic Inflammatory Myopathies. *Rheumatology (Oxford)*. **2007**, 46 (9), 1411–1416.
151. Lutz J, Huwiler KG, Fedczyna T, et al. Increased Plasma Thrombospondin-1 (TSP-1) Levels Are Associated with the TNF Alpha-308A Allele in Children with Juvenile Dermatomyositis. *Clin. Immunol.* **2002**, 103 (3 Pt 1), 260–263.
152. Niewold TB, Kariuki SN, Morgan GA, et al. Gene-Gene-Sex Interaction in Cytokine Gene Polymorphisms Revealed by Serum Interferon Alpha Phenotype in Juvenile Dermatomyositis. *J. Pediatr.* **2010**, 157 (4), 653–657.
153. Pachman LM, Liotta-Davis MR, Hong DK, et al. TNFalpha-308A Allele in Juvenile Dermatomyositis: Association with Increased Production of Tumor Necrosis Factor Alpha, Disease Duration, and Pathologic Calcifications. *Arthritis Rheum.* **2000**, 43 (10), 2368–2377.
154. Pachman LM, Fedczyna TO, Lechman TS, et al. Juvenile Dermatomyositis: The Association of the TNF Alpha-308A Allele and Disease Chronicity. *Curr. Rheumatol. Rep.* **2001**, 3 (5), 379–386.
155. Bohan A, Peter JB. Polymyositis and Dermatomyositis (First of Two Parts). *N. Engl. J. Med.* **1975**, 292 (7), 344–347.
156. Bohan A, Peter JB. Polymyositis and Dermatomyositis (Second of Two Parts). *N. Engl. J. Med.* **1975**, 292 (8), 403–407.
157. Wedderburn LR, Varsani H, Li CKC, et al. International Consensus on a Proposed Score System for Muscle Biopsy Evaluation in Patients with Juvenile Dermatomyositis: A Tool for Potential Use in Clinical Trials. *Arthritis Rheum.* **2007**, 57 (7), 1192–1201.
158. Deakin CT, Yasin SA, Simou S, et al. Muscle Biopsy Findings in Combination With Myositis-Specific Autoantibodies Aid Prediction of Outcomes in Juvenile Dermatomyositis. *Arthritis Rheumatol. (Hoboken, N.J.)* **2016**, 68 (11), 2806–2816.
159. Li CKC, Varsani H, Holton JL, et al. MHC Class I Overexpression on Muscles in Early Juvenile Dermatomyositis. *J. Rheumatol.* **2004**, 31 (3), 605–609.
160. Sallum AME, Kiss MHB, Silva CAA, et al. MHC Class I and II Expression in Juvenile Dermatomyositis Skeletal Muscle. *Clin. Exp. Rheumatol.* **2009**, 27 (3), 519–526.

161. Sallum AME, Marie SKN, Wakamatsu A, et al. Immunohistochemical Analysis of Adhesion Molecule Expression on Muscle Biopsy Specimens from Patients with Juvenile Dermatomyositis. *J. Rheumatol.* **2004**, 31 (4), 801–807.
162. Sakuta R, Murakami N, Jin Y, et al. Diagnostic Significance of Membrane Attack Complex and Vitronectin in Childhood Dermatomyositis. *J. Child Neurol.* **2005**, 20 (7), 597–602.
163. Tezak Z, Hoffman EP, Lutz JL, et al. Gene Expression Profiling in DQA1*0501+ Children with Untreated Dermatomyositis: A Novel Model of Pathogenesis. *J. Immunol.* **2002**, 168 (8), 4154–4163.
164. Shrestha S, Wershil B, Sarwark JF, et al. Lesional and Nonlesional Skin from Patients with Untreated Juvenile Dermatomyositis Displays Increased Numbers of Mast Cells and Mature Plasmacytoid Dendritic Cells. *Arthritis Rheum.* **2010**, 62 (9), 2813–2822.
165. Wargula JC, Lovell DJ, Passo MH, et al. What More Can We Learn from Muscle Histopathology in Children with Dermatomyositis/polymyositis? *Clin. Exp. Rheumatol.* **2006**, 24 (3), 333–343.
166. Soponkanaporn S, Deakin CT, Schutz PW, et al. Expression of Myxovirus-Resistance Protein A: A Possible Marker of Muscle Disease Activity and Autoantibody Specificities in Juvenile Dermatomyositis. *Neuropathol. Appl. Neurobiol.* **2018**.
167. Gitiaux C, Latroche C, Weiss-Gayet M, et al. Myogenic Progenitor Cells Exhibit Type I Interferon-Driven Proangiogenic Properties and Molecular Signature During Juvenile Dermatomyositis. *Arthritis Rheumatol. (Hoboken, N.J.)* **2018**, 70 (1), 134–145.
168. Minetti C, Gattorno M, Repetto S, et al. Chemokine Receptor CCR7 Is Expressed in Muscle Fibers in Juvenile Dermatomyositis. *Biochem. Biophys. Res. Commun.* **2005**, 333 (2), 540–543.
169. Lopez de Padilla CM, Vallejo AN, McNallan KT, et al. Plasmacytoid Dendritic Cells in Inflamed Muscle of Patients with Juvenile Dermatomyositis. *Arthritis Rheum.* **2007**, 56 (5), 1658–1668.
170. Englund P, Nennesmo I, Klareskog L, et al. Interleukin-1alpha Expression in Capillaries and Major Histocompatibility Complex Class I Expression in Type II Muscle Fibers from Polymyositis and Dermatomyositis Patients: Important Pathogenic Features Independent of Inflammatory Cell Clusters in Muscle. *Arthritis Rheum.* **2002**, 46 (4), 1044–1055.
171. Kim E, Cook-Mills J, Morgan G, et al. Increased Expression of Vascular Cell Adhesion Molecule 1 in Muscle Biopsy Samples from Juvenile Dermatomyositis Patients with Short Duration of Untreated Disease Is Regulated by miR-126. *Arthritis Rheum.* **2012**, 64 (11), 3809–3817.
172. Chen Y-W, Shi R, Geraci N, et al. Duration of Chronic Inflammation Alters Gene Expression in Muscle from Untreated Girls with Juvenile Dermatomyositis. *BMC Immunol.* **2008**, 9, 43.
173. Zhao Y, Fedczyna TO, McVicker V, et al. Apoptosis in the Skeletal Muscle of Untreated Children with Juvenile Dermatomyositis: Impact of Duration of Untreated Disease. *Clin. Immunol.* **2007**, 125 (2), 165–172.
174. Lopez De Padilla CM, Vallejo AN, Lacomis D, et al. Extranodal Lymphoid Microstructures in Inflamed Muscle and Disease Severity of New-Onset Juvenile Dermatomyositis. *Arthritis Rheum.* **2009**, 60 (4), 1160–1172.
175. Shinjo SK, Sallum AME, Silva CA, et al. Skeletal Muscle Major Histocompatibility Complex Class I and II Expression Differences in Adult and Juvenile Dermatomyositis. *Clinics (Sao Paulo).* **2012**, 67 (8), 885–890.

176. Iglesias E, Jou C, Bou R, et al. [Importance of muscle biopsy in the diagnosis of juvenile dermatomyositis]. *Anales de pediatria (Barcelona, Spain : 2003)*. Spain February 2014, pp e25-6.
177. Mamyrova G, Rider LG, Ehrlich A, et al. Environmental Factors Associated with Disease Flare in Juvenile and Adult Dermatomyositis. *Rheumatology (Oxford)*. **2017**.
178. Manlhiot C, Liang L, Tran D, et al. Assessment of an Infectious Disease History Preceding Juvenile Dermatomyositis Symptom Onset. *Rheumatology (Oxford)*. **2008**, 47 (4), 526–529.
179. Pachman LM, Lipton R, Ramsey-Goldman R, et al. History of Infection before the Onset of Juvenile Dermatomyositis: Results from the National Institute of Arthritis and Musculoskeletal and Skin Diseases Research Registry. *Arthritis Rheum.* **2005**, 53 (2), 166–172.
180. Pachman LM, Litt DL, Rowley AH, et al. Lack of Detection of Enteroviral RNA or Bacterial DNA in Magnetic Resonance Imaging-Directed Muscle Biopsies from Twenty Children with Active Untreated Juvenile Dermatomyositis. *Arthritis Rheum.* **1995**, 38 (10), 1513–1518.
181. Jia H, Thelwell C, Dilger P, et al. Endothelial Cell Functions Impaired by Interferon in Vitro: Insights into the Molecular Mechanism of Thrombotic Microangiopathy Associated with Interferon Therapy. *Thromb. Res.* **2018**, 163, 105–116.
182. Aanhane E, Schulkens IA, Heusschen R, et al. Different Angioregulatory Activity of Monovalent Galectin-9 Isoforms. *Angiogenesis* **2018**.
183. O'Brien MJ, Shu Q, Stinson WA, et al. A Unique Role for Galectin-9 in Angiogenesis and Inflammatory Arthritis. *Arthritis Res. Ther.* **2018**, 20 (1), 31.
184. Heusschen R, Schulkens IA, van Beijnum J, et al. Endothelial LGALS9 Splice Variant Expression in Endothelial Cell Biology and Angiogenesis. *Biochim. Biophys. Acta* **2014**, 1842 (2), 284–292.
185. Campanella GS V, Colvin RA, Luster AD. CXCL10 Can Inhibit Endothelial Cell Proliferation Independently of CXCR3. *PLoS One* **2010**, 5 (9), e12700.
186. Ladislau L, Suarez-Calvet X, Toquet S, et al. JAK Inhibitor Improves Type I Interferon Induced Damage: Proof of Concept in Dermatomyositis. *Brain* **2018**, 141 (6), 1609–1621.
187. Crescioli C, Sottili M, Bonini P, et al. Inflammatory Response in Human Skeletal Muscle Cells: CXCL10 as a Potential Therapeutic Target. *Eur. J. Cell Biol.* **2012**, 91 (2), 139–149.
188. Nagaraju K, Rider LG, Fan C, et al. Endothelial Cell Activation and Neovascularization Are Prominent in Dermatomyositis. *J. Autoimmune Dis.* **2006**, 3, 2.
189. Sorensen EW, Lian J, Ozga AJ, et al. CXCL10 Stabilizes T Cell-Brain Endothelial Cell Adhesion Leading to the Induction of Cerebral Malaria. *JCI insight* **2018**, 3 (8).
190. Fu H, Kishore M, Gittens B, et al. Self-Recognition of the Endothelium Enables Regulatory T-Cell Trafficking and Defines the Kinetics of Immune Regulation. *Nat. Commun.* **2014**, 5, 3436.
191. Pober JS, Merola J, Liu R, et al. Antigen Presentation by Vascular Cells. *Front. Immunol.* **2017**, 8, 1907.
192. Huber AM, Robinson AB, Reed AM, et al. Consensus Treatments for Moderate Juvenile Dermatomyositis: Beyond the First Two Months. Results of the Second Childhood Arthritis and Rheumatology Research Alliance Consensus Conference. *Arthritis Care Res. (Hoboken)*. **2012**, 64 (4), 546–553.
193. McCann LJ, Pilkington CA, Huber AM, et al. Development of a Consensus Core Dataset in Juvenile Dermatomyositis for Clinical Use to Inform Research. *Ann. Rheum. Dis.* **2018**, 77 (2), 241–250.

194. van Dijkhuizen EP, Deakin CT, Wedderburn LR, et al. Modelling Disease Activity in Juvenile Dermatomyositis: A Bayesian Approach. *Stat. Methods Med. Res.* **2017**, 962280217713233.
195. Lim LSH, Pullenayegum E, Moineddin R, et al. Methods for Analyzing Observational Longitudinal Prognosis Studies for Rheumatic Diseases: A Review & Worked Example Using a Clinic-Based Cohort of Juvenile Dermatomyositis Patients. *Pediatr. Rheumatol. Online J.* **2017**, 15 (1), 18.
196. Higgs BW, Zhu W, Morehouse C, et al. A Phase 1b Clinical Trial Evaluating Sifalimumab, an Anti-IFN-Alpha Monoclonal Antibody, Shows Target Neutralisation of a Type I IFN Signature in Blood of Dermatomyositis and Polymyositis Patients. *Ann. Rheum. Dis.* **2014**, 73 (1), 256–262.
197. Guo X, Higgs BW, Rebelatto M, et al. Suppression of Soluble T Cell-Associated Proteins by an Anti-Interferon-Alpha Monoclonal Antibody in Adult Patients with Dermatomyositis or Polymyositis. *Rheumatology (Oxford)*. **2014**, 53 (4), 686–695.

Galectin-9 and CXCL10 as Biomarkers for Disease Activity in Juvenile Dermatomyositis: A Longitudinal Cohort Study and Multicohort Validation

Judith Wienke, Felicitas Bellutti Enders, Johan Lim, Jorre S. Mertens, Luuk L. van den Hoogen, Camiel A. Wijngaarde, Joo Guan Yeo, Alain Meyer, Henny G. Otten, Ruth D. E. Fritsch-Stork, Sylvia S. M. Kamphuis, Esther P. A. H. Hoppenreijns, Wineke Armbrust, J. Merlijn van den Berg, Petra C. E. Hissink Muller, Janneke Tekstra, Jessica E. Hoogendijk, Claire T. Deakin, Wilco de Jager, Joël A. G. van Roon, W. Ludo van der Pol, Kiran Nistala, Clarissa Pilkington, Marianne de Visser, Thaschawee Arkachaisri, Timothy R. D. J. Radstake, Anneke J. van der Kooi, Stefan Nierkens, Lucy R. Wedderburn, Annet van Royen-Kerkhof*, and Femke van Wijk*

*These authors contributed equally

ABSTRACT

Objective: Objective evaluation of disease activity is challenging in patients with juvenile dermatomyositis (DM) due to a lack of reliable biomarkers, but it is crucial to avoid both under- and overtreatment of patients. Recently, we identified 2 proteins, galectin-9 and CXCL10, whose levels are highly correlated with the extent of juvenile DM disease activity. This study was undertaken to validate galectin-9 and CXCL10 as biomarkers for disease activity in juvenile DM, and to assess their disease specificity and potency in predicting the occurrence of flares.

Methods: Levels of galectin-9 and CXCL10 were measured by multiplex immunoassay in serum samples from 125 unique patients with juvenile DM in 3 international cross-sectional cohorts and a local longitudinal cohort. The disease specificity of both proteins was examined in 50 adult patients with DM or nonspecific myositis (NSM) and 61 patients with other systemic autoimmune diseases.

Results: Both cross-sectionally and longitudinally, galectin-9 and CXCL10 outperformed the currently used laboratory marker, creatine kinase (CK), in distinguishing between juvenile DM patients with active disease and those in remission (area under the receiver operating characteristic curve [AUC] 0.86–0.90 for galectin-9 and CXCL10; AUC 0.66–0.68 for CK). The sensitivity and specificity for active disease in juvenile DM was 0.84 and 0.92, respectively, for galectin-9 and 0.87 and 1.00, respectively, for CXCL10. In 10 patients with juvenile DM who experienced a flare and were prospectively followed up, continuously elevated or rising biomarker levels suggested an imminent flare up to several months before the onset of symptoms, even in the absence of elevated CK levels. Galectin-9 and CXCL10 distinguished between active disease and remission in adult patients with DM or NSM ($P = 0.0126$ for galectin-9 and $P < 0.0001$ for CXCL10) and were suited for measurement in minimally invasive dried blood spots (healthy controls versus juvenile DM, $P = 0.0040$ for galectin-9 and $P < 0.0001$ for CXCL10).

Conclusion: In this study, galectin-9 and CXCL10 were validated as sensitive and reliable biomarkers for disease activity in juvenile DM. Implementation of these biomarkers into clinical practice as tools to monitor disease activity and guide treatment might facilitate personalized treatment strategies.

INTRODUCTION

Juvenile dermatomyositis (DM) is a rare, chronic systemic immune-mediated disease with a high disease burden. In children with juvenile DM, the disease is characterized by inflammation of the skeletal muscles and skin, leading to muscle weakness and a pathognomonic skin rash. Vital organs such as the lung and heart can also be involved. Although the pathogenesis is still largely unknown, environmental and genetic factors may predispose children to the disease.¹⁻⁵ The autoimmune process is characterized by a type I interferon signature and by infiltration of immune cells such as plasmacytoid dendritic cells, B cells, CD4⁺ T cells, and macrophages into the skin and muscle tissue.⁶⁻⁹

Children with juvenile DM are at risk of both under- and overtreatment due to a lack of reliable biomarkers that could be used to gauge the extent of disease activity. Current treatment guidelines recommend immunosuppression for at least 2 years, tapering steroids over the first year, and withdrawing treatment if a patient has been taken off steroids and has achieved disease remission with methotrexate (or an alternative disease-modifying antirheumatic drug) for a minimum of 1 year.¹⁰⁻¹² However, for some patients, this standardized regimen may not be optimal. Approximately 50% of patients do not respond to initial treatment or present with disease flares during follow-up, resulting in additional tissue damage and impaired physical recovery.¹³⁻¹⁵ Of the other 50% of patients, some could likely benefit from a shorter treatment duration, taking into account that overtreatment with steroids can result in serious side effects in children, such as Cushing's syndrome, osteoporosis, and growth delay.¹⁶⁻¹⁸

To determine the rate of medication tapering and to avoid both under- and overtreatment, objective measurement of disease activity and subclinical inflammation is crucial. However, validated and reliable biomarkers for disease activity in juvenile DM are lacking.¹⁹ Disease activity is currently assessed by a combination of muscle enzyme testing and clinical evaluation;^{10,20-22} the latter depends on the experience of the health care professional and the patient's collaboration. Muscle enzymes, including serum creatine kinase (CK) activity, have been shown to correlate only moderately with disease activity in juvenile DM, and the erythrocyte sedimentation rate and C-reactive protein level are rarely elevated in patients with juvenile DM.²³⁻²⁵ Lack of objective tools or biomarkers to monitor the response to therapy also hampers clinical trial design. Thus, there is an unmet need for an objective and reliable measure of disease activity.

Recently, in a cross-sectional cohort of patients with juvenile DM, we demonstrated that 3 proteins, galectin-9, CXCL10, and tumor necrosis factor receptor type II, can distinguish between juvenile DM patients with active disease and those in remission, with galectin-9 and CXCL10 being the most discriminative markers.^{26,27} CXCL10 and galectin-9 can be produced by a variety of cells, both immune and nonimmune, upon stimulation with interferons.^{28,29} CXCL10 has been recognized as a biomarker in several human autoimmune

diseases, including myositis,^{29–33} whereas galectin-9 has been investigated mainly as a biomarker in cancer and viral infections.^{28,34} Reports on the role of galectin-9 in autoimmunity are conflicting, suggesting either an attenuating or an aggravating effect on autoimmune manifestations in experimental models.^{35,36} Its role in human autoimmune diseases has yet to be elucidated.

We aimed to validate galectin-9 and CXCL10 as biomarkers for active disease in patients with juvenile DM, to examine their disease specificity in adult patients with DM, adult patients with nonspecific myositis (NSM), and patients with other systemic autoimmune diseases, to assess their potency in predicting flares, and to test the applicability of the biomarkers in minimally invasive dried blood spots, in order to aid broad implementation into clinical practice.

PATIENTS AND METHODS

Cohorts

In total, 125 unique patients with juvenile DM from 3 independent cross-sectional international cohorts and 1 Dutch prospective cohort participated in the present study, with inclusion between May 2001 and May 2017. Two large cohorts from Utrecht, The Netherlands and London, UK were used for validation of the biomarkers; a third smaller cohort from Singapore was used to assess international generalizability. An overview of all cohorts is shown in Table 1. The internal validation cohort (IVC) from Utrecht does not overlap with the previously reported discovery cohort.²⁶ For specific questions, including disease specificity, longitudinal follow-up, and measurements in dried blood spots, a combination of blood samples from the IVC and blood samples from new patients was used.

Participants

Patients with juvenile DM were included if they met the Bohan and Peter criteria for definite or probable juvenile DM.^{37,38} The Childhood Myositis Assessment Scale (CMAS; scale 0–52),³⁹ Manual Muscle Testing of 8 muscle groups (MMT-8; scale 0–80),⁴⁰ and physician's global assessment of disease activity (PhGA; scale 0–10) were recorded as clinical measures of muscle and global disease activity. In addition, cutaneous assessment tool (CAT) scores measuring the severity of skin disease (scale 0–116)⁴¹ were recorded in Dutch and Singaporean patients. Disease remission was defined according to the updated criteria for clinically inactive disease and, in the case of missing data, was defined by clinical description.⁴²

Table 1. Overview of the juvenile DM cohorts

	Abbreviation	City, country	No. of patients	No. of samples	No. of active disease–remission paired samples
<i>International validation cohorts</i>					
External validation cohort	EVC	London, UK	61	79	16
Internal validation cohort	IVC; JDM NL	Utrecht, The Netherlands	47; 47	83; 58	26; 11
Asian cohort	JDM Sing	Singapore	12	13	–
<i>Analysis-specific subcohorts from Utrecht</i>					
Systemic autoimmune disease cohort		Utrecht, The Netherlands	14	16	2
Longitudinal cohort		Utrecht, The Netherlands	28	286	
Dried blood spot cohort		Utrecht, The Netherlands	7	10	

Data are listed as follows: for the London external validation cohort (EVC), see Figure 1, Supplementary Table 1, and Supplementary Figure 1; for the Utrecht internal validation cohort (IVC), see Figure 1, Supplementary Table 2, and Supplementary Figure 1; for the Juvenile Dermatomyositis The Netherlands (JDM NL) and Juvenile Dermatomyositis Singapore (JDM Sing) cohorts, see Figure 2 and Supplementary Table 4; for the systemic autoimmune disease cohort, see Figure 2 and Supplementary Table 5; for the longitudinal cohort, see Figure 3, Supplementary Table 6, and Supplementary Figure 2; for the dried blood spot cohort, see Figure 4 and Supplementary Table 7.

All other patients were considered to have active disease. Flares were defined as the combination of the following 3 items: a previous response to treatment with the decision to start tapering steroids, worsening of at least 1 of 3 clinical scores (CMAS, PhGA, and CAT) by ≥ 2 points, and the decision to start new immunosuppressive treatment or increase the current dose.

Adult patients with DM and those with NSM were classified according to the European Neuromuscular Centre criteria.⁴³ Myositis was confirmed by biopsy unless typical skin manifestations of DM were present. Patients with cancer-associated myositis were excluded. Disease activity was determined by combined evaluation of muscle strength with the Medical Research Council Muscle Scale,⁴⁴ skin symptoms, and muscle enzyme levels. To determine the disease specificity of the biomarkers, different disease controls were added in the study, including pediatric and adult patients with systemic lupus erythematosus (SLE), pediatric patients with localized scleroderma, adult patients with eosinophilic fasciitis (EF), and pediatric and adult patients with hereditary proximal spinal muscular atrophy (SMA). All controls had either systemic inflammation, inflammation of the skin or muscles, or a noninflammatory neuromuscular disorder.

Patients with SLE fulfilled the American College of Rheumatology classification criteria for SLE.⁴⁵ Active disease was defined as an SLE Disease Activity Index score of ≥ 4 of 105.⁴⁶ Patients with localized scleroderma were diagnosed based on the typical clinical picture, with active disease being defined as a modified Localized Scleroderma Skin Severity Index (mLoSSi) score of ≥ 5 of 162.⁴⁷ Patients with EF were diagnosed based on the clinical picture and histopathologic evaluation of skin biopsy specimens containing the fascia. As the mLoSSi may stay high in these patients due to the presence of extensive, irreversible sclerosis despite a reduction of inflammation, active disease was defined as a PhGA score of ≥ 5 (on 100-mm visual analog scale).⁴⁷ Patients with hereditary proximal SMA, a progressive, noninflammatory neuromuscular disorder, were diagnosed by genetic confirmation of a homozygous loss of function of the survival motor neuron 1 gene;⁴⁸ these patients served as disease controls. Adult healthy volunteers were included as healthy controls.

Ethics approval

The study was approved by the institutional ethics committees of the involved centers (UMC Utrecht [approval nos. METC 15-191 and 12-466], UK [approval no. MREC1/3/22], CHUV Lausanne, CHU Strasbourg, SingHealth centralized IRB, AMC Amsterdam) and conducted according to the Declaration of Helsinki. Written informed consent was obtained prior to inclusion in the study, both from patients and from parents or legal representatives when the patient was younger than 12 years old.

Blood samples

Blood was collected in serum tubes in accordance with the local study protocol (all participating centers). At the UMC Utrecht, blood samples were collected in sodium-heparin tubes in addition to serum tubes. All samples were spun down and aliquoted within 4 hours after collection, and subsequently stored at -80°C until analyzed.

Measurement in dried blood spots

Dried blood spots were made by application of 50 μl sodium-heparin full blood to each spot on Whatman 903 filter paper within 4 hours after the blood sample was obtained. Spotted filter papers were dried for 2 days at room temperature to mimic mail delivery times, and subsequently stored with desiccant in individual air-tight polyethylene bags at -80°C under constant monitoring of humidity levels until analyzed. Two circles of 3.0 mm in diameter (containing ~ 3 μl of whole blood each) were punched from the central part of 1 spot and

eluted in 100 µl buffer (phosphate buffered saline containing 5 ml/liter Tween 20, 10 g/liter bovine serum albumin, and Complete protease inhibitor cocktail with EDTA [1 tablet per 25 ml buffer; Roche]) in 96-well plates. Plates were sealed and placed overnight at 4°C on a microshaker (600 revolutions per minute) and were spun down at 2,100g for 2 minutes. The analysis was performed on the obtained eluate.

Biomarker analysis

Galectin-9 and CXCL10 were measured in 50 µl of serum, plasma, or eluate by multiplex assay (xMAP; Luminex). CXCL10 was measured in undiluted material. Galectin-9 was measured in 10× diluted plasma or serum, except in the serum/plasma samples paired with dried blood spots (in which case galectin-9 was measured undiluted from the eluate and serum/plasma). The multiplex immunoassay was performed as described previously.⁴⁹ Heterophilic immunoglobulins were preabsorbed from all samples with HeteroBlock (Omega Biologicals). Acquisition was performed with a Bio-Rad FlexMAP3D in combination with xPONENT software version 4.2 (Luminex). Data analysis was performed with Bioplex Manager version 6.1.1 (Bio-Rad).

Between measurement of the internal and external validation cohorts in 2015, the recombinant protein for galectin-9 was replaced, which affected the standard curve. Therefore absolute values between these cohorts may not be comparable. Since 2015, the interassay variability has been negligible.⁵⁰ All biomarker analyses were performed at the UMC Utrecht, thereby minimizing intercenter variation. Treating physicians were blinded with regard to biomarker levels, and technicians performing the multiplex assay were blinded with regard to clinical data.

Statistical analysis

Basic descriptive statistics were used to describe the patient population. Statistical analyses were performed using either GraphPad Prism version 7.0 or SPSS Statistics version 21 (IBM). Correlations were assessed using Spearman's rank correlation coefficients. For comparisons between 2 groups, the Mann-Whitney U test (unpaired analysis) or Wilcoxon's matched-pairs signed rank test (paired analysis) was used. For comparisons between multiple groups, nonparametric variants of analysis of variance (ANOVA) with post hoc correction for multiple testing were used (Dunn's post hoc test for Kruskal-Wallis, and Šidak's or Tukey's post hoc test for 2-way ANOVA, as appropriate). Multiplicity-adjusted *P* values less than 0.05 were considered significant.

To assess diagnostic accuracy, area under the receiver operating characteristic (ROC) curves (AUCs) were constructed. Cutoff values for the diagnostic accuracy of galectin-9

and CXCL10 were determined based on the maximal Youden's Index, with a sensitivity of at least 80%.

RESULTS

Cross-sectional validation of galectin-9 and CXCL10

To validate the biomarker potential of galectin-9 and CXCL10, we measured the proteins in blood samples from patients with juvenile DM from 2 independent validation cohorts: an external validation cohort (EVC) from London and an internal validation cohort (IVC) from Utrecht. The clinical characteristics of these cohorts are shown in Supplementary Tables 1 and 2. As observed in the previously reported discovery cohort,²⁶ the levels of galectin-9 and CXCL10 were significantly higher in patients with active disease compared to patients in remission ($P < 0.0001$) (results in Supplementary Figures 1A and B). The levels were highest at the time of diagnosis (before treatment), decreased steadily under treatment, and were comparably low in remission regardless of whether the patient was receiving or not receiving medication while in remission (Figures 1A and B). The wide range of biomarker levels in the group of juvenile DM patients with active disease who were on treatment corresponded to a wide range of clinical disease activity scores within this group (CMAS scores ranging 3–44 in the EVC and 10–52 in the IVC; PhGA scores ranging 2–8 in the EVC and 1–9 in the IVC). Based on the levels of both galectin-9 and CXCL10, we were able to differentiate patients with active disease while receiving medication from patients in remission while receiving medication (Figures 1A and B), which is clinically important to assess the response to treatment. Paired analysis within individual patients, in which we compared samples from a period of active disease and from a period of remission in each patient, showed decreasing biomarker levels in response to therapy and confirmed the high discriminative power of both proteins (each $P = 0.0078$ in the EVC and $P = 0.0002$ in the IVC) (Figures 1C and D).

To further assess the discriminative power of galectin-9 and CXCL10 for distinguishing between a status of active disease and a status of remission in juvenile DM, we examined the AUCs in the 2 separate cohorts. In comparing active disease and remission in patients regardless of their treatment status, the levels of galectin-9 and CXCL10 had AUCs of 0.894 and 0.863, respectively, in the EVC and 0.877 and 0.902, respectively, in the IVC (Figures 1E and F, and Supplementary Table 3). To take into account the effect of treatment, we also assessed the AUC for differentiating active disease from disease remission in patients who were taking medication. During treatment, the levels of galectin-9 and CXCL10 had AUCs of 0.844 and 0.776, respectively, in the EVC and 0.860 and 0.840, respectively, in the IVC

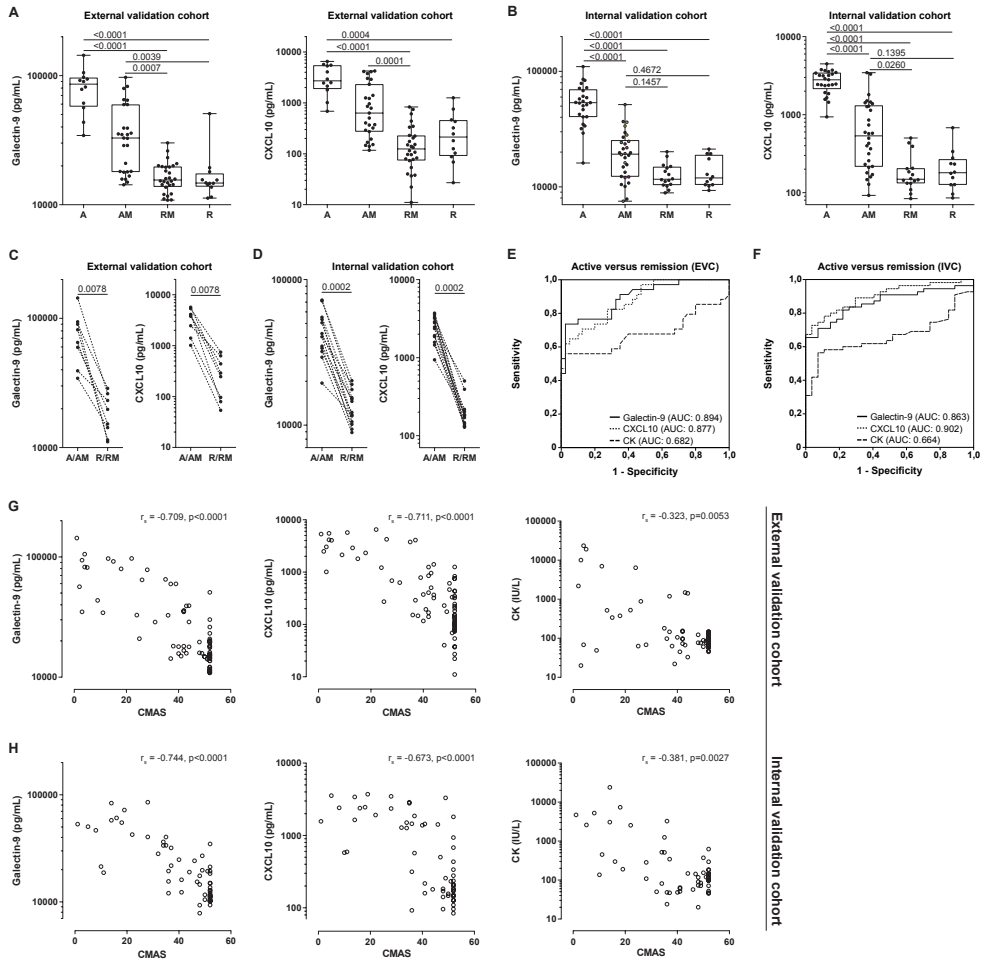


Figure 1. Cross-sectional validation of galectin-9 and CXCL10 as biomarkers for disease activity in juvenile dermatomyositis (DM) in 2 independent validation cohorts.

A and B, Measurement of galectin-9 and CXCL10 by multiplex immunoassay in serum from patients with active disease before start of treatment (group A), active disease while receiving medication (group AM), in remission while receiving medication (group RM), and in remission while not receiving medication (group R), in the external validation cohort (EVC) (n = 12 group A, n = 27 group AM, n = 28 group RM, n = 12 group R) (A) and the internal validation cohort (IVC) (n = 25 group A, n = 30 group AM, n = 16 group RM, n = 12 group R) (B). In group AM, 3 samples from 1 patient (from different time points at least 3 months apart) and 2 samples from 6 patients (from different time points 2–11 months apart) were included. Data are shown as box plots. Each box represents the interquartile range. Lines inside the boxes represent the median (log scale). Lines outside the boxes represent the 10th and 90th percentiles. Symbols represent individual patients. Multiplicity-adjusted P values were determined by Kruskal-Wallis test with Dunnett's post hoc test. C and D, Measurement of galectin-9 and CXCL10 in paired samples from individual patients (regardless of treatment status) during active disease and remission, from the EVC (median time between samples 23 months) (C) and IVC (median time between samples 12 months) (D). P values were determined by Wilcoxon's matched-pairs signed rank test. E and F, Area under the receiver operating characteristic (ROC) curves (AUCs) for diagnostic accuracy of galectin-9, CXCL10, and creatine kinase (CK) in patients (regardless of treatment status) from the EVC (E) and IVC (F). Only patients with complete data for the specific ROC curve were included. G and H, Spearman's rank correlations of galectin-9, CXCL10, and CK levels with Childhood Myositis Assessment Scale (CMAS) scores in the EVC (n = 79) (G) and IVC (n = 61) (H).

(Supplementary Figures 1C and D and Supplementary Table 3). Moreover, galectin-9 and CXCL10 performed better than the current standard laboratory marker, CK, in both cohorts (AUCs for CK, 0.682 in the EVC and 0.662 in the IVC).

To calculate the optimal cutoff value for distinguishing active disease from disease remission, we analyzed the ROC curves in the IVC, as blood samples from this cohort were assessed according to the most recently optimized and standardized protocol of the multiplex immunoassay.⁵⁰ Based on the coordinates of this ROC curve, we determined the cutoff values for discriminating active disease from remission, yielding a cutoff value of 19,396 pg/ml for galectin-9 and 805 pg/ml for CXCL10, with a high sensitivity (0.84 for galectin-9 and 0.87 for CXCL10) and a high negative predictive value (0.83 for galectin-9 and 0.87 for CXCL10) (Table 2); these values ensured a low risk of ongoing inflammation in the case of a test result that was below the cutoff. The specificity of the galectin-9 and CXCL10 cutoff levels was 0.92 and 1.00, respectively, and the positive predictive value was 0.93 and 1.00, respectively.

Consistent with the previously reported discovery cohort,²⁶ the levels of galectin-9 and CXCL10 correlated strongly with 3 clinical scores of global or muscle disease activity: the PhGA, the CMAS, and the MMT-8. The correlation coefficients for association with either of the biomarkers, which ranged between 0.67 and 0.81 ($P < 0.0001$), were notably higher than those for CK ($r_s = 0.32-0.51$, $P < 0.01$) (Figures 1G and H, and Supplementary Figures 1E–G). Thus, these results in 2 independent validation cohorts validate galectin-9 and CXCL10 as strong biomarkers for disease activity in patients with juvenile DM, outperforming the currently used laboratory marker CK.

To assess the international generalizability of galectin-9 and CXCL10, we tested the biomarkers in a small cohort of patients with juvenile DM from a different geographic region (i.e., Singapore). Observations in this cohort confirmed the discriminative potential of galectin-9 and CXCL10 between active disease and remission, and their levels were comparable to those seen in the IVC ($P = 0.0006$ for galectin-9 and $P = 0.0025$ for CXCL10) (Figures 2A and B).

Table 2. Sensitivity, specificity, NPV, and PPV of the determined cutoff values for diagnostic accuracy of galectin-9 and CXCL10 in the juvenile dermatomyositis internal validation cohort

	Cutoff value, pg/ml	Sensitivity	Specificity	NPV	PPV
Galectin-9	19,396	0.839	0.923	0.828	0.929
CXCL10	805	0.871	1	0.867	1

Cutoff values for galectin-9 and CXCL10 were determined based on the maximal Youden's Index with a sensitivity of >0.80 , in order to ensure a low risk of ongoing active inflammation with a biomarker value below the set cutoff. Only 1 sample per patient per category (active disease or in remission) was included in the analysis (i.e., the cohort designated "JDM NL" [Juvenile Dermatomyositis The Netherlands], as shown in Figure 2 and Supplementary Table 5). NPV = negative predictive value; PPV = positive predictive value.

Disease specificity of galectin-9 and CXCL10

We next investigated the disease specificity of galectin-9 and CXCL10 and explored the applicability of each as a biomarker in adult patients with DM or NSM and patients with other systemic autoimmune diseases. The biomarkers were first measured in a cohort of adult patients with DM ($n = 36$), patients with NSM ($n = 14$), and patients with EF ($n = 18$), as well as 43 disease control patients with SMA, a genetic neuromuscular disorder without systemic inflammation, and 22 healthy controls (the characteristics of these subjects are listed in Supplementary Table 4). The levels of both galectin-9 and CXCL10 were elevated in adult patients with active DM ($P < 0.0001$), patients with NSM ($P < 0.0003$), and patients with EF ($P < 0.05$) as compared to healthy controls. Both biomarkers distinguished between active disease and remission in the adult DM cohort ($P = 0.0126$ and $P < 0.0001$ for galectin-9 and CXCL10, respectively), and CXCL10 was also discriminative for disease activity in patients with NSM ($P = 0.0139$) and those with EF ($P = 0.0497$) (Figures 2A and B). As expected, the biomarkers were not elevated in control patients with SMA.

A second cohort consisted of pediatric and adult patients with 2 other systemic immune-mediated diseases: localized scleroderma ($n = 15$) and SLE ($n = 36$) (the characteristics of these patients are listed in Supplementary Table 5). In patients with localized scleroderma and those with SLE, the 2 biomarkers did not distinguish significantly between active disease and remission, but galectin-9 levels in patients with SLE were elevated compared to healthy controls ($P = 0.0105$) (Figures 2C and D).

Thus, these results demonstrate that galectin-9 and CXCL10 are applicable as biomarkers for disease activity in both pediatric and adult patients with myositis.

Prospective analysis and flare prediction

To determine the prognostic value of galectin-9 and CXCL10 during clinical follow-up in patients with juvenile DM, we measured the biomarkers in a prospective cohort of 28 patients, with a median follow-up time of 2.8 years per patient (the characteristics of these patients are listed in Supplementary Table 6). First, we established the biomarker dynamics after diagnosis in 15 patients who reached sustained remission within the first months of treatment and did not have a flare later. The biomarker levels quickly declined after the start of treatment, reached levels below the previously determined cutoff value within several months, and remained low in remission (the “No flare” group, shown in Figures 3A and B). The biomarker dynamics in patients with a flare after the first year (the “Flare >12 months” group; $n = 7$) were similar to those in patients without flares (Figures 3C and D). However, patients who experienced a disease flare in the first year after the start of treatment (the “Flare <12 months” group; $n = 6$) had significantly higher biomarker levels at diagnosis than did patients with later flares ($P = 0.0254$ for galectin-9 and $P = 0.0265$ for CXCL10) (Figures

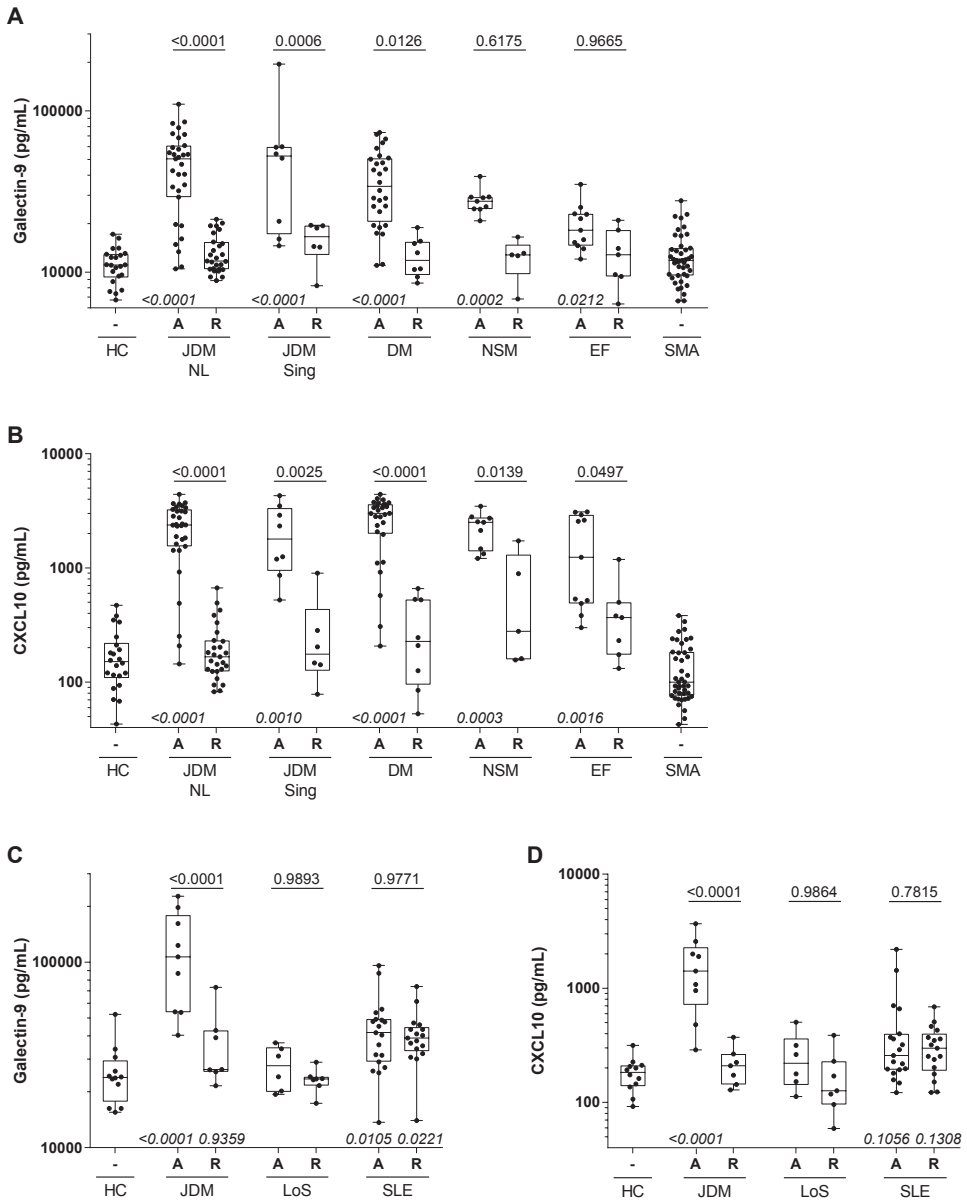


Figure 2. Biomarker potential of galectin-9 and CXCL10 in adult inflammatory myopathies and systemic autoimmune diseases with skin involvement.

A and B, Galectin-9 (A) and CXCL10 (B) were measured in serum samples from patients with juvenile dermatomyositis from The Netherlands (JDM NL) (the internal validation cohort [IVC]) and Singapore validation cohort (JDM Sing), adult patients with DM, adult patients with nonspecific myositis (NSM), adult patients with eosinophilic fasciitis (EF), a mixed cohort of adult and juvenile patients with hereditary proximal spinal muscular atrophy (SMA), and adult healthy controls (HC). C and D, Galectin-9 (C) and CXCL10 (D) were measured in serum samples from the Dutch juvenile DM cohort, juvenile patients with localized scleroderma (LoS), a mixed cohort of juvenile and adult patients with systemic lupus erythematosus (SLE), and adult healthy controls. In A–D, patients were stratified into 2 groups based on disease activity (active [A] or in remission [R] regardless of treatment status).

(Figure 2 continued)

Only 1 sample per patient per activity group was included in the analysis; therefore, the numbers of patients in the IVC differ from those in Figure 1. Data are shown as box plots. Each box represents the interquartile range. Lines inside the boxes represent the median (log scale). Lines outside the boxes represent the 10th and 90th percentiles. Symbols represent individual patients. Multiplicity-adjusted P values above boxes are for comparison between active disease and remission, by 2-way analysis of variance with Šidak's post hoc test for multiple comparisons. Multiplicity-adjusted P values below boxes are for comparison between each disease group and healthy controls, by Kruskal-Wallis test with Dunnett's post hoc test for multiple comparisons. P values >0.999 are not shown.

3C and D). In addition, these patients who experienced a flare at <12 months had elevated biomarker levels over the entire first year (Figures 3C–E). In contrast to the 2 biomarkers, CK activity normalized in 5 of 6 patients (Figure 3E).

To assess the predictive value of the biomarkers for flares after the first year, we analyzed 4 patients for whom longitudinal samples were available within 7 months before a flare (Figure 3F and Supplementary Figure 2). In patients 1 and 2, raised levels of galectin-9 and CXCL10 (even while remaining below the cutoff level) were observed from up to 7 months prior to the flare, with levels that were above the cutoff value up to 6 months prior to the flare for galectin-9 and up to 3 months prior to the flare for CXCL10. These biomarker fluctuations were observed even before clinical symptoms of a flare became apparent. In patients 3 and 4, persistently borderline cutoff values were observed for galectin-9 and CXCL10 in the 12 months prior to occurrence of a flare, and biomarkers were elevated above the cutoff during the flare. In contrast, CK levels did not increase prior to or during a flare in patient 4, and did not demonstrate an increase until the occurrence of a flare in patients 2 and 3. Only in patient 1 did the CK level steadily increase by 3 months prior to a flare. It was also observed that galectin-9 and CXCL10 levels stayed high during continued disease activity after the start of the flare in patients receiving medication, while in 3 of 4 individuals, the CK level decreased to within normal limits by the first time point following the start of the clinical flare, despite continued disease activity.

Thus, these results suggest that persistently high or rising galectin-9 and CXCL10 levels above their cutoff values may be indicative of ongoing (sub)clinical inflammation or an imminent flare, even with a lack of clinical symptoms or elevated CK levels.

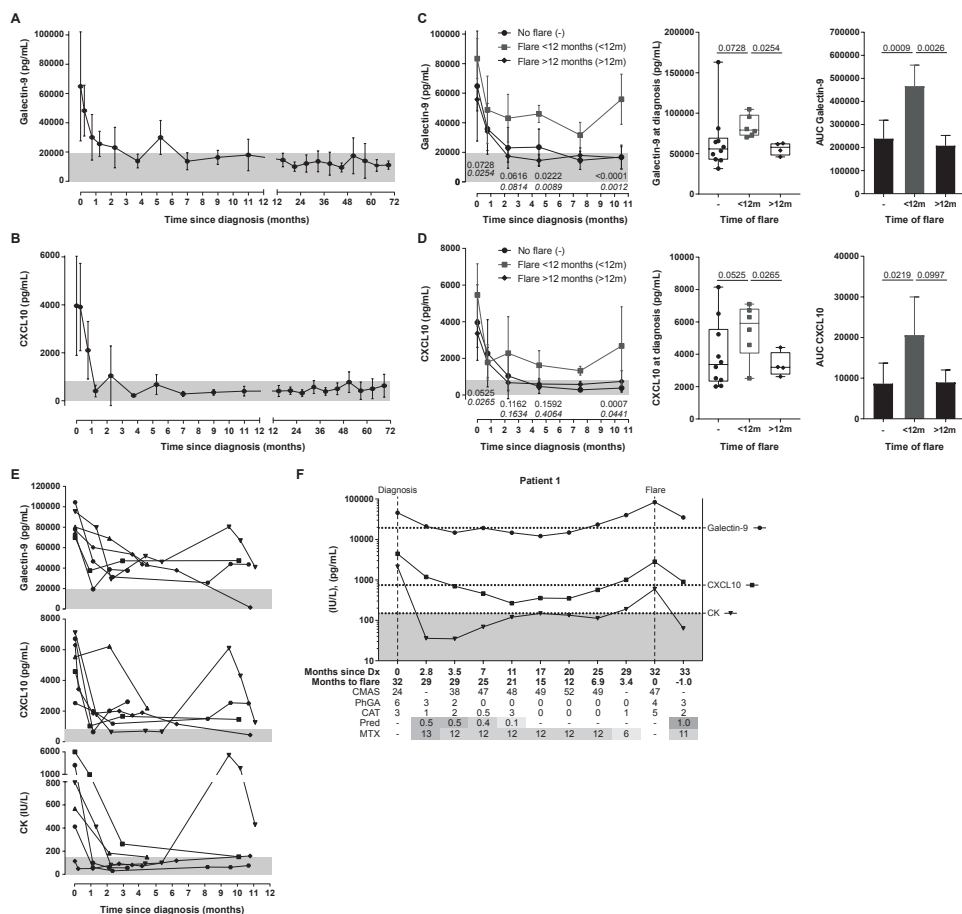


Figure 3. Galectin-9 and CXCL10 serum levels from longitudinal follow-up of patients with juvenile dermatomyositis (DM) in a prospective cohort.

A and B, Dynamics of galectin-9 (A) and CXCL10 (B) serum levels up to 6 years after juvenile DM diagnosis in 15 patients without flares. The first sample was obtained a maximum of 6 months after treatment start. Both patients with and those without intensification of therapy within the first 3 months were included. Each point contains between 3 and 13 samples, pooled over the time span around the data point. The median interval between 2 samples from a patient was 3.6 months. Per patient, 4–14 samples (median 9) were included. Values are the mean±SD (linear scale). C and D, Galectin-9 (C) and CXCL10 (D) serum levels in longitudinal samples from juvenile DM patients with a flare within the first year (<12m) (n = 6), after the first year (>12m) (n = 7), or without flares (n = 15) (same patients as in A and B). Only patients with a first sample obtained a maximum of 6 months after treatment start were included. Left, Longitudinal data (mean±SD) within the first year. Multiplicity-adjusted P values, by 2-way analysis of variance (ANOVA) with Tukey’s post hoc test, were for flare <12 months versus no flare (top) or flare <12 months versus flare >12 months (bottom) Middle, Galectin-9 and CXCL10 levels at diagnosis, before treatment start. Data are shown as box plots. Boxes represent the interquartile range, lines inside the boxes show the median, and lines outside the boxes show the 10th and 90th percentiles. Symbols represent individual patients. All P values, by 2-way ANOVA with Tukey’s post hoc test, were corrected. Right, Total area under the receiver operating characteristic curves (AUCs) for each group, calculated by the trapezoidal method. Values are the mean and 95% confidence interval. P values were determined by one-way ANOVA with Tukey’s post hoc test. E, Galectin-9, CXCL10, and creatine kinase (CK) serum levels in 6 individuals with a flare within the first year after treatment start.

(Figure 3 continued)

In A–F, Gray shading indicates the previously determined cutoffs for galectin-9 and CXCL10 (19,396 pg/ml and 805 pg/ml, respectively) and the standard cutoff for CK (150 IU/liter). F, Levels of galectin-9, CXCL10, and CK measured longitudinally in an individual with a disease flare after the first year. Broken horizontal lines indicate the previously determined cutoffs for galectin-9, CXCL10, and CK. Biomarker levels are shown on a log scale. Shading in the rows for prednisone (Pred) and methotrexate (MTX) represent the relative medication dose (in mg/kg/day for prednisone; in mg/m²/week for MTX). Dark gray shading = high dose; lighter gray shading = low dose. Dx = diagnosis; CMAS = Childhood Myositis Assessment Scale; PhGA = physician's global assessment; CAT = cutaneous assessment tool.

Levels of galectin-9 and CXCL10 in dried blood spots

To facilitate minimally invasive (at-home) biomarker assessment and broad clinical applicability with centralization of diagnostic cores, we assessed galectin-9 and CXCL10 measurements in dried blood spots and paired plasma and serum samples (the patients' characteristics are shown in Supplementary Table 7). Correlation between the biomarker levels in the circulation and biomarker levels in dried blood spots was higher for CXCL10 ($r_s = 0.93$ in plasma and $r_s = 0.96$ in serum) than for galectin-9 ($r_s = 0.62$ in plasma and $r_s = 0.58$ in serum) (Figures 4A and B).

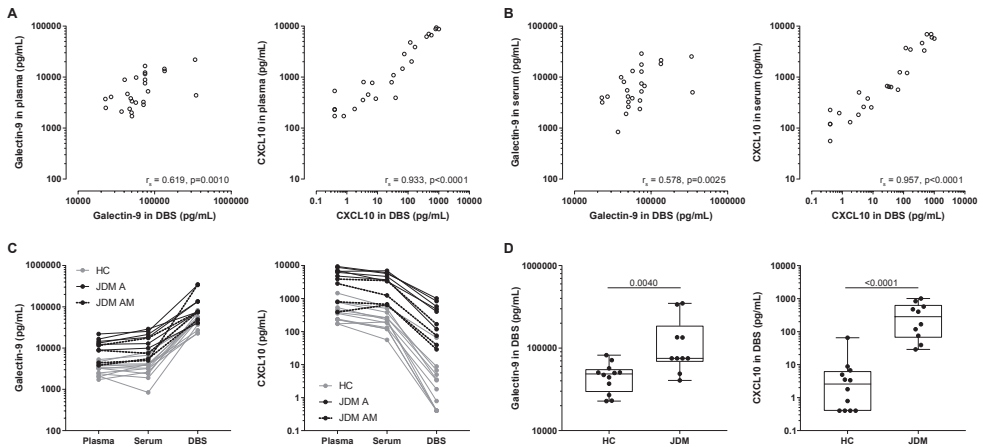


Figure 4. Measurement of galectin-9 and CXCL10 levels in dried blood spots (DBS) as compared to paired plasma and serum samples from patients with active juvenile dermatomyositis (DM).

A and B, Correlations between biomarker levels in the plasma (A) and serum (B) and in DBS (on a double log scale) were assessed using Spearman's correlation coefficients. C, Paired representation of the biomarker levels in the plasma, serum, and DBS from healthy controls (HC), patients with active juvenile DM pre-treatment (JDM A), and patients with active juvenile DM while receiving medication (JDM AM) are shown. D, Biomarker levels in DBS were compared between healthy controls and patients with active juvenile DM. P values were determined by Mann-Whitney U test.

Galectin-9 and CXCL10 levels were similar in the plasma and serum (Figure 4C). Both galectin-9 and CXCL10, as measured in dried blood spots, were capable of discriminating between patients with active juvenile DM and healthy controls ($P = 0.0040$ and $P < 0.0001$, respectively) (Figure 4D), with the healthy control subjects having biomarker levels that were similar to those in patients with juvenile DM in remission (Figure 2). Thus, measurements of both galectin-9 and CXCL10 in dried blood spots are suitable as biomarkers for juvenile DM disease activity.

DISCUSSION

In this study, galectin-9 and CXCL10 were validated as strong, reliable, and sensitive biomarkers for disease activity in juvenile DM, and both were identified as promising biomarkers both in adult patients with DM and in adult patients with NSM. The levels of galectin-9 and CXCL10 strongly distinguished between juvenile DM patients with active disease and juvenile DM patients in remission, even when the patient was receiving immunosuppressive treatment. Furthermore, we showed that galectin-9 and CXCL10 were relatively specific for autoinflammatory myopathies in adult and pediatric patients, as their levels were not as highly increased or did not differentiate between active disease and remission in other autoimmune diseases such as localized scleroderma and SLE. Both cross-sectionally and longitudinally, galectin-9 and CXCL10 outperformed CK, which is commonly used as a laboratory marker for disease activity and is one of the current criteria for determining clinically inactive disease in juvenile DM.^{42,51} Continuously elevated or rising biomarker levels, as determined in a prospective patient cohort, may be indicative of an imminent disease flare up to several months before clinical symptoms, even in the absence of elevated CK levels. The biomarkers may therefore be promising to use in longitudinal follow-up of patients for monitoring of disease activity.

Furthermore, our results showed that galectin-9 and CXCL10 can be reliably measured in the plasma, serum, and minimally invasive dried blood spots from patients with juvenile DM. It has recently been shown that capillary concentrations of CXCL10 correlate with venous concentrations; for galectin-9, this has not yet been established.⁵² The moderate correlation between circulating levels of galectin-9 and levels of galectin-9 in dried blood spots could be attributed to either liberation of intracellularly stored galectin-9 and/or release from its carrier proteins upon elution and dilution.

This study has several strengths. Although many biomarkers are being identified for a variety of diseases, only a few have been implemented into clinical practice, due to a lack of reproducibility and diagnostic accuracy. However, the levels of galectin-9 and CXCL10 have a high discriminative power and strong, reproducible correlation with disease activity.

Thanks to a large international collaborative effort, and despite the rarity of the disease, we have been able to extensively validate galectin-9 and CXCL10 as biomarkers in a large number of patients with juvenile DM from 3 independent cross-sectional cohorts. The additional analyses in a prospective cohort of patients with juvenile DM with a long follow-up time added important information on the value of galectin-9 and CXCL10 in clinical follow-up. In addition to the clinical validation in this study, the biomarkers have undergone a technical validation at the diagnostic department of the UMC Utrecht, which has demonstrated the stability of the biomarkers and reproducibility of the measurements. In addition, we have explored a minimally invasive diagnostic method of measuring the biomarkers in dried blood spots.

The findings of this study need to be interpreted carefully, taking into account the observational nature of the data and the use of a combination of clinical scores and CK levels (the Paediatric Rheumatology International Trials Organisation criteria for clinically inactive disease in juvenile DM) as the gold standard for assessment of disease activity in juvenile DM.^{42,51} Importantly, measurement of galectin-9 and CXCL10 levels can complement, but not replace, clinical assessment by experienced health care professionals. However, both biomarkers outperformed the currently used marker, CK, a finding that underscores the gains that can be achieved by introducing the new biomarkers into clinical practice.

A recent study using the SOMAScan assay also identified both galectin-9 and CXCL10 among the top up-regulated proteins in juvenile DM, correlating with disease activity as assessed by the PhGA.⁵³ CXCL10 levels were previously shown to correlate with disease activity in juvenile DM,^{26,30–32,54} and CXCL10 is well known to be an interferon-inducible chemokine that can be elevated in other types of myositis and autoimmune diseases.^{29,33} In our study, galectin-9 was a specific biomarker for inflammatory myopathies. In patients with juvenile DM, high circulating interferon- α levels have been found, and in one group of patients with juvenile DM, more than 75% of patients had a positive interferon signature.^{55,56} Circulating galectin-9 and CXCL10 levels could therefore be a direct reflection of active, interferon-driven inflammation, which is supported by a recent study in which galectin-9 was demonstrated to be a marker for the interferon signature in SLE and antiphospholipid syndrome.⁵⁷

Since the levels of these biomarkers are known to correlate with the extent of disease activity in various types of tissue, local tissue cells are the main candidate producers of the proteins. Indeed, galectin-9 can be detected not only in the circulation, but also locally within inflamed muscle and skin, where it is mainly present in activated tissue macrophages and capillary endothelial cells (*data not shown*). A similar expression pattern, in tissue mononuclear cells and endothelial cells, was previously demonstrated for CXCL10.^{58,59} Local biomarker production within the inflamed tissue is consistent with our previous observation that the biomarker levels slowly decline after stem cell transplantation, as tissue-infiltrating immune cells (and endothelial cells) are likely to be less affected by immune-ablative preconditioning than are circulating immune cells.²⁷

Implementation of galectin-9 and CXCL10 into clinical practice, as tools to monitor disease activity and guide treatment, might enable personalized treatment strategies for patients with juvenile DM. It is an advantage that both biomarkers performed equally well in our study, suggesting that diagnostic centers can decide to use their biomarker of choice depending on its availability and feasibility. Biomarker levels below the set cutoff value reflect the absence of disease activity, which could allow tapering of immunosuppressive medication. Rising or persistently high levels might be indicative of an insufficient response to therapy and/or an imminent flare, even in the absence of clinical symptoms or elevated CK levels, possibly reflecting subclinical inflammation. Elevated biomarker levels might therefore indicate the need for intensification of treatment or slower tapering of steroids. With this envisioned personalized treatment strategy, we could respond to important patient-reported needs: a recently conducted patient survey by Cure JM, a US patient organization for juvenile myositis, has shown that “predictors for disease flares” and “new treatments, less side effects” are 2 of the top 3 research priorities chosen by patients.⁶⁰

Galectin-9 and CXCL10 may also provide an objective outcome measure for response to therapy in future clinical trials that would be assessing novel therapeutics. Our study has shown that galectin-9 and CXCL10 levels in dried blood spots correlate with venous levels and could differentiate patients with active juvenile DM from healthy controls. Longitudinal assessment of these biomarkers via dried blood spots, which requires further study, has potential for high utility in the future, since dried blood spots can be sampled at home by simple capillary finger-prick. Since protein levels in dried blood spots remain remarkably stable over time, even at room temperature,^{61,62} samples of dried blood spots can be sent to a diagnostic center through regular mail. This enables at-home diagnostics and centralization of diagnostic cores for both clinical care and multicenter studies. It also ensures maximum accessibility of the biomarker measurements for non-expert medical centers, which can also facilitate care in rural areas.

Galectin-9 and CXCL10 measurements could add important information to the complex differential diagnosis of muscle symptoms during follow-up, and might aid in discriminating between steroid-induced myopathy, noninflammatory muscle pain, and muscle inflammation, all of which require different treatment strategies. In these complicated cases, in particular, the biomarkers may also help abrogate the need for invasive diagnostic muscle biopsy or costly magnetic resonance imaging scans, which can sometimes require sedation in young children. This specific potential use of these biomarkers will have to be further investigated in additional prospective studies. In addition, future prospective studies will have to point out 1) whether one biomarker may be superior to the other in answering specific clinical questions concerning juvenile DM, 2) whether the biomarkers are able to detect mild disease activity, 3) whether the biomarkers also have prognostic value in adult patients with myositis, and 4) whether biomarker-guided disease management will improve the outcomes in patients with juvenile DM.

In conclusion, galectin-9 and CXCL10 were identified and extensively validated as strong, reliable, and sensitive biomarkers for disease activity in juvenile DM. Measurement of these biomarkers might facilitate personalized treatment strategies for patients with juvenile DM, by providing a diagnostic monitoring tool to guide treatment.

REFERENCES

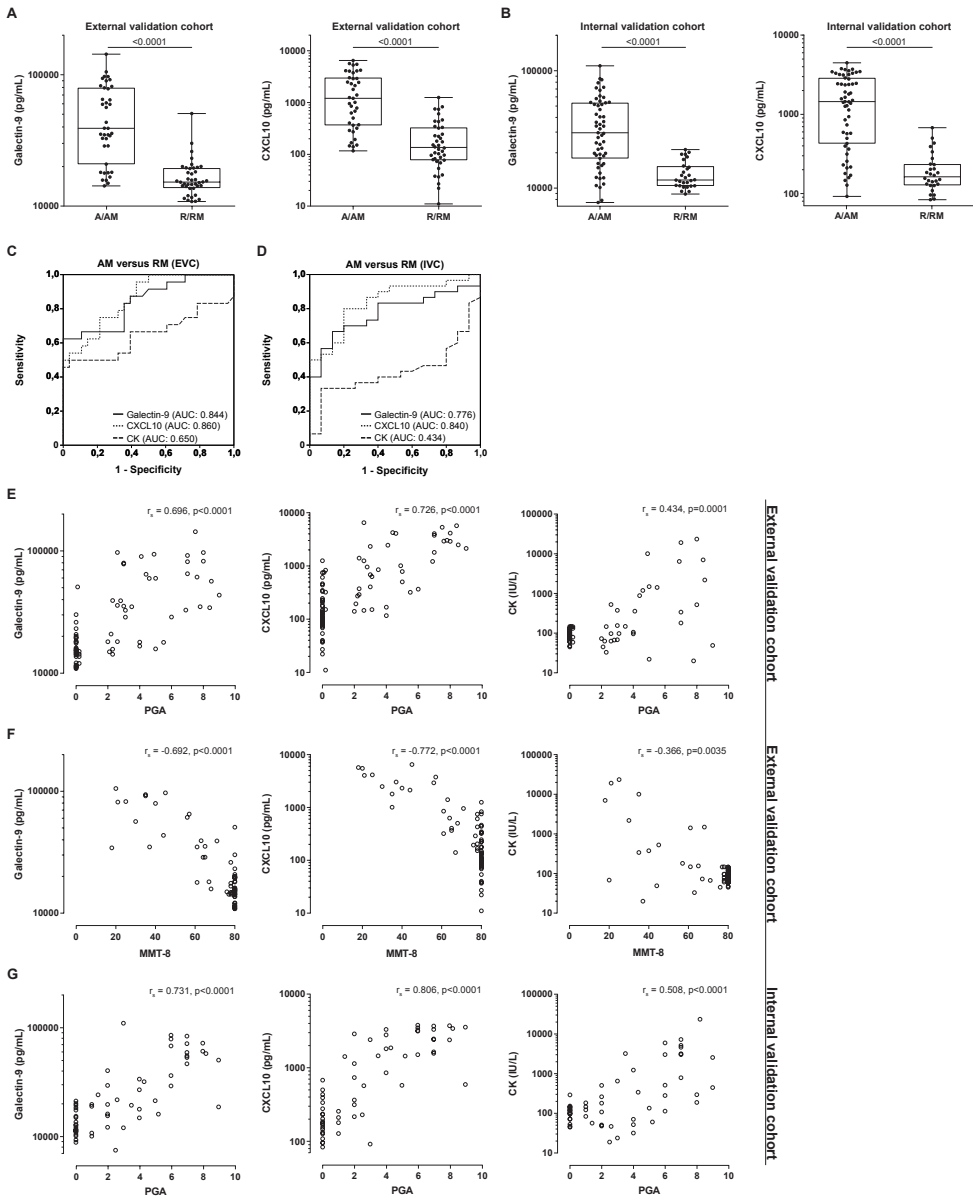
1. Feldman BM, Rider LG, Reed AM, et al. Juvenile Dermatomyositis and Other Idiopathic Inflammatory Myopathies of Childhood. *Lancet (London, England)* **2008**, 371 (9631), 2201–2212.
2. Meyer A, Meyer N, Schaeffer M, et al. Incidence and Prevalence of Inflammatory Myopathies: A Systematic Review. *Rheumatology (Oxford)*. **2015**, 54 (1), 50–63.
3. Pachman LM, Lipton R, Ramsey-Goldman R, et al. History of Infection before the Onset of Juvenile Dermatomyositis: Results from the National Institute of Arthritis and Musculoskeletal and Skin Diseases Research Registry. *Arthritis Rheum.* **2005**, 53 (2), 166–172.
4. Shah M, Targoff IN, Rice MM, et al. Brief Report: Ultraviolet Radiation Exposure Is Associated with Clinical and Autoantibody Phenotypes in Juvenile Myositis. *Arthritis Rheum.* **2013**, 65 (7), 1934–1941.
5. Vegosen LJ, Weinberg CR, O'Hanlon TP, et al. Seasonal Birth Patterns in Myositis Subgroups Suggest an Etiologic Role of Early Environmental Exposures. *Arthritis Rheum.* **2007**, 56 (8), 2719–2728.
6. Lopez De Padilla CM, Vallejo AN, Lacomis D, et al. Extranodal Lymphoid Microstructures in Inflamed Muscle and Disease Severity of New-Onset Juvenile Dermatomyositis. *Arthritis Rheum.* **2009**, 60 (4), 1160–1172.
7. Wedderburn LR, Varsani H, Li CKC, et al. International Consensus on a Proposed Score System for Muscle Biopsy Evaluation in Patients with Juvenile Dermatomyositis: A Tool for Potential Use in Clinical Trials. *Arthritis Rheum.* **2007**, 57 (7), 1192–1201.
8. Vercoulen Y, Bellutti Enders F, Meerding J, et al. Increased Presence of FOXP3+ Regulatory T Cells in Inflamed Muscle of Patients with Active Juvenile Dermatomyositis Compared to Peripheral Blood. *PLoS One* **2014**, 9 (8), e105353.
9. Shrestha S, Wershil B, Sarwark JF, et al. Lesional and Nonlesional Skin from Patients with Untreated Juvenile Dermatomyositis Displays Increased Numbers of Mast Cells and Mature Plasmacytoid Dendritic Cells. *Arthritis Rheum.* **2010**, 62 (9), 2813–2822.
10. Enders FB, Bader-Meunier B, Baildam E, et al. Consensus-Based Recommendations for the Management of Juvenile Dermatomyositis. *Ann. Rheum. Dis.* **2017**, 76 (2), 329–340.
11. Huber AM, Giannini EH, Bowyer SL, et al. Protocols for the Initial Treatment of Moderately Severe Juvenile Dermatomyositis: Results of a Children's Arthritis and Rheumatology Research Alliance Consensus Conference. *Arthritis Care Res. (Hoboken)*. **2010**, 62 (2), 219–225.
12. Huber AM, Robinson AB, Reed AM, et al. Consensus Treatments for Moderate Juvenile Dermatomyositis: Beyond the First Two Months. Results of the Second Childhood Arthritis and Rheumatology Research Alliance Consensus Conference. *Arthritis Care Res. (Hoboken)*. **2012**, 64 (4), 546–553.
13. Huber AM, Lang B, LeBlanc CM, et al. Medium- and Long-Term Functional Outcomes in a Multicenter Cohort of Children with Juvenile Dermatomyositis. *Arthritis Rheum.* **2000**, 43 (3), 541–549.
14. Gowdie PJ, Allen RC, Kornberg AJ, et al. Clinical Features and Disease Course of Patients with Juvenile Dermatomyositis. *Int. J. Rheum. Dis.* **2013**, 16 (5), 561–567.
15. Ravelli A, Trail L, Ferrari C, et al. Long-Term Outcome and Prognostic Factors of Juvenile Dermatomyositis: A Multinational, Multicenter Study of 490 Patients. *Arthritis Care Res. (Hoboken)*. **2010**, 62 (1), 63–72.
16. Ravelli A, Lattanzi B, Consolaro A, et al. Glucocorticoids in Paediatric Rheumatology. *Clin. Exp. Rheumatol.* **2011**, 29 (5 Suppl 68), S148-52.

17. Santiago RA, Silva CAA, Caparbo VF, et al. Bone Mineral Apparent Density in Juvenile Dermatomyositis: The Role of Lean Body Mass and Glucocorticoid Use. *Scand. J. Rheumatol.* **2008**, 37 (1), 40–47.
18. Shiff NJ, Brant R, Guzman J, et al. Glucocorticoid-Related Changes in Body Mass Index among Children and Adolescents with Rheumatic Diseases. *Arthritis Care Res. (Hoboken)*. **2013**, 65 (1), 113–121.
19. Wienke J, Deakin CT, Wedderburn LR, et al. Systemic and Tissue Inflammation in Juvenile Dermatomyositis: From Pathogenesis to the Quest for Monitoring Tools. *Front. Immunol.* **2018**, 9, 2951.
20. Rider LG, Aggarwal R, Pistorio A, et al. 2016 American College of Rheumatology/European League Against Rheumatism Criteria for Minimal, Moderate, and Major Clinical Response in Juvenile Dermatomyositis: An International Myositis Assessment and Clinical Studies Group/Paediatric Rheumatology Inter. *Arthritis Rheumatol. (Hoboken, N.J.)* **2017**, 69 (5), 911–923.
21. Ruperto N, Ravelli A, Pistorio A, et al. The Provisional Paediatric Rheumatology International Trials Organisation/American College of Rheumatology/European League Against Rheumatism Disease Activity Core Set for the Evaluation of Response to Therapy in Juvenile Dermatomyositis: A Prospective va. *Arthritis Rheum.* **2008**, 59 (1), 4–13.
22. Rider LG, Werth VP, Huber AM, et al. Measures of Adult and Juvenile Dermatomyositis, Polymyositis, and Inclusion Body Myositis: Physician and Patient/Parent Global Activity, Manual Muscle Testing (MMT), Health Assessment Questionnaire (HAQ)/Childhood Health Assessment Questionnaire (C-HAQ),. *Arthritis care (&) Res.* **2011**, 63 Suppl 1, S118-57.
23. Guzman J, Petty RE, Malleson PN. Monitoring Disease Activity in Juvenile Dermatomyositis: The Role of von Willebrand Factor and Muscle Enzymes. *J. Rheumatol.* **1994**, 21 (4), 739–743.
24. Rider LG. Assessment of Disease Activity and Its Sequelae in Children and Adults with Myositis. *Curr. Opin. Rheumatol.* **1996**, 8 (6), 495–506.
25. McCann LJ, Juggins AD, Maillard SM, et al. The Juvenile Dermatomyositis National Registry and Repository (UK and Ireland)--Clinical Characteristics of Children Recruited within the First 5 Yr. *Rheumatology (Oxford)*. **2006**, 45 (10), 1255–1260.
26. Bellutti Enders F, van Wijk F, Scholman R, et al. Correlation of CXCL10, Tumor Necrosis Factor Receptor Type II, and Galectin 9 with Disease Activity in Juvenile Dermatomyositis. *Arthritis Rheumatol. (Hoboken, N.J.)* **2014**, 66 (8), 2281–2289.
27. Enders FB, Delemarre EM, Kuemmerle-Deschner J, et al. Autologous Stem Cell Transplantation Leads to a Change in Proinflammatory Plasma Cytokine Profile of Patients with Juvenile Dermatomyositis Correlating with Disease Activity. *Annals of the rheumatic diseases*. England January 2015, pp 315–317.
28. Merani S, Chen W, Elahi S. The Bitter Side of Sweet: The Role of Galectin-9 in Immunopathogenesis of Viral Infections. *Rev. Med. Virol.* **2015**, 25 (3), 175–186.
29. Antonelli A, Ferrari SM, Giuggioli D, et al. Chemokine (C-X-C Motif) Ligand (CXCL)10 in Autoimmune Diseases. *Autoimmun. Rev.* **2014**, 13 (3), 272–280.
30. Reed AM, Peterson E, Bilgic H, et al. Changes in Novel Biomarkers of Disease Activity in Juvenile and Adult Dermatomyositis Are Sensitive Biomarkers of Disease Course. *Arthritis Rheum.* **2012**, 64 (12), 4078–4086.
31. Bilgic H, Ytterberg SR, Amin S, et al. Interleukin-6 and Type I Interferon-Regulated Genes and Chemokines Mark Disease Activity in Dermatomyositis. *Arthritis Rheum.* **2009**, 60 (11), 3436–3446.

32. Baechler EC, Bauer JW, Slattery CA, et al. An Interferon Signature in the Peripheral Blood of Dermatomyositis Patients Is Associated with Disease Activity. *Mol. Med.* **2007**, *13* (1–2), 59–68.
33. Huard C, Gulla S V, Bennett D V, et al. Correlation of Cutaneous Disease Activity with Type 1 Interferon Gene Signature and Interferon Beta in Dermatomyositis. *Br. J. Dermatol.* **2016**.
34. Thijssen VL, Heusschen R, Caers J, et al. Galectin Expression in Cancer Diagnosis and Prognosis: A Systematic Review. *Biochim. Biophys. Acta* **2015**, *1855* (2), 235–247.
35. Panda SK, Facchinetti V, Voynova E, et al. Galectin-9 Inhibits TLR7-Mediated Autoimmunity in Murine Lupus Models. *J. Clin. Invest.* **2018**, *128* (5), 1873–1887.
36. Zeggar S, Watanabe KS, Teshigawara S, et al. Lgals9 Deficiency Attenuates Nephritis and Arthritis in Pristane-Induced Lupus Model of BALB/c Mice. *Arthritis Rheumatol. (Hoboken, N.J.)* **2018**.
37. Bohan A, Peter JB. Polymyositis and Dermatomyositis (First of Two Parts). *N. Engl. J. Med.* **1975**, *292* (7), 344–347.
38. Bohan A, Peter JB. Polymyositis and Dermatomyositis (Second of Two Parts). *N. Engl. J. Med.* **1975**, *292* (8), 403–407.
39. Rider LG, Feldman BM, Perez MD, et al. Development of Validated Disease Activity and Damage Indices for the Juvenile Idiopathic Inflammatory Myopathies: I. Physician, Parent, and Patient Global Assessments. Juvenile Dermatomyositis Disease Activity Collaborative Study Group. *Arthritis Rheum.* **1997**, *40* (11), 1976–1983.
40. Rider LG, Koziol D, Giannini EH, et al. Validation of Manual Muscle Testing and a Subset of Eight Muscles for Adult and Juvenile Idiopathic Inflammatory Myopathies. *Arthritis Care Res. (Hoboken)*. **2010**, *62* (4), 465–472.
41. Huber AM, Dugan EM, Lachenbruch PA, et al. The Cutaneous Assessment Tool: Development and Reliability in Juvenile Idiopathic Inflammatory Myopathy. *Rheumatology (Oxford)*. **2007**, *46* (10), 1606–1611.
42. Almeida B, Campanilho-Marques R, Arnold K, et al. Analysis of Published Criteria for Clinically Inactive Disease in a Large Juvenile Dermatomyositis Cohort Shows That Skin Disease Is Underestimated. *Arthritis Rheumatol. (Hoboken, N.J.)* **2015**, *67* (9), 2495–2502.
43. Hoogendijk JE, Amato AA, Lecky BR, et al. 119th ENMC International Workshop: Trial Design in Adult Idiopathic Inflammatory Myopathies, with the Exception of Inclusion Body Myositis, 10-12 October 2003, Naarden, The Netherlands. *Neuromuscular disorders : NMD*. England May 2004, pp 337–345.
44. *Medical Research Council. Aids to the Examination of the Peripheral Nervous System, Memorandum No. 45, Her Majesty's Stationery Office.*; London, 1981.
45. Hochberg MC. Updating the American College of Rheumatology Revised Criteria for the Classification of Systemic Lupus Erythematosus. *Arthritis and rheumatism*. United States September 1997, p 1725.
46. Yee C-S, Farewell VT, Isenberg DA, et al. The Use of Systemic Lupus Erythematosus Disease Activity Index-2000 to Define Active Disease and Minimal Clinically Meaningful Change Based on Data from a Large Cohort of Systemic Lupus Erythematosus Patients. *Rheumatology (Oxford)*. **2011**, *50* (5), 982–988.
47. Arkachaisri T, Vilaiyuk S, Li S, et al. The Localized Scleroderma Skin Severity Index and Physician Global Assessment of Disease Activity: A Work in Progress toward Development of Localized Scleroderma Outcome Measures. *J. Rheumatol.* **2009**, *36* (12), 2819–2829.

48. Lunn MR, Wang CH. Spinal Muscular Atrophy. *Lancet (London, England)* **2008**, *371* (9630), 2120–2133.
49. de Jager W, Prakken BJ, Bijlsma JWJ, et al. Improved Multiplex Immunoassay Performance in Human Plasma and Synovial Fluid Following Removal of Interfering Heterophilic Antibodies. *J. Immunol. Methods* **2005**, *300* (1–2), 124–135.
50. Scholman RC, Giovannone B, Hiddingh S, et al. Effect of Anticoagulants on 162 Circulating Immune Related Proteins in Healthy Subjects. *Cytokine* **2017**.
51. Lazarevic D, Pistorio A, Palmisani E, et al. The PRINTO Criteria for Clinically Inactive Disease in Juvenile Dermatomyositis. *Ann. Rheum. Dis.* **2013**, *72* (5), 686–693.
52. Neesgaard B, Ruhwald M, Krarup HB, et al. Determination of Anti-HCV and Quantification of HCV-RNA and IP-10 from Dried Blood Spots Sent by Regular Mail. *PLoS One* **2018**, *13* (7), e0201629.
53. Kim H, Biancotto A, Cheung F, et al. Novel Serum Broad-Based Proteomic Discovery Analysis Identifies Proteins and Pathways Dysregulated in Juvenile Dermatomyositis (JDM) Myositis Autoantibody Groups. *Arthritis Rheumatol. (Hoboken, N.J.)* **2017**, *69* (Supplement S10), 26–27.
54. Sanner H, Schwartz T, Flato B, et al. Increased Levels of Eotaxin and MCP-1 in Juvenile Dermatomyositis Median 16.8 Years after Disease Onset; Associations with Disease Activity, Duration and Organ Damage. *PLoS One* **2014**, *9* (3), e92171.
55. Rice GI, Melki I, Fremont M-L, et al. Assessment of Type I Interferon Signaling in Pediatric Inflammatory Disease. *J. Clin. Immunol.* **2017**, *37* (2), 123–132.
56. Rodero MP, Decalf J, Bondet V, et al. Detection of Interferon Alpha Protein Reveals Differential Levels and Cellular Sources in Disease. *J. Exp. Med.* **2017**, *214* (5), 1547–1555.
57. Van den Hoogen LL, Van Roon JAG, Mertens JS, et al. Galectin-9 Is an Easy to Measure Biomarker for the Interferon Signature in Systemic Lupus Erythematosus and Antiphospholipid Syndrome. *Ann. Rheum. Dis.* **2018**, *77* (12), 1810–1814.
58. Fall N, Bove KE, Stringer K, et al. Association between Lack of Angiogenic Response in Muscle Tissue and High Expression of Angiostatic ELR-Negative CXC Chemokines in Patients with Juvenile Dermatomyositis: Possible Link to Vasculopathy. *Arthritis Rheum.* **2005**, *52* (10), 3175–3180.
59. Limongi F. The CXCR3 Chemokines in Inflammatory Myopathies. *Clin. Ter.* **2015**, *166* (1), e56-61.
60. Dave (Cure JM Foundation) M. Patient Perspectives on Juvenile Myositis Research Priorities http://www.curejm.org/medical_professionals/pdfs/2017-05-04 JM-Research-Priorities.pdf (accessed May 31, 2018).
61. McDade TW, Williams S, Snodgrass JJ. What a Drop Can Do: Dried Blood Spots as a Minimally Invasive Method for Integrating Biomarkers into Population-Based Research. *Demography* **2007**, *44* (4), 899–925.
62. De Jesus VR, Zhang XK, Keutzer J, et al. Development and Evaluation of Quality Control Dried Blood Spot Materials in Newborn Screening for Lysosomal Storage Disorders. *Clin. Chem.* **2009**, *55* (1), 158–164.

SUPPLEMENTARY MATERIAL

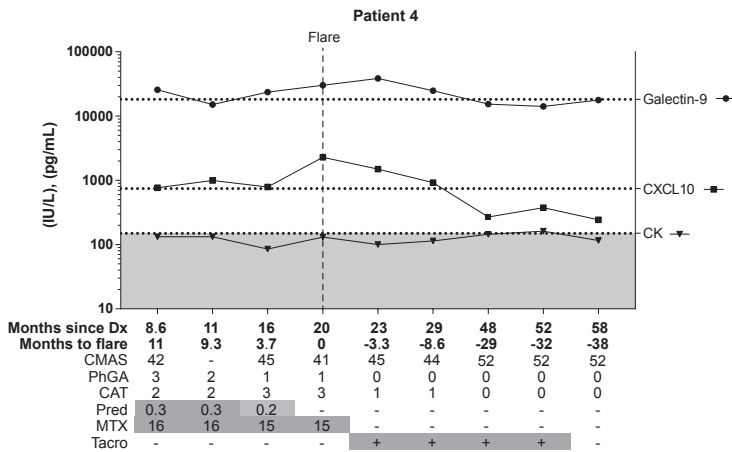
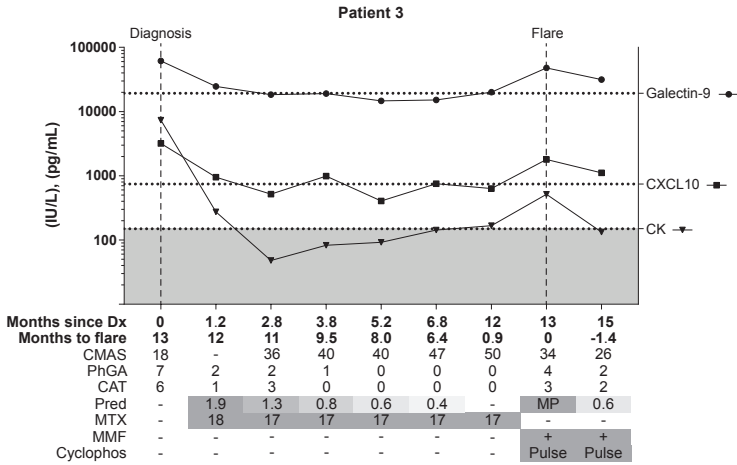
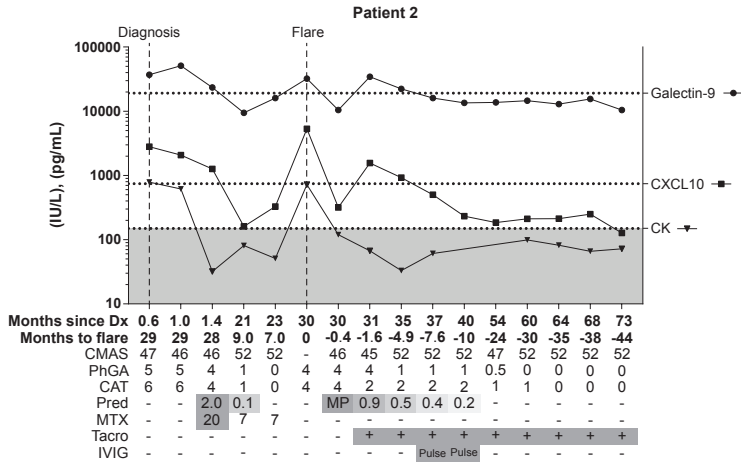


Supplementary figure 1. Cross-sectional validation of galectin-9 and CXCL10 as biomarkers for disease activity in JDM in two independent validation cohorts.

(A&B) Galectin-9 and CXCL10 levels were measured in serum samples from JDM patients by multiplex immunoassay. Patients were stratified into two groups based on disease activity, regardless of medication. Medians and interquartile ranges are shown, on a log scale. Mann-Whitney U test. (A) External validation cohort (EVC) (A/AM: n=39, R/RM: n=40).

(Supplementary figure 1 continued)

(B) Internal validation cohort (IVC) (A/AM: n=55, R/RM: n=28). **(C&D)** ROC curves of galectin-9, CXCL10, and CK in the EVC **(C)** and IVC **(D)**. Only patients with a complete dataset for the specific ROC curve were included in the analysis. ROC curves for patients on medication. Statistic details of the ROC curve analysis are shown in supplementary table 3. **(E&F)** Correlation of galectin-9, CXCL10 and CK with the PGA **(E)** and MMT-8 **(F)** in the EVC. Spearman rank correlation, n=79. **(G)** Correlation of galectin-9, CXCL10 and CK with the PGA in the IVC. Spearman rank correlation, n=67. A = active pre-treatment; AM = active on medication; RM = remission on medication; R = remission off medication; r_s = Spearman r; PGA = physician's global assessment; MMT-8 = manual muscle testing scores of 8 muscle groups. Patient characteristics are shown in table 1 and 2.



Supplementary figure 2. Galectin-9, CXCL10, CK in individual patients with disease flares after the first year.

(Supplementary figure 2 continued)

Galectin-9 and CXCL10 were measured in longitudinal samples from 3 patients with JDM with a disease flare after the first year. Each panel represents one patient. Dotted lines indicate the previously determined cutoff values for galectin-9 and CXCL10 (19396 pg/mL and 805 pg/mL, respectively). Gray shading indicates the cutoff for CK (150 IU/L). Time is in months. CK = creatine kinase, IU = international units, Dx = diagnosis, CMAS = childhood myositis assessment scale, PGA = Physician's global assessment, CAT = cutaneous assessment tool, Pred = prednisone (mg/kg/day), MP = methylprednisolone (Pulse= 3x 20 mg/kg/day), MTX = methotrexate (mg/m²/week), IVIG = intravenous immunoglobulins (Pulse= 2 g/kg per month), Tacro = Tacrolimus, MMF = mycophenolate mofetil, Cyclophos = Cyclophosphamide (Pulse= 750 mg/m² per month). Patient characteristics are shown in supplementary table 7.

Supplementary table 1. Patient characteristics of cross-sectional external validation cohort from London.

External validation cohort (EVC) from London, United Kingdom				
	At diagnosis	Active on medication	Remission on medication	Remission off medication
	A	AM	RM	R
	(n=12)	(n=27)	(n=28)	(n=12)
Age at diagnosis, years	5 (2-15)	6 (2-12)	7 (2-14)	6 (1-13)
Age at sampling, years	5 (3-15)	8 (3-16)	10 (5-16)	12 (6-17)
Sex, % female	66.7	59.3	67.9	75.0
Diagnosis to sampling, months	0 (0-1)	17 (0-107)	34 (7-105)	72 (42-127)
Disease activity				
CMAS (0-52)	7 (1-28) <i>NR=2</i>	39 (3-44)	52 (48-52)	52 (50-52)
PGA (0-10)	7 (3-9) <i>NR=1</i>	4 (2-8)	0 (0-0)	0 (0-0)
MMT-8 score (0-80)	35 (18-56) <i>NR=3</i>	65 (25-78) <i>NR=11</i>	80 (78-80)	80 (78-80)
Autoantibodies				
% of patients ANA positive	58	63	46	42
% of patients MSA positive	88 <i>NR=4</i>	93	77 <i>NR=2</i>	67
Medication, % of patients				
Oral steroids	-	73	7	-
IV steroids	-	36	-	-
Methotrexate	-	85	93	-
Ciclosporin	-	8	-	-
Azathioprine	-	4	14	-
Cyclophosphamide	8	25	-	-
Hydroxychloroquine	-	8	4	-
IV immunoglobulins	8	4	4	-
Etanercept	-	-	4	-
Infliximab	-	13	4	-
None	92	-	-	100

(Continued)

Supplementary table 1. Patient characteristics of cross-sectional external validation cohort from London.

External validation cohort (EVC) from London, United Kingdom				
	At diagnosis	Active on medication	Remission on medication	Remission off medication
	A	AM	RM	R
	(n=12)	(n=27)	(n=28)	(n=12)
Muscle enzymes				
CK, IU/liter	442 (49-19078)	126 (20-23444)	78 (45-147)	87 (48-145)
	<i>NR=2</i>	<i>NR=3</i>		
AST, IU/liter	153 (60-246)	57 (27-876)	49 (26-65)	41 (38-43)
	<i>NR=10</i>	<i>NR=20</i>	<i>NR=21</i>	<i>NR=10</i>
ALT, IU/liter	85 (25-340)	35 (10-482)	23 (6-125)	19 (6-39)
	<i>NR=1</i>	<i>NR=4</i>		
LDH, IU/liter	1410 (686-4676)	793 (404-5478)	590 (405-829)	589 (392-832)
	<i>NR=1</i>	<i>NR=4</i>	<i>NR=1</i>	<i>NR=1</i>
Inflammation markers				
CRP, mg/liter	5 (5-9)	7 (1-10)	4 (3-63)	5 (3-7)
	<i>NR=2</i>	<i>NR=9</i>	<i>NR=5</i>	
ESR, mm/hour	36 (5-124)	13 (1-80)	6 (2-40)	5 (2-26)
	<i>NR=1</i>	<i>NR=1</i>		<i>NR=1</i>

Patients were stratified into four groups based on disease activity and use of medication: active pre-treatment ("A"), active on medication ("AM"), remission on medication ("RM"), remission off medication ("R"). Unless indicated otherwise, values represent median (range). The CMAS and MMT-8 were used to assess muscle strength. ANA were detected by indirect immunofluorescence on Hep-2 cells. All patients in remission had all clinical data available (PGA, CK, CMAS and MMT8). The missing data in the A/AM groups did not affect their classification due to redundancy of de data (CMAS and MMT8). 1 patient in the "A" group had started treatment less than 1 week before sampling and was therefore still included in the pre-treatment group. In the "R" group the median time between stopping immunosuppressive medication and sampling was 12.4 months, with a range of 0.9-93.9 months. *NR=not recorded*, *CMAS =childhood myositis assessment scale*, *PGA = physician's global assessment*, *MMT-8 = manual muscle testing of 8 muscle groups*, *ANA = anti-nuclear antibodies*, *MSA = myositis-specific antibodies*, *IV = intravenous*, *CK = creatine kinase*, *AST = aspartate aminotransferase*, *ALT = alanine aminotransferase*, *LDH = lactate dehydrogenase*, *CRP = C-reactive protein*, *ESR = erythrocyte sedimentation rate*, *IU= international units*

Supplementary table 2. Patient characteristics of cross-sectional internal validation cohort.

Internal validation cohort (IVC) from Utrecht, Netherlands				
	At diagnosis A (n=25)	Active on medication AM (n=30)	Remission on medication RM (n=16)	Remission off medication R (n=12)
Age at diagnosis, years	5 (2-16)	6 (2-18)	8 (3-16)	7 (3-14)
Age at sampling, years	5 (2-16)	7 (2-18)	9 (4-19)	14 (8-25)
Sex, % female	52.0	63.3	56.3	50.0
Diagnosis to sampling, months	0 (0-10)	3 (0-80)	18 (3-113)	93 (37-191)
Disease activity				
CMAS (0-52)	21 (1-52) <i>NR=9</i>	41 (10-52) <i>NR=9</i>	52 (48-52) <i>NR=3</i>	52 (48-52) <i>NR=1</i>
PGA (0-10)	7 (2-9) <i>NR=6</i>	2 (1-9) <i>NR=10</i>	0 (0-0) <i>NR=3</i>	0 (0-0) <i>NR=1</i>
Autoantibodies				
% of patients ANA positive	52	52	44	44
% of patients MSA positive	22 <i>NR=7</i>	18 <i>NR=8</i>	8 <i>NR=3</i>	50 <i>NR=10</i>
Medication, % of patients				
Oral steroids	-	93	44	-
Methotrexate	-	80	56	-
Cyclophosphamide	-	10	-	-
Hydroxychloroquine	-	10	6	-
IV immunoglobulins	-	11	-	-
Mycophenolate mofetil	-	7	13	-
Tacrolimus	-	3	13	-
None	100	-	-	100
Muscle enzymes				
CK, IU/liter	813 (61-23908)	83 (19-5292)	112 (47-146) <i>NR=1</i>	111 (45-293)
AST, IU/liter	186 (30-1343)	34 (9-734)	29 (19-40)	24 (11-42) <i>NR=1</i>
ALT, IU/liter	63 (12-366)	25 (11-1242)	14 (8-28)	18 (8-24) <i>NR=1</i>
LDH, IU/liter	658 (314-1541) <i>NR=3</i>	281 (179-818) <i>NR=8</i>	246 (160-347)	205 (151-261) <i>NR=2</i>

(Continued)

Supplementary table 2. Patient characteristics of cross-sectional internal validation cohort.

Internal validation cohort (IVC) from Utrecht, Netherlands				
	At diagnosis A (n=25)	Active on medication AM (n=30)	Remission on medication RM (n=16)	Remission off medication R (n=12)
Inflammation markers				
CRP, mg/liter	1 (0-28) NR=2	1 (0-8) NR=3	1 (0-6) NR=3	1 (1-9) NR=3
ESR, mm/hour	16 (2-85) NR=3	6 (2-24) NR=4	6 (2-26) NR=1	6 (2-15) NR=1

Patients were stratified into four groups based on disease activity and use of medication: active pre-treatment ("A"), active on medication ("AM"), remission on medication ("RM"), remission off medication ("R"). Unless indicated otherwise, values represent: median (range). The CMAS was used to assess muscle strength. ANA were detected by indirect immunofluorescence on Hep-2 cells. 8 out of 55 active patients had a CMAS>47, but were nonetheless defined as active based on active skin disease and/or active arthritis, rendering an elevated PGA. 3 of these patients also had an elevated CK despite a normal CMAS. All patients in remission were sure to be in remission even with missing data: 1 patient did not have a CMAS available but a clinical description of normal muscle strength. 2 patients did not have a PGA available, but both had a CMAS of 52, no skin symptoms and low muscle enzymes. All patients "at diagnosis" were considered active, also because diagnoses of JDM were certain due to available clinical follow-up data. In the "AM" group 10 patients had missing PGA, 6 of which had evident muscle weakness (by CMAS or clinical description), with or without skin symptoms. The remaining 4 patients in this group had evident skin symptoms (CAT or clinical description). In the "R" group the median time between stopping immunosuppressive medication and sampling was 39.8 months, with a range of 4.7-106.3 months. *NR=not recorded*, *CMAS = childhood myositis assessment scale*, *PGA = physician's global assessment*, *ANA = anti-nuclear antibodies*, *MSA = myositis-specific antibodies*, *IV = intravenous*, *CK = creatine kinase*, *AST = aspartate aminotransferase*, *ALT = alanine aminotransferase*, *LDH = lactate dehydrogenase*, *CRP = C-reactive protein*, *ESR = erythrocyte sedimentation rate*, *IU= international units*.

Supplementary table 3. Analysis of ROC curves for galectin-9 and CXCL10 in external and internal cross-sectional validation cohort.

Cohort	Marker	AUC	Standard Error	Asymptotic Significance	Asymptotic 95% Confidence Interval		N		
					Lower Bound	Upper Bound			
Active versus remission	EC	0.894	0.037	<0.0001	0.821	0.966	n=34 for active		
	CXCL10						0.802	0.953	n=40 for remission
	CK						0.544	0.819	n=5 missing
AM versus RM	EC	0.844	0.055	<0.0001	0.738	0.951	n=24 for active		
	CXCL10						0.764	0.956	n=28 for remission
	CK						0.485	0.815	n=3 missing
Active versus remission	IC	0.863	0.040	<0.0001	0.785	0.941	n=55 for active		
	CXCL10						0.838	0.965	n=27 for remission
	CK						0.547	0.778	n=1 missing
AM versus RM	IC	0.776	0.069	<0.0001	0.640	0.911	n=30 for active		
	CXCL10						0.722	0.958	n=15 for remission
	CK						0.267	0.602	n=1 missing

ROC curves for both the internal and external validation cohort, comparing galectin-9, CXCL10 and CK were constructed, assessing their discriminative power for active disease versus remission. Either all active patients and all patients in remission, regardless of treatment ("active versus remission") or only patients on medication ("AM versus RM") were analyzed. *AUC = area under the curve, AM = active on medication, RM = remission on medication.*

Supplementary table 4. Patient characteristics of cohort with adult inflammatory myopathies and eosinophilic fasciitis.

HC	JDM NL	JDM Sing	DM	NSM	EF	SMA
Utrecht, NL	Utrecht, NL	Singapore	Amsterdam, NL	Amsterdam, NL	Utrecht & Nijmegen, NL	Utrecht, NL
(n=22)	Active Remission disease A/AM (n=31) RM/R (n=27)	Active Remission disease A/AM (n=8) RM/R (n=6)	Active Remission disease A/AM (n=28) RM/R (n=8)	Active Remission disease A/AM (n=9) RM/R (n=5)	Active Remission disease A/AM (n=11) RM/R (n=7)	(n=43)
Age at diagnosis, years	6 (2-18)	7 (4-16)	47 (19-81)	45 (18-69)	59 (30-70)	2 (0-31)
Age at sampling, years	8 (2-18)	12 (7-16)	49 (19-81)	45 (18-69)	61 (34-69)	36 (2-71)
Sex, % female	54.8	50.0	71.4	100.0	63.6	60.5
Diagnosis to sampling, months	0 (0-80)	0 (0-129)	0 (0-195)	0 (0-36)	13 (1-330)	383 (12-830)
Disease activity						
Muscle weakness (% of patients)	81	50	68	88	-	-
(J)DM skin symptoms (% of patients)	90	100	100	0	-	-
CMAS (0-52)	28 (1-52) NR=10	46 (14-52) NR=4	52 (48-52)	-	-	-
EF VAS activity (0-100)	-	-	-	-	41 (7-64) NR=2	2 (0-4) NR=1

(Continued)

Supplementary table 4. Patient characteristics of cohort with adult inflammatory myopathies and eosinophilic fasciitis.

HC	JDM NL		JDM Sing		DM		NSM		EF		SMA
	A/AM	RM/R	A/AM	RM/R	A/AM	RM/R	A/AM	RM/R	A/AM	RM/R	
EF activity (mLoSSI, 0-162)	-	-	-	-	-	-	-	-	30 (14-52)	8 (3-40)	-
SMA motor score (HMFSE, 0-66)	-	-	-	-	-	-	-	-	NR=2	NR=1	4 (0-60) NR=4
Medication, % of patients											
Oral steroids	16	26	13	50	29	50	22	80	27	57	-
Methotrexate	16	33	25	67	4	25	11	40	9	71	-
Azathioprine	-	-	-	-	-	38	-	-	-	-	-
Hydroxychloroquine	3	4	38	67	4	13	22	20	-	-	-
IV immunoglobulins	3	-	-	-	7	-	-	-	-	-	-
Tacrolimus	3.2	4	-	-	4	-	-	-	-	-	-
Mycophenolate Mofetil	3.2	7	13	-	-	-	-	-	-	-	-
Adalimumab	-	-	-	-	-	-	11	-	-	-	-
None	100	81	44	50	68	25	44	0	73	14	100
Muscle enzymes											
CK, IU/liter	658 (52-23908)	109 (45-293)	156 (84-1010)	136 (101-184)	268 (32-12338)	87 (45-481)	1518 (75-5700)	94 (66-149)	37 (35-39)	18 (18-18)	-
AST, IU/liter	88 (12-1343)	28 (11-42)	33 (25-102)	25 (18-31)	46 (14-415)	16 (13-37)	100 (67-133)	19 (15-23)	NR=9	NR=6	-
		NR=1			NR=4		NR=7	NR=1	NR=9	NR=6	
		NR=1			NR=11	NR=3	NR=7	NR=1	NR=8	NR=8	

(Continued)

Supplementary table 4. Patient characteristics of cohort with adult inflammatory myopathies and eosinophilic fasciitis.

HC	JDM NL		JDM Sing		DM		NSM		EF		SMA	
	A/AM	RM/R	A/AM	RM/R	A/AM	RM/R	A/AM	RM/R	A/AM	RM/R		
ALT, IU/liter	-	51 (11-1242)	15 (8-28)	20 (9-71)	14 (11-24)	33 (5-324)	17 (10-59)	60 (13-327)	20 (18-24)	23 (12-70)	30 (20-62)	-
LDH, IU/liter	-	645 (189-1541)	NR=1	318 (237-700)	255 (224-276)	313 (163-613)	182 (163-200)	170 (170-170)	136 (136-136)	215 (194-235)	NR=2	-
		NR=3	NR=2	NR=6	NR=6	NR=11	NR=8	NR=4	NR=9	NR=9	NR=4	NR=9
Inflammation markers												
CRP, mg/liter	-	1 (0-28)	1 (0-9)	1 (0-21)	1 (0-1)	5 (0-129)	5 (2-8)	4 (1-34)	4 (3-14)	10 (9-11)	10 (2-12)	-
		NR=3	NR=6	NR=12	NR=4	NR=2	NR=2	NR=2	NR=2	NR=9	NR=4	NR=4
ESR, mm/hour	-	14 (2-85)	6 (2-26)	13 (2-104)	6 (2-16)	11 (2-130)	6 (3-12)	31 (5-75)	4 (3-14)	13 (5-23)	5 (2-102)	-
		NR=5	NR=2	NR=13	NR=4	NR=3	NR=2	NR=3	NR=2	NR=7	NR=2	NR=2

Patients were stratified based on disease activity, regardless of treatment. Of each patient, only one sample per category (active or remission) was included in the analysis. The internal validation cohort (supplementary table 2) served as the JDM cohort in this analysis, with exclusion of samples from the same patient falling within the same category ('active' or 'remission'). Unless indicated otherwise, values represent: median (range). 6 out of 31 active patients had a CMAS>47, but were defined as active based on active skin disease and/or active arthritis, rendering an elevated PGA. 3 of these patients also had an elevated CK despite a normal CMAS. HC = healthy adult control, JDM = juvenile dermatomyositis, NL = Netherlands (Dutch cohort) DM = adult dermatomyositis, NSM = adult non-specific myositis and overlap myositis, EF = eosinophilic fasciitis, SMA = spinal muscular atrophy, NR=not recorded, CMAS = childhood myositis assessment scale, VAS = visual analogue scale, mLoSSI = modified LS Skin Severity Index, HMFSE = Hammersmith Functional Motor Scale-Expanded, IV = intravenous, CK = creatine kinase, AST = aspartate Aminotransferase, ALT = alanine Aminotransferase, LDH = lactate dehydrogenase, CRP = C-reactive protein, ESR = erythrocyte sedimentation rate.

Supplementary table 5. Patient characteristics of cohort with systemic autoimmune diseases with involvement of the skin.

	HC		JDM		LoS		SLE			
	Utrecht, NL	(n=12)	Active disease A/AM (n=9)	Remission RM/R (n=7)	Utrecht & Nijmegen, NL	Active disease A/AM (n=8)	Remission RM/R (n=7)	Utrecht, NL	Active disease A/AM (n=19)	Remission RM/R (n=17)
Age at diagnosis, years			12 (5-18)	6 (5-14)		10 (3-16)	8 (1-13)		19 (11-37)	23 (11-29)
Age at sampling, years	35 (25-57)		12 (5-18)	10 (7-17)		12.5 (6-16)	14 (7-16)		33 (11-55)	40 (12-56)
Sex, % female	75		66.7	57.1		33.3	71.4		100.0	94.1
Diagnosis to sampling, months			0 (0-38)	36 (5-77)		10.5 (6-66)	47 (10-180)		131 (0-270)	149 (7-472)
Disease activity										
Muscle weakness (% of patients)			78	0		-	-		-	-
CMAS (0-52)			35 (4-52) NR=1	50 (48-52) NR=2		-	-		-	-
JDM skin symptoms (% of patients)			100	0		-	-		-	-
Morphea activity (mLoSSI, 0-162)			-	-		8 (6-22) NR=1	1 (0-5)		-	-
Morphea VAS activity (0-100)			-	-		19 (11-37) NR=1	0 (0-5)		-	-
SLEDAI (0-105)			-	-		-	-		6 (4-26)	2 (0-3)
LE skin disease (% of patients)			-	-		-	-		83	53
									NR=1	

(Continued)

Supplementary table 5. Patient characteristics of cohort with systemic autoimmune diseases with involvement of the skin.

	HC		JDM		LoS		SLE	
	A/AM	RM/R	A/AM	RM/R	A/AM	RM/R	A/AM	RM/R
Medication, % of patients								
Oral steroids	22	71			17	14	68	35
IV steroids	-	-			-	-	-	-
Methotrexate	22	71			17	43	-	-
Ciclosporin	-	-			-	-	-	-
Azathioprine	-	-			-	-	42	6
Cyclophosphamide	-	-			-	-	-	-
Hydroxychloroquine	-	-			-	-	68	53
IV immunoglobulins	-	-			-	-	-	-
Tacrolimus	-	29			-	-	-	-
Mycophenolate Mofetil	-	-			-	29	32	29
Etanercept	-	-			-	-	-	-
Infliximab	-	-			-	-	-	-
None	67	14			83	29	11	29
Muscle enzymes								
CK, IU/liter	1240 (52-3243)	84 (45-370)			33 (24-42) NR=4	84 (59-183)	-	-
AST, IU/liter	112 (18-1343)	22 (12-32)			24 (24-24) NR=5	27 (18-35)	-	-
ALT, IU/liter	85 (14-1242)	16 (11-25)			20 (16-23) NR=1	19 (13-30) NR=1	17 (10-123)	17 (9-40)

(Continued)

Supplementary table 5. Patient characteristics of cohort with systemic autoimmune diseases with involvement of the skin.

	HC		JDM		LoS		SLE	
	A/AM	RM/R	A/AM	RM/R	A/AM	RM/R	A/AM	RM/R
Inflammation markers								
LDH, IU/liter	658 (213-1742)	241 (160-255)	-	-	-	-	-	-
CRP, mg/liter	2 (0-7)	1 (0-5)	5 (5-5)	5 (1-9)	1 (1-13)	2 (1-18)	NR=8	NR=8
ESR, mm/hour	9 (5-33)	7 (2-14)	5 (2-8)	2 (0-6)	16 (2-82)	11 (2-79)	NR=2	NR=2

Patients were stratified based on disease activity, regardless of treatment. Of each patient, only one sample per category (active or remission) was included in the analysis. Unless indicated otherwise, values represent: median (range). 2 out of 9 active patients had a CMAS>47, but were defined as active based on active skin disease. 1 of these patients also had an elevated CK despite a normal CMAS. HC = healthy adult control, JDM = juvenile dermatomyositis, LoS = localized scleroderma, SLE = systemic lupus erythematosus, NR=not recorded, CMAS = childhood myositis assessment scale, VAS = visual analogue scale, mLOSSI = modified LS Skin Severity Index, SLEDAI = Systemic Lupus Erythematosus Disease Activity Index, IV = intravenous, CK = creatine kinase, AST = Aspartate Aminotransferase, ALT = Alanine Aminotransferase, LDH = lactate dehydrogenase, CRP = C-reactive protein, ESR = erythrocyte sedimentation rate, IU = international units.

Supplementary table 6. Patient characteristics of longitudinal cohort.

	JDM		
	Utrecht, NL		
	No flare (n=15)	Flare < 12 months (n=6)	Flare >12 months (n=7)
Age at diagnosis, years	6 (3-15)	9 (2-12)	8 (3-15)
Sex, % female	46.7	66.7	42.9
Diagnosis to sampling, months	0 (0-3)	0 (0-0)	0 (0-9)
Onset of disease to flare, months	-	4 (3-10)	30 (13-53)
Follow-up time, years	2 (1-9)	1 (1-10)	3 (1-6)
Disease activity at diagnosis			
CMAS (0-52)	28 (1-37)	14 (6-14) NR=3	34 (18-47) NR=1
PGA (0-10)	4 (2-9) NR=2	6 (5-7)	5 (3-7)
JDM skin symptoms (% of patients)	100	100	100
Muscle enzymes at diagnosis			
CK, IU/liter	510 (78-4687)	683 (114-6038)	193 (98-7334)
AST, IU/liter	121 (35-1482) NR=1	267 (63-940)	57 (24-400)
ALT, IU/liter	76 (14-1242) NR=1	99 (31-320)	29 (16-77)
LDH, IU/liter	678 (316-958) NR=1	754 (564-1292)	428 (323-1028)
Inflammation markers at diagnosis			
CRP, mg/liter	2 (0-28) NR=3	2 (1-4)	2 (1-7)
ESR, mm/hour	15 (2-121) NR=3	28 (9-45)	10 (5-40)

Patients were stratified into three groups based on the timing of a disease flare: Patients without flares ("no flare", n=15), patients with a flare within the first year after diagnosis ("<12 months", n=6) and patients with a flare after the first year (">12 months", n=7). Of the 7 patients with a flare after the first year, 4 patients had a sample available at diagnosis. These 4 are shown in more detail in figure 3 and supplementary figure 2. CMAS = childhood myositis assessment scale, PGA = physician's global assessment, CK = creatine kinase, AST = aspartate aminotransferase, ALT = alanine aminotransferase, LDH = lactate dehydrogenase, CRP = C-reactive protein, ESR = erythrocyte sedimentation rate, IU = international units.

Supplementary table 7. Patient characteristics of dried blood spot cohort.

	JDM	HC
	Utrecht, NL	Utrecht, NL
	Active disease A/AM (n=10)	(n=12)
Age at diagnosis, years	4 (3-6)	-
Age at sampling, years	4 (3-6)	34 (21-61)
Sex, % female	50.0	66.7
Diagnosis to sampling, months	0 (0-5)	-
Disease activity		
CMAS (0-52)	34 (1-42)	-
JDM skin symptoms (% of patients)	75	-
Medication, % of patients		
Oral steroids	50	-
Methotrexate	50	-
Hydroxychloroquine	10	-
None	50	100
Muscle enzymes		
CK, IU/liter	99 (47-7334)	-
AST, IU/liter	38 (22-400)	-
ALT, IU/liter	25 (12-121)	-
LDH, IU/liter	370 (284-1028)	-
Inflammation markers		
CRP, mg/liter	1 (1-205)	-
ESR, mm/hour	12 (2-85)	-

Only JDM patients with active disease were included in this cohort, and compared to adult healthy controls. HC= healthy adult control, JDM = juvenile dermatomyositis, NR=not recorded, CMAS = childhood myositis assessment scale, CK = creatine kinase, AST = aspartate aminotransferase, ALT = alanine aminotransferase, LDH = lactate dehydrogenase, CRP = C-reactive protein, ESR = erythrocyte sedimentation rate, IU = international units.

Endothelial and inflammatory biomarker profiling at diagnosis reflects clinical heterogeneity of juvenile dermatomyositis and is prognostic for response to treatment

Judith Wienke, Lauren M. Pachman, Gabrielle A. Morgan, Joo Guan Yeo, Maria L. Amoruso, Victoria Hans, Sylvia S.M. Kamphuis, Esther P.A.H. Hoppenreijns, Wineke Armbrust, J. Merlijn van den Berg, Petra C.E. Hissink Muller, Thaschawee Arkachaisri, Femke van Wijk,* and Annet van Royen-Kerkhof*

*These authors contributed equally

Submitted

ABSTRACT

Objectives: In juvenile dermatomyositis (JDM), a heterogeneous systemic immune-mediated vasculopathy, we aim to 1) identify inflammation/endothelial dysfunction-related biomarker profiles reflecting disease severity at diagnosis; 2) establish if biomarker profiles can predict response to treatment.

Methods: 39 markers related to endothelial activation, dysfunction and inflammation were measured in treatment-naive JDM patient serum from two independent cohorts (n=30/n=29) by multiplex technology. Data were analyzed by unsupervised hierarchical clustering, non-parametric tests with correction for multiple testing and Kaplan-Meier and cox-proportional-hazards-model for analysis of time until drug-free remission. Myositis-specific antibodies were measured by immunoprecipitation or line blot.

Results: Severe vasculopathy was associated with low ICAM-1 and high endoglin levels. Unsupervised clustering of the discovery cohort with all markers yielded two distinct patient clusters: the smaller cluster, with high levels of CXCL13, CCL19, galectin-9, CXCL10, TNFR2 and galectin-1 (amongst others), had higher muscle and global disease activity. In the validation cohort, correlations of galectin-9, CXCL10, TNFR2 and galectin-1 with global disease activity were confirmed. Stratification of patients by these 4 markers identified those with more severe symptoms, requiring more intense treatment in the first 3 months. Anti-NXP2 positive patients were more likely to be in this 'at risk' subgroup. High galectin-9, CXCL10, and TNFR2 at diagnosis were predictive of a longer disease course until drug-free remission.

Conclusion: This study confirms the heterogeneity of new-onset JDM using serum biomarkers. Patients with a suboptimal response to treatment present with high levels of galectin-9, CXCL10, TNFR2 and galectin-1. These patients may benefit from more intensive monitoring and/or treatment.

INTRODUCTION

Juvenile Dermatomyositis (JDM) is a rare systemic immune-mediated disease with an incidence of 2-4/million/year.¹ JDM is a heterogeneous disease; patients can develop a spectrum of symptoms, ranging from the typical proximal skeletal muscle weakness and pathognomonic skin rash, to involvement of vital organs such as the lungs, heart, brain and intestines.² The clinical heterogeneity of JDM has been linked to myositis-specific autoantibodies, which may distinguish distinct clinical phenotypes and are prognostic for the disease course and need for second-line therapy.³ Despite this heterogeneity, current treatment guidelines are not yet adapted to subgroup-specific needs.⁴ Stratification of patients, e.g. into high-risk or low-risk groups, may facilitate the development of personalized monitoring and treatment strategies.

Next to inflammation of muscles and skin, vasculopathy is an important hallmark of JDM.^{5,6} It is characterized by loss of capillaries, morphologic changes to endothelium, endothelial activation and small vessel angiopathy.⁵⁻⁸ Complement, immune complexes and anti-endothelial antibodies are involved in its pathogenesis, but a disturbed balance between angiostatic and angiogenic factors also plays a role.⁹⁻¹² The degree of vasculopathy correlates with the expression of interferon-inducible angiostatic chemokines,¹² indicating that vascular injury may be related to the interferon signature.⁵ This interferon signature has been identified in serum and many cell types from patients with JDM, including endothelial cells.¹²⁻¹⁸

The degree of vasculopathy is clinically relevant: pathologic changes in nailfold capillaries are associated with clinical disease activity,¹⁹ and prominent vascular injury in muscle biopsies has been related to severe clinical presentation and outcomes.^{20,21} Recently, Gitiaux et al. identified a subgroup of JDM patients with severe disease, based on trajectories of clinical parameters during follow-up.²⁰ These patients were characterized by severe muscle weakness, frequent limb edema and gastrointestinal involvement, higher myopathological scores (e.g. capillary dropout) and low remission rates.²⁰ Most of these manifestation could be related to vasculopathy.²⁰

Here we used a minimally invasive biomarker-based approach to identify JDM patients with a severe disease course already at diagnosis, in a discovery and independent validation cohort. The biomarker panel included previously described and novel markers related to endothelial activation, endothelial dysfunction, and (interferon-driven) inflammation.^{5,18} Specifically, we investigated whether biomarker profiles were linked to vasculopathy, disease severity and myositis-specific antibodies and whether they predict response to induction therapy and time required to attain drug-free remission.

METHODS

Participants

59 patients meeting the Bohan and Peter criteria for definite or probable JDM ^{22,23} from Chicago, United States (discovery cohort, n=30), Utrecht, Netherlands and Singapore (validation cohort, n=25+4) were included before start of treatment, between March 2004 and June 2018. The childhood myositis scale (CMAS; 0-52; 0-49 for age 4-5 ²⁴ was recorded in both cohorts as a measure of muscle disease activity. Disease activity scores for muscle (DAS-M; 0-11), skin (DAS-S, 0-9) and global disease activity (DAS-T; 0-20) were recorded in the discovery cohort,²⁵ and the physician's global assessment (PGA; 0-10 ²⁶) and cutaneous assessment tool (CAT; 0-116 ²⁷) in the validation cohort. Intensification of treatment was defined as addition of new immunosuppressive medication or increased dose of previous medication. Time to drug-free remission (DFR) was defined as the time in months between the date of start of immunosuppressive treatment and date of withdrawal of all immunosuppressive drugs. End row loops (ERL) were assessed by nailfold capillaroscopy.²⁸ Myositis-specific antibodies (MSA) and anti-RNP antibodies were measured by immunoprecipitation in the discovery cohort and by line blot in the validation cohort. This study was approved by the institutional ethics committees of the involved centers: UMC Utrecht (METC#15-191), SingHealth centralized IRB (CIRB 2014/083/E), Lurie Children's hospital Chicago (IRB#2001-11715 and IRB#2008-13457) and conducted according to the Declaration of Helsinki. Age-appropriate written informed consent was obtained prior to inclusion in the study.

Patient material and biomarker analysis

Serum was spun down and stored at -80°C within four hours after collection. 39 markers related to endothelial activation, dysfunction and inflammation (supplementary table 1) were simultaneously measured in 50 µL of serum by multiplex technology, as described previously (xMAP; Luminex).²⁹

Statistical analysis

Statistical analyses were performed using GraphPad Prism 7.0, SPSS Statistics 21 (IBM) or R3.5.1 (CRAN). Values below detection limit were imputed as 0.5x lowest measured value. For Spearman rank correlations (r_s), imputed values were excluded. Cutoff values for ROC curves were based on the Youden's index. For comparisons between two groups, the

Mann-Whitney U test was used for continuous variables and the Fisher's exact test for categorical variables, with correction for multiple testing by false discovery rate (FDR) as indicated where applicable. $P < 0.05$ or $FDR < 0.05$ were considered statistically significant as indicated. For unsupervised clustering by principal component analysis (PCA) and heatmap analysis with hierarchical clustering (Euclidian/Ward), data were mean-centered and scaled per marker. Five markers with $>30\%$ of values below detection limit were excluded from clustering analyses (PAI-1, fibronectin, OSM, E-sel, TM). For time until drug-free remission, the Kaplan-Meier estimator (dichotomized by median) and cox-proportional-hazards-model with log-transformed data were used with log-rank test.

RESULTS

Patient characteristics

The median age in the discovery and validation cohort was 5.1 and 7.0 years (table 1). The majority of patients were female, with a higher frequency in the discovery cohort (86.7% vs. 62.1%, $p=0.039$), and Caucasian (76-77%). The duration of untreated disease was higher in the discovery cohort (5.9 vs. 3.2 months, $p=0.020$), and treatment intensification was needed in 57% of patients compared to 26% in the validation cohort ($p=0.018$). Muscle disease activity was similar in both cohorts (median CMAS 33). LDH was higher in the validation cohort ($p=0.010$). MSA were more frequently detected in the discovery cohort (17% MSA negative by immunoprecipitation compared to 55% MSA negative by line blot in the validation cohort). Anti-TIF1 γ antibodies were more frequent in the discovery cohort (57% vs 14%), while the frequencies of anti-MDA5 and anti-NXP2 antibodies were similar (7% and 10/17%).

Table 1. Baseline characteristics of patients from discovery and validation cohort.

	Discovery cohort	Validation cohort	
	Chicago, USA (n=30)	Netherlands + Singapore (n=25 + n=4)	P value
Age at sampling (years), <i>median (IQR)</i>	5.1 (4.8)	7 (8.3)	0.192
Sex, % female	86.7	62.1	0.039
Ethnicity (%Caucasian/Hispanic/Afro-American/Asian)	77/20/3/0	76/0/10/14	0.012
Duration of untreated disease (months), <i>median (IQR)</i>	5.9 (11.2)	3.2 (7.7)	0.020
Intensification of treatment in first 3 months, %	57	26	0.018
Disease activity at diagnosis			
CMAS (0-52; 0-49 for age 4-5), <i>median (IQR)</i>	33 (21)	33 (26)	0.334
	NR=1	NR=4	
PGA (0-10), <i>median (IQR)</i>	-	6 (4)	n/a
		NR=4	
DAS Total (0-20), <i>median (IQR)</i>	12 (4)	-	n/a
DAS Muscle (0-11), <i>median (IQR)</i>	6 (4)	-	n/a
DAS Skin (0-9), <i>median (IQR)</i>	5 (1)	-	n/a
CAT (0-116), <i>median (IQR)</i>	-	5 (8)	n/a
Muscle enzymes at diagnosis			
CK (IU/liter), <i>median (IQR)</i>	131 (592)	510 (4219)	0.053
LDH (IU/liter), <i>median (IQR)</i>	364 (190)	497 (479)	0.010
	NR=1	NR=4	
AST (IU/liter), <i>median (IQR)</i>	46 (45)	65 (266)	0.118
		NR=2	
ALT (IU/liter), <i>median (IQR)</i>	26 (26)	45 (89)	0.158
	NR=1		

(Continued)

Table 1. Baseline characteristics of patients from discovery and validation cohort.

	Discovery cohort		Validation cohort	
Myositis-specific antibodies (%)				
Negative	20	55.2	0.006	
MDA5	6.7	6.8	1.000	
Mi-2 indeterminate	6.7	-	n/a	
NXP2 total	10.0	17.1	0.472	
NXP2 positive	10.0	10.3		
NXP2 weakly positive	-	6.8		
SAE1	-	6.9	n/a	
TIF1γ total	56.6	13.7	0.001	
TIF1γ only	40	13.7		
TIF1γ + Mi-2 ind	3.3	-		
TIF1γ + Mi-2	13.3	-		

For continuous variables, medians and interquartile ranges (IQR) are shown. For categorical variables, frequencies are shown (%). P values for continuous variables were calculated by Mann-Whitney U test. P values for categorical variables were calculated by Fisher’s exact test (2 categories) or Chi squared test (>2 categories). Myositis-specific antibodies were measured by immunoprecipitation in the discovery cohort and by line blot in the validation cohort at Sanquin (Amsterdam, NL). NR = Not reported, DAS = disease activity scale, CMAS = Childhood myositis assessment scale, PGA = physician’s global assessment, CAT = cutaneous assessment tool, CK = creatine kinase activity, LDH = lactate dehydrogenase, AST = aspartate aminotransferase, ALT = alanine aminotransferase.

Biomarker profiles are related to muscle disease activity

To investigate the heterogeneity of biomarker profiles in treatment-naive JDM patients, we performed unsupervised hierarchical clustering in the discovery cohort, which split into two distinct clusters of 8 and 22 patients. The smaller cluster (#1) stood out due to significantly higher levels of CXCL13, CCL19, Gal-9, TNFR2, Gal-1, CXCL10, CXCL9, IL-18, YKL-40, CCL2, CCL4, VEGF, E-sel, ICAM-1 and CCL18 and lower levels of fetuin than the larger cluster (#2) (figure 1A-B, supplementary table 2). To assess whether distinct biomarker profiles corresponded to clinical profiles, we compared disease characteristics between the clusters (figure 1C and supplementary table 3). Total disease activity (DAS-T), was significantly higher in cluster 1 than 2 ($p=0.0265$), due to significantly higher muscle disease activity (DAS-M $p=0.0486$ and CMAS $p=0.0110$; figure 1C). Skin disease activity and creatine kinase activity (CK) were comparable, but cluster 1 had higher lactate dehydrogenase (LDH, $p=0.0285$). Multidimensional PCA identified muscle disease activity as an important factor explaining biomarker profile variance, and confirmed that patients with the highest DAS-M spatially overlapped with cluster 1 (figure 1D). ERL scores were similar between the clusters. 12 of the 16 differentially expressed biomarkers between the clusters correlated with DAS-T, DAS-M or CMAS: CXCL13, CCL19, Gal-9, TNFR2, Gal-1, CXCL10, CXCL9, IL-18, YKL-40, CCL2, CCL4 and ICAM-1 ($|r_s|=0.35-0.67$, $p<0.05$; table 2). High levels of these markers may therefore identify a subgroup of patients with more severe disease.

Figure 1. Heterogeneity in biomarker profiles corresponds with differences in clinical disease activity.

A panel of biomarkers for endothelial dysfunction and inflammation (supplementary table 1) was measured in serum of 30 treatment-naive JDM patients (discovery cohort) by multiplex assay. (A) Unsupervised hierarchical clustering of 30 patients in discovery cohort by values of 34 mean-centered and scaled markers by Euclidian distance and Wards' method yields two distinct patient clusters (#1/#2). Numbers represent unique patient identifiers (not ranked). (B) Levels of the six most significantly different markers between cluster 1 ($n=8$) and cluster 2 ($n=22$) based on Mann-Whitney U test with correction for multiple testing by FDR. Medians and FDR are indicated. (C) Clinical scores for global (DAS-T), skin (DAS-S) and muscle (DAS-M and CMAS) disease activity and muscle enzymes (CK and LDH) compared between the two clusters. P values of Mann-Whitney U test are shown. (D) Principal component analysis (PCA) based on 34 mean-centered markers shows patients stratified by cluster (left panel), DAS-S (middle panel) and DAS-M (right panel). Colors in middle and right panel represent categories of DAS-S and DAS-M. Closed circles represent individual patients, open circles represent cluster centers. *DAS = disease activity scale, DAS-T = DAS total, DAS-S = DAS skin, DAS-M = DAS muscle, CMAS = Childhood myositis assessment scale, PGA = physician's global assessment, CPK = creatine phosphokinase activity, LDH = lactate dehydrogenase, PC = principal component*

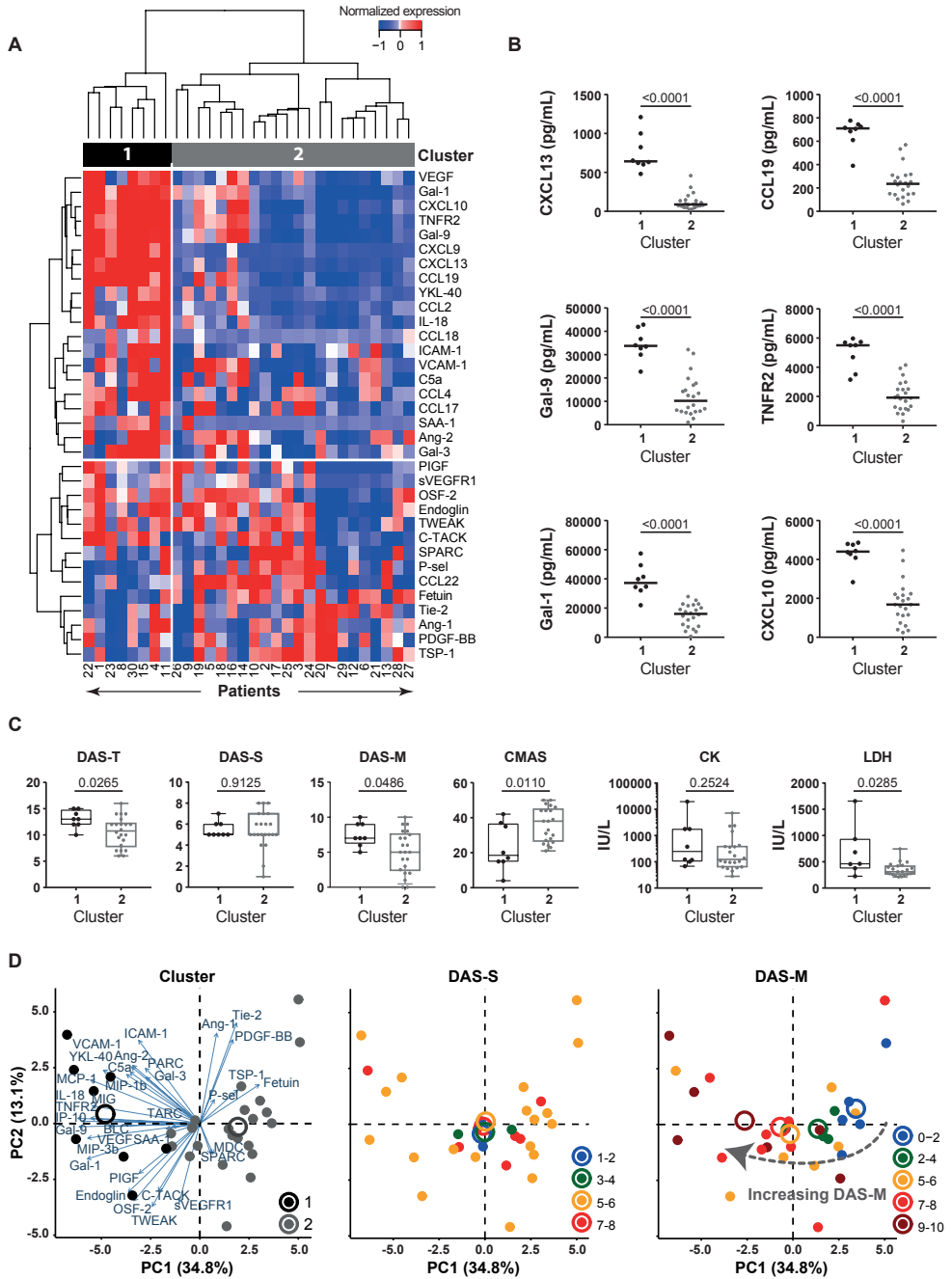


Figure 1. Heterogeneity in biomarker profiles corresponds with differences in clinical disease activity.

Table 2. Spearman rank correlations of biomarkers with clinical scores for disease activity.

	Discovery cohort			Validation cohort	
	DAS-T	DAS-M	CMAS	PGA	CMAS
	(n=30)	(n=30)	(n=29)	(n=25)	(n=25)
CXCL13	0.538**	0.539**	-0.476**	NS	NS
CCL19	0.541**	0.553**	-0.497**	NS	NS
Gal-9	0.519**	0.496**	-0.428*	0.403*	NS
TNFR2	0.518**	0.489**	-0.377*	0.439*	NS
Gal-1	0.471**	0.495**	NS	0.486*	NS
CXCL10	0.505**	0.458*	-0.397*	0.445*	NS
CXCL9	0.432*	NS	NS	NS	NS
IL-18	0.503**	0.415*	-0.490**	NS	NS
YKL-40	0.465**	0.524**	-0.667****	NS	NS
CCL2	0.557**	0.566**	-0.532**	NS	NS
CCL4	0.388*	NS	-0.396*	NS	NS
VEGF	NS	NS	NS	NS	NS
E-sel	NS	NS	NS	NS	NS
ICAM-1	NS	NS	-0.515**	NS	NS
Fetuin	NS	NS	NS	NS	NS
CCL18	NS	NS	NS	NS	NS

Biomarkers with significantly different levels between cluster 1 and 2 are shown. For biomarkers with out of range values (CXCL9 and E-sel), these imputed values were excluded from the analysis to prevent skewing of data. DAS = Disease activity scale, DAS-T = Total DAS, DAS-M = Muscle DAS, CMAS = Childhood myositis assessment score, PGA = Physician's global assessment. **** $P < 0.0001$, *** $P < 0.001$, ** $P < 0.01$, * $P < 0.05$, NS = not significant.

Association of biomarker profiles with vasculopathy

We next assessed which markers showed a direct correlation to ERL scores ($n=29$, discovery cohort). ERL scores correlated negatively with endoglin ($r_s = -0.67$, $p < 0.0001$), TSP-1 and VEGF, and positively with ICAM-1 ($|r_s| = 0.42-0.47$, $p < 0.05$; figure 2A). Patients with ERL < 4 , indicating severe vasculopathy, had significantly higher endoglin and lower ICAM-1 than patients with ERL > 4 ($p = 0.0120/p = 0.0079$; figure 2B). For endoglin, the area under the curve (AUC) in a receiver operating curve (ROC) identifying patients with low as opposed to high ERL was 0.771 ($p = 0.0129$). The optimal cutoff value at 2286 pg/mL yielded a sensitivity of 85.7% and specificity of 73.3% for patients with low ERL. For ICAM-1, the AUC was 0.786 ($p = 0.0088$) and the cutoff at 386425 pg/mL yielded a sensitivity of 85.7% and specificity of 80%. Combination of the two markers in a prediction model improved the AUC to 0.833 ($P = 0.0023$), but did not yield a higher sensitivity (79%) or specificity (80%) than ICAM-1 alone.

The presence of low levels of ICAM-1 may thus be suitable to identify patients with severe vasculopathy.

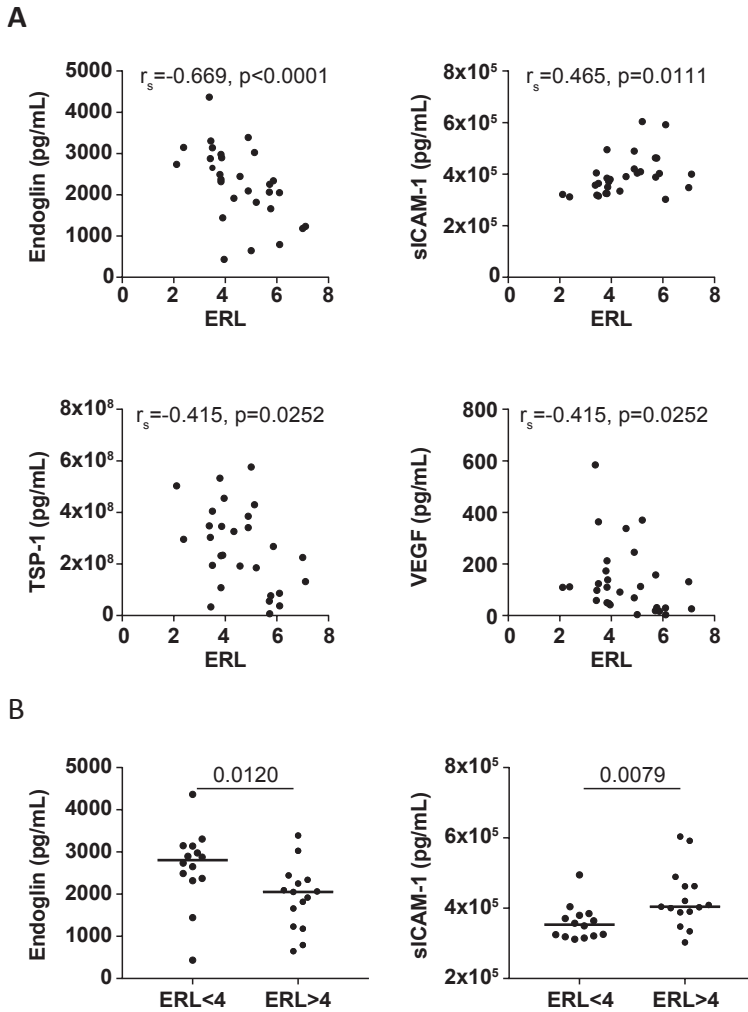


Figure 2. Correlation of biomarkers with end row loop scores.

A panel of biomarkers for endothelial dysfunction and inflammation (supplementary table 1) was measured in serum of 30 treatment-naïve JDM patients (discovery cohort) by multiplex assay. End row loop scores were assessed by nailfold capillaroscopy. (A) Spearman rank correlations (r_s) between serum biomarker levels measured by multiplex immunoassay and ERL scores assessed by nailfold capillaroscopy in 29 JDM patients of the discovery cohort. (B) Patients stratified into two groups by low (<4) and higher (>4) ERL score. P values for Mann-Whitney U test are indicated. *ERL* = end row loops.

Validation of biomarker and clinical profiles in independent cohort

To validate the association between biomarker profiles and clinical disease, the same biomarker panel was measured in an independent validation cohort (n=29). The 16 markers identifying patients with severe (muscle) disease activity in the discovery cohort, were again assessed for correlations with clinical disease activity. 4 markers correlated significantly with clinical disease activity in both cohorts: Gal-9, TNFR2, Gal-1 and CXCL10 ($r_s=0.40-0.52$ with DAS-T/PGA; table 2 and figure 3A-D). Reciprocal analysis of the two cohorts by the same criteria, i.e. 1) clustering of the validation cohort by all markers, 2) selection of markers identifying a more severely affected subgroup and 3) subsequent correlation with clinical disease parameters, yielded the same four markers. Next, we examined whether these markers would be able and sufficient to identify severely affected patients. Hierarchical clustering of the two cohorts with these 4 markers yielded 2 distinct patient clusters in each cohort (n=9/n=21 in discovery cohort and n=6/n=23 in validation cohort ; figure 3E-F and supplementary table 4). Indeed, in both cohorts the smaller subgroup of patients with high levels of all Gal-9, TNFR2, Gal-1 and CXCL10 (cluster 1 (D=discovery/V=validation)) had significantly higher total and muscle disease activity than cluster 2: cluster 1D had higher DAS-T ($p=0.0078$), higher DAS-M ($p=0.0181$) and lower CMAS ($p=0.0148$) than cluster 2D and cluster 1V had higher PGA ($p=0.0013$) and lower CMAS ($p=0.0053$) than cluster 2V (figure 3G-H and supplementary table 4). Skin disease activity did not differ in the discovery cohort, but was significantly higher in cluster 1V than cluster 2V (CAT, $p=0.0131$). In both cohorts, LDH was higher in cluster 1 than 2. Thus, the combination of high Gal-9, TNFR2, Gal-1 and CXCL10 may be sufficient to identify a subgroup of patients with severe global and muscle disease. To assess the potency of each individual marker for identifying severely affected patients, patients were stratified into severe (>75th percentile of PGA/DAS-T/DAS-M or <25th percentile of CMAS) and non-severe (muscle or global) disease, and the AUC in ROC curves were determined for each marker. TNFR2 had the highest AUC for severe muscle (AUC=0.80) and global (AUC=0.73) disease, with a sensitivity of 80% and 69% and specificity of 82% and 76% at a cutoff of 3010 pg/mL (supplementary table 5). Due to the high correlations between the markers ($r_s=0.76-0.95$) a combined model was not constructed. In conclusion, Gal-9, TNFR2, Gal-1 and CXCL10 can identify severely affected patients at diagnosis, with TNFR2 being the best indicator.

Figure 3. Gal-9, CXCL10, TNFR2 and Gal-1 as biomarkers for stratification of patients with severe JDM.

A panel of biomarkers for endothelial dysfunction and inflammation (supplementary table 1) was measured in serum of 59 treatment-naïve JDM patients by multiplex assay. (A-D) Spearman rank correlations (r_s) of Gal-9 (A), TNFR2 (B), CXCL10 (C) and Gal-1 (D) with global disease activity: DAS-T in discovery cohort (left panels) and PGA in validation cohort (right panels). **** $P<0.0001$, *** $P<0.001$, ** $P<0.01$, * $P<0.05$. (E-F) Unsupervised hierarchical clustering of discovery cohort (E) and validation cohort (F) by expression of Gal-9, TNFR2, CXCL10 and Gal-1. Numbers represent unique patient identifiers (not ranked). (G-H) Clinical measures of disease activity in cluster 1 and 2 from figures E and F in discovery cohort (G) and validation cohort (H). P values of Mann-Whitney U test are indicated. DAS = disease activity scale, DAS-T = DAS total, DAS-S = DAS skin, DAS-M = DAS muscle, CMAS = Childhood myositis assessment scale, PGA = physician's global assessment, CPK = creatine phosphokinase activity, LDH = lactate dehydrogenase. Clusters: 1/2 "D" = Discovery cohort, 1/2 "V" = Validation cohort.

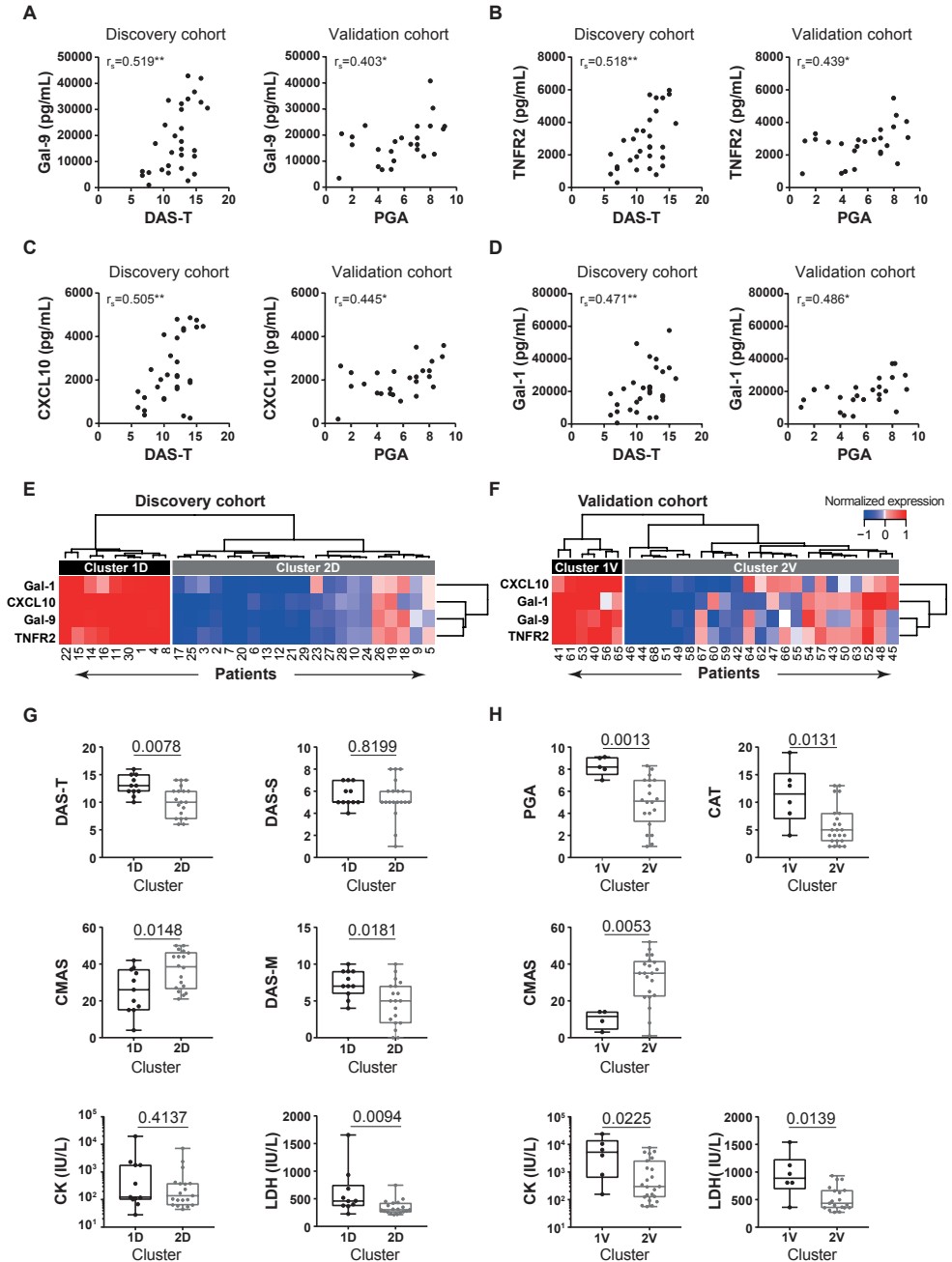


Figure 3. Gal-9, CXCL10, TNFR2 and Gal-1 as biomarkers for stratification of patients with severe JDM.

Association of biomarker profiles with myositis-specific autoantibodies

As MSA serotypes were previously linked to disease phenotypes, including (muscle) disease severity,^{2,3} we compared MSA frequencies between the biomarker-based clusters. The cohorts were combined into one to yield sufficient patients per MSA category. Clustering by Gal-9, CXCL10, TNFR2 and Gal-1 expression produced two clusters (1C and 2C, C="combined cohorts", figure 4A). Patients with anti-NXP2 antibodies were significantly more frequent in cluster 1C than cluster 2C ($p=0.0236$, figure 4A-B). Moreover, 2 of the 3 anti-NXP2 positive patients in cluster 2C were weakly positive, possibly indicating these could have been false positive measurements. If so, this would further increase the difference between anti-NXP2 frequencies in cluster 1C and 2C. The frequencies of MSA negative anti-TIF1 γ positive patients were comparable. Patient numbers for anti-SAE1 and anti-MDA5 were too small to statistically compare the clusters, but it was notable that all 4 patients with anti-MDA5 autoantibodies were in cluster 2C. In conclusion, MSA serotypes were not directly linked to the biomarker-based patient clusters, but anti-NXP2 positive patients were more likely to be in the severe cluster with high biomarker levels.

Figure 4. Gal-9, CXCL10, TNFR2 and Gal-1 as biomarkers for patient stratification and prognosis of response to therapy.

A panel of biomarkers for endothelial dysfunction and inflammation (supplementary table 1) was measured in serum of 59 treatment-naïve JDM patients by multiplex assay. (A) Unsupervised hierarchical clustering of 59 patients in discovery and validation cohort combined, by expression of Gal-9, CXCL10, TNFR2 and Gal-1. Color bar represents different MSA serotypes, as indicated in the heatmap legend. Numbers represent unique patient identifiers (not ranked). (B) Cumulative frequencies of MSA serotypes in cluster 1C and 2C (C="combined cohorts"). P values of Chi squared test with MSA negative, anti-TIF1 γ , and anti-NXP2 positive patients are indicated. *ns* = not significant. (C) Cumulative frequencies of patients needing intensification of treatment within the first 3 months in cluster 1C and 2C. P values of Fisher's exact test is indicated. (D) Differentiating capacity of gal-9, CXCL10, TNFR2 and Gal-1 for patients requiring intensification of treatment in the combined cohort, discovery cohort and validation cohort. P values of Mann Whitney U test are indicated. (E) Cumulative frequencies of patients with 1) time to DFR>4 years, 2) time to DFR<4 years, 3) less than <4 years of follow-up time still on medication and 4) unknown medication use and time to DFR in clusters 1C and 2C. (F) Kaplan Meier curves of months from diagnosis (Dx) until remission off immunosuppressive treatment. Patients were stratified by median values of Gal-9, CXCL10, TNFR2 and Gal-1 (into high/low, n=29/30). P values of log-rank test are indicated. MSA = myositis-specific antibodies, Disc = Discovery cohort, Val = Validation cohort, DFR = drug-free remission, FU = follow-up.

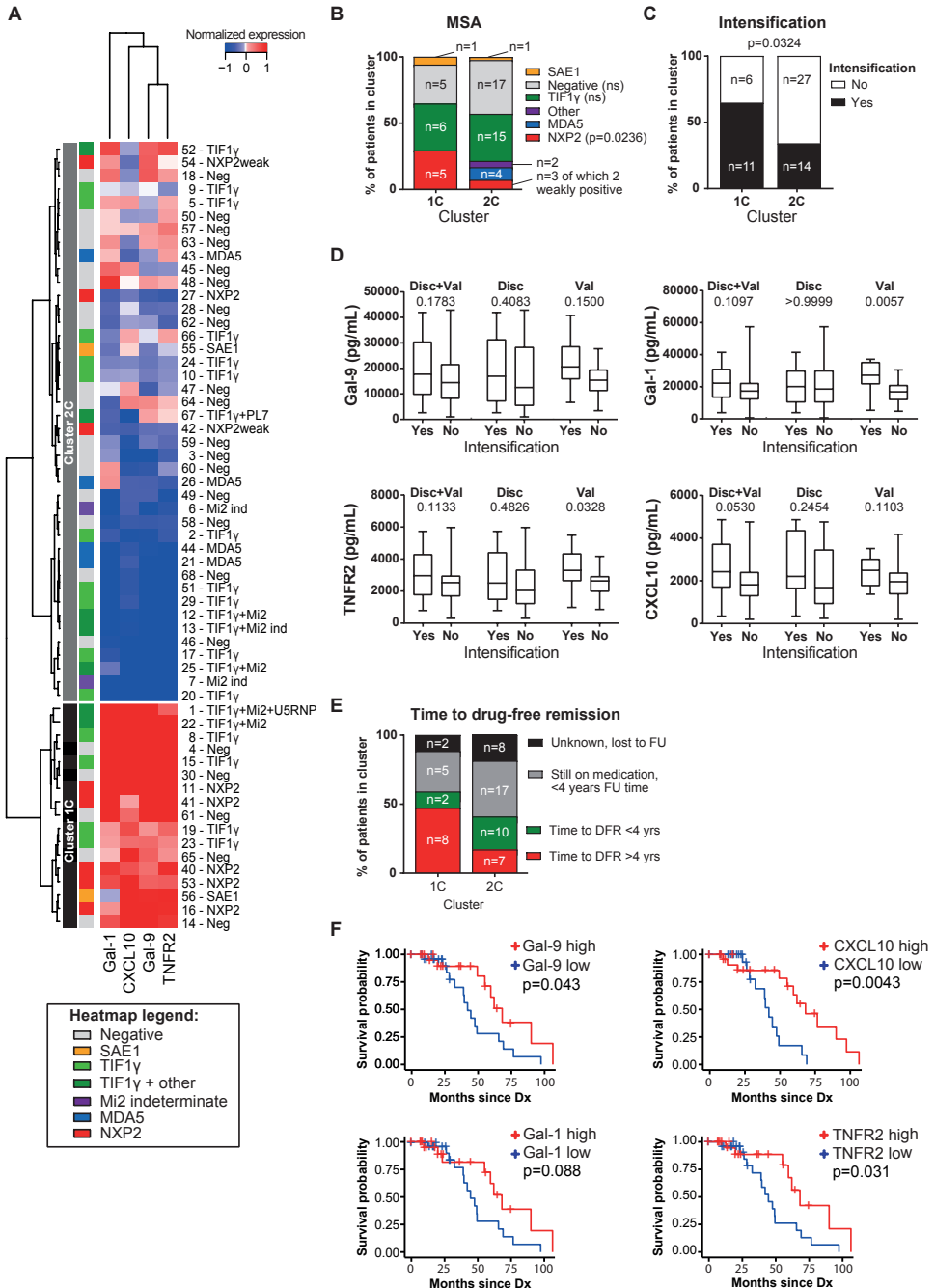


Figure 4. Gal-9, CXCL10, TNFR2 and Gal-1 as biomarkers for patient stratification and prognosis of response to therapy.

Prognostic value of biomarkers for suboptimal response to initial treatment

Next, we assessed whether high levels of Gal-9, CXCL10, TNFR2 and/or Gal-1 could be prognostic for a suboptimal response to initial treatment. The frequency at which intensification of treatment was required within the first 3 months was significantly higher in cluster 1C than 2C, suggesting that indeed high biomarker levels may identify a risk group (64.7% vs. 34.1% of patients, $p=0.0324$; figure 4C). Although the combination of biomarkers could identify these 'at risk' patients, the single biomarkers only showed a trend towards being higher in patients needing intensification in the combined cohort (CXCL10: $p=0.0530$, Gal-1: $p=0.1097$, Gal-9: $p=0.1783$, TNFR2: $p=0.1133$; figure 4D). In the validation cohort, Gal-1 and TNFR2 potentially identified patients needing intensification (Gal-1 $p=0.0057$, TNFR2 $p=0.0328$; figure 4D). Thus, the combination of the 4 markers Gal-9, CXCL10, TNFR2 and Gal-1 can identify patients at risk for a suboptimal response to induction therapy, with Gal-1 and TNFR2 possibly being the most potent.

Prognostic value of biomarkers for time to drug-free remission

Finally, we examined whether patients with high Gal-9, CXCL10, TNFR2 and/or Gal-1 at diagnosis would need a longer time to attain drug-free remission (DFR). 24 out of 59 patients had attained DFR at the time of analysis (median follow-up time of 4.0 years). Of the 10 patients in cluster 1C with a known time until DFR or more than 4 years of follow-up, 8 (80%) were still on medication after 4 years, whereas this was the case for only 7 out of 17 (41%) in cluster 2C ($p<0.05$; figure 4E). Kaplan-Meier survival analysis with dichotomization of the single biomarkers into "high" and "low" by median values showed that patients with high CXCL10, Gal-9, or TNFR2 at diagnosis needed significantly longer to attain DFR than patients with low biomarker levels ($p<0.05$; figure 4F), although the Kaplan-Meier curves showed cross-overs indicating that confounding factors may play a role. In cox-proportional-hazards-model, high biomarker levels showed a trend towards conferring a higher risk of 'not getting off treatment' compared to low levels (Gal-9: Hazard ratio (HR)=0.32, $p=0.06$; TNFR2: HR=0.24, $p=0.08$; CXCL10: HR=0.39, $p=0.1$; Gal-1: HR=0.41, $p=0.1$). Patients with ERL scores <4 , indicating severe vasculopathy, also showed a trend towards needing longer to attain DFR (Kaplan-Meier log-rank $p=0.069$). Taken together, patients with high Gal-9, CXCL10 or TNFR2 at diagnosis may be at risk for a longer disease course.

DISCUSSION

Here, we have shown that patients with juvenile dermatomyositis are heterogeneous not only in their clinical presentation, but also in their biomarker profiles at diagnosis. In two independent cohorts we have identified a subgroup of patients, constituting approximately one third of patients, characterized by high levels of Gal-9, CXCL10, TNFR2 and Gal-1, higher muscle and global disease activity, at risk of requiring intensification of initial treatment and a longer time to reach drug-free remission. These biomarkers can thus identify a severely affected subgroup at diagnosis, and may be prognostic for the disease course. Patients with anti-NXP2 antibodies were more likely to be in this severe subgroup.

Our results are in line with the findings by Gitiaux et al., identifying approximately one third of patients as severely affected.²⁰ To our surprise, in our study the severe subgroup did not have more severe vasculopathy by ERL scores, and vasculopathy-associated biomarkers endoglin, ICAM-1, TSP-1 and VEGF did not aid in the identification of this subgroup. However, the correlation of VEGF and endoglin with vasculopathy is consistent with a recent publication showing that both proteins are upregulated in lesions with active capillary injury in JDM muscle.⁷ Endoglin and VEGF were also previously found to be expressed in dermatomyositis muscle.^{30,31} Soluble endoglin has more widely been described as an anti-angiogenic molecule and marker for vasculopathy.³² TSP-1 was previously suggested to be an anti-angiogenic regulator³³ with a vasculopathic role in patients with JDM (in particular patients with the TNF-308A allele).³⁴ We found a positive association between ICAM-1 levels and ERL scores. Since endothelial activation is one of the hallmarks of JDM-associated vasculopathy,³⁵ and soluble ICAM-1 levels correlate with endothelial surface ICAM-1 expression,³⁶ we could only speculate that lower soluble ICAM-1 may be found in patients with severe vasculopathy due to systemic loss of endothelial cells, leading to a lower total production of soluble ICAM-1.

Two of the 4 identified severity markers, Gal-9 and CXCL10, are known IFN-related proteins.^{37,38} The correlation between severe muscle disease activity and high levels of IFN-related markers or interferon signature (in blood and biopsies) has been previously demonstrated at disease onset^{14,39,40} and during follow-up¹⁷ in patients with JDM. A higher interferon signature was also associated with a longer time to reach clinically inactive disease.⁴⁰ Gal-9, CXCL10 and TNFR2 specifically correlate with muscle disease activity during follow-up in JDM, and Gal-9 and CXCL10 have recently been validated as biomarkers for disease activity in JDM.^{18,41} Moreover, patients experiencing a disease flare within the first year after start of treatment, had higher levels of Gal-9 and CXCL10 at diagnosis.⁴¹ TNFR2 levels were found to be high in adult DM patients with a high type I interferon score, and neutralization of the interferon signature by an anti-interferon- α monoclonal antibody resulted in decreased levels of TNFR2, suggesting that TNFR2 may also be related to interferon-driven inflammation.⁴² The increased expression of circulating interferon-inducible proteins in severely affected

patients further supports the pathogenic role for interferons in JDM immunopathology. Gal-1 has not been previously linked to dermatomyositis, but degeneration of injured muscles induces high expression of Gal-1 and its expression may increase muscle regeneration in experimental models.^{43,44} In addition, Gal-1 is an antiviral effector molecule expressed by endothelial cells and a negative regulator of both T cell recruitment to the endothelium and transendothelial migration.⁴⁵⁻⁴⁷ In line with our results, the anti-NXP2 antibody serotype was previously associated with more severe muscle disease, whereas anti-MDA5 positive patients were less likely to be weak.³ In contrast with previous publications, we did not observe high levels of interferon-related markers in patients with anti-MDA5 antibodies.⁴⁸ JDM is a very rare disease, which hampers the collection of large samples numbers for study purposes. A unique strength of our study is that we were able to perform biomarker profiling in two large, independent cohorts of treatment-naïve patients. We could thereby analyze the unmodified disease signatures in different patients without possible treatment-effects on biomarker profiles. Although the cohorts showed some differences in baseline characteristics (e.g. duration of untreated disease, MSA, requirement of intensification, ethnicity), we were able to validate our findings, showing that Gal-9, TNFR2, Gal-1 and CXCL10 are robust markers for the identification of a severe subgroup of patients. Further validation in a large prospective cohort will allow for the construction of prediction models for the need for intensification of treatment and time to drug-free remission. We speculate that patients in the 'at risk' group could benefit from more intensive monitoring during induction-treatment in order to detect suboptimal response to therapy in an early phase. This early detection would promote a swift intensification of treatment. Future studies will have to point out whether more aggressive or targeted initial treatment (e.g. JAK-inhibition or anti-interferon antibodies) could also be an option in these patients.^{49,50} Considering the longer time to remission, it may be useful to discuss expectations of treatment length and the possible effect on cumulative medication dose with patients and parents, as these may have implications for the long-term outcomes. In conclusion, this study underlines the clinical and serological heterogeneity of JDM and provides easy-to-measure serum biomarkers Gal-9, TNFR2, CXCL10 and Gal-1 that may be used to identify severely affected patients with a suboptimal response to standard immunosuppressive treatment.

REFERENCES

1. Meyer A, Meyer N, Schaeffer M, et al. Incidence and Prevalence of Inflammatory Myopathies: A Systematic Review. *Rheumatology (Oxford)*. **2015**, *54* (1), 50–63.
2. Shah M, Mamyrova G, Targoff IN, et al. The Clinical Phenotypes of the Juvenile Idiopathic Inflammatory Myopathies. *Medicine (Baltimore)*. **2013**, *92* (1), 25–41.
3. Tansley SL, Simou S, Shaddick G, et al. Autoantibodies in Juvenile-Onset Myositis: Their Diagnostic Value and Associated Clinical Phenotype in a Large UK Cohort. *J. Autoimmun.* **2017**, *84*, 55–64.
4. Enders FB, Bader-Meunier B, Baildam E, et al. Consensus-Based Recommendations for the Management of Juvenile Dermatomyositis. *Ann. Rheum. Dis.* **2017**, *76* (2), 329–340.
5. Wienke J, Deakin CT, Wedderburn LR, et al. Systemic and Tissue Inflammation in Juvenile Dermatomyositis: From Pathogenesis to the Quest for Monitoring Tools. *Front. Immunol.* **2018**, *9*, 2951.
6. Papadopoulou C, McCann LJ. The Vasculopathy of Juvenile Dermatomyositis. *Front. Pediatr.* **2018**, *6*, 284.
7. Baumann M, Gumpold C, Mueller-Felber W, et al. Pattern of Myogenesis and Vascular Repair in Early and Advanced Lesions of Juvenile Dermatomyositis. *Neuromuscul. Disord.* **2018**, *28* (12), 973–958.
8. Kim E, Cook-Mills J, Morgan G, et al. Increased Expression of Vascular Cell Adhesion Molecule 1 in Muscle Biopsy Samples from Juvenile Dermatomyositis Patients with Short Duration of Untreated Disease Is Regulated by miR-126. *Arthritis Rheum.* **2012**, *64* (11), 3809–3817.
9. Goncalves FGP, Chimelli L, Sallum AME, et al. Immunohistological Analysis of CD59 and Membrane Attack Complex of Complement in Muscle in Juvenile Dermatomyositis. *J. Rheumatol.* **2002**, *29* (6), 1301–1307.
10. Kissel JT, Mendell JR, Rammohan KW. Microvascular Deposition of Complement Membrane Attack Complex in Dermatomyositis. *N. Engl. J. Med.* **1986**, *314* (6), 329–334.
11. Karasawa R, Tamaki M, Sato T, et al. Multiple Target Autoantigens on Endothelial Cells Identified in Juvenile Dermatomyositis Using Proteomics. *Rheumatology (Oxford)*. **2018**, *57* (4), 671–676.
12. Fall N, Bove KE, Stringer K, et al. Association between Lack of Angiogenic Response in Muscle Tissue and High Expression of Angiostatic ELR-Negative CXC Chemokines in Patients with Juvenile Dermatomyositis: Possible Link to Vasculopathy. *Arthritis Rheum.* **2005**, *52* (10), 3175–3180.
13. Gitiaux C, Latroche C, Weiss-Gayet M, et al. Myogenic Progenitor Cells Exhibit Type I Interferon-Driven Proangiogenic Properties and Molecular Signature During Juvenile Dermatomyositis. *Arthritis Rheumatol. (Hoboken, N.J.)* **2018**, *70* (1), 134–145.
14. O'Connor KA, Abbott KA, Sabin B, et al. MxA Gene Expression in Juvenile Dermatomyositis Peripheral Blood Mononuclear Cells: Association with Muscle Involvement. *Clin. Immunol.* **2006**, *120* (3), 319–325.
15. Rice GI, Melki I, Fremont M-L, et al. Assessment of Type I Interferon Signaling in Pediatric Inflammatory Disease. *J. Clin. Immunol.* **2017**, *37* (2), 123–132.
16. Rodero MP, Decalf J, Bondet V, et al. Detection of Interferon Alpha Protein Reveals Differential Levels and Cellular Sources in Disease. *J. Exp. Med.* **2017**, *214* (5), 1547–1555.

17. Reed AM, Peterson E, Bilgic H, et al. Changes in Novel Biomarkers of Disease Activity in Juvenile and Adult Dermatomyositis Are Sensitive Biomarkers of Disease Course. *Arthritis Rheum.* **2012**, 64 (12), 4078–4086.
18. Bellutti Enders F, van Wijk F, Scholman R, et al. Correlation of CXCL10, Tumor Necrosis Factor Receptor Type II, and Galectin 9 with Disease Activity in Juvenile Dermatomyositis. *Arthritis Rheumatol. (Hoboken, N.J.)* **2014**, 66 (8), 2281–2289.
19. Schmeling H, Stephens S, Goia C, et al. Nailfold Capillary Density Is Importantly Associated over Time with Muscle and Skin Disease Activity in Juvenile Dermatomyositis. *Rheumatology (Oxford)*. **2011**, 50 (5), 885–893.
20. Gitiaux C, De Antonio M, Aouizerate J, et al. Vasculopathy-Related Clinical and Pathological Features Are Associated with Severe Juvenile Dermatomyositis. *Rheumatology (Oxford)*. **2016**, 55 (3), 470–479.
21. Wargula JC, Lovell DJ, Passo MH, et al. What More Can We Learn from Muscle Histopathology in Children with Dermatomyositis/polymyositis? *Clin. Exp. Rheumatol.* **2006**, 24 (3), 333–343.
22. Bohan A, Peter JB. Polymyositis and Dermatomyositis (First of Two Parts). *N. Engl. J. Med.* **1975**, 292 (7), 344–347.
23. Bohan A, Peter JB. Polymyositis and Dermatomyositis (Second of Two Parts). *N. Engl. J. Med.* **1975**, 292 (8), 403–407.
24. Quinones R, Morgan GA, Amoruso M, et al. Lack of Achievement of a Full Score on the Childhood Myositis Assessment Scale by Healthy Four-Year-Olds and Those Recovering from Juvenile Dermatomyositis. *Arthritis Care Res. (Hoboken)*. **2013**, 65 (10), 1697–1701.
25. Bode RK, Klein-Gitelman MS, Miller ML, et al. Disease Activity Score for Children with Juvenile Dermatomyositis: Reliability and Validity Evidence. *Arthritis Rheum.* **2003**, 49 (1), 7–15.
26. Rider LG, Feldman BM, Perez MD, et al. Development of Validated Disease Activity and Damage Indices for the Juvenile Idiopathic Inflammatory Myopathies: I. Physician, Parent, and Patient Global Assessments. Juvenile Dermatomyositis Disease Activity Collaborative Study Group. *Arthritis Rheum.* **1997**, 40 (11), 1976–1983.
27. Huber AM, Dugan EM, Lachenbruch PA, et al. Preliminary Validation and Clinical Meaning of the Cutaneous Assessment Tool in Juvenile Dermatomyositis. *Arthritis Rheum.* **2008**, 59 (2), 214–221.
28. Christen-Zaech S, Seshadri R, Sundberg J, et al. Persistent Association of Nailfold Capillaroscopy Changes and Skin Involvement over Thirty-Six Months with Duration of Untreated Disease in Patients with Juvenile Dermatomyositis. *Arthritis Rheum.* **2008**, 58 (2), 571–576.
29. de Jager W, Prakken BJ, Bijlsma JWJ, et al. Improved Multiplex Immunoassay Performance in Human Plasma and Synovial Fluid Following Removal of Interfering Heterophilic Antibodies. *J. Immunol. Methods* **2005**, 300 (1–2), 124–135.
30. Grundtman C, Tham E, Ulfgren A-K, et al. Vascular Endothelial Growth Factor Is Highly Expressed in Muscle Tissue of Patients with Polymyositis and Patients with Dermatomyositis. *Arthritis Rheum.* **2008**, 58 (10), 3224–3238.
31. Konttinen YT, Mackiewicz Z, Povilenaite D, et al. Disease-Associated Increased HIF-1, alphavbeta3 Integrin, and Flt-1 Do Not Suffice to Compensate the Damage-Inducing Loss of Blood Vessels in Inflammatory Myopathies. *Rheumatol. Int.* **2004**, 24 (6), 333–339.

32. Venkatesha S, Toporsian M, Lam C, et al. Soluble Endoglin Contributes to the Pathogenesis of Preeclampsia. *Nat. Med.* **2006**, *12* (6), 642–649.
33. Jimenez B, Volpert O V, Crawford SE, et al. Signals Leading to Apoptosis-Dependent Inhibition of Neovascularization by Thrombospondin-1. *Nat. Med.* **2000**, *6* (1), 41–48.
34. Lutz J, Huwiler KG, Fedczyna T, et al. Increased Plasma Thrombospondin-1 (TSP-1) Levels Are Associated with the TNF Alpha-308A Allele in Children with Juvenile Dermatomyositis. *Clin. Immunol.* **2002**, *103* (3 Pt 1), 260–263.
35. Nagaraju K, Rider LG, Fan C, et al. Endothelial Cell Activation and Neovascularization Are Prominent in Dermatomyositis. *J. Autoimmune Dis.* **2006**, *3*, 2.
36. Kjaergaard AG, Dige A, Krog J, et al. Soluble Adhesion Molecules Correlate with Surface Expression in an in Vitro Model of Endothelial Activation. *Basic Clin. Pharmacol. Toxicol.* **2013**, *113* (4), 273–279.
37. Van den Hoogen LL, Van Roon JAG, Mertens JS, et al. Galectin-9 Is an Easy to Measure Biomarker for the Interferon Signature in Systemic Lupus Erythematosus and Antiphospholipid Syndrome. *Ann. Rheum. Dis.* **2018**, *77* (12), 1810–1814.
38. Antonelli A, Ferrari SM, Giuggioli D, et al. Chemokine (C-X-C Motif) Ligand (CXCL10) in Autoimmune Diseases. *Autoimmun. Rev.* **2014**, *13* (3), 272–280.
39. Soponkanaporn S, Deakin CT, Schutz PW, et al. Expression of Myxovirus-Resistance Protein A: A Possible Marker of Muscle Disease Activity and Autoantibody Specificities in Juvenile Dermatomyositis. *Neuropathol. Appl. Neurobiol.* **2018**.
40. Moneta GM, Pires Marafon D, Marasco E, et al. Muscle Expression of Type I and Type II Interferons Is Increased in Juvenile Dermatomyositis and Related to Clinical and Histological Features. *Arthritis Rheumatol. (Hoboken, N.J.)* **2018**.
41. Wienke J, Bellutti Enders F, Lim J, et al. Galectin-9 and CXCL10 as Biomarkers for Disease Activity in Juvenile Dermatomyositis: A Longitudinal Cohort Study and Multi-Cohort Validation. *Arthritis Rheumatol. (Hoboken, N.J.)* **2019**.
42. Guo X, Higgs BW, Rebelatto M, et al. Suppression of Soluble T Cell-Associated Proteins by an Anti-Interferon-Alpha Monoclonal Antibody in Adult Patients with Dermatomyositis or Polymyositis. *Rheumatology (Oxford)*. **2014**, *53* (4), 686–695.
43. Cerri DG, Rodrigues LC, Stowell SR, et al. Degeneration of Dystrophic or Injured Skeletal Muscles Induces High Expression of Galectin-1. *Glycobiology* **2008**, *18* (11), 842–850.
44. Chan J, O'Donoghue K, Gavina M, et al. Galectin-1 Induces Skeletal Muscle Differentiation in Human Fetal Mesenchymal Stem Cells and Increases Muscle Regeneration. *Stem Cells* **2006**, *24* (8), 1879–1891.
45. Garner OB, Yun T, Pernet O, et al. Timing of Galectin-1 Exposure Differentially Modulates Nipah Virus Entry and Syncytium Formation in Endothelial Cells. *J. Virol.* **2015**, *89* (5), 2520–2529.
46. Norling L V, Sampaio ALF, Cooper D, et al. Inhibitory Control of Endothelial Galectin-1 on in Vitro and in Vivo Lymphocyte Trafficking. *FASEB J. Off. Publ. Fed. Am. Soc. Exp. Biol.* **2008**, *22* (3), 682–690.
47. He J, Baum LG. Endothelial Cell Expression of Galectin-1 Induced by Prostate Cancer Cells Inhibits T-Cell Transendothelial Migration. *Lab. Invest.* **2006**, *86* (6), 578–590.

48. Ono N, Kai K, Maruyama A, et al. The Relationship between Type 1 IFN and Vasculopathy in Anti-MDA5 Antibody-Positive Dermatomyositis Patients. *Rheumatology (Oxford)*. **2018**.
49. Ladislau L, Suarez-Calvet X, Toquet S, et al. JAK Inhibitor Improves Type I Interferon Induced Damage: Proof of Concept in Dermatomyositis. *Brain* **2018**, *141* (6), 1609–1621.
50. Higgs BW, Zhu W, Morehouse C, et al. A Phase 1b Clinical Trial Evaluating Sifalimumab, an Anti-IFN-Alpha Monoclonal Antibody, Shows Target Neutralisation of a Type I IFN Signature in Blood of Dermatomyositis and Polymyositis Patients. *Ann. Rheum. Dis.* **2014**, *73* (1), 256–262.

SUPPLEMENTARY MATERIAL

Supplementary table 1. List of measured biomarkers and abbreviations.

Abbreviation/name	Biomarker
Ang-1	Angiopoietin-1
Ang-2	Angiopoietin-2
Tie-2	Angiopoietin-1 receptor
C5a	Complement 5a
CCL2	Monocyte chemoattractant protein-1
CCL4	Macrophage inflammatory protein 1 β , MIP-1 β
CCL17	Thymus- and activation-regulated chemokine, TARC
CCL18	Pulmonary and activation-regulated chemokine, PARC
CCL19	Macrophage inflammatory protein 3 β , MIP-3 β
CCL22	Macrophage-derived chemokine, MDC
CCL27	Cutaneous T-cell attracting chemokine, C-TACK
CXCL9	Monokine induced by gamma interferon, MIG
CXCL10	Interferon gamma-induced protein, IP-10
CXCL13	B-Lymphocyte chemoattractant, BLC
Endoglin	Endoglin
E-sel	E-selectin
Fetuin	Fetuin
Fibronectin	Fibronectin
Gal-1	Galectin-1
Gal-3	Galectin-3
Gal-9	Galectin-9
IL-18	Interleukin 18
OSM	Oncostatin M
OSF-2	Periostin
PIGF	Placental growth factor
PAI-1	Plasminogen activator inhibitor
PDGF-BB	Platelet-derived growth factor BB

(Continued)

Supplementary table 1. List of measured biomarkers and abbreviations.

Abbreviation/name	Biomarker
P-sel	P-selectin
SAA-1	Serum amyloid A1
ICAM-1	Intercellular adhesion molecule 1
sVEGFR1	Soluble VEGF receptor 1
SPARC	Secreted protein acidic and rich in cysteine
VCAM-1	Vascular cell adhesion protein 1
TM	Thrombomodulin
TSP-1	Thrombospondin-1
TNFR2	Tumor necrosis factor receptor 2
TWEAK	Tumor necrosis factor-related weak inducer of apoptosis
VEGF	Vascular endothelial growth factor
YKL-40	Chitinase-3-like protein 1

Biomarkers measured by multiplex assay in treatment-naive patient serum.

Supplementary table 2. Biomarker levels in the two clusters identified by biomarker-based unsupervised hierarchical clustering of patients in the discovery cohort.

Marker	Cluster 1 (n=8)	Cluster 2 (n=22)	P value	FDR
CXCL13	642.3 (348.9)	88.2 (74.9)	<0.0001	<0.0001
CCL19	710.7 (110.1)	235.3 (163.9)	<0.0001	<0.0001
Gal-9	33756.5 (9924.1)	10235.1 (11469.7)	<0.0001	<0.0001
TNFR2	5506.4 (1914.7)	1917.9 (1448.3)	<0.0001	<0.0001
Gal-1	37251.4 (14729.8)	16039.7 (14347.9)	<0.0001	<0.0001
CXCL10	4404.6 (650.1)	1680.2 (1197.2)	<0.0001	<0.0001
CXCL9	1198.1 (651.1)	38.3 (71.5)	<0.0001	0.0002
IL-18	756.7 (625.9)	207 (227.3)	<0.0001	0.0002
YKL-40	155315 (392327.4)	42406 (38300.1)	0.0002	0.0009
CCL2	2987.6 (2442.6)	500.9 (532.1)	0.0011	0.0043
CCL4	277.4 (147.1)	172 (98.4)	0.0025	0.0089
VEGF	291.6 (234)	79.9 (95)	0.0052	0.0168
E-sel	<i>25% out of range</i>	<i>81.8% out of range</i>	0.0057	0.0170
ICAM-1	475982.7 (190565.7)	367525.4 (80448.1)	0.0072	0.0201
Fetuin	206615000 (52602500)	267685000 (62940000)	0.0080	0.0209
CCL18	133588 (263212.8)	62923.7 (41849.8)	0.0134	0.0328
C5a	116892.1 (108459)	80599.8 (80283.4)	0.0446	0.1024
Gal-3	38365.1 (30138.1)	21183.4 (10616.2)	0.0516	0.1118
SAA-1	1966200 (2699225)	169318.6 (265189.3)	0.0564	0.1157
VCAM-1	5869650 (3292400)	4415050 (1871150)	0.0710	0.1384
sVEGFR1	1715.1 (1061.5)	808.4 (1617.8)	0.0775	0.1439
P-sel	253756.5 (140506.5)	392762.2 (281097.2)	0.0871	0.1541
PIGF	15.7 (15.8)	8.2 (27.3)	0.0915	0.1541
Fibronectin	<i>87.5% out of range</i>	<i>59.1% out of range</i>	0.1051	0.1541
CCL27	1886 (1031.5)	1303.5 (703.5)	0.1067	0.1541
Endoglin	2711 (1166.1)	2285.8 (1490.8)	0.1067	0.1541
CCL17	334.6 (229.1)	204.8 (160.8)	0.1067	0.1541
Ang-2	4774.3 (3604.7)	2916.7 (2144)	0.1176	0.1638

(Continued)

Supplementary table 2. Biomarker levels in the two clusters identified by biomarker-based unsupervised hierarchical clustering of patients in the discovery cohort.

Marker	Cluster 1 (n=8)	Cluster 2 (n=22)	P value	FDR
CCL22	1358.4 (493.8)	1603.5 (844.7)	0.1555	0.2091
OSF-2	8265.5 (844)	7696.4 (2065.3)	0.1852	0.2331
TWEAK	10344.1 (2735.2)	9266.9 (3951.9)	0.1852	0.2331
TM	<i>75% out of range</i>	<i>59.1% out of range</i>	0.2658	0.3239
TSP-1	207455000 (191505000)	282175000 (290085500)	0.3363	0.3974
OSM	<i>0% out of range</i>	<i>50% out of range</i>	0.3484	0.3996
PAI-1	<i>62.5% out of range</i>	<i>50% out of range</i>	0.4601	0.5127
PDGF-BB	10080.2 (6533)	11339.8 (5876.5)	0.6291	0.6816
Tie-2	3735.2 (794)	3741.7 (948.4)	0.6559	0.6914
Ang-1	40905.4 (31268.4)	37147.7 (17758.6)	0.6960	0.7143
SPARC	41572.7 (81332.3)	31450 (118798.8)	0.7937	0.7937

Median values with interquartile ranges are shown. For markers with more than 30% of values below the detection limit, frequencies of out of range values are indicated. P values for Mann-Whitney U test before (P value) and after correction for multiple testing by false discovery rate (FDR) are shown.

Supplementary table 3. Clinical characteristics of patients from two clusters in discovery cohort identified by unsupervised hierarchical clustering of 34 markers.

	Cluster 1 (n=8)	Cluster 2 (n=22)	P value
Age at sampling (years), <i>median (IQR)</i>	8.2 (10)	4.2 (4.2)	0.0395
Sex, % <i>female</i>	87.5	86.4	>0.9999
Duration of untreated disease (months), <i>median (IQR)</i>	9.4 (21)	5.8 (5.9)	0.5042
Intensification of treatment in first 3 months, %	50.0	59.1	0.6976
Time until remission off medication (years), <i>median (IQR)</i>	65.1 (24.4)	47.5 (26.5)	0.08
Disease activity at diagnosis			
CMAS (0-52; 0-49 for age 4-5), <i>median (IQR)</i>	18.5 (21.5)	38 (18.5) NR=1	0.011
DAS Total (0-20), <i>median (IQR)</i>	13 (2.8)	10.8 (4.5)	0.0265
DAS Muscle (0-11), <i>median (IQR)</i>	7 (2.8)	5 (5.3)	0.0486
DAS Skin (0-9), <i>median (IQR)</i>	5 (1)	5 (2)	0.9125
ERL (normal ≥ 7), <i>median (IQR)</i>	4.6 (1.4) NR=1	4.1 (2.3)	0.7934
Muscle enzymes at diagnosis			
CK (IU/liter), <i>median (IQR)</i>	249 (1666)	123.5 (327.3)	0.2524
LDH (IU/liter), <i>median (IQR)</i>	462 (555) NR=1	310.5 (159)	0.0285
AST (IU/liter), <i>median (IQR)</i>	52.5 (137.3)	44 (33)	0.3996
ALT (IU/liter), <i>median (IQR)</i>	31 (97.8)	26 (28.5) NR=1	0.3674

For continuous variables, medians and interquartile ranges (IQR) are shown. For categorical variables, frequencies are shown (%). P values for continuous variables were calculated by Mann-Whitney U test. P values for categorical variables were calculated by Fisher's exact test. NR = Not reported, CMAS = Childhood myositis assessment scale, DAS = disease activity scale, ERL = end row loops, CK = creatine kinase activity, LDH = lactate dehydrogenase, AST = aspartate aminotransferase, ALT = alanine aminotransferase.

Supplementary table 4. Clinical characteristics of patients from clusters identified by unsupervised hierarchical clustering of 34 markers in the discovery and validation cohorts.

	Discovery cohort			Validation cohort		
	Cluster 1D (n=9)	Cluster 2D (n=22)	P value	Cluster 1V (n=6)	Cluster 2V (n=23)	P value
Age at sampling (years), median (IQR)	8.2 (9.4)	4.2 (3.7)	0.0144	7.8 (6)	6.9 (9.1)	0.969
Sex, % female	88.9	85.7	>0.9999	50.0	65.2	0.6457
Duration of untreated disease (months), median (IQR)	5 (18.8)	5.9 (10.1)	0.5333	1.9 (4.7)	3.6 (8.7)	0.2317
Intensification of treatment in first 3 months, %	66.7	52.3	0.6908	66.7	18.2	0.0384
Disease activity at diagnosis						
DAS Total (0-20), median (IQR)	13 (3)	10.5 (4.5)	0.0078	-	-	-
CMAS (0-52; 0-49 for age 4-5), median (IQR)	26 (21)	38 (20) NR=1	0.0148	11.5 (9.5)	35 (19)	0.0053
DAS Muscle (0-11), median (IQR)	8 (2.5)	5 (4.7)	0.0181	-	-	-
DAS Skin (0-9), median (IQR)	5 (1.5)	5 (1.5)	0.8199	-	-	-
PGA (0-10), median (IQR)	-	-	-	8.2 (1.6) NR=1	5.1 (3.7) NR=3	0.0013
CAT (0-116), median (IQR)	-	-	-	11.5 (8.3)	5 (5)	0.0131
ERL (normal \geq 7), median (IQR)	4.2 (1.5) NR=1	4.3 (2.2)	0.5412	-	-	-

(Continued)

Supplementary table 4. Clinical characteristics of patients from clusters identified by unsupervised hierarchical clustering of 34 markers in the discovery and validation cohorts.

	Discovery cohort			Validation cohort		
	Cluster 1D (n=9)	Cluster 2D (n=22)	P value	Cluster 1V (n=6)	Cluster 2V (n=23)	P value
Muscle enzymes at diagnosis						
CK (IU/liter), median (IQR)	375 (192.4)	109 (310.5)	0.4137	5209 (13216.5)	298 (2411)	0.0225
LDH (IU/liter), median (IQR)	462 (437)	305 (154) NR=1	0.0094	888 (532.8)	434 (314) NR=4	0.0139
AST (IU/liter), median (IQR)	58 (223.5)	43 (28.5)	0.3543	404.5 (564.2)	61 (110.5) NR=2	0.008
ALT (IU/liter), median (IQR)	38 (167)	23 (17) NR=1	0.0309	160.5 (188.5)	32 (54)	0.0168

For continuous variables, medians and interquartile ranges (IQR) are shown. For categorical variables, frequencies are shown (%). P values for continuous variables were calculated by Mann-Whitney U test. P values for categorical variables were calculated by Fisher's exact test. NR = Not reported, DAS = disease activity scale, CMAAS = Childhood myositis assessment scale, PGA = physician's global assessment, CAT = cutaneous assessment tool, ERL = end row loops, CK = creatine kinase activity, LDH = lactate dehydrogenase, AST = aspartate aminotransferase, ALT = alanine aminotransferase.

Supplementary table 5. Receiver operating curves for identification of severe muscle and global disease at diagnosis by single biomarkers.

Biomarker	Severe disease	AUC ROC	P value	ROC	Cutoff value	Sensitivity	Specificity	NPV	PPV
Gal-9	Muscle	0.788	0.0009		19687 pg/mL	0.73	0.77	0.89	0.52
	Global	0.722	0.015		19687 pg/mL	0.69	0.74	0.89	0.43
CXCL10	Muscle	0.727	0.009		2425 pg/mL	0.67	0.77	0.87	0.50
	Global	0.707	0.0233		2425 pg/mL	0.62	0.74	0.87	0.40
TNFR2	Muscle	0.802	0.0005		3010 pg/mL	0.80	0.82	0.92	0.60
	Global	0.731	0.0116		3010 pg/mL	0.69	0.76	0.90	0.45
Gal-1	Muscle	0.797	0.0006		21236 pg/mL	0.80	0.70	0.91	0.48
	Global	0.721	0.0158		21236 pg/mL	0.69	0.65	0.88	0.36

Patients were stratified into patients with severe or non-severe muscle and global disease by the 75th percentile as following: patients with CMAS values below the 25th percentile of the cohort or DAS-M values above the 75th percentile of cohort were considered to have severe muscle disease. Patients with PGA or DAS-T above the 75th percentile of the respective score were considered to have severe global disease. Patients below the 75th percentile of PGA, DAS-T or DAS-M and above the 25th percentile of CMAS were considered to have non-severe muscle or global disease. *ROC = receiver operating curve, AUC = area under the curve, NPV = negative predictive value, PPV = positive predictive value, DAS-T = Total DAS, DAS-M = Muscle DAS, CMAS = Childhood myositis assessment score, PGA = Physician's global assessment.*

Distinctive biomarker profiles of endothelial activation and dysfunction in treatment-naïve rare systemic autoimmune diseases: implications for cardiovascular risk

Judith Wienke, Jorre S. Mertens, Samuel Garcia, Johan Lim, Camiel A. Wijngaarde, Joo Guan Yeo, Alain Meyer, Lucas L. van den Hoogen, Janneke Tekstra, Jessica E. Hoogendijk, Henny G. Otten, Ruth D.E. Fritsch-Stork, Wilco de Jager, Anneke J. van der Kooi, W. Ludo van der Pol, Thaschawee Arkachaisri, Timothy R.D.J. Radstake, Annet van Royen-Kerkhof,* and Femke van Wijk PhD*
Dutch juvenile myositis consortium#

*These authors contributed equally

#Sylvia S.M. Kamphuis, Esther P.A.H. Hoppenreijns, Wineke Armbrust, J. Merlijn van den Berg, Petra C.E. Hissink Muller

Submitted

ABSTRACT

Background: Vasculopathy is an important hallmark of systemic chronic inflammatory connective tissue diseases (CICTD), and is associated with increased cardiovascular risk. We investigated disease-specific biomarker profiles associated with endothelial dysfunction, angiogenic homeostasis and (tissue) inflammation, and their relation to disease activity in rare CICTD.

Methods: 38 serum proteins associated with endothelial (dys)function and inflammation were measured by multiplex-immunoassay in treatment-naive patients with localized scleroderma (LoS, 30), eosinophilic fasciitis (EF, 8), or (juvenile) dermatomyositis (34), 119 (follow-up) samples during treatment, and 65 controls. Data were analyzed by unsupervised clustering, Spearman correlations, non-parametric t-test and ANOVA.

Results: The systemic CICTD EF and dermatomyositis had distinct biomarker profiles, with 'signature' markers galectin-9 (dermatomyositis) and CCL18, fetuin, fibronectin, CXCL9, CCL4, galectin-1, and TSP-1 (EF). In LoS, CCL18, CXCL9, and CXCL10 were subtly increased. Furthermore, dermatomyositis and EF shared upregulation of markers related to interferon (CXCL10, CCL2), endothelial activation (VCAM-1), inhibition of angiogenesis (angiopoietin-2, sVEGFR-1) and inflammation/leukocyte chemo-attraction (CCL19, CXCL13, IL-18, YKL-40), as well as disturbance of the Angiopoietin-Tie receptor system and VEGF-VEGFR system. These profiles were related to disease activity, and largely normalized during treatment. However, a subgroup of CICTD patients showed continued elevation of galectin-9, CXCL10, IL-18, TNFR2, CXCL13, YKL-40 and/or VCAM-1 during clinically inactive disease, possibly indicating subclinical interferon-driven inflammation and/or endothelial dysfunction.

Conclusions: CICTD-specific biomarker profiles revealed an anti-angiogenic, interferon-driven environment during active disease, with incomplete normalization under treatment. This warrants further investigation into monitoring of vascular biomarkers during clinical follow-up, or targeted interventions to minimize cardiovascular risk in the long-term.

INTRODUCTION

Vasculopathy is an important hallmark of many chronic inflammatory connective tissue diseases (CICTD) affecting the skin. The vasculopathic component is well documented in (juvenile) dermatomyositis ((J)DM), systemic lupus erythematosus (SLE) and scleroderma/systemic sclerosis (SSc).¹⁻⁵ Increasing evidence suggests that vasculopathic changes can also be present, although to a lesser extent, in rare scleroderma-spectrum disorders such as localized scleroderma (LoS), eosinophilic fasciitis (EF) and mixed connective tissue disease (MCTD).⁶⁻¹¹ Endothelial dysfunction has important clinical implications in CICTD: it is associated with severe complications such as skin ulceration, renal, cardiac, and pulmonary involvement.^{1,12} Moreover, especially in systemic CICTD vasculopathy contributes to morbidity and mortality through accelerated atherosclerosis, leading to an increased risk of cardiovascular events.^{1,13,14} In LoS, a more localized CICTD with little systemic inflammation, the risk of cardiovascular disease is not increased.¹⁵ For patients with EF, a disease characterized by severe systemic inflammation, long-term implications for cardiovascular risk are still unknown, but may be considerable.

Although multiple pathophysiologic events play a role in the development of vasculopathic changes, chronic immune activation has emerged as an important contributing factor.¹⁶ Deposition of complement and immune complexes and direct immune cell-mediated endothelial injury can cause endothelial loss.¹⁷ Moreover, serum factors in CICTD can directly affect endothelial function: patient sera can induce adhesion molecule expression on cultured endothelial cells, while reducing angiogenesis, normal capillary morphogenesis, endothelial proliferation, migration and tube formation.¹⁸⁻²⁰ Anti-endothelial antibodies present in these sera²¹ and a disturbed balance between angiogenic and angiostatic stimuli may contribute to vasculopathic changes.^{22,23} Especially interferon-driven inflammation has been linked to the development of vasculopathic changes through direct and indirect angiostatic effects.²⁴⁻²⁶ Notably, overexpression of type I interferons (IFN) is observed in many CICTD.^{1,2,7,27} A classic example of an angiogenic system that may be disturbed during inflammation is the Angiopoietin-Tie receptor system.^{28,29} The vascular endothelial growth factor (VEGF) system may also be affected in inflammation, and elevated VEGF is considered a biomarker for disturbed angiogenesis.^{30,31} Finally, soluble adhesion molecules (e.g. ICAM-1 and VCAM-1) are considered reliable and representative markers for endothelial activation.^{23,31,32}

Thus, in many IFN-driven CICTD vasculopathy may play an important role in the disease pathology. However, it is yet unclear whether disturbances of circulating factors associated with endothelial dysfunction or activation show overlapping or distinct patterns between diseases, and whether they are related to disease activity. Here, we investigated disease-specific biomarker profiles associated with endothelial dysfunction, angiogenic homeostasis and (tissue) inflammation in a unique set of treatment-naive patients with rare

systemic and localized CICTD involving skin and/or muscles (LoS, EF, (dermato)myositis and mixed connective tissue disease) as well as healthy controls and neuromuscular control patients. We relate these biomarker profiles to disease activity and persistent low-grade inflammation, which may have implications for the long-term cardiovascular risk.

METHODS

Participants

Patients with (juvenile) dermatomyositis ((J)DM), mixed connective tissue disease with myositis (MCTD), localized scleroderma (LoS), eosinophilic fasciitis (EF), as well as healthy controls (HC) and neuromuscular control patients with hereditary proximal spinal muscular atrophy (SMA, a progressive, non-inflammatory neuromuscular disorder with a suspected vasculopathic component due to impaired endocytosis),³³ were recruited between January 2006 and June 2017 in tertiary referral centres in the Netherlands, Singapore, and France. This study was approved by the institutional ethics committees of the involved centres (UMC Utrecht (NL47875.041.14, NL13046.091.06), AMC Amsterdam, SingHealth centralized IRB (CIRB2014/083/E), CHU Strasbourg) and conducted according to the Declaration of Helsinki. Age-appropriate written informed consent was obtained prior to study inclusion.

Disease classification and disease activity criteria

Patients with JDM were included if they met the Bohan and Peter criteria for definite or probable JDM.^{34,35} As clinical measures of muscle and global disease activity, the childhood myositis scale (CMAS; 0-52) and physician's global assessment (PGA; 0-10) were recorded. Clinically inactive disease was defined according to the updated criteria for JDM;^{36,37} all other patients were considered active. Adult patients with dermatomyositis were classified according to the ENMC criteria.³⁸ Myositis was confirmed by biopsy unless typical skin manifestations of dermatomyositis were present. Patients with cancer-associated myositis were excluded. Disease activity was determined by combined evaluation of muscle strength with the medical research council scale, skin symptoms and muscle enzymes. Patients with myositis and presence of anti-RNP antibodies were classified as mixed connective tissue disease.³⁹ Patients with localized scleroderma were diagnosed based on the typical clinical picture. Treatment-naïve patients were considered active. In follow-up samples, inactive disease was defined as a modified LoS Skin Severity Index (mLoSSi) ≤ 5 out of 162.⁴⁰ Adult patients with eosinophilic fasciitis were diagnosed based on the clinical picture and

histopathological evaluation of skin biopsies containing the fascia. As the mLoSSi may stay high in these patients due to extensive irreversible sclerosis despite improved inflammatory symptoms, inactive disease was defined as a PGA for activity ≤ 5 out of 100.⁴⁰ Paediatric and adult patients with hereditary proximal spinal muscular atrophy served as disease controls. Confirmation of a homozygous loss of function of the *survival motor neuron 1* gene was obtained in all SMA patients.⁴¹ Adult healthy volunteers were included as healthy controls.

Biomarker analysis

Blood was collected in serum tubes, according to the local study protocol. All samples were spun down within four hours after collection and stored at -80°C until analysis. 38 analytes were measured in 50 μL of serum by multiplex technology in all samples simultaneously, as described previously (xMAP; Luminex,⁴²): Angiopoietin-1 (Ang-1), angiopoietin-2 (Ang-2), angiopoietin-1 receptor (Tie-2), CXCL13, CCL2, CCL4, CCL17, CCL18, CCL19, CCL22, CCL27, CXCL9, CXCL10, CXCL12, Endoglin, E-selectin (E-sel), Fetuin, Fibronectin, galectin-1 (Gal-1), galectin-3 (Gal-3), galectin-9 (Gal-9), interleukin 18 (IL-18), oncostatin M (OSM), periostin (OSF-2), placental growth factor (PIGF), plasminogen activator inhibitor (PAI-1), platelet-derived growth factor BB (PDGF-BB), P-selectin (P-sel), serum amyloid A1 (SAA-1), SPARC, soluble ICAM-1 (ICAM-1), soluble VCAM-1 (VCAM-1), soluble VEGF receptor 1 or Flt-1 (sVEGFR1), thrombomodulin (TM), thrombospondin-1 (TSP-1), TNF receptor-2 (TNFR2), TWEAK, vascular endothelial growth factor (VEGF), and YKL-40. Tie-1 was measured separately by ELISA assay (R&D, DY5907).

Statistical analysis

Statistical analyses were performed using GraphPad Prism 7.0, SPSS Statistics 21 (IBM) and R 3.5.1 (CRAN). Multiplex values below the detection limit were imputed as 0.5x lowest measured value. For correlations, assessed by Spearman rank, imputed values were excluded. To correct for multiple testing, Kruskal-Wallis tests with Dunn's posthoc test were performed for each disease separately, stratified by activity (i.e. treatment-naive, active on medication, inactive and HC). Multiplicity adjusted p values of these tests are reported in the tables and legends. For comparison between SMA and HC, the Mann-Whitney U test was used with correction for multiple testing by false discovery rate (FDR). For paired analyses, the Wilcoxon matched-pairs signed rank test with FDR correction was used. Multiplicity adjusted P values or FDR less than 0.05 were considered statistically significant as indicated in the figure legends. For unsupervised clustering by principal component analysis (PCA) and heatmap analysis with hierarchical clustering by 1-Pearson correlation with average linkage, data were mean-centered and scaled per analyte. Analytes with more than 30% of measured values below the detection limit were excluded from the clustering analyses

(OSM and CXCL9). K-means clustering was performed based on median analyte expression within the groups.

RESULTS

Patient characteristics

We included 146 unique CICTD patients with (J)DM (72), MCTD with myositis (1), LoS (55) or EF (18), 43 control patients with SMA and 22 HC (table 1 and 2). Among CICTD patients, 72 samples were taken before start of treatment and 119 during treatment and/or inactive disease. The age at sampling differed significantly between the treatment-naive disease groups ($p < 0.0001$), as most myositis patients were juvenile, whereas the majority of other patients were adults. The gender distribution was similar between groups. As expected, patients with EF had significantly higher VAS disease activity and mLoSSI scores than patients with LoS ($p = 0.0017$ and $p = 0.0031$). Muscle enzymes were highest in the myositis group.

Table 1. Clinical characteristics of treatment-naive patients and controls.

	Eosinophilic fasciitis	Localized scleroderma	(Dermato)myositis	Spinal muscular atrophy	Healthy controls	
	EF	LoS	(J)DM+MCTD	SMA	HC	P value
	Netherlands	Netherlands	Netherlands, France & Singapore	Netherlands	Netherlands	
	n=8	n=30	n=33 + 1	n=43	n=22	
Age at diagnosis (years), median (IQR)	64.9 (17.1)	35.5 (40.4)	8.4 (9.5)	1.5 (1.7)	-	<0.0001
Age at sampling (years), median (IQR)	65.1 (12.8)	41.9 (35.1)	8.4 (9.5)	35.7 (28.4)	31 (21)	<0.0001
Sex, % female	62.5	66.7	55.9	60.5	68.2	0.8750
Pediatric patients,%	0.0	16.7	91.2	23.3	0.0	
Clinical disease activity scores						
Muscle weakness (% of patients)	-	-	91.2	-	-	n/a
(J)DM skin symptoms (% of patients)	-	-	94.1	-	-	n/a
CMAS (0-52), median (IQR)	-	-	28.0 (22.3) NR=12	-	-	n/a
PGA (0-10), median (IQR)	-	-	6.0 (1.8) NR=9	-	-	n/a
EF/LoS VAS activity (0-100), median (IQR)	46.5 (11.8) NR=2	20.5 (21.3) NR=2	-	-	-	0.0054

(Continued)

Table 1. Clinical characteristics of treatment-naïve patients and controls.

	Eosinophilic fasciitis	Localized scleroderma	(Dermato)myositis	Spinal muscular atrophy	Healthy controls	P value
	Netherlands	Netherlands	(J)DM+MCTD Netherlands, France & Singapore	Netherlands	Netherlands	
	n=8	n=30	n=33 + 1	n=43	n=22	
EF/LoS mLoSSI (0-162), median (IQR)	42.5 (18.3) NR=2	16 (12.5) NR=2	-	-	HC	0.0035
EF/LoS VAS damage (0-100), median (IQR)	17.5 (20) NR=2	12 (17) NR=1	-	-	Netherlands	0.5839
EF/LoS LoSDI (0-162), median (IQR)	8.5 (6.8) NR=2	6 (6.5) NR=2	-	-	SMA	0.8560
SMA motor score (HMFSE, 0-66)	-	-	-	4 (36) NR=4	-	n/a
Laboratory parameters						
% ANA positive	42.9 NR=1	60.0 NR=10	59.4 NR=2	-	-	0.7006
CRP, mg/liter	10 (1) NR=6	5 (1.5) NR=26	1 (2) NR=3	-	-	0.0172
ESR, mm/hour	16 (7) NR=5	5 (7.8) NR=18	16 (10) NR=5	-	-	0.0126
ALT, IU/liter	20.5 (9.5) NR=4	20.5 (7.8) N=18	48.5 (83.3)	-	-	0.0031

(Continued)

Table 1. Clinical characteristics of treatment-naive patients and controls.

	Eosinophilic fasciitis	Localized scleroderma	(Dermato)myositis	Spinal muscular atrophy	Healthy controls	
	EF	LoS	(J)DM+MCTD	SMA	HC	
	Netherlands	Netherlands	Netherlands, France & Singapore	Netherlands	Netherlands	
	n=8	n=30	n=33 + 1	n=43	n=22	P value
AST, IU/liter	24 (20.5) NR=5	-	102 (480) NR=1	-	-	0.0060
CK, IU/liter	37 (2) NR=6	-	659 (2865.3)	-	-	0.0032
LDH, IU/liter	214.5 (20.5) NR=6	-	642 (480) NR=3	-	-	0.0214

Three patients (2 JDM, 1 LoS) in whom treatment was started max 1 week before sampling, were also considered treatment-naive. For continuous variables, medians and interquartile ranges (IQR) are shown. For categorical variables, frequencies are shown. For comparison between two groups, the Mann-Whitney U test was used for continuous variables and the Fisher's exact test for categorical variables. For comparison between more than two groups, the Kruskal-Wallis test was used for continuous variables and the chi-squared test for categorical variables. NR = not reported. HC = healthy controls (n=22); LoS = Localized scleroderma (n=30), EF = eosinophilic fasciitis (n=8), (J)DM = (juvenile) dermatomyositis (n=33), MCTD = mixed connective tissue disease (n=1), SMA = spinal muscular atrophy (n=43).

Table 2. Clinical characteristics of patients with CICTD during different disease states.

	Eosinophilic fasciitis				Localized scleroderma				(Juvenile) Dermatomyositis			
	EF Netherlands				LoS Netherlands				(JDM Netherlands, France & Singapore			
	TN n=8	AM n=6	Inact n=8	P value	TN n=30	AM n=17	Inact n=18	P value	TN n=33	AM n=29	Inact n=41	P value
Age at diagnosis (years), median (IQR)	64.9 (17.1)	62.6 (9.1)	56.3 (15.4)	0.1936	35.5 (40.4)	44.6 (45.1)	19.1 (27.1)	0.3578	8.4 (9.5)	11.5 (9.9)	12.8 (8.5)	0.0063
Age at sampling (years), median (IQR)	65.1 (12.8)	61.3 (10.9)	51.9 (15)	0.2790	41.9 (35.1)	16.1 (46.8)	17.3 (29.1)	0.2233	8.4 (9.5)	6.3 (7.7)	8 (8.7)	0.8664
Sex, % female	62.5	66.7	25.0	0.2053	66.7	58.8	55.6	0.7195	57.6	65.5	58.5	0.7275
Clinical disease activity scores												
Muscle weakness (% of patients)	-	-	-	-	-	-	-	-	90.9	62.1	0.0	<0.0001
(JDM skin symptoms (% of patients)	-	-	-	-	-	-	-	-	93.9	75.0	0.0	<0.0001
CMAS (0-52), median (IQR)	-	-	-	-	-	-	-	-	28.0 (22.3)	48 (15.5)	52 (0)	<0.0001
PGA (0-10), median (IQR)	-	-	-	-	-	-	-	-	NR=12	NR=10	NR=12	
EF/LoS VAS activity (0-100), median (IQR)	46.5 (11.8)	17.5 (11.8)	2 (2)	0.0007	20.5 (21.3)	16 (10)	0 (3)	<0.0001	6.0 (1.8)	2 (2.5)	0 (0)	<0.0001
	NR=2	NR=1	NR=1		NR=2	NR=1	NR=1		NR=9	NR=11	NR=4	

(Continued)

Table 2. Clinical characteristics of patients with CICTD during different disease states.

	Eosinophilic fasciitis			Localized scleroderma			(Juvenile) Dermatomyositis			
	EF Netherlands			LoS Netherlands			(JDM) Netherlands, France & Singapore			
	TN n=8	AM n=6	Inact n=8	TN n=30	AM n=17	Inact n=18	TN n=33	AM n=29	Inact n=41	P value
EF/LoS mLoSSI (0-162), median (IQR)	42.5 (18.3)	25.5 (4)	9 (8.5)	16 (12.5)	9 (6)	2 (3)	-	-	-	<0.0001
EF/LoS VAS damage (0-100), median (IQR)	NR=2	44.5 (38.5)	10 (11.5)	NR=2	NR=1	NR=1	-	-	-	0.1566
EF/LoS LoSDI (0-162), median (IQR)	NR=2	8.5 (2.5)	5 (2)	NR=1	NR=1	NR=1	-	-	-	0.8471
	NR=2	NR=3	NR=2	NR=2	NR=11	NR=4	NR=5	NR=5	NR=6	
Laboratory parameters										
% ANA positive	42.9	50.0	16.7	60.0	27.3	25.0	61.3	55.6	43.6	0.3792
	NR=1	NR=2	NR=2	NR=10	NR=6	NR=2	NR=2	NR=2	NR=2	
CRP, mg/liter	10 (1)	-	10 (5)	5 (1.5)	2 (3)	3 (4)	1 (2)	1 (1.5)	1 (1.5)	0.3260
	NR=6	NR=5	NR=5	NR=26	NR=12	NR=10	NR=3	NR=3	NR=10	
ESR, mm/hour	16 (7)	5 (1.5)	3.5 (5.3)	5 (7.8)	2 (2.3)	5 (3)	16 (10)	8 (9)	6 (7.5)	0.0001
	NR=5	NR=3	NR=2	NR=18	NR=11	NR=4	NR=5	NR=5	NR=6	

(Continued)

Table 2. Clinical characteristics of patients with CICTD during different disease states.

	Eosinophilic fasciitis				Localized scleroderma				(Juvenile) Dermatomyositis			
	EF Netherlands				LoS Netherlands				(JDM) Netherlands, France & Singapore			
	TN n=8	AM n=6	Inact n=8	P value	TN n=30	AM n=17	Inact n=18	P value	TN n=33	AM n=29	Inact n=41	P value
ALT, IU/liter	20.5 (9.5)	37 (20.5)	39 (30)	0.1277	20.5 (7.8)	21 (11)	20.5 (17)	0.6511	48.5 (83.3)	25 (13)	15 (6.5)	<0.0001
AST, IU/liter	24 (20.5)	-	NR=2		NR=18	NR=10	NR=4		102 (480)	28 (13)	26 (11)	<0.0001
CK, IU/liter	37 (2)	-	-		-	32.5 (9.5)	97.5 (62.5)		NR=1	659 (2865.3)	114 (49.8)	<0.0001
LDH, IU/liter	214.5 (20.5)	-	-		-	NR=15	NR=10		NR=4	642 (480)	238 (69)	<0.0001
	NR=6	NR=6							NR=3	NR=5	NR=8	
Immunosuppressive medication												
Oral steroids	0.0	83.3	62.5	0.7978	0.0	35.3	11.1	0.0019	6.1	86.2	34.1	<0.0001
Methotrexate	0.0	66.7	75.0	>0.999	0.0	64.7	55.6	<0.0001	6.1	72.4	3.7	<0.0001
Cyclophosphamide	0.0	0.0	0.0		0.0	0.0	0.0		0.0	10.3	0.0	
IV immunoglobulins	0.0	0.0	0.0		0.0	0.0	0.0		0.0	14.3	0.0	

(Continued)

Table 2. Clinical characteristics of patients with CICTD during different disease states.

	Eosinophilic fasciitis				Localized scleroderma				(Juvenile) Dermatomyositis			
	EF				LoS				(J)DM			
	Netherlands		Inact		Netherlands		Inact		Netherlands, France & Singapore		Inact	
	TN n=8	AM n=6	Inact n=8	P value	TN n=30	AM n=17	Inact n=18	P value	TN n=33	AM n=29	Inact n=41	P value
Hydroxychloroquine	0.0	0.0	0.0		0.0	0.0	0.0		0.0	20.7	14.6	
Tacrolimus	0.0	0.0	0.0		0.0	0.0	0.0		0.0	6.9	2.4	
Mycophenolate Mofetil	0.0	0.0	0.0		3.3	0.0	5.6		0.0	6.9	4.9	
Azathioprine	0.0	0.0	0.0		0.0	0.0	0.0		0.0	0.0	7.3	
Other	0.0	16.7 ^a	0.0		0.0	0.0	0.0		0.0	0.0	0.0	
None	100.0	0.0	12.5	0.0001	96.7	21.4	38.9	<0.0001	93.9	0.0	3.7	<0.0001

For continuous variables, medians and interquartile ranges (IQR) are shown. For categorical variables, frequencies are shown. For comparison between two groups, the Mann-Whitney U test was used for continuous variables and the Fisher's exact test for categorical variables. For comparison between more than two groups, the Kruskal-Wallis test was used for continuous variables and the chi-squared test for categorical variables. *NR = not reported. If data were available for less than 2 subjects per category, they were not shown ("–"). Three patients (2 JDM, 1 LoS) in whom treatment was started max 1 week before sampling, were also considered 'active at diagnosis': (a) Imatinib. NR = not reported, HC = healthy controls, LoS = Localized scleroderma, EF = eosinophilic fasciitis, (J)DM = (juvenile) dermatomyositis, SMA = spinal muscular atrophy.*

Unsupervised clustering reveals distinct biomarker profiles in treatment-naive myositis, EF and LoS

A panel of 38 markers for endothelial (dys)function and inflammation was measured in serum of treatment-naive patients and controls by multiplex immunoassay. Unsupervised principal component analysis (PCA) showed that patients with (J)DM, EF and LoS clustered separately based on their biomarker profiles (figure 1A), with (J)DM and EF patients being most distinct from HC. One patient with MCTD-associated myositis clustered close to the (J)DM cluster, suggesting a similar biomarker profile despite the distinct disease background. Patients with LoS and SMA had biomarker profiles similar to HC, indicating low/absent systemic inflammation. 30 proteins were differentially expressed between at least one disease and HC (FDR<0.05; supplementary table 1). Seven of these were increased in all three CICTD: Gal-9, CXCL10, TNFR2, IL-18, CXCL13, CCL19, and VCAM-1 (figure 1B). (J)DM and EF additionally shared upregulation of Ang-2, CCL2, ICAM-1, YKL-40 and sVEGFR1. CXCL9 and CCL18 were significantly increased in LoS and EF. Random forest analysis showed that Gal-9, CCL18 and CXCL10 were the most important analytes to distinguish the CICTD from HC and each other (figure 1C). To identify disease-specific analyte signatures, we performed K-means clustering, which revealed 7 analyte clusters (supplementary figure 1). Analyte cluster 1, with the highest expression in (J)DM, contained Gal-9, CCL2, PIGF, and sVEGFR1 (figure 1D). Cluster 2 and 3, with similarly elevated levels in (J)DM and EF, consisted of CXCL10, VCAM-1, Ang-2, TNFR2, CCL19, OSF-2, IL-18, CXCL13, VEGF, and YKL-40 (figure 1E-F). Analytes in cluster 4, CCL18, Fetuin, CXCL9, CCL4, ICAM-1, and Gal-1, were specifically high in EF (figure 1G). Clusters 5-7 showed mixed expression patterns across groups, with high Gal-3 in (J)DM, high fibronectin and TSP-1 in EF and low SPARC in (J)DM and EF. These results suggest that patients with LoS, a localized CICTD, have a limited systemic biomarker signature, whereas patients with the systemic CICTD (J)DM and EF have clear and distinct, but also overlapping biomarker profiles. In both diseases, IFN-related and chemo-attractant proteins (CXCL10, TNFR2, IL-18, CXCL13, CCL19, CCL2, YKL-40), endothelial activation markers (ICAM-1, VCAM-1) and the anti-angiogenic Ang-2 and sVEGFR1 were highly expressed, whereas Gal-9 and CCL18, amongst others, were more disease-specific.

Figure 1. Unsupervised clustering reveals distinct biomarker profiles in treatment-naive myositis, EF and LoS. (A) Principal component analysis of treatment-naive patients with different CICTD and controls based on 34 mean-centered analytes. Open circles represent cluster centres. (B) Venn diagram of analytes that were significantly upregulated compared to controls ($p < 0.05$), per disease group. (C) Analyte importance in Random Forest analysis of CICTD and HC. (E-G) Dot plots of individual biomarker values across all groups, ordered per analyte cluster as shown in supplementary figure 1 (D=cluster 1, E=cluster 2, F=cluster 3, G=cluster 4). Bars represent medians. P value of Kruskal-Wallis test are indicated. Red = (J)DM, orange = EF, purple = SMA, blue = LoS, black = HC. HC = healthy controls (n=22), LoS = Localized scleroderma (n=30), EF = eosinophilic fasciitis (n=8), Myos = myositis, (J)DM = (juvenile) dermatomyositis (n=33), SMA = spinal muscular atrophy (n=43).

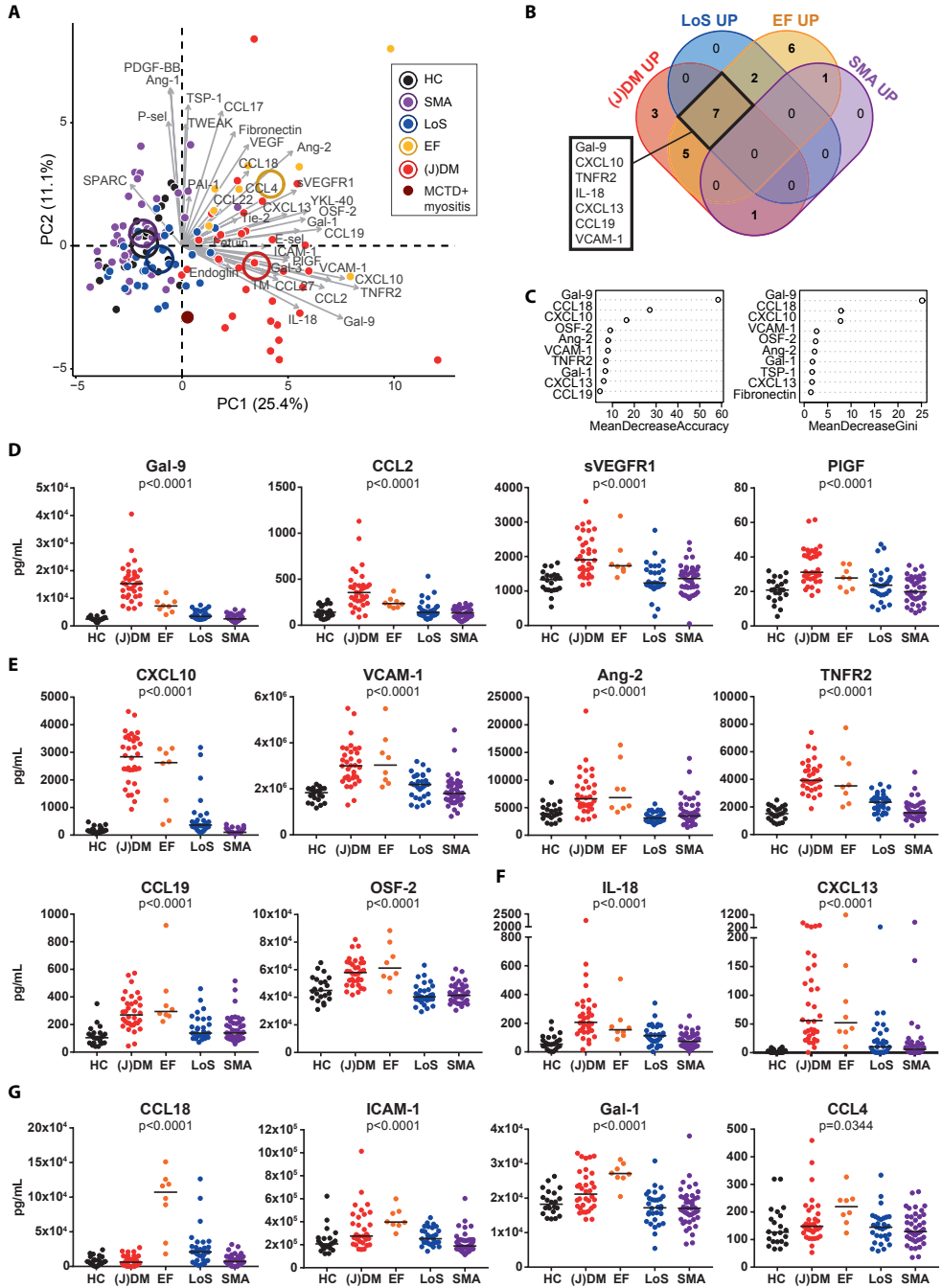


Figure 1. Unsupervised clustering reveals distinct biomarker profiles in treatment-naive myositis, EF and LoS.

Relation of biomarker profiles with disease activity

To assess whether the biomarker profiles were related to disease activity and would normalize during treatment, we analyzed HC and CICTD patients before start of treatment (treatment naive, “TN”), during active disease on medication (“AM”) and during clinically inactive disease by PCA. The biomarker profiles were most distinct from HC before treatment and became more similar to HC during treatment and subsequent inactive disease (figure 2A, B and C), suggesting that the biomarker profiles are highly associated with disease activity. In LoS, these differences were small, again indicating that the systemic effects are limited in this rather localized disease. To investigate which of the biomarkers were most related to disease activity, we performed three separate analyses in each CICTD: we analyzed differential biomarker expression 1) between treatment-naive and inactive disease and 2) between longitudinal paired samples taken during active disease and after follow-up, and 3) assessed correlations with clinical measures of disease activity. Results of these separate analyses are shown in supplementary table 2, 3 and 4 and summarized in the Venn diagrams in figure 2D. In (J)DM, 13 markers were related to disease activity in all three analyses: Gal-9, CXCL10, TNFR2, CCL2, ICAM-1, VCAM-1, OSF-2, YKL-40, sVEGFR1, CCL27, CCL19, Ang-2, and Gal-1 (figure 2D). In EF, 8 markers were related to disease activity in all analyses, showing considerable overlap with the biomarkers in (J)DM: CCL18, TNFR2, CCL2, ICAM-1, OSF-2, CCL19, Gal-1, and Tie-1. In LoS, only CCL18 was identified in all three analyses. The heatmaps in figure 2E and paired samples in figure 2F-H (EF, (J)DM and LoS, respectively) show the considerable reduction of these core biomarkers from active to inactive disease.

In conclusion, many of the disease-specific analytes, including vasculopathy-associated markers, are related to disease activity and decrease to near-normal levels during treatment.

Figure 2. Relation of biomarker profiles with disease activity in CICTD diseases.

(A-C) Principal component analysis of patients with (J)DM (A), EF (B) and LoS (B) before treatment (“TN”, red), with active disease on medication (“AM”, orange), with inactive disease (“Inact”, green) and healthy controls (“HC”, grey). Open circles represent cluster centres. (D) Venn diagrams of significant analytes from 3 analyses per disease group: differential biomarker expression 1) between treatment-naive patients and patients with inactive disease and 2) between longitudinal paired samples taken during active disease and after follow-up, and 3) correlations with clinical measures of disease activity. (E) Heatmap of (J)DM and EF patients with different disease states based on normalized expression of core activity-related analytes from figure 2D. (F-H) Analyte levels in active and paired follow-up samples in EF (F, n=5), (J)DM (G, n=24) and LoS (H, n=10). (J) DM = (juvenile) dermatomyositis, EF = eosinophilic fasciitis, LoS = localized scleroderma.

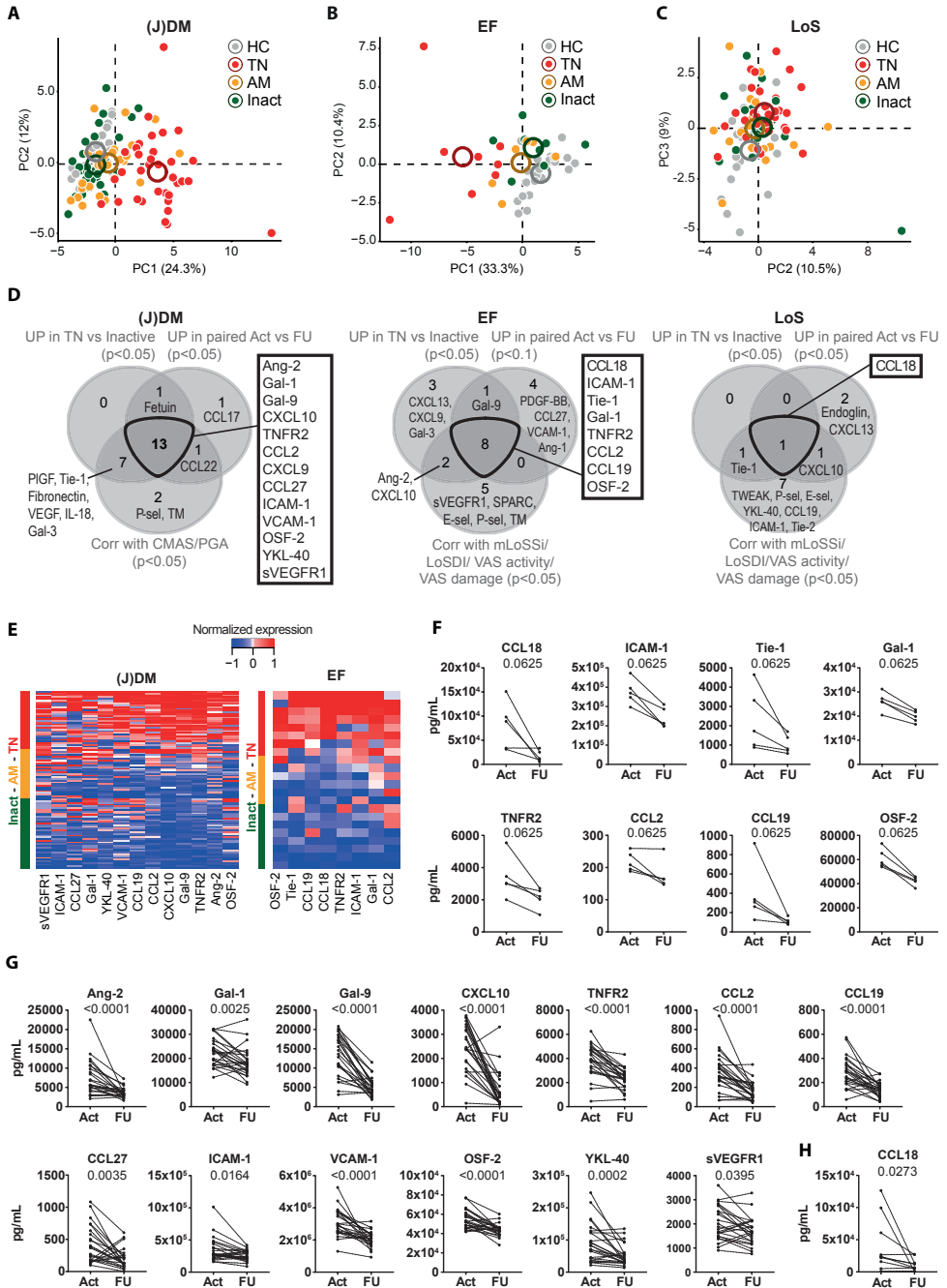


Figure 2. Relation of biomarker profiles with disease activity in CICTD diseases.

Homeostasis of angiogenic systems

To identify disturbances in the angiogenic homeostasis, we focused on the two important angiogenesis-regulating Ang-Tie and VEGF-PlGF-VEGFR systems. Under homeostatic conditions, the activation of the Tie-1/Tie-2 receptor complex by its ligand Ang-1 is key for endothelial proliferation and survival. Under inflammatory conditions however, this interaction is antagonized on multiple levels by 1) cleavage of Tie-1, destabilizing the receptor complex, 2) induction of the antagonistic alternative Tie receptor ligand Ang-2, and 3) release of the soluble decoy receptor Tie-2. These inflammation-induced changes can compromise vascular integrity (figure 3A).^{28,29} In active (J)DM and EF, Ang-2 levels were more than twofold increased compared to inactive disease, whereas Ang-1 levels were not significantly changed (figure 3B and C). The Ang-2/Ang-1 ratio, representing the balance of angiostatic over angiogenic signals, was significantly elevated in active (J)DM ($p < 0.0001$), however unaffected in EF and LoS (figure 3D). Soluble, cleaved Tie-1 was higher during active than inactive disease ($p < 0.05$; figure 3B and C), especially in (J)DM and EF. These results indicate that in active (J)DM, and to a lesser extent in EF, homeostatic Ang-Tie signaling is compromised. The Ang-2/Ang-1 balance in these disease is shifted towards an anti-angiogenic environment, which is further aggravated by destabilization of the Tie-receptor complex (figure 3A-B).^{28,29}

In the VEGF system, the VEGF receptor ligands VEGF and PlGF induce pro-angiogenic signaling, which may be antagonized by the soluble decoy receptor sVEGFR1. sVEGFR1 was significantly increased during active (J)DM and EF compared to controls ($p < 0.01$; figure 3B&C). VEGF was increased during active EF ($p = 0.0323$) and PlGF was increased during active (J)DM ($p < 0.0001$). These disturbances normalized during inactive disease (figure 3B). In LoS, none of these components were affected. Taken together, in active (J)DM and EF the Ang-Tie system is shifted towards an anti-angiogenic balance and the VEGF-PlGF-VEGFR system is disturbed.

Figure 3. Homeostasis of angiogenic systems.

(A) Schematic representation of angiogenic disturbances in active (J)DM and EF. Under homeostatic conditions, angiopoietin (Ang)-1 binds to its cell-surface receptor Tie-2 on endothelial cells, which induces heterodimerization of Tie-2 with its cell-bound co-receptor Tie-1, forming a stable signaling complex leading to endothelial cell proliferation and survival. In homeostasis, Ang-2 also acts as a Tie-2 agonist. However, under inflammatory conditions, the ectodomain of Tie-1 is cleaved, resulting in and destabilization of the Tie-2/Tie-1 complex and reduced signaling. Moreover, Tie-1 cleavage inhibits Ang-2 agonist activity, thus converting its role into a Tie-2 antagonist, reducing endothelial proliferation and survival. Simultaneously, levels of Ang-2 are increased, whereas Ang-1 and surface Tie-2 are decreased in inflammation. Lastly, soluble Tie-2 can be released during inflammation, acting as a decoy receptor for the angiopoietins. Eventually, the combination of these changes lead to loss of vascular integrity in inflammation.^{28,29} (B) Fold change ("FC") of median biomarker values in treatment-naïve patients compared to inactive disease (left panel, p values from supplementary table 2) or healthy controls (right panel, p values from supplementary table 1). Multiplicity adjusted P values of Kruskal-Wallis test are indicated. (C) Tukey boxplots of analytes before start of treatment ("TN"), during active disease on medication ("AM") or inactive disease ("Inact") and in healthy controls ("HC"). P values of Kruskal-Wallis test are indicated.

(Figure 3 continued)

As Tie-1 was measured on different ELISA plates for different diseases, values can only be compared within diseases but not to HC. (D) Dot plots of Ang-2/Ang-1 ratio in treatment-naïve patients. P values of Kruskal-Wallis test with Dunn' post hoc test are indicated. Dotted line indicates cutoff for normal values set at mean+2 standard deviations of HC. HC = healthy controls, (J)DM = (juvenile) dermatomyositis, EF = eosinophilic fasciitis, LoS = localized scleroderma. *P<0.05, **P<0.01, ***P<0.001, ****P<0.0001.

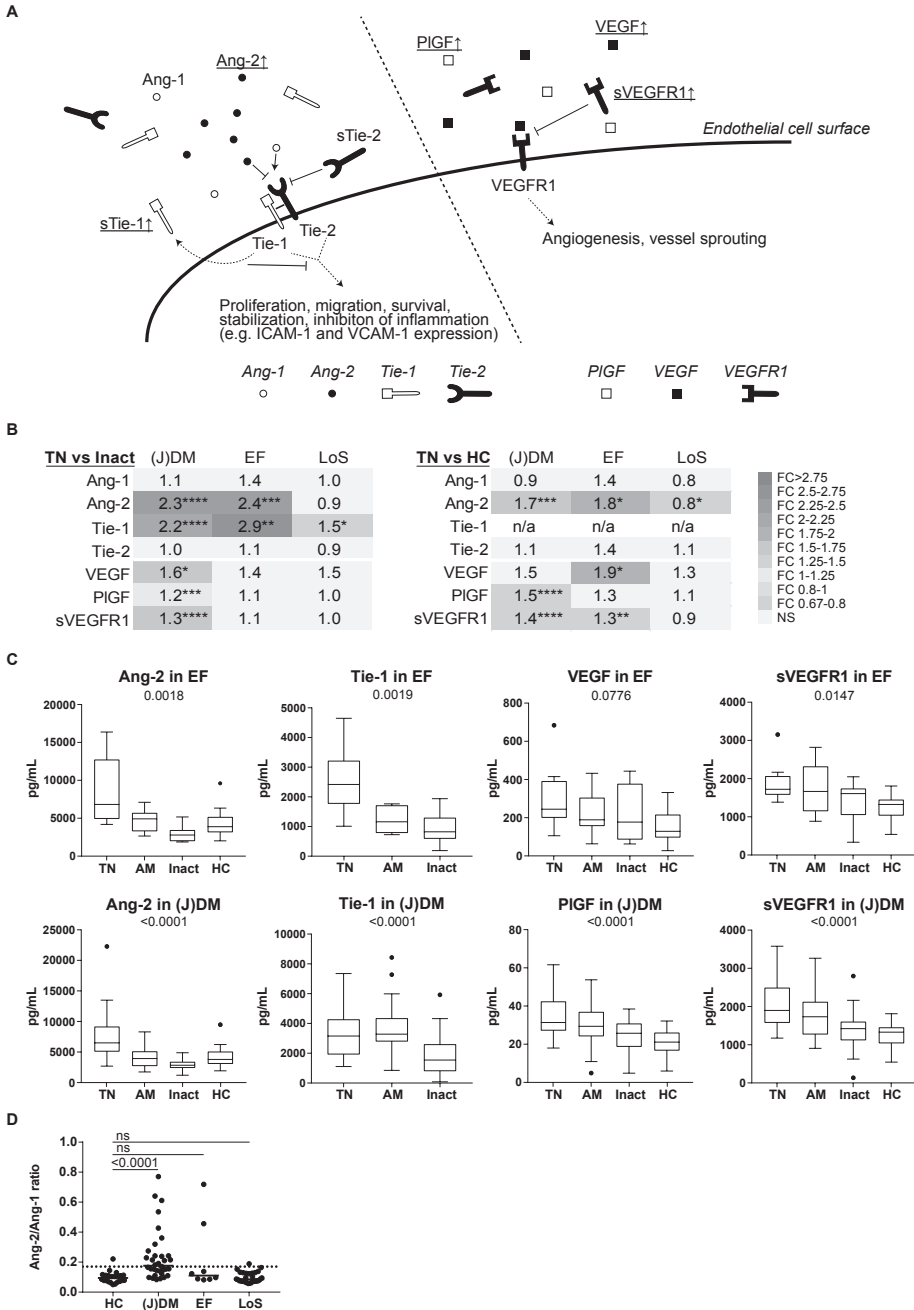


Figure 3. Homeostasis of angiogenic systems.

Biomarker normalization during inactive disease

In (J)DM and EF, biomarker profiles of patients with inactive disease were more similar to HC than of patients with active disease (figure 2A-B). To examine whether biomarker profiles of patients completely normalized during clinically inactive disease, we compared clinically inactive patients to HC by PCA. Patients with inactive disease were still distinct from HC (figure 4A). We observed remarkably elevated levels of the 12 analytes shared between (J)DM and EF in figure 1B: Gal-9, CXCL10, IL-18, TNFR2, CXCL13, CCL19, and VCAM-1 were still elevated in a subgroup (of up to 59%) of patients in both diseases (figure 4B). Ang-2 was rather decreased (figure 4B). In addition, patients with inactive (J)DM had significantly lower CCL27, Fetuin and P-sel than HC (supplementary table 5). 50% of patients with inactive EF had increased fibronectin, and overall Gal-3 and SPARC were lower than in HC. This indicates that (a subgroup of) patients with clinically inactive CICTD can still have abnormal levels of markers indicating interferon-driven inflammation, leukocyte chemo-attraction, endothelial activation or angiogenic disturbance, possibly indicating continued subclinical inflammation and/or endothelial dysfunction. The observed differences were not due to medication effects, since we did not find differences between inactive patients on and off treatment (*data not shown*).

DISCUSSION

Vasculopathy is an important hallmark of many CICTD affecting the skin. It is associated with chronic inflammation and can lead to severe complications, including an increased risk of cardiovascular events.^{1,12-14} To date, it is unknown how biomarker profiles associated with vasculopathy compare between different CICTD. Here, we are the first to show that different interferon-associated, treatment-naive CICTD can be separated based on their biomarker signatures related to both inflammation and endothelial dysfunction/activation. (J)DM and EF, characterized by systemic inflammation, showed clear systemic biomarker signatures, with disease-specific markers such as Gal-9 and CCL18. In LoS, a more localized disease with little systemic inflammation, subtle biomarker changes were observed as well. Markers shared among diseases were related to interferon (CXCL10, CCL2), endothelial activation (VCAM-1), inhibition of angiogenesis (angiopoietin-2, sVEGFR1) or inflammation/leukocyte chemo-attraction (CCL19, OSF-2, CXCL13, IL-18, and YKL-40). Remarkably, a subgroup of CICTD patients showed continued biomarker disturbances during clinically inactive disease, indicating that an anti-angiogenic interferon-dominated environment and endothelial activation may linger subclinically and possibly affect long-term outcome and cardiovascular risk.

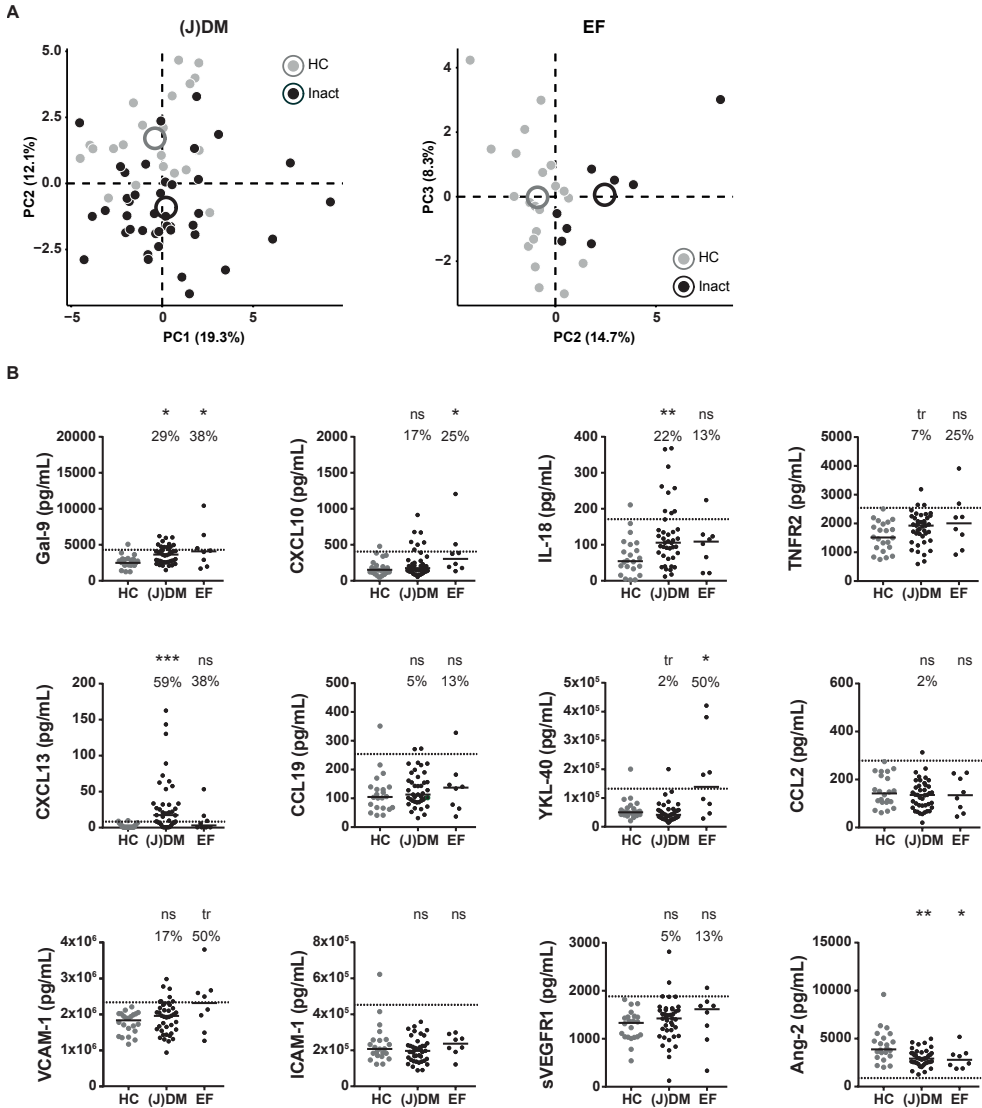


Figure 4. Incomplete biomarker profile normalization during clinically inactive disease.

(A) Principal component analysis of inactive patients (“Inact”) compared to healthy controls (“HC”). Open circles represent cluster centres. (B) Biomarker values in inactive (J)DM and EF compared to controls, in biomarkers with continuously elevated or reduced levels. Dotted line indicates cutoff for normal values set at mean±2 standard deviations of HC. Percentages indicate percentage of patients above cutoff, per disease. P values from Kruskal-Wallis test per disease with Dunn’s posthoc test are indicated: *P<0.05, **P<0.01, ***P<0.001, ****P<0.0001. (J)DM= (Juvenile) dermatomyositis, EF = eosinophilic fasciitis.

Elevated levels of IFN-inducible chemokines CXCL10, CXCL9, and CCL2, which serve as potent chemo-attractants promoting leukocyte recruitment to inflamed tissues, were present in the three different CICTD, supporting previous studies.^{43–47} We found higher circulating levels in (J)DM and EF compared to LoS, reflecting the compartmentalization of the diseases. These chemokines can be produced within DM muscle and LoS skin, and their overexpression in DM muscle correlates with the severity of vasculopathy, such as loss of capillaries.^{43,44,48,49} Type I interferons can directly exert an angiostatic effect on endothelial cells,⁵⁰ or indirectly via induction of e.g. CXCL9, and CXCL10.^{48,51} Moreover, the type I IFN signature has been associated with endothelial (progenitor cell) dysfunction and a higher risk of cardiovascular events in SLE, SSc and DM.^{24–26,52–54} Gal-9 and CXCL10 have been recently validated as biomarkers for (J)DM and in the current study high levels of Gal-9 were found to be (J)DM specific.⁴⁶ Although the effects of Gal-9 on endothelial cells are largely context-dependent, at higher concentrations direct angiostatic effects have been demonstrated.⁵⁵ Thus, the observed presence of interferon-related biomarkers during active and even inactive disease, may indicate that an anti-angiogenic environment is present in patients with CICTD for a prolonged period.

Also IL-18, one of the core cytokines upregulated in all three CICTD, has been shown to induce endothelial progenitor cell dysfunction in SLE,⁵⁶ correlates with intima media thickness and severity of coronary atherosclerosis in the general population,^{57,58} and is predictive of cardiovascular mortality.^{59,60}

In line with previous observations, soluble adhesion molecules (ICAM-1 and VCAM-1) were increased in active (and inactive) DM, EF and to a lesser extent in LoS,^{61–64} reflecting increased surface expression on endothelial cells as described in DM muscle and skin of SSc patients.^{63,65–67} Elevated adhesion molecule expression may enhance leukocyte migration into tissues, perpetuating and/or aggravating local (chronic) inflammation. Increased serum ICAM-1 and/or VCAM-1 are related to coronary artery calcification, and manifest or future cardiovascular disease and cardiovascular mortality in SLE,^{68,69} and an increased risk of clinical cardiovascular disease and atherosclerosis in the general population.⁷⁰ These observations imply that prolonged overexpression of soluble adhesion molecules in CICTD patients may reflect an increased cardiovascular risk in the long term.

We observed that the Angiopoietin-Tie receptor system was disturbed in active (J)DM and EF, with high anti-angiogenic Ang-2, disrupting homeostatic Ang/Tie signaling. Also others have found high Ang-2 in (J)DM, which decreased during treatment.^{71,72} In SSc, similarly increased Ang-2 levels were described,^{73,74} being highest in patients with advanced capillary damage.^{73,75}

Levels of VEGF, PlGF and sVEGFR1 were increased during active (J)DM and EF, which normalized during treatment. High levels of sVEGFR1 are disruptive for angiogenesis.⁷⁶ High serum VEGF, normalizing during treatment, was previously reported in DM, LoS, SLE and MCTD.^{30,68,77–81} Although high levels of the pro-angiogenic molecule VEGF may seem beneficial for angiogenesis, higher VEGF levels have been associated with more severe

vasculopathy: increased VEGF correlated with higher intima media thickness in SLE⁷⁸, with lower capillary density in SSc,⁸² and with pulmonary arterial hypertension, atherosclerosis and myositis in MCTD.⁷⁹ In (J)DM, increased VEGF expression in inflamed muscle and vasculitic lesions correlated with the degree of angiopathy.^{80,81,83} Similarly, high PIGF was related to the development of digital ulcers in SSc.⁸⁴ Taken together, this suggests that in CICTD vasculature is either unresponsive to increased VEGF or PIGF, that VEGF or PIGF upregulation may be an insufficient compensatory mechanism, or that vascular morphology becomes disturbed due to prolonged overexpression.^{22,48,85,86}

Together our results suggest that the identified biomarker profiles reflect on multiple levels a systemic environment of disturbed endothelial function associated with vasculopathy and increased current and/or future cardiovascular risk, especially in CICTD with systemic inflammation. This may have important implications for EF, as in these patients an increased risk of cardiovascular events has not been investigated but may be considerable. In LoS, the more localized nature with little systemic disturbances may translate into the absence of an increased cardiovascular risk.¹⁵

This study has several strengths. Most importantly, samples were taken before start of treatment to capture disease-specific biomarker signatures free of medication effects. All markers and samples were measured simultaneously, enabling us to study their interrelation in the relevant angiopoietic systems. We were able to include relatively large numbers of treatment-naive patients, considering the rarity of the diseases, although for some (e.g. EF) the numbers were still small. Moreover, we collected (paired) follow-up samples to study the development of biomarker profiles during treatment and inactive disease. It would be interesting to follow-up the relationship between prolonged elevation of interferon- and vasculopathy-related markers during clinically inactive disease and the cardiovascular risk profile, especially in patients with EF for which these implications are still unknown. The results of this study have to be interpreted keeping in mind the observational nature of the cohort, with differing sample numbers between diseases, and unmatched controls. Based on these biomarker data in serum, we can only speculate whether these biomarker profiles are similarly represented in the tissues, as within affected tissues, biomarker concentrations may significantly differ from circulating concentrations.

We observed inflammatory and anti-angiogenic biomarker disturbances not only in treatment-naive patients with (J)DM and EF, but also during treatment and, less pronounced, during clinically inactive disease. This suggests that even with well-controlled symptoms, these biomarkers may reflect subclinical inflammation or (mild) endothelial dysfunction. If so, there may be a window of opportunity to support future treat-to-target treatment strategies with biomarker profiling, to achieve not only clinical, but also 'molecular remission'. Such a definition could be useful in long-term clinical follow-up of both inflammatory and vasculopathic disease aspects. Moreover, it may warrant the consideration of a targeted treatment to reduce the anti-angiogenic component in CICTD. For instance, vitamin D has been proposed to restore myeloid angiogenic cell function by reducing the expression

of CXCL10.⁸⁷ Direct targeting of the anti-angiogenic interferon signature by JAK-inhibition or anti-IFN monoclonal antibodies could also be considered.^{72,88} Although endothelial dysfunction can be reduced by control of inflammation,⁸⁹ conventional and more general immunosuppressive therapy which is currently used, often combining prednisone, methotrexate, hydroxychloroquine or other DMARDs, may not sufficiently target the anti-angiogenic IFN signature. Other considerations to reduce vasculopathy and concurrent cardiovascular risk in patients with CICTD may be to ‘hit hard’ at onset of disease, reducing the duration of active disease as the serum evidence of endothelial dysfunction is most pronounced in this period. Future studies will have to point out whether a treat-to-target approach for the vasculopathic component of CICTD may be beneficial in the long term, by monitoring endothelial dysfunction with established biomarkers for vasculopathy, also in patients with clinically inactive disease.^{31,90} Lastly, we identified several new biomarkers which highly correlate with clinical disease activity in (J)DM, LoS or EF, including Ang-2, ICAM-1, Gal-1, TNFR2, CCL2, CCL19, OSF-2 and CCL18.⁹¹ These may potentially serve as novel monitoring tools for disease activity in clinical follow-up.

In conclusion, we have identified disease-specific biomarker profiles in CICTD, which demonstrated an interferon-driven anti-angiogenic environment conducive to leukocyte recruitment to inflamed tissues. These biomarker profiles were related to disease activity, but did not completely normalize during clinically inactive disease. These findings warrant future studies into monitoring of biomarkers for inflammation and endothelial dysfunction during clinical follow-up of patients, possibly supporting a treat-to target approach to minimize cardiovascular risk in the long term.

REFERENCES

1. Gabrielli A, Avedimento E V, Krieg T. Scleroderma. *N. Engl. J. Med.* **2009**, 360 (19), 1989–2003.
2. Wienke J, Deakin CT, Wedderburn LR, et al. Systemic and Tissue Inflammation in Juvenile Dermatomyositis: From Pathogenesis to the Quest for Monitoring Tools. *Front. Immunol.* **2018**, 9, 2951.
3. Vincze M, Der H, Kerekes G, et al. Decreased Flow-Mediated Dilatation with Increased Arterial Stiffness and Thickness as Early Signs of Atherosclerosis in Polymyositis and Dermatomyositis Patients. *Clin. Rheumatol.* **2014**, 33 (11), 1635–1641.
4. Lahoria R, Selcen D, Engel AG. Microvascular Alterations and the Role of Complement in Dermatomyositis. *Brain* **2016**, 139 (Pt 7), 1891–1903.
5. Mak A, Kow NY, Schwarz H, et al. Endothelial Dysfunction in Systemic Lupus Erythematosus - a Case-Control Study and an Updated Meta-Analysis and Meta-Regression. *Sci. Rep.* **2017**, 7 (1), 7320.
6. Soltesz P, Bereczki D, Szodoray P, et al. Endothelial Cell Markers Reflecting Endothelial Cell Dysfunction in Patients with Mixed Connective Tissue Disease. *Arthritis Res. Ther.* **2010**, 12 (3), R78.
7. Mertens JS, Seyger MMB, Thurlings RM, et al. Morphea and Eosinophilic Fasciitis: An Update. *Am. J. Clin. Dermatol.* **2017**, 18 (4), 491–512.
8. Kowalewski C, Kozłowska A, Gorska M, et al. Alterations of Basement Membrane Zone and Cutaneous Microvasculature in Morphea and Extragenital Lichen Sclerosus. *Am. J. Dermatopathol.* **2005**, 27 (6), 489–496.
9. Helmbold P, Fiedler E, Fischer M, et al. Hyperplasia of Dermal Microvascular Pericytes in Scleroderma. *J. Cutan. Pathol.* **2004**, 31 (6), 431–440.
10. Herson S, Brechignac S, Piette JC, et al. Capillary Microscopy during Eosinophilic Fasciitis in 15 Patients: Distinction from Systemic Scleroderma. *Am. J. Med.* **1990**, 88 (6), 598–600.
11. Rozboril MB, Maricq HR, Rodnan GP, et al. Capillary Microscopy in Eosinophilic Fasciitis. A Comparison with Systemic Sclerosis. *Arthritis Rheum.* **1983**, 26 (5), 617–622.
12. Gitiaux C, De Antonio M, Aouizerate J, et al. Vasculopathy-Related Clinical and Pathological Features Are Associated with Severe Juvenile Dermatomyositis. *Rheumatology (Oxford)*. **2016**, 55 (3), 470–479.
13. Silverberg JI, Kwa L, Kwa MC, et al. Cardiovascular and Cerebrovascular Comorbidities of Juvenile Dermatomyositis in US Children: An Analysis of the National Inpatient Sample. *Rheumatology (Oxford)*. **2018**, 57 (4), 694–702.
14. Weng M-Y, Lai EC-C, Kao Yang Y-H. Increased Risk of Coronary Heart Disease among Patients with Idiopathic Inflammatory Myositis: A Nationwide Population Study in Taiwan. *Rheumatology (Oxford)*. **2019**.
15. Hesselvig JH, Kofoed K, Wu JJ, et al. Localized Scleroderma, Systemic Sclerosis and Cardiovascular Risk: A Danish Nationwide Cohort Study. *Acta Derm. Venereol.* **2018**, 98 (3), 361–365.
16. Faccini A, Kaski JC, Camici PG. Coronary Microvascular Dysfunction in Chronic Inflammatory Rheumatoid Diseases. *Eur. Heart J.* **2016**, 37 (23), 1799–1806.
17. Murdaca G, Colombo BM, Cagnati P, et al. Endothelial Dysfunction in Rheumatic Autoimmune Diseases. *Atherosclerosis* **2012**, 224 (2), 309–317.

18. Borghini A, Manetti M, Nacci F, et al. Systemic Sclerosis Sera Impair Angiogenic Performance of Dermal Microvascular Endothelial Cells: Therapeutic Implications of Cyclophosphamide. *PLoS One* **2015**, *10* (6), e0130166.
19. Barbasso Helmers S, Englund P, Engstrom M, et al. Sera from Anti-Jo-1-Positive Patients with Polymyositis and Interstitial Lung Disease Induce Expression of Intercellular Adhesion Molecule 1 in Human Lung Endothelial Cells. *Arthritis Rheum.* **2009**, *60* (8), 2524–2530.
20. Yap HK, Ng SC, Lee BW, et al. Modulation of MHC Expression on Human Endothelial Cells by Sera from Patients with Systemic Lupus Erythematosus. *Clin. Immunol. Immunopathol.* **1993**, *68* (3), 321–326.
21. Meroni P, Ronda N, Raschi E, et al. Humoral Autoimmunity against Endothelium: Theory or Reality? *Trends Immunol.* **2005**, *26* (5), 275–281.
22. Liakouli V, Cipriani P, Marrelli A, et al. Angiogenic Cytokines and Growth Factors in Systemic Sclerosis. *Autoimmun. Rev.* **2011**, *10* (10), 590–594.
23. Chora I, Guiducci S, Manetti M, et al. Vascular Biomarkers and Correlation with Peripheral Vasculopathy in Systemic Sclerosis. *Autoimmun. Rev.* **2015**, *14* (4), 314–322.
24. Ono N, Kai K, Maruyama A, et al. The Relationship between Type 1 IFN and Vasculopathy in Anti-MDA5 Antibody-Positive Dermatomyositis Patients. *Rheumatology (Oxford)*. **2018**.
25. Somers EC, Zhao W, Lewis EE, et al. Type I Interferons Are Associated with Subclinical Markers of Cardiovascular Disease in a Cohort of Systemic Lupus Erythematosus Patients. *PLoS One* **2012**, *7* (5), e37000.
26. Ladislau L, Suarez-Calvet X, Toquet S, et al. JAK Inhibitor Improves Type I Interferon Induced Damage: Proof of Concept in Dermatomyositis. *Brain* **2018**, *141* (6), 1609–1621.
27. Van den Hoogen LL, Van Roon JAG, Mertens JS, et al. Galectin-9 Is an Easy to Measure Biomarker for the Interferon Signature in Systemic Lupus Erythematosus and Antiphospholipid Syndrome. *Ann. Rheum. Dis.* **2018**, *77* (12), 1810–1814.
28. Kim M, Allen B, Korhonen EA, et al. Opposing Actions of Angiopoietin-2 on Tie2 Signaling and FOXO1 Activation. *J. Clin. Invest.* **2016**, *126* (9), 3511–3525.
29. Korhonen EA, Lampinen A, Giri H, et al. Tie1 Controls Angiopoietin Function in Vascular Remodeling and Inflammation. *J. Clin. Invest.* **2016**, *126* (9), 3495–3510.
30. Kikuchi K, Kubo M, Kadono T, et al. Serum Concentrations of Vascular Endothelial Growth Factor in Collagen Diseases. *Br. J. Dermatol.* **1998**, *139* (6), 1049–1051.
31. Mostmans Y, Cutolo M, Giddelo C, et al. The Role of Endothelial Cells in the Vasculopathy of Systemic Sclerosis: A Systematic Review. *Autoimmun. Rev.* **2017**, *16* (8), 774–786.
32. Teixeira V, Tam L-S. Novel Insights in Systemic Lupus Erythematosus and Atherosclerosis. *Front. Med.* **2017**, *4*, 262.
33. Hosseinbarkoobe S, Peters M, Torres-Benito L, et al. The Power of Human Protective Modifiers: PLS3 and CORO1C Unravel Impaired Endocytosis in Spinal Muscular Atrophy and Rescue SMA Phenotype. *Am. J. Hum. Genet.* **2016**, *99* (3), 647–665.
34. Bohan A, Peter JB. Polymyositis and Dermatomyositis (First of Two Parts). *N. Engl. J. Med.* **1975**, *292* (7), 344–347.

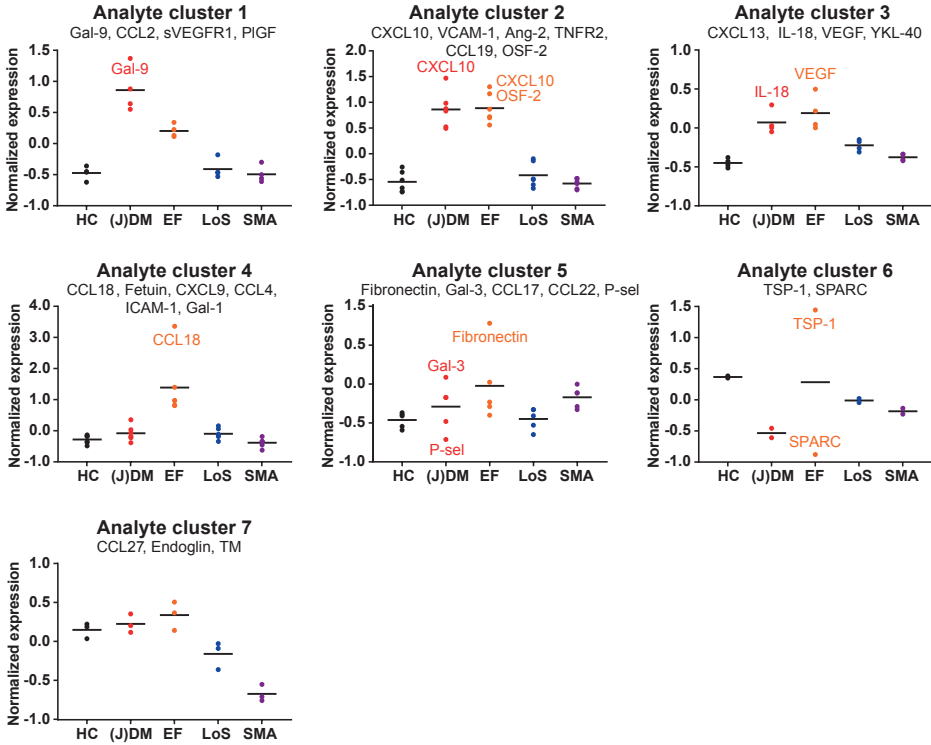
35. Bohan A, Peter JB. Polymyositis and Dermatomyositis (Second of Two Parts). *N. Engl. J. Med.* **1975**, 292 (8), 403–407.
36. Almeida B, Campanilho-Marques R, Arnold K, et al. Analysis of Published Criteria for Clinically Inactive Disease in a Large Juvenile Dermatomyositis Cohort Shows That Skin Disease Is Underestimated. *Arthritis Rheumatol. (Hoboken, N.J.)* **2015**, 67 (9), 2495–2502.
37. Lazarevic D, Pistorio A, Palmisani E, et al. The PRINTO Criteria for Clinically Inactive Disease in Juvenile Dermatomyositis. *Ann. Rheum. Dis.* **2013**, 72 (5), 686–693.
38. Hoogendijk JE, Amato AA, Lecky BR, et al. 119th ENMC International Workshop: Trial Design in Adult Idiopathic Inflammatory Myopathies, with the Exception of Inclusion Body Myositis, 10-12 October 2003, Naarden, The Netherlands. *Neuromuscular disorders : NMD.* England May 2004, pp 337–345.
39. Vianna MAAG, Borges CTL, Borba EF, et al. Myositis in Mixed Connective Tissue Disease: A Unique Syndrome Characterized by Immunohistopathologic Elements of Both Polymyositis and Dermatomyositis. *Arq. Neuropsiquiatr.* **2004**, 62 (4), 923–934.
40. Arkachaisri T, Vilaiyuk S, Li S, et al. The Localized Scleroderma Skin Severity Index and Physician Global Assessment of Disease Activity: A Work in Progress toward Development of Localized Scleroderma Outcome Measures. *J. Rheumatol.* **2009**, 36 (12), 2819–2829.
41. Wadman RI, Stam M, Gijzen M, et al. Association of Motor Milestones, SMN2 Copy and Outcome in Spinal Muscular Atrophy Types 0-4. *Journal of neurology, neurosurgery, and psychiatry.* England April 2017, pp 365–367.
42. de Jager W, Prakken BJ, Bijlsma JWJ, et al. Improved Multiplex Immunoassay Performance in Human Plasma and Synovial Fluid Following Removal of Interfering Heterophilic Antibodies. *J. Immunol. Methods* **2005**, 300 (1–2), 124–135.
43. O'Brien JC, Rainwater YB, Malviya N, et al. Transcriptional and Cytokine Profiles Identify CXCL9 as a Biomarker of Disease Activity in Morphea. *J. Invest. Dermatol.* **2017**, 137 (8), 1663–1670.
44. Mertens JS, de Jong EMGJ, Pandit A, et al. Regarding “Transcriptional and Cytokine Profiles Identify CXCL9 as a Biomarker of Disease Activity in Morphea”. *J. Invest. Dermatol.* **2018**, 138 (5), 1212–1215.
45. Bellutti Enders F, van Wijk F, Scholman R, et al. Correlation of CXCL10, Tumor Necrosis Factor Receptor Type II, and Galectin 9 with Disease Activity in Juvenile Dermatomyositis. *Arthritis Rheumatol. (Hoboken, N.J.)* **2014**, 66 (8), 2281–2289.
46. Wienke J, Bellutti Enders F, Lim J, et al. Galectin-9 and CXCL10 as Biomarkers for Disease Activity in Juvenile Dermatomyositis: A Longitudinal Cohort Study and Multi-Cohort Validation. *Arthritis Rheumatol. (Hoboken, N.J.)* **2019**.
47. Reed AM, Peterson E, Bilgic H, et al. Changes in Novel Biomarkers of Disease Activity in Juvenile and Adult Dermatomyositis Are Sensitive Biomarkers of Disease Course. *Arthritis Rheum.* **2012**, 64 (12), 4078–4086.
48. Fall N, Bove KE, Stringer K, et al. Association between Lack of Angiogenic Response in Muscle Tissue and High Expression of Angiostatic ELR-Negative CXC Chemokines in Patients with Juvenile Dermatomyositis: Possible Link to Vasculopathy. *Arthritis Rheum.* **2005**, 52 (10), 3175–3180.
49. Antonelli A, Ferrari SM, Giuggioli D, et al. Chemokine (C-X-C Motif) Ligand (CXCL)10 in Autoimmune Diseases. *Autoimmun. Rev.* **2014**, 13 (3), 272–280.

50. Jia H, Thelwell C, Dilger P, et al. Endothelial Cell Functions Impaired by Interferon in Vitro: Insights into the Molecular Mechanism of Thrombotic Microangiopathy Associated with Interferon Therapy. *Thromb. Res.* **2018**, 163, 105–116.
51. Lasagni L, Francalanci M, Annunziato F, et al. An Alternatively Spliced Variant of CXCR3 Mediates the Inhibition of Endothelial Cell Growth Induced by IP-10, Mig, and I-TAC, and Acts as Functional Receptor for Platelet Factor 4. *J. Exp. Med.* **2003**, 197 (11), 1537–1549.
52. Lee PY, Li Y, Richards HB, et al. Type I Interferon as a Novel Risk Factor for Endothelial Progenitor Cell Depletion and Endothelial Dysfunction in Systemic Lupus Erythematosus. *Arthritis Rheum.* **2007**, 56 (11), 3759–3769.
53. Ekholm L, Kahlenberg JM, Barbasso Helters S, et al. Dysfunction of Endothelial Progenitor Cells Is Associated with the Type I IFN Pathway in Patients with Polymyositis and Dermatomyositis. *Rheumatology (Oxford)*. **2016**, 55 (11), 1987–1992.
54. Eloranta M-L, Franck-Larsson K, Lovgren T, et al. Type I Interferon System Activation and Association with Disease Manifestations in Systemic Sclerosis. *Ann. Rheum. Dis.* **2010**, 69 (7), 1396–1402.
55. Aanhan E, Schulkens IA, Heusschen R, et al. Different Angioregulatory Activity of Monovalent Galectin-9 Isoforms. *Angiogenesis* **2018**.
56. Kahlenberg JM, Thacker SG, Berthier CC, et al. Inflammasome Activation of IL-18 Results in Endothelial Progenitor Cell Dysfunction in Systemic Lupus Erythematosus. *J. Immunol.* **2011**, 187 (11), 6143–6156.
57. Yamagami H, Kitagawa K, Hoshi T, et al. Associations of Serum IL-18 Levels with Carotid Intima-Media Thickness. *Arterioscler. Thromb. Vasc. Biol.* **2005**, 25 (7), 1458–1462.
58. Hulthe J, McPheat W, Samnegard A, et al. Plasma Interleukin (IL)-18 Concentrations Is Elevated in Patients with Previous Myocardial Infarction and Related to Severity of Coronary Atherosclerosis Independently of C-Reactive Protein and IL-6. *Atherosclerosis* **2006**, 188 (2), 450–454.
59. Formanowicz D, Wanic-Kossowska M, Pawliczak E, et al. Usefulness of Serum Interleukin-18 in Predicting Cardiovascular Mortality in Patients with Chronic Kidney Disease—Systems and Clinical Approach. *Sci. Rep.* **2015**, 5, 18332.
60. Blankenberg S, Tiret L, Bickel C, et al. Interleukin-18 Is a Strong Predictor of Cardiovascular Death in Stable and Unstable Angina. *Circulation* **2002**, 106 (1), 24–30.
61. Kubo M, Ihn H, Yamane K, et al. Increased Serum Levels of Soluble Vascular Cell Adhesion Molecule-1 and Soluble E-Selectin in Patients with Polymyositis/dermatomyositis. *Br. J. Dermatol.* **2000**, 143 (2), 392–398.
62. Bloom BJ, Miller LC, Blier PR. Soluble Adhesion Molecules in Pediatric Rheumatic Diseases. *J. Rheumatol.* **2002**, 29 (4), 832–836.
63. Figarella-Branger D, Schleinitz N, Boutiere-Albanese B, et al. Platelet-Endothelial Cell Adhesion Molecule-1 and CD146: Soluble Levels and in Situ Expression of Cellular Adhesion Molecules Implicated in the Cohesion of Endothelial Cells in Idiopathic Inflammatory Myopathies. *J. Rheumatol.* **2006**, 33 (8), 1623–1630.
64. Ihn H, Fujimoto M, Sato S, et al. Increased Levels of Circulating Intercellular Adhesion Molecule-1 in Patients with Localized Scleroderma. *J. Am. Acad. Dermatol.* **1994**, 31 (4), 591–595.

65. Kjaergaard AG, Dige A, Krog J, et al. Soluble Adhesion Molecules Correlate with Surface Expression in an in Vitro Model of Endothelial Activation. *Basic Clin. Pharmacol. Toxicol.* **2013**, *113* (4), 273–279.
66. Sallum AME, Kiss MHB, Silva CAA, et al. Difference in Adhesion Molecule Expression (ICAM-1 and VCAM-1) in Juvenile and Adult Dermatomyositis, Polymyositis and Inclusion Body Myositis. *Autoimmun. Rev.* **2006**, *5* (2), 93–100.
67. Lee JS, Park HS, Yoon HS, et al. CD34 Stromal Expression Is Inversely Proportional to Smooth Muscle Actin Expression and Extent of Morphea. *J. Eur. Acad. Dermatol. Venereol.* **2018**, *32* (12), 2208–2216.
68. Rho YH, Chung CP, Oeser A, et al. Novel Cardiovascular Risk Factors in Premature Coronary Atherosclerosis Associated with Systemic Lupus Erythematosus. *J. Rheumatol.* **2008**, *35* (9), 1789–1794.
69. Gustafsson JT, Simard JF, Gunnarsson I, et al. Risk Factors for Cardiovascular Mortality in Patients with Systemic Lupus Erythematosus, a Prospective Cohort Study. *Arthritis Res. Ther.* **2012**, *14* (2), R46.
70. Blankenberg S, Barbaux S, Tiret L. Adhesion Molecules and Atherosclerosis. *Atherosclerosis* **2003**, *170* (2), 191–203.
71. Conklin LS, Merkel PA, Pachman LM, et al. Serum Biomarkers of Glucocorticoid Response and Safety in Anti-Neutrophil Cytoplasmic Antibody-Associated Vasculitis and Juvenile Dermatomyositis. *Steroids* **2018**, *140*, 159–166.
72. Guo X, Higgs BW, Rebelatto M, et al. Suppression of Soluble T Cell-Associated Proteins by an Anti-Interferon-Alpha Monoclonal Antibody in Adult Patients with Dermatomyositis or Polymyositis. *Rheumatology (Oxford)*. **2014**, *53* (4), 686–695.
73. Michalska-Jakubus M, Kowal-Bielecka O, Chodorowska G, et al. Angiotensin-1 and -2 Are Differentially Expressed in the Sera of Patients with Systemic Sclerosis: High Angiotensin-2 Levels Are Associated with Greater Severity and Higher Activity of the Disease. *Rheumatology (Oxford)*. **2011**, *50* (4), 746–755.
74. Dunne J V, Keen KJ, Van Eeden SF. Circulating Angiotensin and Tie-2 Levels in Systemic Sclerosis. *Rheumatol. Int.* **2013**, *33* (2), 475–484.
75. Riccieri V, Vasile M, Macri V, et al. Successful Immunosuppressive Treatment of Dermatomyositis: A Nailfold Capillaroscopy Survey. *J. Rheumatol.* **2010**, *37* (2), 443–445.
76. Kendall RL, Thomas KA. Inhibition of Vascular Endothelial Cell Growth Factor Activity by an Endogenously Encoded Soluble Receptor. *Proc. Natl. Acad. Sci. U. S. A.* **1993**, *90* (22), 10705–10709.
77. Dzikowska-Bartkowiak B, Zebrowska A, Wagrowska-Danielewicz M, et al. [Systemic sclerosis and scleroderma circumscripta--disturbances of selected serum parameters which are responsible for vascular changes and CD34 expression in involved skin]. *Przegl. Lek.* **2009**, *66* (12), 1040–1045.
78. Colombo BM, Cacciapaglia F, Puntoni M, et al. Traditional and Non Traditional Risk Factors in Accelerated Atherosclerosis in Systemic Lupus Erythematosus: Role of Vascular Endothelial Growth Factor (VEGATS Study). *Autoimmun. Rev.* **2009**, *8* (4), 309–315.
79. Distler JHW, Strapatsas T, Huscher D, et al. Dysbalance of Angiogenic and Angiostatic Mediators in Patients with Mixed Connective Tissue Disease. *Ann. Rheum. Dis.* **2011**, *70* (7), 1197–1202.
80. Chai K-X, Chen Y-Q, Fan P-L, et al. STROBE: The Correlation of Cyr61, CTGF, and VEGF with Polymyositis/dermatomyositis. *Medicine (Baltimore)*. **2018**, *97* (34), e11775.

81. Grundtman C, Tham E, Ulfgren A-K, et al. Vascular Endothelial Growth Factor Is Highly Expressed in Muscle Tissue of Patients with Polymyositis and Patients with Dermatomyositis. *Arthritis Rheum.* **2008**, *58* (10), 3224–3238.
82. Choi J-J, Min D-J, Cho M-L, et al. Elevated Vascular Endothelial Growth Factor in Systemic Sclerosis. *J. Rheumatol.* **2003**, *30* (7), 1529–1533.
83. Baumann M, Gumpold C, Mueller-Felber W, et al. Pattern of Myogenesis and Vascular Repair in Early and Advanced Lesions of Juvenile Dermatomyositis. *Neuromuscul. Disord.* **2018**, *28* (12), 973–958.
84. Avouac J, Meune C, Ruiz B, et al. Angiogenic Biomarkers Predict the Occurrence of Digital Ulcers in Systemic Sclerosis. *Ann. Rheum. Dis.* **2012**, *71* (3), 394–399.
85. Distler O, Distler JHW, Scheid A, et al. Uncontrolled Expression of Vascular Endothelial Growth Factor and Its Receptors Leads to Insufficient Skin Angiogenesis in Patients with Systemic Sclerosis. *Circ. Res.* **2004**, *95* (1), 109–116.
86. Manetti M, Guiducci S, Ibba-Manneschi L, et al. Mechanisms in the Loss of Capillaries in Systemic Sclerosis: Angiogenesis versus Vasculogenesis. *J. Cell. Mol. Med.* **2010**, *14* (6A), 1241–1254.
87. Reynolds JA, Rosenberg AZ, Smith CK, et al. Brief Report: Vitamin D Deficiency Is Associated With Endothelial Dysfunction and Increases Type I Interferon Gene Expression in a Murine Model of Systemic Lupus Erythematosus. *Arthritis Rheumatol. (Hoboken, N.J.)* **2016**, *68* (12), 2929–2935.
88. Higgs BW, Zhu W, Morehouse C, et al. A Phase 1b Clinical Trial Evaluating Sifalimumab, an Anti-IFN-Alpha Monoclonal Antibody, Shows Target Neutralisation of a Type I IFN Signature in Blood of Dermatomyositis and Polymyositis Patients. *Ann. Rheum. Dis.* **2014**, *73* (1), 256–262.
89. Parker B, Al-Husain A, Pemberton P, et al. Suppression of Inflammation Reduces Endothelial Microparticles in Active Systemic Lupus Erythematosus. *Ann. Rheum. Dis.* **2014**, *73* (6), 1144–1150.
90. Tselios K, Sheane BJ, Gladman DD, et al. Optimal Monitoring For Coronary Heart Disease Risk in Patients with Systemic Lupus Erythematosus: A Systematic Review. *J. Rheumatol.* **2016**, *43* (1), 54–65.
91. Mertens JS, de Jong EMGJ, van den Hoogen LL, et al. The Identification of CCL18 as Biomarker of Disease Activity in Localized Scleroderma. *J. Autoimmun.* **2019**.

SUPPLEMENTARY MATERIAL



Supplementary figure 1. K-means clustering of analytes by median analyte expression per group.

Biomarkers were mean-centered and scaled. Each dot represents the median expression of an analyte per disease; bars represent median normalized expression values of analytes in each cluster per disease. Red = myositis, orange = EF, purple = SMA, blue = LoS, black = HC. *HC* = healthy controls ($n=22$), *LoS* = Localized scleroderma ($n=30$), *EF* = eosinophilic fasciitis ($n=8$), *(J)DM* = (juvenile) dermatomyositis ($n=33$), *SMA* = spinal muscular atrophy ($n=43$).

Supplementary table 1. Differential expression of analytes between each disease group and healthy controls.

Analyte	P value compared to HC			
	(J)DM	EF	LoS	SMA
CXCL10	<0.0001	<0.0001	0.0001	0.3196
TNFR2	<0.0001	<0.0001	0.0002	0.7558
Gal-9	<0.0001	<0.0001	0.0007	0.9059
VCAM-1	<0.0001	<0.0001	0.0030	0.8295
CCL19	<0.0001	<0.0001	0.0030	0.0516
CXCL13	<0.0001	0.0001	0.0006	0.0727
IL-18	<0.0001	0.0010	0.0083	0.4079
Ang-2	0.0007	0.0149	0.0428*	0.7558
YKL-40	0.0141	0.0026	0.1459	0.6596
ICAM-1	0.0052	0.0002	0.0543	0.7558
CCL2	<0.0001	0.0133	0.5175	0.7558
sVEGFR1	<0.0001	0.0062	0.3192	0.7558
OSF-2	<0.0001	0.0050	0.0879	0.3892
TSP-1	<0.0001*	0.0365	0.0568	0.0516
SPARC	0.0016*	0.0199*	0.3092	0.4079
PIGF	<0.0001	0.1679	0.2791	0.9668
Gal-3	0.0239	0.2354	0.8355	0.6596
P-sel	0.0245*	0.3491	0.2995	0.6596
Gal-1	0.0814	0.0003	0.2541	0.4079
Fibronectin	0.1886	0.0013	0.6384	0.8005
Fetuin	0.1651	0.0098	0.3742	0.0716
VEGF	0.2044	0.0323	0.2092	0.7558
CCL4	0.3165	0.0432	0.4540	0.9059
CCL18	0.3206	0.0000	0.0003	0.9653
CXCL9	0.4302	0.0007	0.0225	0.4079
CCL17	0.3725	0.0209	0.2930	0.0374

(Continued)

Supplementary table 1. Differential expression of analytes between each disease group and healthy controls.

Analyte	P value compared to HC			
	(J)DM	EF	LoS	SMA
TM	0.2921	0.0519	0.3189	0.0355*
CCL22	0.0255	0.4353	0.4746	0.0106
Endoglin	0.4112	0.4735	0.4241	0.0355*
CCL27	0.2501	0.3198	0.0439*	0.0010*
E-sel	0.0942	0.2714	0.4931	0.9059
Ang-1	0.1565	0.2456	0.1483	0.0716
PDGF-BB	0.2091	0.3170	0.0868	0.8295
Tie-2	0.4878	0.1184	0.2505	0.8005
PAI-1	0.1862	0.3705	1.0000	0.8067
OSM	0.9740	0.4797	0.3397	0.6596
TWEAK	0.3653	0.5325	0.2693	0.9059

Multiplicity-adjusted p values from Kruskal-Wallis test with Dunn's post hoc test per disease group as described in methods ((J)DM, EF, LoS) or Mann-Whitney U test with correction for multiple testing by false discovery rate (SMA). *Lower in disease than in healthy controls. (J)DM = (juvenile) dermatomyositis, EF = eosinophilic fasciitis, LoS = localized scleroderma, SMA = spinal muscular atrophy.

Supplementary table 2. Differential expression of analytes between treatment-naive and inactive patients per autoimmune disease.

JDM				EF				LoS			
Analyte	Treatment-naive	Inactive	Pvalue	Analyte	Treatment-naive	Inactive	Pvalue	Analyte	Treatment-naive	Inactive	Pvalue
CXCL10	2838.4 (130.9)	176.1 (149.9)	<0.0001	Ang-2	6829.3 (4859.1)	2791.7 (207.2)	0.0004	CCL18	20711.8 (20711.8)	8801.2 (8801.2)	0.0106
Gal-9	15298.7 (7642.7)	3648.4 (2035.7)	<0.0001	Gal-1	27136.2 (2871.4)	182741 (2664.3)	0.0015	Tie-1	862.7 (862.7)	596.5 (596.5)	0.0157
Ang-2	6616 (3856.8)	2918.5 (993.2)	<0.0001	CXCL9	33.7 (5.1)	0.6 (0)	0.0019	CXCL10	355.4 (355.4)	224.5 (224.5)	0.0570
TNFR2	3926.3 (1272.5)	1928.2 (634.1)	<0.0001	Tie-1	2417.0 (1177.2)	821.0 (431.1)	0.0054	TNFR2	2313.2 (2313.2)	1815.8 (1815.8)	0.0951
CCL2	355.3 (174.8)	135.5 (82.4)	<0.0001	ICAM-1	3975477 (101313)	237245 (64430.3)	0.0056	ICAM-1	250750 (250750)	212207.4 (212207.4)	0.1021
VCAM-1	3003700 (116600)	1955200 (686600)	<0.0001	CXCL13	52.2 (68)	3.1 (10.7)	0.0058	Tie-2	9481.8 (9481.8)	10931.3 (10931.3)	0.1099
CCL19	269.2 (150.6)	113.3 (69.9)	<0.0001	OSF-2	61212.8 (17206)	42648.2 (5245.6)	0.0059	VEGF	162.9 (162.9)	113.6 (113.6)	0.1253
OSF-2	57917.4 (13237.3)	44909.2 (8795.1)	<0.0001	CCL2	236.1 (60.5)	134.9 (130.2)	0.0072	OSF-2	40509.2 (40509.2)	45052.7 (45052.7)	0.1305
sVEGFR1	1903.6 (868.3)	1424 (424.7)	<0.0001	Gal-3	15040 (5499.7)	9869.8 (1989)	0.0081	YKL-40	68906.1 (68906.1)	60151.5 (60151.5)	0.1696
Tie-1	3363.9 (2278.3)	15571 (1783.2)	<0.0001	CCL19	295 (93.8)	1371 (80.8)	0.0081	TWEAK	8810.5 (8810.5)	9693.1 (9693.1)	0.1923
YKL-40	88423.7 (67864.2)	41356 (29813.4)	<0.0001	CCL18	107239.9 (45249.5)	11626.6 (16055)	0.0125	TM	3903.8 (3903.8)	4349.3 (4349.3)	0.1992
CCL27	442.7 (503.9)	184.2 (170.4)	<0.0001	CXCL10	2628 (1926.7)	303.9 (228.5)	0.0206	P-sel	151646.1 (151646.1)	207612.6 (207612.6)	0.2128

(Continued)

Supplementary table 2. Differential expression of analytes between treatment-naive and inactive patients per autoimmune disease.

Analyte	JDM			EF			LoS				
	Treatment-naive	Inactive	Pvalue	Analyte	Treatment-naive	Inactive	Pvalue	Analyte	Treatment-naive	Inactive	Pvalue
ICAM-1	275289.8 (193250)	197295.4 (81742)	<0.0001	Gal-9	7219.4 (2886.9)	4098.9 (2311.2)	0.0339	Ang-2	3159 (3159)	3478.6 (3478.6)	0.2167
IL-18	206.4 (164.7)	105.7 (73.5)	<0.0001	CCL17	436.4 (240.4)	283.1 (113)	0.0645	CCL27	233 (233)	289.2 (289.2)	0.2181
CXCL13	56 (111)	17.4 (27)	0.0001	IL-18	154 (54.9)	108.7 (70)	0.0703	VCAM-1	2187700 (2187700)	2430700 (2430700)	0.2357
PIGF	31.2 (14.8)	25.5 (12.1)	0.0002	Endoglin	1201.5 (354.1)	756 (580.1)	0.0847	PIGF	23.4 (23.4)	24.6 (24.6)	0.2368
Gal-1	21187.9 (7973.2)	16220.8 (4696.8)	0.0006	TNFR2	3530.3 (2437)	2006.5 (862.4)	0.0951	Gal-9	3387 (3387)	3129.8 (3129.8)	0.2477
Fibronectin	128670000 (62059000)	85405000 (68522000)	0.0024	Tie-2	11758.3 (3231.9)	10265.7 (3587.3)	0.1099	Gal-1	17414.4 (17414.4)	18929.5 (18929.5)	0.2618
Gal-3	17760.6 (11401.6)	12472 (3641.3)	0.0036	sVEGFR1	1732.3 (248.7)	1617 (507.6)	0.1105	Fetuin	70713000 (70713000)	83920500 (83920500)	0.2895
Fetuin	66404000 (33243750)	56796000 (21176000)	0.0296	VEGF	243.9 (143.4)	175.4 (155)	0.1253	CXCL9	0.6 (0.6)	0.6 (0.6)	0.3078
VEGF	186.7 (167.6)	114 (115)	0.0350	Fetuin	95045500 (14890750)	86922000 (23701500)	0.1993	PDGF-BB	11313.9 (11313.9)	11182.2 (11182.2)	0.3109
SPARC	68508.8 (85640)	99881.3 (105426)	0.0441*	E-sel	52801 (5596.2)	2763.5 (1415)	0.1446	CCL17	322.1 (322.1)	296.1 (296.1)	0.3289
CCL17	293.1 (237.4)	355.8 (273.1)	0.0526	YKL-40	112085.6 (286149.5)	138447.8 (166018.8)	0.1696	CCL19	137.6 (137.6)	132.9 (132.9)	0.3711

(Continued)

Supplementary table 2. Differential expression of analytes between treatment-naive and inactive patients per autoimmune disease.

Analyte	JDM			EF			LoS				
	Treatment-naive	Inactive	Pvalue	Analyte	Treatment-naive	Inactive	Pvalue	Analyte	Treatment-naive	Inactive	Pvalue
TM	4202 (1371)	3697.6 (1280.7)	0.0661	TWEAK	8921.2 (3687.1)	8107.3 (2559.2)	0.1923	CXCL13	10.1 (10.1)	9.5 (9.5)	0.3942
Endoglin	1176.7 (583.1)	1053.1 (387.7)	0.1421	TM	4669.8 (1509.9)	3771.7 (1206.4)	0.1992	SPARC	108609.8 (108609.8)	99712 (99712)	0.3995
PAI-1	1699650 (952600)	1598300 (754100)	0.1942	CCL22	876.5 (480.7)	759.4 (223)	0.2101	OSM	4.9 (4.9)	2.3 (2.3)	0.4023
CXCL9	0.6 (0)	0.6 (0)	0.2700	P-sel	21074.8 (250070.3)	131233.9 (110300.6)	0.2201	sVEGFR1	1241.2 (1241.2)	1292 (1292)	0.4048
TSP-1	76018500 (96052750)	79297000 (76788000)	0.3347	CCL4	219.3 (60.8)	140.4 (84.8)	0.2331	Fibronectin	92328000 (92328000)	103430000 (103430000)	0.4055
CCL22	972.7 (526.4)	1048.3 (625.2)	0.3577	VCAM-1	3033600 (1350925)	2310650 (758500)	0.2357	IL-18	112.3 (112.3)	111.4 (111.4)	0.4350
CCL4	148.1 (63.8)	130 (70)	0.3648	Ang-1	56468.1 (21464)	40731.7 (10752)	0.2505	CCL22	871.4 (871.4)	845.3 (845.3)	0.4454
PDGF-BB	10792.3 (5600.1)	11793.2 (6206.6)	0.3746	PDGF-BB	14108 (2683.5)	14004.1 (4189.5)	0.2687	CCL2	134.4 (134.4)	138.1 (138.1)	0.4614
CCL18	6324.9 (11403.4)	5341.7 (6260.9)	0.3760	CCL27	409.6 (142.8)	265.4 (110.6)	0.3870	CCL4	143.8 (143.8)	142.6 (142.6)	0.4647
Ang-1	35332 (32320.3)	33011.3 (22430.3)	0.3971	Fibronectin	202250000 (66467500)	213640000 (83640000)	0.4182	Ang-1	34669.9 (34669.9)	33701.6 (33701.6)	0.4700
E-sel	5813.6 (3596.9)	5616.5 (3708.4)	0.4208	SPARC	24957.5 (84467.3)	41506.2 (43980.9)	0.4190	TSP-1	116560000 (116560000)	117985000 (117985000)	0.4859
P-sel	102330.3 (151987.7)	110112.9 (119501)	0.4212	OSM	5.2 (4.9)	8.6 (17.3)	0.4815	E-sel	4210.7 (4210.7)	4006.8 (4006.8)	0.5641

(Continued)

Supplementary table 2. Differential expression of analytes between treatment-naive and inactive patients per autoimmune disease.

Analyte	(J)DM			EF			LoS				
	Treatment-naive	Inactive	Pvalue	Analyte	Treatment-naive	Inactive	Pvalue	Analyte	Treatment-naive	Inactive	Pvalue
Tie-2	9673.7 (4476.5)	9682.9 (4264.6)	0.4310	TSP-1	206985000 (89205000)	150770000 (98608000)	0.4859	Endoglin	1085.5 (1085.5)	1252.3 (1252.3)	0.5943
OSM	1.4 (4.5)	2.5 (5.3)	0.4814	PIGF	27.9 (10.5)	24.6 (20.8)	0.5405	PAI-1	1915500 (1915500)	1958400 (1958400)	0.7721
TWEAK	9448.5 (3422.6)	9302.7 (3138.7)	0.4912	PAI-1	2384600 (347175)	1540200 (727975)	0.6065	Gal-3	14132.2 (14132.2)	12881.2 (12881.2)	1.0000

Median (IQR) are shown for biomarker values. Multiplicity-adjusted p values from Kruskal-Wallis test with Dunn's post hoc test per disease group as described in methods. (J)DM = (juvenile) dermatomyositis, EF = eosinophilic fasciitis, LoS = localized scleroderma. *Lower in active disease than remission.

Supplementary table 3. Differential expression of analytes between active and paired follow-up samples per autoimmune disease.

Analyte	(J)DM				EF				LoS					
	Active	Follow-up	Pvalue	FDR	Analyte	Active	Follow-up	Pvalue	FDR	Analyte	Active	Follow-up	Pvalue	FDR
TNFR2	3914.8 (1580.3)	2283 (1096.7)	<0.0001	<0.0001	CCL2	140.8(28.2)	136.4 (73.2)	0.0625	0.1875	CXCL10	94.8 (112.1)	109.5 (28)	0.0020	0.0742
CXCL10	2432.6 (1546.5)	298.9 (778.5)	<0.0001	<0.0001	CCL19	8518.4 (3428.5)	8797 (314.5)	0.0625	0.1875	CXCL13	9672.3 (2524.1)	9715.1 (1974.5)	0.0059	0.1113
Gal-9	14107.5 (8226.4)	4449.4 (2725.6)	<0.0001	<0.0001	CCL27	208.4 (44.6)	164.2 (13)	0.0625	0.1875	Endoglin	131.5 (94.9)	126.3 (97.3)	0.0195	0.2474
CCL2	336.2 (162.4)	142.3 (107)	<0.0001	<0.0001	TNFR2	197.2 (22.1)	194.7 (69.2)	0.0625	0.1875	CCL18	165.2 (54.6)	142.4 (50.6)	0.0273	0.2598
VCAM-1	2966750 (1243425)	2090900 (532800)	<0.0001	<0.0001	Gal-1	367.4 (112.8)	305.1 (80.6)	0.0625	0.1875	CXCL9	329.7 (221)	378.4 (209.9)	0.0591	0.4488
CCL19	2873 (147.6)	145.8 (83.1)	<0.0001	0.0001	Gal-9	309.8 (74.2)	101.3 (26.1)	0.0625	0.1875	CCL19	147.7 (73.6)	141.8 (35.1)	0.1055	0.5010
OSF-2	52480.9 (12113.6)	43203.5 (6817.8)	<0.0001	0.0001	OSF-2	589.2 (203.1)	567.8 (219.4)	0.0625	0.1875	Gal-9	846.9 (342.8)	1019.7 (372.9)	0.1055	0.5010
Ang-2	5668.9 (5326)	3295.7 (1293.4)	<0.0001	0.0001	Ang-1	344.1 (296.4)	249.3 (72.8)	0.0625	0.1875	TM	259.8 (241.8)	243.1 (130.4)	0.1055	0.5010
YKL-40	82729.7 (82809.9)	38764.4 (27775.4)	0.0002	0.0009	PDGF-BB	62 (53.2)	12.8 (160.1)	0.0625	0.1875	Tie-2	321 (45.9)	7.9 (5.7)	0.1309	0.5525
Gal-1	22996.6 (8665.7)	17551.7 (5197.5)	0.0025	0.0096	CCL18	276 (5.7)	36.1 (8.1)	0.0625	0.1875	P-sel	23.1 (8)	23.2 (12.3)	0.1602	0.5533
CCL27	319.1 (411.9)	131.7 (155.3)	0.0035	0.0121	ICAM-1	250.3 (118.5)	221.7 (74.4)	0.0625	0.1875	PDGF-BB	182.6 (111.6)	149.2 (142.1)	0.1602	0.5533
ICAM-1	275289.8 (154686.4)	267510.6 (117838.6)	0.0164	0.0520	VCAM-1	1258.8 (2129.8)	507.1 (362.2)	0.0625	0.1875	SPARC	507.7 (405.3)	179.2 (253.3)	0.1925	0.5652

(Continued)

Supplementary table 3. Differential expression of analytes between active and paired follow-up samples per autoimmune disease.

Analyte	(J)DM				EF				LoS					
	Active	Follow-up	Pvalue	FDR	Analyte	Active	Follow-up	Pvalue	FDR	Analyte	Active	Follow-up	Pvalue	FDR
sVEGFR1	1828.1 (1082.1)	1666.7 (829.5)	0.0395	0.1085	Tie-1	3032.4 (460.5)	2205.8 (523)	0.0625	0.1875	CCL4	1963.2 (533.2)	1669.2 (755.3)	0.1934	0.5652
CCL22	1008.9 (644.7)	808 (797.9)	0.0425	0.1085	CXCL10	60977.8 (151386.6)	113023.7 (97221.3)	0.1250	0.2566	IL-18	85703.2 (96095)	80512 (114146.6)	0.2754	0.6800
CCL17	312.1 (210.7)	388.4 (290.8)	0.0457	0.1085	Endoglin	1710.4 (103.4)	1790.2 (465.8)	0.1250	0.2566	OSF-2	1414.4 (475.2)	14211 (583.2)	0.2754	0.6800
Fetuin	64154500 (35428500)	55077500 (23557500)	0.0457	0.1085	Ang-2	26051 (1409.6)	19835.9 (3508.9)	0.1250	0.2566	OSM	17870.4 (4745.2)	17572.6 (7588.2)	0.2863	0.6800
SPARC	68508.8 (69405.8)	98814 (90706.9)	0.0526	0.1177	Tie-2	7077.3 (2292.6)	4278 (912)	0.1250	0.2566	TNFR2	3649.1 (2384.1)	2888.8 (359.9)	0.3223	0.7204
IL-18	217.9 (167.6)	176.9 (160.8)	0.0839	0.1772	PAI-1	152726 (98219.5)	153293.4 (169052.4)	0.1250	0.2566	Gal-3	248744.5 (203124.3)	264158.8 (211076.3)	0.3750	0.7793
Fibronectin	126905000 (64742500)	107590000 (65888000)	0.0951	0.1902	TSP-1	5274.9 (1689.5)	5588.3 (4512.4)	0.1250	0.2566	E-sel	4159.7 (2413.9)	3958.8 (2411.3)	0.4316	0.7793
CXCL13	39.9 (69.6)	29.7 (53.5)	0.1245	0.2366	CXCL9	4588.8 (1757.1)	4292.8 (1791.9)	0.1875	0.3656	PAI-1	3119.4 (733.8)	3602 (1364.9)	0.4316	0.7793
CCL4	145.5 (52.7)	150.1 (80.1)	0.1875	0.3393	TWEAK	1155.6 (377.4)	1060.9 (261.4)	0.3125	0.4875	TWEAK	954.9 (146.5)	11691 (530.1)	0.4922	0.7793
TSP-1	82022000 (105487300)	69715000 (71706250)	0.2292	0.3865	CCL17	57290.9 (9820.6)	42802.2 (2633.3)	0.3125	0.4875	ICAM-1	49378.6 (10906.1)	43637.6 (9578.5)	0.4922	0.7793
CXCL9	0.6 (0)	0.6 (0)	0.2340	0.3865	PIGF	68194 (63867.6)	45011.5 (18475.6)	0.3125	0.4875	VCAM-1	34707.4 (5654.9)	35513.1 (12420.6)	0.4922	0.7793

(Continued)

Supplementary table 3. Differential expression of analytes between active and paired follow-up samples per autoimmune disease.

Analyte	(J)DM				EF				LoS					
	Active	Follow-up	Pvalue	FDR	Analyte	Active	Follow-up	Pvalue	FDR	Analyte	Active	Follow-up	Pvalue	FDR
Tie-1	2960.5 (2047)	2538.4 (1466.8)	0.2897	0.4586	Gal-3	7104.3 (3070.6)	3954 (1468.8)	0.3125	0.4875	TSP-1	3580.6 (1080.4)	3568.8 (8171)	0.4922	0.7793
VEGF	186.7 (164.6)	172.5 (105.7)	0.3449	0.5041	OSM	9186.9 (4087.5)	9003.6 (3431.7)	0.3125	0.4875	CCL22	10220.1 (2714.4)	10672.6 (1475)	0.5566	0.8461
E-sel	6083.3 (2878.7)	6345.2 (4836.8)	0.3449	0.5041	CXCL13	15611.6 (7749.9)	10696.3 (1367.3)	0.4375	0.5884	CCL17	11482 (1603.2)	10819.2 (1487.3)	0.6250	0.8482
PDGF-BB	11414.5 (6210.6)	12672.9 (8219.8)	0.3596	0.5061	VEGF	121450.5 (34341.9)	84101.3 (116507.7)	0.4375	0.5884	VEGF	72045.8 (56579.7)	62911.4 (46077.5)	0.6250	0.8482
Gal-3	15362.1 (9678.3)	14542.9 (90271)	0.4223	0.5732	YKL-40	89038.4 (64399.3)	11892.7 (16042.3)	0.4375	0.5884	Ang-1	23746.7 (34809.8)	9245 (8267.7)	0.6250	0.8482
PIGF	29.9 (16.5)	28.7 (13.3)	0.4908	0.6431	Fibronectin	2511400 (421200)	1656300 (1150200)	0.4375	0.5884	sVEGFR1	2228900 (910275)	1713300 (1460125)	0.6953	0.9111
OSM	1.4 (4.8)	2.6 (9.9)	0.5595	0.7088	SPARC	369435.8 (47639.3)	212675 (85091.9)	0.5839	0.7386	CCL27	288180.8 (152513.7)	202054.7 (111236.5)	0.7695	0.9433
P-sel	119075.5 (167015.7)	141127.4 (177866.3)	0.5838	0.7156	IL-18	2705600 (728200)	1891500 (595100)	0.6250	0.7386	YKL-40	2312650 (360650)	2234650 (1032575)	0.7695	0.9433
Ang-1	33313.8 (41250.2)	40019.7 (20014.3)	0.6431	0.7637	CCL22	12003.9 (5957.7)	14716.7 (2239.5)	0.6250	0.7386	Ang-2	12728.3 (2813.8)	11568.9 (3817)	0.8457	1.0000
TWEAK	9106.4 (4399.9)	8970.2 (3228.9)	0.7469	0.8566	Fetuin	87163000 (10079000)	91655000 (23170000)	0.6250	0.7386	PIGF	66193500 (34697500)	87709500 (31423500)	0.9219	1.0000
PAI-1	1612800 (908375)	1656300 (861350)	0.7898	0.8566	CCL4	164410000 (24490000)	200400000 (28140000)	0.8125	0.9054	Tie-1	113435000 (63260500)	100780000 (39156000)	0.9219	1.0000

(Continued)

Supplementary table 3. Differential expression of analytes between active and paired follow-up samples per autoimmune disease.

Analyte	(J)DM			EF			LoS							
	Active	Follow-up	Pvalue	FDR	Analyte	Active	Follow-up	Pvalue	FDR	Analyte	Active	Follow-up	Pvalue	FDR
CCL18	6394.6 (13200.5)	7639.8 (7335.9)	0.7951	0.8566	E-sel	278400000 (37650000)	1706900000 (400000000)	0.8125	0.9054	CCL2	127975000 (53345000)	123710000 (37645000)	1.0000	1.0000
Endoglin	1174.6 (535)	1052.9 (335.9)	0.8115	0.8566	sVEGFR1	5.5 (4.7)	10.2 (6)	1.0000	1.0000	Gal-1	9.8 (21.5)	3.8 (24.4)	1.0000	1.0000
TM	4323.4 (1431.5)	4177.2 (1662.6)	0.8774	0.9011	P-sel	1.7 (34.2)	0.6 (0)	1.0000	1.0000	Fetuin	2 (25.3)	0.6 (0.2)	1.0000	1.0000
Tie-2	9938.6 (3025.3)	10388.5 (2007.9)	0.9888	0.9888	TM	1726.4 (2310)	806.9 (664)	1.0000	1.0000	Fibronectin	6541 (461.5)	639.6 (421.9)	1.0000	1.0000

Median (IQR) are shown for biomarker values. Wilcoxon matched-pairs signed rank test with correction for multiple testing by false discovery rate (FDR). (J)DM = (juvenile) dermatomyositis, EF = eosinophilic fasciitis, LoS = localized scleroderma.

Supplementary table 4. Spearman rank correlations of analytes with clinical measures of disease activity per autoimmune disease.

	(J)DM			EF			LoS				
	CMAS	PGA		mLoSSI	VAS activity	LoSDI	VAS damage	mLoSSI	VAS activity	LoSDI	VAS damage
Ang-2	-0.68****	0.66****		0.74***	0.66**	0.39 ^{TR}	NS	0.40**	0.41***	NS	NS
CXCL10	-0.62****	0.83****		0.69**	0.52*	NS	NS	0.39**	0.31*	NS	NS
Gal-9	-0.61****	0.79****		0.68**	0.71***	NS	NS	0.31*	NS	NS	0.25*
TNFR2	-0.6****	0.71****		0.68**	0.76***	NS	NS	-0.27*	-0.23 ^{TR}	NS	NS
sVEGFR1	-0.58****	0.52****		0.66**	0.47 ^{TR}	0.56*	0.67**	0.27*	0.27*	NS	NS
VCAM-1	-0.51****	0.50****		0.55*	0.67**	NS	NS	0.26*	0.24 ^{TR}	NS	NS
CCL2	-0.49****	0.64****		0.47*	0.42 ^{TR}	NS	NS	NS	-0.31*	NS	NS
PIGF	-0.44****	0.49****		0.52*	NS	0.62**	NS	NS	-0.27*	0.36**	0.36**
CXCL13	-0.46****	0.43****		0.68**	NS	0.45 ^{TR}	NS	NS	NS	0.28*	0.25 ^{TR}
YKL-40	-0.41****	0.48****		0.56*	NS	NS	NS	NS	NS	NS	NS
IL-18	-0.38**	0.41****		0.55*	NS	NS	NS	NS	NS	NS	NS
Tie-1	-0.37**	0.54****		0.52*	NS	NS	NS	NS	NS	NS	NS
ICAM-1	-0.36**	0.41****		0.49*	NS	NS	NS	NS	NS	NS	NS
Fibronectin	-0.50****	0.28*		0.44 ^{TR}	0.46*	NS	NS	NS	NS	NS	NS
VEGF	-0.32**	0.34**		NS	0.58**	NS	NS	NS	NS	NS	NS
Gal-1	-0.30*	0.45****									
CCL19	-0.28*	0.38**									

(Continued)

Supplementary table 4. Spearman rank correlations of analytes with clinical measures of disease activity per autoimmune disease.

	(J)DM			EF			LoS				
	CMAS	PGA		mLoSSI	VAS activity	LoSDI	VAS damage	mLoSSI	VAS activity	LoSDI	VAS damage
Gal-3	-0.28*	0.30*									
CCL22	0.26*	NS									
P-sel	-0.26*	NS									
OSF-2	NS	0.35**									
CCL27	NS	0.34**									
TM	NS	0.25*									

(J)DM = (juvenile) dermatomyositis (n=70), EF = eosinophilic fasciitis (n=19), LoS = localized scleroderma (n=62), CMAS = childhood myositis assessment scale, PGA = physician's global assessment, mLoSSI = modified LoS Skin Severity Index, LoSDI = LoS Damage Index, LoSDI = LoS damage index, VAS = visual analogue scale, rs= spearman rank correlation coefficient. NS= not significant, TR = trend (P<0.1), *P<0.05, **P<0.01, ***P<0.001, ****P<0.0001.

Supplementary table 5. Differential expression of analytes between autoimmune disease patients with inactive disease and healthy controls.

(J)DM		EF	
Analyte	P value	Analyte	P value
TSP-1	<0.0001*	Fibronectin	0.0035
CXCL13	0.0001	Gal-3	0.0080*
CCL27	0.0013*	SPARC	0.0204*
Ang-2	0.0028*	YKL-40	0.0305
Fetuin	0.0049*	Ang-2	0.0309*
IL-18	0.0092	CXCL10	0.0399
P-sel	0.0234*	Gal-9	0.0463
Gal-9	0.0240	VCAM-1	0.0633
CCL22	0.0347	Endoglin	0.0746
SPARC	0.0537	CCL18	0.0876
CCL17	0.0541	TNFR2	0.1066
PAI-1	0.0549	IL-18	0.1247
PIGF	0.0554	E-sel	0.1387
Fibronectin	0.0572	P-sel	0.1585
E-sel	0.0601	Fetuin	0.1805
YKL-40	0.0846	sVEGFR1	0.1887
Gal-1	0.0868	VEGF	0.2134
TNFR2	0.0896	CXCL13	0.2206
sVEGFR1	0.1248	CCL27	0.2244
PDGF-BB	0.1475	CCL22	0.2496
Ang-1	0.1681	CCL4	0.2806
VCAM-1	0.1827	CCL2	0.2836
Endoglin	0.2182	Ang-1	0.2971
CCL19	0.2209	OSF-2	0.3135
ICAM-1	0.2261	PIGF	0.3162
CXCL10	0.2275	ICAM-1	0.3187
CCL2	0.2355	Tie-2	0.3499
TM	0.2632	CCL19	0.3636

(Continued)

Supplementary table 5. Differential expression of analytes between autoimmune disease patients with inactive disease and healthy controls.

(J)DM		EF	
Analyte	P value	Analyte	P value
VEGF	0.3013	TM	0.3778
Tie-2	0.3405	CCL17	0.3879
CXCL9	0.3507	TSP-1	0.4110
Gal-3	0.3650	CXCL9	0.4134
TWEAK	0.3690	PAI-1	0.4440
CCL18	0.4077	PDGF-BB	0.4676
OSF-2	0.4316	Gal-1	0.4744
CCL4	0.4746	OSM	0.6125
OSM	0.5409	TWEAK	0.9324

Multiplicity-adjusted p values from Kruskal-Wallis test with Dunn's post hoc test per disease group as described in methods. *Lower in disease than in healthy controls. (J)DM = (juvenile) dermatomyositis, EF = eosinophilic fasciitis.

PART II



Human placental bed transcriptomic profiling reveals inflammatory activation of endothelial cells in preeclampsia

Laura Brouwers,* **Judith Wienke**,* Michal Mokry, Peter G.J. Nikkels, Tatjana E. Vogelvang, Arie Franx, Femke van Wijk,# and Bas B. van Rijn#

*,# These authors contributed equally

Submitted

ABSTRACT

Aims: Preeclampsia is a complex disorder of pregnancy presenting as hypertension and proteinuria as a result of extensive systemic endothelial dysfunction, and poor development of the spiral arteries underlying the placenta. However, functional characteristics of endothelial cells (ECs) within the human placental bed are unknown. Here, we determined transcriptional profiles of human placental bed ECs in women with severe preeclampsia, compared to ECs from women with normal pregnancy outcome, in addition to a comprehensive biomarker panel of systemic inflammation, endothelial cell function and activation markers.

Methods & results: Biopsy samples were obtained from the uterus at the site of the placental bed of five women with severe preeclampsia with fetal growth restriction and four controls with uneventful pregnancies undergoing Caesarean section. CD31⁺CD146⁺ ECs were isolated by enzymatic digestion followed by flow cytometry-assisted cell sorting and RNA-sequencing using a CEL-Seq2 preparation protocol. Data were analyzed by unsupervised principal component analysis and hierarchical clustering, gene set enrichment (GSEA) and standardized pathway analysis. In addition, circulating markers of endothelial function and systemic inflammation were measured in women with preeclampsia and fetal growth restriction (N=20) and controls (N=20) by multiplex immunoassay. Transcriptional profiling showed differentially expressed genes in placental bed ECs (FDR <0.05), with upregulation of prostaglandin D2 synthase, olfactomedin 1 and interleukin-3 receptor subunit alpha, and downregulation of serine peptidase inhibitor kazal type 5 and sestrin 3 in preeclampsia. Pathway analysis of upregulated genes identified enhanced activity of pathways associated with vasoconstriction, platelet activation and the innate immune response in preeclampsia-derived placental bed ECs. In addition, GSEA showed a significant enrichment of genes upregulated in human umbilical vein endothelial cells (HUVECS) treated with PE plasma, and genes downregulated in HUVEC stimulated with VEGF or PIGF compared to their unstimulated counterparts, suggestive of a VEGF- and PIGF deprived state in preeclampsia ECs. Unsupervised clustering of subjects by endothelium-related circulating markers identified separate profiles for healthy pregnancy and preeclampsia, in particular for those women with low platelets and elevated liver enzymes. Analytes most contributing to this were sFLT-1, endoglin, PIGF, leptin, SAA-1 and sICAM-1.

Conclusions: Transcriptional profiling of human placental bed ECs and profiling of circulating markers reveals involvement of endothelial cell immune activation in women who have preeclampsia with defective remodeling of spiral arteries.

INTRODUCTION

Preeclampsia is a serious multisystem vascular disorder characterized by new-onset hypertension and proteinuria, as well as vascular impairment of many organ systems e.g. the liver, kidneys, and brain, that affects about 1-5% of women in the second half of pregnancy. Endothelial cell dysfunction is generally acknowledged as its key pathophysiological feature.¹ Severe, or early onset, preeclampsia is often associated with fetal growth restriction (FGR) as a result of insufficient placental function due to underdevelopment of the maternal arteries supporting placental growth.^{2,3} Women who experience preeclampsia are at an increased risk of arterial disease, including atherosclerosis, ischemic heart disease and stroke later in life, and preeclampsia is now considered as one of the strongest sex-specific risk factors for major cardiovascular events in women of a young age.^{4,5} The cause of preeclampsia and the sequence of events leading to the disease is unclear. However, impaired physiological transformation of the uterine vascular bed underlying the placenta (i.e. the placental bed), known as spiral artery remodeling, is thought to be the essential first stage preceding the symptomatic phase of generalized endothelial dysfunction in most cases.⁶ Spiral artery remodeling is necessary for adequate blood flow to the developing placenta and fetus, and is histologically characterized by reorganization of vascular wall components including ECs, smooth muscle cells and the elastic lamina and new formation of a fibrinous layer within the vessel wall. It has been suggested that intramural invasion and EC replacement in response to migration of extravillous trophoblasts into the placental bed is a key mechanism for successful remodeling of spiral arteries.⁷ In preeclampsia and FGR, spiral artery remodeling is often impaired or absent, leading to altered blood flow to the placenta. In spiral arteries with defective remodeling, histological signs of loss of EC function have been observed, e.g. thrombotic lesions and infiltration of foam cells and lipid deposits into the intimal and medial layer termed 'acute atherosclerosis'.⁸⁻¹¹ It has been hypothesized that these processes at the maternal-fetal interface and the generalized maternal endothelial dysfunction and subsequent hypertension of preeclampsia are linked and result from the release of inflammatory and antiangiogenic factors into the maternal circulation.¹² Similar to other arterial disorders, e.g. during the early stages of atherosclerosis, women with preeclampsia consistently show increased activation of the systemic inflammatory response both during pregnancy and in the non-pregnant state, including elevated levels of C-reactive protein (CRP), interleukin (IL)-6 and IL-8.¹³ In addition, endothelial cell activation is suggested by elevated levels of several endothelial and vascular cell activation molecules, i.e. E-selectin and sVCAM-1.¹⁴ Specific to preeclampsia are high levels of the anti-angiogenic factors sFLT-1 and endoglin and low levels of the pro-angiogenic agent PlGF, which are released in abundance by the placenta, and are thought to contribute to impaired EC function by sustaining an anti-angiogenic environment.^{5,15} Additionally, the complex homeostatic balance of vascular tone, which is normally maintained by the endothelium,

is disturbed, leading to dysregulated and elevated blood pressure.^{16,17} ECs exposed to serum from women with preeclampsia show signs of dysfunction in vitro, indicating the presence of circulating factors involved in systemic endothelial dysfunction.^{18,19} Furthermore, women with preeclampsia have an increased risk of future cardiovascular disease, in particular for atherosclerosis, implying that a vulnerable maternal vascular constitution may contribute to both disorders by an increased susceptibility to EC dysfunction independent of pregnancy.^{4,11,20}

Due to the practical and technical challenge of getting access to tissue from the human placental bed and isolating tissue-specific ECs from human tissue for reliable transcriptomic analysis, little is known about the functional changes of ECs at the maternal-fetal interface during preeclampsia. Here, we applied flow cytometry assisted cell sorting of ECs for RNA-sequencing to investigate preeclampsia-induced changes in the transcriptomic profile of ECs within the human placental bed. We applied cluster and pathway analyses to identify functional changes in ECs associated with abnormal spiral artery remodeling typical of preeclampsia and FGR, in addition to circulating markers representative of systemic inflammation and endothelial activation by multiplex immunoassay.

METHODS

Patient selection and definitions

This study was part of the Spiral Artery Remodeling (SPAR) study. SPAR is a prospective multicenter study investigating spiral artery remodeling and pathology in women with and without preeclampsia and/or fetal growth restriction (FGR). Detailed description of the study design and sampling protocol was previously published.¹¹ In short, all women with a clinical indication for a Caesarean section for either preeclampsia or FGR, or both, were asked to participate in the study. In addition, women who delivered by primary elective Caesarean section after an uneventful pregnancy and without any major underlying pathology were enrolled as controls. We defined preeclampsia according to the most recent definition of the International Society for the Study of Hypertension in Pregnancy, as new-onset hypertension ($\geq 140/90$ mmHg) after 20 weeks of gestation in combination with significant proteinuria (≥ 300 mg/24h or protein/creatinine ratio ≥ 0.3 mg/mg), maternal organ dysfunction (i.e. renal insufficiency, liver involvement, neurological or hematological complications) or the presence of FGR.²¹ Preeclampsia complicated by HELLP syndrome, which is considered a more severe form of the same condition, was defined according to the presence of two or more of the following criteria: hemolysis (defined as serum lactate dehydrogenase (LDH) >600 U/L and/or haptoglobin 0.3 g/L), elevated liver enzymes (serum

aspartate aminotransferase (AST) >50 U/L and/or serum alanine aminotransferase (ALT) >50 U/L), and a low platelet count (<100x10⁹/L).²² FGR was defined as an ultrasonographical estimated fetal weight or abdominal circumference below the tenth percentile or a reduction in the standardized growth curves of ≥ 20 percentiles.²³ Placental insufficiency had to be the suspected cause of preeclampsia and FGR, and cases with confirmed chromosomal and/or congenital abnormalities were excluded. Further details and definitions used in the study can be found in our previous publication.¹¹

For this study we chose to include women with severe disease on the basis of early-onset, i.e. onset and delivery of preeclampsia before 34 completed weeks of gestation, and the presence of FGR as confirmation of the placental origin of the disease. For EC transcriptomics we included only primiparous women, N=5 with preeclampsia, and N=4 women with healthy pregnancies. For the multiplex immunoassay, we included 20 patients with severe preeclampsia and FGR with histologically confirmed spiral artery pathology, and 20 healthy women with uneventful pregnancies with histologically confirmed normal spiral artery remodeling as controls. All patients were delivered by elective Caesarean sections, without any signs of labour, e.g. contractions or rupture of membranes. All patients provided written informed consent prior to participation. This study was reviewed and approved by the Institutional Ethical Review Board of the University Medical Center Utrecht, protocol reference number: 16-198 and was prospectively monitored for any adverse events.

Placental bed biopsies

After delivery of the neonate and the placenta, as per routine procedures, the placental bed was manually located and two biopsies of the central placental bed from the inner uterine myometrial wall were obtained according to a pre-specified protocol published previously.¹¹ In addition to the placental bed site, biopsies were taken from the incision site when the placenta was not situated on this part of the uterine wall.

Isolation of placental bed ECs

The biopsy samples were collected in medium consisting of RPMI 1640 (Gibco) supplemented with Penicillin/Streptomycin (Gibco), L-glutamine (Gibco) and 10% fetal calf serum (FCS, Biowest) and minced into pieces of 1 mm³ in PBS (Gibco). The biopsies were enzymatically digested with 1 mg/mL collagenase IV (Sigma) in medium for 60 minutes at 37°C in a tube shaker under constant agitation at 120 rpm. To dissolve the remaining biopsy pieces after digestion and remove any remaining lumps, the biopsies were pipetted up and down multiple times and poured over a 100 μ m Cell Strainer (BD Falcon). Cells were subsequently washed in staining buffer consisting of cold PBS supplemented with 2% FCS

and 0.1% sodium-azide (Severn Biotech Ltd.) and filtered through a 70 μm cell strainer. For FACS sorting, the cells were incubated with surface antibodies against CD45, CD31 (PECAM-1), CD146 (MCAM), CD54 (ICAM-1), CD144 (VE-cadherin), CD105 (Endoglin), and CD309 (VEGFR2) (Supplementary Table 1) for 20 minutes in staining buffer at 4°C, washed in the same buffer and filtered through a 50 μm cell strainer (Falcon, BD). 2000 cells of the CD45-CD31⁺CD146⁺ cell population were sorted into eppendorfs containing 125 μL PBS on one of the two available FACSria™ II or III machines (BD). After sorting, 375 μL Trizol LS (Thermo Fisher Scientific) was added to each vial and vials were stored at -80°C until RNA isolation.

RNA isolation

For RNA isolation, vials were thawed at room temperature and 100 μL chloroform was added to each vial. The vials were shaken well and spun down at 12000g for 15 minutes at 4°C. The aqueous phase was transferred into a new tube and RNA was mixed with 1 μL of GlycoBlue (Invitrogen) and precipitated with 250 μL isopropanolol. Cells were incubated at -20°C for one hour and subsequently spun down at 12000g for 10 minutes. The supernatant was carefully discarded and the RNA pellet was washed twice with 375 μL 75% ethanol. Vials were stored at -80°C until library preparation.

Whole transcriptome sequencing and data analysis

Low input RNA sequencing libraries from biological sorted cell population replicates were prepared using the Cel-Seq2 Sample Preparation Protocol²⁴ and sequenced as 2 x 75bp paired-end on a NextSeq 500 (Utrecht Sequencing Facility). The reads were demultiplexed and aligned to human cDNA reference using the BWA (0.7.13).²⁵ Multiple reads mapping to the same gene with the same unique molecular identifier (UMI, 6bp long) were counted as a single read. RNA sequencing data were normalized per million reads and differentially expressed genes were identified using the DESeq2 package in R 3.4.3 (CRAN). Genes with $\text{padj} < 0.05$ were considered differentially expressed. For principal component analysis (PCA), the 1000 most variable genes were used and data were mean-centered per gene. For pathway analysis with Toppgene Suite, genes with nominal p value < 0.05 were used.²⁶

GSEA

For GSEA, we screened published datasets in the GEO NCBI database repository containing expression profiling data on human ECs, for datasets related to angiogenesis, pregnancy,

endothelial activation, stimulation with hormones or inflammatory mediators, shear stress, hypoxia, growth patterning and other factors considered relevant in preeclampsia. Gene sets of 50-500 genes were created from published gene sets based on differentially expressed genes with $P < 0.05$. GSEA was performed by 1000 random permutations of the phenotypic subgroups to establish a null distribution of enrichment score against which a (normalized) enrichment score and nominal p values were calculated.²⁷ Gene sets with $p < 0.05$ were considered statistically significant.

Multiplex immunoassay

Blood was collected in serum tubes within 4 hours before Caesarean section and spun down at 4000g at 4°C. Serum was stored at -80°C until analysis. The multiplex immunoassay for 67 analytes was performed as described previously, measuring all analytes simultaneously in 50 μ L of serum (xMAP; Luminex).²⁸ Heterophilic immunoglobulins were pre-absorbed from all samples with HeteroBlock (Omega Biologicals). Acquisition was performed with a Bio-Rad FlexMAP 3D in combination with xPONENT software version 4.2 (Luminex). Data analysis was performed with Bioplex Manager 6.1.1 (Bio-Rad).

Data analysis multiplex immunoassay

Multiplex data were analyzed using GraphPad Prism 7.0, SPSS Statistics 24 (IBM) and R 3.4.3 (CRAN). Out of range values on the lower end were imputed as 0.5x lowest measured value; out of range values on the upper end were imputed as 2x highest measured value. Analytes with more than 35% of measured values below the lower or above the upper limit of detection were excluded from the analyses (Granzyme B, Galectin-7, TRANCE-sRANKL, MIF, TNF α , IL-4, IL-1RA). For comparisons between two groups, the Mann-Whitney U test was used, with correction for multiple testing of all 60 analytes by Bonferroni or FDR as indicated where applicable. For principal component analysis (PCA) and heatmap analysis, data were mean-centered per analyte. Unsupervised hierarchical clustering was performed by Ward's method with Euclidian distance. Random forest analysis was performed via <http://www.metaboanalyst.ca/> with standard settings. Correlations were assessed by spearman rank correlation. Adjusted p -values < 0.05 were considered significant.

RESULTS

Baseline characteristics

Maternal and pregnancy baseline characteristics for both the EC transcriptomics and the multiplex immunoassay are presented in Supplementary Table 2 and 3. Two patients with preeclampsia were excluded from the biomarker analyses due to cross-reactivity with the multiplex beads, which can lead to false-positive results. One additional preeclampsia case was excluded when histopathology did not confirm defective spiral artery remodeling. Baseline characteristics for both analyses were very similar. Women with preeclampsia were less often of white European descent and were more often obese, with both factors being known risk factors for the disorder. As expected, preeclampsia was associated with nulliparity, lower gestational age and birth weight.

Placental bed endothelial cell transcriptomics

CD31⁺CD146⁺ ECs isolated from placental bed biopsies and sorted through flow cytometry-assisted cell sorting, were subsequently successfully prepared for RNA-sequencing by Cel-Seq2 protocol. High expression of key endothelial genes such as Van Willebrand Factor, PECAM1 (CD31), MCAM (CD146) endoglin, claudin-5, CCL14, Tie1, CD34, and CTGF in addition to expression of 65 out of 72 endothelial-specific genes identified by Chi et al. confirmed endothelial cell identity (Supplementary Figure 1A).²⁹ In addition, the maternal origin of ECs was confirmed by high expression of the female-specific XIST gene and absent expression of the male-specific SRY gene in all samples. In addition to overlapping gene expression signatures which were found between patients with preeclampsia and healthy pregnancies, we identified five individual differentially expressed genes (Figure 1A), including three significantly upregulated genes and two downregulated genes associated with preeclampsia ($p_{adj} < 0.05$; Figure 1B). Upregulated genes were prostaglandin D2 synthase (PTGDS), olfactomedin 1 (OFLM1) and IL-3 receptor subunit alpha (IL3RA). Downregulated genes were serine peptidase inhibitor Kazal type 5 (SPINK5) and sestrin 3 (SESN3). Three additional up- and three downregulated genes were identified with $p_{adj} < 0.10$ (Figure 1B), including nestin. Heatmap analysis comparing expression of the differentially expressed genes in preeclampsia with healthy pregnant controls is shown in Figure 1C. In order to perform pathway analysis of upregulated genes in preeclampsia we lowered the significance threshold (to a nominal p -value < 0.05) to study potentially enriched pathways involved in preeclampsia pathogenesis, and identified 6 significantly enriched pathways (Figure 1D) related to both innate immune activation and platelet activation within the transcriptional profile of the placental bed ECs. Comparison of EC transcriptional

profiles at two sites within the uterus, i.e. the incision and the placental bed site, between preeclampsia and healthy pregnancy, revealed partially overlapping gene signatures of upregulated and downregulated genes, including PTGDS and SPINK5 (Supplementary Figure 1B and 1C). Subsequent GSEA analysis showed significant enrichment of genes

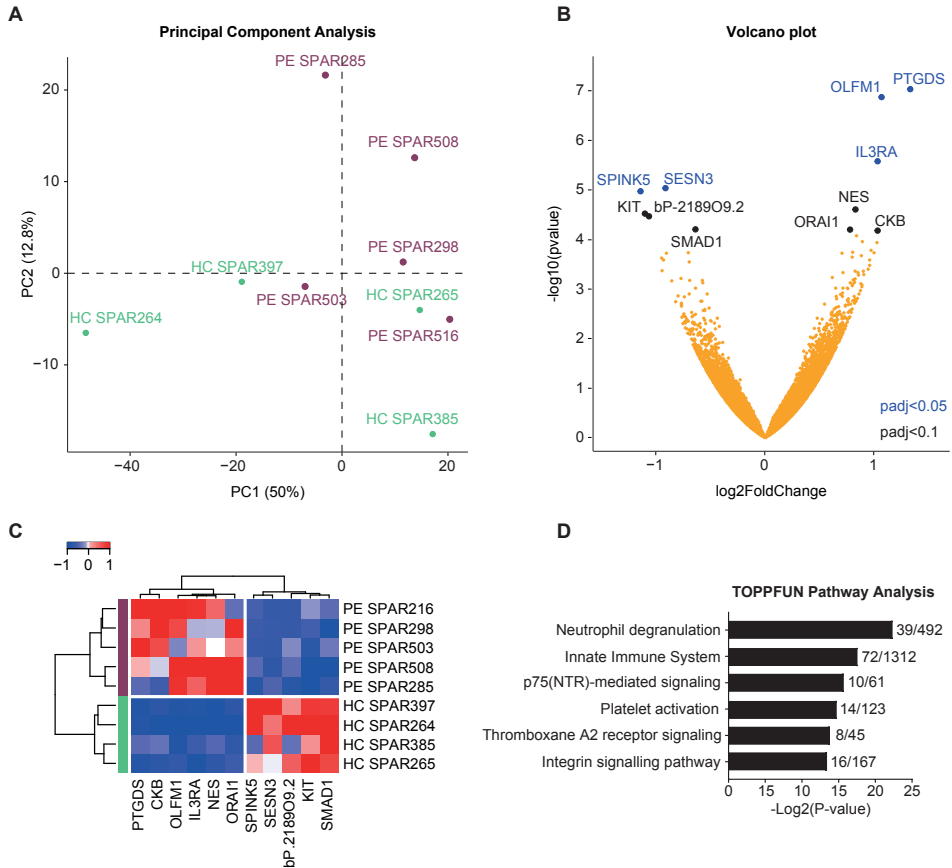


Figure 1. Transcriptomic profiling of spiral artery endothelial cells from the placental bed, comparing preeclampsia with FGR and healthy pregnancy.

2000 CD45-CD31+CD146+ endothelial cells were isolated from each biopsy by flow cytometry assisted cell sorting and RNA was sequenced by CEL-seq2 protocol. (A) Principal component analysis of preeclampsia cases and healthy controls using the 1000 genes with the highest variance (purple = preeclampsia, green = healthy controls). Genes were mean-centered. (B) Volcano plot showing differentially expressed genes with a $p_{adj} < 0.05$ (blue) and $p_{adj} < 0.1$ (black). (C) Heatmap of differentially expressed genes with a $p_{adj} < 0.1$. Genes were mean-centered and hierarchically clustered by Ward's method and Euclidian distance. (D) Pathway analysis in ToppGene Suite on the 617 upregulated genes in preeclampsia compared to healthy pregnancy with a nominal p-value < 0.05 . Numbers indicate the number of overlapping upregulated genes in endothelial cells from preeclampsia samples, compared to the total known genes in the indicated pathway. Abbreviations: PE, preeclampsia (in this study early onset, in combination with fetal growth restriction); HC, healthy pregnancy; SPINK5, serine peptidase inhibitor Kazal type 5; SESN3, sestrin 3, KIT, KIT proto-oncogene receptor tyrosine kinase; SMAD1, Mothers against decapentaplegic homolog 1; PTGDS, prostaglandin D2 synthase; OLFM1, olfactomedin 1; IL3RA, interleukin 3 receptor subunit alpha; NES, nestin; ORAI1, Calcium release-activated calcium channel protein 1; CKB, creatine kinase B.

upregulated in human umbilical vein endothelial cells (HUVECs) treated with plasma from patients with preeclampsia (figure 2A), indicating that circulating factors may partly induce the transcriptional phenotype observed in placental bed ECs from preeclamptic patients. In addition, GSEA showed significant enrichment of genes downregulated in HUVEC stimulated with VEGF or PIGF compared to their unstimulated counterparts, suggesting a VEGF- and PIGF deprived state in ECs of women with preeclampsia (figure 2B, 2C and 2D). Taken together, this analysis points towards significant enrichment of EC transcriptional changes which may be partly due to circulating factors involved in the pathogenesis of preeclampsia.

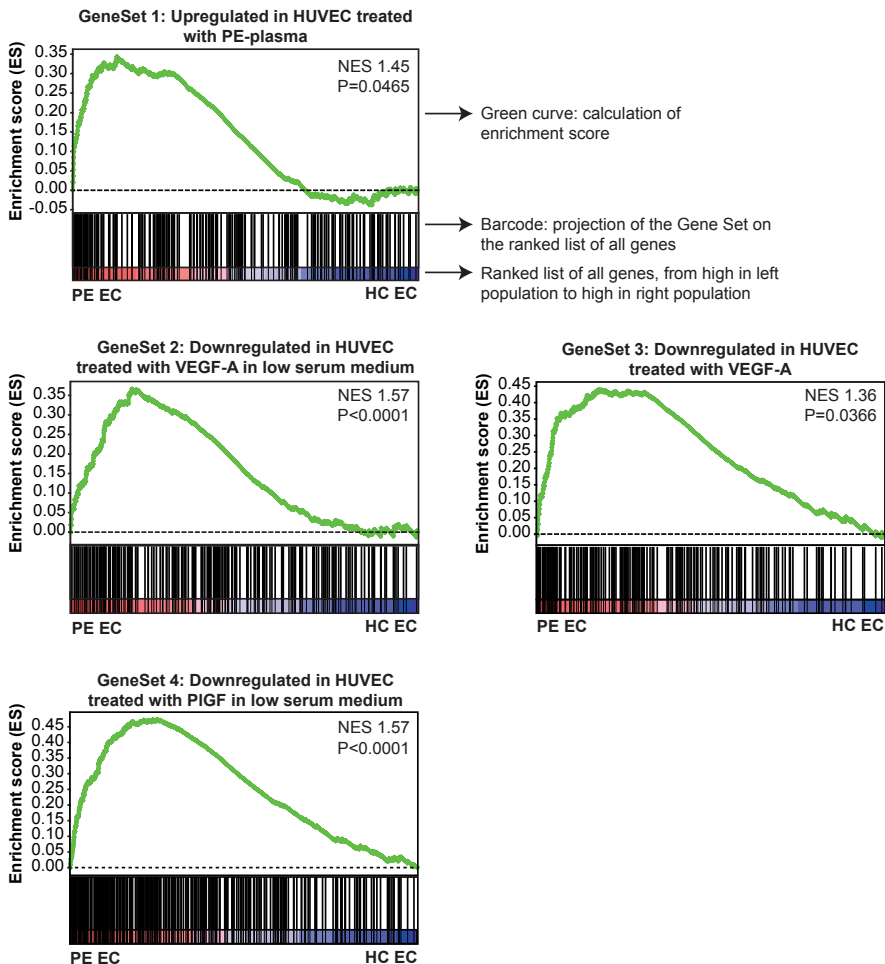


Figure 2. Gene set enrichment analysis (GSEA) showing significant enrichment of genes in published endothelial cell datasets.

GSEA were run for all published datasets with endothelial cells (ECs) stimulated with factors relevant in preeclampsia. (#1) GSEA with our preeclampsia cases showed significant enrichment for upregulated genes in HUVECS treated with PE plasma, and genes downregulated in HUVECS stimulated with VEGF (#2,3) or PIGF (#4).

Markers of systemic inflammation and EC activation

As the findings of GSEA analysis indicated that the presence or absence of circulating factors, known to be involved in preeclampsia, may have pathophysiological effects on EC transcriptomics, we performed biomarker profiling to further elucidate systemic disturbances of relevant proteins. To determine endothelial-related effects in preeclampsia we measured markers associated with inflammation, endothelial activation and endothelial dysfunction during the active disease state of preeclampsia patients compared with women with healthy pregnancy outcomes. Baseline characteristics are summarized in Supplementary Table 3. Using a comprehensive panel, we observed clear and distinct biomarker signatures associated with preeclampsia compared with normal pregnancy by principal component analysis (Figure 3A), with a similar separation of groups observed using unsupervised hierarchical clustering, with the exception of five individuals (Figure 3B). No clinical, histological or laboratory parameters could be identified to explain these exceptions, which merits further investigation. Analytes most contributing to separation of the two groups were identified as sFLT-1, endoglin and PIGF by random forest analysis, with an out-of-bag (OOB) error of 0.0 (Figure 3C). Accordingly, the sFLT-1/PIGF ratio was significantly increased in preeclampsia (Supplementary Figure 2), further confirming the preeclampsia phenotype. In addition to the sFlt-1/PIGF ratio, which is an established marker in preeclampsia, we also identified differences in leptin, and the acute phase reactant SAA-1 as highly discriminative factors, supporting the hypothesis that preeclampsia is associated with a pro-inflammatory phenotype (Figure 3D). This was further confirmed by increased levels of individual pro-inflammatory proteins IL-6, TNF-R1, and CCL4 in preeclampsia, as compared to normal pregnant controls (Supplementary Table 4). Levels of endothelial activation markers sICAM-1 and E-selectin were also significantly higher in preeclampsia patients, further confirming the presence of systemic endothelial activation (Figure 3D, Supplementary Table 4).

To further explore heterogeneity within preeclampsia, unbiased analysis within the case group was performed. PCA and hierarchical clustering separated the case group into two clusters (Figure 4A and B). Strikingly, review of clinical and biochemical parameters revealed the presence of the clinically recognized severe preeclampsia phenotype of HELLP syndrome, in 6 out of 7 cases clustering separately. Analytes most contributing to this separation of preeclampsia with and without HELLP were identified as Ang-1, PDGF-BB, RPB4 and Apelin by random forest analysis with an OOB error of 0.294 (Figure 4C). All of these analytes were lower in patients with HELLP syndrome, which is likely due to the decreased platelet count in these women (*data not shown*). In addition, sFLT-1, SAA-1, adipsin, chemerin, and clusterin were higher in women with preeclampsia complicated by HELLP syndrome, although this effect was less obvious after adjustment for multiple testing (Supplementary Table 5).

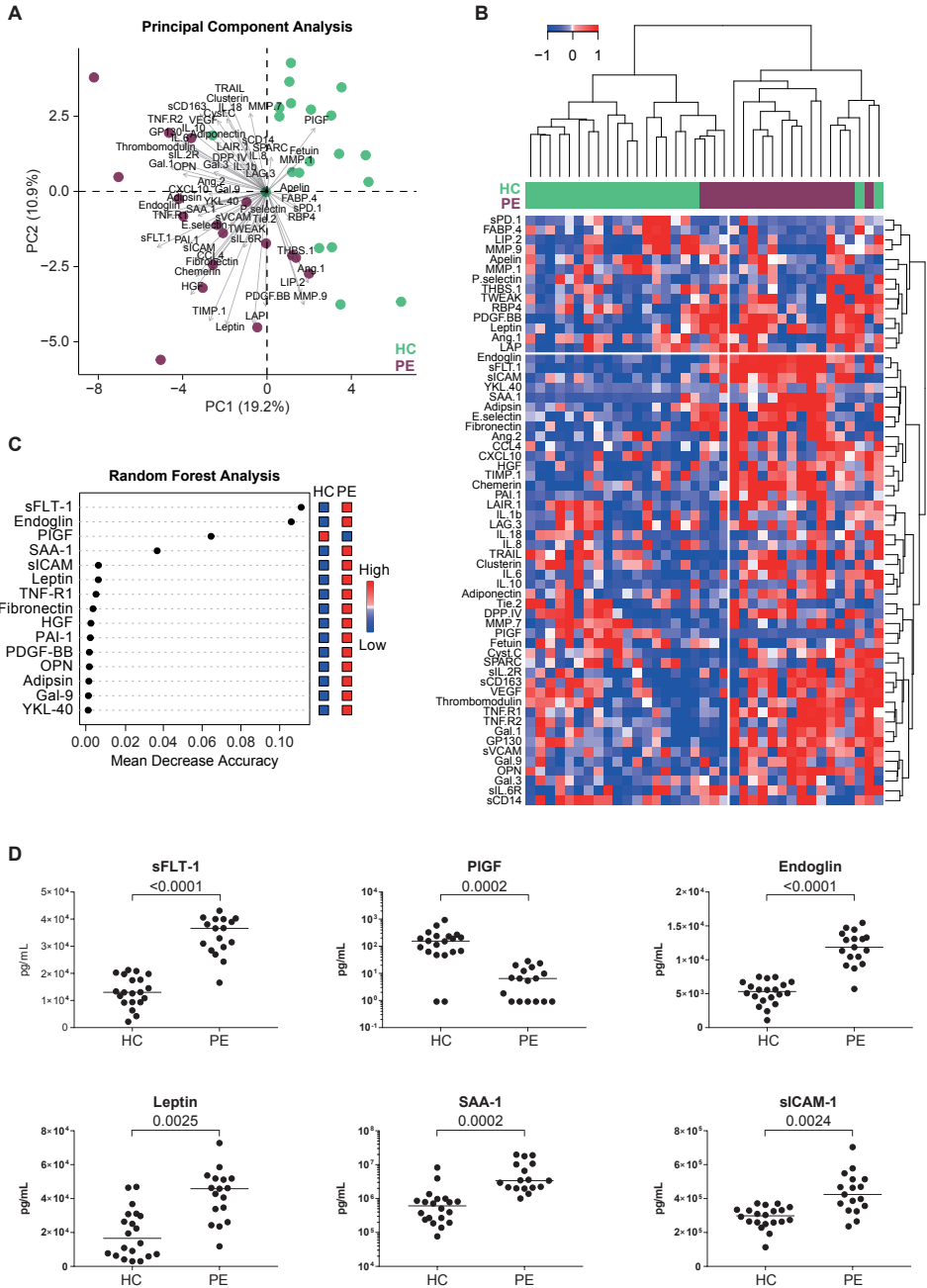


Figure 3. Systemic biomarker profiling of markers related to inflammation, endothelial activation and endothelial dysfunction, comparing pre-eclampsia with FGR and healthy pregnancy.

(Figure 3 continued)

Biomarkers were analyzed in serum by multiplex immunoassay. (A) Principal component analysis of preeclampsia cases and healthy controls using all 60 markers (purple = preeclampsia, green = healthy controls). Analytes were mean-centered. (B) Heatmap with hierarchical clustering of all 60 markers. Markers were mean-centered and patients were clustered by Ward's method with Euclidian distance. (C) Random Forest analysis with 1000 trees yielding an out-of-bag error of 0.00 and showing the analytes most important for separation of preeclampsia and healthy groups. Analytes were mean-centered. (D) Scatter dot plots of sFLT-1, PIGF, Endoglin, Leptin, SAA-1, and sICAM-1. Line represents median; FDR with correction for multiple testing of 60 analytes is indicated. Mann-Whitney U test. Abbreviations: PE, preeclampsia (in this study early onset, in combination with fetal growth restriction); HC, healthy pregnancy; Multiplex Immunoassay abbreviations may be found in the Supplementary Tables.

DISCUSSION

In this study we used state of the art techniques to isolate ECs from the human placental bed to allow for transcriptomic profiling, comparing pregnancies complicated by preeclampsia with healthy pregnant controls. To our knowledge, our data provide the first transcriptomic analysis of human ECs isolated from this highly specialized vascular bed lying within the uterus at the maternal-fetal interface. We identified at least 5 differentially expressed genes (PTGDS, OLFM1, IL3RA, SPINK5 and SESN3) and pathways related to innate immune activation and platelet activation associated with preeclampsia. For two of these, PTGDS and SPINK5, differential expression was confirmed both at the site of the uterus underlying the placenta, as well as at a second biopsy site elsewhere in the uterus, suggesting that some of the transcriptional changes observed in ECs from preeclampsia are confined to the placental bed while others are present in the entire uterus. While overall transcriptomic profiling showed similarities between the two groups for individual genes, the pathway analysis identified distinct signatures associated with the disease. Consistent with other studies, EC activation and inflammation observed in the placental bed, could be found in the profiles of several key circulating markers of endothelial activation including the well-known markers sFLT-1, endoglin and PIGF, as well as markers of inflammation including SAA-1 and leptin, further confirming the preeclampsia phenotype.

Our study provides proof-of-concept data that ECs derived from the placental bed in women with confirmed pathology of the spiral arteries underlying the placenta, indeed show signs of altered gene expression similar to endothelial activation and inflammation observed in other vascular beds. Although these findings need to be followed up in additional experiments, some of the differentially expressed genes have been associated with preeclampsia in previous studies, and may be considered as plausible candidates for involvement in the pathophysiology of the disease, as summarized below.

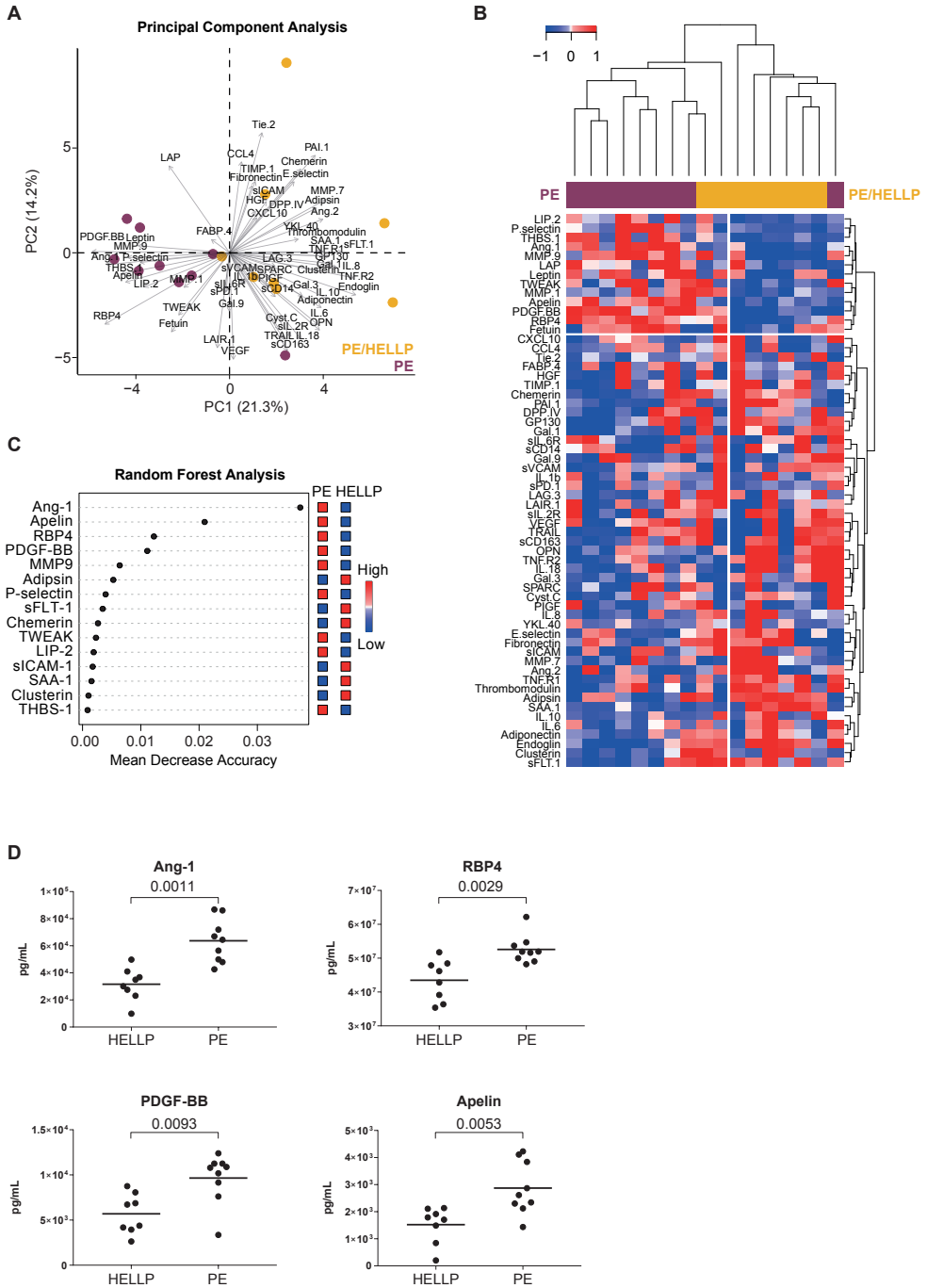


Figure 4. Systemic biomarker profiling of markers related to inflammation, endothelial activation and endothelial dysfunction within preeclampsia and a subgroup with HELLP syndrome.

(Figure 4 continued)

Biomarkers were analyzed in serum by multiplex immunoassay. (A) Principal component analysis of preeclampsia cases with and without HELLP using all 60 markers (purple = preeclampsia without HELLP, yellow = preeclampsia with HELLP). Analytes were mean-centered. (B) Heatmap with hierarchical clustering of all 60 markers. Markers were mean-centered and patients were clustered by Ward's method with Euclidian distance. (C) Random Forest analysis with 1000 trees yielding an out-of-bag error of 0.294 and showing the analytes most important for separation of preeclampsia with and without HELLP syndrome. Analytes were mean-centered. (D) Scatter dot plots of Ang-1, RBP4, PDGF-BB, and apelin. Line represents median; nominal p value without correction for multiple testing is indicated. Mann-Whitney U test. Abbreviations: PE, preeclampsia (in this study early onset, in combination with fetal growth restriction, without HELLP); HELLP, hemolysis, elevated liver enzymes, low platelets syndrome; Multiplex Immunoassay abbreviations may be found in the Supplementary Tables.

PTGDS, upregulated in preeclampsia, catalyzes the conversion of prostaglandin H2 to prostaglandin D2 (PGD2) and is important for inhibition of platelet aggregation, relaxation and contraction of smooth muscle and reduction of vascular permeability.^{30,31} ECs are known to produce PTGDS under shear stress, which is likely present in the case of insufficient remodeling and high blood pressure in preeclampsia.³²⁻³⁴ PGD2 may be involved in inflammation through recruitment of T helper (Th) type 2 cells.³⁵ Although many studies show increased Th1 type and decreased Th2 type immunity in preeclampsia, at least as many reports demonstrate the opposite.¹³ PTGDS upregulation has been associated with uterine contraction and spontaneous preterm birth, which may be linked to preeclampsia due to belief of some that spontaneous preterm birth serves as an internal rescue mechanism aiming to protect both mother and baby from damaging effects of prolonged preeclamptic and growth restricted pregnancy.³⁶⁻⁴¹ Studies on olfactomedin 1 (Olfm-1) in the context of reproduction are limited. Human recombinant Olfm-1 suppresses the attachment of spheroids onto endometrial cells and downregulation of Olfm-1 during the receptive period may favor embryo attachment for successful implantation.⁴² IL-3RA is a receptor for IL-3. IL-3 was shown to mediate positive signals for embryo implantation and to promote placental development and fetal growth.⁴³ IL-3RA receptor expression on EC increases migration of dendritic cells into tissues, which may regulate the Th1/Th2 balance within the decidua to maintain a Th2-dominant state, which is essential for maintenance of pregnancy.⁴⁴⁻⁴⁶ A pathologic implication of high IL3-RA expression in reproduction has not been reported. Nestin (NES), a type VI intermediate filament protein known to participate in remodeling of the cell, was borderline upregulated in preeclampsia. In animal models, NES upregulation characterizes vascular remodeling secondary to hypertension. In comparison to multiple other reproductive tissues, NES is most strongly expressed by ECs of newly vascularized tissues.^{47,48} In humans, urinary NES levels are significantly increased in preeclampsia patients and positively correlate with proteinuria, which is a key feature of the preeclampsia phenotype.⁴⁸ The SPINK5 gene, downregulated in ECs from preeclamptic patients, codes for the protein LEKT1, a serine protease inhibitor. Polymorphisms in SPINK5 have been associated with hypersensitivity of the immune system, especially in skin (atopy).⁴⁹ Other

members of the SPINK family (i.e. SPINK1) have been shown to be highly up-regulated in decidua of recurrent pregnancy loss and to be predictive of preeclampsia, but no evidence is available for similar functions of SPINK5.⁵⁰ Finally, Sestrin 3, which was downregulated in preeclampsia in our study, reduces the levels of intracellular reactive oxygen species and is stress-induced.⁵¹ It is required for normal regulation of blood glucose, insulin resistance, plays a role in lipid storage in obesity and is associated with increasing severity of coronary artery disease.^{52,53} SESN3 has not previously been investigated in reproduction.

Pathway analysis of the genes enriched in ECs from preeclampsia identified 6 upregulated pathways, involving the innate immune system and platelet activation. GSEA indicated that disturbances in circulating factors, especially related to angiogenesis, may contribute to the transcriptional changes observed in EC from preeclamptic patients. Systemic biomarker profiling by multiplex immunoassay confirmed immune activation and a disturbed balance between angiogenic and angiostatic factors in preeclampsia, which was most pronounced in patients with low platelets and elevated liver enzymes. These results indicate that inflammation and disturbed angiogenic signaling is not only present locally, in EC from the placental bed, but also systemically. Our findings are suggestive of the fact that this anti-angiogenic state plays a role in the generalized endothelial dysfunction key to preeclampsia, as well as contributes to the disturbed EC function at the placental bed, which may explain the increased susceptibility to endothelial cell erosion and lack of endothelial repair observed in defective spiral artery remodeling.¹⁵

Strengths of our study include the use of transcriptomics to investigate ECs from the human placental bed in patients with pregnancy complicated by severe preeclampsia and controls. This can only be performed on fresh tissue with 24/7 availability of dedicated clinicians and laboratory staff, as well as the use of state-of-the-art techniques for isolating very pure ECs from the placental bed with histologically confirmed defective spiral artery remodeling. Additionally, we confirmed the preeclampsia phenotype by extensive biomarker profiling to identify associated systemic markers of inflammation, endothelial dysfunction and soluble angiogenic factors. Limitations of this study include the limited availability of biopsy samples per group, which did not allow us to extensively confirm our findings in additional experiments e.g. immunohistochemistry or at the protein level. In addition, pregnancies of women with severe preeclampsia generally lead to delivery at an earlier gestational age than in women with planned Caesarean sections in the control group. In theory, the alterations in EC function attributed to preeclampsia may partly be influenced by this difference in gestational age. However, many of the markers we found to be discriminatory, confirmed the preeclampsia phenotype both at the EC, as well as at the systemic level.

In conclusion, we identified several candidate genes which were differentially expressed in endothelial cells from the placental bed that have a role in inflammatory response, vascular function and endothelial dysfunction, in addition to the known signs of generalized endothelial and inflammatory activation in preeclampsia. Our results underline the importance of maintaining vascular integrity by appropriate adaptation of ECs to the

challenges of pregnancy, and contribute to the understanding of the impact of endothelial health on pregnancy outcome, as well as the similarities in the pathophysiology between preeclampsia and later-life arterial disease.

REFERENCES

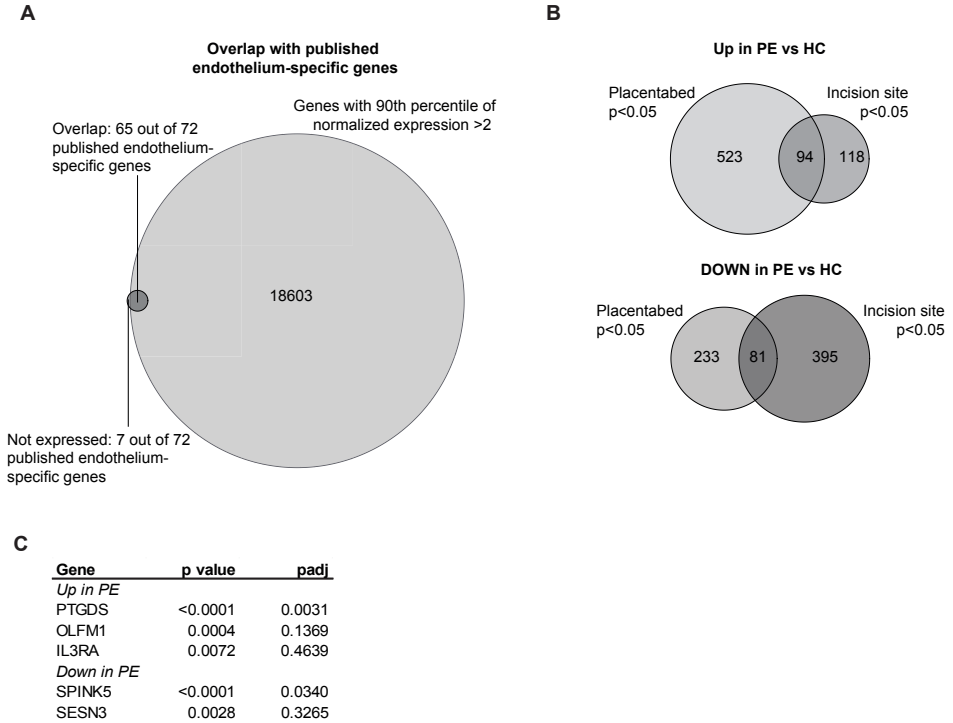
1. Powe CE, Levine RJ, Karumanchi SA. Preeclampsia, a Disease of the Maternal Endothelium: The Role of Antiangiogenic Factors and Implications for Later Cardiovascular Disease. *Circulation* **2011**, *123* (24), 2856–2869.
2. Duley L. The Global Impact of Pre-Eclampsia and Eclampsia. *Semin. Perinatol.* **2009**, *33* (3), 130–137.
3. Kuklina E V, Ayala C, Callaghan WM. Hypertensive Disorders and Severe Obstetric Morbidity in the United States. *Obstet. Gynecol.* **2009**, *113* (6), 1299–1306.
4. Bellamy L, Casas J-P, Hingorani AD, et al. Pre-Eclampsia and Risk of Cardiovascular Disease and Cancer in Later Life: Systematic Review and Meta-Analysis. *BMJ* **2007**, *335* (7627), 974.
5. de Jager SCA, Meeuwse JAL, van Pijpen FM, et al. Preeclampsia and Coronary Plaque Erosion: Manifestations of Endothelial Dysfunction Resulting in Cardiovascular Events in Women. *Eur. J. Pharmacol.* **2017**, *816*, 129–137.
6. Brosens I, Pijnenborg R, Vercruysse L, et al. The “Great Obstetrical Syndromes” are Associated with Disorders of Deep Placentation. *Am. J. Obstet. Gynecol.* **2011**, *204* (3), 193–201.
7. Fisher SJ. Why Is Placentation Abnormal in Preeclampsia? *Am. J. Obstet. Gynecol.* **2015**, *213* (4 Suppl), S115-22.
8. Lyall F, Robson SC, Bulmer JN. Spiral Artery Remodeling and Trophoblast Invasion in Preeclampsia and Fetal Growth Restriction: Relationship to Clinical Outcome. *Hypertens. (Dallas, Tex. 1979)* **2013**, *62* (6), 1046–1054.
9. Staff AC, Dechend R, Pijnenborg R. Learning from the Placenta: Acute Atherosclerosis and Vascular Remodeling in Preeclampsia—Novel Aspects for Atherosclerosis and Future Cardiovascular Health. *Hypertens. (Dallas, Tex. 1979)* **2010**, *56* (6), 1026–1034.
10. Staff AC, Johnsen GM, Dechend R, et al. Preeclampsia and Uteroplacental Acute Atherosclerosis: Immune and Inflammatory Factors. *J. Reprod. Immunol.* **2014**, *101–102*, 120–126.
11. Veerbeek JHW, Brouwers L, Koster MPH, et al. Spiral Artery Remodeling and Maternal Cardiovascular Risk: The Spiral Artery Remodeling (SPAR) Study. *J. Hypertens.* **2016**, *34* (8), 1570–1577.
12. Roberts JM. The Perplexing Pregnancy Disorder Preeclampsia: What Next? *Physiol. Genomics* **2018**, *50* (6), 459–467.
13. Visser N, van Rijn BB, Rijkers GT, et al. Inflammatory Changes in Preeclampsia: Current Understanding of the Maternal Innate and Adaptive Immune Response. *Obstet. Gynecol. Surv.* **2007**, *62* (3), 191–201.
14. Docheva N, Romero R, Chaemsaihong P, et al. The Profiles of Soluble Adhesion Molecules in The “great Obstetrical Syndromes”(). *J. Matern. Fetal. Neonatal Med.* **2019**, *32* (13), 2113–2136.
15. Ngene NC, Moodley J. Role of Angiogenic Factors in the Pathogenesis and Management of Pre-Eclampsia. *Int. J. Gynaecol. Obstet.* **2018**, *141* (1), 5–13.
16. Lopes van Balen VA, van Gansewinkel TAG, de Haas S, et al. Physiological Adaptation of Endothelial Function to Pregnancy: Systematic Review and Meta-Analysis. *Ultrasound Obstet. Gynecol.* **2017**, *50* (6), 697–708.
17. McLaughlin K, Audette MC, Parker JD, et al. Mechanisms and Clinical Significance of Endothelial Dysfunction in High-Risk Pregnancies. *Can. J. Cardiol.* **2018**, *34* (4), 371–380.

18. Alma LJ, Bokslag A, Maas AHM, et al. Shared Biomarkers between Female Diastolic Heart Failure and Pre-Eclampsia: A Systematic Review and Meta-Analysis. *ESC Hear. Fail.* **2017**, *4* (2), 88–98.
19. Roberts JM, Taylor RN, Musci TJ, et al. Preeclampsia: An Endothelial Cell Disorder. *Am. J. Obstet. Gynecol.* **1989**, *161* (5), 1200–1204.
20. Wu P, Haththotuwa R, Kwok CS, et al. Preeclampsia and Future Cardiovascular Health: A Systematic Review and Meta-Analysis. *Circ. Cardiovasc. Qual. Outcomes* **2017**, *10* (2).
21. Tranquilli AL, Dekker G, Magee L, et al. The Classification, Diagnosis and Management of the Hypertensive Disorders of Pregnancy: A Revised Statement from the ISSHP. *Pregnancy hypertension*. Netherlands April 2014, pp 97–104.
22. Tranquilli AL, Brown MA, Zeeman GG, et al. The Definition of Severe and Early-Onset Preeclampsia. Statements from the International Society for the Study of Hypertension in Pregnancy (ISSHP). *Pregnancy Hypertens.* **2013**, *3* (1), 44–47.
23. Terwisscha van Scheltinga J, Scherjon S, van Dillen J. NVOG-Richtlijn Foetale Groeirestrictie (FGR). *Ned. Ver. voor Obstet. en Gynaecol.* **2017**, [Dutch gui].
24. Hashimshony T, Senderovich N, Avital G, et al. CEL-Seq2: Sensitive Highly-Multiplexed Single-Cell RNA-Seq. *Genome Biol.* **2016**, *17*, 77.
25. Li H, Durbin R. Fast and Accurate Long-Read Alignment with Burrows-Wheeler Transform. *Bioinformatics* **2010**, *26* (5), 589–595.
26. Chen J, Bardes EE, Aronow BJ, et al. ToppGene Suite for Gene List Enrichment Analysis and Candidate Gene Prioritization. *Nucleic Acids Res.* **2009**, *37* (Web Server issue), W305-11.
27. Subramanian A, Tamayo P, Mootha VK, et al. Gene Set Enrichment Analysis: A Knowledge-Based Approach for Interpreting Genome-Wide Expression Profiles. *Proc. Natl. Acad. Sci. U. S. A.* **2005**, *102* (43), 15545–15550.
28. Scholman RC, Giovannone B, Hiddingh S, et al. Effect of Anticoagulants on 162 Circulating Immune Related Proteins in Healthy Subjects. *Cytokine* **2017**.
29. Chi J-T, Chang HY, Haraldsen G, et al. Endothelial Cell Diversity Revealed by Global Expression Profiling. *Proc. Natl. Acad. Sci. U. S. A.* **2003**, *100* (19), 10623–10628.
30. Lichtenstein SH, Carvell GE, Simons DJ. Responses of Rat Trigeminal Ganglion Neurons to Movements of Vibrissae in Different Directions. *Somatosens. Mot. Res.* **1990**, *7* (1), 47–65.
31. Omori K, Morikawa T, Kunita A, et al. Lipocalin-Type Prostaglandin D Synthase-Derived PGD2 Attenuates Malignant Properties of Tumor Endothelial Cells. *J. Pathol.* **2018**, *244* (1), 84–96.
32. Burton GJ, Woods AW, Jauniaux E, et al. Rheological and Physiological Consequences of Conversion of the Maternal Spiral Arteries for Uteroplacental Blood Flow during Human Pregnancy. *Placenta* **2009**, *30* (6), 473–482.
33. Miyagi M, Miwa Y, Takahashi-Yanaga F, et al. Activator Protein-1 Mediates Shear Stress-Induced Prostaglandin D Synthase Gene Expression in Vascular Endothelial Cells. *Arterioscler. Thromb. Vasc. Biol.* **2005**, *25* (5), 970–975.
34. Taba Y, Sasaguri T, Miyagi M, et al. Fluid Shear Stress Induces Lipocalin-Type Prostaglandin D(2) Synthase Expression in Vascular Endothelial Cells. *Circ. Res.* **2000**, *86* (9), 967–973.

35. Saito S, Tsuda H, Michimata T. Prostaglandin D2 and Reproduction. *Am. J. Reprod. Immunol.* **2002**, 47 (5), 295–302.
36. Connealy BD, Carreno CA, Kase BA, et al. A History of Prior Preeclampsia as a Risk Factor for Preterm Birth. *Am. J. Perinatol.* **2014**, 31 (6), 483–488.
37. Enquobahrie DA, Williams MA, Qiu C, et al. Early Pregnancy Peripheral Blood Gene Expression and Risk of Preterm Delivery: A Nested Case Control Study. *BMC Pregnancy Childbirth* **2009**, 9, 56.
38. Kumar S, Palaia T, Hall CE, et al. Role of Lipocalin-Type Prostaglandin D2 Synthase (L-PGDS) and Its Metabolite, Prostaglandin D2, in Preterm Birth. *Prostaglandins Other Lipid Mediat.* **2015**, 118–119, 28–33.
39. Liu B, Yang J, Luo W, et al. Prostaglandin D2 Is the Major Cyclooxygenase-1-Derived Product in Prepartum Mouse Uteri Where It Mediates an Enhanced in Vitro Myometrial Contraction. *Eur. J. Pharmacol.* **2017**, 813, 140–146.
40. Shiki Y, Shimoya K, Tokugawa Y, et al. Changes of Lipocalin-Type Prostaglandin D Synthase Level during Pregnancy. *J. Obstet. Gynaecol. Res.* **2004**, 30 (1), 65–70.
41. Wikstrom A-K, Stephansson O, Cnattingius S. Previous Preeclampsia and Risks of Adverse Outcomes in Subsequent Nonpreeclamptic Pregnancies. *Am. J. Obstet. Gynecol.* **2011**, 204 (2), 148.e1-6.
42. Kodithuwakku SP, Ng P-Y, Liu Y, et al. Hormonal Regulation of Endometrial Olfactomedin Expression and Its Suppressive Effect on Spheroid Attachment onto Endometrial Epithelial Cells. *Hum. Reprod.* **2011**, 26 (1), 167–175.
43. Fishman P, Falach-Vaknine E, Zigelman R, et al. Prevention of Fetal Loss in Experimental Antiphospholipid Syndrome by in Vivo Administration of Recombinant Interleukin-3. *J. Clin. Invest.* **1993**, 91 (4), 1834–1837.
44. de la Rosa G, Longo N, Rodriguez-Fernandez JL, et al. Migration of Human Blood Dendritic Cells across Endothelial Cell Monolayers: Adhesion Molecules and Chemokines Involved in Subset-Specific Transmigration. *J. Leukoc. Biol.* **2003**, 73 (5), 639–649.
45. Lim LHK, Burdick MM, Hudson SA, et al. Stimulation of Human Endothelium with IL-3 Induces Selective Basophil Accumulation in Vitro. *J. Immunol.* **2006**, 176 (9), 5346–5353.
46. Miyazaki S, Tsuda H, Sakai M, et al. Predominance of Th2-Promoting Dendritic Cells in Early Human Pregnancy Decidua. *J. Leukoc. Biol.* **2003**, 74 (4), 514–522.
47. Mokry J, Nemecek S. Angiogenesis of Extra- and Intraembryonic Blood Vessels Is Associated with Expression of Nestin in Endothelial Cells. *Folia Biol. (Praha)*. **1998**, 44 (5), 155–161.
48. Yang X, Ding Y, Yang M, et al. Nestin Improves Preeclampsia-Like Symptoms by Inhibiting Activity of Cyclin-Dependent Kinase 5. *Kidney Blood Press. Res.* **2018**, 43 (2), 616–627.
49. Hubiche T, Ged C, Benard A, et al. Analysis of SPINK 5, KLK 7 and FLG Genotypes in a French Atopic Dermatitis Cohort. *Acta Derm. Venereol.* **2007**, 87 (6), 499–505.
50. Krieg SA, Fan X, Hong Y, et al. Global Alteration in Gene Expression Profiles of Deciduas from Women with Idiopathic Recurrent Pregnancy Loss. *Mol. Hum. Reprod.* **2012**, 18 (9), 442–450.
51. Rhee SG, Bae SH. The Antioxidant Function of Sestrins Is Mediated by Promotion of Autophagic Degradation of Keap1 and Nrf2 Activation and by Inhibition of mTORC1. *Free Radic. Biol. Med.* **2015**, 88 (Pt B), 205–211.

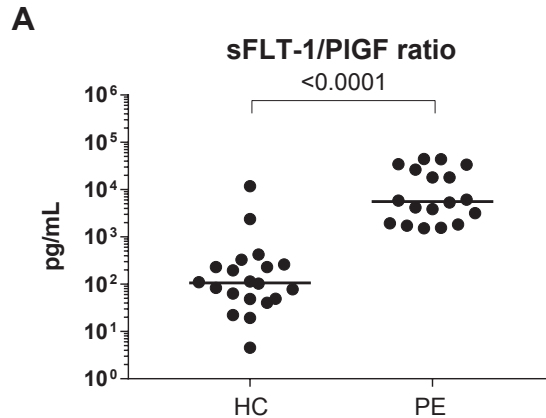
52. Nascimento EB, Osler ME, Zierath JR. Sestrin 3 Regulation in Type 2 Diabetic Patients and Its Influence on Metabolism and Differentiation in Skeletal Muscle. *Am. J. Physiol. Endocrinol. Metab.* **2013**, 305 (11), E1408-14.
53. Ye J, Wang M, Xu Y, et al. Sestrins Increase in Patients with Coronary Artery Disease and Associate with the Severity of Coronary Stenosis. *Clin. Chim. Acta.* **2017**, 472, 51–57.

SUPPLEMENTARY MATERIAL



Supplementary Figure 1. Endothelial identity and overlap of upregulated and downregulated genes in placental bed with incision site.

(A) Overlap between 72 endothelium-specific genes published by Chi *et al.* and all genes with 90th percentile of normalized expression >2 in endothelial cells from the placental bed (irrespective of preeclampsia or healthy controls).²⁹ (B) Overlap between upregulated and downregulated genes in preeclampsia compared to healthy pregnancies in placental bed and incision site, with a nominal p -value <0.05. (C) P value and $padj$ of differential gene expression between preeclampsia and healthy controls at the incision site, for significantly differentially expressed genes with a $padj$ <0.05 in placental bed. *Abbreviations:* PE, preeclampsia (in this study early onset, in combination with fetal growth restriction); HC, healthy pregnancy; PTGDS, prostaglandin D2 synthase; OLFM1, olfactomedin 1; IL3RA, interleukin 3 receptor subunit alpha; SPINK5, serine peptidase inhibitor Kazal type 5; SESN3,sestrin 3.



Supplementary Figure 2. Ratio between serum sFLT-1 and PIGF in preeclampsia and healthy pregnancy. Scatter dot plots of sFLT-1/PIGF ratio.

Line represents median; nominal p -value without correction for multiple testing is indicated and calculated by Mann-Whitney U test. *Abbreviations:* PE, preeclampsia (in this study early onset, in combination with fetal growth restriction); HC, healthy pregnancy; sFLT-1, soluble fms-like tyrosine kinase-1; sICAM, soluble Intercellular Adhesion Molecule; PIGF, Placental growth factor.

Supplementary Table 1. Antibodies used for flow cytometry assisted cell sorting.

CD marker	Name	Fluorochrome	Company	Catalog no.	Clone
CD31	PECAM-1	FITC	BD	555445	WM59
CD144	VE-Cadherin	PE	BD	561714	55-7H1
CD146	MCAM	PerCP-Cy5.5	Biologend	342014	SHM-57
CD309	VEGFR2	Pe-Cy7	Biologend	359912	7D4-6
CD54	ICAM-1	APC	BD	559771	HA58
CD105	Endoglin	eFluor450	eBioscience	48-1057-42	SN6
CD45	Leukocyte common antigen	Pacific Orange	Life technologies	MHCD4530	HI30

Abbreviations: CD, cluster of differentiation; PECAM-1, Platelet-endothelial cell adhesion molecule-1; VE-Cadherin, vascular endothelial cadherin; MCAM, melanoma cell adhesion molecule; VEGFR2, Vascular endothelial growth factor receptor 2; ICAM-1, Intercellular Adhesion Molecule 1; FITC, Fluorescein isothiocyanate; PE, Phycoerythrin; PerCP-Cy5.5, Peridinin-chlorophyll proteins- Cyanine5.5; Pe-Cy7, Phycoerythrin-cyanine 7; APC, Allophycocyanin.

Supplementary Table 2. Baseline characteristics for nulliparous women with preeclampsia and healthy pregnancy included for endothelial cell transcriptional profile comparison.

	Healthy control <i>n</i> =4	Preeclampsia <i>n</i> =5	<i>p</i> -value
General characteristics			
Age (years)	35.3 (5.3)	28.2 (7.1)	0.145
White European (%)	4 (100%)	2 (40.0%)	0.058
BMI (kg/m ²)	26.6 (5.5)	28.1 (5.6)	0.699
Obesity (%)	2 (50.0%)	2 (40.0%)	0.764
Smoking (%)	0 (0.0%)	0 (0.0%)	n/a
General and obstetric history			
Pre-existent hypertension (%)	0 (0.0%)	0 (0.0%)	n/a
Pre-existent kidney disease (%)	0 (0.0%)	0 (0.0%)	n/a
Pre-existent Diabetes (%)	0 (0.0%)	0 (0.0%)	n/a
Nulliparity (%)	4 (100.0%)	5 (100.0%)	n/a
Pregnancy characteristics			
Early onset (%)	n/a	5 (100%)	n/a
FGR (%)	n/a	5 (100%)	n/a
HELLP (%)	n/a	2 (40%)	n/a
GDM with insulin use (%)	0 (0.0%)	0 (0.0%)	n/a
HPP (%)	1 (25%)	1 (20%)	0.858
Maternal characteristics			
Systolic blood pressure (mmHg)	122 (10)	162 (22)	0.010
Diastolic blood pressure (mmHg)	76 (8)	101 (9)	0.003
Antihypertensive treatment oral (%)	0 (0.0%)	4 (80.0%)	0.016
Antihypertensive treatment iv (%)	0 (0.0%)	1 (20.0%)	0.343
Antepartum MgSO ₄ iv (%)	0 (0.0%)	4 (80.0%)	0.016
Antepartum CCS (%)	0 (0.0%)	5 (100%)	0.003
Neonatal characteristics			
GA at delivery (days)	277 (7)	216 (16)	<0.001
Birthweight (grams)	3529 (525)	1135 (338)	<0.001
Birthweight <3 rd percentile (%)	0 (0.0%)	4 (80.0%)	<0.001
Fetal sex, male (%)	2 (50%)	3 (60%)	0.764

Values are presented as means (standard deviations) or as numbers (%). *P*-values were calculated by the χ^2 test for continuous variables and Fisher's exact test for categorical variables. Abbreviations: BMI, Body Mass Index; Obesity was defined as an BMI >30kg/m²; FGR, fetal growth restriction; HELLP, Hemolysis Elevated Liver enzymes Low Platelets syndrome; GDM, gestational diabetes mellitus, HPP, hemorrhage post-partum, defined as blood loss >1000mL; iv, intravenous; MgSO₄, magnesiumsulphate; CCS, corticosteroid treatment; GA, gestational age (days); n/a; not applicable.

Supplementary Table 3. Maternal and pregnancy baseline characteristics in women with severe preeclampsia (with and without HELLP syndrome) and healthy pregnancy for the multiplex immunoassay comparison of systemic biomarkers for inflammation, endothelial activation and dysfunction.

	Healthy control n=20	Preeclampsia n=17	p-value†	Preeclampsia n=9	Preeclampsia with HELLP syndrome n=8	p-value‡
General characteristics						
Age (years)	33.6 (3.9)	31.0 (5.6)	0.110	30.0 (6.5)	33.8 (5.7)	0.228
White European (%)	20 (100.0%)	10 (58.8%)	0.001	4 (44.4%)	6 (75%)	0.201
BMI (kg/m ²)	23.2 (2.2)	25.3 (4.9)	0.094	28.0	22.3	0.016
Obesity (%)	0 (0.0%)	3 (20.0%)	0.036	3 (37.5%)	0 (0.0%)	0.070
Smoking (%)	0 (0.0%)	1 (5.9%)	0.272	1 (11.1%)	0 (0.0%)	0.331
General and obstetric history						
Pre-existent hypertension (%)	0 (0.0%)	2 (11.8%)	0.115	1 (11.1%)	1 (12.5%)	0.929
Pre-existent kidney disease (%)	1 (5.0%)	0 (0.0%)	0.350	0 (0%)	0 (0%)	n/a
Pre-existent Diabetes (%)	0 (0.0%)	0 (0.0%)	n/a	0 (0%)	0 (0%)	n/a
Nulliparity (%)	5 (25.0%)	12 (70.6%)	0.006	6 (66.7%)	6 (75.0%)	0.707
CS in history (%)*	13 (86.7%)	2 (40.0%)	0.037	2 (66.7%)	0 (0.0%)	0.136
HDP in history (%)*	0 (0.0%)	2 (40.0%)	0.010	2 (66.7%)	0 (0.0%)	0.136
FGR in history (%)*	0 (0.0%)	2 (40.0%)	0.010	2 (66.7%)	0 (0.0%)	0.136
Pregnancy characteristics						
Early onset (%)	n/a	17 (100%)	n/a	9 (100%)	8 (100%)	n/a
FGR (%)	n/a	17 (100%)	n/a	9 (100%)	8 (100%)	n/a
HELLP (%)	n/a	8 (47.1%)	n/a	n/a	8 (100%)	n/a
GDM with insulin use (%)	0 (0.0%)	0 (0.0%)	n/a	0 (0%)	0 (0%)	n/a
HPP (%)	1 (5.0%)	0 (0.0%)	0.350	0 (0%)	0 (0%)	n/a

(Continued)

Supplementary Table 3. Maternal and pregnancy baseline characteristics in women with severe preeclampsia (with and without HELLP syndrome) and healthy pregnancy for the multiplex immunoassay comparison of systemic biomarkers for inflammation, endothelial activation and dysfunction.

	Healthy control n=20	Preeclampsia n=17	p-value†	Preeclampsia n=9	Preeclampsia with HELLP syndrome n=8	p-value‡
Maternal characteristics						
Systolic blood pressure (mmHg)	120 (8)	169 (23)	<0.001	164 (21)	171 (26)	0.567
Diastolic blood pressure (mmHg)	75 (7)	108 (10)	<0.001	105 (10)	108 (12)	0.591
Antihypertensive treatment oral (%)	0 (0.0%)	14 (82.4%)	<0.001	8 (88.9%)	6 (75.0%)	0.453
Antihypertensive treatment iv (%)	0 (0.0%)	7 (41.2%)	0.001	2 (22.2%)	5 (62.5%)	0.092
Antepartum MgSO4 iv (%)	0 (0.0%)	13 (76.5%)	<0.001	7 (77.8%)	6 (75.0%)	0.893
Antepartum CCS (%)	0 (0.0%)	17(100.0%)	<0.001	9 (100%)	8 (100%)	n/a
Neonatal characteristics						
GA at delivery (days)	276 (4)	214 (14)	<0.001	215.1 (12.1)	211.9 (16.0)	0.642
Birthweight (grams)	3528 (400)	1048 (278)	<0.001	1015.8 (277.6)	1095.9 (274.2)	0.554
Birthweight <3 rd percentile (%)	0 (0.0%)	14 (82.4%)	<0.001	9 (100%)	5 (62.5%)	0.043
Fetal sex, male (%)	8 (40.0%)	8 (47.1%)	0.666	4 (44.4%)	4 (50.0%)	0.819

Values are presented as means (standard deviations) or as numbers (%). P values were calculated by the χ^2 test for continuous variables and Fisher's exact test for categorical variables. *Obstetric history is calculated amongst multiparous patients only. †P-value between healthy pregnancy and all cases of preeclampsia with FGR; ‡ p-value between cases of preeclampsia with and without HELLP syndrome. Abbreviations: BMI, Body Mass Index; Obesity was defined as an BMI >30kg/m²; CS, Caesarean section; HDP, hypertensive disease of pregnancy; FGR, fetal growth restriction; HELLP, Hemolysis Elevated Liver enzymes Low Platelets syndrome; GDM, gestational diabetes mellitus; HPP, hemorrhage post-partum, defined as blood loss >1000ml; iv, intravenous; MgSO₄, magnesiumsulphate; CCS, corticosteroid treatment; GA, gestational age (days); n/a; not applicable.

Supplementary Table 4. Individual marker comparison by multiplex immunoassay between preeclampsia and healthy pregnancy.

Marker	Healthy controls <i>n</i> =20	Preeclampsia <i>n</i> =17	Nominal <i>p</i> *	Corrected <i>p</i> -value [†]	FDR [‡]
sFLT-1	13021 (9818)	36593 (10929)	<0.001	<0.001	0.000
Endoglin	5322 (2499)	11854 (3664)	<0.001	<0.001	0.000
SAA-1	611653 (698678)	3370800 (8368350)	<0.001	0.001	0.000
PIGF	154 (175)	6 (15)	<0.001	0.001	0.000
sICAM	298010 (74524)	424138 (170489)	<0.001	0.012	0.002
Leptin	16590 (24017)	45833 (21860)	<0.001	0.015	0.003
Fibronectin	3940350 (85956650)	264720000 (252699500)	<0.001	0.026	0.004
YKL-40	49269 (31248)	80929 (103123)	0.001	0.043	0.005
TNF-R1	5112 (1609)	6921 (2129)	0.001	0.082	0.009
HGF	713 (527)	1122 (713)	0.002	0.092	0.009
PAI-1	260281 (169489)	445399 (774301)	0.002	0.096	0.009
Chemerin	21215 (9372)	29814 (14405)	0.002	0.125	0.010
sIL-2R	215 (421)	645 (583)	0.002	0.148	0.011
CCL4	78 (32)	112 (39)	0.004	0.227	0.016
TIMP-1	221695 (50772)	277035 (103473)	0.006	0.365	0.024
IL-6	6 (7)	13 (11)	0.007	0.401	0.025
E-selectin	37510 (22478)	63530 (38702)	0.010	0.575	0.032
OPN	31031 (9983)	46889 (31280)	0.010	0.575	0.032
CXCL10	316 (196)	439 (180)	0.019	1.137	0.060
PDGF-BB	5304 (2909)	8074 (6557)	0.021	1.232	0.062
Gal-9	22030 (6233)	26245 (15174)	0.022	1.336	0.064
Adipsin	536 (359)	853 (680)	0.026	1.562	0.071
IL-10	3 (6)	6 (9)	0.037	2.209	0.096
GP130	42194 (6669)	44972 (7236)	0.046	2.753	0.114
FABP-4	25018 (12684)	20040 (9522)	0.048	2.856	0.114
sIL-6R	25297 (11062)	32534 (11260)	0.051	3.066	0.118
sPD-1	441 (299)	316 (129)	0.059	3.529	0.131
Gal-1	22035 (5283)	25366 (9627)	0.100	5.989	0.214

(Continued)

Supplementary Table 4. Individual marker comparison by multiplex immunoassay between preeclampsia and healthy pregnancy.

Marker	Healthy controls <i>n</i> =20	Preeclampsia <i>n</i> =17	Nominal <i>p</i>*	Corrected <i>p</i>-value[†]	FDR[‡]
sVCAM	2641450 (593475)	3175200 (1198850)	0.106	6.376	0.220
LAP	4290 (2123)	5201 (1938)	0.116	6.986	0.232
TNF-R2	1371 (422)	1546 (860)	0.120	7.207	0.232
Ang-2	2494 (2018)	4489 (6135)	0.170	10.215	0.319
VEGF	7 (6)	8 (5)	0.185	11.091	0.335
RBP4	47079500 (6995250)	49048000 (7432500)	0.190	11.402	0.335
Gal-3	15908 (10207)	20115 (14824)	0.235	14.077	0.402
Thrombomodulin	2575 (1384)	2951 (2346)	0.247	14.808	0.411
IL-8	21 (37)	28 (16)	0.259	15.569	0.421
TWEAK	4314 (1083)	4715 (2219)	0.273	16.355	0.429
SPARC	1804650 (3669059)	681058 (2634289)	0.286	17.166	0.429
Fetuin	255200000 (108872500)	250070000 (73740000)	0.286	17.167	0.429
Apelin	1824 (1317)	2122 (1143)	0.322	19.315	0.471
Adiponectin	90217000 (45889250)	110140000 (61881500)	0.345	20.687	0.493
MMP-1	92106 (85164)	75686 (42535)	0.361	21.634	0.503
LAG-3	854 (482)	756 (434)	0.411	24.632	0.547
Clusterin	197982 (41166)	180935 (60490)	0.411	24.635	0.547
sCD163	8483 (6436)	10977 (5644)	0.428	25.688	0.558
MMP-7	2865 (4093)	2013 (3626)	0.465	27.871	0.581
THBS-1	126100000 (125142500)	77871000 (154575000)	0.465	27.871	0.581
Ang-1	52821 (16822)	47937 (33180)	0.522	31.330	0.639
LIP-2	230467 (449878)	260186 (133947)	0.626	37.549	0.747
DPP-IV	1065650 (579388)	1139300(648400)	0.648	38.854	0.747
MMP-9	31766000 (31350250)	33745000 (27716000)	0.648	38.854	0.747
Tie-2	2026 (1417)	1701 (618)	0.703	42.193	0.796
LAIR-1	1331 (517)	1512 (594)	0.784	47.032	0.871
Cyst C	646181 (434890)	724342 (596285)	0.807	48.443	0.881

(Continued)

Supplementary Table 4. Individual marker comparison by multiplex immunoassay between preeclampsia and healthy pregnancy.

Marker	Healthy controls <i>n</i> =20	Preeclampsia <i>n</i> =17	Nominal <i>p</i> *	Corrected <i>p</i> -value [†]	FDR [‡]
IL-1b	5 (5)	5 (3)	0.855	51.293	0.900
P-selectin	304331 (269833)	287851 (240170)	0.855	51.295	0.900
IL-18	162 (203)	168 (279)	0.903	54.178	0.934
TRAIL	84 (127)	88 (122)	0.951	57.045	0.964
sCD14	2418500 (1386475)	2267000 (2090233)	0.964	57.812	0.964

Values are median concentrations (pg/ml) with interquartile ranges, *p*-value was calculated with Mann-Whitney-U tests. *Analytes with more than 35% of measured values below the lower or above the upper limit of detection. [†]*P*-value adjusted for multiple testing by Bonferroni. [‡]*P*-value adjusted for multiple testing by False Discovery Rate (FDR).

Abbreviations: FDR, false discovery rate; sFLT-1, soluble fms-like tyrosine kinase-1; SAA-1, serum amyloid A1; PIGF, placental growth factor; sICAM, soluble Intercellular Adhesion Molecule; YKL-40, human cartilage glycoprotein 39; TNF-R1, tumor necrosis factor-receptor 1; HGF, hepatocyte growth factor; PAI-1, plasminogen activator inhibitor-1; sIL-2R, soluble interleukin-2 receptor; TIMP-1, Tissue Inhibitor of Metalloproteinase 1; IL-6, interleukin 6; OPN, osteopontin; PDGF-BB, Platelet-derived growth factor subunit B; Gal-9, galectin 9; IL-10, interleukin 10; GPI30, glycoprotein 130; FABP-4, Fatty acid-binding protein 4; sIL-6R, soluble interleukin 6 receptor; sPD-1, soluble programmed cell death protein 1; Gal-1, galectin 1; sVCAM, soluble Vascular cell adhesion protein; LAP, leucine-amino-peptidase; TNF-R2, tumor necrosis factor receptor 2; Ang-2, Angiopoietin 2; VEGF, vascular endothelial cell growth factor; RBP4, Retinol binding protein 4; Gal-3, galectin 3; IL-8, interleukin 8; TWEAK, TNF (tumor necrosis factor)-related weak inducer of apoptosis; SPARC, secreted protein acidic and rich in cysteine; MMP-1, matrix metalloprotease 1; LAG-3, Lymphocyte-activation gene 3; sCD-163, soluble cluster of differentiation 163; MMP-7, matrix metalloprotease 7; THBS-1, Thrombospondin 1; Ang-1, Angiopoietin 1; LIP-2, Lipase 2; DPP-IV, Dipeptidyl peptidase-4; MMP-9, matrix metalloprotease 9; Tie-2, Tyrosine kinase with immunoglobulin-like and EGF-like domains 2; LAIR-1, Leukocyte-associated immunoglobulin-like receptor 1; Cyst C, Cystatin C; IL-1b, interleukin 1 beta; IL-18, interleukin 18; TRAIL, Tumor necrosis factor-related apoptosis-inducing ligand; sCD14, soluble cluster of differentiation 14.

Supplementary Table 5. Individual marker comparison by multiplex immunoassay between women with preeclampsia with or without HELLP syndrome.

Marker	Preeclampsia n=9	Preeclampsia with HELLP syndrome n=8	Nominal p*	Corrected p-value[†]	FDR[‡]
Ang-1	64475 (30089)	32536 (15733)	0.001	0.064	0.064
RBP4	51902000 (4672000)	44490500 (11239000)	0.003	0.171	0.086
Apelin	2613 (1764)	1747 (1054)	0.005	0.316	0.105
PDGF-BB	10789 (2871)	5552 (3771)	0.009	0.560	0.124
sFLT-1	29677 (11717)	40018 (6668)	0.012	0.741	0.124
P-selectin	361210 (678401)	199624 (212380)	0.012	0.741	0.124
LIP-2	308570 (235993)	216820 (68172)	0.016	0.969	0.138
SAA-1	2152800 (1799600)	10419500 (16176975)	0.021	1.255	0.144
Adipsin	609 (652)	992 (148)	0.024	1.419	0.144
Clusterin	173716 (31083)	205257 (83254)	0.027	1.613	0.144
MMP-9	38172000 (18494500)	15480500 (27122425)	0.027	1.613	0.144
PAI-1	329237 (602442)	702866 (873613)	0.034	2.056	0.144
IL-10	5 (7)	10 (19)	0.043	2.598	0.144
LAG-3	693 (284)	955 (343)	0.043	2.598	0.144
IL-8	26 (9)	36 (22)	0.043	2.598	0.144
Endoglin	10456 (3512)	13188 (2584)	0.043	2.598	0.144
Chemerin	24906 (14321)	35253 (8072)	0.043	2.598	0.144
THBS-1	181170000 (222636500)	61244500 (92863250)	0.043	2.598	0.144
E-selectin	41700(35183)	74198 (42960)	0.054	3.258	0.171
GP130	43643(14851)	48886 (7553)	0.068	4.050	0.193
sICAM	357172 (195616)	466600 (181756)	0.068	4.050	0.193
Gal-1	22128 (8862)	29001 (10229)	0.083	4.996	0.217
Ang-2	2365 (4026)	5696 (7261)	0.083	4.996	0.217
TNF-R1	5749 (1907)	7199 (2544)	0.102	6.113	0.235
TNF-R2	1412 (650)	1910 (923)	0.102	6.113	0.235
LAP	5420 (2165)	4558 (1746)	0.102	6.113	0.235
Leptin	51168 (18453)	39824 (22068)	0.112	6.728	0.249

(Continued)

Supplementary Table 5. Individual marker comparison by multiplex immunoassay between women with preeclampsia with or without HELLP syndrome.

Marker	Preeclampsia n=9	Preeclampsia with HELLP syndrome n=8	Nominal p*	Corrected p-value†	FDR‡
Fibronectin	210150000 (218089825)	329035000 (329784250)	0.123	7.364	0.263
TWEAK	5407 (2120)	4317 (735)	0.149	8.935	0.298
Tie-2	1699 (697)	2150 (1201)	0.149	8.935	0.298
Thrombomodulin	2526 (2500)	3394 (2003)	0.178	10.676	0.334
DPP-IV	1073200 (626920)	1258550 (512500)	0.178	10.676	0.334
MMP-1	76927 (45814)	67427 (64107)	0.211	12.658	0.384
Fetuin	251270000 (57415000)	213730000 (79657500)	0.290	17.390	0.497
TIMP-1	251428 (88968)	281139 (75567)	0.290	17.390	0.497
FABP-4	22066 (11863)	19132 (6272)	0.336	20.155	0.530
sVCAM	3028100 (939800)	3379500 (1542825)	0.336	20.155	0.530
Adiponectin	91688000 (57801500)	121705000 (66442500)	0.336	20.155	0.530
OPN	44073 (18272)	52769 (47517)	0.386	23.189	0.580
MMP-7	1999 (2219)	2894 (5488)	0.386	23.189	0.580
SPARC	1433700 (2914207)	622578 (1582056)	0.441	26.485	0.646
IL-6	13 (10)	15 (11)	0.501	30.035	0.698
HGF	944 (854)	1189 (612)	0.501	30.035	0.698
Gal-3	20115 (13396)	23106 (23100)	0.630	37.826	0.824
sCD14	2543500 (2219787)	2167300 (2068225)	0.630	37.826	0.824
IL-1b	5 (4)	5 (5)	0.665	39.889	0.824
VEGF	8 (4)	6 (6)	0.700	41.998	0.824
IL-18	168 (250)	185 (327)	0.700	42.019	0.824
sIL-2R	645 (642)	717 (574)	0.700	42.019	0.824
Cyst C	724342 (916234)	727035 (514915)	0.700	42.019	0.824
Gal-9	23763 (16392)	27282 (14181)	0.700	42.019	0.824
CCL4	105 (39)	114 (72)	0.773	46.370	0.875
sPD-1	326 (176)	302 (54)	0.773	46.370	0.875

(Continued)

Supplementary Table 5. Individual marker comparison by multiplex immunoassay between women with preeclampsia with or without HELLP syndrome.

Marker	Preeclampsia <i>n</i> =9	Preeclampsia with HELLP syndrome <i>n</i> =8	Nominal <i>p</i> *	Corrected <i>p</i> -value [†]	FDR [‡]
CXCL10	418 (164)	440 (410)	0.847	50.843	0.924
sCD163	8599 (4445)	11659 (8178)	0.847	50.843	0.924
PIGF	6(14)	4 (16)	0.883	52.963	0.946
sIL-6R	32534(13135)	32003 (10516)	0.923	55.398	0.955
LAIR-1	1512 (557)	1482 (693)	0.923	55.401	0.955
TRAIL	88 (101)	65 (154)	0.961	57.683	0.978
YKL-40	80929 (74124)	105167 (126816)	1.000	60.000	1.000

Values are median concentrations (pg/ml) with interquartile ranges, *P*-value was calculated with Mann-Whitney-U tests. [†]*P*-value adjusted for multiple testing by Bonferroni. [‡]*P*-value adjusted for multiple testing by False Discovery Rate (FDR).

Abbreviations: HELLP, hemolysis, elevated liverenzymen, low platelets; FDR, false discovery rate; Ang-1, Angiopoietin 1; RBP4, Retinol binding protein 4; PDGF-BB, Platelet-derived growth factor subunit B; sFLT-1, soluble fms-like tyrosine kinase-1; LIP-2, Lipase 2; SAA-1, serum amyloid A1; MMP-9, matrix metalloprotease 9; PAI-1, plasminogen activator inhibitor-1; IL-10, interleukin 10; LAG-3, Lymphocyte-activation gene 3; IL-8, interleukin 8; THBS-1, Thrombospondin 1; GPI30, glycoprotein 130; sICAM, soluble Intercellular Adhesion Molecule; Gal-1, galectin 1; Ang-2, Angiopoietin 2; TNR-R1, tumor necrosis factor-receptor 1; TNF-R2, tumor necrosis factor receptor 2; LAP, leucine-amino-peptidase; TWEAK, TNF (tumor necrosis factor)-related weak inducer of apoptosis; Tie-2, Tyrosine kinase with immunoglobulin-like and EGF-like domains 2; DPP-IV, Dipeptidyl peptidase-4; TIMP-1, MMP-1, matrix metalloprotease 1; Tissue Inhibitor of Metalloproteinase 1; FABP-4, Fatty acid-binding protein 4; sVCAM, soluble Vascular cell adhesion protein; OPN, osteopontin; MMP-7, matrix metalloprotease 7; SPARC, secreted protein acidic and rich in cysteine; IL-6, interleukin 6; HGF, hepatocyte growth factor; Gal-3, galectin 3; sCD14, soluble cluster of differentiation 14, IL-1b, interleukin 1 beta; VEGF, vascular endothelial cell growth factor; IL-18, interleukin 18; sIL-2R, soluble interleukin-2 receptor; Cyst C, Cystatin C; Gal-9, galectin 9; sPD-1, soluble programmed cell death protein 1; sCD-163, soluble cluster of differentiation 163; PIGF, placental growth factor; sIL-6R, soluble interleukin 6 receptor; LAIR-1, Leukocyte-associated immunoglobulin-like receptor 1; TRAIL, Tumor necrosis factor-related apoptosis-inducing ligand; YKL-40, human cartilage glycoprotein 39.

Human regulatory T cells at the maternal- fetal interface show functional site-specific adaptation with tumor- infiltrating-like features

Judith Wienke, Laura Brouwers, Leone van der Burg, Michal Mokry, Rianne Scholman, Peter Nikkels, Bas van Rijn, and Femke van Wijk

Manuscript in preparation

ABSTRACT

Objectives: Regulatory T cells (Tregs) in tissues show functional adaptation to their local microenvironment. Here, we investigate the transcriptional adaptation of human uterine Tregs (uTregs) to the peculiar environment of the maternal-fetal interface during pregnancy, where Tregs have a crucial role in maintaining immune tolerance against the semi-allogeneic fetus.

Methods: Placental bed biopsy samples were obtained from women with uncomplicated pregnancies undergoing primary Caesarean section. Biopsies were enzymatically digested and CD3⁺CD4⁺CD25^{hi}CD127⁻ uTregs, blood Tregs (bTregs) and CD4⁺ non-Tregs (Tconv) from both compartments were isolated by flow cytometry-assisted cell sorting for transcriptomic profiling.

Results: uTregs showed enhanced expression of Treg signature markers compared to bTregs, including FOXP3, CTLA4 and TIGIT. The uTreg core signature, defined by genes specifically upregulated or downregulated in uTreg compared to bTreg and uTconv, was indicative of late-stage effector Treg differentiation and chronic activation with high expression of immune checkpoints TACI, GITR, TNFR2, OX-40, CD30, 4-1BB, molecules associated with suppressive capacity (CTLA4, ENTPD1, HAVCR2, IL10, IL2RA, LAG3, LAYN, LGALS1, PDCD1, TOX2), Treg activation (HLA-DR, CD80, LRR32), and transcription factors MAF, PRDM1, BATF, and VDR, as well as downregulated SATB1. uTregs at the maternal-fetal interface mirrored uTconv Th1 polarization, with high expression of T-bet and CXCR3. uTregs further had high expression of residency marker CD69 and showed functional adaptation to their microenvironment with transcriptional characteristics of tissue-resident memory T cells, and increased expression of several cytokine and chemokine receptors (CCR1, CXCR6, CCR5, IL-1 receptor family) indicating high responsiveness to environmental cues. Moreover, their core signature was specifically shared with the specialized transcriptional profile of tumor-infiltrating Tregs. Remarkably, this highly differentiated effector profile similar to tumor-infiltrating Tregs was more pronounced at the maternal-fetal interface compared to a distant uterine tissue site.

Conclusion: uTregs at the maternal-fetal interface specifically acquire a highly differentiated effector Treg profile similar to tumor-infiltrating Tregs, which is more pronounced even compared to a distant uterine tissue site. This introduces the novel concept of site-specific transcriptional adaptation of human Tregs within one organ.

INTRODUCTION

In the past decade, T cells have been identified in a spectrum of human and murine non-lymphoid tissues.^{1,2} T cells residing in tissues for prolonged periods are thought to serve as first-line responders to infections.^{1,2} These tissue-resident memory T cells (TRM) do not recirculate and are characterized by expression of signature molecules such as CD69, which prevents their tissue egress.^{1,3–8} TRM adapt to their tissue environments by acquiring a specialized functional phenotype that depends on micro-environmental cues.^{9,10} Also regulatory T cells (Tregs), which are critical gatekeepers of immune homeostasis,¹¹ have been recently identified in various murine and human tissues.^{12–17} Like TRM, Tregs can become resident and adapt to their microenvironment.^{12,14,15,18–20} Tissue-resident Tregs gain a polarized phenotype compared to circulating Tregs, with functional specialization depending on the tissue or organ, which is controlled on a transcriptional level.^{12,14,16,21,22} Although increasing evidence in mice supports this functional adaptation of Tregs to non-lymphoid tissue environments,²³ studies investigating tissue adaptation of human Treg are still scarce. Only recently, the first transcriptional profiles of Tregs in healthy human tissues were published.^{14,15} A human tissue environment in which transcriptional adaptation of Tregs has gained interest due to the important therapeutic implications, is the tumor environment.²⁴ Tumor-infiltrating Tregs (TITR) have been shown to display a unique and specialized transcriptional signature,²⁵ which is associated with activation and functional specialization of Tregs at these sites, including increased suppressive capacity.^{25–27} In tissues, and especially in tumors, Tregs undergo differentiation reminiscent of effector Tregs. Effector Tregs are a subset of Tregs with potent suppressive capacity, which are characterized by expression of CD45RO, and increased CD25, CTLA-4, and HLA-DR.^{28–31} Furthermore, effector Tregs (in tissues and tumors) express high levels of immune checkpoint molecules OX-40, 4-1BB, GITR, CD30, TIGIT, ICOS and transcription factors such as PRDM1 (blimp-1) and BATF.^{22,25–27,31–34} Effector Tregs can mirror effector T helper (Th) cell polarization, by acquiring coexpression of FOXP3 with chemokine receptors and transcription factors associated with Th1 (CXCR3, T-bet), Th2 (GATA3, IRF4) or Th17 (RORC, STAT3) differentiation.^{22,35–38} This specific polarization has been associated with an enhanced suppressive efficacy towards the matching T effector response.^{31,35–37,39–45} Since most of these insights have been generated in mice, it is still largely unknown whether these principles also apply to human tissue Tregs. As recently highlighted by Sharma *et al.*,⁴⁶ one of the most interesting, but yet elusive tissue sites for Treg function in humans is the maternal-fetal interface.

Pregnancy is a mystifying biological process when viewed from an immunological perspective, as it poses a unique challenge to the maternal immune system.^{47,48} While peripheral immunity against pathogens needs to remain intact⁴⁹, the semi-allogeneic fetus and placenta, which may harbor foreign paternal antigens, have to be tolerized. This suggests that the maternal immune response is delicately balanced during pregnancy,

requiring tight regulation especially of the local immune response at the maternal-fetal interface, while maintaining systemic immune responses.^{47,48,50} The requirement for local regulation of the maternal immune response is underlined by the fact that human decidual T cells can recognize and actively respond to fetal cord blood cells.⁵¹ Accordingly, maternal Tregs have been shown to be indispensable for successful embryo implantation and pregnancy outcome in murine pregnancy, as they contribute to maternal-fetal tolerance on multiple levels.^{47,52,53} Specifically, depletion of maternal Tregs caused pregnancy loss due to immunological rejection of the fetus.^{53,54} In humans, maternal Tregs have been shown to be abundantly present in the gravid uterus,^{55–62} and normal human pregnancy is characterized by increased numbers of Tregs in the periphery and at the maternal–fetal interface.^{56,61,63,64} In patients with preeclampsia, a severe hypertensive disorder of pregnancy, and patients with recurrent miscarriages, Treg numbers are reduced both at the maternal-fetal interface and in the periphery,^{57,65–70} which implies that also in humans local presence of Tregs in the pregnant uterus is required for successful pregnancy outcome. However, most previous studies investigating the maternal, uterine immune system in humans have been limited by the practical challenge of acquiring exclusively maternal material and have therefore made use of decidua derived from the post-partum placenta, which can be contaminated by fetal immune cells. Moreover, the functional and transcriptomic profile of human Tregs from the maternal-fetal interface and its relation to Tregs from other human tissues remains to be elucidated.

We hypothesize that resident Tregs in the gravid human uterus acquire a specialized functional profile to effectively regulate the local maternal immune response. Here, we investigated functional adaptation and specialization of highly purified human, exclusively maternal, resident uterine Tregs in myometrial biopsies from the maternal-fetal interface. We performed transcriptomic profiling and functional *in vitro* assays, as well as flow cytometry to study their phenotypic heterogeneity on protein level in single cell resolution. Furthermore, to identify tissue (site)-specific functional adaptation, we compared these Tregs to uterine Tregs from a distant uterine control site and maternal peripheral blood Tregs, in addition to the tissue- and site-matched resident CD4⁺ non-Treg T cells. Lastly, we compared the specific profile of functional adaptation of uTregs to known Treg signatures from other human and murine tissue sites, including tumors. In short, we identified a functional profile representing late-stage effector Treg differentiation, chronic activation, and Th1-like polarization, in uterine Tregs from the maternal-fetal interface, which revealed a remarkable overlap with tumor-infiltrating Treg signatures. Moreover, this functional adaptation represented not only local adaptation to the uterine tissue environment, but was specifically pronounced at the maternal-fetal interface, implying tissue site-specific adaptation within the uterus.

METHODS

Participants and biopsies

This study is part of the Spiral Artery Remodeling (SPAR) cohort study. Detailed description of the study set-up and protocol was previously published.⁷¹ We included 20 women who delivered by primary elective Caesarean section, i.e. without contractions or rupture of membranes, after an uneventful pregnancy and without any major underlying pathology, five of which were included for transcriptomics of T cell populations, 4 for suppression assays, and 11 for flow cytometry. The baseline characteristics are provided in supplementary table 1. All patients received study information and signed informed consent prior to participation. This study was reviewed and approved by the local Institutional Ethical Review Board of the University Medical Center Utrecht (16-198). One tube of sodium-heparin blood was taken before Caesarean section. After delivery of the neonate and placenta the placental bed was manually located and two biopsies of the central placental bed from the inner uterine myometrial wall were obtained as previously described.⁷¹ Additionally, biopsies were taken from the incision site when the placenta was not situated on this part of the uterine wall.

Lymphocyte isolation

Peripheral blood mononuclear cells (PBMC) were isolated from blood diluted 1:1 with basic medium (RPMI 1640 (Gibco) with Penicillin/Streptomycin (Gibco), L-glutamine (Gibco)), by ficoll-density centrifugation (GE Healthcare-Biosciences, AB). PBMC were washed in basic medium with 2% fetal calf serum (FCS, Biowest) and PBS or staining buffer consisting of cold PBS supplemented with 2% FCS and 0.1% sodium-azide (Severn Biotech Ltd.). The biopsy samples were collected in basic medium supplemented with 10% FCS and minced into pieces of 1 mm³ in PBS (Gibco). The biopsies were enzymatically digested with 1 mg/mL collagenase IV (Sigma) in medium for 60 minutes at 37°C in a tube shaker under constant agitation at 120 rpm. To dissolve the remaining biopsy pieces after digestion and remove any remaining lumps, the biopsies were pipetted up and down multiple times and poured over a 100 µm Cell Strainer (BD Falcon). Cells were subsequently washed in staining buffer and filtered through a 70 µm cell strainer and prepared for flow cytometry or flow-cytometry assisted cell sorting.

Flow cytometry

For flow cytometric experiments without restimulation, PBMC and uterine cells were first incubated in Fixable viability dye eFluor506 (eBioscience) 1:300 in PBS for 20 min at 4°C, and washed in PBS. For surface staining cells were incubated with the antibodies shown in supplementary table 2 for 20 minutes in staining buffer at 4°C, and subsequently washed in the same buffer. Cells were permeabilized with 1 part fixation/permeabilization concentrate and 3 parts fixation/permeabilization diluent (eBioscience) for 30 minutes at 4°C and subsequently incubated overnight with intracellular antibodies (supplementary table 2) in 10x diluted Permeabilization buffer (Perm, eBioscience) 4°C. The next day, cells were washed with Perm and measured on the LSR Fortessa (BD). For intracellular cytokine measurement, PBMC and uterine cells were first incubated with surface staining, washed, and then restimulated with 20 ng/ml phorbol 12-myristate 13-acetate (PMA) and 1 µg/ml ionomycin for 4 hours with addition of Monensin (GolgiStop, BD Bioscience) during the last 3.5 hours at 37°C. Afterwards, cells were stained with the viability dye, permeabilized, intracellularly stained and measured as described above.

Cell sorting

Cells were incubated with surface antibodies (supplementary table 2) for 20 minutes in staining buffer at 4°C, washed in the same buffer and filtered through a 50 µm cell strainer (Falcon, BD). For suppression assays, cells of the CD3⁺CD4⁺CD25⁺CD127⁻ cell population (Tregs) and CD3⁺CD4⁺CD25⁻ cell population (Tconv) were directly sorted into tubes with 500µL FCS on a FACSAria™ III (BD). For RNA sequencing, 2000 cells of the CD3⁺CD4⁺CD25⁺CD127⁻ cell population (Tregs) and CD3⁺CD4⁺CD25⁻CD45RA⁻ (CD69⁺ from biopsies, CD69⁻ from blood) cell population (Tconv) were sorted into Eppendorfs containing 125 µL PBS. After sorting, 375 µL Trizol LS (Thermo Fisher Scientific) was added to each vial and vials were stored at -80°C until RNA isolation.

Suppression assays and cytokine measurement

After sorting, peripheral blood and uterine Tregs and Tconv were washed in PBS and resuspended in basic medium with 10% human AB serum (Sanquin). Previously isolated and frozen healthy donor (HC) PBMC were labelled with 2µM CellTrace Violet (ThermoFisher) as described previously.⁷² Treg or Tconv populations were added to 15.000 HC PBMC at different ratios and cells were co-incubated for 4 days at 37°C. Supernatants were collected for cytokine measurement by multiplex assay before cells were stained with surface antibodies for CD3, CD4 and CD8 as described above and measured on a FACS Canto (BD).

Whole transcriptome sequencing

For RNA isolation, the vials were thawed at room temperature and 100 μ L chloroform was added to each vial. The vials were shaken well and spun down at 12000xg for 15 minutes at 4°C. The aqueous phase was transferred into a new tube and RNA was mixed with 1ul of GlycoBlue (Invitrogen) and precipitated with 250 μ L isopropanol. Cells were incubated at -20°C for one hour and subsequently spun down at 12000xg for 10 minutes. The supernatant was carefully discarded and the RNA pellet was washed twice with 375 μ L 75% ethanol. Vials were stored at -80°C until library preparation. Low input RNA sequencing libraries from biological sorted cell population replicates were prepared using the Cel-Seq2 Sample Preparation Protocol⁷³ and sequenced as 2 x 75bp paired-end on a NextSeq 500 (Utrecht Sequencing Facility). The reads were demultiplexed and aligned to human cDNA reference using the BWA (0.7.13).⁷⁴ Multiple reads mapping to the same gene with the same unique molecular identifier (UMI, 6bp long) were counted as a single read.

7

Data analysis

RNA sequencing data were normalized per million reads and differentially expressed genes were identified using the DESeq2 package in R 3.5.1 (CRAN), with correction for donor batch. Genes with adjusted p value (padj) <0.05 were considered differentially expressed. Principal component analysis (PCA) was performed in DESeq2 based on gene expression of all genes. Pathway enrichment analysis was conducted in Toppgene Suite publicly available online portal and pathways with Bonferroni-corrected p-values <0.05 were considered statistically significant.⁷⁵ For heatmap analysis, gene expression was mean-centered and scaled per gene and hierarchical clustering was performed with Ward's method and Euclidian distance. Gene set enrichment analysis (GSEA⁷⁶) was conducted by 1000 random permutations of the phenotypic subgroups to establish a null distribution of enrichment score against which a normalized enrichment score and FDR-corrected q values were calculated. Gene sets were either obtained from provided data in publications or by analyzing raw data using GEO2R (NCBI tool).⁷⁷ An overview of used signatures is provided in supplementary table 3. For flow cytometric data, median fluorescent intensities (MFI) and percentages of positive cells were analyzed in FlowJo (LLC). For graphic representation, data were analyzed in GraphPad Prism (GraphPad Software). To assess significance between groups, Two-way ANOVA with Tukey post hoc test was used and p values <0.05 were considered statistically significant.

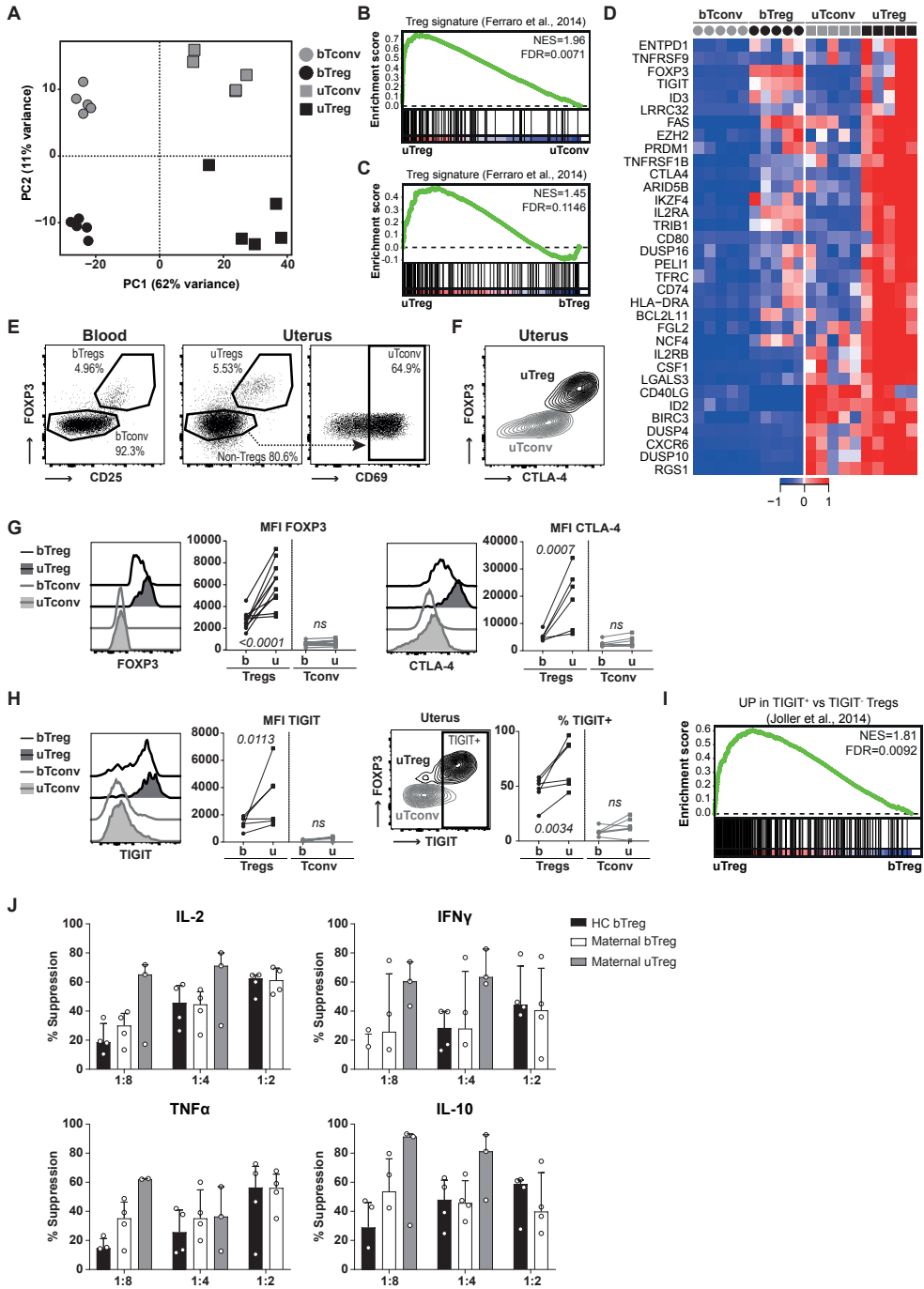


Figure 1. Tregs at the maternal-fetal interface are bona fide Tregs.

RESULTS

Uterine Tregs are bona fide suppressive Tregs

The frequency of CD25^{hi}FOXP3⁺ regulatory T cells (Tregs) within the CD4⁺ T cell population was similar between blood and uterine tissue and ranged from 2.5 to 13.5% (supplementary figure 1A). For transcriptomic analysis, the CD3⁺CD4⁺CD25^{hi}CD127⁻ population (Tregs) and CD3⁺CD4⁺CD25⁻CD45RA⁻ memory T cells (Tconv) were FACS sorted from peripheral blood and myometrial biopsies from 5 women with uncomplicated pregnancies undergoing Caesarean section. In myometrium, Tconv were selected for CD69 positivity. The sorting strategy is shown in supplementary figure 1B. Confirming the maternal origin of the sorted cells, the female-specific gene XIST was highly expressed in all samples, whereas transcripts of the male-specific gene SRY were undetectable in all samples, including pregnancies with male offspring (supplementary figure 1C). Principal component analysis (PCA) of transcriptomic profiles showed that uterine Tregs (uTregs) from the maternal-fetal interface are clearly distinct from blood-derived Tregs (bTregs), and that also uterine T conv (uTconv) and blood-derived Tconv (bTconv) clearly cluster apart (figure 1A). Notably, PC1, mounting the difference between the cell sources, accounted for >60% of the variance, whereas PC2, explaining variance between Treg and Tconv populations, accounted for only 11% of the variance. To assess whether the sorted population of uTregs were bona fide Tregs, we analyzed enrichment of a published core Treg gene signature⁷⁸ in uTregs compared to uTconv and bTregs by gene set enrichment analysis (GSEA). Expression of Treg core signature genes was not only enriched compared to uTconv, but, remarkably, also more pronounced in uTregs than in bTregs, indicating that uTregs are bona fide Tregs with enhanced expression of Treg core signature genes (figure 1B-C). Indeed, expression of many Treg markers from the published Treg signature⁷⁸ was higher in uTreg than bTreg (figure 1D). Expression of the Treg-identifying molecules FOXP3 and CTLA-4 was confirmed to be higher in uTregs than bTregs on protein level (figure 1E-G). Also TIGIT, a key checkpoint

7

(Figure 1 continued)

(A) Principal component analysis of bTregs, bTconv, uTregs and uTconv. (B+C) Gene set enrichment analysis (GSEA) with published Treg signature gene set 78 comparing uTreg and uTconv (B) and uTreg and bTreg (C). NES = normalized enrichment score. (D) Heatmap of genes in leading edge of GSEA analysis comparing enrichment of published Treg signature genes in uTregs and bTregs. Expression values were mean-centered and scaled per gene. (E) Gating strategy of bTregs, uTregs and uTconv. (F) Expression of CTLA-4 in uTregs. (G) Ex vivo protein expression of core Treg molecules FOXP3, CTLA4, and CD25 measured by flow cytometry. (H) Ex vivo protein expression of Treg signature molecule TIGIT measured by flow cytometry. (I) GSEA of TIGIT⁺ Treg signature.⁷⁹ (J) Suppression assay assessing cytokine production of anti-CD3 stimulated (or unstimulated) healthy CD4⁺ T cells in the supernatant by multiplex immunoassay after 4 days of coculture with healthy donor bTregs, maternal bTregs, or uTregs at a 1:8, 1:4 and 1:2 ratio. MFI = median fluorescent intensity.

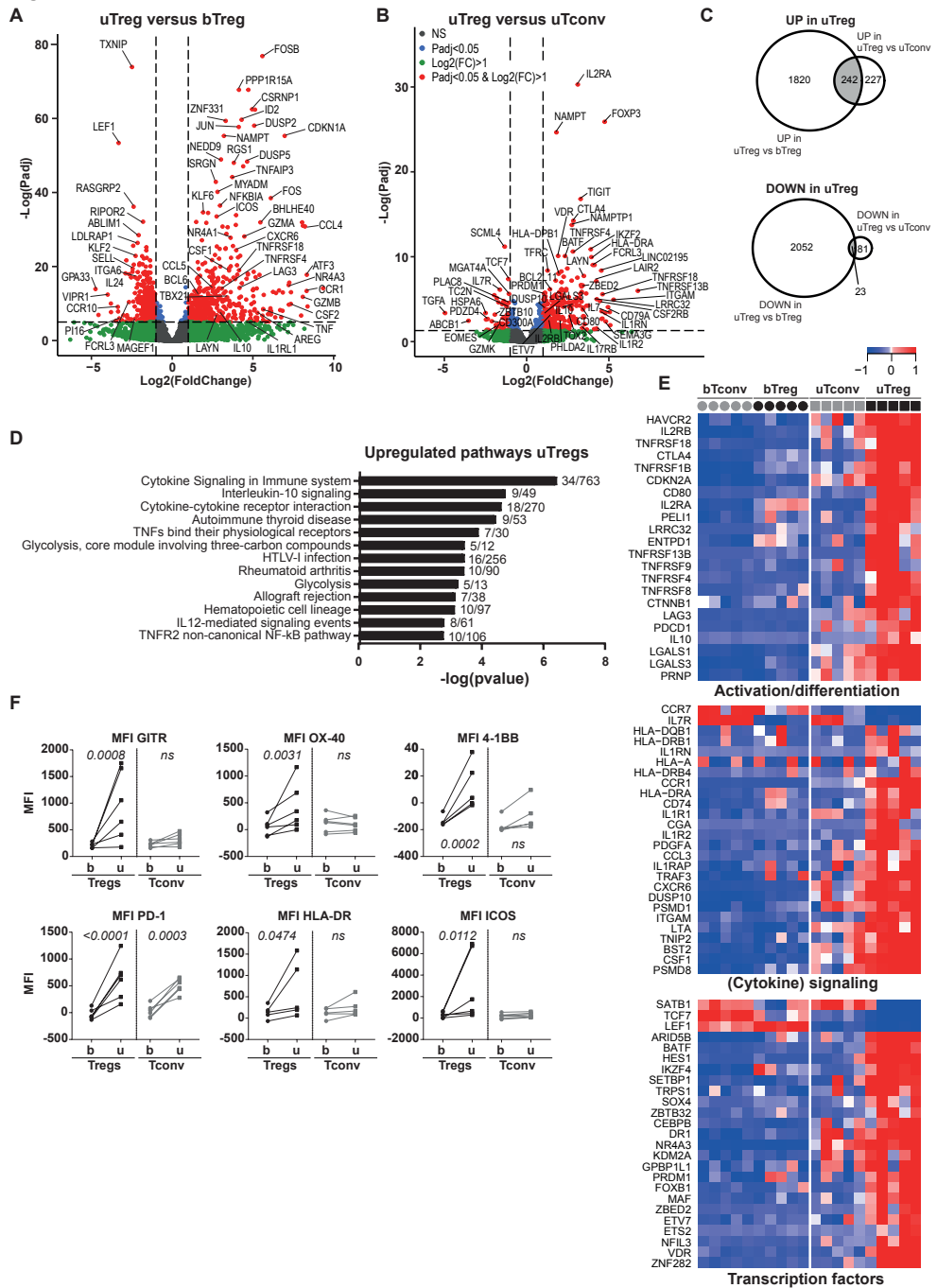


Figure 2. The uTreg core signature.

molecule associated with specialized suppressive function,⁷⁹ was highly expressed in uTregs, with the majority uTregs being positive for TIGIT (figure 1H). Consistently, GSEA showed significant enrichment of a previously identified TIGIT⁺ Treg signature (figure 1I).⁷⁹ Suppression assays, although technically challenging due to low cell numbers, confirmed the suppressive potential of uTregs on proliferation and cytokine production of healthy donor peripheral blood-derived CD4⁺ T cells (Figure 1J and supplementary figure 1D-E). 2 out of 4 uTreg donors showed particularly high suppressive capacity of uTregs on cytokine production of IL-2, IL-10, IFN γ and TNF α , already at a 1:8 (Treg:Tconv) ratio, compared to bTregs. These results confirm that the sorted uTregs are bona fide functional Tregs, with enhanced expression of Treg signature genes.

The uTreg signature is indicative of an activated and effector Treg profile

To investigate the functional adaptation of uTregs to the specific environment of the maternal-fetal interface, we determined both their functional differentiation and (T helper) polarization, both of which may be influenced by the tissue environment.^{13,17,18,33,80–82} To identify the uTreg-specific transcriptional signature, we assessed their differential gene expression with both bTregs and uTconv. A large number of genes were differentially expressed between uTregs and bTregs (figure 2A). Differential gene expression analysis showed significant upregulation of 2062 genes and downregulation of 2075 genes in uTregs compared to bTregs (padj<0.05). To isolate the uTreg specific signature, we also compared gene expression between uTreg and uTconv, yielding 469 upregulated and 104 downregulated genes in uTreg compared to uTconv, including the Treg-identifying genes FOXP3, IL2RA, CTLA4, TIGIT and IKZF2 (padj<0.05; figure 2B) To pinpoint uTreg-specific genes, we overlapped their differentially expressed genes with bTreg and uTconv (figure 2C). This resulted in 242 genes specifically upregulated (231 after removal of duplicate genes) and 23 genes specifically downregulated in uTreg compared to both bTreg and uTconv (supplementary table 4). Among the 23 downregulated genes were ITGA6, IL7R,

(Figure 2 continued)

(A+B) Volcanoplot of differential gene expression between uTregs and bTregs (A) or uTregs and uTconv (B) (C) Venn diagrams yielding genes specifically upregulated (padj<0.05, upper panel) or downregulated (padj<0.05, lower panel) in uTreg compared to bTreg and uTconv. (D) Pathway analysis (ToppGene pathways) of 242 genes specifically upregulated in uTregs. P-values<0.05 after Bonferroni correction were considered significant. (E) Heatmap showing gene expression of genes in top 5 pathways and selected downregulated genes in the uTreg core signature, related to Treg activation or effector differentiation (upper panel), (cytokine) signaling (middle panel; including downregulated CCR7 and IL7R) and transcription factors (lower panel). Expression values were mean-centered and scaled per gene. (F). Protein expression of GITR (TNFRSF18), OX-40 (TNFRSF4), 4-1BB (TNFRSF9), PD-1 (PDCD1), HLA-DR and ICOS. Padj of Two-way ANOVA with Tukey post hoc test. MFI = median fluorescent intensity; NS = Not significant. .

CCR7, TTC39C, PLAC8, ATF7IP2, ABLIM1, MGAT4A, PRKCB, GIMAPs as well as transcription factors TCF7, LEF1, and SATB1, indicating late-stage differentiation of Tregs.^{83,84} Pathway analysis of the 231 upregulated genes yielded cytokine signaling, TNF receptor signaling, and glycolysis as important upregulated pathways (figure 2D). Selected genes from the top 5 pathways included molecules related to Treg activation and effector differentiation, such as immune checkpoints of the TNF receptor superfamily (TNFRSF13B (TACI), TNFRSF18 (GITR), TNFRSF1B (TNFR2), TNFRSF4 (OX-40), TNFRSF8 (CD30), TNFRSF9 (4-1BB)) and HLA-DR, CD80, and LRRC32. Also molecules associated with suppressive capacity (CTLA4, ENTPD1, HAVCR2, IL10, IL2RA, LAG3, LAYN, LGALS1, PDCD1, and TOX2) were highly expressed in uTregs (figure 2E).^{22,31} Furthermore, cytokine receptors of the IL-1 and IL-2 family (IL1R1, IL1R2, IL1RAP, IL1RN, IL2RA, IL2RB) and specific chemokine receptors (CCR1, CXCR6) showed increased and specific expression in uTregs (figure 2E). Transcription factors that were specifically upregulated in uTregs included BATF, CEBPB, ETS2, ETV7, HES1, IKZF4, MAF, NFIL3, PRDM1, VDR, and ZBTB32 among others (figure 2E). This transcriptomic profile, and especially high expression of BATF, PRDM1, and immune checkpoint molecules, reflects previously identified crucial signatures of effector Treg differentiation and function, especially in tissues.^{29,32,33,85–87} We confirmed upregulation of the important immune checkpoints associated with effector Treg differentiation/chronic stimulation GITR, OX-40, 4-1BB, and PD-1, HLA-DR, and ICOS in uTregs on protein level, which again showed their specifically high levels in uTregs even compared to uTconv (figure 2F). Since increased expression of many of these genes pointed towards an activated phenotype, we confirmed this by demonstrating significant enrichment of published gene sets generated by activating Treg *in vitro* with TCR stimulation or cytokine stimulation, in uTregs (supplementary figure 2, supplementary table 3).^{88–92} Taken together, these findings indicate that uTreg at the maternal-fetal interface have a highly differentiated transcriptional signature suggestive of a specialized function with high suppressive capacity and high responsiveness to environmental cues, which is reflective of late-stage effector differentiation and chronic activation.

uTregs have a tissue-resident phenotype and share transcriptional specialization with uTconv

To examine whether uTregs at the maternal-fetal interface represent a resident population or rather transiently infiltrating cells, we assessed the expression of tissue-residency related markers and gene signatures. uTregs had a significantly higher gene and protein expression of key residency molecule CD69 than bTregs and bTconv, similar to uTconv (figure 3A-B). Expression analysis and GSEA with published human TRM signatures showed a pattern of upregulated and downregulated genes as previously described in CD4⁺ (and CD8⁺) TRM from the lung and skin (figure 3B-C),^{4,15,93} confirming the tissue-resident profile in uTregs as compared to bTregs. To further assess the tissue-specific adaptation of T cells at the

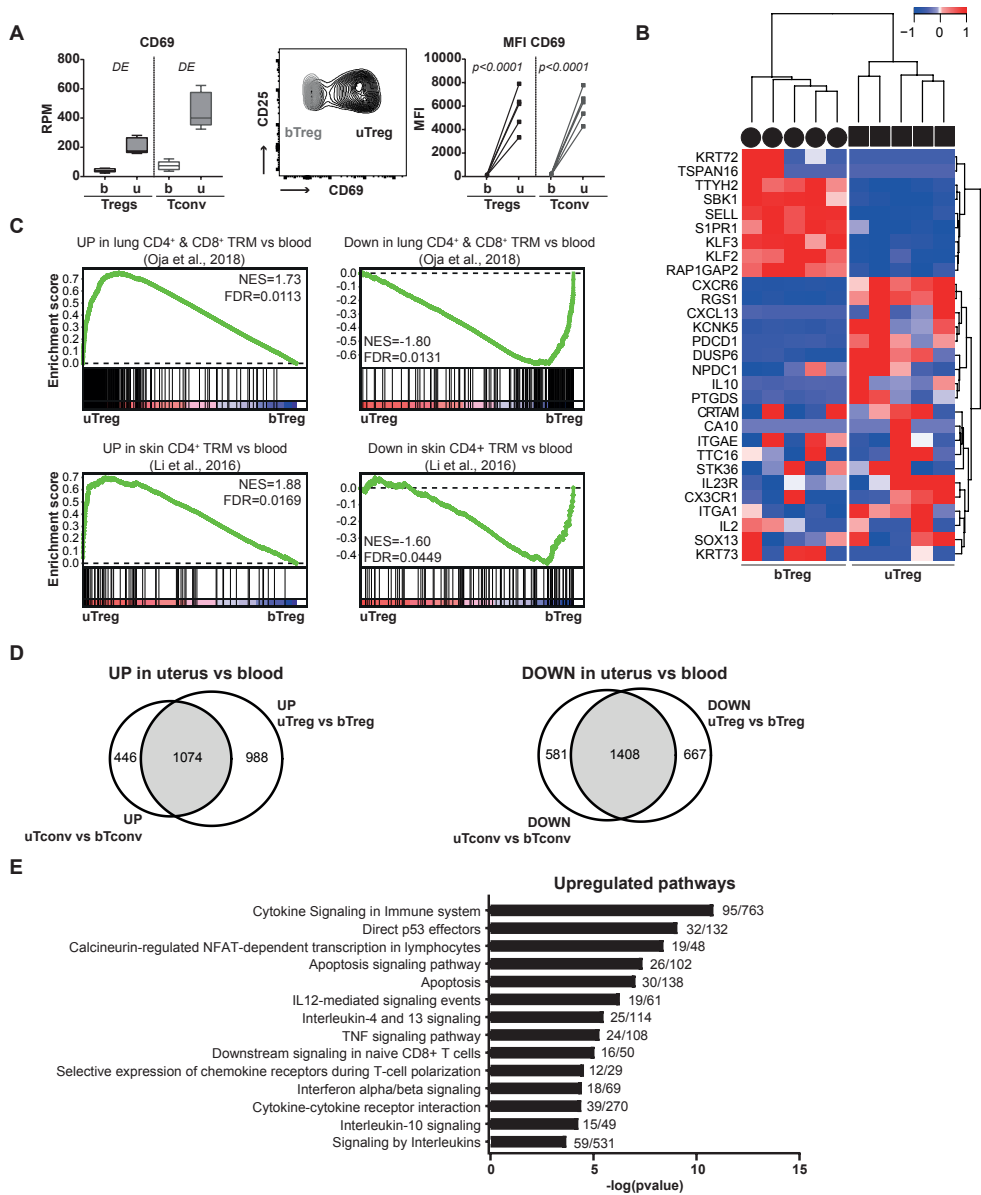


Figure 3. Tregs at the maternal-fetal interface have a tissue-resident profile.

(A) Gene and protein expression of CD69 in sorted T cell populations. MFI = median fluorescent intensity. Two-way ANOVA with Tukey post hoc test. (B) Heatmap of published human core tissue-resident gene expression⁴ in uTreg compared to bTreg. Expression values were mean-centered and scaled per gene. (C) Gene set enrichment analysis (GSEA) with published genes identifying human lung CD4⁺ and CD8⁺ TRM compared to blood memory cells; left panel⁹³) and genes upregulated in skin CD4⁺ TRM compared to blood CD4⁺ T cells (right panel¹⁵), in uTregs vs bTregs. NES = normalized enrichment score. (D) Venn diagrams of upregulated and downregulated genes ($padj < 0.05$) shared between Tregs and CD4⁺ Tconv from the maternal-fetal interface, compared to their blood-derived counterparts. (E) Pathway analysis (ToppGene pathways) of the 1074 shared upregulated genes in uTreg and uTconv. P-values < 0.05 after Bonferroni correction were considered significant.

maternal-fetal interface, we overlapped the genes that were significantly upregulated or downregulated in uTregs and uTconv compared to their counterparts from blood. The Venn diagrams in figure 3D show that a large proportion of upregulated and downregulated genes was shared between uTregs and uTconv (1074 up and 1408 down), which suggests that the specific tissue environment at the maternal-interface accounts for a significant part of their adapted transcriptional profile. Pathway analysis demonstrated that shared upregulated genes were involved in cytokine signaling (figure 3E). Downregulated pathways were reflective of ribosomal processes involved in RNA translation (supplementary figure 3). Taken together, uTregs have a TRM signature which reflects a shared adaptation to the tissue environment of the maternal-fetal interface between uTregs and uTconv.

uTregs mirror uTconv Th1 polarization with a predominance of T-bet⁺CXCR3⁺ Tregs

Effector Tregs can acquire different T helper phenotypes with coexpression of FOXP3 and lineage-defining transcription factors T-bet (TBX21, Th1), GATA3 (Th2), RORγt (RORC, Th17), as well as lineage-associated cytokine and chemokine receptors.³⁸ We investigated whether uTregs and uTconv underwent a, possibly shared, T helper polarization. uTregs showed significantly increased expression of Th1-related TBX21 compared to bTreg, which mirrored the increased expression of TBX21 in uTconv compared to bTconv (figure 4A). Th2-related GATA3 and Th17-related RORC were not significantly differentially expressed between uTreg and bTreg (and uTconv and bTconv), although RORC showed a trend towards downregulation, which was confirmed on protein level (Figure 4A-B). Increased expression of T-bet was also confirmed on protein level, with a 6-87% (median 22%) of uTregs showing positivity for T-bet (figure 4C-D). Also the Th1-related cytokine receptor IL18R1 was increased in both uTregs and uTconv compared to their counterparts in blood on gene and protein level (figure 4E). Investigation of chemokine receptor expression, which is related both T helper polarization and tissue-specific homing,^{94,95} showed that chemokine receptors related to naive Tregs and lymphoid tissue environments CCR7 and CXCR5 were downregulated in uTregs compared to bTregs, on gene and protein level (figure 4F-G). Chemokine receptors upregulated in uTregs included CCR2, CCR5, CXCR3, CXCR4, CCR1, and CXCR6 (figure 4F and H), which largely mirrored expression by uTconv. CCR1 and CXCR6 were particularly upregulated in uTregs, both previously identified as part of the conserved murine tissue Treg signature.²¹ The Th1-associated CXCR3^{35,96} and Th1/inflammation-associated CCR5,⁹⁶⁻⁹⁹ had significantly higher gene and protein expression in uTregs and uTconv compared to their counterparts from blood (figure 4F and H). Although the variable percentage of T-bet⁺ Tregs suggests heterogeneity in uTreg subspecialization, virtually all uTregs (and uTconv) were positive for CXCR3 (84-100%, median 93%), and the majority expressed CCR5 (22-83%, median 62%) (figure 4I). Consistent with these findings, a previously published gene

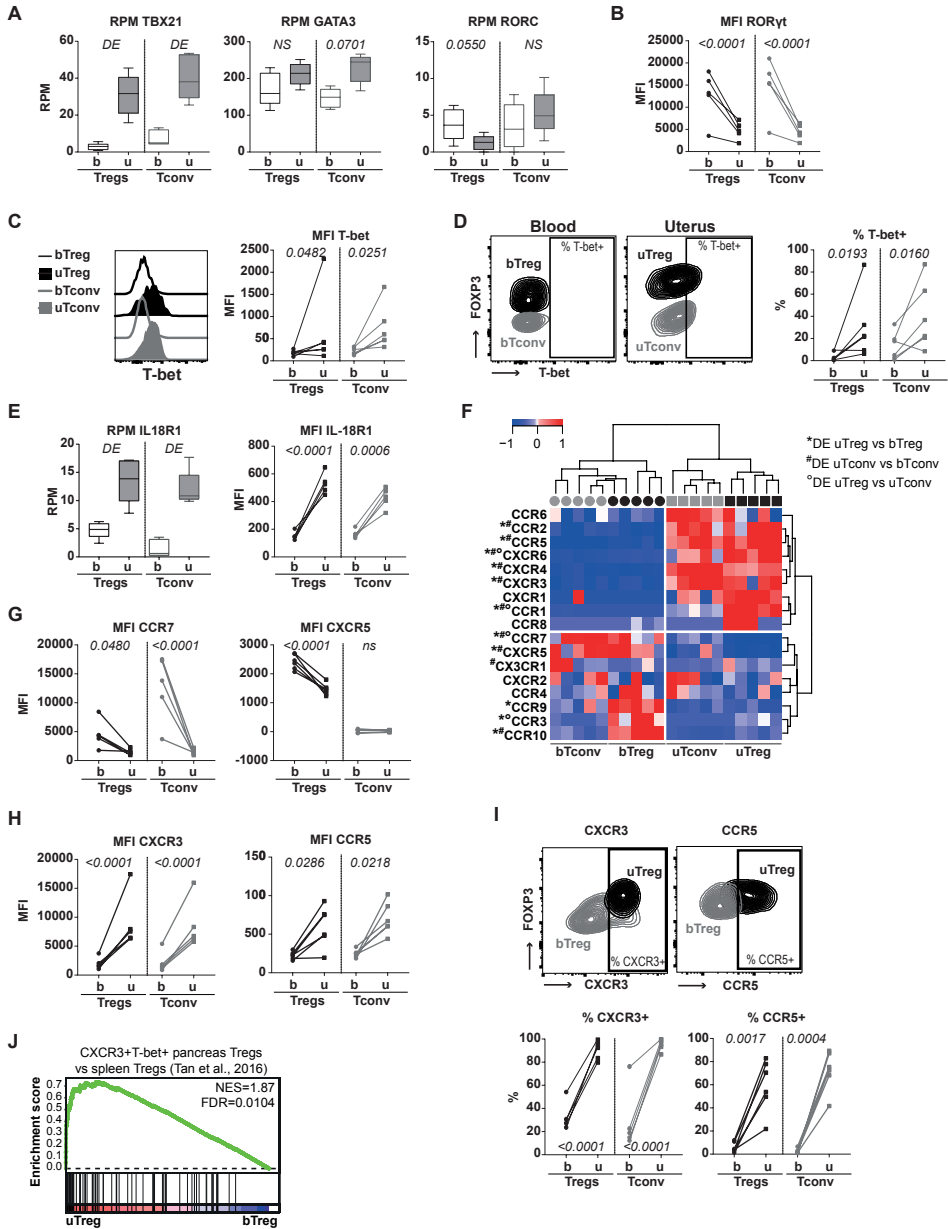


Figure 4. uTreg and uTconv polarization at the maternal-fetal interface.

(A) Gene expression of lineage-defining transcription factors TBX21 (T-bet), GATA3 (GATA-3), and RORC (ROR γ t). P values from differential gene expression analysis. (B-D) Protein expression of ROR γ t (B) and T-bet (C+D). MFI = median fluorescent intensity. P values of two-way ANOVA with Tukey posthoc test. (E) Gene and protein expression of IL18R1 (IL-18R1). (F) Heatmap showing gene expression of chemokine receptors. Expression values were mean-centered and scaled per gene. DE = differentially expressed. (G-I) Protein expression of chemokine receptors downregulated (G) and upregulated (H+I) in uTregs. P values of two-way ANOVA with Tukey posthoc test. (J) Gene set enrichment analysis with published gene set of CXCR3⁺T-bet⁺ Tregs from the pancreas of prediabetic mice,³⁷ comparing uTregs and bTregs. NES = normalized enrichment score.

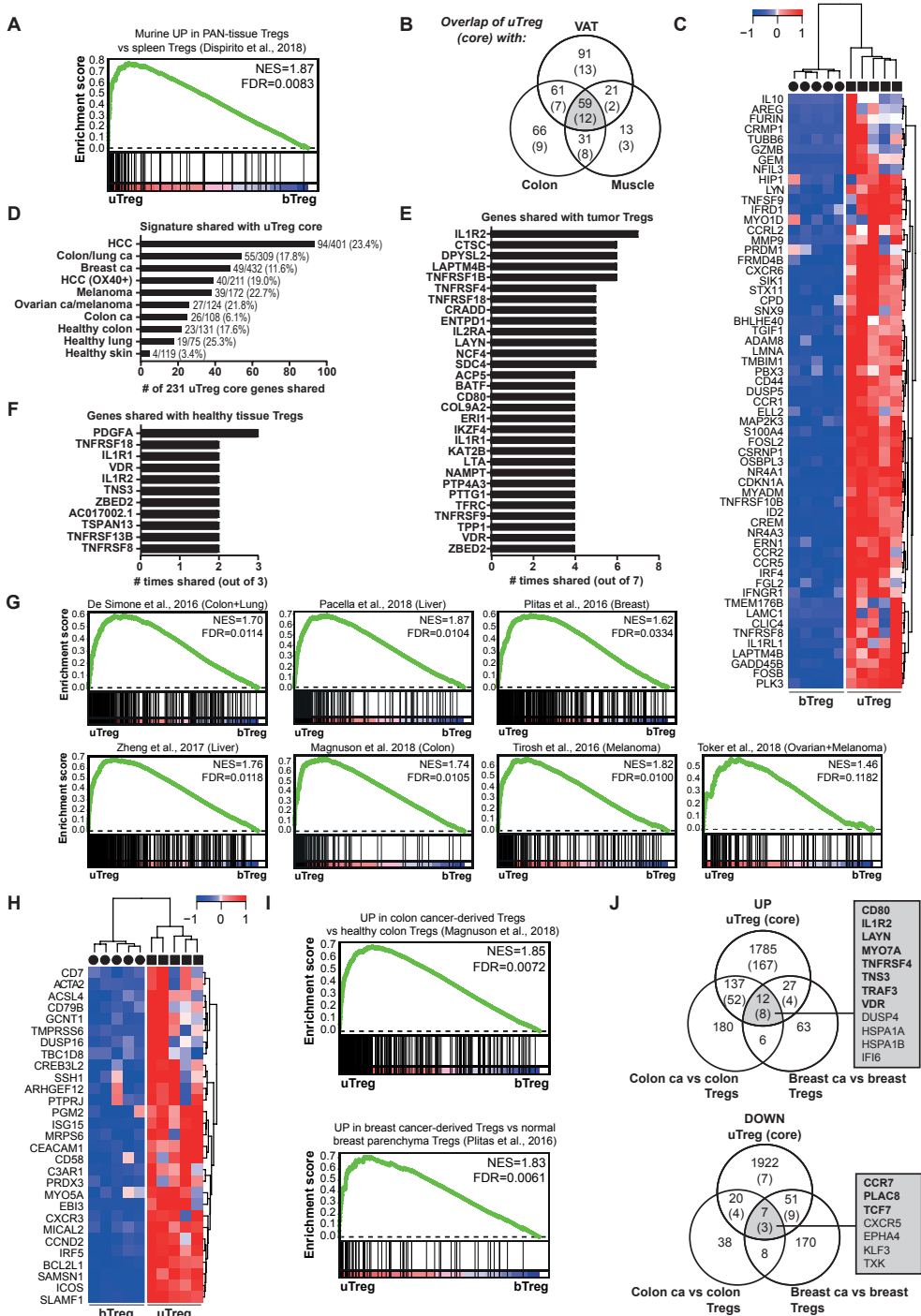


Figure 5. uTregs have a functional profile similar to tumor-infiltrating Tregs.

signature of T-bet⁺CXCR3⁺ Tregs from the pancreas of prediabetic mice was highly enriched in uTregs compared to bTregs (figure 4J).³⁷ In conclusion, uTregs at the maternal-fetal interface show Th1 polarization mirroring uTconv, with high expression of Th1-related markers T-bet and CXCR3. Furthermore, uTregs express an array of chemokine receptors, some of which uTreg-specific and others shared with uTconv, with which they can integrate a variety of locally produced signals. uTreg and uTconv cells may therefore rely on both unique and shared cues to guide their migration to and retention at the uterine maternal-fetal interface.

The core uTreg signature from the maternal-fetal interface overlaps with tumor-infiltrating Treg signatures

uTregs at the maternal-fetal interface displayed profiles of effector Treg differentiation/chronic activation and Th1 polarization. We wondered whether these highly differentiated uTregs from the maternal-fetal interface would resemble Tregs from other human and murine tissue sites or would show a uniquely adapted profile. Well-studied murine tissue Treg populations include Tregs from visceral adipose tissue (VAT), muscle, and intestines.^{12,13,21,80,100} Each population has been shown to display a tissue-specific phenotype with expression of certain 1) transcription factors, 2) chemokine receptors and 3) preference towards a T helper (Th) lineage differentiation when compared to spleen Tregs.^{12,13,17,21,80} Next to these tissue-specific signatures, a murine PAN-tissue signature, shared by VAT, muscle and intestinal Tregs, was identified.²¹

(Figure 5 continued)

(A) Gene set enrichment analysis with a published murine PAN-tissue gene signature,²¹ comparing uTregs and bTregs. (B) Venn diagram showing the numbers of genes upregulated in uTregs compared to bTregs ($p_{adj} < 0.05$) (and genes in the uTreg core signature in parentheses), which are represented in tissue-specific and tissue-shared published murine gene signatures.²¹ VAT = Visceral adipose tissue Tregs. (C) Heatmap showing the expression of the 59 genes that were part of the murine PAN-tissue signature and upregulated in uTregs compared to bTregs ($p_{adj} < 0.05$).²¹ Expression values were mean-centered and scaled per gene. (D) The number of genes shared between the uTreg core signature and published human TITR signatures or healthy tissue Treg signatures.^{14,15,25,102-107} Numbers behind bars indicate the number of shared genes out of the total number of genes in the specific signature. (E) The genes that were most often shared between the uTreg core signature and human TITR signatures (shared in $>3/7$ signatures). (E) The genes that were most often shared between the uTreg core signature and human healthy tissue Treg signatures (shared in $>1/3$ signatures). (G) Gene set enrichment analysis (GSEA) with published TITR-specific signatures in uTregs vs bTregs.^{25,102-107} NES = normalized enrichment score. (H) Heatmap showing expression of genes in the leading edge of $>2/7$ GSEA analyses from (G), which were not represented in the uTreg core signature. Expression values were mean-centered and scaled per gene. (I) GSEA with published gene signatures specific to Tregs from tumor-tissue compared to the healthy tissue counterpart in uTregs vs bTregs.^{26,107} (J) Venn diagrams showing shared genes between uTregs and genes specifically upregulated in Tregs from tumor-tissue compared to the healthy tissue counterpart.^{26,107}

GSEA in figure 5A shows that the shared murine PAN-tissue Treg signature was also strongly enriched in uTregs, again highlighting its generalized expression in tissue Tregs, apparently even conserved across species. Overlaying significantly upregulated genes in uTreg (versus bTreg) with the murine tissue-specific or tissue-shared Treg signatures,²¹ yielded a large amount of shared genes between uTregs and murine VAT-, colon- and muscle-derived Tregs (figure 5B, numbers in each field represent overlap of the specific field with significantly upregulated genes in uTreg). 59 genes were shared among all 3 murine tissues and uTregs, including IL1RL1 (receptor for IL-33, ST2), AREG, IL10, IRF4, GZMB, TNFRSF9, BHLHE40, NR4A1, NR4A3, and CCR2, many of which have been described as crucial regulators for effector and/or tissue Treg function (figure 5C).^{13,32,40,85–87,101} 12 of the 59 genes were even part of the uTreg-specific core signature as defined in figure 2 (CCR1, CXCR6, ELL2, FGL2, GEM, IL10, LAPTM4B, SNX9, TNFRSF8, NFIL3, NR4A3, and PRDM1). This indicates that uTreg display features of tissue adaptation, which are highly conserved across tissues and species.

In the human setting, the investigation of tissue-derived Tregs, especially from healthy tissues, has proven challenging, and only limited data are available. To assess how the uTreg tissue profile compares to other human Treg tissue profiles, we analyzed enrichment of the three previously published gene sets of significantly upregulated genes in skin, colon and lung Treg compared to blood Treg (supplementary table 3).^{14,15} All three of these signatures were significantly enriched in uTregs compared to bTregs, indicating that the tissue profile of uTregs shows similarities with human Tregs from various tissue sites (supplementary figure 4). Human Tregs infiltrating the unique tissue-environment of tumors (TITR) have been studied slightly more extensively. Comparison of genes significantly upregulated in uTregs versus bTregs with seven recently published gene signatures of TITR infiltrating a variety of human tumors (supplementary table 3),^{25,102–107} yielded a remarkable overlap with each of the TITR signatures with up to 65% shared with uTregs (supplementary table 5). Of the 41 genes that were shared among ≥ 4 of the 7 TITR signatures (supplementary table 6), a notable 31 were also part of the 231 genes in the uTreg core signature. Figure 5D shows the genes that were shared between the uTreg core signature and each of the TITR signatures and healthy tissue-derived Treg signatures. Remarkably, 94 (40.7%) of the 231 core uTreg genes were overlapping with specifically upregulated genes from HCC-infiltrating Tregs,¹⁰⁵ 55 with the unique TITR signature identified by De Simone et al,²⁵ 49 with breast cancer TITR genes,¹⁰² and 40 with OX-40⁺ Treg from cirrhotic/tumor liver tissue (figure 5D).¹⁰⁶ Importantly, the 231 uTreg core signature genes showed less overlap with healthy tissue-derived Treg specific signatures from human healthy colon, lung and skin. The genes that were most often shared between uTregs and TITR were IL1R2 (7/7), TNFRSF1B, CTSC, DPYSL2, LAPTM4B (6/7), TNFRSF4, TNFRSF18, LAYN, IL2RA, ENTPD1, NCF4, SDC4 and CRADD (5/7) (figure 5E), whereas with healthy tissue-Treg signatures PDGFA was most often shared (3/3) (figure 5F). GSEA showed that also many of the non-overlapping genes from the published TITR signatures were significantly enriched in uTreg compared to bTreg (figure 5G). Genes

in the leading edge of $\geq 3/7$ tumor-specific GSEA analyses that were highly expressed in uTregs compared to bTregs, but not part of the uTreg core (mostly because their high expression was shared with uTconv), are shown in figure 5H. These included CREB3L2 (6/7) EB13, GCNT1, ICOS (5/7), ACTA2, ARHGEF12, BCL2L1, CCND2, PRDX3, SLAMF1 (4/7), CXCR3, CD7, CAECAM1, CD79B, and MICAL2 (3/7), amongst others. Remarkably, genes specifically upregulated in breast cancer-infiltrating Tregs compared to Tregs from normal breast parenchyma and significantly upregulated in colon cancer Tregs compared to healthy colon Tregs showed a particularly high enrichment in uTregs, suggesting that uTregs are not just similar to Tregs from breast or colon tissue, but specifically to the highly differentiated/activated Tregs from the tumor environment (figure 5I).^{26,107} By overlapping these cancer-versus-healthy tissue Treg signatures with significantly upregulated genes in uTregs (versus bTregs), we identified 12 ‘cancer-specific’ genes expressed by uTregs (figure 5J): CD80, IL1R2, LAYN, MYO7A, TNFRSF4, TNS3, TRAF3, VDR, DUSP4, HSPA1A, HSPA1B, and IFI6. The first 8 of these were also part of the uTreg-specific core signature, again highlighting the specificity c.q. importance of receptors IL1R2, LAYN, TNFRSF4, CD80 and transcription factor VDR for human Tregs in a tumor(-like) microenvironment. Also tumor-specific downregulated genes were shared with the uTreg core signature: CCR7, PLAC8, and TCF7. In conclusion, these results indicate that uTreg from the maternal-fetal interface have a transcriptional core signature which is shared specifically with the specialized transcriptional profile of tumor-infiltrating Tregs.

Uterine Tregs show site-specific adaptation

Next we wondered whether uTreg would be merely adapted to the microenvironment in uterine tissue, or specifically adapted to the tissue site at the maternal-interface. To investigate this site-specific adaptation within one tissue, we compared uTregs from the maternal-fetal interface, i.e. placental bed (^{pb}uTregs), to uTregs from a distant uterine site, i.e. the incision site made during Caesarean section (^{inc}uTregs). Confirmation of Treg identity and TRM signature for ^{inc}uTregs are shown in supplementary figure 5A-F. The differentially expressed genes between ^{inc}uTregs and bTregs were similar to those between ^{pb}uTregs and bTregs (figure 6A). Also PCA showed that gene expression profiles of ^{pb}uTregs and ^{inc}uTregs were rather similar, compared to bTregs (figure 6B). However, direct comparison of ^{pb}uTregs and ^{inc}uTregs revealed a substantial difference between the two populations (figure 6B-C). First, protein expression of the core Treg transcription factor FOXP3 was lower in ^{inc}uTregs than ^{pb}uTregs, comparable to bTregs (figure 6D). This was not due to ^{inc}uTreg contamination with bTregs, as expression of CD69 was similar between ^{pb}uTregs and ^{inc}uTregs (supplementary figure 5D). Protein expression of other core Treg genes CTLA4 and TIGIT was also lower in ^{inc}uTregs than ^{pb}uTregs (figure 6D). This indicates that ^{pb}uTregs, derived from the maternal-fetal interface, have a more pronounced expression of Treg

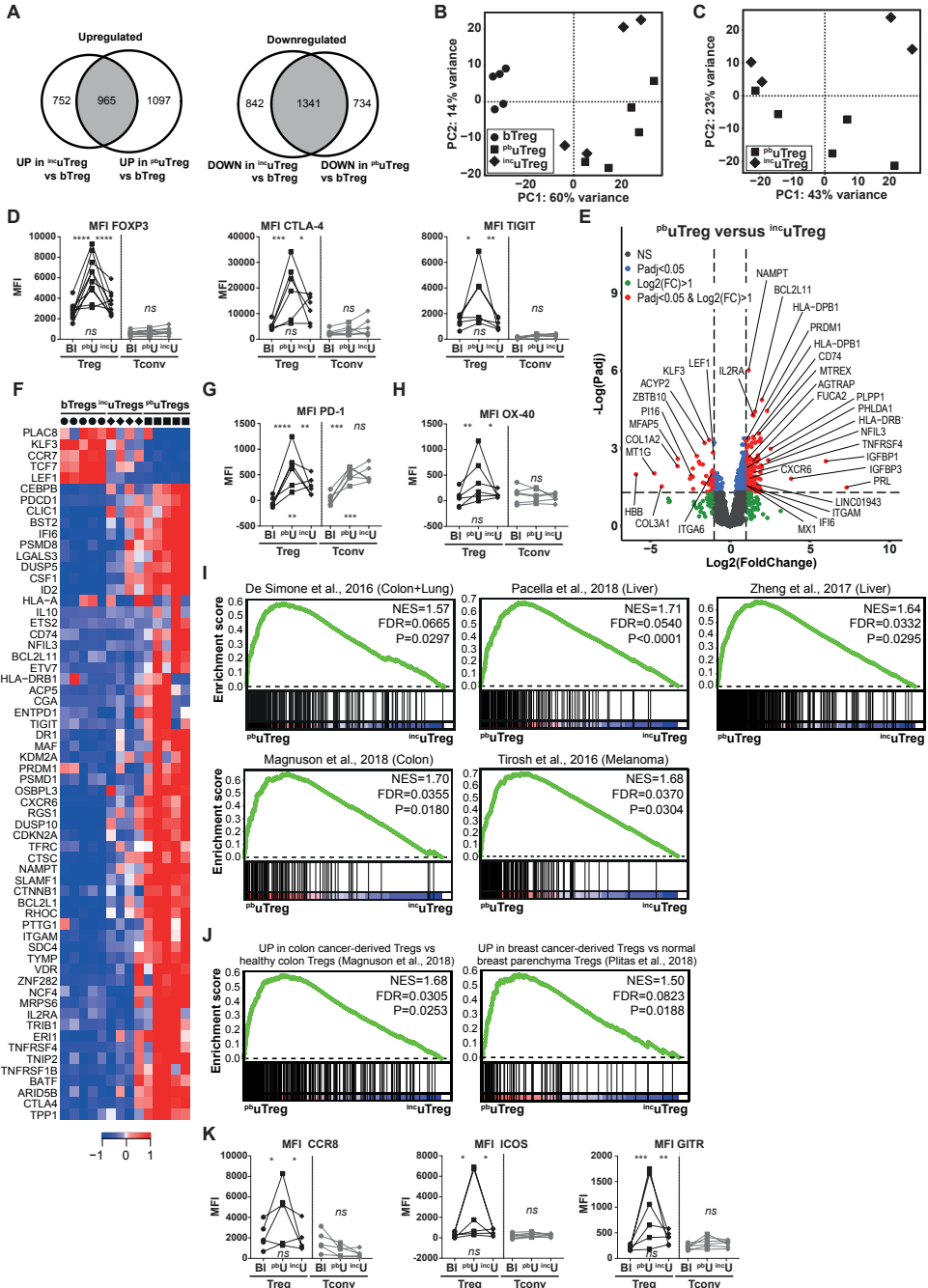


Figure 6. uTregs show site-specific adaptation to the maternal-fetal interface.

(Figure 6 continued)

(A) Venn diagrams of genes upregulated (left panel) and downregulated (right panel) in both ^{inc}uTregs and ^{pbu}uTregs compared to bTregs. (B) PCA of bTregs, ^{pbu}uTregs and ^{inc}uTregs. (C) PCA of ^{pbu}uTregs and ^{inc}uTregs. (D) Protein expression of FOXP3, CTLA-4, and TIGIT. Padj of Two-way ANOVA with Tukey post hoc test for protein. Left upper p-value: blood vs placental bed; right upper p-value: placental bed vs incision site; lower p-value: blood vs incision site. MFI = median fluorescent intensity; NS = Not significant. (E) Volcanoplot of differentially expressed genes between ^{pbu}uTregs and ^{inc}uTregs. (F) Heatmap with previously highlighted genes in this manuscript which were differentially expressed between ^{pbu}uTregs and ^{inc}uTregs. Expression values were mean-centered and scaled per gene. (G+H) Protein expression of PD-1 (G) and OX-40 (H). Padj of Two-way ANOVA with Tukey post hoc test for protein. Left upper p-value: blood vs placental bed; right upper p-value: placental bed vs incision site; lower p-value: blood vs incision site. MFI = median fluorescent intensity; NS = Not significant. (I) Gene set enrichment analysis (GSEA) with published TITR -specific signatures in ^{pbu}uTregs vs ^{inc}uTregs.^{25,102–107} NES = normalized enrichment score. (J) GSEA with published gene signatures specific to Tregs from tumor-tissue compared to the healthy tissue counterpart in ^{pbu}uTregs vs ^{inc}uTregs.^{26,107} (K) Protein expression of CCR8, ICOS and GITR. Padj of Two-way ANOVA with Tukey post hoc test for protein. Left upper p-value: blood vs placental bed; right upper p-value: placental bed vs incision site; lower p-value: blood vs incision site. MFI = median fluorescent intensity; NS = Not significant. ****P<0.0001, ***P<0.001, **P<0.01, *P<0.05.

signature markers, suggesting enhanced activation/differentiation in comparison with their uterine counterparts from the incision site. Differential gene expression analysis revealed 576 upregulated and 126 downregulated genes in ^{pbu}uTregs versus ^{inc}uTregs (figure 6E). The heatmap in figure 6F shows a selection of previously highlighted genes in this manuscript that proved to be differentially expressed between ^{pbu}uTregs and ^{inc}uTregs. These results suggest that Tregs cannot only adapt to the microenvironment within a certain tissue, but will specifically adapt to the environmental cues at a specific tissue site. Pathway analysis showed that upregulated genes ^{pbu}uTregs versus ^{inc}uTregs were related to PD-1 signaling, cytokine signaling, TCR signaling, and T helper cell differentiation (supplementary figure 5G). Indeed, PD-1 was higher expressed in ^{pbu}uTregs and ^{inc}uTregs on gene and protein level (figure 6F-G), and GSEA showed enrichment of a TCR-activated Treg signature in ^{pbu}uTregs compared to ^{inc}uTregs (supplementary figure 5H). Furthermore, ^{pbu}uTreg-specific core genes associated with effector Treg differentiation including TNFRSF4 (OX-40 protein, figure 6H) and transcription factors BATF, MAF, PRDM1, and VDR, among others, were significantly higher expressed in ^{pbu}uTreg than in ^{inc}uTreg (figure 6F), again suggesting that ^{pbu}uTreg show more pronounced differentiation towards an effector Treg phenotype. Since ^{pbu}uTregs appeared to be especially differentiated at the maternal-fetal interface, we assessed whether the TITR-like profile of ^{pbu}uTregs was also more pronounced than in ^{inc}uTregs. Remarkably, 5 out of 7 tested published TITR signatures were significantly enriched in ^{pbu}uTregs compared to ^{inc}uTregs (P<0.05; figure 6I). More specifically, GSEA with signatures differentiating between TITR and their counterparts from a matched healthy tissue site, showed significant enrichment in ^{pbu}uTregs compared to ^{inc}uTregs (figure 6J). CCR8 and ICOS, which were present in 6 out of 7 TITR signatures, as well as TNFRSF18 (GITR), were significantly higher expressed in ^{pbu}uTregs than in ^{inc}uTregs and bTregs on protein level (figure 6K). CCR8 has been shown to be highly enriched in tumor Treg cells and associated

with a poor prognosis in several cancers.^{25,26,81} Thus, ^{pb}uTregs at the maternal-fetal interface specifically acquire a highly differentiated effector profile similar to tumor-infiltrating Tregs, which is more pronounced even compared to a uterine tissue site distant from the maternal-fetal interface.

DISCUSSION

Here, we demonstrate for the first time that human uterine Tregs have a highly differentiated transcriptional profile, which is specifically enriched at the maternal-fetal interface and is reminiscent of the specialized and highly effective profile of tumor-infiltrating Tregs. With these findings we answer a long-standing question on how Tregs are functionally specialized at the maternal-fetal interface to modulate local effector T cell responses, preventing an allo-reaction against the fetus. Moreover, we introduce the novel concept of site-specific adaptation of Tregs within one organ or tissue. This again substantiates the notion that Tregs are capable of adapting their transcriptional program driven by micro-environmental cues.^{12,14,16,21,22}

We have demonstrated that uTregs at the maternal-fetal interface display a highly activated and late-stage differentiated effector profile (as suggested by expression of BATF and PRDM1, and downregulation of SATB1),^{32,34,83,84,86} with increased expression of molecules associated with enhanced suppressive capacity (CTLA4, ENTPD1, HAVCR2, IL10, LGALS1, TIGIT) and abundant expression of TNFR superfamily members ((TNFRSF13B (TACI), TNFRSF18 (GITR), TNFRSF1B (TNFR2), TNFRSF4 (OX-40), TNFRSF8 (CD30), TNFRSF9 (4-1BB)). Also others have found that non-lymphoid-tissue Tregs display an activated phenotype compared to lymphoid-organ and circulating Tregs,^{13,18,80} and both BATF and the TNFRSF-NF- κ B signaling axis have been described as crucial in the survival of Tregs and maintenance of a stable effector Treg phenotype, especially in tissues.^{16,28,32,33,85,86,108} It is now recognized that Tregs adapt to their tissue environments, with common adaptations across many tissues, such as increased expression of IL10, IL1RL1 (encoding ST2, an IL-33 receptor subunit), AREG (encoding amphiregulin), CTLA4, TIGIT, BATF and IRF4, and a low expression of LEF1 and TCF7 compared to lymphoid tissue Tregs, but, importantly, also tissue-specific signatures.^{12,13,16,17,21} These tissue-specific transcriptomic profiles counter the notion that tissue Tregs merely have a more activated, effector or memory state than lymphoid-organ Tregs. Rather, they have a specialized adapted program,¹⁰⁰ likely matching the specific requirements of a certain tissue site.^{10,17,21,109,110}

Although site-specific distribution of T cell composition and maturation in the human intestinal tract has been previously reported,¹¹¹ to our knowledge, the concept of site-specific transcriptional adaptation of Tregs within one tissue or organ is novel, taking into account

that tumors represent a completely altered tissue and not a different site within the same organ. We show that uTregs display features suggestive of a high responsiveness to micro-environmental cues, such as a range of TNF receptor superfamily members and chemokine receptors. With such a matrix of options to detect signals from the microenvironment, Tregs are likely able to adjust not only to the tissue or organ of their residence, but even to specific sites within that tissue, based on the cues provided by surrounding cells. Most likely, the implantation of the placenta, i.e. the multitude of signals produced by myometrium-invading trophoblast,¹¹² are the primary cues effectuating micro-environmental changes at the maternal-fetal interface. It has been shown that trophoblast attracts Tregs to the maternal-fetal interface by production of hCG and CXCL16, the ligand for CXCR6.^{113,114} Moreover, in vitro co-culture of HLA-G⁺ extravillous trophoblast with CD4⁺ T cells increased Treg numbers and the FOXP3 expression level,^{115,116} indicating that Tregs may also be locally induced or expanded by trophoblast. Thus, it is likely that signals produced by invading trophoblast at the maternal-fetal interface account for at least some of the site-specific transcriptional adaptations in uTregs.

The T helper response at the maternal-fetal interface has been previously suggested to be skewed away from a pro-inflammatory Th1 response, to prevent a pathogenic alloreaction against the fetus, resulting in a Th2 dominant response during the second trimester. However, during the third trimester, a pro-inflammatory Th1 response was described to be essential for initiation of labor.(reviewed in⁴⁸) In line with this, our findings indicate that the T helper response in the uterus at term is dominated by Th1 polarization, but that it is very well-controlled. The highly differentiated population of uTregs at the maternal-fetal interface appears to be specifically equipped to effectively suppress Th1 responses. Most importantly, although we observed heterogeneity of T-bet protein expression in uTreg, CXCR3 expression was remarkably homogeneous, with 84-100% of uTregs being CXCR3⁺. CXCR3 (and T-bet) expressing Tregs have been shown to be especially adept to suppress Th1 responses.^{35,37,45,96} Furthermore, the majority of uTregs expressed TIGIT, OX-40 and/or CCR5. Tregs expressing TIGIT have been described to preferentially inhibit Th1 and Th17 responses,⁷⁹ a subpopulation of OX-40 expressing Tregs are thought to differentiate into Th1-suppressing Tregs,¹¹⁷ and also CCR5 expression on Tregs has been associated with more effective suppression of Th1 responses.⁹⁷ Thus, the necessary pro-inflammatory Th1 response at the maternal-fetal interface at term appears to be controlled by specifically differentiated and Th1-polarized Tregs. So far, Th1-like Tregs have been described mainly in inflammatory environments, such as infections, autoimmune diseases and transplantation reactions,^{45,96,118–120} whereas tissue-resident Tregs have been mostly characterized as being Th2-skewed (VAT, muscle)^{17,21} or Th17 skewed (intestines).⁸⁰ DiSpirito et al. however recently also identified a subset of T-bet expressing Tregs in muscle and colon,²¹ indicating that they can be present also in steady-state tissues.

We are the first to study exclusively maternal, myometrial tissue-resident Tregs from the maternal-fetal interface. Although Tregs at the human maternal-fetal interface have been

studied previously, investigations had to resort to the use of more easily accessible decidua, due to the difficulty of acquiring human myometrium. Since decidual tissue is of fetal origin, it may not only be contaminated with fetal immune cells, but it also does not allow for studying the unique, and specifically maternal, uterine environment underlying the placenta, in which the complex process of spiral artery remodeling takes place. The only publications that we know of investigating FOXP3 expression in actual human placental bed biopsies demonstrated that the percentage of FOXP3⁺ T cells was significantly decreased in patients with pre-eclampsia, and FOXP3 mRNA expression was reduced in endometrial biopsies of infertile women, highlighting the importance of functional Tregs for a healthy pregnancy.^{57,121} From human decidual data, it is known that the frequency of clonally expanded populations of effector Treg cells is increased in decidua of 3rd trimester cases compared to 1st trimester cases.¹²² Decidual Tregs were found to display a more pronounced suppressive phenotype than in blood, with increased expression of FOXP3, CTLA-4, CD25, HLA-DR, ICOS, GITR, and OX-40, which recapitulates our findings.^{58,59,63,123} Very recently, three types of functional regulatory T cells were identified at the human maternal-fetal interface, of which the CD25^{hi}FOXP3⁺ population matches the here studied population.¹¹⁶ Decidual CD25^{hi}FOXP3⁺ Tregs effectively suppressed CD4⁺ and CD8⁺ T cell proliferation and IFN γ and TNF α production. Transcripts identified by qPCR array as specific for this subset were IL2RA, FOXP3, TIGIT, CD39, LRRC32, ST2, BATF, and CCR8, as well as increased expression of CCR5, IL10, and GITR compared to blood Tregs,¹¹⁶ which confirms our findings of an activated Treg phenotype at the maternal-fetal interface. A previously published study investigating chemokine receptor expression of CXCR3, CCR4 and CCR6 in decidual Tregs by flow cytometry, showed that CCR6⁺CXCR3⁺ Th1 cells were increased, CCR6⁺CCR4⁺ Th17 cells were nearly absent, whereas CCR4⁺ Th2 frequencies were similar in blood and decidua,⁵⁸ which is also in line with our findings. Remarkably, in murine gravid uterus, CCR5 expression on Tregs was related to suppressive capacity: CCR5⁺ effector Tregs were more suppressive compared to their CCR5⁻ counterparts.¹²⁴ Furthermore, also in human TITR CCR5 was highly expressed, even specifically compared to the healthy colon-derived Tregs, and also here CCR5 expression on Tregs correlated with an increased suppressive capacity.^{107,125} Taken together, this indicates that the here identified activated phenotype of myometrial uTregs has overlapping characteristics with decidual Tregs. We observed that uTregs from the maternal-fetal interface are highly responsive to their micro-environment. They display a peculiar differentiated effector phenotype similar to TITR, defined by high gene expression of IL1R2, LAYN, CD80, VDR, and TNFRSF4, amongst others, with specific enrichment of TITR signatures compared to Treg signatures from matched, unaffected tissue sites. This observation may be explained by recent insights on the similarity of the immune environment at the maternal-fetal interface and tumors.⁴⁸ Both the receptivity of the myometrium towards implantation of the blastocyst and the invasiveness of the trophoblast show striking similarities with implantation of tumor metastases in healthy tissues.^{126,127} Tumor cells can modulate their immune environment into an anti-inflammatory

milieu and have been shown to recruit and/or induce suppressor cells among which high numbers of suppressive Tregs.^{128,129} Just as in tumors, a tolerogenic mode of antigen presentation with indirect allorecognition of low levels of antigens predominates at the maternal-fetal interface.¹³⁰ Also others have reported striking similarities between the early Treg responses to embryo and tumor implantation.⁵⁴ And not only Tregs, but also neutrophils in decidua basalis have been shown to be similar to tumor-associated neutrophils.¹³¹ These findings imply that the micro-environment at the maternal-fetal interface may be a unique mammalian tissue site that under challenged, but physiological conditions resembles a tumor micro-environment. The tumor environment represents an actively remodeling tissue site distinct from a steady-state tissue, with low-grade inflammation, and newly infiltrating/invading cells. These dynamic characteristics are shared with the maternal-fetal interface and may account for the unique transcriptional adaptation of Tregs.

Although we observed global changes in gene expression patterns in uTregs, flow cytometry revealed an expression gradient of many markers across the uTreg population, suggesting that uTregs consist of a heterogenic population with different stages of differentiation and possibly sub-specialization. Single cell sequencing techniques and mass cytometry are indeed starting to reveal the heterogeneity of Treg populations in tissues and tumors.^{16,27,104,105,132–134} Treg heterogeneity may even contribute to their suppressive potential: IL-35 (encoded by EBI3) and IL-10 expressing heterogenic Treg subpopulations in the tumor micro-environment have been recently shown to induce CD8⁺ Tconv exhaustion.¹³⁵ Considering the striking similarities between uTreg and TITR and the high expression of IL-35 and IL-10 in uTregs, this could also be a potential mechanism employed by uTregs at the maternal-fetal interface, which is in line with a recent report showing partial CD8⁺ effector dysfunction in the human decidua.¹³⁶

A unique strength of our study is that we were able to study a highly specific and pure maternal Treg cell subset isolated by FACS sorting from human tissue biopsies, of which we compared the transcriptomic profiles by state of the art low-input CEL-Seq protocol, not only to their counterpart in blood, but also to a tissue and site-specific Treg control population and matched Tconv. Moreover, we have validated our key findings on protein level in single cell resolution by flow cytometry. This revealed that some of the differences found on RNA level were even more pronounced on protein level. As we were only able to study T cells from biopsies acquired in term pregnancies, due to the practical limitation of delivery of the infant and placenta, it would be interesting to investigate term-dependent changes in uTreg profiles in future studies. It should be taken into account that protocols for tissue digestion may induce transcriptional changes.¹³⁷ However, many of the uTreg specific genes identified here, were previously found not to be affected in human lung-derived Tregs by a tissue digestion protocol which was similar to but harsher than the isolation method used here.¹⁴ Our findings have important implications. TITR are currently under heavy investigation as targets in cancer immunotherapy. However, we demonstrate that signatures identified in TITR are not as unique as previously assumed, and that they may be shared by Tregs with

specialized functions in other human tissues that may still be unknown. On the other hand, our results may lead to new targets for cancer immunotherapy, since profiling of Tregs in a variety of tissues under physiological, but not necessarily steady-state conditions, may help to identify truly TITR-specific expression patterns. Moreover, increased understanding of immunoregulatory mechanisms at the maternal-fetal interface during healthy pregnancy gives not only unique insights into human immunobiology of pregnancy, but also aids to elucidate the pathological changes in Tregs in pregnancy disorders such as preeclampsia, fetal growth restriction or recurrent miscarriage, as many studies have pointed towards a role for Treg defects of deficiency in these disorders.^{65–67,113,122,138,139} Lastly, functional adaptation of human Tregs to different tissues and specific tissue sites is still largely unexplored. The receptivity of Tregs to their environmental stimuli and subsequent sub-specialization may be exploited for therapeutic purposes.

In conclusion, we have shown that human Tregs show functional adaptation with tumor-infiltrating-like features specifically at the maternal-fetal interface, which introduces the novel concept of tissue site-specific transcriptional adaptation of human Tregs.

REFERENCES

1. Szabo PA, Miron M, Farber DL. Location, Location, Location: Tissue Resident Memory T Cells in Mice and Humans. *Sci. Immunol.* **2019**, *4* (34).
2. Snyder ME, Finlayson MO, Connors TJ, et al. Generation and Persistence of Human Tissue-Resident Memory T Cells in Lung Transplantation. *Sci. Immunol.* **2019**, *4* (33).
3. Thome JJC, Yudanin N, Ohmura Y, et al. Spatial Map of Human T Cell Compartmentalization and Maintenance over Decades of Life. *Cell* **2014**, *159* (4), 814–828.
4. Kumar BV, Ma W, Miron M, et al. Human Tissue-Resident Memory T Cells Are Defined by Core Transcriptional and Functional Signatures in Lymphoid and Mucosal Sites. *Cell Rep.* **2017**, *20* (12), 2921–2934.
5. Hombrink P, Helbig C, Backer RA, et al. Programs for the Persistence, Vigilance and Control of Human CD8(+) Lung-Resident Memory T Cells. *Nat. Immunol.* **2016**, *17* (12), 1467–1478.
6. Purwar R, Campbell J, Murphy G, et al. Resident Memory T Cells (T(RM)) Are Abundant in Human Lung: Diversity, Function, and Antigen Specificity. *PLoS One* **2011**, *6* (1), e16245.
7. Sathaliyawa T, Kubota M, Yudanin N, et al. Distribution and Compartmentalization of Human Circulating and Tissue-Resident Memory T Cell Subsets. *Immunity* **2013**, *38* (1), 187–197.
8. Booth JS, Toapanta FR, Salerno-Goncalves R, et al. Characterization and Functional Properties of Gastric Tissue-Resident Memory T Cells from Children, Adults, and the Elderly. *Front. Immunol.* **2014**, *5*, 294.
9. Tanoue T, Atarashi K, Honda K. Development and Maintenance of Intestinal Regulatory T Cells. *Nat. Rev. Immunol.* **2016**, *16* (5), 295–309.
10. Chaudhry A, Rudensky AY. Control of Inflammation by Integration of Environmental Cues by Regulatory T Cells. *J. Clin. Invest.* **2013**, *123* (3), 939–944.
11. Sakaguchi S, Miyara M, Costantino CM, et al. FOXP3+ Regulatory T Cells in the Human Immune System. *Nat. Rev. Immunol.* **2010**, *10* (7), 490–500.
12. Cipolletta D, Feuerer M, Li A, et al. PPAR- γ Is a Major Driver of the Accumulation and Phenotype of Adipose Tissue Treg Cells. *Nature* **2012**, *486* (7404), 549–553.
13. Burzyn D, Kuswanto W, Kolodin D, et al. A Special Population of Regulatory T Cells Potentiates Muscle Repair. *Cell* **2013**, *155* (6), 1282–1295.
14. Niedzielska M, Israelsson E, Angermann B, et al. Differential Gene Expression in Human Tissue Resident Regulatory T Cells from Lung, Colon, and Blood. *Oncotarget* **2018**, *9* (90), 36166–36184.
15. Li J, Olshansky M, Carbone FR, et al. Transcriptional Analysis of T Cells Resident in Human Skin. *PLoS One* **2016**, *11* (1), e0148351.
16. Miragaia RJ, Gomes T, Chomka A, et al. Single-Cell Transcriptomics of Regulatory T Cells Reveals Trajectories of Tissue Adaptation. *Immunity* **2019**, *50* (2), 493–504.e7.
17. Delacher M, Imbusch CD, Weichenhan D, et al. Genome-Wide DNA-Methylation Landscape Defines Specialization of Regulatory T Cells in Tissues. *Nat. Immunol.* **2017**, *18* (10), 1160–1172.
18. Feuerer M, Herrero L, Cipolletta D, et al. Lean, but Not Obese, Fat Is Enriched for a Unique Population of Regulatory T Cells That Affect Metabolic Parameters. *Nat. Med.* **2009**, *15* (8), 930–939.
19. Thome JJC, Bickham KL, Ohmura Y, et al. Early-Life Compartmentalization of Human T Cell Differentiation and Regulatory Function in Mucosal and Lymphoid Tissues. *Nat. Med.* **2016**, *22* (1), 72–77.

20. Whibley N, Tucci A, Powrie F. Regulatory T Cell Adaptation in the Intestine and Skin. *Nat. Immunol.* **2019**, *20* (4), 386–396.
21. DiSpirito JR, Zemmour D, Ramanan D, et al. Molecular Diversification of Regulatory T Cells in Nonlymphoid Tissues. *Sci. Immunol.* **2018**, *3* (27).
22. Liston A, Gray DHD. Homeostatic Control of Regulatory T Cell Diversity. *Nat. Rev. Immunol.* **2014**, *14* (3), 154–165.
23. Bilate AM, Bousbaine D, Mesin L, et al. Tissue-Specific Emergence of Regulatory and Intraepithelial T Cells from a Clonal T Cell Precursor. *Sci. Immunol.* **2016**, *1* (2), eaaf7471.
24. Ahmadzadeh M, Pasetto A, Jia L, et al. Tumor-Infiltrating Human CD4(+) Regulatory T Cells Display a Distinct TCR Repertoire and Exhibit Tumor and Neoantigen Reactivity. *Sci. Immunol.* **2019**, *4* (31).
25. De Simone M, Arrigoni A, Rossetti G, et al. Transcriptional Landscape of Human Tissue Lymphocytes Unveils Uniqueness of Tumor-Infiltrating T Regulatory Cells. *Immunity* **2016**, *45* (5), 1135–1147.
26. Plitas G, Konopacki C, Wu K, et al. Regulatory T Cells Exhibit Distinct Features in Human Breast Cancer. *Immunity* **2016**, *45* (5), 1122–1134.
27. Azizi E, Carr AJ, Plitas G, et al. Single-Cell Map of Diverse Immune Phenotypes in the Breast Tumor Microenvironment. *Cell* **2018**, *174* (5), 1293–1308.e36.
28. Cuadrado E, van den Biggelaar M, de Kivit S, et al. Proteomic Analyses of Human Regulatory T Cells Reveal Adaptations in Signaling Pathways That Protect Cellular Identity. *Immunity* **2018**, *48* (5), 1046–1059.e6.
29. Miyara M, Yoshioka Y, Kitoh A, et al. Functional Delineation and Differentiation Dynamics of Human CD4+ T Cells Expressing the FoxP3 Transcription Factor. *Immunity* **2009**, *30* (6), 899–911.
30. Ito T, Hanabuchi S, Wang Y-H, et al. Two Functional Subsets of FOXP3+ Regulatory T Cells in Human Thymus and Periphery. *Immunity* **2008**, *28* (6), 870–880.
31. Cretney E, Kallies A, Nutt SL. Differentiation and Function of Foxp3(+) Effector Regulatory T Cells. *Trends Immunol.* **2013**, *34* (2), 74–80.
32. Cretney E, Xin A, Shi W, et al. The Transcription Factors Blimp-1 and IRF4 Jointly Control the Differentiation and Function of Effector Regulatory T Cells. *Nat. Immunol.* **2011**, *12* (4), 304–311.
33. Hayatsu N, Miyao T, Tachibana M, et al. Analyses of a Mutant Foxp3 Allele Reveal BATF as a Critical Transcription Factor in the Differentiation and Accumulation of Tissue Regulatory T Cells. *Immunity* **2017**, *47* (2), 268–283.e9.
34. Cretney E, Leung PS, Trezise S, et al. Characterization of Blimp-1 Function in Effector Regulatory T Cells. *J. Autoimmun.* **2018**, *91*, 73–82.
35. Koch MA, Tucker-Heard G, Perdue NR, et al. The Transcription Factor T-Bet Controls Regulatory T Cell Homeostasis and Function during Type 1 Inflammation. *Nat. Immunol.* **2009**, *10* (6), 595–602.
36. Yang B-H, Hagemann S, Mamareli P, et al. Foxp3(+) T Cells Expressing ROR γ Represent a Stable Regulatory T-Cell Effector Lineage with Enhanced Suppressive Capacity during Intestinal Inflammation. *Mucosal Immunol.* **2016**, *9* (2), 444–457.
37. Tan TG, Mathis D, Benoist C. Singular Role for T-BET+CXCR3+ Regulatory T Cells in Protection from Autoimmune Diabetes. *Proc. Natl. Acad. Sci. U. S. A.* **2016**, *113* (49), 14103–14108.

38. Duhén T, Duhén R, Lanzavecchia A, et al. Functionally Distinct Subsets of Human FOXP3⁺ Treg Cells That Phenotypically Mirror Effector Th Cells. *Blood* **2012**, *119* (19), 4430–4440.
39. Chaudhry A, Rudra D, Treuting P, et al. CD4⁺ Regulatory T Cells Control TH17 Responses in a Stat3-Dependent Manner. *Science* **2009**, *326* (5955), 986–991.
40. Zheng Y, Chaudhry A, Kas A, et al. Regulatory T-Cell Suppressor Program Co-Opts Transcription Factor IRF4 to Control T(H)2 Responses. *Nature* **2009**, *458* (7236), 351–356.
41. Yu F, Sharma S, Edwards J, et al. Dynamic Expression of Transcription Factors T-Bet and GATA-3 by Regulatory T Cells Maintains Immunotolerance. *Nat. Immunol.* **2015**, *16* (2), 197–206.
42. Ohnmacht C, Park J-H, Cording S, et al. MUCOSAL IMMUNOLOGY. The Microbiota Regulates Type 2 Immunity through ROR γ mat(+) T Cells. *Science* **2015**, *349* (6251), 989–993.
43. Wohlfert EA, Grainger JR, Bouladoux N, et al. GATA3 Controls Foxp3(+) Regulatory T Cell Fate during Inflammation in Mice. *J. Clin. Invest.* **2011**, *121* (11), 4503–4515.
44. Wang Y, Su MA, Wan YY. An Essential Role of the Transcription Factor GATA-3 for the Function of Regulatory T Cells. *Immunity* **2011**, *35* (3), 337–348.
45. Hall AO, Beiting DP, Tato C, et al. The Cytokines Interleukin 27 and Interferon-Gamma Promote Distinct Treg Cell Populations Required to Limit Infection-Induced Pathology. *Immunity* **2012**, *37* (3), 511–523.
46. Sharma A, Rudra D. Emerging Functions of Regulatory T Cells in Tissue Homeostasis. *Front. Immunol.* **2018**, *9*, 883.
47. Erlebacher A. Mechanisms of T Cell Tolerance towards the Allogeneic Fetus. *Nat. Rev. Immunol.* **2013**, *13* (1), 23–33.
48. Mor G, Aldo P, Alvero AB. The Unique Immunological and Microbial Aspects of Pregnancy. *Nat. Rev. Immunol.* **2017**, *17* (8), 469–482.
49. Svensson-Arvelund J, Ernerudh J, Buse E, et al. The Placenta in Toxicology. Part II: Systemic and Local Immune Adaptations in Pregnancy. *Toxicol. Pathol.* **2014**, *42* (2), 327–338.
50. Pearson H. Reproductive Immunology: Immunity's Pregnant Pause. *Nature*. England November 2002, pp 265–266.
51. Powell RM, Lissauer D, Tamblyn J, et al. Decidual T Cells Exhibit a Highly Differentiated Phenotype and Demonstrate Potential Fetal Specificity and a Strong Transcriptional Response to IFN. *J. Immunol.* **2017**, *199* (10), 3406–3417.
52. Rowe JH, Ertelt JM, Xin L, et al. Pregnancy Imprints Regulatory Memory That Sustains Anergy to Fetal Antigen. *Nature* **2012**, *490* (7418), 102–106.
53. Aluvihare VR, Kallikourdis M, Betz AG. Regulatory T Cells Mediate Maternal Tolerance to the Fetus. *Nat. Immunol.* **2004**, *5* (3), 266–271.
54. Chen T, Darrasse-Jeze G, Bergot A-S, et al. Self-Specific Memory Regulatory T Cells Protect Embryos at Implantation in Mice. *J. Immunol.* **2013**, *191* (5), 2273–2281.
55. Feyaerts D, Benner M, van Cranenbroek B, et al. Human Uterine Lymphocytes Acquire a More Experienced and Tolerogenic Phenotype during Pregnancy. *Sci. Rep.* **2017**, *7* (1), 2884.

56. Sasaki Y, Sakai M, Miyazaki S, et al. Decidual and Peripheral Blood CD4+CD25+ Regulatory T Cells in Early Pregnancy Subjects and Spontaneous Abortion Cases. *Mol. Hum. Reprod.* **2004**, 10 (5), 347–353.
57. Sasaki Y, Darmochwal-Kolarz D, Suzuki D, et al. Proportion of Peripheral Blood and Decidual CD4(+) CD25(bright) Regulatory T Cells in Pre-Eclampsia. *Clin. Exp. Immunol.* **2007**, 149 (1), 139–145.
58. Mjosberg J, Berg G, Jenmalm MC, et al. FOXP3+ Regulatory T Cells and T Helper 1, T Helper 2, and T Helper 17 Cells in Human Early Pregnancy Decidua. *Biol. Reprod.* **2010**, 82 (4), 698–705.
59. Dimova T, Nagaeva O, Stenqvist A-C, et al. Maternal Foxp3 Expressing CD4+ CD25+ and CD4+ CD25- Regulatory T-Cell Populations Are Enriched in Human Early Normal Pregnancy Decidua: A Phenotypic Study of Paired Decidual and Peripheral Blood Samples. *Am. J. Reprod. Immunol.* **2011**, 66 Suppl 1, 44–56.
60. Tilburgs T, Scherjon SA, van der Mast BJ, et al. Fetal-Maternal HLA-C Mismatch Is Associated with Decidual T Cell Activation and Induction of Functional T Regulatory Cells. *J. Reprod. Immunol.* **2009**, 82 (2), 148–157.
61. Tilburgs T, Roelen DL, van der Mast BJ, et al. Evidence for a Selective Migration of Fetus-Specific CD4+CD25bright Regulatory T Cells from the Peripheral Blood to the Decidua in Human Pregnancy. *J. Immunol.* **2008**, 180 (8), 5737–5745.
62. Jin L-P, Chen Q-Y, Zhang T, et al. The CD4+CD25 Bright Regulatory T Cells and CTLA-4 Expression in Peripheral and Decidual Lymphocytes Are down-Regulated in Human Miscarriage. *Clin. Immunol.* **2009**, 133 (3), 402–410.
63. Heikkinen J, Mottonen M, Alanen A, et al. Phenotypic Characterization of Regulatory T Cells in the Human Decidua. *Clin. Exp. Immunol.* **2004**, 136 (2), 373–378.
64. Somerset DA, Zheng Y, Kilby MD, et al. Normal Human Pregnancy Is Associated with an Elevation in the Immune Suppressive CD25+ CD4+ Regulatory T-Cell Subset. *Immunology* **2004**, 112 (1), 38–43.
65. Jung YJ, Park Y, Kim H-S, et al. Abnormal Lymphatic Vessel Development Is Associated with Decreased Decidual Regulatory T Cells in Severe Preeclampsia. *Am. J. Reprod. Immunol.* **2018**, 80 (1), e12970.
66. Ebina Y, Shimada S, Deguchi M, et al. Divergence of Helper, Cytotoxic, and Regulatory T Cells in the Decidua from Miscarriage. *Am. J. Reprod. Immunol.* **2016**, 76 (3), 199–204.
67. Bao SH, Wang XP, De Lin Q, et al. Decidual CD4+CD25+CD127dim/- Regulatory T Cells in Patients with Unexplained Recurrent Spontaneous Miscarriage. *Eur. J. Obstet. Gynecol. Reprod. Biol.* **2011**, 155 (1), 94–98.
68. Yang H, Qiu L, Chen G, et al. Proportional Change of CD4+CD25+ Regulatory T Cells in Decidua and Peripheral Blood in Unexplained Recurrent Spontaneous Abortion Patients. *Fertil. Steril.* **2008**, 89 (3), 656–661.
69. Darmochwal-Kolarz D, Saito S, Rolinski J, et al. Activated T Lymphocytes in Pre-Eclampsia. *Am. J. Reprod. Immunol.* **2007**, 58 (1), 39–45.
70. Santner-Nanan B, Peek MJ, Khanam R, et al. Systemic Increase in the Ratio between Foxp3+ and IL-17-Producing CD4+ T Cells in Healthy Pregnancy but Not in Preeclampsia. *J. Immunol.* **2009**, 183 (11), 7023–7030.
71. Veerbeek JHW, Brouwers L, Koster MPH, et al. Spiral Artery Remodeling and Maternal Cardiovascular Risk: The Spiral Artery Remodeling (SPAR) Study. *J. Hypertens.* **2016**, 34 (8), 1570–1577.

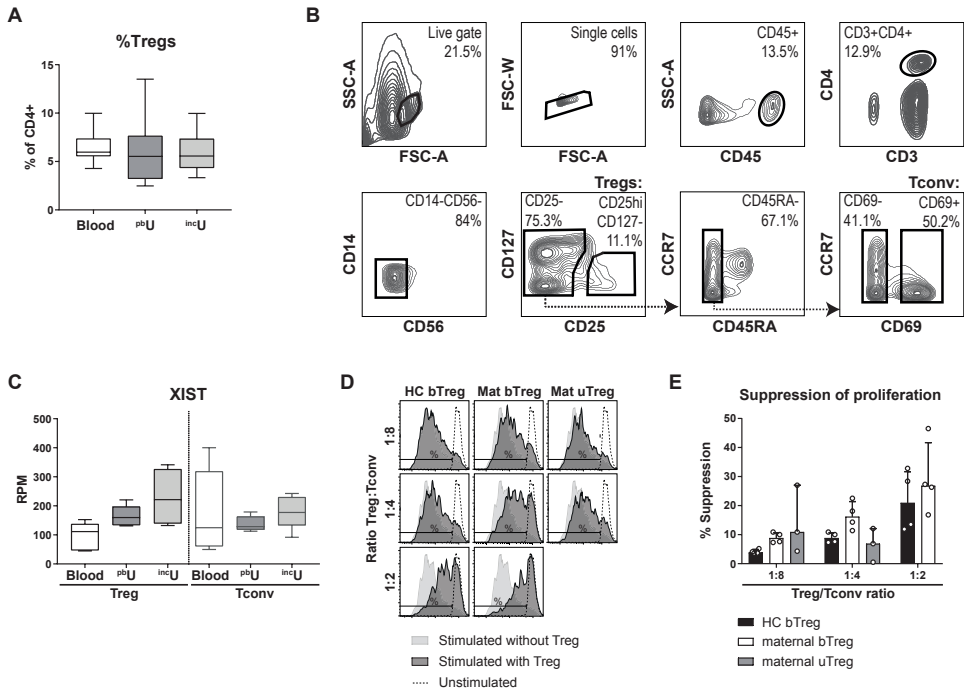
72. Petrelli A, Wehrens EJ, Scholman RC, et al. Self-Sustained Resistance to Suppression of CD8⁺ Teff Cells at the Site of Autoimmune Inflammation Can Be Reversed by Tumor Necrosis Factor and Interferon-Gamma Blockade. *Arthritis Rheumatol. (Hoboken, N.J.)* **2016**, 68 (1), 229–236.
73. Hashimshony T, Senderovich N, Avital G, et al. CEL-Seq2: Sensitive Highly-Multiplexed Single-Cell RNA-Seq. *Genome Biol.* **2016**, 17, 77.
74. Li H, Durbin R. Fast and Accurate Long-Read Alignment with Burrows-Wheeler Transform. *Bioinformatics* **2010**, 26 (5), 589–595.
75. Chen J, Bardes EE, Aronow BJ, et al. ToppGene Suite for Gene List Enrichment Analysis and Candidate Gene Prioritization. *Nucleic Acids Res.* **2009**, 37 (Web Server issue), W305-11.
76. Subramanian A, Tamayo P, Mootha VK, et al. Gene Set Enrichment Analysis: A Knowledge-Based Approach for Interpreting Genome-Wide Expression Profiles. *Proc. Natl. Acad. Sci. U. S. A.* **2005**, 102 (43), 15545–15550.
77. Edgar R, Domrachev M, Lash AE. Gene Expression Omnibus: NCBI Gene Expression and Hybridization Array Data Repository. *Nucleic Acids Res.* **2002**, 30 (1), 207–210.
78. Ferraro A, D'Alise AM, Raj T, et al. Interindividual Variation in Human T Regulatory Cells. *Proc. Natl. Acad. Sci. U. S. A.* **2014**, 111 (12), E1111–20.
79. Joller N, Lozano E, Burkett PR, et al. Treg Cells Expressing the Coinhibitory Molecule TIGIT Selectively Inhibit Proinflammatory Th1 and Th17 Cell Responses. *Immunity* **2014**, 40 (4), 569–581.
80. Sefik E, Geva-Zatorsky N, Oh S, et al. MUCOSAL IMMUNOLOGY. Individual Intestinal Symbionts Induce a Distinct Population of RORgamma(+) Regulatory T Cells. *Science* **2015**, 349 (6251), 993–997.
81. Halim L, Romano M, McGregor R, et al. An Atlas of Human Regulatory T Helper-like Cells Reveals Features of Th2-like Tregs That Support a Tumorigenic Environment. *Cell Rep.* **2017**, 20 (3), 757–770.
82. Vasanthakumar A, Moro K, Xin A, et al. The Transcriptional Regulators IRF4, BATF and IL-33 Orchestrate Development and Maintenance of Adipose Tissue-Resident Regulatory T Cells. *Nat. Immunol.* **2015**, 16 (3), 276–285.
83. Kitagawa Y, Ohkura N, Kidani Y, et al. Guidance of Regulatory T Cell Development by Satb1-Dependent Super-Enhancer Establishment. *Nat. Immunol.* **2017**, 18 (2), 173–183.
84. Beyrer M, Thabet Y, Muller R-U, et al. Repression of the Genome Organizer SATB1 in Regulatory T Cells Is Required for Suppressive Function and Inhibition of Effector Differentiation. *Nat. Immunol.* **2011**, 12 (9), 898–907.
85. Vasanthakumar A, Liao Y, Teh P, et al. The TNF Receptor Superfamily-NF-kappaB Axis Is Critical to Maintain Effector Regulatory T Cells in Lymphoid and Non-Lymphoid Tissues. *Cell Rep.* **2017**, 20 (12), 2906–2920.
86. Vasanthakumar A, Moro K, Xin A, et al. The Transcriptional Regulators IRF4, BATF and IL-33 Orchestrate Development and Maintenance of Adipose Tissue-Resident Regulatory T Cells. *Nat. Immunol.* **2015**, 16 (3), 544.
87. Vasanthakumar A, Kallies A. Interleukin (IL)-33 and the IL-1 Family of Cytokines-Regulators of Inflammation and Tissue Homeostasis. *Cold Spring Harb. Perspect. Biol.* **2019**, 11 (3).

88. Nagar M, Jacob-Hirsch J, Vernitsky H, et al. TNF Activates a NF-kappaB-Regulated Cellular Program in Human CD45RA-Regulatory T Cells That Modulates Their Suppressive Function. *J. Immunol.* **2010**, *184* (7), 3570–3581.
89. Yu A, Snowwhite I, Vendrame F, et al. Selective IL-2 Responsiveness of Regulatory T Cells through Multiple Intrinsic Mechanisms Supports the Use of Low-Dose IL-2 Therapy in Type 1 Diabetes. *Diabetes* **2015**, *64* (6), 2172–2183.
90. He F, Chen H, Probst-Kepper M, et al. PLAU Inferred from a Correlation Network Is Critical for Suppressor Function of Regulatory T Cells. *Mol. Syst. Biol.* **2012**, *8*, 624.
91. Sadlon TJ, Wilkinson BG, Pederson S, et al. Genome-Wide Identification of Human FOXP3 Target Genes in Natural Regulatory T Cells. *J. Immunol.* **2010**, *185* (2), 1071–1081.
92. Beyer M, Classen S, Chemnitz J, et al. No Title <https://www.ncbi.nlm.nih.gov/geo/query/acc.cgi?acc=GSE16835> (accessed May 28, 2019).
93. Oja AE, Piet B, Helbig C, et al. Trigger-Happy Resident Memory CD4(+) T Cells Inhabit the Human Lungs. *Mucosal Immunol.* **2018**, *11* (3), 654–667.
94. Siewert C, Menning A, Dudda J, et al. Induction of Organ-Selective CD4+ Regulatory T Cell Homing. *Eur. J. Immunol.* **2007**, *37* (4), 978–989.
95. Duhon T, Geiger R, Jarrossay D, et al. Production of Interleukin 22 but Not Interleukin 17 by a Subset of Human Skin-Homing Memory T Cells. *Nat. Immunol.* **2009**, *10* (8), 857–863.
96. Littringer K, Moresi C, Rakebrandt N, et al. Common Features of Regulatory T Cell Specialization During Th1 Responses. *Front. Immunol.* **2018**, *9*, 1344.
97. Yurchenko E, Tritt M, Hay V, et al. CCR5-Dependent Homing of Naturally Occurring CD4+ Regulatory T Cells to Sites of Leishmania Major Infection Favors Pathogen Persistence. *J. Exp. Med.* **2006**, *203* (11), 2451–2460.
98. Zhang N, Schroppe B, Lal G, et al. Regulatory T Cells Sequentially Migrate from Inflamed Tissues to Draining Lymph Nodes to Suppress the Alloimmune Response. *Immunity* **2009**, *30* (3), 458–469.
99. Wysocki CA, Jiang Q, Panoskaltis-Mortari A, et al. Critical Role for CCR5 in the Function of Donor CD4+CD25+ Regulatory T Cells during Acute Graft-versus-Host Disease. *Blood* **2005**, *106* (9), 3300–3307.
100. Panduro M, Benoist C, Mathis D. Tissue Tregs. *Annu. Rev. Immunol.* **2016**, *34*, 609–633.
101. Arpaia N, Green JA, Moltedo B, et al. A Distinct Function of Regulatory T Cells in Tissue Protection. *Cell* **2015**, *162* (5), 1078–1089.
102. Plitas G, Rudensky AY. Regulatory T Cells: Differentiation and Function. *Cancer Immunol. Res.* **2016**, *4* (9), 721–725.
103. Toker A, Nguyen LT, Stone SC, et al. Regulatory T Cells in Ovarian Cancer Are Characterized by a Highly Activated Phenotype Distinct from That in Melanoma. *Clin. Cancer Res.* **2018**, *24* (22), 5685–5696.
104. Tirosh I, Izar B, Prakadan SM, et al. Dissecting the Multicellular Ecosystem of Metastatic Melanoma by Single-Cell RNA-Seq. *Science* **2016**, *352* (6282), 189–196.
105. Zheng C, Zheng L, Yoo J-K, et al. Landscape of Infiltrating T Cells in Liver Cancer Revealed by Single-Cell Sequencing. *Cell* **2017**, *169* (7), 1342–1356.e16.

106. Pacella I, Procaccini C, Focaccetti C, et al. Fatty Acid Metabolism Complements Glycolysis in the Selective Regulatory T Cell Expansion during Tumor Growth. *Proc. Natl. Acad. Sci. U. S. A.* **2018**, *115* (28), E6546–E6555.
107. Magnuson AM, Kiner E, Ergun A, et al. Identification and Validation of a Tumor-Infiltrating Treg Transcriptional Signature Conserved across Species and Tumor Types. *Proc. Natl. Acad. Sci. U. S. A.* **2018**, *115* (45), E10672–E10681.
108. Ferrandino F, Grazioli P, Bellavia D, et al. Notch and NF-kappaB: Coach and Players of Regulatory T-Cell Response in Cancer. *Front. Immunol.* **2018**, *9*, 2165.
109. Ulges A, Schmitt E, Becker C, et al. Context- and Tissue-Specific Regulation of Immunity and Tolerance by Regulatory T Cells. *Adv. Immunol.* **2016**, *132*, 1–46.
110. Sather BD, Treuting P, Perdue N, et al. Altering the Distribution of Foxp3(+) Regulatory T Cells Results in Tissue-Specific Inflammatory Disease. *J. Exp. Med.* **2007**, *204* (6), 1335–1347.
111. Senda T, Dogra P, Granot T, et al. Microanatomical Dissection of Human Intestinal T-Cell Immunity Reveals Site-Specific Changes in Gut-Associated Lymphoid Tissues over Life. *Mucosal Immunol.* **2019**, *12* (2), 378–389.
112. Dong M, Ding G, Zhou J, et al. The Effect of Trophoblasts on T Lymphocytes: Possible Regulatory Effector Molecules—a Proteomic Analysis. *Cell. Physiol. Biochem.* **2008**, *21* (5–6), 463–472.
113. Schumacher A, Brachwitz N, Sohr S, et al. Human Chorionic Gonadotropin Attracts Regulatory T Cells into the Fetal-Maternal Interface during Early Human Pregnancy. *J. Immunol.* **2009**, *182* (9), 5488–5497.
114. Huang Y, Zhu X-Y, Du M-R, et al. Human Trophoblasts Recruited T Lymphocytes and Monocytes into Decidua by Secretion of Chemokine CXCL16 and Interaction with CXCR6 in the First-Trimester Pregnancy. *J. Immunol.* **2008**, *180* (4), 2367–2375.
115. Tilburgs T, Crespo AC, van der Zwan A, et al. Human HLA-G+ Extravillous Trophoblasts: Immune-Activating Cells That Interact with Decidual Leukocytes. *Proc. Natl. Acad. Sci. U. S. A.* **2015**, *112* (23), 7219–7224.
116. Salvany-Celades M, van der Zwan A, Benner M, et al. Three Types of Functional Regulatory T Cells Control T Cell Responses at the Human Maternal-Fetal Interface. *Cell Rep.* **2019**, *27* (9), 2537–2547.e5.
117. Piconese S, Timperi E, Pacella I, et al. Human OX40 Tunes the Function of Regulatory T Cells in Tumor and Nontumor Areas of Hepatitis C Virus-Infected Liver Tissue. *Hepatology* **2014**, *60* (5), 1494–1507.
118. Dominguez-Villar M, Baecher-Allan CM, Hafler DA. Identification of T Helper Type 1-Like, Foxp3+ Regulatory T Cells in Human Autoimmune Disease. *Nat. Med.* **2011**, *17* (6), 673–675.
119. McClymont SA, Putnam AL, Lee MR, et al. Plasticity of Human Regulatory T Cells in Healthy Subjects and Patients with Type 1 Diabetes. *J. Immunol.* **2011**, *186* (7), 3918–3926.
120. Imanguli MM, Cowen EW, Rose J, et al. Comparative Analysis of FoxP3(+) Regulatory T Cells in the Target Tissues and Blood in Chronic Graft versus Host Disease. *Leukemia* **2014**, *28* (10), 2016–2027.
121. Jasper MJ, Tremellen KP, Robertson SA. Primary Unexplained Infertility Is Associated with Reduced Expression of the T-Regulatory Cell Transcription Factor Foxp3 in Endometrial Tissue. *Mol. Hum. Reprod.* **2006**, *12* (5), 301–308.
122. Tsuda S, Zhang X, Hamana H, et al. Clonally Expanded Decidual Effector Regulatory T Cells Increase in Late Gestation of Normal Pregnancy, but Not in Preeclampsia, in Humans. *Front. Immunol.* **2018**, *9*, 1934.

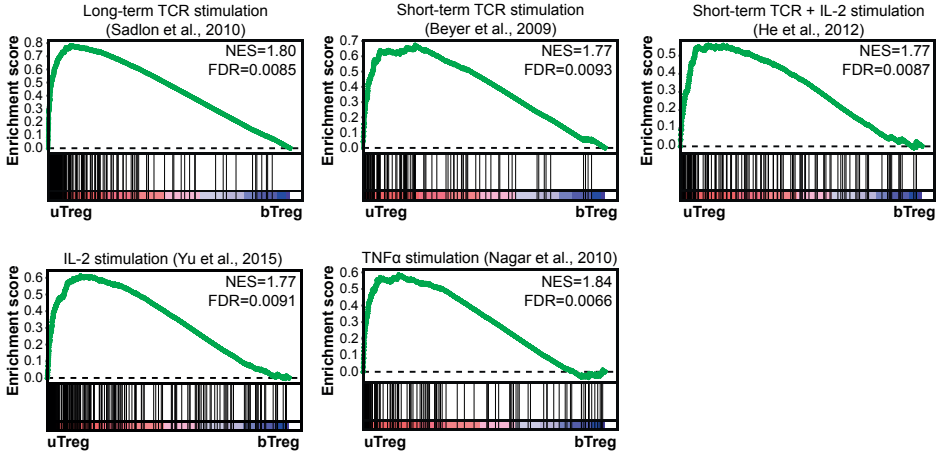
123. Nagamatsu T, Barrier BF, Schust DJ. The Regulation of T-Cell Cytokine Production by ICOS-B7H2 Interactions at the Human Fetomaternal Interface. *Immunol. Cell Biol.* **2011**, 89 (3), 417–425.
124. Kallikourdis M, Andersen KG, Welch KA, et al. Alloantigen-Enhanced Accumulation of CCR5+ “Effector” Regulatory T Cells in the Gravid Uterus. *Proc. Natl. Acad. Sci. U. S. A.* **2007**, 104 (2), 594–599.
125. Ward ST, Li KK, Hepburn E, et al. The Effects of CCR5 Inhibition on Regulatory T-Cell Recruitment to Colorectal Cancer. *Br. J. Cancer* **2015**, 112 (2), 319–328.
126. Beaman KD, Jaiswal MK, Katara GK, et al. Pregnancy Is a Model for Tumors, Not Transplantation. *Am. J. Reprod. Immunol.* **2016**, 76 (1), 3–7.
127. Holtan SG, Creedon DJ, Haluska P, et al. Cancer and Pregnancy: Parallels in Growth, Invasion, and Immune Modulation and Implications for Cancer Therapeutic Agents. *Mayo Clin. Proc.* **2009**, 84 (11), 985–1000.
128. Lin W-W, Karin M. A Cytokine-Mediated Link between Innate Immunity, Inflammation, and Cancer. *J. Clin. Invest.* **2007**, 117 (5), 1175–1183.
129. Deng G. Tumor-Infiltrating Regulatory T Cells: Origins and Features. *Am. J. Clin. Exp. Immunol.* **2018**, 7 (5), 81–87.
130. Collins MK, Tay C-S, Erlebacher A. Dendritic Cell Entrapment within the Pregnant Uterus Inhibits Immune Surveillance of the Maternal/fetal Interface in Mice. *J. Clin. Invest.* **2009**, 119 (7), 2062–2073.
131. Amsalem H, Kwan M, Hazan A, et al. Identification of a Novel Neutrophil Population: Proangiogenic Granulocytes in Second-Trimester Human Decidua. *J. Immunol.* **2014**, 193 (6), 3070–3079.
132. Zhang L, Yu X, Zheng L, et al. Lineage Tracking Reveals Dynamic Relationships of T Cells in Colorectal Cancer. *Nature* **2018**, 564 (7735), 268–272.
133. Norton SE, Ward-Hartstonge KA, McCall JL, et al. High-Dimensional Mass Cytometric Analysis Reveals an Increase in Effector Regulatory T Cells as a Distinguishing Feature of Colorectal Tumors. *J. Immunol.* **2019**, 202 (6), 1871–1884.
134. Wen T, Aronow BJ, Rochman Y, et al. Single-Cell RNA Sequencing Identifies Inflammatory Tissue T Cells in Eosinophilic Esophagitis. *J. Clin. Invest.* **2019**, 130.
135. Sawant D V, Yano H, Chikina M, et al. Adaptive Plasticity of IL-10(+) and IL-35(+) Treg Cells Cooperatively Promotes Tumor T Cell Exhaustion. *Nat. Immunol.* **2019**.
136. van der Zwan A, Bi K, Norwitz ER, et al. Mixed Signature of Activation and Dysfunction Allows Human Decidual CD8(+) T Cells to Provide Both Tolerance and Immunity. *Proc. Natl. Acad. Sci. U. S. A.* **2018**, 115 (2), 385–390.
137. van den Brink SC, Sage F, Vertesy A, et al. Single-Cell Sequencing Reveals Dissociation-Induced Gene Expression in Tissue Subpopulations. *Nat. Methods* **2017**, 14 (10), 935–936.
138. Inada K, Shima T, Ito M, et al. Helios-Positive Functional Regulatory T Cells Are Decreased in Decidua of Miscarriage Cases with Normal Fetal Chromosomal Content. *J. Reprod. Immunol.* **2015**, 107, 10–19.
139. Jianjun Z, Yali H, Zhiqun W, et al. Imbalance of T-Cell Transcription Factors Contributes to the Th1 Type Immunity Predominant in Pre-Eclampsia. *Am. J. Reprod. Immunol.* **2010**, 63 (1), 38–45.

SUPPLEMENTARY MATERIAL



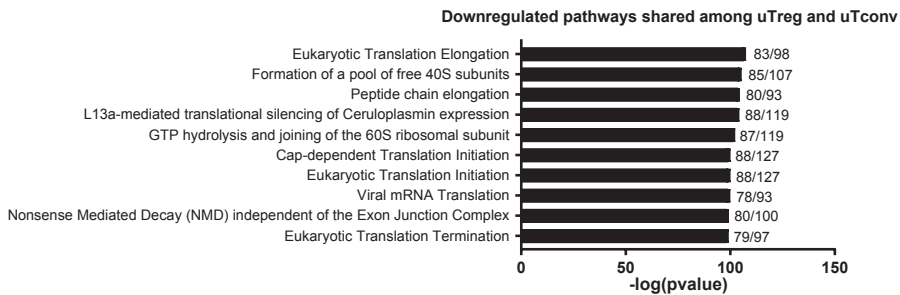
Supplementary figure 1. uTregs derived from the maternal-fetal interface are bona fide maternal Tregs.

(A) Ex vivo frequency of CD25+FOXP3+ cells among CD4+ T cells from blood, maternal-fetal interface (pbU) and incision site (incU). (B) Sorting strategy for uTregs and uTconv in the uterus. (C) Expression of female-specific gene XIST in all sorted T cell subsets. (D+E) Suppression assay assessing proliferation of healthy donor CD4+ T cells by CTV dilution assay, after 4 days of coculture with healthy donor bTregs, maternal bTregs, or uTregs at a 1:8, 1:4 and 1:2 ratio (n=4).



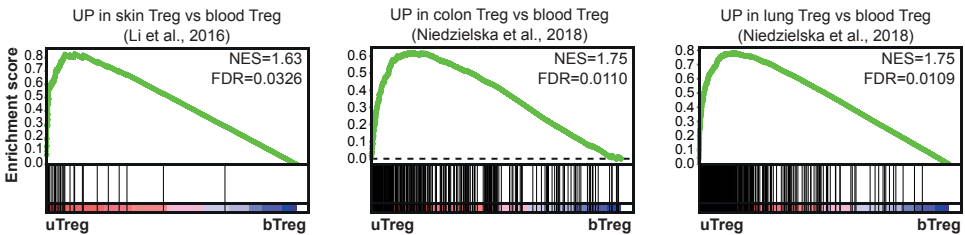
Supplementary figure 2. Enrichment of gene signatures of *in vitro* activated Tregs.

Gene set enrichment analysis with genes upregulated in Tregs stimulated *in vitro* with TCR stimulation, IL-2 or TNF α , comparing uTregs and bTregs. ^{88–92} NES = normalized enrichment score.



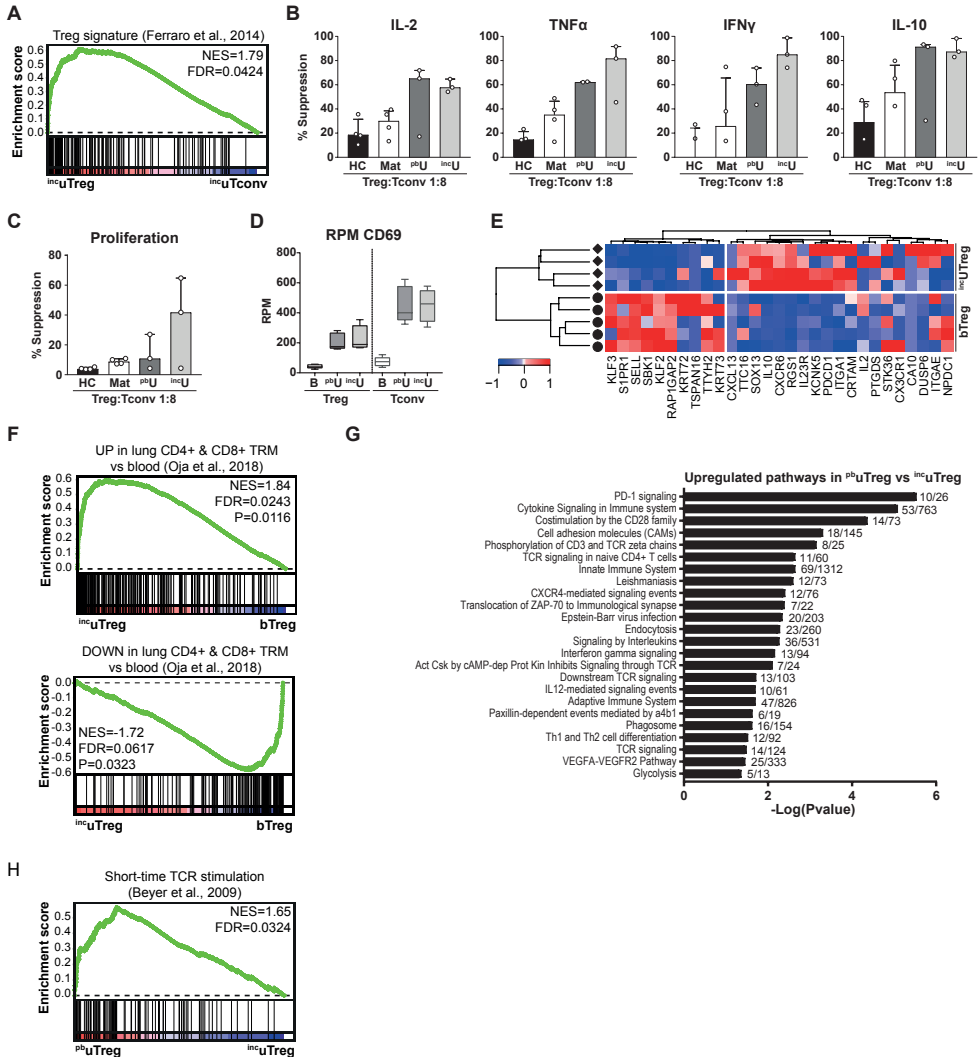
Supplementary figure 3. Downregulated pathways shared among uTregs and uTconv

Pathway analysis (ToppGene Suite) of downregulated pathways shared among uTreg and uTconv. P-values<0.05 after Bonferroni correction were considered significant.



Supplementary figure 4. uTregs from the maternal-fetal interface share similarities were human Tregs from healthy tissue sites.

Gene set enrichment analysis with published genes which are significantly upregulated in tissue Tregs from healthy skin¹⁵, colon¹⁴ or lung¹⁴ compared to blood Tregs, in uTregs versus bTregs.



Supplementary figure 5. uTregs from the incision site are bona fide Tregs and have a tissue-resident profile. (A) GSEA with published Treg signature gene set comparing *incuTreg* and *incuTconv*.⁷⁸ (B+C) Suppression assay assessing proliferation of anti-CD3 stimulated (or unstimulated) healthy CD4⁺ T cells by CTV dilution assay (C) and cytokine production in the supernatant by multiplex immunoassay (B), after 4 days of coculture with healthy donor bTregs, maternal bTregs, or uTregs at a 1:8, 1:4 and 1:2 ratio. (D) Gene expression of CD69. (E) Heatmap with published human core tissue-resident genes⁴ in *incuTregs* vs *bTregs* (F). Gene set enrichment analysis (GSEA) with published genes identifying human lung CD4⁺ and CD8⁺ TRM compared to blood memory cells; left panel⁹³) and genes upregulated in skin CD4⁺ TRM compared to blood CD4⁺ T cells (right panel¹⁵), in *incuTregs* vs *bTregs*. NES = normalized enrichment score. (G) Pathway analysis (ToppGene Suite) with 576 genes upregulated in *pbuTregs* vs *incuTregs*. P-values<0.05 after Bonferroni correction were considered significant. (H) GSEA with gene set of upregulated genes in *in vitro* stimulated Tregs.⁹² NES = normalized enrichment score.

Supplementary table 1. Clinical characteristics of 20 human subjects undergoing caesarian section

Maternal characteristics	
Age (years), <i>mean (st.dev)</i>	34 (2.3)
White ethnicity, <i>n (%)</i>	19 (95%)
Gravida (n), <i>mean (st.dev)</i>	2.3 (1.0)
Para (n), <i>mean (st.dev)</i>	1.0 (0.7)
Nulliparous, <i>n (%)</i>	4 (20%)
Pregravid BMI (kg/m ²), <i>mean (st.dev)</i>	24.4 (5.2)
Neonatal characteristics	
Gestation age at birth (days), <i>mean (st.dev)</i>	275 (5)
Birthweight (grams), <i>mean (st.dev)</i>	3535 (480)
Birthweight (percentile), <i>mean (st.dev)</i>	60 (30)
FGR (birthweight <p10), <i>n (%)</i>	0 (0%)
LGA (birthweight >p95), <i>n (%)</i>	2 (10%)
Male sex, <i>n (%)</i>	6 (30%)
Apgar at 5 min post partum, <i>mean (st.dev)</i>	8.7 (0.8)
Apgar at 10 min post partum, <i>mean (st.dev)</i>	9.6 (0.9)

Supplementary table 2. Antibodies used for sorting and flow cytometric analysis

Cell sorting					
<i>Antibody</i>	<i>Fluorochrome</i>	<i>Clone</i>	<i>Dilution (x)</i>	<i>Catalog no</i>	<i>Company</i>
CD69	FITC	FN50	25	130-113-523	Miltenyi
CCR7	PE	3D12	25	12-1979-42	eBioscience
CD4	PerCP-Cy5.5	RPA-T4	200	2102650	Sony Biotechnology
CD25	PE-Cy7	M-A251	25	557741	BD
CD127	AF647	HCD127	50	2356590	Sony Biotechnology
CD14	APC-Cy7	MphiP9	200	557831	BD
CD56?	PE-CF594	B159		562289	BD
CD45RA	PacBlue	HI100	200	2120590	Sony Biotechnology
CD3	BV510	OKT3	200	317332	Biolegend
CD45RA	BV711	HI30	400	304050	Biolegend

(Continued)

Supplementary table 2. Antibodies used for sorting and flow cytometric analysis

Flow cytometry					
<i>Surface antibody</i>	<i>Fluorochrome</i>	<i>Clone</i>	<i>Dilution (x)</i>	<i>Catalog no</i>	<i>Company</i>
CCR5	FITC	2D7/CCR5	25	555992	BD
CCR8	PE	L263G8	100	360603	Biologend
CD134 (OX-40)	PerCP-Cy5.5	Ber-ACT35	50	350010	Biologend
CD137 (4-1BB)	APC	4B4-1	50	550890	BD
CD14	V500	M5E2	100	561391	BD
CD25	BV711	2A3	50	563159	BD
CD3	APC-eF780	UCHT1	400	47-0038-42	eBioscience
CD4	PE-Cy5	RPA-T4	50	555348	BD
CD56	BV510	HCD56	50	2191700	Sony Biotechnology
CD69	PE-Cy7	FN50	50	557745	BD
CXCR3	BV605	G025H7	12.5	2368640	Sony Biotechnology
CXCR5	PerCP-Cy5.5	TG2/CXCR5	200	TG2/CXCR5	AntibodyChain
GITR	FITC	#110416	25	FAB689F	R&D
HLA-DR	PerCP-Cy5.5	L243	100	307630	Biologend
ICOS	APC	ISA3	25	17-9948-42	eBioscience
IL18R1	FITC	H44	12.5	11-7183-42	eBioscience
PD-1	APC	MIH4	12.5	558694	BD
TIGIT	PerCP-eF710	MBSA43	50	46-9200-42	eBioscience
<i>Intracellular antibody</i>	<i>Fluorochrome</i>	<i>Clone</i>	<i>Dilution (x)</i>	<i>Catalog no</i>	<i>Company</i>
CTLA-4	PE	BNI3	12.5	555853	BD
FOXP3	eFluor450	PCH101	50	48-4776-42	eBioscience
Ki67	AF647	B56	200	558615	BD
ROR γ t	APC	AFKJS-9	200	17-6988-82	eBioscience
T-bet	PE-CF594	O4-46	25	562467	BD
<i>eBioscience™ Fixable Viability Dye</i>	<i>eFluor506</i>		<i>300</i>	<i>65-0866-14</i>	<i>ThermoFisher</i>

Supplementary table 3. Gene signatures used for gene set enrichment analysis and overlap with uTreg signature

Figure	Reference			Geneset origin			Criteria for geneset		
	Author, year	GEO NCBI	Organism	Tissue compartment	Publ/GEO2R	Pvalue/Padj	FC	Comparison	
1B, S5A	Ferraro et al., 2014	-	Human	Peripheral blood	Publication			Treg signature vs Tconv	
1I	Joller et al., 2014	-	Mouse	Spleen	Publication	P<0.05	FC>2	TIGIT+ vs TIGIT- Tregs	
2B, S5E	Kumar et al., 2017	GSE94964	Human	Lung and spleen	Publication	Padj<0.05		CD69+ vs CD69- (shared among CD4+ and CD8+ from lung and spleen)	
2D	Niedzielska et al., 2018	-	Human	Colon & lung vs peripheral blood	Publication	Padj<0.05	L2FC>2	Lung/Colon CD4+ vs blood CD4+	
3C	Li et al., 2016	GSE74158	Human	Skin vs peripheral blood	GEO2R	Padj<0.05		Skin CD4+ vs blood CD4+	
3C, S5F	Oja et al., 2018	-	Human	Lung vs peripheral blood	Publication	Padj<0.05		Shared between lung CD4+ and CD8+ TRM vs Blood TEM	
4J	Tan et al., 2016	-	Mouse	Pancreas prediabetic T1D mice vs spleen	Publication	<0.05	FC>2	Splenic CXCR3+ versus CXCR3- Tregs (T-bet+)	
5ABC	Dispirito et al., 2018	-	Mouse	VAT, muscle, Colon vs spleen	Publication	<0.05	FC>2	VAT/muscle/colon Tregs vs spleen Tregs	
5DEGH	Plitas et al., 2016	-	Human	Breast cancer vs breast parenchyma vs peripheral blood	Publication	Padj<0.05		UP in breast cancer Treg vs breast cancer Tconv AND UP in breast cancer Treg vs Blood Treg	
5DEGH	Toker et al., 2018	-	Human	Epithelial ovarian cancer (mostly high-grade serous) or melanoma	Publication	Padj<0.1		PD1intCOSHi population (Tregs) vs Tconv	
5DEGH, 6I	Tirosch et al., 2016	-	Human	Single cell melanoma	Publication	<0.01 (CD4) <0.05 (CD8)	FC>2	Meloma Treg vs CD4 Tconv and CD8 Tconv	

(Continued)

Supplementary table 3. Gene signatures used for gene set enrichment analysis and overlap with uTreg signature

Figure	Reference		Geneset origin		Criteria for geneset			
	Author, year	GEO NCBI	Organism	Tissue compartment	Publ/GEO2R	Pvalue/Padj	FC	Comparison
5DEGH, 6I	Zheng et al., 2017	-	Human	Hepatocellular carcinoma single cell seq	Publ S3 Cluster	Padj<0.05	FC>2	Genes specific for Treg cluster identified by single cell seq
5DEGH, 6I	De Simone et al., 2016	-	Human	Colon and lung cancer vs colon and lung parenchyma vs blood vs Tconv	Publication			UP in TITR vs parenchyma vs blood vs Tconv
5DEGH, 6I	Pacella et al., 2018	-	Human	Liver cirrhosis and tumor (CT) or from the peripheral blood (PB) of patients with chronic HCV infection and hepatocellular carcinoma (HCC)	Publication		FC>2	Upregulated in Treg CT OX40+ versus Treg PB OX40-, and not in Treg CT OX40-, Treg PB OX40+ and all Tconv counterparts
5DEGH, 6I	Magnuson et al., 2018	-	Human	Colon cancer vs healthy colon	Publication			Tumor-Treg specific in mouse and human and correlation with FOXP3 expression
5DF	Li et al., 2016	GSE74158	Human	Skin vs peripheral blood	GEO2R	Padj<0.05		UP in skin Treg vs skin Tconv AND UP in skin Treg vs Blood Treg
5DF	Niedzielska et al., 2018	-	Human	Colon & lung vs peripheral blood	Publication	Padj<0.05	L2FC>2	UP in lung/colon Treg vs lung/colon Tconv AND UP in lung/colon Treg vs Blood Treg
5I, 6J	Pilitas et al., 2016	-	Human	Breast cancer vs breast parenchyma	Publication	Padj<0.05		UP in Breast cancer Tregs vs healthy breast parenchyma Tregs

(Continued)

Supplementary table 3. Gene signatures used for gene set enrichment analysis and overlap with uTreg signature

Figure	Reference		Geneset origin			Criteria for geneset		
	Author, year	GEO NCBI	Organism	Tissue compartment	Publ/GEO2R	Pvalue/Padj	FC	Comparison
5IJ, 6J	Magnuson et al., 2018	-	Human	Colon cancer vs healthy colon	Publication			Mean overall fold change, or high fold change in at least two patients. Mean FoldChange > 2 and nominal pvalue <0.02, or FoldChange >4 (UP), or <0.25 (DN).
S2	Nagar et al., 2010	GSE18893	Human	Peripheral blood	GEO2R	P<0.05	L2FC>0.5	50ng/mL TNFa stim vs unstim sorted Tregs (2 and 24 hrs combined in GEO2R)
S2	Yu et al., 2015	GSE49817	Human	Peripheral blood	GEO2R	Padj<0.05	UP FC>1.5, DOWN all FC	Sorted Treg stimulated with IL-2 24 hrsvs unstimulated Tregs
S2	He et al., 2012	GSE11292	Human	Peripheral blood	GEO2R	P<0.01	FC>10	Sorted Treg stim with anti-CD3/CD28 and IL-2 for 3 hours vs unstimulated Tregs
S2	Sadlon et al., 2010	GSE20934	Human	Cord blood	GEO2R	P<0.05	FC>2	Cord blood Treg expanded with dynabeads for 8 days + PMA/ionomycin vs resting Tregs at day 4
S2, S5H	Beyer et al., 2009	GSE16835	Human	Peripheral blood	GEO2R	Padj<0.05	FC>3	Tregs undergoing short time stimulation with anti-CD3/CD28 vs ex vivo Treg
S4	Li et al., 2016	GSE74158	Human	Skin vs peripheral blood	GEO2R	Padj<0.05		Skin Treg vs blood Treg
S4	Niedzielska et al., 2018	-	Human	Colon & lung vs peripheral blood	Publication	Padj<0.05	L2FC>2	Lung/Colon Treg vs blood Treg

Supplementary table 4. Upregulated and downregulated genes in the uTreg-specific core signature

Gene	uTreg core UP			UP vs bTreg			UP vs uTconv		
	Ensembl	baseMean	Log2(FC)	Pvalue	Padj	Log2(FC)	Pvalue	Padj	
AC006064.4	ENSG00000269968	153.4	1.22	1.09E-07	2.43E-06	0.75	9.81E-04	4.01E-02	
AC017002.1	ENSG00000240350	24.1	2.69	6.15E-09	1.78E-07	3.09	3.19E-11	2.93E-08	
AC080038.1	ENSG00000011028	5.4	3.80	1.31E-05	1.87E-04	3.12	6.80E-05	5.38E-03	
AC126603.1	ENSG00000258628	76.9	1.49	1.00E-09	3.39E-08	1.09	4.15E-06	5.25E-04	
AC132825.2	ENSG00000243655	163.7	0.89	5.90E-05	7.19E-04	0.73	8.51E-04	3.65E-02	
AC147651.4	ENSG00000237181	7.6	1.49	3.93E-04	3.73E-03	1.78	2.30E-05	2.23E-03	
ACP5	ENSG00000102575	28.6	1.58	2.39E-05	3.21E-04	1.92	2.74E-07	5.31E-05	
ADAMT55	ENSG00000154736	13.3	2.94	2.54E-07	5.30E-06	2.21	1.78E-05	1.85E-03	
ADPRH	ENSG00000144843	8.3	1.56	7.12E-05	8.48E-04	1.92	1.15E-06	1.81E-04	
ADRM1	ENSG00000130706	66.0	0.83	3.27E-04	3.20E-03	0.75	9.77E-04	4.00E-02	
AGTRAP	ENSG00000177674	44.8	1.36	7.07E-09	2.01E-07	0.84	1.67E-04	1.10E-02	
AK4	ENSG00000162433	5.6	4.35	6.96E-08	1.62E-06	1.91	4.74E-04	2.40E-02	
AKIRIN2	ENSG00000135334	44.4	1.48	8.04E-07	1.51E-05	1.31	8.68E-06	1.02E-03	
AL390719.1	ENSG00000217801	15.6	1.55	2.11E-07	4.49E-06	1.05	7.25E-05	5.67E-03	
ARHGAP11B	ENSG00000187951	13.7	1.33	2.30E-05	3.09E-04	0.97	8.87E-04	3.75E-02	
ARID5B	ENSG00000150347	203.1	0.88	3.06E-06	5.11E-05	1.04	3.32E-08	1.06E-05	
ARL3	ENSG00000138175	26.3	0.93	6.30E-04	5.58E-03	0.88	7.74E-04	3.39E-02	
ASMTL	ENSG00000169093	29.1	0.73	4.78E-03	3.08E-02	0.84	1.10E-03	4.28E-02	
ATP1B3	ENSG00000069849	166.3	1.01	7.06E-08	1.64E-06	0.73	7.58E-05	5.89E-03	
ATP6V1B2	ENSG00000147416	79.2	0.87	3.09E-06	5.15E-05	0.60	9.05E-04	3.80E-02	

(Continued)

Supplementary table 4. Upregulated and downregulated genes in the uTreg-specific core signature

Gene	uTreg core UP			UP vs bTreg			UP vs uTconv		
	Ensembl	baseMean	Padj	Log2(FC)	Pvalue	Padj	Log2(FC)	Pvalue	Padj
B3GAT1	ENSG00000109956	8.9	3.45	1.28E-08	3.49E-07	3.19	2.59E-08	8.67E-06	
B4GALT5	ENSG00000158470	43.0	1.38	4.06E-10	1.47E-08	1.07	3.57E-07	6.56E-05	
BABAM2	ENSG00000158019	40.5	1.07	4.84E-05	6.05E-04	1.10	2.14E-05	2.14E-03	
BATF	ENSG00000156127	130.8	2.52	5.88E-16	6.25E-14	2.33	4.39E-14	8.43E-11	
BCL2L11	ENSG00000153094	371	0.94	4.88E-05	6.10E-04	1.42	1.11E-09	6.88E-07	
BPGM	ENSG00000172331	18.7	1.47	6.12E-06	9.56E-05	1.32	2.40E-05	2.31E-03	
BST2	ENSG00000130303	59.7	1.66	7.32E-12	3.62E-10	0.82	3.35E-04	1.85E-02	
BTG3	ENSG00000154640	97.0	2.33	1.13E-21	2.79E-19	0.91	7.65E-05	5.92E-03	
C15orf39	ENSG00000167173	14.3	1.01	2.49E-03	1.79E-02	1.24	1.78E-04	1.14E-02	
CAMK1	ENSG00000134072	22.1	2.67	2.90E-15	2.75E-13	1.75	6.98E-09	3.01E-06	
CAVIN3	ENSG00000170955	17.0	3.95	5.62E-08	1.33E-06	2.07	4.95E-04	2.46E-02	
CCDC71L	ENSG00000253276	15.8	0.98	6.83E-03	4.13E-02	1.38	1.46E-04	9.89E-03	
CCL3	ENSG00000277632	4.7	3.15	5.15E-05	6.40E-04	2.37	6.85E-04	3.11E-02	
CCL3	ENSG00000278567	5.1	3.74	9.33E-06	1.39E-04	3.49	1.01E-05	1.16E-03	
CCR1	ENSG00000163823	12.1	8.33	3.68E-16	4.06E-14	2.05	2.57E-05	2.43E-03	
CD74	ENSG0000019582	1077.4	1.00	2.59E-04	2.62E-03	1.55	1.62E-08	5.90E-06	
CD80	ENSG00000121594	4.0	3.26	2.86E-06	4.81E-05	3.41	5.52E-07	9.56E-05	
CDKN1C	ENSG00000273707	13.9	2.64	5.31E-06	8.39E-05	1.89	3.50E-04	1.91E-02	
CDKN2A	ENSG00000147889	52.1	2.47	8.83E-14	6.42E-12	1.10	5.31E-04	2.59E-02	
CEBPB	ENSG00000172216	63.7	1.73	9.23E-12	4.48E-10	0.89	2.17E-04	1.32E-02	

(Continued)

Supplementary table 4. Upregulated and downregulated genes in the uTreg-specific core signature

Gene	uTreg core UP			UP vs bTreg			UP vs uTconv		
	Ensembl	baseMean	Log2(FC)	Pvalue	Padj	Log2(FC)	Pvalue	Padj	
CFAP20	ENSG00000070761	85.8	1.21	3.41E-07	6.90E-06	0.87	1.62E-04	1.07E-02	
CGA	ENSG00000135346	4.2	6.00	3.41E-07	6.90E-06	4.78	3.00E-06	4.19E-04	
CHST11	ENSG00000171310	117.7	0.86	2.00E-05	2.75E-04	0.87	1.22E-05	1.36E-03	
CHSY1	ENSG00000131873	39.9	1.12	1.22E-07	2.71E-06	0.75	1.95E-04	1.22E-02	
COL9A2	ENSG00000049089	10.0	3.83	3.30E-10	1.22E-08	2.68	7.45E-07	1.26E-04	
COMT	ENSG00000093010	62.9	0.90	9.89E-08	2.23E-06	0.82	5.96E-07	1.02E-04	
COX17	ENSG00000138495	95.7	0.90	2.08E-06	3.61E-05	0.76	4.03E-05	3.52E-03	
CRADD	ENSG00000169372	6.6	2.29	3.04E-05	3.96E-04	1.95	1.28E-04	8.97E-03	
CSF1	ENSG00000184371	48.9	3.53	4.64E-22	1.22E-19	1.33	5.67E-05	4.59E-03	
CTLA4	ENSG00000163599	91.2	1.89	3.58E-09	1.09E-07	2.84	1.39E-18	5.85E-15	
CTNNA1	ENSG00000044115	22.5	1.39	2.76E-07	5.70E-06	0.83	8.39E-04	3.62E-02	
CTNNB1	ENSG00000168036	132.7	0.36	6.81E-03	4.11E-02	0.69	2.13E-07	4.42E-05	
CTSC	ENSG00000109861	155.9	2.06	1.81E-16	2.11E-14	1.28	1.93E-07	4.08E-05	
CXCR6	ENSG00000172215	65.7	3.97	9.30E-28	4.08E-25	1.34	4.86E-05	4.11E-03	
CXorf40A	ENSG00000197620	33.9	0.96	8.49E-06	1.27E-04	0.98	2.66E-06	3.75E-04	
CXorf40B	ENSG00000197021	22.0	0.98	3.29E-04	3.22E-03	1.26	3.42E-06	4.55E-04	
DNAJC12	ENSG00000108176	7.3	2.82	3.85E-05	4.92E-04	2.13	8.35E-04	3.61E-02	
DPYSL2	ENSG00000092964	37.6	1.04	5.08E-04	4.65E-03	1.42	2.10E-06	3.07E-04	
DR1	ENSG00000117505	105.7	0.42	2.43E-04	2.48E-03	0.36	9.99E-04	4.04E-02	
DUSP10	ENSG00000143507	32.9	2.91	2.01E-25	7.34E-23	1.13	8.16E-07	1.37E-04	

(Continued)

Supplementary table 4. Upregulated and downregulated genes in the uTreg-specific core signature

Gene	uTreg core UP			UP vs bTreg			UP vs uTconv		
	Ensembl	baseMean	Log2(FC)	Pvalue	Padj	Log2(FC)	Pvalue	Padj	
DYNLL1	ENSG00000088986	347.0	0.92	4.14E-06	6.68E-05	0.70	4.83E-04	2.43E-02	
EIF2AK3	ENSG00000172071	11.5	1.65	3.04E-06	5.08E-05	1.01	1.02E-03	4.06E-02	
ELL2	ENSG0000018985	12.2	2.11	5.86E-06	9.19E-05	1.40	1.17E-03	4.55E-02	
ENO1	ENSG00000074800	971.5	1.54	1.27E-11	5.98E-10	0.74	1.08E-03	4.24E-02	
ENTPD1	ENSG00000138185	72.2	0.50	2.68E-03	1.91E-02	0.88	1.39E-07	3.13E-05	
ER1	ENSG00000104626	26.5	1.43	6.70E-09	1.91E-07	1.03	9.45E-06	1.10E-03	
ETS2	ENSG00000157557	17.9	2.36	1.88E-07	4.04E-06	2.21	4.31E-07	7.77E-05	
ETV7	ENSG0000010030	27.6	1.40	4.05E-05	5.16E-04	1.56	3.97E-06	5.05E-04	
EVA1B	ENSG00000142694	12.9	1.21	1.54E-03	1.19E-02	1.62	2.69E-05	2.53E-03	
FABP5	ENSG00000164687	21.0	1.72	2.55E-06	4.35E-05	1.66	3.21E-06	4.34E-04	
FAM3C	ENSG00000196937	13.2	2.39	7.45E-11	3.09E-09	1.56	1.21E-06	1.88E-04	
FGL2	ENSG00000127951	13.2	1.50	7.55E-06	1.14E-04	1.24	8.51E-05	6.52E-03	
FKBP1A	ENSG00000088832	236.1	0.94	1.02E-05	1.49E-04	0.81	1.26E-04	8.83E-03	
FKBP1C	ENSG00000198225	18.5	0.95	3.00E-04	2.98E-03	1.29	9.63E-07	1.58E-04	
FOXB1	ENSG00000171956	3.2	2.44	8.75E-04	7.40E-03	3.48	1.26E-05	1.40E-03	
FUCA2	ENSG00000001036	19.3	1.52	2.65E-07	5.51E-06	0.97	3.56E-04	1.92E-02	
G3BP2	ENSG00000138757	142.0	1.59	1.96E-24	6.72E-22	0.47	1.18E-03	4.57E-02	
GADD45A	ENSG00000116717	36.1	2.38	1.94E-09	6.19E-08	1.84	1.71E-06	2.60E-04	
GADD45G	ENSG00000130222	17.4	6.43	1.48E-15	1.47E-13	1.88	3.63E-06	4.70E-04	
GAPDH	ENSG00000111640	955.4	1.30	1.20E-09	4.00E-08	0.76	3.52E-04	1.91E-02	

(Continued)

Supplementary table 4. Upregulated and downregulated genes in the uTreg-specific core signature

Gene	uTreg core UP			UP vs bTreg			UP vs uTconV		
	Ensembl	baseMean	Log2(FC)	Pvalue	Padj	Log2(FC)	Pvalue	Padj	
GEM	ENSG00000164949	10.8	8.39	1.33E-11	6.23E-10	5.29	3.64E-08	1.15E-05	
GLUD1	ENSG00000148672	91.8	0.69	2.18E-04	2.26E-03	0.68	1.88E-04	1.19E-02	
GPAT3	ENSG00000138678	6.8	2.33	3.17E-06	5.26E-05	1.48	4.98E-04	2.47E-02	
GPBP1L1	ENSG00000159592	50.4	0.47	4.79E-03	3.08E-02	0.57	4.53E-04	2.34E-02	
GPR137B	ENSG00000077585	15.1	2.38	7.35E-13	4.49E-11	0.83	1.07E-03	4.21E-02	
GSTO1	ENSG00000148834	85.1	0.80	2.46E-04	2.50E-03	0.74	6.33E-04	2.97E-02	
HAVCR2	ENSG00000135077	25.3	1.40	1.94E-07	4.17E-06	0.85	6.14E-04	2.89E-02	
HES1	ENSG00000114315	12.2	5.22	7.09E-08	1.65E-06	3.65	3.14E-07	5.87E-05	
HLA-A	ENSG00000223980	729.5	0.70	1.28E-03	1.02E-02	0.75	5.52E-04	2.66E-02	
HLA-A	ENSG00000224320	848.3	0.64	1.12E-03	9.07E-03	0.67	6.20E-04	2.91E-02	
HLA-A	ENSG00000227715	787.4	0.66	1.87E-03	1.41E-02	0.71	8.26E-04	3.58E-02	
HLA-A	ENSG00000235657	781.5	0.63	3.15E-03	2.18E-02	0.69	1.15E-03	4.48E-02	
HLA-DQB1	ENSG00000225824	33.0	1.33	9.31E-04	7.78E-03	1.32	8.50E-04	3.65E-02	
HLA-DRA	ENSG00000204287	12.0	1.31	7.35E-03	4.37E-02	2.75	1.18E-07	2.78E-05	
HLA-DRA	ENSG00000227993	11.6	1.41	5.81E-03	3.61E-02	3.35	2.57E-09	1.39E-06	
HLA-DRA	ENSG00000228987	13.6	1.56	1.52E-03	1.18E-02	3.34	4.79E-10	3.27E-07	
HLA-DRA	ENSG00000234794	13.2	1.88	3.23E-05	4.18E-04	3.94	6.25E-14	1.10E-10	
HLA-DRB1	ENSG00000228080	111.4	1.54	3.13E-03	2.17E-02	2.75	2.70E-07	5.27E-05	
HLA-DRB1	ENSG00000229074	113.7	1.84	3.53E-04	3.42E-03	2.88	7.09E-08	1.92E-05	
HLA-DRB4	ENSG00000227357	20.9	1.55	1.97E-03	1.48E-02	2.20	1.43E-05	1.55E-03	

(Continued)

Supplementary table 4. Upregulated and downregulated genes in the uTreg-specific core signature

Gene	uTreg core UP			UP vs bTreg			UP vs uTconv		
	Ensembl	baseMean	Padj	Log2(FC)	Pvalue	Padj	Log2(FC)	Pvalue	Padj
HLA-DRB4	ENSG00000231021	21.3	8.79E-04	1.88	7.43E-05	8.79E-04	2.57	8.73E-08	2.25E-05
HNRNPLL	ENSG00000143889	87.6	1.26E-03	0.79	1.13E-04	1.26E-03	0.71	4.60E-04	2.35E-02
IFT27	ENSG00000100360	21.3	3.25E-02	0.70	5.11E-03	3.25E-02	0.90	2.45E-04	1.45E-02
IGFLR1	ENSG00000126246	59.4	2.61E-04	0.81	1.88E-05	2.61E-04	1.10	4.67E-09	2.19E-06
IKZF4	ENSG00000123411	26.2	3.93E-02	0.81	6.43E-03	3.93E-02	1.53	5.39E-07	9.42E-05
IL10	ENSG00000136634	28.3	2.84E-08	3.05	8.34E-10	2.84E-08	2.56	1.05E-07	2.55E-05
IL1R1	ENSG00000115594	22.0	1.45E-04	1.47	9.82E-06	1.45E-04	1.19	1.91E-04	1.20E-02
IL1R2	ENSG00000115590	12.2	6.52E-03	4.22	7.54E-04	6.52E-03	4.25	6.07E-04	2.88E-02
IL1RAP	ENSG00000196083	18.1	3.01E-02	0.87	4.66E-03	3.01E-02	0.97	1.31E-03	4.91E-02
IL1RN	ENSG00000136689	5.1	8.31E-04	3.51	6.95E-05	8.31E-04	4.56	1.72E-06	2.60E-04
IL2RA	ENSG00000134460	114.7	5.87E-04	0.98	4.67E-05	5.87E-04	3.11	2.43E-35	5.14E-31
IL2RB	ENSG00000100385	224.5	3.62E-10	1.96	7.34E-12	3.62E-10	1.22	1.76E-05	1.84E-03
ITGAM	ENSG00000169896	19.0	1.22E-06	3.14	5.08E-08	1.22E-06	3.07	5.50E-08	1.59E-05
JMJD4	ENSG00000081692	43.8	1.88E-05	1.02	1.03E-06	1.88E-05	0.66	8.98E-04	3.79E-02
JOSD2	ENSG00000161677	29.9	1.47E-04	1.14	9.96E-06	1.47E-04	0.85	5.78E-04	2.76E-02
KAT2B	ENSG00000114166	31.9	1.16E-06	1.39	4.80E-08	1.16E-06	0.81	6.97E-04	3.12E-02
KCNK5	ENSG00000164626	5.1	9.64E-08	4.87	3.11E-09	9.64E-08	2.59	4.64E-07	8.23E-05
KDM2A	ENSG00000173120	123.4	1.42E-05	1.05	7.55E-07	1.42E-05	0.69	9.00E-04	3.79E-02
KLHL2	ENSG00000109466	12.8	4.22E-03	1.18	4.52E-04	4.22E-03	1.12	5.40E-04	2.61E-02
LAG3	ENSG00000089692	25.1	6.07E-15	4.17	4.64E-17	6.07E-15	1.59	1.61E-04	1.07E-02

(Continued)

Supplementary table 4. Upregulated and downregulated genes in the uTreg-specific core signature

Gene	uTreg core UP			UP vs bTreg			UP vs uTconv		
	Ensembl	baseMean	Log2(FC)	Pvalue	Padj	Log2(FC)	Pvalue	Padj	
LAPTM4B	ENSG00000104341	47.7	1.76	1.25E-12	7.21E-11	0.80	5.00E-04	2.47E-02	
LAYN	ENSG00000204381	10.0	2.84	1.24E-08	3.38E-07	3.48	1.82E-11	1.83E-08	
LGALS1	ENSG00000100097	340.4	2.90	6.11E-17	7.82E-15	1.39	5.08E-05	4.21E-03	
LGALS3	ENSG00000131981	197.5	2.00	7.97E-14	5.84E-12	1.26	1.72E-06	2.60E-04	
LINC01943	ENSG00000280721	29.5	2.91	2.85E-10	1.08E-08	2.56	1.46E-08	5.56E-06	
LINC02195	ENSG00000236481	6.4	2.65	4.25E-07	8.39E-06	4.54	3.45E-12	4.29E-09	
LRRC32	ENSG00000137507	8.4	2.49	3.39E-04	3.31E-03	4.27	3.07E-08	1.01E-05	
LTA	ENSG00000231408	9.2	2.43	9.72E-08	2.20E-06	1.33	3.39E-04	1.87E-02	
MAF	ENSG00000178573	290.5	0.98	1.98E-06	3.45E-05	1.07	2.51E-07	4.95E-05	
MAPKAPK3	ENSG00000114738	62.8	1.97	5.20E-16	5.60E-14	0.72	1.28E-03	4.86E-02	
MAST4	ENSG00000069020	181.9	1.25	2.74E-11	1.23E-09	0.96	1.79E-07	3.88E-05	
MB21D2	ENSG00000180611	19.9	3.33	6.67E-11	2.78E-09	1.68	1.70E-04	1.11E-02	
MCM6	ENSG00000076003	29.5	0.77	7.50E-04	6.49E-03	0.95	2.43E-05	2.32E-03	
MGST2	ENSG00000085871	15.3	0.87	1.58E-03	1.22E-02	1.65	1.19E-08	4.67E-06	
MIF-AS1	ENSG00000218537	60.7	0.79	2.99E-04	2.97E-03	0.73	6.10E-04	2.88E-02	
MRNIP	ENSG00000161010	220.6	0.76	4.93E-07	9.62E-06	0.49	1.02E-03	4.07E-02	
MTREX	ENSG00000039123	91.6	2.46	1.62E-14	1.38E-12	1.68	7.36E-08	1.94E-05	
MT-RNR1	ENSG00000211459	4450.1	1.73	1.53E-20	3.19E-18	0.60	1.28E-03	4.86E-02	
MTRNR2L1	ENSG00000256618	2315.5	1.43	4.17E-16	4.53E-14	0.60	6.77E-04	3.09E-02	
MTRNR2L10	ENSG00000256045	141.2	1.65	1.64E-13	1.14E-11	0.69	1.24E-03	4.76E-02	

(Continued)

Supplementary table 4. Upregulated and downregulated genes in the uTreg-specific core signature

Gene	uTreg core UP			UP vs bTreg			UP vs uTconv		
	Ensembl	baseMean	Log2(FC)	Pvalue	Padj	Log2(FC)	Pvalue	Padj	
MYOIE	ENSG00000157483	8.8	3.20	1.51E-11	6.97E-10	2.40	1.67E-09	9.51E-07	
MYO7A	ENSG00000137474	10.7	1.67	1.49E-04	1.62E-03	1.90	1.54E-05	1.64E-03	
NAB1	ENSG00000138386	13.0	2.29	1.79E-09	5.76E-08	1.86	6.71E-08	1.84E-05	
NAMPT	ENSG00000105835	64.2	3.21	2.78E-59	5.23E-56	1.81	3.15E-29	2.22E-25	
NAMPTP1	ENSG00000229644	17.8	4.02	1.48E-23	4.55E-21	2.75	5.12E-18	1.80E-14	
NCF4	ENSG00000100365	43.6	0.78	1.81E-03	1.38E-02	1.15	4.20E-06	5.29E-04	
NDFIP2	ENSG00000102471	26.4	3.80	5.28E-20	1.00E-17	1.32	9.62E-05	7.21E-03	
NDUFV2	ENSG00000178127	124.3	0.60	1.60E-03	1.24E-02	0.60	1.26E-03	4.82E-02	
NFIL3	ENSG00000165030	18.9	5.24	6.56E-17	8.27E-15	2.36	1.15E-07	2.76E-05	
NINJ1	ENSG00000131669	109.4	2.23	7.31E-17	9.16E-15	1.18	5.11E-06	6.31E-04	
NMB	ENSG00000197696	13.6	2.25	2.23E-09	7.02E-08	1.61	2.46E-06	3.51E-04	
NR4A3	ENSG00000119508	39.3	7.22	7.00E-18	9.99E-16	0.80	5.07E-04	2.50E-02	
OGG1	ENSG00000114026	39.8	1.04	4.55E-07	8.94E-06	0.66	6.41E-04	2.98E-02	
OTUD1	ENSG00000165312	33.1	1.41	5.30E-05	6.56E-04	1.63	2.61E-06	3.70E-04	
PARBP	ENSG00000185480	13.3	1.55	2.16E-03	1.59E-02	1.70	6.88E-04	3.11E-02	
PDCD1	ENSG00000276977	48.4	4.09	8.79E-26	3.41E-23	1.16	3.57E-04	1.92E-02	
PDGFA	ENSG00000197461	11.0	1.65	1.48E-05	2.09E-04	1.39	9.53E-05	7.17E-03	
PELI1	ENSG00000197329	38.8	1.31	3.30E-06	5.42E-05	1.96	7.41E-12	8.24E-09	
PGAM1P8	ENSG00000255200	37.6	1.24	1.04E-07	2.34E-06	0.70	1.33E-03	4.94E-02	
PGK1	ENSG00000102144	412.2	1.33	3.42E-10	1.26E-08	0.81	1.09E-04	7.95E-03	

(Continued)

Supplementary table 4. Upregulated and downregulated genes in the uTreg-specific core signature

Gene	uTreg core UP		UP vs bTreg			UP vs uTconv		
	Ensembl	baseMean	Log2(FC)	Pvalue	Padj	Log2(FC)	Pvalue	Padj
PGM2L1	ENSG00000165434	96.0	1.13	1.90E-08	5.04E-07	0.82	2.90E-05	2.69E-03
PHLDA1	ENSG00000139289	302.4	4.72	2.67E-72	1.82E-68	0.77	1.22E-03	4.68E-02
PHLDA2	ENSG00000181649	10.3	4.91	2.64E-12	1.41E-10	1.68	6.70E-05	5.34E-03
PHLDA2	ENSG00000274538	10.6	4.59	1.19E-13	8.49E-12	1.90	2.36E-06	3.39E-04
PHTF2	ENSG00000006576	43.3	1.65	1.03E-15	1.05E-13	0.67	2.62E-04	1.52E-02
PIGT	ENSG00000124155	43.2	0.70	1.85E-03	1.40E-02	0.83	1.71E-04	1.11E-02
PIM3	ENSG00000198355	173.1	2.55	3.74E-17	4.95E-15	1.04	4.16E-04	2.19E-02
PKM	ENSG00000067225	645.7	1.18	6.06E-06	9.47E-05	1.22	3.07E-06	4.27E-04
PLPP1	ENSG00000067113	55.9	3.51	7.01E-12	3.50E-10	2.17	1.10E-05	1.24E-03
PMAIP1	ENSG00000141682	41.3	2.33	4.27E-14	3.29E-12	1.17	4.97E-05	4.14E-03
PMVK	ENSG00000163344	40.2	1.04	2.94E-06	4.94E-05	0.69	1.26E-03	4.80E-02
PRDM1	ENSG00000057657	221.3	0.75	7.56E-05	8.92E-04	1.12	3.43E-09	1.72E-06
PRDX1	ENSG00000117450	77.6	0.57	3.67E-03	2.47E-02	0.72	2.27E-04	1.35E-02
PRNP	ENSG00000171867	62.5	1.90	2.57E-10	9.77E-09	0.92	1.35E-03	4.99E-02
PSMD1	ENSG00000173692	78.1	0.56	6.80E-04	5.95E-03	0.53	9.62E-04	3.97E-02
PSMD8	ENSG00000099341	126.4	0.51	3.59E-04	3.47E-03	0.59	3.06E-05	2.83E-03
PTP4A3	ENSG00000184489	9.6	1.72	6.52E-04	5.75E-03	1.80	2.79E-04	1.59E-02
PTP4A3	ENSG00000275575	7.4	1.66	3.52E-03	2.40E-02	1.98	5.20E-04	2.55E-02
PTTG1	ENSG00000164611	34.7	1.40	1.14E-05	1.64E-04	1.55	1.08E-06	1.71E-04
PXK	ENSG00000168297	14.5	1.14	1.04E-04	1.18E-03	0.95	6.53E-04	3.02E-02

(Continued)

Supplementary table 4. Upregulated and downregulated genes in the uTreg-specific core signature

Gene	uTreg core UP			UP vs bTreg			UP vs uTconv		
	Ensembl	baseMean	Log2(FC)	Pvalue	Padj	Log2(FC)	Pvalue	Padj	
RAB10	ENSG00000084733	52.4	0.92	4.96E-07	9.67E-06	0.60	5.66E-04	2.70E-02	
RAC1	ENSG00000136238	238.4	0.62	3.09E-04	3.06E-03	0.66	9.74E-05	7.27E-03	
RBKS	ENSG00000171174	71	2.49	5.12E-06	8.13E-05	1.79	2.02E-04	1.24E-02	
RCAN2	ENSG00000172348	101	7.23	3.94E-12	2.04E-10	2.78	3.20E-05	2.93E-03	
RDH10	ENSG00000121039	21.8	2.01	4.25E-08	1.04E-06	2.20	1.49E-09	8.77E-07	
RHBD2	ENSG00000005486	119.4	1.02	3.31E-05	4.29E-04	0.78	1.35E-03	4.99E-02	
RHPN2	ENSG00000131941	87.0	1.20	9.09E-11	3.73E-09	1.07	4.40E-09	2.15E-06	
RNF145	ENSG00000145860	102.7	0.49	2.29E-03	1.68E-02	0.50	1.27E-03	4.84E-02	
RNF187	ENSG00000168159	79.1	0.81	2.16E-04	2.24E-03	0.75	5.21E-04	2.55E-02	
SAT1	ENSG00000130066	194.6	0.79	1.03E-03	8.44E-03	0.94	1.07E-04	7.82E-03	
SDC4	ENSG00000124145	39.0	3.53	1.11E-22	3.14E-20	1.83	1.47E-08	5.56E-06	
SDF4	ENSG00000078808	115.6	0.85	9.96E-05	1.14E-03	0.77	3.34E-04	1.85E-02	
SEC14L1	ENSG00000129657	64.4	0.88	1.17E-04	1.30E-03	0.76	7.62E-04	3.35E-02	
SETBP1	ENSG00000152217	4.7	3.11	6.49E-06	1.01E-04	1.83	7.08E-04	3.16E-02	
SGMS1	ENSG00000198964	21.7	0.86	1.02E-03	8.41E-03	1.19	5.65E-06	6.90E-04	
SIGLEC17P	ENSG00000171101	15.4	5.68	5.02E-15	4.70E-13	3.41	3.33E-10	2.35E-07	
SIPA1L1	ENSG00000197555	36.4	1.50	4.21E-09	1.25E-07	1.07	8.86E-06	1.03E-03	
SLC16A1	ENSG00000155380	9.0	1.59	3.33E-05	4.31E-04	1.49	4.48E-05	3.86E-03	
SLC27A2	ENSG00000140284	4.6	4.87	5.27E-07	1.02E-05	3.45	8.25E-06	9.79E-04	
SLC5A3	ENSG00000198743	33.6	1.96	2.69E-16	3.06E-14	0.69	6.94E-04	3.12E-02	

(Continued)

Supplementary table 4. Upregulated and downregulated genes in the uTreg-specific core signature

Gene	uTreg core UP		UP vs bTreg			UP vs uTconv		
	Ensembl	baseMean	Log2(FC)	Pvalue	Padj	Log2(FC)	Pvalue	Padj
SLC7A5	ENSG00000103257	72.9	3.63	2.77E-23	8.34E-21	1.45	1.83E-05	1.88E-03
SLCO4A1	ENSG00000101187	4.8	3.53	5.97E-07	1.15E-05	2.08	2.27E-04	1.35E-02
SMOX	ENSG00000088826	6.0	4.83	5.65E-08	1.34E-06	2.20	1.63E-04	1.07E-02
SNAP47	ENSG00000143740	41.5	2.09	3.46E-12	1.81E-10	1.16	4.04E-05	3.52E-03
SNX5	ENSG00000089006	76.3	0.52	2.92E-04	2.91E-03	0.56	5.66E-05	4.59E-03
SNX9	ENSG00000130340	38.7	1.64	7.13E-07	1.35E-05	1.38	2.01E-05	2.04E-03
SOX4	ENSG00000124766	12.6	1.89	2.02E-04	2.12E-03	2.21	1.46E-05	1.58E-03
SPATS2L	ENSG00000196141	90.6	1.55	1.12E-19	2.01E-17	0.81	4.40E-07	7.87E-05
SRGN	ENSG00000122862	1731.7	2.71	1.15E-46	1.36E-43	0.69	2.21E-04	1.33E-02
SURF4	ENSG00000148248	73.2	1.49	3.46E-10	1.27E-08	0.74	1.20E-03	4.64E-02
SUSD6	ENSG00000100647	70.5	1.14	3.47E-06	5.68E-05	0.80	9.72E-04	3.99E-02
SYT11	ENSG00000132718	44.7	0.69	4.55E-04	4.24E-03	1.08	4.90E-08	1.48E-05
TFR3	ENSG00000072274	78.9	1.02	3.36E-08	8.38E-07	1.28	3.30E-12	4.29E-09
TGIF2-RAB5IF	ENSG00000259399	8.7	0.98	7.50E-03	4.44E-02	1.24	6.52E-04	3.02E-02
TMED3	ENSG00000166557	67.3	0.59	2.95E-04	2.94E-03	0.77	1.49E-06	2.30E-04
TMEM173	ENSG00000184584	225.7	0.87	6.27E-06	9.77E-05	0.65	6.75E-04	3.09E-02
TNFRSF13B	ENSG00000240505	4.5	3.63	6.63E-06	1.02E-04	6.76	1.88E-09	1.05E-06
TNFRSF18	ENSG00000186891	58.6	4.15	3.77E-22	1.03E-19	2.19	3.20E-08	1.04E-05
TNFRSF1B	ENSG00000028137	539.9	1.11	9.86E-06	1.46E-04	1.20	1.91E-06	2.85E-04
TNFRSF4	ENSG00000186827	95.2	3.07	7.53E-17	9.38E-15	2.82	1.04E-14	2.45E-11
TNFRSF8	ENSG00000120949	2.8	2.44	3.66E-03	2.47E-02	4.56	2.11E-05	2.12E-03

(Continued)

Supplementary table 4. Upregulated and downregulated genes in the uTreg-specific core signature

Gene	uTreg core UP			UP vs bTreg			UP vs uTconv		
	Ensembl	baseMean	Log2(FC)	Pvalue	Padj	Log2(FC)	Pvalue	Padj	
TNFRSF9	ENSG00000049249	74.3	1.55	9.01E-11	3.70E-09	1.13	1.06E-06	1.69E-04	
TNIP2	ENSG00000168884	77.4	0.95	4.76E-04	4.41E-03	0.92	6.80E-04	3.09E-02	
TNS3	ENSG00000136205	19.4	2.25	2.74E-12	1.45E-10	0.92	4.31E-04	2.26E-02	
TOX2	ENSG00000124191	14.5	2.31	1.08E-04	1.22E-03	2.66	8.41E-06	9.93E-04	
TP53INP2	ENSG00000078804	15.0	4.26	1.64E-14	1.39E-12	1.03	9.85E-04	4.01E-02	
TP1	ENSG00000111669	218.1	1.50	2.84E-08	7.24E-07	0.99	2.46E-04	1.45E-02	
TPP1	ENSG00000166340	187.5	0.66	1.12E-03	9.09E-03	0.68	6.95E-04	3.12E-02	
TRAF1	ENSG00000056558	64.5	1.45	4.55E-08	1.11E-06	1.13	1.29E-05	1.42E-03	
TRAF3	ENSG00000131323	27.8	0.58	7.40E-03	4.39E-02	0.84	1.07E-04	7.82E-03	
TRPS1	ENSG00000104447	17.6	1.09	3.84E-04	3.66E-03	0.94	1.34E-03	4.98E-02	
TSPAN13	ENSG00000106537	5.8	6.96	5.27E-06	8.34E-05	5.08	1.82E-04	1.16E-02	
TSPAN17	ENSG00000048140	25.6	0.84	2.46E-03	1.77E-02	0.95	5.64E-04	2.70E-02	
TTYH3	ENSG00000136295	5.3	2.36	6.21E-05	7.51E-04	1.80	9.18E-04	3.84E-02	
U623171	ENSG00000272666	5.2	3.30	5.54E-07	1.07E-05	1.82	9.99E-04	4.04E-02	
UBASH3B	ENSG00000154127	30.9	1.24	1.72E-06	3.03E-05	1.17	3.10E-06	4.28E-04	
VDR	ENSG00000114424	67.0	1.87	2.58E-13	1.73E-11	1.92	3.81E-14	8.05E-11	
VMP1	ENSG00000062716	123.1	0.53	9.93E-05	1.13E-03	0.56	3.13E-05	2.88E-03	
ZBED2	ENSG00000177494	5.9	5.64	8.61E-11	3.54E-09	3.31	2.96E-10	2.16E-07	
ZBTB32	ENSG00000011590	5.6	2.22	7.03E-04	6.13E-03	3.74	3.04E-07	5.74E-05	
ZNF282	ENSG00000170265	34.4	2.44	4.55E-10	1.63E-08	2.04	8.74E-08	2.25E-05	
ZNRF1	ENSG00000186187	29.0	2.72	6.38E-15	5.90E-13	1.37	1.31E-05	1.43E-03	

(Continued)

Supplementary table 4. Upregulated and downregulated genes in the uTreg-specific core signature

Gene	uTreg core DOWN			DOWN vs bTreg			DOWN vs uTconv		
	Ensembl	baseMean		Log2(FC)	Pvalue	Padj	Log2(FC)	Pvalue	Padj
ABLIM1	ENSG0000009204	1316		-2.07	5.82E-32	3.36E-29	-0.84	3.61E-06	4.70E-04
AL157935.1	ENSG0000227218	19.5		-1.55	4.81E-08	1.16E-06	-1.00	5.53E-04	2.66E-02
APBA2	ENSG0000034053	17.8		-1.10	1.54E-03	1.20E-02	-1.44	1.55E-05	1.64E-03
ATF7IP2	ENSG0000166669	56.4		-1.44	1.84E-12	1.02E-10	-0.95	3.88E-06	4.97E-04
BEX2	ENSG0000133134	42.6		-2.54	4.66E-20	8.90E-18	-1.20	3.25E-05	2.96E-03
CCR7	ENSG0000126353	605.6		-1.83	2.50E-13	1.68E-11	-0.94	1.80E-04	1.15E-02
GCSAM	ENSG0000174500	29.7		-1.25	4.56E-04	4.25E-03	-1.96	8.19E-09	3.39E-06
GIMAP4	ENSG0000133574	251.1		-1.63	3.65E-23	1.07E-20	-0.81	1.02E-06	1.65E-04
GIMAP7	ENSG0000179144	352.4		-2.13	1.31E-21	3.20E-19	-0.74	1.01E-03	4.06E-02
IL7R	ENSG0000168685	1201.0		-0.71	8.53E-03	4.92E-02	-1.62	1.27E-09	7.65E-07
ITGA6	ENSG0000091409	53.7		-2.28	4.53E-20	8.72E-18	-0.90	5.64E-04	2.70E-02
LDLRAP1	ENSG0000157978	166.2		-2.14	8.14E-30	4.19E-27	-0.62	1.32E-03	4.91E-02
LEF1	ENSG0000138795	241.9		-3.31	2.49E-57	4.22E-54	-0.77	3.16E-04	1.78E-02
LINC02273	ENSG0000245954	42.9		-1.82	2.72E-08	6.96E-07	-1.81	2.20E-08	7.49E-06
MGAT4A	ENSG0000071073	100.1		-1.09	5.05E-09	1.48E-07	-1.07	5.30E-09	2.38E-06
PLAC8	ENSG0000145287	136.7		-1.02	1.12E-06	2.04E-05	-1.09	1.17E-07	2.78E-05
PRKCB	ENSG0000166501	114.2		-1.23	1.27E-12	7.30E-11	-0.85	1.19E-06	1.86E-04
RARRES3	ENSG0000133321	208.5		-0.62	4.25E-04	4.00E-03	-0.70	5.82E-05	4.67E-03
RBL2	ENSG0000103479	105.8		-0.96	7.38E-08	1.71E-06	-0.64	3.14E-04	1.78E-02
SATB1	ENSG0000182568	163.1		-0.80	1.10E-03	8.91E-03	-1.26	2.07E-07	4.34E-05

(Continued)

Supplementary table 4. Upregulated and downregulated genes in the uTreg-specific core signature

Gene	uTreg core DOWN		DOWN vs bTreg			DOWN vs uTconv		
	Ensembl	baseMean	Log2(FC)	Pvalue	Padj	Log2(FC)	Pvalue	Padj
TCF7	ENSG0000081059	493.4	-1.75	1.84E-25	6.80E-23	-1.11	4.86E-11	4.28E-08
TTC39C	ENSG00000168234	158.1	-1.36	6.25E-25	2.18E-22	-0.71	1.30E-07	2.98E-05
TTC9	ENSG00000133985	40.7	-0.99	8.71E-04	7.37E-03	-1.15	9.23E-05	7.02E-03

Supplementary table 5. Overlap of tumor-infiltrating Treg signatures with significantly upregulated genes in uTregs vs bTregs (% of overlapping genes/genes in signature)

Overlap between uTregs and tumor-infiltrating Treg signatures						
Tirosh et al 76/172 (44%)	Zheng et al 226/401 (56%)	De Simone et al. 93/309 (30%)	Pacella et al. 91/211 (43%)	Toker et al. 42/124 (34%)	Magnuson et al. 70/108 (65%)	Pitas et al. 105/423 (25%)
ACP5	ACP5	ACAA2	ACP5	ARHGEF12	ANXA4	ACSL4
AGTRAP	ACSL4	ACP5	ACTG2	BCL2L1	ARHGEF12	ACTG2
ANXA2	ACTN4	ACSL4	AKAP13	CD80	ATF3	ADPRH
B4GALT1	AKIRIN2	ACTG2	AKIRIN2	COL5A1	BATF	AKAP5
BATF	APOBEC3C	ADPRH	APOBEC3C	CRADD	BCL2L1	ASB2
BIRC3	APOBEC3G	AKAP5	ARID5B	CREB3L2	CAPG	ATP6V1A
BST2	ARHGEF12	ARHGEF12	ATP6V1B2	CTSC	CCR5	ATP6V1C2
C17orf49	ARID5B	ARNTL2	ATP6V1D	DPYSL2	CD74	AURKA
C3AR1	ARPP19	AURKA	B3GAT1	GADD45A	CD80	BCL2
CAPI	ASB2	BATF	BCL2L1	GCNT1	CDKN1A	C3AR1
CCND2	ASXL2	BCL2L1	CAMK1	HIP1	CPD	CCND2
CD79B	ATP1B1	CD7	CCDC6	ICOS	CREB3L2	CCRL2
CLIC1	ATP6V1C2	CDK6	CCND2	ILIR1	CREM	CD40LG
CMC2	BATF	CEACAM1	CD2	ILIR2	CTNNA1	CD7
COX17	BCL2L1	CGA	CD4	IL2RA	CTSH	CD79B
CRADD	BIRC3	COL9A2	CD63	KAT2B	CXCR3	CD80
CTLA4	BST2	CRADD	CD7	KBTD8	CYFIP1	CDK6
CTNNB1	BTG3	CREB3L2	CD74	KSRI	DUSP4	CGA

(Continued)

Supplementary table 5. Overlap of tumor-infiltrating Treg signatures with significantly upregulated genes in uTregs vs bTregs (% of overlapping genes/genes in signature)

Overlap between uTregs and tumor-infiltrating Treg signatures						
Tirosh et al 76/172 (44%)	Zheng et al 226/401 (56%)	De Simone et al. 93/309 (30%)	Pacella et al. 91/211 (43%)	Toker et al. 42/124 (34%)	Magnuson et al. 70/108 (65%)	Pitas et al. 105/423 (25%)
CTSC	C21orf91	CSF1	CD79B	LAPTM4B	ENTPD1	KKS2
CXCR3	C3AR1	CTLA4	CDK2AP1	LAYN	FAM126A	COL9A2
CXCR6	CCL20	CTSC	GEACAM1	LRRC32	FAM129A	CORO1C
DPYSL2	CCND2	DPYSL2	CLIC1	LTA	FNDC3B	COX17
EIF4A1	CCR1	EML2	COL5A1	MAST4	FURIN	CPXM1
ENO1	CCR5	ENTPD1	COL9A2	MYO5A	GCNT1	CRADD
EPS15	CD2	ER11	COMMD7	NAMPT	GRN	CREB3L2
ER11	CD63	ETV7	GRADD	NCOA3	HIF1A	CSF1
ICOS	CD7	EVA1B	CREB3L2	NETO2	HIVEP3	CTSC
IFI6	CD74	FBXO45	CST7	PDGFA	ICOS	DPYSL2
IL1R2	CD79B	FKBP1A	CTNNA1	PHACTR2	IKZF4	DYNC1I2
IL2RA	CD80	FNDC3B	CTSC	PHTF2	IL1R2	EGR3
IL2RB	CD82	FUCA2	CXCR6	PTP4A3	IL1RL1	ENTPD1
IL2RG	CD83	GADD45A	DPYSL2	SAT1	IRAK2	ETV7
ISG15	CDIP1	GCNT1	ENO1	SEC14L1	IRF5	FAM126A
LGALS1	CDKN1A	HAP1	ENTPD1	SGMS1	ISG15	FNDC3B
LGALS3	CDKN2A	HAVCR2	ER11	SLAMF1	LAMP2	FUCA2
LY6E	GEACAM1	HIVEP3	FBLN7	SLC16A1	LAPTM4B	GALM
MAPKAPK3	CLIC1	ICOS	GALM	SOX4	MAP2K3	GCNT1
MRPS6	CMTM6	IGFLR1	GAPDH	TNFRSF13B	MAPKAPK2	GEM

(Continued)

Supplementary table 5. Overlap of tumor-infiltrating Treg signatures with significantly upregulated genes in uTregs vs bTregs (% of overlapping genes/genes in signature)

Overlap between uTregs and tumor-infiltrating Treg signatures						
Tirosh et al 76/172 (44%)	Zheng et al 226/401 (56%)	De Simone et al. 93/309 (30%)	Pacella et al. 91/211 (43%)	Toker et al. 42/124 (34%)	Magnuson et al. 70/108 (65%)	Pitas et al. 105/423 (25%)
MX1	COL9A2	IKZF4	GLA	TNFRSF1B	MAPKAPK3	HAVCR2
MYL6	CREB3L2	IL1R2	GRAMD4	TPP1	MRPS6	HIVEP3
NAMPT	CREM	IL1RL1	HLA-DRB4	WLS	MVP	HMOX1
NCF4	CSF1	IL2RA	HSP90AA1	ZBTB32	MXD1	HSPA1A
NDUVF2	CST7	IL2RB	IFI27		NAMPT	ICOS
NFKB1Z	CTLA4	KAT2B	IFI35		NCF4	IFT27
OAS1	CTNNA1	KLHDC7B	IL18R1		NDRG1	IKZF4
PELI1	CTNNB1	LAPTM4B	IL1R1		NINJ1	IL1A
PGK1	CTSC	LAX1	IL1R2		OSBPL3	IL1R1
PHTF2	CTSD	LAYN	IRF4		PICALM	IL1R2
PLP2	CXCR3	LEPROT	ITGB2		PLP2	IL1RL1
PRDM1	CXCR6	LTA	KAT2B		PMAIP1	IL1RN
PRDX3	DDIT4	MAP1LC3A	LAPTM4B		RHBDD2	IL2RA
PRNP	DDX24	MAST4	LAX1		RHOC	IL4R
PTTG1	DPYSL2	MGST2	LAYN		SAMSN1	IRAK2
RPS27L	DUSP2	MICAL2	LGALS1		SDC4	IRF5
S100A4	DUSP4	MINPP1	LTA		SEC14L1	KSRI
S100A6	DYNLL1	MREG	MAPK6		SKAP2	LAPTM4B
SAMSN1	EDARADD	NAB1	MFIH1A1		SNX9	LAYN

(Continued)

Supplementary table 5. Overlap of tumor-infiltrating Treg signatures with significantly upregulated genes in uTregs vs bTregs (% of overlapping genes/genes in signature)

Overlap between uTregs and tumor-infiltrating Treg signatures						
Tirosh et al 76/172 (44%)	Zheng et al 226/401 (56%)	De Simone et al. 93/309 (30%)	Pacella et al. 91/211 (43%)	Toker et al. 42/124 (34%)	Magnuson et al. 70/108 (65%)	Pitas et al. 105/423 (25%)
SAT1	ENO1	NCF4	MGST2		SSH1	MAP2K3
SDC4	ENTPD1	NDFIP2	MYO5A		TMBIM1	MGST2
SDF4	ER11	NETO2	MZB1		TNFRSF18	MICAL2
SLAMF1	ETV7	NUSAP1	NAB1		TNFRSF1B	MIR155HG
SNX5	FAM129A	PAM	NFIL3		TNFRSF4	MRPS6
SPPL2A	FBLN7	PARD6G	PAM		TNFRSF8	MYO1E
SQSTM1	FKBP1A	PDGFA	PMAIP1		TNFRSF9	NAGA
TANK	FOS	PRDX3	PMVK		TNIP2	NCF4
TFRC	FOSL2	PTP4A3	PRDX5		TRAF1	NEDD9
TMED9	FYCO1	PTTG1	PRNP		TRAF3	NFKB2
TMEM173	GABARAPL1	RBKS	PSTPIP1		UEVLD	NR4A1
TNFRSF18	GADD45A	RDH10	RGS1		VIM	NTRK1
TNFRSF1B	GADD45G	RNF145	RHOB		ZNRF1	PARD6G
TNFRSF4	GALM	RYBP	SAMID9			PARPBP
TPM4	GAPDH	SECTM1	SCD			PDGFA
TPP1	GCNT1	SLC16A1	SDC4			PDIA6
TXN	GOLGA8A	SNAP47	SETBP1			PHLDA1
TYMP	GPI	SOX4	SFT2D1			PIK3API
VDR	GRN	SPATS2L	SH2D1A			PSEN1

(Continued)

Supplementary table 5. Overlap of tumor-infiltrating Treg signatures with significantly upregulated genes in uTregs vs bTregs (% of overlapping genes/genes in signature)

Overlap between uTregs and tumor-infiltrating Treg signatures						
Tirosh et al 76/172 (44%)	Zheng et al 226/401 (56%)	De Simone et al. 93/309 (30%)	Pacella et al. 91/211 (43%)	Toker et al. 42/124 (34%)	Magnuson et al. 70/108 (65%)	Pitas et al. 105/423 (25%)
GSTO1	SSH1	SSH1	SH2D2A			PTP4A3
HAVCR2	SYT11	SYT11	SLC20A1			PTTG1
HERPUD1	TFRC	TFRC	SOC31			RBBP8
HLA-DQB1	THADA	THADA	SPPL2A			RBKS
HLA-DRB1	TMEM184C	TMEM184C	TFRC			RHOC
HLA-J	TNFRSF18	TNFRSF18	TMCO1			SDC4
HNRNP1L	TNFRSF4	TNFRSF4	TMEM109			SETBP1
HSPA1A	TNFRSF8	TNFRSF8	TNFRSF1B			SH2D2A
HSPB1	TNFRSF9	TNFRSF9	TNS3			SLAMF1
ICOS	TOX2	TOX2	TP11			SLC4A2
IFI6	TPP1	TPP1	TTYH3			SLCO4A1
IGFLR1	TRAF3	TRAF3	ZBED2			SNX5
IKZF4	TSPAN17	TSPAN17	ZBTB32			SPATS2L
IL10RB	VDR	VDR	ZFAND5			THADA
IL18R1	YIPF6	YIPF6	ZFP36L1			TNFRSF18
IL1R1	ZBED2	ZBED2				TNFRSF1B
IL1R2	ZNF282	ZNF282				TNFRSF4
IL2RA						TNFRSF8
IL2RB						TNFRSF9

(Continued)

Supplementary table 5. Overlap of tumor-infiltrating Treg signatures with significantly upregulated genes in uTregs vs bTregs (% of overlapping genes/genes in signature)

Overlap between uTregs and tumor-infiltrating Treg signatures						
Tirosh et al 76/172 (44%)	Zheng et al 226/401 (56%)	De Simone et al. 93/309 (30%)	Pacella et al. 91/211 (43%)	Toker et al. 42/124 (34%)	Magnuson et al. 70/108 (65%)	Pitas et al. 105/423 (25%)
IL4R						TNIP2
IQGAP1						TNIP3
IRF5						TNS3
ISG15						TRAF1
IVNS1ABP						TYMP
KAT2B						UBASH3B
KDM5B						VDR
KIF20B						VRK2
LAPTM4A						XXYL1
LAPTM4B						ZBED2
LAT2						
LAYN						
LDHA						
LEPROT						
LGALS1						
LGALS3						
LINC00963						
LRPAP1						
LTA						

(Continued)

Supplementary table 5. Overlap of tumor-infiltrating Treg signatures with significantly upregulated genes in uTregs vs bTregs (% of overlapping genes/genes in signature)

Overlap between uTregs and tumor-infiltrating Treg signatures						
Tirosh et al 76/172 (44%)	Zheng et al 226/401 (56%)	De Simone et al. 93/309 (30%)	Pacella et al. 91/211 (43%)	Toker et al. 42/124 (34%)	Magnuson et al. 70/108 (65%)	Pitas et al. 105/423 (25%)
	LYST					
	MAF					
	MAP2K3					
	MAPKAPK3					
	MAST4					
	MCL1					
	MICAL2					
	MIR497HG					
	MKNIK1					
	MRPS6					
	MYO5A					
	MZB1					
	NAMPT					
	NCF4					
	NCOA3					
	NDFIP2					
	NEDD9					
	NRBP1					
	OAS1					

(Continued)

Supplementary table 5. Overlap of tumor-infiltrating Treg signatures with significantly upregulated genes in uTregs vs bTregs (% of overlapping genes/genes in signature)

Overlap between uTregs and tumor-infiltrating Treg signatures						
Tirosh et al 76/172 (44%)	Zheng et al 226/401 (56%)	De Simone et al. 93/309 (30%)	Pacella et al. 91/211 (43%)	Toker et al. 42/124 (34%)	Magnuson et al. 70/108 (65%)	Pitas et al. 105/423 (25%)
	P2RY10					
	PAM					
	PDCD1					
	PDIA6					
	PELI1					
	PFKFB3					
	PGK1					
	PHACTR2					
	PHLDA1					
	PHPT1					
	PHTF2					
	PIM3					
	PKM					
	PLTP					
	PMAIP1					
	PMF1					
	PMF1-BGLAP					
	PPP1CB					
	PRDM1					

(Continued)

Supplementary table 5. Overlap of tumor-infiltrating Treg signatures with significantly upregulated genes in uTregs vs bTregs (% of overlapping genes/genes in signature)

Overlap between uTregs and tumor-infiltrating Treg signatures						
Tirosh et al 76/172 (44%)	Zheng et al 226/401 (56%)	De Simone et al. 93/309 (30%)	Pacella et al. 91/211 (43%)	Toker et al. 42/124 (34%)	Magnuson et al. 70/108 (65%)	Pitas et al. 105/423 (25%)
	PRDX1					
	PRDX3					
	PRDX5					
	PRF1					
	PRKARIA					
	PRNP					
	PTP4A1					
	PTP4A3					
	PTPN22					
	PTPN7					
	PTTG1					
	RAB10					
	RAB11FIP1					
	RAB8B					
	RALGDS					
	RBPJ					
	RGS1					
	RHBDD2					
	RHOC					

(Continued)

Supplementary table 5. Overlap of tumor-infiltrating Treg signatures with significantly upregulated genes in uTregs vs bTregs (% of overlapping genes/genes in signature)

Overlap between uTregs and tumor-infiltrating Treg signatures						
Tirosh et al 76/172 (44%)	Zheng et al 226/401 (56%)	De Simone et al. 93/309 (30%)	Pacella et al. 91/211 (43%)	Toker et al. 42/124 (34%)	Magnuson et al. 70/108 (65%)	Pitas et al. 105/423 (25%)
	RNF19A					
	RPS27L					
	SAMSN1					
	SAT1					
	SCO2					
	SDC4					
	SDF4					
	SERPINE2					
	SFT2D1					
	SH2D2A					
	SKAP2					
	SLA					
	SLAMF1					
	SLC16A1					
	SLC3A2					
	SLC5A3					
	SNX9					
	SPATS2L					
	SPPL2A					

(Continued)

Supplementary table 5. Overlap of tumor-infiltrating Treg signatures with significantly upregulated genes in uTregs vs bTregs (% of overlapping genes/genes in signature)

Overlap between uTregs and tumor-infiltrating Treg signatures						
Tirosh et al 76/172 (44%)	Zheng et al 226/401 (56%)	De Simone et al. 93/309 (30%)	Pacella et al. 91/211 (43%)	Toker et al. 42/124 (34%)	Magnuson et al. 70/108 (65%)	Pitas et al. 105/423 (25%)
	SGSTM1					
	SRA1					
	SRGN					
	STAT3					
	SURF4					
	SYT11					
	TANK					
	TFRC					
	THADA					
	TMCO1					
	TMEM173					
	TMEM50A					
	TMX1					
	TNFAIP3					
	TNFRSF13B					
	TNFRSF18					
	TNFRSF1B					
	TNFRSF4					
	TNFRSF9					

(Continued)

Supplementary table 5. Overlap of tumor-infiltrating Treg signatures with significantly upregulated genes in uTregs vs bTregs (% of overlapping genes/genes in signature)

Overlap between uTregs and tumor-infiltrating Treg signatures						
Tirosh et al 76/172 (44%)	Zheng et al 226/401 (56%)	De Simone et al. 93/309 (30%)	Pacella et al. 91/211 (43%)	Toker et al. 42/124 (34%)	Magnuson et al. 70/108 (65%)	Pitas et al. 105/423 (25%)
	TNIP3					
	TOX2					
	TPI1					
	TPM4					
	TPP1					
	TRAF1					
	TRAF3					
	TRPS1					
	TSPAN13					
	TSPYL2					
	TYMP					
	UBASH3B					
	VDR					
	VMP1					
	ZBED2					
	ZBTB32					
	ZFP36L1					

Supplementary table 6. Genes most often shared between 7 tumor-infiltrating Treg signatures

Name	# Signatures shared	DE ^{pb} uTreg vs bTreg?	DE ^{pb} uTreg vs ^{inc} Treg?	In uTreg core?
IL1R2	7	Yes	No	Yes
TNFRSF1B	6	Yes	Yes	Yes
CTSC	6	Yes	Yes	Yes
LAPTM4B	6	Yes	No	Yes
DPYSL2	6	Yes	No	Yes
CREB3L2	6	Yes	No	No
ICOS	6	Yes	No	No
CCR8	6	No	No	No
CSF2RB	6	No	No	No
GLRX	6	No	No	No
MAGEH1	6	No	No	No
ENTPD1	5	Yes	Yes	Yes
IL2RA	5	Yes	Yes	Yes
NCF4	5	Yes	Yes	Yes
SDC4	5	Yes	Yes	Yes
TNFRSF4	5	Yes	Yes	Yes
CRADD	5	Yes	No	Yes
LAYN	5	Yes	No	Yes
TNFRSF18	5	Yes	No	Yes
BCL2L1	5	Yes	Yes	No
GCNT1	5	Yes	No	No
TIGIT	5	No	Yes	No
EBI3	5	No	No	No
F5	5	No	No	No
FOXP3	5	No	No	No
GBP2	5	No	No	No
IKZF2	5	No	No	No
IL12RB2	5	No	No	No
TBC1D8	5	No	No	No
ACP5	4	Yes	Yes	Yes
BATF	4	Yes	Yes	Yes
ERI1	4	Yes	Yes	Yes
NAMPT	4	Yes	Yes	Yes
PTTG1	4	Yes	Yes	Yes
TFRC	4	Yes	Yes	Yes

(Continued)

Supplementary table 6. Genes most often shared between 7 tumor-infiltrating Treg signatures

Name	# Signatures shared	DE ^{pb}uTreg vs bTreg?	DE ^{pb}uTreg vs ^{inc}Treg?	In uTreg core?
TPP1	4	Yes	Yes	Yes
VDR	4	Yes	Yes	Yes
CD80	4	Yes	No	Yes
COL9A2	4	Yes	No	Yes
IKZF4	4	Yes	No	Yes
IL1R1	4	Yes	No	Yes
KAT2B	4	Yes	No	Yes
LTA	4	Yes	No	Yes
PTP4A3	4	Yes	No	Yes
TNFRSF9	4	Yes	No	Yes
ZBED2	4	Yes	No	Yes
MRPS6	4	Yes	Yes	No
SLAMF1	4	Yes	Yes	No
ARHGEF12	4	Yes	No	No
CCND2	4	Yes	No	No
CD7	4	Yes	No	No
CD79B	4	Yes	No	No
HTATIP2	4	No	Yes	No
CARD16	4	No	Yes	No
SIRPG	4	No	Yes	No
DFNB31	4	No	No	No
DUSP16	4	No	No	No
FCRL3	4	No	No	No
FLVCR2	4	No	No	No
GBP5	4	No	No	No
MYO5C	4	No	No	No
SYNGR2	4	No	No	No
TMPRSS6	4	No	No	No
UGP2	4	No	No	No

T cell interaction with activated endothelial cells induces sustained CD69 expression independent of T cell activation: priming for tissue-residency?

Judith Wienke, Eva M. Struijf, Fjodor Yousef Yengej, Marlot van der Wal, Annet van Royen-Kerkhof, and Femke van Wijk

Manuscript in preparation

ABSTRACT

Objectives: Endothelial cells are obligate interaction partners for T cells trafficking into tissues during inflammation. It is still elusive whether and how noncognate interactions between activated endothelial cells and T cells influence T cell function.

Methods: Human microvascular endothelial cells (EC) or human umbilical vein endothelial cells (HUVEC) were stimulated for 3 days with TNF α and/or IFN γ . Bulk or subsets of T cells were FAC-sorted and cocultured with activated EC for up to 7 days. EC and T cell phenotypes were assessed by flow cytometry. T cell proliferation was measured by CellTrace Violet dilution assay. Soluble mediators in cultured medium of EC were analyzed by multiplex immunoassay.

Results: TNF α and/or IFN γ stimulated EC expressed increased levels of adhesion molecules ICAM-1 and VCAM-1, and MHC-I and MHC-II molecules but negligible levels of costimulatory molecules CD80 and CD86. Coculture of T cells with activated, but not resting, EC induced CD69 expression without activation (CD25, Ki67) or proliferation. The dynamic of CD69 expression induced by EC was distinct from that induced by cognate antigen recognition, with rapid induction and rather stable expression up to 7 days of coculture. These effects could be recapitulated with HUVEC. CD69 induction by activated EC was higher in memory than naive CD4⁺ and CD8⁺ T cells, and most pronounced in CD8⁺ effector memory T cells. Early CD69 induction was mostly mediated by IL-15, whereas later effects were also mediated by interactions with ICAM-1 and/or VCAM-1. Cognate antigen recognition was not involved, and transmigration did not further enhance CD69 expression by T cells. CD69⁺ T cells displayed a phenotype associated with tissue-residency, with higher levels of CD49a, CD103, CXCR6, PD-1 and CD57 than their CD69⁻ counterparts, and downregulation of CD62L and S1PR1. EC-induced CD69⁺ T cells were poised for high production of pro-inflammatory cytokines TNF α and IFN γ and showed increased expression of T helper 1 transcription factor T-bet.

Conclusion: Activated EC can induce a specialized phenotype in T cells with sustained CD69 expression, increased cytokine response and a marker profile reminiscent of tissue-resident memory T cells. Interaction with activated EC during transmigration into inflamed tissues may be a first event priming T cells for tissue-residency.

INTRODUCTION

Endothelial cells (EC) play a crucial role in the homeostasis of immune responses. During tissue inflammation, caused by infection or inflammatory diseases, EC become actively engaged in response to pro-inflammatory cytokines.¹ Especially the T cell-derived cytokines IFN γ and TNF α are important cues for EC. They can induce the expression of costimulatory molecules^{2–4} and adhesion molecules (VCAM-1, ICAM-1) on EC and increase the secretion of leukocyte chemo-attractants.^{1,5,6} By elevated expression of chemo-attractant and adhesion molecules, activated EC recruit leukocytes, among which T cells, to the inflamed tissue sites and facilitate their transmigration from the circulation into the tissue. This process is crucial to the surveillance and effector functions of the immune system, such as eradication of invading pathogens, but can also contribute to the immunopathogenesis of immune-mediated inflammatory diseases.

Transmigration of immune cells across the endothelium is a complex and slow process, which is regulated at different stages. First, the migratory capacity of T cells is primed by antigen recognition in lymph nodes, where T cells become activated by antigen-presenting cells.^{7–9} Typical markers of T cell activation include CD25,¹⁰ ICOS,¹¹ Ki67,¹⁰ and CD69, an early marker upregulated within hours after stimulation and associated with subsequent T cell proliferation.^{10,12,13} These antigen-experienced T cells are recruited to sites of inflammation through the chemo-attractants released by activated EC and tissue cells. T cells are captured from the circulation by interactions of integrins expressed by T cells upon activation, and both selectins and integrins like ICAM-1 and VCAM-1 on EC.^{14–18} Subsequently, T cells adhere to EC and migrate through the endothelial layer into the tissue.^{2,19} Since the process of transmigration involves prolonged, close interaction between T cells and EC, it is likely that this process might induce functional changes in transiting T cells that prepare them for the tissue environment. However, the exact changes induced by noncognate interactions between EC and T cells are still elusive.

T cells can either transiently pass through tissues to perform their effector function and subsequently re-enter circulation, or they can become resident and stay in tissues for prolonged periods, to respond quickly to (re-) infection with a previously encountered pathogen. These tissue-resident memory T cells (TRM), which were identified as a subset of effector memory T cells residing in tissues without recirculation, have gained interest over the past decade due to their specialized characteristics and clinical relevance for vaccines and cancer immunotherapies.^{20–22} TRM are characterized by high and sustained expression of CD69,^{23–28} which prevents tissue egress by sequestering sphingosine 1 phosphate receptor 1 (S1PR1) from the cellular surface.^{29,30} In activated T cells, short-term expression of CD69 is suggested to temporarily limit egress from lymph nodes, while constitutive expression, as found in TRM, enables long-term tissue-residency.³¹ Also in inflammatory diseases, tissue-infiltrating T cells show increased expression of CD69^{32–34} and

TRM have been implicated in the chronicity of immune-mediated inflammatory diseases.³⁵ TRMs are poised to rapidly respond to pathogens by secretion of cytokines like IFN γ , and have a decreased turnover rate compared to circulating memory cells.^{24,31,36} Furthermore, CD49a, CD103, CXCR6, CD57 and PD-1 were described as core markers for TRM, as their expression patterns best discriminate between CD69⁺ and CD69⁻ cells in different types of tissues.^{24,37–39} Despite the huge efforts made in elucidating human TRM phenotype and function, key events in induction of the TRM program are still poorly understood. Also the potential role of the endothelium in the activation of T cells migrating to inflamed tissue sites is still under discussion.⁶

We hypothesized that the transmigration through activated endothelium into inflamed tissues may prime T cells for tissue-residency and initialize the specialized phenotype of TRM. Here, we used an *in vitro* coculture system of cytokine-activated EC and highly purified T cell populations to investigate the effect of EC on T cell activation and phenotype and elucidate the involved mechanisms.

METHODS

Endothelial cell culture

The human dermal microvascular endothelium cell line (HMEC-1, ATCC) was cultured in MCDB-131 medium (*Life Technologies*), supplemented with 10 mM L-glutamine (*Gibco*), 10 ng/ml epidermal growth factor (EGF) (*Invitrogen*), 1 μ g/ml hydrocortisone (*Sigma*), 1% Penicillin Streptomycin (p/s, *Gibco*) and 10% fetal calf serum (FCS) (*Biowest*). Medium was refreshed every 3–4 days and cells were suspended at confluence, using 0.05% Trypsin (*Gibco*). All cell cultures and incubations in this study were performed in a 5% CO₂ incubator at 37°C. For phenotyping, 250,000 HMEC-1 cells were stimulated with 10 ng/ml tumor necrosis factor α (TNF α , *Miltenyi*) and/or 10 ng/ml interferon γ (IFN γ , *eBioscience*) for three days in 12-wells plates, to form a confluent layer of stimulated endothelial cells. HMEC-1 were detached using 0.25 mL trypsin 0.5% EDTA (*Life Technologies*) and stained with surface antibodies for flow cytometric analysis (see below).

Lymphocyte isolation

Peripheral Blood Mononuclear Cells (PBMCs) were isolated from fresh healthy donor blood by Ficoll-Paque™ PLUS (*GE Healthcare*) density centrifugation. PBMCs were frozen at -80°C in RPMI 1640 (*Gibco*) + 1% p/s + 1% L-glutamine (basic medium) supplemented

with 20% FCS and 10% DMSO (*Honeywell*), until use. CD3⁺ bulk T cells, CD3⁺ memory (CD3⁺CD45RO⁺CD45RA⁻) or naive (CD3⁺CD45RO⁻CD45RA⁺) T cells, CD8⁺ memory subsets (CD3⁺CD8⁺CD45RA^{+/−}CCR7^{+/−}(CD27^{+/−})) and HLA-DR⁺CD14⁺CD11c⁺ conventional dendritic cells (cDc) were obtained by fluorescence-activated cell sorting (FACS) of thawed PBMCs in MACS buffer (phosphate buffered saline (PBS, *Gibco*) + 2 mM EDTA (*VWR chemicals*) + 2% FCS). The four CD8⁺ memory T cell subsets were defined as central memory (CM, CD45RA⁻CCR7⁺), terminally differentiated CD45RA⁺ effector memory (TEMRA, CD45RA⁺CCR7⁻) and two subsets of effector memory (EM, CD27⁺ and CD27⁻, both CD45RA⁻CCR7⁻). Cells were sorted using a FACSAria™ III cell sorter. For proliferation assays, T cells were labelled with 2 μM celltrace violet (CTV, *Life Technologies*) and proliferation was assessed by CTV dilution assay by flow cytometry.

Endothelial cell-T cell coculture

HMEC-1 cells were first grown in culture medium (basic medium + 10% FCS) in round-bottom 96-well plates (12.500 cells/well) overnight. HMEC-1 cells were then stimulated with 10 ng/ml TNFα and/or 10 ng/ml IFNγ for three days. After three days, TNFα and IFNγ were washed away with PBS and 50.000 sorted T cells were added per well, either with or without blocking antibodies. In control conditions, T cells were cultured in the absence of EC (negative control), in the presence of resting EC (negative control) in the presence of 1 μg/mL soluble anti-CD3 or anti-CD3/CD28 human T-activator Dynabeads™ (1:50, *Gibco*) and/or 10.000 cDCs (positive controls) as indicated in the figure legends. Samples were incubated for different time periods up to 7 days as indicated in the figure legends and protein expression levels were analyzed using flow cytometry (see below). Monoclonal antibodies blocking interleukin (IL)-15, transforming growth factor β (TGF-β), ICAM-1, and VCAM-1 were added to the coculture in different concentrations as indicated. Monoclonal antibody blocking HLA-ABC was added to the coculture in a concentration of 35 μg/mL. Details on blocking antibodies are provided in supplementary table 1. To assess the effects of HMEC-1 cultured medium on T cells, supernatant of cultured HMEC-1 was transferred to T cells and diluted 1:1 with culture medium. Protein levels of IL-15, TGF-β, soluble ICAM-1 and soluble VCAM-1 were analyzed in undiluted HMEC-1 supernatants by multiplex immunoassay.

Transmigration assay

HMEC-1 cells were grown in the upper wells of 24-wells Transwell® cell culture chambers, with a Polycarbonate Membrane with 5.0μm pores (*Costar*). Upper wells contained 200 μl culture medium, while lower wells contained 800 μl, to prevent hydrostatic gradients.

Endothelial cells were stimulated with TNF α and IFN γ as described above. To induce a chemotactic gradient, lower wells contained culture medium with 10% FCS and 0.44 ng/ml interferon-inducible protein 10 (IP-10, *Peprotech*), while upper wells contained CD3⁺ memory cells (250,000 cells/well) in medium without FCS and IP-10. After one day of incubation, CD69 expression levels of migrated and non-migrated cells were measured using flow cytometry. The HMEC-1 cell layer was tested for integrity using a trypan-blue-albumin complex diffusion assay. In short, 800 μ l Hanks' balanced salt solution (HBSS, *Gibco*) was added to the lower wells and 200 μ l of a 10 ml HBSS mixture containing 900 μ l Trypan Blue (*Sigma*) and 80mg BSA (*Sigma*) was added to the upper well. Wells were incubated for 5 minutes, at room temperature with continuous shaking, and dye leakage to the lower compartment was assessed with the naked eye, as described previously.⁴⁰

Flow cytometry

Viability of all cells was assessed with fixable viability dye eF506 (*eBioscience*[™]), by 30 minute staining at 4°C in PBS. Flow cytometry stainings were prepared by adding fluorochrome-conjugated antibodies to (PBS, *Sigma*) with 2% FCS and either 0,1% NaN₃ (*Severn Biotech Ltd.*) or 2 mM EDTA. In addition, 2% normal mouse serum (*Fitzgerald*) was added to inhibit aspecific antibody-binding by Fc γ receptors. Before surface staining, cells were rinsed twice. Cells were incubated for 20 minutes at 4 °C with the surface antibody staining and then rinsed twice again. For intracellular and intranuclear staining, cells were fixated and permeabilized with 1:3 Fixation/Permeabilization concentrate and Fixation/Permeabilization diluent (*Invitrogen*) for 30 minutes at 4°C. Intracellular staining was performed in permeabilization buffer (*Invitrogen*), at 4°C and for 25 minutes. Expression levels of secreted cytokines were intracellularly measured after four hours of restimulation with 20 ng/ml Phorbol 12-myristate 13-acelate (PMA, *Sigma*) and 1 μ g/ml ionomycin (*Sigma*) in basic medium supplemented with 10% AB serum (*Sanquin*) in the presence of 1:1500 diluted GolgiStop (*BD bioscience*). Cells were subsequently rested for 90 minutes at 37°C. For optimal measurement of CD69 in PMA/ionomycin stimulated samples, CD69, CD3, CD4 and CD8 were stained prior to stimulation. Viability and intracellular stainings were performed after stimulation, as described above. Median fluorescent intensities (MFI) per sample were measured in FACS buffer using the flow cytometer BD FACSCanto[™] II. Flow cytometry data were analyzed with FlowJo[™] V10 software (*FlowJo, LLC*). GraphPad Prism 7.02 (GraphPad Software Inc) was used for graphic display of the results.

RESULTS

Activated EC induce T cell CD69 expression, but not proliferation

To study the effect of the activation state of EC on T cell function, HMEC-1 (from now on referred to as EC) were stimulated with IFN γ and/or TNF α for 3 days. EC stimulated with IFN γ and TNF α expressed high levels of adhesion molecules ICAM-1 and VCAM-1, HLA-DR, HLA-ABC and CD40, but negligible levels of CD80 and CD86 (supplementary figure 1). Total CD3 $^+$ T cells co-incubated with stimulated, but not resting EC, showed increased expression of early activation marker CD69 (figure 1A and B). Additional activation of T cells by T cell receptor (TCR) stimulation with soluble anti-CD3 did not further increase CD69 expression as induced by activated EC. The combination of the cytokines TNF α and IFN γ in the absence of EC did not induce CD69 expression in T cells, indicating that the effect was mediated by EC. Although co-incubation with activated EC induced CD69 expression, which is usually associated with subsequent proliferation,^{10,12,13} we did not observe T cell proliferation (figure 1C). A control condition with T cells co-incubated with conventional dendritic cells (cDC) showed that the proliferative capacity of these T cells was intact. Expression of two other markers associated with T cell proliferation, Ki67 and CD25,¹⁰ was also low (figure 1D). This indicates that activated EC induce CD69 expression in T cells, without inducing proliferation or conventional activation. In all follow-up experiments, T cells in coculture with EC were not stimulated with anti-CD3.

Activated EC induce a T cell CD69 expression dynamic distinct from conventional TCR stimulation

To investigate the dynamics of this unusual activation-independent CD69 expression induced by EC, we assessed its expression over time in CD4 $^+$ and CD8 $^+$ T cells. As a control for conventional TCR stimulation-induced CD69 expression, T cells were stimulated with anti-CD3/anti-CD28 beads. EC-induced CD69 expression was rapid, showing an increase already after 2.5 hours, which peaked at 18 hours and maintained a subsequently slightly lower, but rather stable expression up to 7 days of coculture (figure 2A). Bead-induced CD69 expression showed a slower increase, with a peak at 18-42 hours and a sharp decline afterwards. This indicates that activated EC can induce rapid and sustained CD69 expression in T cells, a dynamic distinct from CD69 expression induced by TCR stimulation. Again, in contrast to bead-stimulated T cells, EC-stimulated T cells did not proliferate (figure 2B). Whereas the expression pattern of CD69 was similar in CD4 $^+$ and CD8 $^+$ T cells, the peak fluorescent intensity of CD69 induced by EC was higher in CD8 $^+$ T cells. Remarkably, in CD8 $^+$ T cells EC induced an even higher fluorescent intensity of CD69 than beads.

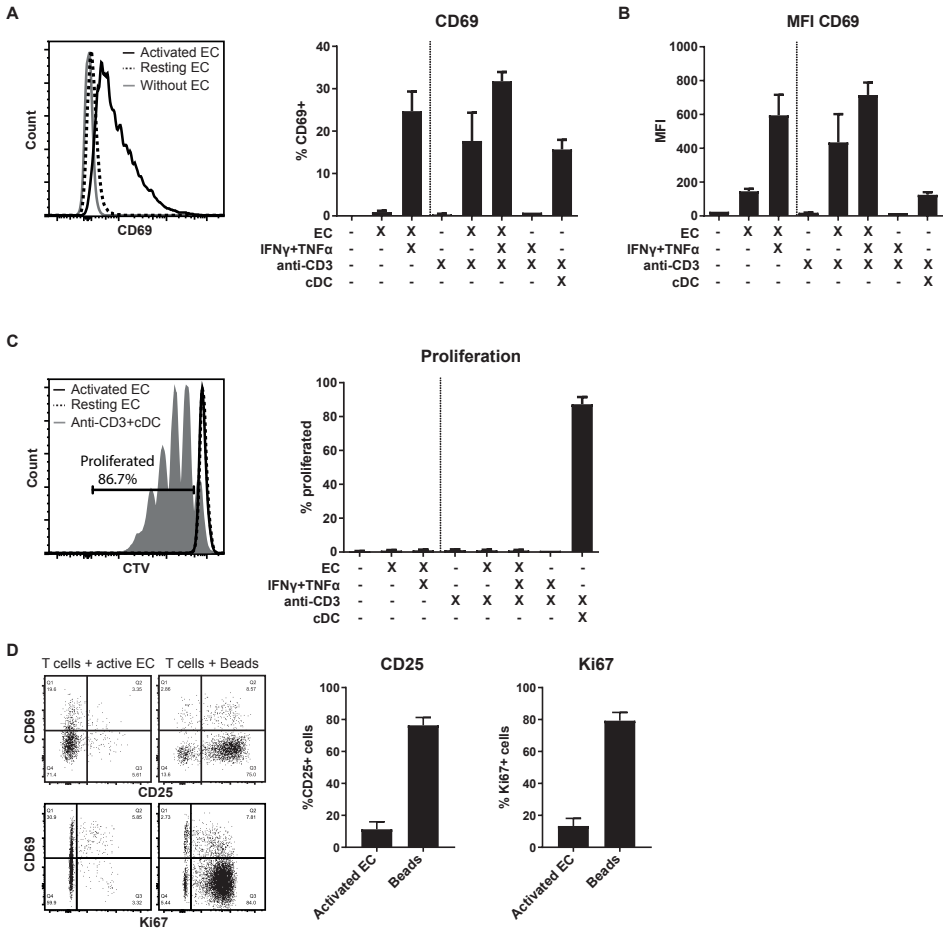


Figure 1. Activated EC induce CD69 expression in T cells, without proliferation or activation.

EC were left unstimulated or stimulated with TNF α and IFN γ for 3 days before addition of FACS sorted CD3⁺ T cells to the coculture, in the presence or absence of soluble anti-CD3 stimulation. Conventional dendritic cells (cDC) were added as a positive control to induce T cell proliferation. CD69 expression was analyzed by flow cytometry after 4 days of coculture by percentage of positive cells (A) and median fluorescent intensity (MFI) (B). Proliferation was assessed by CellTrace Violet (CTV) dilution assay (C). (D) Expression of CD25 and Ki67 after 4 days of coculture with activated EC or anti-CD3/CD28 beads. N=3, mean+SEM.

To assess whether the capability to induce CD69 was specific to human microvascular EC or would be a general feature of EC, we repeated these experiments with human umbilical vein EC (HUVEC). The dynamic of CD69 expression induced by HMEC-1 (up to now called EC) and HUVEC was essentially identical, indicating that this is a global endothelial effect (supplementary figure 2). Taken together, activated EC induce sustained CD69 expression (without proliferation) in T cells, with a dynamic distinct from CD69 expression induced by TCR stimulation.

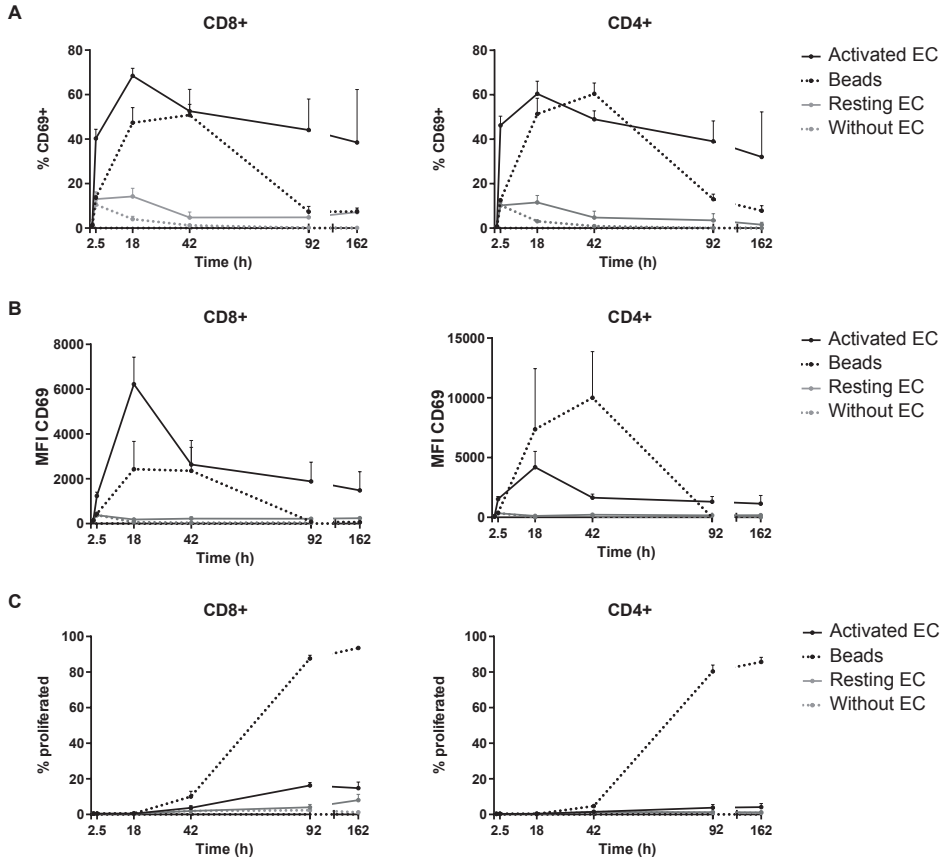


Figure 2. Activated EC induce sustained CD69 expression on T cells.

EC were left unstimulated (resting) or stimulated with 10 ng/mL TNF α and IFN γ for 3 days (activated) before addition of FACS sorted CD3 $^+$ T cells to the coculture. CD69 expression and proliferation were assessed at various time points of the coculture. As a positive control, T cells were cultured with anti-CD3/CD28 beads. (A) Percentage of CD69 $^+$ cells within CD4 $^+$ and CD8 $^+$ T cells. (B) Median fluorescent intensity (MFI) of CD69 expression on T cells. (C) Percentage of proliferated T cells assessed by CellTrace Violet dilution assay. N=3, mean+SEM.

EC-induced CD69 expression is most pronounced in effector memory CD8 $^+$ T cells

To assess which T cell subsets were most responsive to CD69 induction, FAC-sorted naive (CD45RA $^-$ CD45RO $^-$) and memory (CD45RA $^-$ CD45RO $^+$) CD3 $^+$ T cells were separately cocultured with EC. Both CD4 $^+$ and CD8 $^+$ memory T cells showed higher CD69 expression than their naive counterparts, and CD8 $^+$ memory T cells in particular had the highest and most stable expression of CD69 over time (figure 3A). To identify which subpopulation(s) of CD8 $^+$ memory T cells were responsive to CD69 induction, we sorted 4 different subsets

of CD8⁺ T cells: central memory (CM, CD45RA⁺CCR7⁺), terminally differentiated CD45RA⁺ effector memory (TEMRA, CD45RA⁺CCR7⁻) and two subsets of effector memory (EM, CD27⁺ and CD27⁻, both CD45RA⁺CCR7⁻) CD8⁺ T cells. After coculture with activated EC, the two CD27^{+/−} effector memory subsets, and especially the CD27⁻ subset which is associated with increased effector function,⁴¹ showed the highest and most stable CD69 expression (figure 3B). These results indicate that CD8⁺ effector memory T cells are most responsive to induction and maintenance of CD69 expression by activated EC.

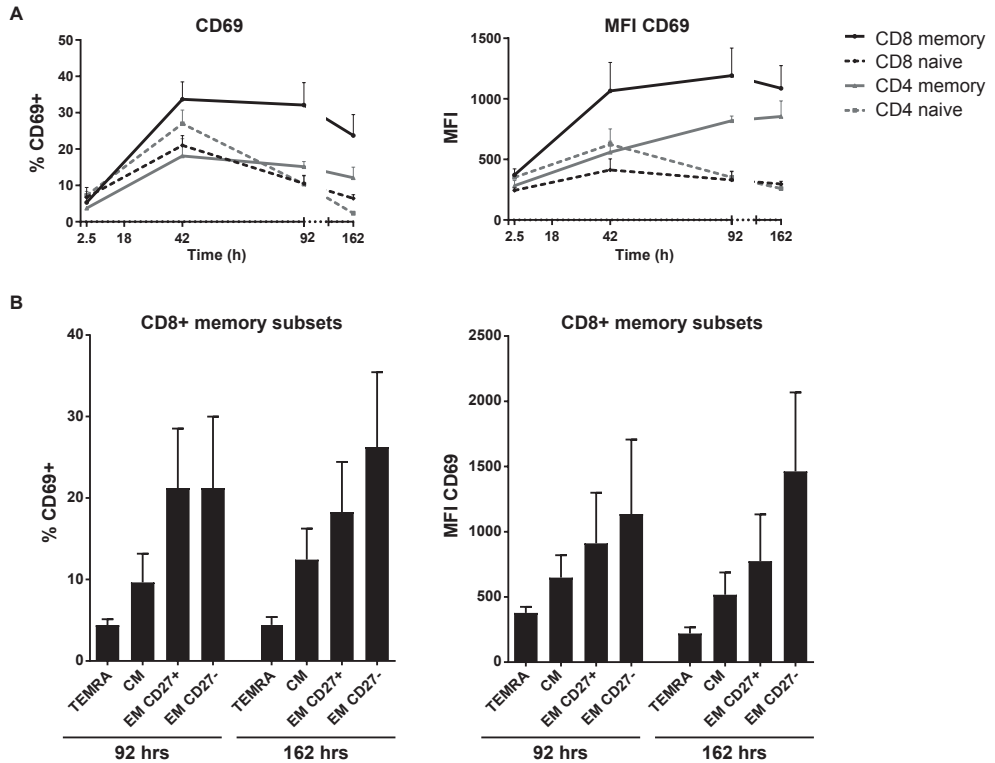


Figure 3. EC-induced CD69 expression is most pronounced in effector memory CD8⁺ T cells.

EC were stimulated with 10 ng/mL TNF α and IFN γ for 3 days before addition of FACS sorted naive CD3⁺ or memory CD3⁺ T cells to the coculture. CD69 expression was assessed at various time points of the coculture by flow cytometry. (A) Percentage of CD69⁺ cells (left panel) and median fluorescent intensity (MFI) of CD69 expression on naive and memory CD4⁺ and CD8⁺ T cells (right panel). N=4, mean+SEM. (B) Percentage of CD69⁺ cells (left panel) and median fluorescent intensity (MFI) of CD69 expression (right panel) on sorted CD8⁺ memory T cell subsets after coculture with activated EC. TEMRA = terminally differentiated CD45RA⁺ effector memory T cells (CD45RA⁺CCR7⁻), CM = central memory T cells (CD45RA⁺CCR7⁺), EM = effector memory T cells (CD45RA⁺CCR7⁻). N=6, mean+SEM.

EC-induced CD69 expression is partly mediated by synergistic action of IL-15, ICAM-1 and VCAM-1

To elucidate the mechanism behind the EC-mediated induction of CD69, we separated effects mediated by cell-contact and soluble factors by culturing T cells in the direct presence of EC or their cultured medium. EC culture supernatants induced a rapid, but lower CD69 expression on CD8⁺ T cells than direct coculture with EC (figure 4A). Supernatant-induced CD69 expression was also less stable, possibly due to consumption of the soluble factors. This indicated that soluble factors likely contributed to, but were not solely responsible for CD69 induction, thereby attributing an important role to direct cell-contact.

EC showed differential upregulation of adhesion and costimulatory molecules in response to stimulation with IFN γ and TNF α (supplementary figure 1). To identify candidate molecules which could mediate CD69 induction by cell-contact or in solution, we analyzed the differential effect of IFN γ and/or TNF α stimulated EC on CD69 expression by T cells. Both direct coculture and supernatant of TNF α -stimulated EC induced higher levels of CD69 than IFN γ -stimulated EC (figure 4B), indicating that molecules upregulated by EC upon TNF α stimulation contributed most to CD69 induction. EC stimulated with both cytokines effected only slightly more CD69 expression than EC stimulated with only TNF α , which suggested that the IFN γ -mediated effect was small. Expression of ICAM-1 and VCAM-1 on EC was most dependent on TNF α stimulation, thereby mirroring the identified pattern of CD69 induction, which rendered them plausible candidate molecules. Soluble levels of ICAM-1 and VCAM-1 as measured in culture supernatants of activated EC were also induced by TNF α stimulation (figure 4C). Low expression of co-stimulatory molecules CD80 and CD86, and MHC molecules, was most dependent on IFN γ stimulation and therefore less likely involved in CD69 induction (supplementary figure 1).

Two soluble factors, IL-15 and TGF- β , have been previously shown to increase CD69 expression on T cells.⁴²⁻⁴⁴ In culture supernatant of activated EC IL-15 levels were similarly induced by IFN γ and TNF α stimulation, whereas TGF- β appeared to be constitutively produced and downregulated by IFN γ stimulation (figure 4D). Although these patterns did not match the preferential pattern of CD69 induction by TNF α -stimulated EC, we empirically blocked their actions in memory T cell-EC cocultures, as well as that of ICAM-1 and VCAM-1. Blockade of IL-15, ICAM-1 and VCAM-1 resulted in a dose-dependent reduction of CD69 expression, indicating that these factors are likely involved in EC-mediated CD69 induction (figure 4E). Early during culture after 18 hours, blockade of IL-15 reduced CD69-induction on T cells by up to 40-45% (figure 4E-F). Blockade of ICAM-1 also caused a small reduction in CD69 expression, whereas blockade of TGF- β and VCAM-1 had no effect. Combined blockade showed that IL-15 contributed most to early induction of CD69 expression on T cells, with a possible small additional role for ICAM-1 (figure 4F). After 4 days of coculture, the effects of IL-15 blockade were comparable, but blockade of TGF- β showed variable effects, rather increasing than decreasing CD69 expression. Combined blockade of these

two cytokines had an effect similar to blockade of IL-15 alone. Blockade of ICAM-1 caused a small reduction in CD69 expression, whereas blockade of VCAM-1 had no effect. However, combined blockade of ICAM-1 and VCAM-1 showed a synergistic effect after 4 days of coculture, reducing CD69 expression by up to 50%. The combined action of blockade of all 4 molecules caused a further reduction of CD69 expression to up to 65% on day 4. This indicates that likely a multitude of signals provided by activated EC induces CD69 expression in T cells, and that it is partly mediated by the synergistic action of IL-15, ICAM-1 and VCAM-1. We observed similar effects in CD4⁺ T cells, suggesting that they respond to similar signals provided by EC (supplementary figure 3).

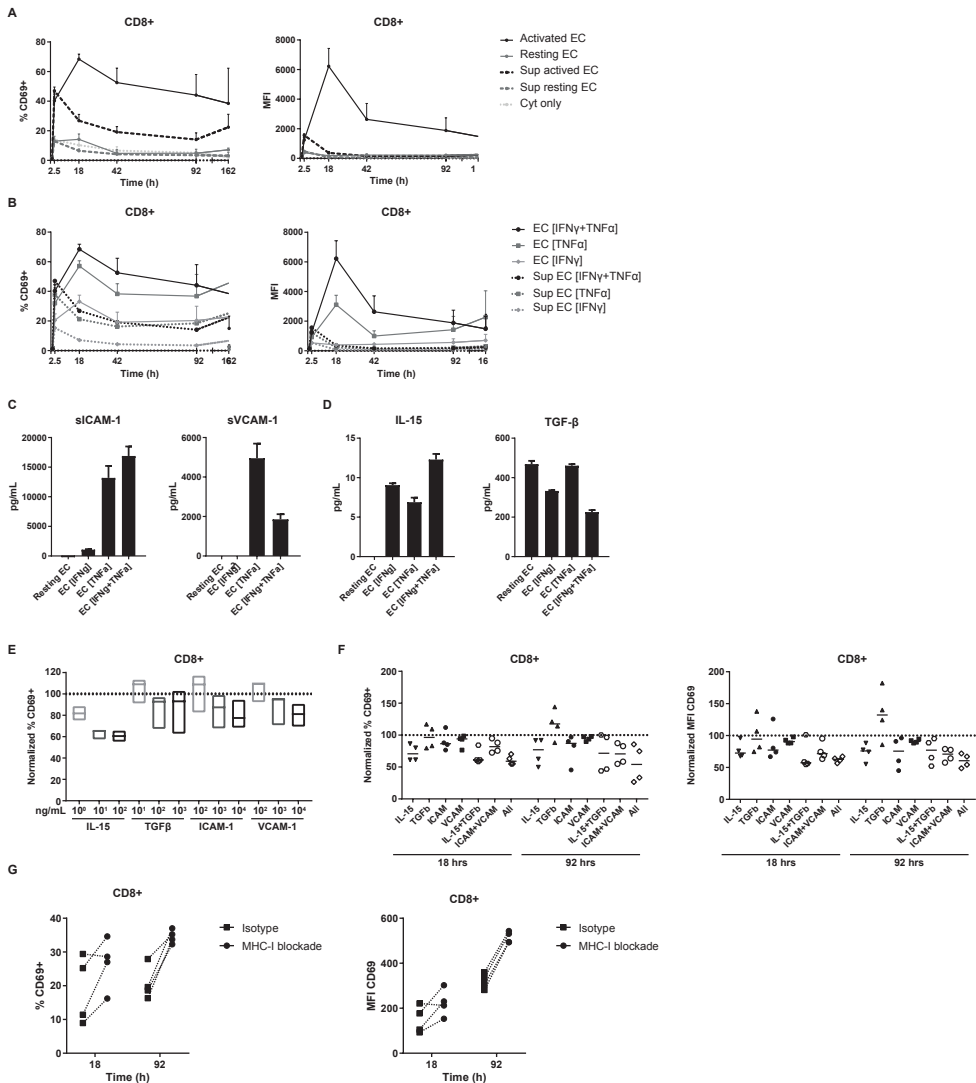


Figure 4. EC-induced CD69 expression on CD8⁺ T cells is partly mediated by synergistic action of IL-15, ICAM-1 and VCAM-1.

(Figure 4 continued)

(A+B) EC were left unstimulated (resting) or stimulated with 10 ng/mL TNF α and/or IFN γ for 3 days (activated) before addition of FACS sorted CD3 $^+$ T cells to the coculture or EC cultured medium. CD69 expression and proliferation were assessed at various time points of the coculture. (A) Percentage of CD69 $^+$ cells (left panel) and median fluorescent intensity (MFI) of CD69 within CD8 $^+$ T cells after coculture with TNF α +IFN γ -stimulated EC, their cultured medium (sup), or TNF α +IFN γ alone. N=3, mean+SEM. (B) Percentage of CD69 $^+$ cells (left panel) and median fluorescent intensity (MFI) of CD69 within CD8 $^+$ T cells after coculture with TNF α and/or IFN γ -stimulated EC or their cultured medium (sup). N=3, mean+SEM. (C+D) Levels of soluble ICAM-1 and VCAM-1 (C) and IL-15 and TGF- β (D) measured in cultured medium of resting or TNF α and/or IFN γ -stimulated EC after 3 days, by multiplex immunoassay. N=3, mean+SEM. (E+F) Coculture of TNF α +IFN γ stimulated EC with FACS sorted memory CD3 $^+$ T cells in the presence of increasing concentrations of monoclonal antibodies blocking IL-15, TGF- β , ICAM-1 and/or VCAM-1. (E) The percentage of CD69 expressing cells was measured by flow cytometry after 18 hours and normalized to the percentage of CD69 $^+$ cells in the condition with isotype control (set to 100). N=3, median. (F) The percentage of CD69 expressing cells and median fluorescent intensity (MFI) of CD69 was measured by flow cytometry after 18 and 92 hours and normalized to the condition with isotype control (set to 100). N=4, median. (G) Coculture of TNF α +IFN γ stimulated EC with FAC-sorted memory CD3 $^+$ T cells in the presence 35 μ g/mL monoclonal antibody blocking HLA-ABC or isotype control. The percentage of CD69 expressing cells and median fluorescent intensity (MFI) of CD69 was measured by flow cytometry after 18 and 92 hours. N=4.

Lastly, to test whether cognate antigen recognition contributed to CD69 expression, we cocultured CD8 $^+$ T cells and EC in the presence of an MHC-I blocking antibody. Blockade of MHC-I-TCR interactions did not reduce, but rather increased CD69 expression. This indicates that MHC-I-TCR interaction is not required for CD69 induction and that most observed effects are mediated by noncognate interactions with EC. This was further supported by the superior effect of TNF α -stimulated EC over IFN γ -stimulated EC, even though IFN γ more potently induced MHC expression.

T cell – EC interaction as a priming signal for tissue-residency

Since both soluble and contact-dependent signals appeared to contribute to induction of CD69 by activated EC, this process may be relevant *in vivo* for T cells transmigrating into tissues. *In vivo*, T cells are attracted into tissues upon infection or inflammation, under which conditions endothelial cells will have an activated phenotype similar to the here induced phenotype.¹ We hypothesized that the unusual activation-independent CD69 expression induced by interaction with activated EC may represent one of the first signs of T cells adopting a specialized program that primes them for prolonged residency in tissues. To investigate this hypothesis, we analyzed the co-expression of TRM-associated markers with CD69. As previously shown, after 4 days of coculture expression levels of activation markers CD25 and Ki67, but also ICOS and CTLA-4, were significantly lower in EC-stimulated than in bead-activated T cells and not increased compared to T cells cultured without EC (Figure 5A), again indicating that CD69 expression in these cells does not represent conventional activation. Memory/effector marker CD38 showed an intermediate increase in response

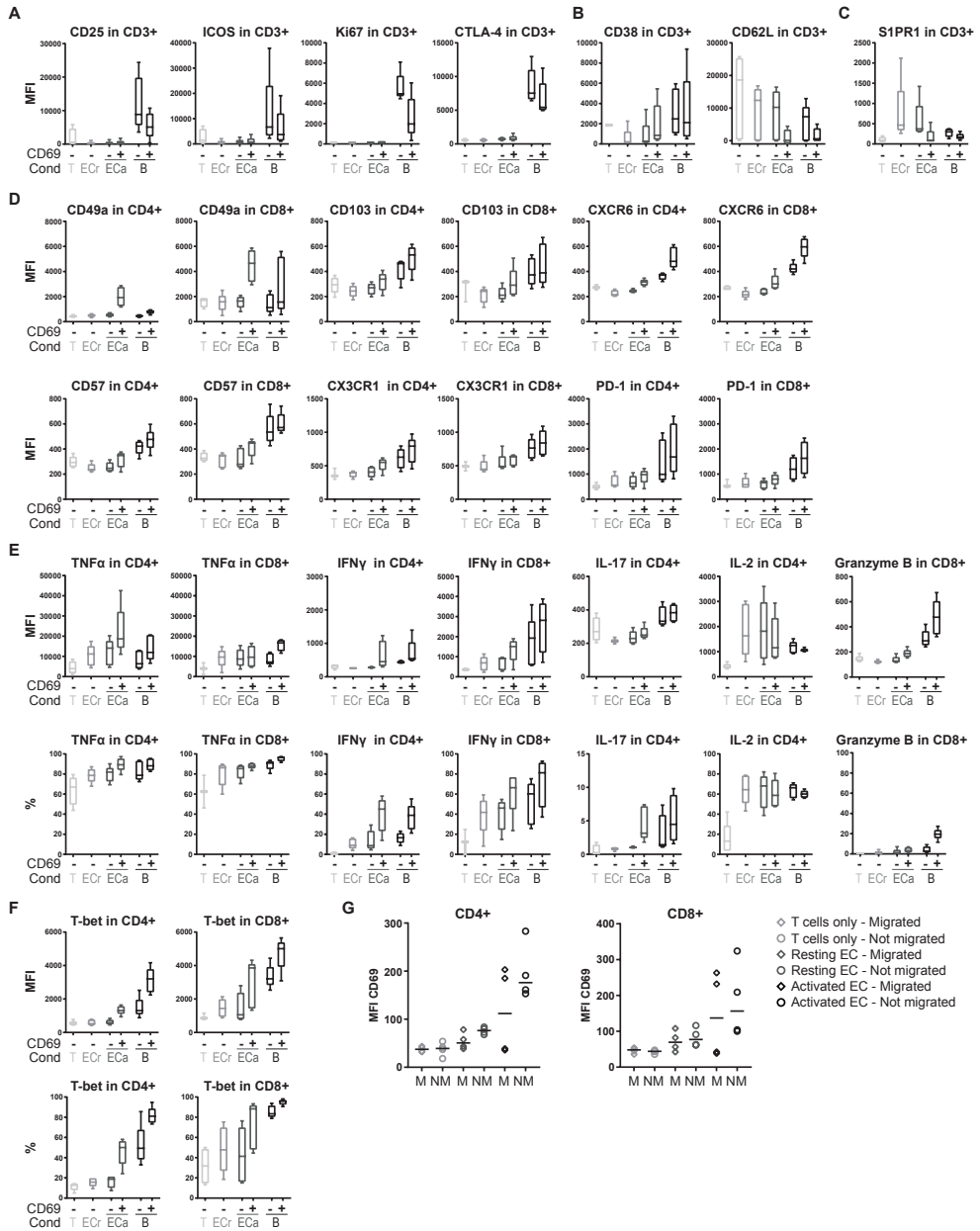


Figure 5. Expression of molecules associated with activation and/or tissue-residency on T cells upon stimulation with activated EC

(A-F) Coculture of TNF α +IFN γ resting or stimulated EC or anti-CD3/CD28 beads with FACS sorted memory CD3⁺ T cells. Expression of activation markers (A) and effector/memory markers (B) was assessed by flow cytometry after 4 days of coculture. Expression of markers associated with tissue-residency (C-D), cytokines (E) and transcription factors (F) was assessed by flow cytometry after 7 days of coculture. Cytokine expression was measured intracellularly after restimulation. N=5, boxplots with median. (G) T cells were seeded on top of a confluent layer of resting or activated EC in a transwell system.

(Figure 5 continued)

CD69 expression of migrated T cells ("M", in lower chamber) and non-migrated T cells ("NM", in upper chamber) was assessed by flow cytometry after 18 hours. N=4, median. Cond = condition, T =T cells only (CD69⁻), ECr = resting EC (CD69⁻), ECa = activated EC (CD69⁻ and CD69⁺), B = anti-CD3/CD28 beads (CD69⁻ and CD69⁺)

to co-culture with EC, especially in CD69⁺ T cells, compared to CD69⁻ and bead-activated cells (Figure 5B). Expression levels of CD62L were specifically downregulated in CD69⁺ compared to CD69⁻ cells, indicating specialization towards an effector phenotype.

Markers associated with tissue-residency were assessed after 7 days of coculture. S1PR1 was upregulated in CD69⁻ cells in response to co-culture with EC, but downregulated in CD69⁺ cells, as also described for TRM (Figure 5C). Remarkably, the TRM-associated marker CD49a (ITGAM1) showed specific upregulation in CD69⁺ cells cocultured with EC, but not beads, both in CD4⁺ and CD8⁺ T cells (Figure 5D). Expression of other TRM-related markers CD103 (ITGAE), CXCR6, CD57, CX3CR1 and PD-1 were all slightly higher in CD69⁺ compared to CD69⁻ T cells cocultured with EC, but lower than in T cells stimulated with beads.

Intracellular cytokine expression was assessed after 7 days of coculture and restimulation. T cells cocultured with activated EC were poised for production of pro-inflammatory cytokines TNF α and IFN γ (Figure 5E). We observed high expression of TNF α specifically in CD4⁺CD69⁺ cells cocultured with EC, which was even higher than in bead-stimulated CD4⁺ T cells, and expressed in 80-100% of CD4⁺ cells. IFN γ expression was higher in CD69⁺ than CD69⁻ negative cells, and comparable between EC-stimulated and bead-stimulated T cells. IL-17 expression was increased in CD69⁺ cells compared to CD69⁻ cells, whereas IL-2 expression was induced by EC and beads irrespective of CD69 expression. Absence of granzyme B expression indicated that the high cytokine response of CD69⁺ T cells cocultured with EC was likely not reflective of direct cytotoxicity towards EC. Increased expression of Th1-related transcription factor T-bet in 25-60% of CD4⁺CD69⁺ and 45-95% of CD8⁺CD69⁺ was consistent with increased IFN γ -production in CD69⁺ cells (Figure 5F). Taken together, CD69⁺ T cells induced by activated EC do not appear to be activated, but rather express TRM-associated markers at higher levels than their CD69⁻ counterparts, and specialize into Th1-like effector memory T cells with an increased pro-inflammatory cytokine response upon stimulation.

Lastly, we investigated whether transmigration, an inevitable process during T cell extravasation that could represent one of the cues for CD69 induction, would induce CD69 expression. Transmigration through endothelium, as opposed to mere interaction with endothelium, is accompanied by vast cytoskeletal rearrangements in T cells, which could also induce intracellular signaling.⁴⁵ Transmigration of memory CD4⁺ and CD8⁺ cells through a layer of stimulated EC did not further enhance CD69 expression. In two experiments, CD69 expression levels were unchanged, while in the remaining experiments CD69 levels

were even slightly decreased after migration (Figure 5G). Thus, close interaction with EC rather than transmigration appears to induce CD69 expression.

DISCUSSION

In this study, we have demonstrated that activated endothelial cells can induce sustained CD69 expression on T cells in the absence of TCR stimulation, without inducing proliferation or activation. The dynamic of this sustained CD69 expression was clearly distinct from TCR-dependent (anti-CD3/anti-CD28)-induced T cell activation.⁴⁶ The EC-mediated induction of CD69 expression was partly dependent on IL-15, VCAM-1 and ICAM-1. Moreover, EC-induced CD69⁺ T cells expressed multiple markers that are associated with tissue-residency in T cells. Therefore close interaction with endothelial cells during transmigration, appears to be one of the first cues priming tissue-infiltrating T cells for tissue-residency. In TRM, high and sustained expression of CD69 prevents tissue egress by sequestering S1PR1 from the cellular surface.^{29,30} Our observations are consistent with the described “activated yet resting” functional phenotype of TRM,⁴⁷ which are also characterized by sustained CD69 expression and an increased cytokine response.

It has been shown previously that interaction with endothelial cells, and especially transmigration,^{48–52} can influence T cell function, and even induce proliferation.^{49–52} However, a thorough literature search to compare our findings of sustained CD69 expression and low-level activation with studies using similar experimental contexts, revealed that almost all studies investigating endothelial-T cell interactions stimulate T cells by providing TCR stimulation during the coculture. This may have influenced the observed T cell behaviour. Especially if T cell isolation methods could not account for a high purity of T cells, this may have led to some contamination with antigen-presenting cells, which can induce T cell proliferation in the presence of TCR-stimulation. In our study, these effects were excluded by the absence of TCR-stimulation and a very high purity of FACS sorted T cells.

To our knowledge, the only three studies determining T cell phenotypes after endothelial coculture without providing TCR stimulation were published by Sancho *et al.*, Iannone *et al.* and Berg *et al.*^{42,53,54} All three studies confirmed our findings of increased CD69 expression without CD25 induction by cytokine-activated EC. Sancho *et al.* also described induction of IFN γ production (but not IL-2 or TNF α), without proliferation, and the preferential CD69 expression in CD8⁺ memory T cells. Both Sancho *et al.* and Berg *et al.* showed that CD69 expression was dependent on LFA-1/ICAM-1 interaction, and Sancho demonstrated that it was enhanced in the presence of IL-15. IL-15 is known to activate naive and memory T cells by induction of CD69, followed by proliferation, but was later also shown to be a crucial factor for TRM development.^{39,55–57} Similar to our results, Berg *et al.* showed that

migration did not further enhance CD69 expression, indicating that the mere interaction with EC is sufficient for CD69 induction, whereas Sancho *et al.* found that transmigrated T cells showed higher CD69 expression than non-migrated cells.^{42,54}

EC-induced CD69 expression on T cells was previously interpreted as a sign of activation, despite the absence of proliferation and CD25 expression.

Based on the combined results from previous studies and our study, including downregulation of S1PR1 which limits egress from tissues, we would now conclude that EC-stimulated T cells display, at best, non-conventional features of activation. We would like to propose an alternative hypothesis in which interaction of effector memory T cells with activated endothelial cells primes T cells for tissue-residency. This is also in line with follow-up experiments by Berg *et al.* showing that EC-T cell interaction enhances T cell responsiveness to antigenic challenge and increases T cell motility, features required for and conducive to TRM fate. In addition, transmigration has been shown to increase T cell survival in an ICAM-1 dependent manner, which could partly prepare them for the longevity of TRM in tissues.^{23,58,59}

Although TRM phenotypes and functions in healthy human tissues are extensively described, the process of TRM induction remains a major outstanding question in the field.^{24,25,31,36}

The relevance to study this fundamental process was underlined by the finding that TRM induction is a new and promising vaccine-strategy in murine models, which induces long-lasting and cross-strain protection against viral infection.^{20,21} During and after transmigration, TRM *in vivo* are exposed to a wealth of tissue derived signals for long periods of time. The absence of a tissue environment in the *in vitro* assays in this study may explain why we did not observe enhanced expression of CD69 in migrated compared to non-migrated cells. Also induction of (high levels of) some of the markers associated with tissue-residency may require tissue-specific signals that were not provided in our experimental setting.

The importance of specific microenvironmental tissue-derived signals in TRM development was emphasized by studies investigating TRM from different sites within one tissue. For example, dermis-derived CD4⁺ TRMs lack expression of CD103, while epidermis-derived CD4⁺ TRMs express CD103.⁶⁰ As tissue environments give specific cues to differentially regulate functional and phenotypical characteristics, TRM may represent a very plastic T cell population, and both CD4⁺ and CD8⁺ TRMs may have the ability to up- and downregulate all described TRM markers depending on the microenvironmental cues present at their specific tissue site.^{31,36,61} The context of the tissue environment may therefore support a two-step model for development of TRM: first, interaction with or transmigration through endothelium primes T cells for increased receptivity towards environmental signals and increased migratory capacity, inducing an “activated yet resting” state and CD69 upregulation preventing tissue egress. Second, microenvironmental signals from the tissue environment further shape, support and consolidate the specific TRM profile that is ‘required’ at a certain tissue site. This hypothesis for TRM development is consistent with

a previously suggested model of T cell trafficking, which also emphasizes a role for the endothelium in shaping T cell function.⁶²

A microenvironmental state which heavily shapes endothelial and immune cell phenotype and function is inflammation. Endothelial cells respond to pro-inflammatory cytokines by upregulating their surface expression of adhesion and costimulatory molecules, and secretion of chemotactic factors.¹ This leads to a physiological enhanced recruitment of T cells to the inflamed tissue sites, to fight potential invading pathogens, but can also contribute to the immunopathogenesis of immune-mediated inflammatory diseases. Recruitment and infiltration of activated T cells can cause a positive feedback loop of inflammation, in which endothelial cells are continuously activated by T cell-derived cytokines TNF α and IFN γ , and activated T cells keep being recruited. This may ultimately lead to a state of chronic inflammation as observed in autoimmune diseases. Interestingly, in some autoimmune diseases the majority of T cells are non-specifically recruited bystander T cells and not antigen-specific T cells.⁶³ Our findings indicate that these cells may be recruited and primed by non-cognate interactions with activated endothelial cells.

The inflammatory response exhibited by endothelial cells likely contributes to the outcomes of T cell-endothelial interactions. For example, in chronically inflamed tissues with a Th1 response, endothelial cells produce CXCL10⁶⁴ and increase expression of adhesion molecules like E-selectin,⁶⁵ which favours recruitment of more Th1 cells, sustaining a positive feedback loop of Th1 influx.⁶⁶ It is therefore not only of interest to study T cell-endothelial interactions to elucidate the biological steps during TRM development for use in vaccination strategies, but also to gain insights into the role of endothelial-T cell interactions in chronic inflammatory diseases, which may provide novel therapeutic targets.

In our *in vitro* experimental setting with allogeneic EC, we cannot rule out that direct allorecognition of EC by T cells may have accounted for some of the observed effects,^{6,49,67} although direct allorecognition accounting for CD69 expression is unlikely due to the lack of induction of CD25 expression, proliferation and the absence of effect of the MHC-1 blockade, as also observed by Sancho *et al.*⁴² To be able to conclude with more certainty that soluble factors only partly account for CD69 induction by activated EC, a follow-up experiment should be to compare direct cocultures of EC and T cells with transwell-cocultures. This will reduce the effects of consumption of soluble factors and give a more balanced comparison of the two conditions. Since we observed the effects of endothelial cells on T cell phenotype and function only in an artificial *in vitro* system, it would be important to further investigate the hypothesis concerning priming for tissue-residency in more detail *in vitro*, as well as *in vivo*, to also take into account the effect of a tissue environment. Important differences in endothelial traits between mice and man will however pose a challenge to translating findings from experimental models to the human situation.⁶ Transcriptional profiling of EC-induced CD69⁺ T cells may give insights into whether the changes in gene expression induced by activated EC are similar to those observed in *ex vivo* profiled TRM. Important to note, although extensive phenotypic profiles have been determined for TRM, none of

the protein and gene expression profiles are exclusively found in and identified for all TRM. Therefore, the lack of recirculation remains the only criterion that can prove tissue-residency at this point.²⁰

In conclusion, we have constructed an *in vitro* system using activated EC, with which we were able to recapitulate some of the peculiar phenotypical and functional characteristics of TRM, including sustained expression of CD69 and markers associated with tissue-residency, and an “activated yet resting” state poised for rapid cytokine production. These findings support our hypothesis that interaction with EC may be one of the first events priming transmigrating T cells for the specific functional requirements of tissue-residency.

REFERENCES

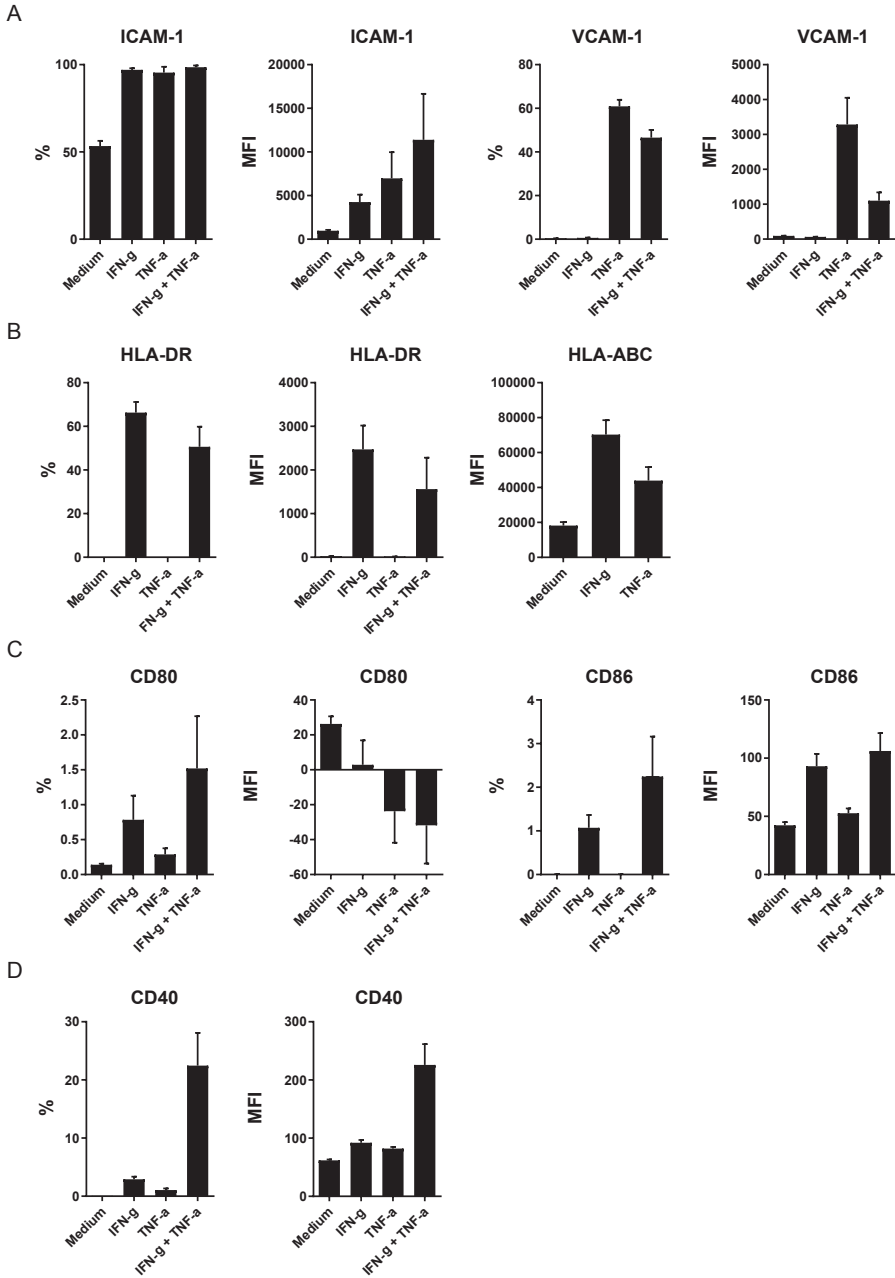
1. Pober JS, Sessa WC. Evolving Functions of Endothelial Cells in Inflammation. *Nat. Rev. Immunol.* **2007**, 7(10), 803–815.
2. Karmann K, Hughes CC, Schechner J, et al. CD40 on Human Endothelial Cells: Inducibility by Cytokines and Functional Regulation of Adhesion Molecule Expression. *Proc. Natl. Acad. Sci. U. S. A.* **1995**, 92(10), 4342–4346.
3. Khayyamian S, Hutloff A, Buchner K, et al. ICOS-Ligand, Expressed on Human Endothelial Cells, Costimulates Th1 and Th2 Cytokine Secretion by Memory CD4+ T Cells. *Proc. Natl. Acad. Sci. U. S. A.* **2002**, 99(9), 6198–6203.
4. Migone TS, Zhang J, Luo X, et al. TL1A Is a TNF-like Ligand for DR3 and TR6/DcR3 and Functions as a T Cell Costimulator. *Immunity* **2002**, 16(3), 479–492.
5. Choi J, Enis DR, Koh KP, et al. T Lymphocyte-Endothelial Cell Interactions. *Annu. Rev. Immunol.* **2004**, 22, 683–709.
6. Carman C V, Martinelli R. T Lymphocyte-Endothelial Interactions: Emerging Understanding of Trafficking and Antigen-Specific Immunity. *Front. Immunol.* **2015**, 6, 603.
7. Brownlie RJ, Zamojska R. T Cell Receptor Signalling Networks: Branched, Diversified and Bounded. *Nat. Rev. Immunol.* **2013**, 13(4), 257–269.
8. Acuto O, Di Bartolo V, Michel F. Tailoring T-Cell Receptor Signals by Proximal Negative Feedback Mechanisms. *Nat. Rev. Immunol.* **2008**, 8(9), 699–712.
9. Smith-Garvin JE, Koretzky GA, Jordan MS. T Cell Activation. *Annu. Rev. Immunol.* **2009**, 27, 591–619.
10. Motamedi M, Xu L, Elahi S. Correlation of Transferrin Receptor (CD71) with Ki67 Expression on Stimulated Human and Mouse T Cells: The Kinetics of Expression of T Cell Activation Markers. *J. Immunol. Methods* **2016**, 437, 43–52.
11. Hutloff A, Dittrich AM, Beier KC, et al. ICOS Is an Inducible T-Cell Co-Stimulator Structurally and Functionally Related to CD28. *Nature* **1999**, 397(6716), 263–266.
12. Simms PE, Ellis TM. Utility of Flow Cytometric Detection of CD69 Expression as a Rapid Method for Determining Poly- and Oligoclonal Lymphocyte Activation. *Clin. Diagn. Lab. Immunol.* **1996**, 3(3), 301–304.
13. Mardiney M 3rd, Brown MR, Fleisher TA. Measurement of T-Cell CD69 Expression: A Rapid and Efficient Means to Assess Mitogen- or Antigen-Induced Proliferative Capacity in Normals. *Cytometry* **1996**, 26(4), 305–310.
14. Butcher EC, Picker LJ. Lymphocyte Homing and Homeostasis. *Science* **1996**, 272(5258), 60–66.
15. Pietschmann P, Cush JJ, Lipsky PE, et al. Identification of Subsets of Human T Cells Capable of Enhanced Transendothelial Migration. *J. Immunol.* **1992**, 149(4), 1170–1178.
16. Mackay CR. Homing of Naive, Memory and Effector Lymphocytes. *Curr. Opin. Immunol.* **1993**, 5(3), 423–427.
17. Oppenheimer-Marks N, Davis LS, Bogue DT, et al. Differential Utilization of ICAM-1 and VCAM-1 during the Adhesion and Transendothelial Migration of Human T Lymphocytes. *J. Immunol.* **1991**, 147(9), 2913–2921.

18. Shimizu Y, Newman W, Tanaka Y, et al. Lymphocyte Interactions with Endothelial Cells. *Immunol. Today* **1992**, *13* (3), 106–112.
19. Hollenbaugh D, Mischel-Petty N, Edwards CP, et al. Expression of Functional CD40 by Vascular Endothelial Cells. *J. Exp. Med.* **1995**, *182* (1), 33–40.
20. Mueller SN, Mackay LK. Tissue-Resident Memory T Cells: Local Specialists in Immune Defence. *Nat. Rev. Immunol.* **2016**, *16* (2), 79–89.
21. Zens KD, Chen JK, Farber DL. Vaccine-Generated Lung Tissue-Resident Memory T Cells Provide Heterosubtypic Protection to Influenza Infection. *JCI insight* **2016**, *1* (10).
22. Gebhardt T, Palendira U, Tschärke DC, et al. Tissue-Resident Memory T Cells in Tissue Homeostasis, Persistent Infection, and Cancer Surveillance. *Immunol. Rev.* **2018**, *283* (1), 54–76.
23. Thome JJC, Yudanin N, Ohmura Y, et al. Spatial Map of Human T Cell Compartmentalization and Maintenance over Decades of Life. *Cell* **2014**, *159* (4), 814–828.
24. Kumar BV, Ma W, Miron M, et al. Human Tissue-Resident Memory T Cells Are Defined by Core Transcriptional and Functional Signatures in Lymphoid and Mucosal Sites. *Cell Rep.* **2017**, *20* (12), 2921–2934.
25. Hombrink P, Helbig C, Backer RA, et al. Programs for the Persistence, Vigilance and Control of Human CD8(+) Lung-Resident Memory T Cells. *Nat. Immunol.* **2016**, *17* (12), 1467–1478.
26. Purwar R, Campbell J, Murphy G, et al. Resident Memory T Cells (T(RM)) Are Abundant in Human Lung: Diversity, Function, and Antigen Specificity. *PLoS One* **2011**, *6* (1), e16245.
27. Sathaliyawala T, Kubota M, Yudanin N, et al. Distribution and Compartmentalization of Human Circulating and Tissue-Resident Memory T Cell Subsets. *Immunity* **2013**, *38* (1), 187–197.
28. Booth JS, Toapanta FR, Salerno-Goncalves R, et al. Characterization and Functional Properties of Gastric Tissue-Resident Memory T Cells from Children, Adults, and the Elderly. *Front. Immunol.* **2014**, *5*, 294.
29. Shioh LR, Rosen DB, Brdickova N, et al. CD69 Acts Downstream of Interferon-Alpha/beta to Inhibit S1P1 and Lymphocyte Egress from Lymphoid Organs. *Nature* **2006**, *440* (7083), 540–544.
30. Cibrian D, Sanchez-Madrid F. CD69: From Activation Marker to Metabolic Gatekeeper. *Eur. J. Immunol.* **2017**, *47* (6), 946–953.
31. Wong MT, Ong DEH, Lim FSH, et al. A High-Dimensional Atlas of Human T Cell Diversity Reveals Tissue-Specific Trafficking and Cytokine Signatures. *Immunity* **2016**, *45* (2), 442–456.
32. Cush JJ, Lipsky PE. Phenotypic Analysis of Synovial Tissue and Peripheral Blood Lymphocytes Isolated from Patients with Rheumatoid Arthritis. *Arthritis Rheum.* **1988**, *31* (10), 1230–1238.
33. Laffon A, Garcia-Vicuna R, Humbria A, et al. Upregulated Expression and Function of VLA-4 Fibronectin Receptors on Human Activated T Cells in Rheumatoid Arthritis. *J. Clin. Invest.* **1991**, *88* (2), 546–552.
34. Afeltra A, Galeazzi M, Ferri GM, et al. Expression of CD69 Antigen on Synovial Fluid T Cells in Patients with Rheumatoid Arthritis and Other Chronic Synovitis. *Ann. Rheum. Dis.* **1993**, *52* (6), 457–460.
35. Clark RA. Resident Memory T Cells in Human Health and Disease. *Sci. Transl. Med.* **2015**, *7* (269), 269rv1.
36. Oja AE, Piet B, Helbig C, et al. Trigger-Happy Resident Memory CD4(+) T Cells Inhabit the Human Lungs. *Mucosal Immunol.* **2018**, *11* (3), 654–667.
37. Nizard M, Roussel H, Diniz MO, et al. Induction of Resident Memory T Cells Enhances the Efficacy of Cancer Vaccine. *Nat. Commun.* **2017**, *8*, 15221.

38. Schenkel JM, Masopust D. Tissue-Resident Memory T Cells. *Immunity* **2014**, *41* (6), 886–897.
39. Mackay LK, Rahimpour A, Ma JZ, et al. The Developmental Pathway for CD103(+)CD8+ Tissue-Resident Memory T Cells of Skin. *Nat. Immunol.* **2013**, *14* (12), 1294–1301.
40. Rotrosen D, Gallin JI. Histamine Type I Receptor Occupancy Increases Endothelial Cytosolic Calcium, Reduces F-Actin, and Promotes Albumin Diffusion across Cultured Endothelial Monolayers. *J. Cell Biol.* **1986**, *103* (6 Pt 1), 2379–2387.
41. Romero P, Zippelius A, Kurth I, et al. Four Functionally Distinct Populations of Human Effector-Memory CD8+ T Lymphocytes. *J. Immunol.* **2007**, *178* (7), 4112–4119.
42. Sancho D, Yanez-Mo M, Tejedor R, et al. Activation of Peripheral Blood T Cells by Interaction and Migration through Endothelium: Role of Lymphocyte Function Antigen-1/intercellular Adhesion Molecule-1 and Interleukin-15. *Blood* **1999**, *93* (3), 886–896.
43. Kanegane H, Tosato G. Activation of Naive and Memory T Cells by Interleukin-15. *Blood* **1996**, *88* (1), 230–235.
44. Tiemessen MM, Kunzmann S, Schmidt-Weber CB, et al. Transforming Growth Factor-Beta Inhibits Human Antigen-Specific CD4+ T Cell Proliferation without Modulating the Cytokine Response. *Int. Immunol.* **2003**, *15* (12), 1495–1504.
45. Dupre L, Houmadi R, Tang C, et al. T Lymphocyte Migration: An Action Movie Starring the Actin and Associated Actors. *Front. Immunol.* **2015**, *6*, 586.
46. Cebrian M, Yague E, Rincon M, et al. Triggering of T Cell Proliferation through AIM, an Activation Inducer Molecule Expressed on Activated Human Lymphocytes. *J. Exp. Med.* **1988**, *168* (5), 1621–1637.
47. Shires J, Theodoridis E, Hayday AC. Biological Insights into TCRgammadelta+ and TCRalphabeta+ Intraepithelial Lymphocytes Provided by Serial Analysis of Gene Expression (SAGE). *Immunity* **2001**, *15* (3), 419–434.
48. Nourshargh S, Marelli-Berg FM. Transmigration through Venular Walls: A Key Regulator of Leukocyte Phenotype and Function. *Trends Immunol.* **2005**, *26* (3), 157–165.
49. Shiao SL, Kirkiles-Smith NC, Shepherd BR, et al. Human Effector Memory CD4+ T Cells Directly Recognize Allogeneic Endothelial Cells in Vitro and in Vivo. *J. Immunol.* **2007**, *179* (7), 4397–4404.
50. Lim WC, Olding M, Healy E, et al. Human Endothelial Cells Modulate CD4(+) T Cell Populations and Enhance Regulatory T Cell Suppressive Capacity. *Front. Immunol.* **2018**, *9*, 565.
51. Mestas J, Hughes CC. Endothelial Cell Costimulation of T Cell Activation through CD58-CD2 Interactions Involves Lipid Raft Aggregation. *J. Immunol.* **2001**, *167* (8), 4378–4385.
52. Samsonov D, Geehan C, Woda CB, et al. Differential Activation of Human T Cells to Allogeneic Endothelial Cells, Epithelial Cells and Fibroblasts in Vitro. *Transplant. Res.* **2012**, *1* (1), 4.
53. Iannone F, Corrigan VM, Kingsley GH, et al. Evidence for the Continuous Recruitment and Activation of T Cells into the Joints of Patients with Rheumatoid Arthritis. *Eur. J. Immunol.* **1994**, *24* (11), 2706–2713.
54. Berg L-P, James MJ, Alvarez-Iglesias M, et al. Functional Consequences of Noncognate Interactions between CD4+ Memory T Lymphocytes and the Endothelium. *J. Immunol.* **2002**, *168* (7), 3227–3234.
55. Mackay LK, Wynne-Jones E, Freestone D, et al. T-Box Transcription Factors Combine with the Cytokines TGF-Beta and IL-15 to Control Tissue-Resident Memory T Cell Fate. *Immunity* **2015**, *43* (6), 1101–1111.

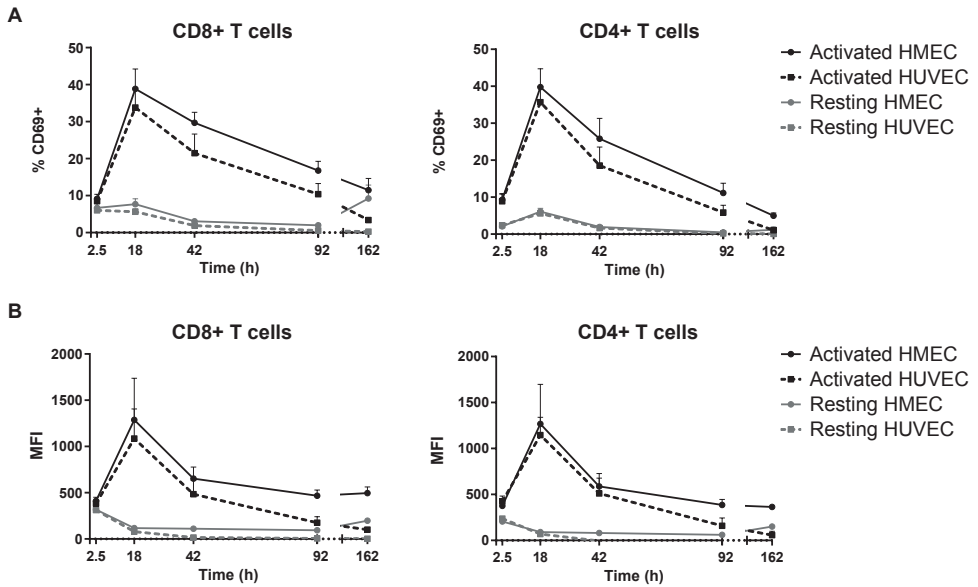
56. Strutt TM, Dhume K, Finn CM, et al. IL-15 Supports the Generation of Protective Lung-Resident Memory CD4 T Cells. *Mucosal Immunol.* **2018**, *11* (3), 668–680.
57. Holz LE, Prier JE, Freestone D, et al. CD8(+) T Cell Activation Leads to Constitutive Formation of Liver Tissue-Resident Memory T Cells That Seed a Large and Flexible Niche in the Liver. *Cell Rep.* **2018**, *25* (1), 68–79.e4.
58. Borthwick NJ, Akbar AA, Buckley C, et al. Transendothelial Migration Confers a Survival Advantage to Activated T Lymphocytes: Role of LFA-1/ICAM-1 Interactions. *Clin. Exp. Immunol.* **2003**, *134* (2), 246–252.
59. Kumar B V, Kratchmarov R, Miron M, et al. Functional Heterogeneity of Human Tissue-Resident Memory T Cells Based on Dye Efflux Capacities. *JCI insight* **2018**, *3* (22).
60. Watanabe R, Gehad A, Yang C, et al. Human Skin Is Protected by Four Functionally and Phenotypically Discrete Populations of Resident and Recirculating Memory T Cells. *Sci. Transl. Med.* **2015**, *7* (279), 279ra39.
61. Wakim LM, Woodward-Davis A, Bevan MJ. Memory T Cells Persisting within the Brain after Local Infection Show Functional Adaptations to Their Tissue of Residence. *Proc. Natl. Acad. Sci. U. S. A.* **2010**, *107* (42), 17872–17879.
62. Marelli-Berg FM, Okkenhaug K, Mirenda V. A Two-Signal Model for T Cell Trafficking. *Trends Immunol.* **2007**, *28* (6), 267–273.
63. Panayi GS, Lanchbury JS, Kingsley GH. The Importance of the T Cell in Initiating and Maintaining the Chronic Synovitis of Rheumatoid Arthritis. *Arthritis and rheumatism*. United States July 1992, pp 729–735.
64. Luster AD, Unkeless JC, Ravetch J V. Gamma-Interferon Transcriptionally Regulates an Early-Response Gene Containing Homology to Platelet Proteins. *Nature* **1985**, *315* (6021), 672–676.
65. Doukas J, Pober JS. IFN-Gamma Enhances Endothelial Activation Induced by Tumor Necrosis Factor but Not IL-1. *J. Immunol.* **1990**, *145* (6), 1727–1733.
66. Austrup F, Vestweber D, Borges E, et al. P- and E-Selectin Mediate Recruitment of T-Helper-1 but Not T-Helper-2 Cells into Inflamed Tissues. *Nature* **1997**, *385* (6611), 81–83.
67. Tafllin C, Charron D, Glotz D, et al. Regulation of the CD4+ T Cell Allo-Immune Response by Endothelial Cells. *Hum. Immunol.* **2012**, *73* (12), 1269–1274.

SUPPLEMENTARY MATERIAL



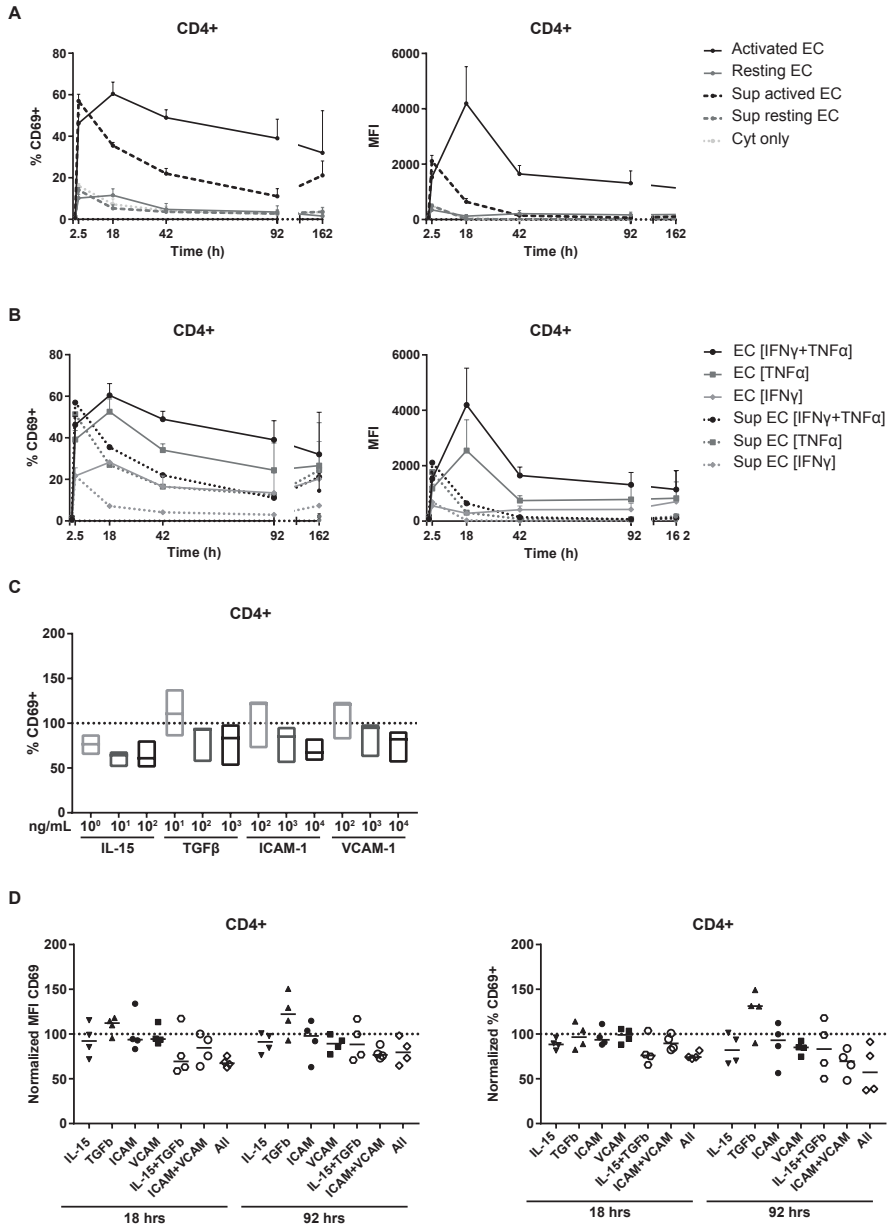
Supplementary figure 1. Expression of adhesion molecules, MHC molecules and costimulatory molecules on EC in response to stimulation with TNF α and/or IFN γ .

EC were incubated with 10 ng/mL TNF α and/or IFN γ for 3 days and expression was analyzed by flow cytometry. *N*=4; mean \pm SEM.



Supplementary figure 2. Dynamic of CD69 induction on T cells by HMEC-1 and HUVEC.

HMEC-1 and HUVEC were left unstimulated (resting) or stimulated with 10 ng/mL TNF α and IFN γ for 3 days before addition of FACS sorted CD3 $^+$ T cells to the coculture. CD69 expression on CD8 $^+$ and CD4 $^+$ T cells was analyzed by flow cytometry at different time points. (A) Percentage of CD69 $^+$ cells among T cells. (B) Median fluorescent intensity (MFI) of CD69 expression on T cells. $N=4$, *mean*+*SEM*.



Supplementary figure 3. EC-induced CD69 expression on CD4⁺ T cells is partly mediated by synergistic action of IL-15, ICAM-1 and VCAM-1.

(A+B) EC were left unstimulated (resting) or stimulated with 10 ng/mL TNF α and/or IFN γ for 3 days (activated) before addition of FACS sorted CD3⁺ T cells to the coculture or EC cultured medium. CD69 expression and proliferation were assessed at various time points of the coculture. (A) Percentage of CD69⁺ cells (left panel) and median fluorescent intensity (MFI, right panel) of CD69 within CD4⁺ T cells after coculture with TNF α +IFN γ -stimulated EC, their cultured medium (sup=supernatant), or TNF α +IFN γ alone. *N*=3, *mean*+*SEM*. (B) Percentage of CD69⁺ cells (left panel) and median fluorescent intensity (MFI, right panel) of CD69 within CD4⁺ T cells after coculture with TNF α and/or IFN γ -stimulated EC or their cultured medium (sup).

(Supplementary Figure 3 continued)

N=3, *mean*+*SEM*. (C+D) Coculture of TNF α +IFN γ stimulated EC with FACS sorted memory CD3⁺ T cells in the presence of increasing concentrations of monoclonal antibodies blocking IL-15, TGF- β , ICAM-1 and/or VCAM. (C) The percentage of CD69 expressing cells was measured by flow cytometry after 18 hours and normalized to the percentage of CD69⁺ cells in the condition with isotype control (set to 100). *N*=3, *median*. (D) The percentage of CD69 expressing cells and median fluorescent intensity (MFI) of CD69 was measured by flow cytometry after 18 and 92 hours and normalized to the condition with isotype control (set to 100). *N*=4, *median*.

Supplementary table 1. Blocking antibodies used in the coculture experiments.

Antigen	Company	Clone	Source
IL-15	eBioscience™	ct2nu	Mouse anti-human
TGF-β	Biologend	19D8	Mouse anti-human
VCAM-1	R&D systems	BBIG-V1	Mouse anti-human
ICAM-1	Biologend	HCD54	Mouse anti-human
IgG1 κ Isotype control	eBioscience™	P3.6.2.8.1	Mouse anti-human
HLA-ABC	Bioceros BV	W6/32	Mouse anti-human
IgG2a κ Isotype control	eBioscience™	eBM2a	Mouse anti-human

GENERAL DISCUSSION

TOWARDS PRECISION MEDICINE IN JUVENILE DERMATOMYOSITIS

Juvenile dermatomyositis, a chronic inflammatory disease in children, is characterized by interferon-driven inflammation of muscles and skin leading to muscle weakness and a typical skin rash. Patients are currently treated according to a standardized treatment regimen consisting of immunosuppressive medication (mostly prednisone and methotrexate) for a duration of at least two years. However, not all patients respond well to this standardized regimen, which indicates that there is room for improvement in the treatment of patients with JDM. In this thesis, we aimed to explore the potential of biomarker-based diagnostic strategies to facilitate precision medicine, i.e. personalized treatment strategies, in patients with JDM.

The first, and currently most important application for biomarker-based strategies is monitoring of disease activity during clinical follow-up. As reviewed in **chapter 2**, objective assessment in patients with JDM is currently challenging due to suboptimal tools for clinical assessment and a lack of validated and reliable biomarkers. In **chapter 3**, we have validated two previously identified biomarkers for disease activity in JDM, galectin-9 and CXCL10,¹ in three independent international cohorts. In **chapter 4**, we have identified galectin-1 and TNFR2, next to galectin-9 and CXCL10 as promising biomarkers for response to treatment of JDM patients. In **chapter 5**, we identified autoimmune disease-specific biomarker profiles of endothelial dysfunction and inflammation, which were still detectable during clinically inactive disease in a subgroup of patients, indicating that these patients may still have had subclinical inflammation.

Biomarker guided monitoring of disease activity

As previously outlined by Macleod et al. (*Lancet series 'Increasing value and reducing waste'; 2014*) "few identified biomarkers have been confirmed by subsequent research and few have entered routine clinical practice". Thus, although many biomarkers are being identified for a variety of diseases, only few are implemented into clinical practice due to a lack of reproducibility and diagnostic accuracy. In **chapter 3** we have shown that galectin-9 and CXCL10 are robust biomarkers, yielding reproducible results and having a high diagnostic accuracy. This suggest that both biomarkers could be promising candidates for clinical implementation. The goal of this implementation is to use galectin-9 and CXCL10 as tools to guide therapy: biomarker levels below the set cut-off reflect the absence of disease activity, which could allow tapering of immunosuppressive medication. Rising or persistently high levels might be indicative of an insufficient response to therapy and/or an imminent flare, even in the absence of clinical symptoms. Elevated biomarker levels may therefore

indicate the need for intensification of treatment or slower tapering of steroids. In this way, medication dosing can be adjusted to specific needs of a patient: reduction of over- and under-treatment can reduce medication side effects and disease flares and can thereby improve outcomes. With this personalized treatment strategy we respond to important patient-reported needs: a recently conducted patient survey by *CureJM*, the North-American patient organization for juvenile myositis, has shown that “predictors for disease flares” and “new treatments, less side effects” were two of the top-three research priorities chosen by patients.² Finally, galectin-9 and CXCL10 may also provide an objective outcome measure for response to therapy in future clinical trials assessing novel therapeutics.

Experimental implementation of biomarkers

An important question to be answered before implementation as monitoring tools is whether galectin-9 and CXCL10 are capable of adding information to the currently used ‘monitoring tool set’ in the clinic, such as clinical assessment and/or laboratory evaluation of other blood parameters. To this end, we set up a 2-year period for experimental diagnostic measurements with the aim of technically optimizing routine measurements of galectin-9 and CXCL10 at the diagnostic department, and establishing the added clinical value of the biomarkers. The technical validation has rendered stable measurements with an inter-assay variability of <15%, which is well within diagnostic standards (figure 1A). During these two years the biomarkers were measured routinely at the diagnostic department in over 200 samples from more than 50 patients with JDM in clinical follow-up. Although we have not analyzed the final results of their added value yet, we have already observed individual cases in which the biomarkers started to rise up to 3-6 months before clinical symptoms of a flare became apparent (figure 1B), which confirms the potential for flare prediction as presented in **chapter 3**. If confirmed in larger patient numbers in a prospective follow-up study, for which we have recently received funding, the future implication could be to already increase medication dosing or slow down tapering of steroids when biomarker levels start to increase or reach the cut-off value. This could prevent a disease flare and the ensuing tissue damage and delay in physical recovery.

The path towards precision medicine

With the 2-year experimental implementation period ending on the 1st of July 2019, we will have successfully validated and implemented galectin-9 and CXCL10 measurements into routine diagnostic care for patients with JDM in the Netherlands. One of our next aims will be international implementation of the biomarkers. The optimal follow-up step would be to perform a clinical study comparing disease outcome parameters of patients receiving

conventional monitoring and the standardized treatment regimen, with patients receiving biomarker-guided monitoring and personalized treatment. Important outcomes to record would be the cumulative medication dose, rate and severity of medication side effects, the frequency and severity of flares, the frequency and type of second-line therapies needed and long-term physical and societal outcome including cardiorespiratory fitness, fatigue, and school/work participation. The rarity of the disease however, makes such a clinical study a challenging next step requiring a large international collaboration with strict adherence to study protocols. An alternative, which we would propose to employ in any case, is to keep collecting information on the performance and added value of the biomarkers in a large group of, hopefully also international, patients, and connect this with other layers of information on disease activity acquired by clinical assessment including patient-reported outcomes such as pain and fatigue, imaging, biopsy scoring, cardiopulmonary function tests and other laboratory investigations. This may also give insights into specific questions such as whether one biomarker may be superior in answering specific clinical questions concerning JDM (e.g. skin vs muscle involvement), and whether the biomarkers are able to detect mild or even subclinical disease activity. In this way, it may be possible to conclude whether biomarker-guided disease management will improve outcomes of patients with JDM. As suggested in **chapter 5**, some biomarkers may indeed reflect subclinical inflammation during clinically inactive disease. Subclinical inflammation could still cause further damage to tissues, impairing long-term outcomes.³ The path towards precision medicine may therefore also include the definition of not only clinical remission, but also ‘molecular remission’, to limit prolonged subclinical inflammation and the associated damage and increased cardiovascular risk.

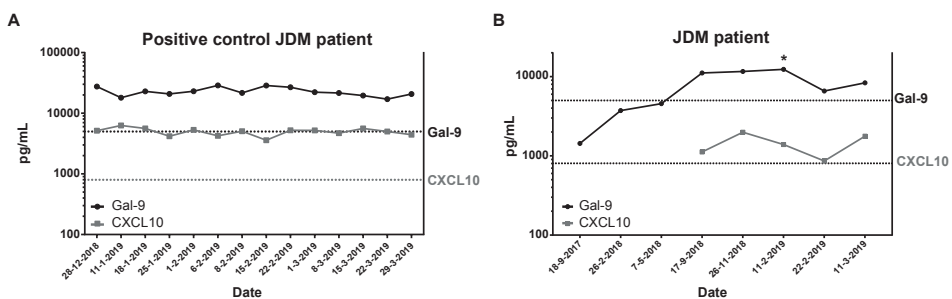


Figure 1. Experimental implementation of biomarker measurements.

(A) Galectin-9 and CXCL10 were measured in one serum sample from a treatment-naive JDM patient at 14 sequential time points 1 week apart to assess the inter-assay variability of the multiplex assay. (B) Experimental diagnostic measurements of galectin-9 and CXCL10 in a patient experiencing a flare (indicated with *). Dotted lines represent cut-off values for active disease.

Molecular classification of autoimmune diseases

Biomarker profiling in systemic autoimmune diseases may not only aid in the identification of biomarkers for use as monitoring tools. As already demonstrated by the distinct clinical phenotypes associated with different myositis-specific autoantibodies in idiopathic inflammatory myopathies,^{4,5} serological or even molecular (as opposed to clinical) stratification of diseases may lead to improved classification of disease entities. As in anti-MDA5⁺ positive patients, such molecular subgroups may even present with a wide spectrum of clinical symptoms that would clinically not be recognized as one disease entity.⁶ However, shared disease processes leading to these serological/molecular similarities, may also respond to similar, targeted treatments. Identification of disease entity-specific biomarkers or pathways may therefore not only provide clues towards the pathogenesis of the disease, but may also identify subgroups of patients who respond well to specific treatments, which opens new options for molecular subgroup-specific patient trials. Thus, molecular classification of patients may lead to identification of disease entities which transcend clinical disease groups, and may be more relevant for targeting of the biological processes underlying autoimmune diseases.

Dried blood spots

In **chapter 3**, we have started a technical innovation by testing the biomarker measurements in dried blood spots, which could enable at-home diagnostics. Due to the promising pilot data, we have now extended our analysis to >100 samples (figure 2). Analyses in these samples confirm our results from **chapter 3**, showing that CXCL10 is a very promising marker to be measured in dried blood spots and the correlation of CXCL10 in DBS and plasma is superior to the correlation of galectin-9 (figure 2A). Remarkably, CXCL10 levels in DBS mirror the levels measured in plasma closely (although the absolute values differ), and result in the same conclusions with respect to the cut-off values, i.e. disease activity (figure 2B). Thus, CXCL10 has a high potential as biomarker in dried blood spots, which are minimally invasive monitoring tools that could enable at-home diagnostics. The next step will be to confirm the correlation between biomarker (especially CXCL10) levels in capillary dried blood spots with plasma levels, as all dried blood spots measurements were done with venous blood so far.

Measurements in dried blood spots can also have implications for accessibility of clinical care for patients living further away from tertiary care centres or even in rural areas, as dried blood spots can be sent by regular mail. They can thereby also play a role in the centralization of diagnostic core centres. CXCL10 measurements in dried blood spots may be an interesting application for adult patients with dermatomyositis and adult/juvenile

patients with other interferon-driven autoimmune diseases as well, since CXCL10 has been shown to be widely implicated in interferon-associated autoimmune diseases.⁷

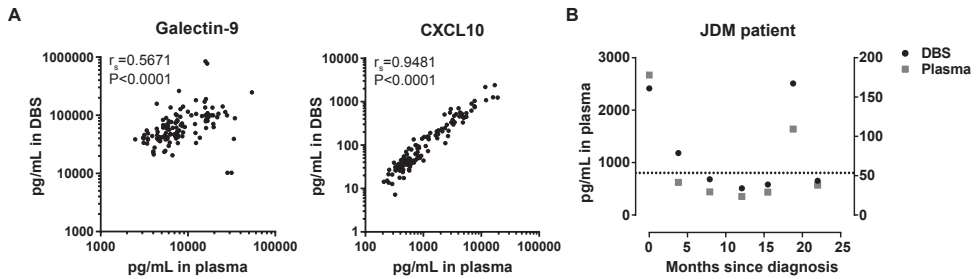


Figure 2. CXCL10 measurements in dried blood spots.

(A) Spearman rank correlation of CXCL10 (left) and galectin-9 (right) values in dried blood spots and plasma. (B). CXCL10 values in plasma and dried blood spots measured in one JDM patient over time.

Biomarker guided prediction of response to treatment

Another clinical application of galectin-9 and CXCL10 (and galectin-1 and TNFR2) that we have addressed in **Chapter 4** is prediction of response to therapy. High levels of these markers identify a group of patients who require intensification of therapy more often and need a longer time to attain clinical remission off medication. This may suggest that these patients could benefit from more intensive monitoring during initial treatment in order to detect suboptimal response to therapy in an early phase. This early detection would promote a swift intensification of treatment. However, perhaps an even better, additional option could be to consider targeted treatment of these patients with different immunosuppressive drugs. Galectin-9 and CXCL10 are typical interferon-inducible proteins, which implies they reflect the magnitude of interferon-driven inflammation, as also suggested by a recent publication.⁸ High levels of these proteins may thus identify patients with high interferon signatures, who could possibly benefit from first-line treatment with drugs directly targeting the interferon signature (e.g. JAK-inhibitors or anti-interferon antibodies),^{9,10} instead of conventional immunosuppression with prednisone and methotrexate to which they apparently respond sub-optimally. Two recently conducted pilot studies with JAK inhibitor Baricitinib among 4 refractory patients with JDM, and one study treating a severe patient with Ruxolitinib showed promising results for JAK inhibition in JDM.¹¹⁻¹³ The interest in blockade of type I interferons as a new treatment strategy in dermatomyositis is highlighted by multiple recently started clinical trials investigating JAK inhibition (Tofacitinib) or other means of interferon blockade (PF-06823859, an interferon- β 1 blocker, and IFN α -Kinoid, a vaccine that induces autoantibodies against IFN α).¹⁴⁻¹⁷

GALECTIN-9 AND CXCL10: CAUSE OR CONSEQUENCE IN JDM?

Chapter 3, 4 and 5 indicate that galectin-9 and CXCL10 are clearly implicated in the disease process of JDM. Galectin-9 and CXCL10 are reflective of disease activity (**Chapter 3**), their levels can identify patients with a more severe phenotype that respond sub-optimally to treatment (**Chapter 4**), and especially galectin-9 seems quite disease-specific for dermatomyositis (**Chapter 3 and 5**). This raises the question whether galectin-9 and CXCL10 are actively contributing to the disease pathology (“cause”), or are rather innocent bystanders only reflecting the underlying pathologic process (“consequence”).

Galectin-9 and CXCL10 as a consequence of the disease process of JDM and its relation with the IFN-signature

Galectin-9 and CXCL10 expression can be induced in multiple immune and non-immune cell types by stimulation with interferons,^{7,18} which could defend their role as bystanders and rather appoint the interferons (or process/cell responsible for interferon production) as culprit. Indeed, in a recent study measuring circulating IFN α with a highly sensitive assay, JDM patients had even higher levels of circulating IFN α than patients with the typical interferon-driven autoimmune disease SLE.¹⁹ Concordantly, an interferon signature has been identified in serum and many cell types from patients with JDM, including endothelial cells, which highlights that the effects of interferon stimulation are sensed throughout the body.^{19–27} It was also observed that neither isolated circulating plasmacytoid dendritic cells – which are generally thought to be the main producers of the type 1 IFNs (IFN α and IFN β) in JDM – nor other circulating immune cell subsets from JDM patients expressed more IFN α than cells from healthy controls, suggesting that a non-circulating cellular source may be responsible for IFN α production in JDM.¹⁹ This is in line with our observation that after stem cell transplantation and concomitant eradication of circulating immune cells, galectin-9 and CXCL10 levels stayed high over several months, which suggests that these proteins are not primarily produced by circulating immune cells, but rather by non-circulating immune or tissue cells.^{19,28} To examine galectin-9 production in inflamed tissues, we performed immunohistochemic stainings on paraffin-embedded muscle and skin biopsies from patients with active disease and controls with non-inflammatory muscle diseases, such as Duchenne’s muscular dystrophy. We observed that galectin-9 production was evident in tissue-infiltrating macrophages and capillary endothelium, both in skin and muscle of JDM patients, whereas galectin-9 staining was entirely absent in the control biopsies (figure 3). A similar expression pattern, in tissue mononuclear cells and endothelial cells, was previously demonstrated for CXCL10.^{21,29}

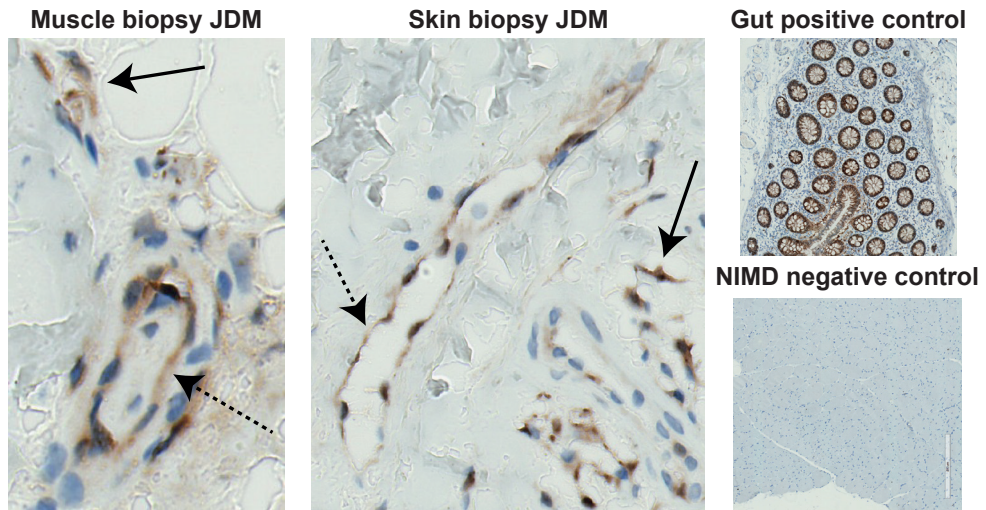


Figure 3. Immunohistochemical staining of galectin-9 in muscle and skin biopsies of patients with JDM. Positive control gut tissue and negative control muscle biopsy of a patient with a non-inflammatory muscular disorder (NIMD). Brown staining = galectin-9; Black arrows indicate tissue macrophages; Dotted arrows indicate capillary endothelium.

To assess the stimuli that may induce galectin-9 and CXCL10 expression in endothelial cells, we incubated human microvascular endothelial cells with different stimuli, among which the three interferons (IFN α , IFN β and IFN γ). Galectin-9 production was most potently induced by stimulation with IFN β and the combination of TNF α and IFN γ (Figure 4). Interestingly, although galectin-9 and CXCL10 levels show a very high correlation in JDM patients, CXCL10 showed a slightly different pattern with the highest induction by IFN γ with or without TNF α . This may indicate that more than one interferon contributes to the production of the biomarkers in JDM, which is in line with a recent study describing both type I and type II interferon signatures, as well as TNF α expression in muscle biopsies from treatment-naïve JDM patients.³⁰ In conclusion, it is very likely that galectin-9 and CXCL10 production by macrophages and endothelial cells in inflamed muscle and skin (but perhaps also by circulating immune cells) is induced by interferons, which are abundantly present in JDM.

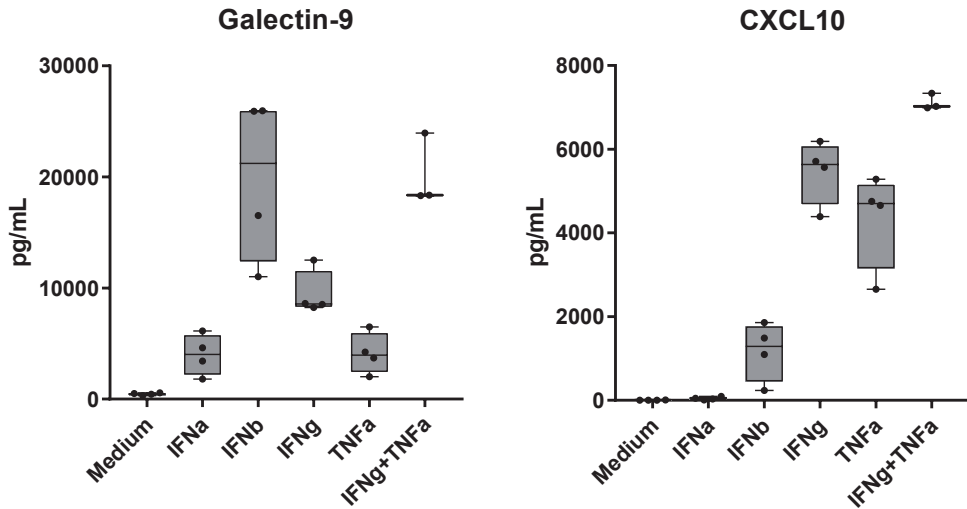


Figure 4. Galectin-9 and CXCL10 production by human microvascular endothelial cells.

HMECs were incubated with the indicated stimuli for 3 days. Galectin-9 and CXCL10 were measured in culture supernatant by multiplex assay.

Galectin-9 and CXCL10 as contributors to disease pathogenesis of JDM

The possible pathological roles of galectin-9 and CXCL10 could either concern immune functions or vasculopathy. CXCL10 is well-known for its potent function as a chemoattractant, promoting leukocyte recruitment to inflamed tissues.³¹ Especially Th1 cells are responsive to CXCL10 mediated chemo-attraction through high expression of its receptor CXCR3. By attracting IFN γ -producing Th1 cells to inflamed tissues, CXCL10 plays a role in a positive feedback loop, since IFN γ is a strong inducer of CXCL10 production by tissue cells.^{7,31} Moreover, CXCL10 has angiostatic properties^{21,32} and overexpression of CXCL10 in DM muscle correlates with the severity of vasculopathy.²¹ Although the effects of galectin-9 on endothelial cells are largely context-dependent, at higher concentrations and for some splicing variants direct angiostatic effects have been demonstrated.^{33–35}

Increased levels of galectin-9 have been described not only in autoimmune diseases,^{8,36} but also in many infectious diseases.^{37–39} Galectin-9 was shown to be an antiviral effector molecule that can inhibit infection with human cytomegalovirus.⁴⁰ At the same time, an immunoregulatory role has been attributed to galectin-9 based on its immunomodulatory effects on T cells. Galectin-9 can limit Th1 responses by inducing apoptosis in IFN γ -producing Th1 cells through interaction with its receptor TIM-3 *in vitro* and *in vivo*.⁴¹ Galectin-9 also inhibits Th17 differentiation.⁴² Th2 cells are resistant to galectin-9 induced death⁴³ and galectin-9 even aids in the amplification of Th2 responses induced by IgD.⁴⁴

Next to limiting Th1 responses and increasing Th2 responses, galectin-9 has been shown to induce regulatory T cells (Tregs) from naive T cells⁴² and increase their stability and function.^{45,46} In line with these results, implying an immunoregulatory role for galectin-9, galectin-9 has been shown to suppress B cell receptor signaling^{47,48} and induce tolerogenic macrophage programming and polarization to an M2 phenotype.^{49,50} Investigations in experimental models even showed that intraperitoneal galectin-9 injection in lupus-prone MRL/lpr and NZB/W F1 mice ameliorated the disease phenotype.^{51,52} Lastly, the galectin-9/TIM-3 axis has been implicated in maternal-fetal tolerance, with increased circulating galectin-9 levels during pregnancy, which was highest in women carrying male fetuses.⁵³ Taken together, these functions imply an immunoregulatory role for galectin-9. However, challenging its immunoregulatory role *in vivo*, galectin-9 deficiency has been recently found to protect against pristane-induced lupus in mice.⁵⁴ Although this study has been received as ‘perplexing’ by the scientific community,⁵⁵ also galectin-9 deficient mice with respiratory tularemia infection exhibited improved lung pathology, reduced cell death and reduced leukocyte infiltration compared to their galectin-9 proficient counterparts.⁵⁶ These findings suggest that galectin-9 may also play a role in the induction or maintenance of inflammation under specific conditions. Other studies substantiating a role of galectin-9 in T cell activation or stability showed that galectin-9 is critical for mucosal adaptive immunity, especially Th17 cells,⁵⁷ and that low concentrations of galectin-9 can induce T cell expansion, Th1 differentiation, and activation.^{58,59} Moreover, galectin-9 binding is crucial for 4-1BB signaling, a costimulatory receptor on T cells which is highly expressed in autoimmune diseases.^{60–62} Taken together, the conflicting results on the immunoregulatory function of galectin-9 *in vivo* and *in vitro* may suggest a highly dynamic, context-dependent role for galectin-9, which is probably dependent on the galectin-9 mode of expression (gene or protein), splicing variant and concentration, presence of specific immune cell populations, or mouse model used.^{55,63–65} Also, differences between mice and man may account for some of the observed differences, which warrants further investigations into the immunoregulatory or immunopathogenic role of galectin-9 in human inflammatory diseases.

THE INTERPLAY BETWEEN ENDOTHELIUM AND (T CELL) IMMUNITY

In this thesis we have discussed different examples of interactions between endothelial cells and the immune system. In JDM, endothelial cells are activated and contribute to the inflammatory process, but are also lost due to damage inflicted by an activated immune system (**chapter 2, 4 and 5**). During active disease, patients with JDM have a dysbalance between circulating angiogenic and angiostatic factors (**chapter 4 and 5**), and prolonged

inflammation may contribute to increased long-term cardiovascular risk (**discussed in chapter 5**). In preeclampsia, we identified immune-activation related pathways in endothelial cells from the maternal-fetal interface, and many circulating markers reflective of immune activation and angiogenic dysbalance, suggesting that immune activation may be one of the mechanisms contributing to the observed endothelial dysfunction (**chapter 6**). In **chapter 8**, we have demonstrated that activated endothelial cells can influence the T cell phenotype, inducing sustained CD69 expression and possibly priming T cells for tissue-residency.

Mutual regulation of endothelial cell and T cell function

These examples of endothelial-immune interaction suggest a mutual crosstalk between the vascular and immune systems, which was indeed demonstrated previously in cancer.⁶⁶ In the tumor microenvironment, abnormal vasculature with suboptimal blood flow is often observed, which hampers the penetration of drugs, such as immune checkpoint inhibitors, into the tumor. Tian *et al.* showed that destabilisation of tumor vessels (by loss of pericytes, the cells surrounding the endothelial vessel wall) also causes a specific defect in T cell infiltration, but not in infiltration of other leukocytes. The other way around, CD4⁺ (but not CD8⁺) T cell depletion, and specifically depletion of activated Th1 cells, resulted in a loss of pericyte coverage, i.e. vessel destabilisation and increased vessel permeability. Specifically, vessel normalization was shown to depend on activated Th1 cells and further improved by immune checkpoint blockade, which induces T cell activation. These effects were only observed in tumors and during wound healing, but not in steady-state tissues. Some parallels may be drawn between these interactions in tumor environments and chapters in this thesis. In JDM and preeclampsia, which are both disorders characterized by local inflammation in tissues, abnormal vessel (re)generation is thought to play an important role in the disease pathogenesis (**chapter 2, 4, 5 and 6**). In JDM and at the maternal-fetal interface, activated CD4⁺ T cell infiltrates are present in the local tissues, and at the maternal-fetal interface they are polarized towards a Th1 profile (**chapter 2 and 7**). More specifically, we have shown that Tregs at the maternal-fetal interface have functional profiles similar to tumor-infiltrating Tregs (**chapter 7**), possibly indicating that this micro-environment is similar to the tumor micro-environment. Some of the principles of endothelial-T cell interaction in the tumor environment may therefore also apply to the maternal-fetal interface. One could for example speculate that signals provided by activated Th1 cells localized in the vicinity of vessels at the maternal-fetal interface may play a role in successful remodeling of spiral arteries. Tian *et al.* also showed that stimulation of endothelial cells with Th1-derived stimuli IFN γ and CD40L induced expression of adhesion molecules and chemoattractant chemokines CXCL9, CXCL10 and CXCL11 by endothelial cells, which enforced a positive feedback loop of T cell recruitment and infiltration. The authors concluded that activated Th1 cells regulate multiple pathways necessary for vessel

normalization in the tumor microenvironment (and wound healing). This study therefore supports a mutual regulation of endothelial cells and T cells under inflammatory conditions as found in the tumor microenvironment and during wound healing.⁶⁶ In JDM, during active disease, i.e. inflammation, levels of interferons and specifically CXCL10 are increased, and endothelial cells express high level of adhesion molecules. As in tumor environments, the combination of these features may enforce a positive feedback loop of T cell recruitment and infiltration in inflamed muscle in JDM (**chapter 2, 3, 4 and 5**). Moreover, activated endothelial cells can shape the phenotype of these transiting T cells and may prepare them for prolonged residency in inflamed muscle tissue (**chapter 8**). These processes may therefore contribute to the chronicity of inflammation in JDM. Thus, both at the maternal-fetal interface and in JDM, a close interaction between and perhaps even mutual regulation of endothelial cells and T cells may be of importance.

Inflammation shaping the endothelium

As already suggested by Tian et al.,⁶⁶ endothelial cells are shaped by their microenvironment. Not only do endothelial cells display different phenotypes depending on their tissue site, which are thought to be induced by signals provided by the local microenvironment, they also respond to additional micro-environmental cues such as pro-inflammatory cytokines, by adjusting their expression of surface molecules and secreted factors, and changing their angiogenic behaviour.^{67–69} The T cell-derived cytokines IFN γ and TNF α are important cues for endothelial cells. They have been shown to upregulate the expression of costimulatory molecules^{70–72} and induce the expression of adhesion molecules (VCAM-1, ICAM-1) on endothelial cells.^{69,73,74} Moreover, inflammatory cytokines, but especially IFN γ , can increase MHC-I and -II expression on endothelial cells, which are already constitutively expressed.^{73–75} These inflammatory changes in endothelial cells, induced by cues from the microenvironment such as IFN γ , with increased expression of adhesion molecules, costimulatory receptors and MHC molecules, are all observed in JDM (**chapter 2**) and to a lesser extent in preeclampsia (**chapter 6**).^{76–80}

On the other hand, T cell-derived cytokines can inhibit angiogenesis: TGF β , IFN γ and TNF α negatively regulate endothelial cell growth in vitro and in vivo.^{69,73} Also the interferon-inducible chemokines CXCL9, CXCL10 and CXCL11 exert direct antiangiogenic properties via their receptor CXCR3.³² Other angiostatic effects of inflammation are disturbance of the essential Angiopoietin-Tie receptor axis and VEGF-VEGFR system, by induction of angiostatic Ang-2 and sVEGFR1, respectively.^{81–83} Thus, endothelial phenotype and function is heavily shaped by micro-environmental, and especially inflammatory cues. The angiostatic effects of inflammation-induced soluble factors likely contribute to the vasculopathic component observed in many autoimmune diseases such as JDM (**chapter 2, 4 and 5**),

including microvascular changes in skin and muscle, and possibly the defective spiral artery remodeling in preeclampsia (**chapter 6**).

Endothelium shaping T cell responses

Since endothelial cells are obligate interaction partners for trafficking immune cells, they can serve as a critical checkpoint for adjusting or controlling immune reactions in tissues, e.g. by tuning the activation and differentiation of transmigrating immune cells (**chapter 8**). The phenotypical and functional heterogeneity exhibited by endothelial cells in response to their local microenvironment, be it the specific tissue of their residence or inflammatory changes, likely contributes to the outcomes of these endothelial-immune cell interactions. Endothelial cells secrete cytokines that regulate and control the recruitment and transmigration of T cells.⁸⁴ The expression of MHC molecules facilitates another important function of endothelial cells: their ability to present and cross-present auto- and allo-antigens *in vitro* and *in vivo*.^{85–90} Through this function endothelial cells can recruit antigen-specific T cells.^{91–94} Especially Treg recruitment to sites of inflammation is favored by their ability to recognize auto-antigens presented by endothelial cells.⁹⁵ Also the antigen presenting function of endothelial cells is tuned by the microenvironment, such as inflammation,⁷⁴ and diapedesis across inflamed endothelium has been shown to have broadly pro-inflammatory or “priming” effects on immune cells (**chapter 8** and⁹⁶). The expression level of MHC-I on endothelial tissues, which is notably high in JDM,^{76,77} has a direct impact on the migration efficiency of autoreactive T cells *in vivo*.⁹⁷ The interaction between autoreactive T cells with activated, antigen-presenting endothelium, may thus initiate and/or perpetuate the autoimmune reaction in JDM (**chapter 2**). Since human decidual T cells have been shown to recognize and actively respond to fetal cells,⁹⁸ antigen-dependent recruitment of T cells by endothelial cells (presenting fetal antigens) may also play a role in T(reg) cell infiltration at the maternal-fetal interface (**chapter 7**). Due to absence of costimulatory molecules CD80 and CD86, endothelial cells cannot prime naive T cells, but as they are equipped with a range of costimulatory molecules, they can stimulate antigen-experienced T cells.^{99–103} Interaction with endothelial cells has been shown to induce activation, proliferation and secretion of pro-inflammatory cytokines in memory T cells, *in vitro* and *in vivo*.^{71,99–101,104–106} Interaction with endothelium can even mediate T cell differentiation and/or skew a certain T helper response: under inflammatory conditions in the presence of IFN γ , microvascular endothelial cells mediate selective expansion of Tregs and Th17 cells.¹⁰⁷ In chronically inflamed tissues with a Th1 response, endothelial cells produce CXCL10¹⁰⁸ and increase expression of adhesion molecules like E-selectin,¹⁰⁹ which favors recruitment of more Th1 cells, sustaining a positive feedback loop of Th1 influx.¹¹⁰ This may also be a relevant process in JDM, where CXCL10 levels are high and expression of adhesion molecules on endothelial cells is increased (**chapter 2, 3, 4, and 5**). In a Th2 dominant chronic inflammatory environment, endothelial

cells respond by producing chemokines such as CCL26 and express adhesion molecules such as VCAM-1, which favor recruitment Th2 cells.¹¹¹ The specific expression patterns of co-stimulatory/co-inhibitory molecules found on endothelium are thought to strongly influence the above processes.¹¹² Thus, the end result of the interaction between endothelial cells and T cells depends on the integration of micro-environmental signals including cytokines, the presence of costimulatory molecules and the avidity of TCR-MHC-peptide complex interaction, and will subsequently determine the nature of the T cell response in tissues.

Implications for the maternal-fetal interface

At the maternal-fetal interface, interactions between endothelial cells and their surrounding cells/signals are crucial for the successful development of spiral arteries, which ensure sufficient blood supply to the developing fetus.¹¹³ The importance of successful spiral artery remodeling is illustrated by the severe consequences of defective remodeling, resulting in pregnancy disorders such as preeclampsia and fetal growth restriction.¹¹⁴ Although the exact cues required for adequate spiral artery remodeling are still elusive, a dysbalance between angiogenic and angiostatic mediators is thought to play a role (**chapter 6**).^{114,115} Moreover, during preeclampsia signs of inflammation are evident both locally at the maternal-fetal interface, and systemically (**chapter 6**). Inflammation-induced changes in endothelial function may therefore also play a role in defective spiral artery remodeling. Treg presence at the maternal-fetal interface may represent one of the mechanisms for local regulation of inflammatory responses (**chapter 7**). As shown in **chapter 7**, these Tregs are specifically differentiated and adapted to effectively suppress local T effector responses. Paradoxically however, despite the requirement of a tolerogenic environment, low-grade inflammation may also be physiologically necessary during some stages of pregnancy, for instance to induce labor.¹¹⁶ Thus, adequate adaptation of endothelial cells and immune cells to the microenvironment at the maternal-fetal interface likely requires a dynamic, pregnancy stage-specific regulation of inflammation and angiogenesis.

TISSUE-RESIDENT T(REG) CELL DIFFERENTIATION AND ADAPTATION

Tissue-resident memory T cells (TRM) have been identified in many tissues and organs, in mice and man.¹¹⁷ Their main role is surveillance of tissues to protect the host against invading pathogens, but additional roles related to tissue homeostasis are starting to emerge.^{118–121} Moreover, TRM may play active roles in chronic inflammation as seen in

autoimmune diseases.¹²² Tissue-resident Tregs have also been identified in a variety of tissues and are thought to be crucial for local immune homeostasis.^{123–128} Although the unique properties of TRM have gained increasing attention in the past decade, the specificity of their (transcriptional) program and functional properties are still elusive. There are some common features, which have been identified in TRM from different tissue sites in mice and man,^{127,129–132} but also tissue-specific features have been identified.^{123,124,127,129,130,133} One of the main questions yet to be answered is how these common and tissue-specific characteristics of TRM are induced and maintained, and whether this is dependent on tissue-specific cues. Especially the influence of the local micro-environment on the transcriptional and functional profile of TRM and tissue-resident Tregs is still largely unexplored.

The context of the tissue micro-environment in TRM differentiation

In **chapter 7** we demonstrate that tissue-resident Tregs at the maternal-fetal interface acquire a specialized functional profile reminiscent of tumor-infiltrating Tregs, that is specifically adapted not only to the uterine environment, but to the tissue-site at the maternal-fetal interface.

It has been established that a range of signals or features can be required for the successful generation and/or maintenance of TRM, including TGF β (skin, lung, gut, brain^{134–138}), IL-2 (lung^{139,140}), IL-15 (skin, lung, liver^{134,135,139,141}), IL-33 (gut¹³⁷), IFN γ (lung¹⁴²), TNF α (gut¹³⁷) or a combination of cytokines,¹³⁷ CXCR3 ligands (gut¹⁴³), and 4-1BB/4-1BBL (lung¹⁴⁴). Interestingly, CD4⁺ IFN γ producing T cells may even prepare the tissue microenvironment for the entry of CD8⁺ TRM by inducing the production of CXCR3 ligands, as demonstrated in vaginal tissues and lung. In this model, the subsequent differentiation into TRM is aided by tissue-derived factors such as TGF β .^{142,145,146} Although continuous TCR stimulation is essential for induction and maintenance of tissue-resident Tregs,¹⁴⁷ this may not be the case for conventional CD4⁺ and CD8⁺ TRM.^{137,139}

The context of the tissue environment may therefore support a stepwise model for development of TRM: first, endothelial cells and T cells are activated by an (inflammatory) trigger (figure 5). Subsequently, interaction with or transmigration through endothelium primes T cells for increased receptivity towards environmental signals and increased migratory capacity, inducing an “activated yet resting” state and sustained CD69 expression, as demonstrated in **chapter 8**. CD69 is considered an important feature for the identification of human tissue-resident memory T cells,^{117,131} also due to its role CD69 in limiting tissue egress by sequestering sphingosine 1 phosphate receptor 1 from the cellular surface.^{148,149} Lastly, micro-environmental signals from the tissue environment may further shape, support and consolidate the specific TRM profile at a certain tissue site (**chapter 7**). This hypothesis for TRM development is consistent with a previously suggested model of T cell trafficking, which also emphasizes a role for the endothelium in shaping T cell function.⁹²

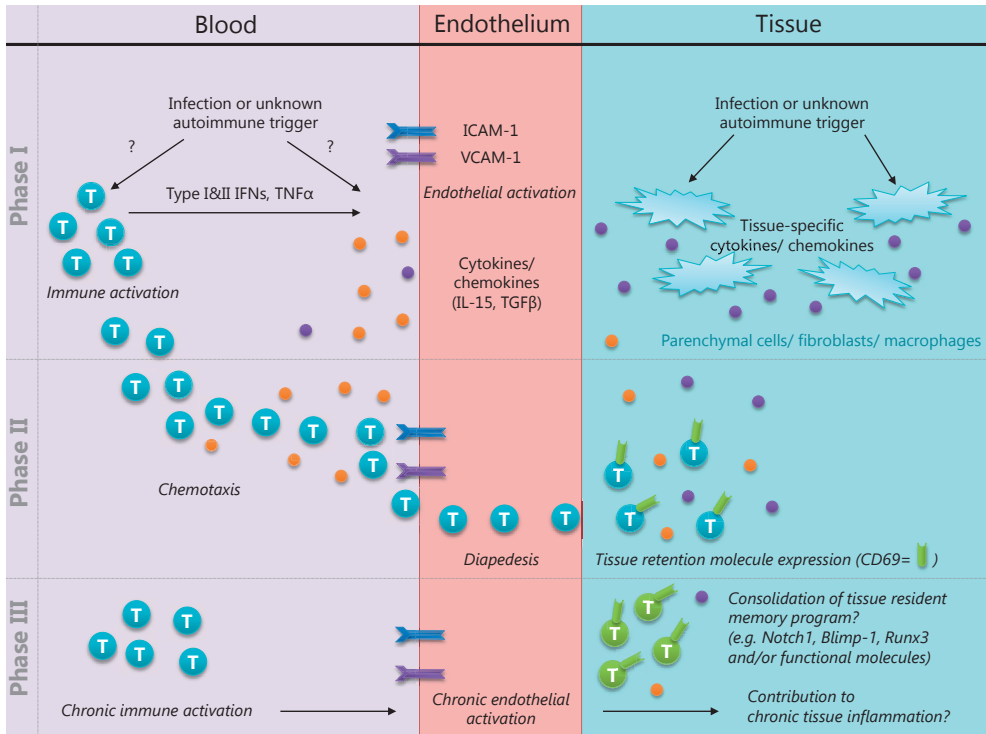


Figure 5. Potential stepwise TRM differentiation of CD4⁺ T cells.

Stages of differentiation and/or adaptation of tissue-infiltrating T cells

Although CD69 is an important molecule regulating T cell maintenance in tissues, not all T cells in tissues express CD69. One theory is that the CD69⁻ cells have recently arrived and are transitioning into CD69⁺ T cells.¹³⁴ In this sense, also within tissues the differentiation into stable TRM may be a stepwise process, as previously suggested.^{127,134,147,150} On the other hand, CD69⁻ cells could represent T cells which transiently pass through tissues and re-enter the circulation, without undergoing the full differentiation into TRM.

Also at the maternal-fetal interface we observed that most, but not all, Tregs (and Tconv) expressed CD69, with a range in the expression intensity (**chapter 7**). This suggests that also within the tissue Treg population, CD69 is not uniformly expressed. One of the control populations analyzed in this study, i.e. CD69⁻ Tconv from the uterus, could shed light on the differentiation and/or migration stage of CD69⁻ T cells in tissues. Comparing gene expression of blood-derived circulating CD4⁺ T cells, CD69⁺ tissue-resident cells, and CD69⁻ tissue-derived T cells by principal component analysis showed that the transcriptional profile of both CD69⁻ and CD69⁺ tissue T cells was clearly distinct from blood-derived T cells (figure 6A). Moreover, the transcriptional profile of CD69⁻ CD4⁺ T cells appeared to be intermediate

between that of blood-derived and CD69⁺ tissue cells. Although this does not exclude the possibility that CD69⁻ are transient bypassers which adapt their transcriptional profile to the tissue environment before re-entering circulating, this could suggest that CD69⁻ tissue CD4⁺ cells are in the process of differentiating into CD69⁺ TRM. To assess which genes could play a role in such a step-wise differentiation, we overlaid the genes that were 1) significantly upregulated in CD69⁻ tissue cells compared to CD69⁻ blood CD4⁺ T cells and 2) significantly upregulated in CD69⁺ compared to CD69⁻ tissue CD4⁺ T cells, implying a stepwise upregulation from blood, to CD69⁻ tissue T cells to CD69⁺ tissue T cells. The same approach was employed to identify genes that were downregulated in a stepwise manner. The analysis yielded 105 gradually upregulated and 45 gradually downregulated genes (figure 6B). The heatmap, which also includes the same populations from a uterine control site, as well as regulatory T cells (Tregs) shows that based on these genes, CD69⁻ CD4⁺ T cells from tissue cluster closer to blood-derived T cells than TRM. Tregs from tissue cluster close to the CD69⁺ fraction, which would imply that they have also undergone full differentiation into TRM. Further investigations will have to point out whether some of these genes are indeed involved in a stepwise differentiation of circulating T cells into TRM. This may lead to the identification of key transcriptional regulators of tissue-residency in human T(reg) cells and may provide insights into the developmental cues and programs that underlie stable tissue-residency.

CONCLUSION

In conclusion, tissues are highly dynamic immune environments, in which local cues provide essential signals for the generation, maintenance and regulation of endothelial cells, T cells and their interactions. In inflammation these tissue microenvironments are changed by pro-inflammatory signals, which induce and sustain feedback loops of disturbed endothelial function and T cell homing and activation, further contributing to the inflammatory process which can lead to chronic inflammation. Stopping this feedback loop with targeted treatments is therefore of utmost importance to restore tissue and immune homeostasis in chronic inflammatory diseases.

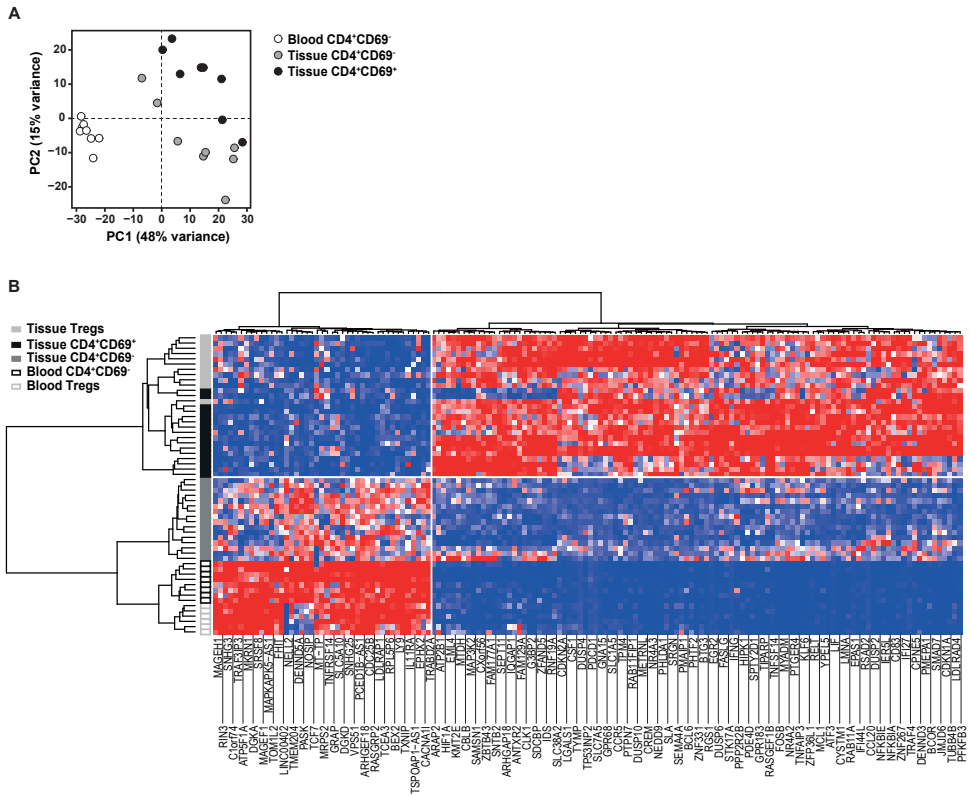


Figure 6. Differentiation stage of CD69⁻ CD4⁺ T cells in tissues.

A) Principal component analysis of transcriptional profile of blood- and tissue-derived CD69⁻ and CD69⁺ CD4⁺ T cells. B) Heatmap of genes displaying step-wise upregulation or downregulation from blood, to CD69⁻ tissue CD4⁺ T cells to CD69⁺ tissue CD4⁺ T cells, as well as Tregs from both compartments.

REFERENCES

1. Bellutti Enders F, van Wijk F, Scholman R, et al. Correlation of CXCL10, Tumor Necrosis Factor Receptor Type II, and Galectin 9 with Disease Activity in Juvenile Dermatomyositis. *Arthritis Rheumatol. (Hoboken, N.J.)* **2014**, 66 (8), 2281–2289.
2. Dave (Cure JM Foundation) M. Patient Perspectives on Juvenile Myositis Research Priorities http://www.curejm.org/medical_professionals/pdfs/2017-05-04 JM-Research-Priorities.pdf (accessed May 31, 2018).
3. Blom KJ, Takken T, Huijgen BCH, et al. Trajectories of Cardiorespiratory Fitness in Patients with Juvenile Dermatomyositis. *Rheumatology (Oxford)*. **2017**, 56 (12), 2204–2211.
4. Betteridge Z, Tansley S, Shaddick G, et al. Frequency, Mutual Exclusivity and Clinical Associations of Myositis Autoantibodies in a Combined European Cohort of Idiopathic Inflammatory Myopathy Patients. *J. Autoimmun.* **2019**, 101, 48–55.
5. Mariampillai K, Granger B, Amelin D, et al. Development of a New Classification System for Idiopathic Inflammatory Myopathies Based on Clinical Manifestations and Myositis-Specific Autoantibodies. *JAMA Neurol.* **2018**, 75 (12), 1528–1537.
6. Vuillard C, Pineton de Chambrun M, de Prost N, et al. Clinical Features and Outcome of Patients with Acute Respiratory Failure Revealing Anti-Synthetase or Anti-MDA-5 Dermato-Pulmonary Syndrome: A French Multicenter Retrospective Study. *Ann. Intensive Care* **2018**, 8 (1), 87.
7. Antonelli A, Ferrari SM, Giuggioli D, et al. Chemokine (C-X-C Motif) Ligand (CXCL)10 in Autoimmune Diseases. *Autoimmun. Rev.* **2014**, 13 (3), 272–280.
8. Van den Hoogen LL, Van Roon JAG, Mertens JS, et al. Galectin-9 Is an Easy to Measure Biomarker for the Interferon Signature in Systemic Lupus Erythematosus and Antiphospholipid Syndrome. *Ann. Rheum. Dis.* **2018**, 77 (12), 1810–1814.
9. Ladislau L, Suarez-Calvet X, Toquet S, et al. JAK Inhibitor Improves Type I Interferon Induced Damage: Proof of Concept in Dermatomyositis. *Brain* **2018**, 141 (6), 1609–1621.
10. Higgs BW, Zhu W, Morehouse C, et al. A Phase 1b Clinical Trial Evaluating Sifalimumab, an Anti-IFN-Alpha Monoclonal Antibody, Shows Target Neutralisation of a Type I IFN Signature in Blood of Dermatomyositis and Polymyositis Patients. *Ann. Rheum. Dis.* **2014**, 73 (1), 256–262.
11. Kim H, Dill S, O'Brien M, et al. P43 Preliminary Response to Janus Kinase (JAK) Inhibition with Baricitinib in Refractory Juvenile Dermatomyositis. In *3rd Global Conference on Myositis*; 2019; p 46.
12. Papadopoulou C, Hong Y, Omoyinmi E, et al. Janus Kinase 1/2 Inhibition with Baricitinib in the Treatment of Juvenile Dermatomyositis. *Brain* **2019**, 142 (3), e8.
13. Aeschlimann FA, Fremond M-L, Duffy D, et al. A Child with Severe Juvenile Dermatomyositis Treated with Ruxolitinib. *Brain* **2018**, 141 (11), e80.
14. Ducreux J, Houssiau FA, Vandepapeliere P, et al. Interferon Alpha Kinoid Induces Neutralizing Anti-Interferon Alpha Antibodies That Decrease the Expression of Interferon-Induced and B Cell Activation Associated Transcripts: Analysis of Extended Follow-up Data from the Interferon Alpha Kinoid Phase I/II. *Rheumatology (Oxford)*. **2016**, 55 (10), 1901–1905.
15. ClinicalTrials.gov NCT02980198 <https://clinicaltrials.gov/ct2/show/NCT02980198?recrs=abdfi&cond=Dermatomyositis&rank=9>.

16. ClinicalTrials.gov NCT03181893 <https://clinicaltrials.gov/ct2/show/NCT03181893?recrs=abdfi&cond=Dermatomyositis&rank=10>.
17. ClinicalTrials.gov NCT03002649.
18. Merani S, Chen W, Elahi S. The Bitter Side of Sweet: The Role of Galectin-9 in Immunopathogenesis of Viral Infections. *Rev. Med. Virol.* **2015**, 25 (3), 175–186.
19. Rodero MP, Decalf J, Bondet V, et al. Detection of Interferon Alpha Protein Reveals Differential Levels and Cellular Sources in Disease. *J. Exp. Med.* **2017**, 214 (5), 1547–1555.
20. Gitiaux C, Lacroche C, Weiss-Gayet M, et al. Myogenic Progenitor Cells Exhibit Type I Interferon-Driven Proangiogenic Properties and Molecular Signature During Juvenile Dermatomyositis. *Arthritis Rheumatol. (Hoboken, N.J.)* **2018**, 70 (1), 134–145.
21. Fall N, Bove KE, Stringer K, et al. Association between Lack of Angiogenic Response in Muscle Tissue and High Expression of Angiostatic ELR-Negative CXC Chemokines in Patients with Juvenile Dermatomyositis: Possible Link to Vasculopathy. *Arthritis Rheum.* **2005**, 52 (10), 3175–3180.
22. O'Connor KA, Abbott KA, Sabin B, et al. MxA Gene Expression in Juvenile Dermatomyositis Peripheral Blood Mononuclear Cells: Association with Muscle Involvement. *Clin. Immunol.* **2006**, 120 (3), 319–325.
23. Niewold TB, Kariuki SN, Morgan GA, et al. Elevated Serum Interferon-Alpha Activity in Juvenile Dermatomyositis: Associations with Disease Activity at Diagnosis and after Thirty-Six Months of Therapy. *Arthritis Rheum.* **2009**, 60 (6), 1815–1824.
24. Piper CJM, Wilkinson MGL, Deakin CT, et al. CD19(+)CD24(hi)CD38(hi) B Cells Are Expanded in Juvenile Dermatomyositis and Exhibit a Pro-Inflammatory Phenotype After Activation Through Toll-Like Receptor 7 and Interferon-Alpha. *Front. Immunol.* **2018**, 9, 1372.
25. Rice GI, Melki I, Fremont M-L, et al. Assessment of Type I Interferon Signaling in Pediatric Inflammatory Disease. *J. Clin. Immunol.* **2017**, 37 (2), 123–132.
26. Baechler EC, Bilgic H, Reed AM. Type I Interferon Pathway in Adult and Juvenile Dermatomyositis. *Arthritis Res. Ther.* **2011**, 13 (6), 249.
27. Reed AM, Peterson E, Bilgic H, et al. Changes in Novel Biomarkers of Disease Activity in Juvenile and Adult Dermatomyositis Are Sensitive Biomarkers of Disease Course. *Arthritis Rheum.* **2012**, 64 (12), 4078–4086.
28. Enders FB, Delemarre EM, Kuemmerle-Deschner J, et al. Autologous Stem Cell Transplantation Leads to a Change in Proinflammatory Plasma Cytokine Profile of Patients with Juvenile Dermatomyositis Correlating with Disease Activity. *Annals of the rheumatic diseases*. England January 2015, pp 315–317.
29. Limongi F. The CXCR3 Chemokines in Inflammatory Myopathies. *Clin. Ter.* **2015**, 166 (1), e56-61.
30. Moneta GM, Pires Marafon D, Marasco E, et al. Muscle Expression of Type I and Type II Interferons Is Increased in Juvenile Dermatomyositis and Related to Clinical and Histological Features. *Arthritis Rheumatol. (Hoboken, N.J.)* **2018**.
31. Karin N, Razon H. Chemokines beyond Chemo-Attraction: CXCL10 and Its Significant Role in Cancer and Autoimmunity. *Cytokine* **2018**, 109, 24–28.

32. Lasagni L, Francalanci M, Annunziato F, et al. An Alternatively Spliced Variant of CXCR3 Mediates the Inhibition of Endothelial Cell Growth Induced by IP-10, Mig, and I-TAC, and Acts as Functional Receptor for Platelet Factor 4. *J. Exp. Med.* **2003**, 197 (11), 1537–1549.
33. Aanhane E, Schulkens IA, Heusschen R, et al. Different Angioregulatory Activity of Monovalent Galectin-9 Isoforms. *Angiogenesis* **2018**.
34. O'Brien MJ, Shu Q, Stinson WA, et al. A Unique Role for Galectin-9 in Angiogenesis and Inflammatory Arthritis. *Arthritis Res. Ther.* **2018**, 20 (1), 31.
35. Heusschen R, Schulkens IA, van Beijnum J, et al. Endothelial LGALS9 Splice Variant Expression in Endothelial Cell Biology and Angiogenesis. *Biochim. Biophys. Acta* **2014**, 1842 (2), 284–292.
36. Nakajima R, Miyagaki T, Oka T, et al. Elevated Serum Galectin-9 Levels in Patients with Atopic Dermatitis. *J. Dermatol.* **2015**, 42 (7), 723–726.
37. Chagan-Yasutan H, Ndhlovu LC, Lacuesta TL, et al. Galectin-9 Plasma Levels Reflect Adverse Hematological and Immunological Features in Acute Dengue Virus Infection. *J. Clin. Virol.* **2013**, 58 (4), 635–640.
38. McSharry BP, Forbes SK, Cao JZ, et al. Human Cytomegalovirus Upregulates Expression of the Lectin Galectin 9 via Induction of Beta Interferon. *J. Virol.* **2014**, 88 (18), 10990–10994.
39. Dembele BPP, Chagan-Yasutan H, Niki T, et al. Plasma Levels of Galectin-9 Reflect Disease Severity in Malaria Infection. *Malar. J.* **2016**, 15 (1), 403.
40. Machala EA, Avdic S, Stern L, et al. Restriction of Human Cytomegalovirus Infection by Galectin-9. *J. Virol.* **2019**, 93 (3).
41. Zhu C, Anderson AC, Schubart A, et al. The Tim-3 Ligand Galectin-9 Negatively Regulates T Helper Type 1 Immunity. *Nat. Immunol.* **2005**, 6 (12), 1245–1252.
42. Seki M, Oomizu S, Sakata K-M, et al. Galectin-9 Suppresses the Generation of Th17, Promotes the Induction of Regulatory T Cells, and Regulates Experimental Autoimmune Arthritis. *Clin. Immunol.* **2008**, 127 (1), 78–88.
43. Bi S, Hong PW, Lee B, et al. Galectin-9 Binding to Cell Surface Protein Disulfide Isomerase Regulates the Redox Environment to Enhance T-Cell Migration and HIV Entry. *Proc. Natl. Acad. Sci. U. S. A.* **2011**, 108 (26), 10650–10655.
44. Shan M, Carrillo J, Yeste A, et al. Secreted IgD Amplifies Humoral T Helper 2 Cell Responses by Binding Basophils via Galectin-9 and CD44. *Immunity* **2018**, 49 (4), 709–724.e8.
45. Wu C, Thalhamer T, Franca RF, et al. Galectin-9-CD44 Interaction Enhances Stability and Function of Adaptive Regulatory T Cells. *Immunity* **2014**, 41 (2), 270–282.
46. Madireddi S, Eun S-Y, Mehta AK, et al. Regulatory T Cell-Mediated Suppression of Inflammation Induced by DR3 Signaling Is Dependent on Galectin-9. *J. Immunol.* **2017**, 199 (8), 2721–2728.
47. Cao A, Alluqmani N, Buhari FHM, et al. Galectin-9 Binds IgM-BCR to Regulate B Cell Signaling. *Nat. Commun.* **2018**, 9 (1), 3288.
48. Giovannone N, Liang J, Antonopoulos A, et al. Galectin-9 Suppresses B Cell Receptor Signaling and Is Regulated by I-Branching of N-Glycans. *Nat. Commun.* **2018**, 9 (1), 3287.
49. Daley D, Mani VR, Mohan N, et al. Dectin 1 Activation on Macrophages by Galectin 9 Promotes Pancreatic Carcinoma and Peritumoral Immune Tolerance. *Nat. Med.* **2017**, 23 (5), 556–567.

50. Li Z-H, Wang L-L, Liu H, et al. Galectin-9 Alleviates LPS-Induced Preeclampsia-Like Impairment in Rats via Switching Decidual Macrophage Polarization to M2 Subtype. *Front. Immunol.* **2018**, *9*, 3142.
51. Moritoki M, Kadowaki T, Niki T, et al. Galectin-9 Ameliorates Clinical Severity of MRL/lpr Lupus-Prone Mice by Inducing Plasma Cell Apoptosis Independently of Tim-3. *PLoS One* **2013**, *8* (4), e60807.
52. Panda SK, Facchinetti V, Voynova E, et al. Galectin-9 Inhibits TLR7-Mediated Autoimmunity in Murine Lupus Models. *J. Clin. Invest.* **2018**, *128* (5), 1873–1887.
53. Enninga EAL, Harrington SM, Creedon DJ, et al. Immune Checkpoint Molecules Soluble Program Death Ligand 1 and Galectin-9 Are Increased in Pregnancy. *Am. J. Reprod. Immunol.* **2018**, *79* (2).
54. Zeggar S, Watanabe KS, Teshigawara S, et al. Role of Lgals9 Deficiency in Attenuating Nephritis and Arthritis in BALB/c Mice in a Pristane-Induced Lupus Model. *Arthritis Rheumatol. (Hoboken, N.J.)* **2018**, *70* (7), 1089–1101.
55. Panda AK, Das BK. Perplexing Role of Galectin 9 in Experimental Lupus Models: Comment on the Article by Zeggar et Al. *Arthritis & rheumatology (Hoboken, N.J.)*. United States September 2018, pp 1530–1531.
56. Steichen AL, Simonson TJ, Salmon SL, et al. Alarmin Function of Galectin-9 in Murine Respiratory Tularemia. *PLoS One* **2015**, *10* (4), e0123573.
57. Liang C-C, Li C-S, Weng I-C, et al. Galectin-9 Is Critical for Mucosal Adaptive Immunity through the T Helper 17-IgA Axis. *Am. J. Pathol.* **2018**, *188* (5), 1225–1235.
58. Gooden MJM, Wiersma VR, Samplonius DF, et al. Galectin-9 Activates and Expands Human T-Helper 1 Cells. *PLoS One* **2013**, *8* (5), e65616.
59. Lhuillier C, Barjon C, Niki T, et al. Impact of Exogenous Galectin-9 on Human T Cells: CONTRIBUTION OF THE T CELL RECEPTOR COMPLEX TO ANTIGEN-INDEPENDENT ACTIVATION BUT NOT TO APOPTOSIS INDUCTION. *J. Biol. Chem.* **2015**, *290* (27), 16797–16811.
60. Bitra A, Doukov T, Wang J, et al. Crystal Structure of Murine 4-1BB and Its Interaction with 4-1BBL Support a Role for Galectin-9 in 4-1BB Signaling. *J. Biol. Chem.* **2018**, *293* (4), 1317–1329.
61. Nielsen MA, Andersen T, Etzerodt A, et al. A Disintegrin and Metalloprotease-17 and Galectin-9 Are Important Regulators of Local 4-1BB Activity and Disease Outcome in Rheumatoid Arthritis. *Rheumatology (Oxford)*. **2016**, *55* (10), 1871–1879.
62. Madireddi S, Eun S-Y, Lee S-W, et al. Galectin-9 Controls the Therapeutic Activity of 4-1BB-Targeting Antibodies. *J. Exp. Med.* **2014**, *211* (7), 1433–1448.
63. Vaitaitis GM, Wagner DHJ. Galectin-9 Controls CD40 Signaling through a Tim-3 Independent Mechanism and Redirects the Cytokine Profile of Pathogenic T Cells in Autoimmunity. *PLoS One* **2012**, *7* (6), e38708.
64. Veenstra RG, Taylor PA, Zhou Q, et al. Contrasting Acute Graft-versus-Host Disease Effects of Tim-3/galectin-9 Pathway Blockade Dependent upon the Presence of Donor Regulatory T Cells. *Blood* **2012**, *120* (3), 682–690.
65. Heusschen R, Griffioen AW, Thijssen VL. Galectin-9 in Tumor Biology: A Jack of Multiple Trades. *Biochim. Biophys. Acta* **2013**, *1836* (1), 177–185.
66. Tian L, Goldstein A, Wang H, et al. Mutual Regulation of Tumour Vessel Normalization and Immunostimulatory Reprogramming. *Nature* **2017**, *544* (7649), 250–254.
67. Aird WC. Phenotypic Heterogeneity of the Endothelium: I. Structure, Function, and Mechanisms. *Circ. Res.* **2007**, *100* (2), 158–173.

68. Aird WC. Phenotypic Heterogeneity of the Endothelium: II. Representative Vascular Beds. *Circ. Res.* **2007**, *100* (2), 174–190.
69. Pober JS, Sessa WC. Evolving Functions of Endothelial Cells in Inflammation. *Nat. Rev. Immunol.* **2007**, *7* (10), 803–815.
70. Karmann K, Hughes CC, Schechner J, et al. CD40 on Human Endothelial Cells: Inducibility by Cytokines and Functional Regulation of Adhesion Molecule Expression. *Proc. Natl. Acad. Sci. U. S. A.* **1995**, *92* (10), 4342–4346.
71. Khayyamian S, Hutloff A, Buchner K, et al. ICOS-Ligand, Expressed on Human Endothelial Cells, Costimulates Th1 and Th2 Cytokine Secretion by Memory CD4+ T Cells. *Proc. Natl. Acad. Sci. U. S. A.* **2002**, *99* (9), 6198–6203.
72. Migone TS, Zhang J, Luo X, et al. TL1A Is a TNF-like Ligand for DR3 and TR6/DcR3 and Functions as a T Cell Costimulator. *Immunity* **2002**, *16* (3), 479–492.
73. Choi J, Enis DR, Koh KP, et al. T Lymphocyte-Endothelial Cell Interactions. *Annu. Rev. Immunol.* **2004**, *22*, 683–709.
74. Carman C V, Martinelli R. T Lymphocyte-Endothelial Interactions: Emerging Understanding of Trafficking and Antigen-Specific Immunity. *Front. Immunol.* **2015**, *6*, 603.
75. Pober JS, Collins T, Gimbrone MAJ, et al. Lymphocytes Recognize Human Vascular Endothelial and Dermal Fibroblast Ia Antigens Induced by Recombinant Immune Interferon. *Nature* **1983**, *305* (5936), 726–729.
76. Li CKC, Varsani H, Holton JL, et al. MHC Class I Overexpression on Muscles in Early Juvenile Dermatomyositis. *J. Rheumatol.* **2004**, *31* (3), 605–609.
77. Sallum AME, Kiss MHB, Silva CAA, et al. MHC Class I and II Expression in Juvenile Dermatomyositis Skeletal Muscle. *Clin. Exp. Rheumatol.* **2009**, *27* (3), 519–526.
78. Shinjo SK, Sallum AME, Silva CA, et al. Skeletal Muscle Major Histocompatibility Complex Class I and II Expression Differences in Adult and Juvenile Dermatomyositis. *Clinics (Sao Paulo)*. **2012**, *67* (8), 885–890.
79. Sallum AME, Kiss MHB, Silva CAA, et al. Difference in Adhesion Molecule Expression (ICAM-1 and VCAM-1) in Juvenile and Adult Dermatomyositis, Polymyositis and Inclusion Body Myositis. *Autoimmun. Rev.* **2006**, *5* (2), 93–100.
80. Sallum AME, Marie SKN, Wakamatsu A, et al. Immunohistochemical Analysis of Adhesion Molecule Expression on Muscle Biopsy Specimens from Patients with Juvenile Dermatomyositis. *J. Rheumatol.* **2004**, *31* (4), 801–807.
81. Korhonen EA, Lampinen A, Giri H, et al. Tie1 Controls Angiopoietin Function in Vascular Remodeling and Inflammation. *J. Clin. Invest.* **2016**, *126* (9), 3495–3510.
82. Kim M, Allen B, Korhonen EA, et al. Opposing Actions of Angiopoietin-2 on Tie2 Signaling and FOXO1 Activation. *J. Clin. Invest.* **2016**, *126* (9), 3511–3525.
83. Cindrova-Davies T, Sanders DA, Burton GJ, et al. Soluble FLT1 Sensitizes Endothelial Cells to Inflammatory Cytokines by Antagonizing VEGF Receptor-Mediated Signalling. *Cardiovasc. Res.* **2011**, *89* (3), 671–679.
84. Marelli-Berg FM, Jarmin SJ. Antigen Presentation by the Endothelium: A Green Light for Antigen-Specific T Cell Trafficking? *Immunol. Lett.* **2004**, *93* (2–3), 109–113.

85. Greening JE, Tree TIM, Kotowicz KT, et al. Processing and Presentation of the Islet Autoantigen GAD by Vascular Endothelial Cells Promotes Transmigration of Autoreactive T-Cells. *Diabetes* **2003**, 52 (3), 717–725.
86. Savage CO, Brooks CJ, Harcourt GC, et al. Human Vascular Endothelial Cells Process and Present Autoantigen to Human T Cell Lines. *Int. Immunol.* **1995**, 7 (3), 471–479.
87. Vora M, Yssel H, de Vries JE, et al. Antigen Presentation by Human Dermal Microvascular Endothelial Cells. Immunoregulatory Effect of IFN-Gamma and IL-10. *J. Immunol.* **1994**, 152 (12), 5734–5741.
88. von Oppen N, Schurich A, Hegenbarth S, et al. Systemic Antigen Cross-Presented by Liver Sinusoidal Endothelial Cells Induces Liver-Specific CD8 T-Cell Retention and Tolerization. *Hepatology* **2009**, 49 (5), 1664–1672.
89. Limmer A, Ohl J, Kurts C, et al. Efficient Presentation of Exogenous Antigen by Liver Endothelial Cells to CD8+ T Cells Results in Antigen-Specific T-Cell Tolerance. *Nat. Med.* **2000**, 6 (12), 1348–1354.
90. Hirose S, Vokali E, Raghavan VR, et al. Steady-State Antigen Scavenging, Cross-Presentation, and CD8+ T Cell Priming: A New Role for Lymphatic Endothelial Cells. *J. Immunol.* **2014**, 192 (11), 5002–5011.
91. Manes TD, Pober JS. Antigen Presentation by Human Microvascular Endothelial Cells Triggers ICAM-1-Dependent Transendothelial Protrusion By, and Fractalkine-Dependent Transendothelial Migration Of, Effector Memory CD4+ T Cells. *J. Immunol.* **2008**, 180 (12), 8386–8392.
92. Marelli-Berg FM, Okkenhaug K, Miranda V. A Two-Signal Model for T Cell Trafficking. *Trends Immunol.* **2007**, 28 (6), 267–273.
93. Marelli-Berg FM, James MJ, Dangerfield J, et al. Cognate Recognition of the Endothelium Induces HY-Specific CD8+ T-Lymphocyte Transendothelial Migration (Diapedesis) in Vivo. *Blood* **2004**, 103 (8), 3111–3116.
94. Savinov AY, Wong FS, Stonebraker AC, et al. Presentation of Antigen by Endothelial Cells and Chemoattraction Are Required for Homing of Insulin-Specific CD8+ T Cells. *J. Exp. Med.* **2003**, 197 (5), 643–656.
95. Fu H, Kishore M, Gittens B, et al. Self-Recognition of the Endothelium Enables Regulatory T-Cell Trafficking and Defines the Kinetics of Immune Regulation. *Nat. Commun.* **2014**, 5, 3436.
96. Nourshargh S, Marelli-Berg FM. Transmigration through Venular Walls: A Key Regulator of Leukocyte Phenotype and Function. *Trends Immunol.* **2005**, 26 (3), 157–165.
97. Lozanoska-Ochser B, Peakman M. Level of Major Histocompatibility Complex Class I Expression on Endothelium in Non-Obese Diabetic Mice Influences CD8 T Cell Adhesion and Migration. *Clin. Exp. Immunol.* **2009**, 157 (1), 119–127.
98. Powell RM, Lissauer D, Tamblyn J, et al. Decidual T Cells Exhibit a Highly Differentiated Phenotype and Demonstrate Potential Fetal Specificity and a Strong Transcriptional Response to IFN. *J. Immunol.* **2017**, 199 (10), 3406–3417.
99. Marelli-Berg FM, Hargreaves RE, Carmichael P, et al. Major Histocompatibility Complex Class II-Expressing Endothelial Cells Induce Allospecific Nonresponsiveness in Naive T Cells. *J. Exp. Med.* **1996**, 183 (4), 1603–1612.
100. Ma W, Pober JS. Human Endothelial Cells Effectively Costimulate Cytokine Production By, but Not Differentiation Of, Naive CD4+ T Cells. *J. Immunol.* **1998**, 161 (5), 2158–2167.

101. Perez VL, Henault L, Lichtman AH. Endothelial Antigen Presentation: Stimulation of Previously Activated but Not Naive TCR-Transgenic Mouse T Cells. *Cell. Immunol.* **1998**, *189* (1), 31–40.
102. Epperson DE, Pober JS. Antigen-Presenting Function of Human Endothelial Cells. Direct Activation of Resting CD8 T Cells. *J. Immunol.* **1994**, *153* (12), 5402–5412.
103. Dengler TJ, Pober JS. Human Vascular Endothelial Cells Stimulate Memory but Not Naive CD8+ T Cells to Differentiate into CTL Retaining an Early Activation Phenotype. *J. Immunol.* **2000**, *164* (10), 5146–5155.
104. Shiao SL, McNiff JM, Pober JS. Memory T Cells and Their Costimulators in Human Allograft Injury. *J. Immunol.* **2005**, *175* (8), 4886–4896.
105. Sage PT, Varghese LM, Martinelli R, et al. Antigen Recognition Is Facilitated by Invadosome-like Protrusions Formed by Memory/effector T Cells. *J. Immunol.* **2012**, *188* (8), 3686–3696.
106. Denton MD, Geehan CS, Alexander SI, et al. Endothelial Cells Modify the Costimulatory Capacity of Transmigrating Leukocytes and Promote CD28-Mediated CD4(+) T Cell Alloactivation. *J. Exp. Med.* **1999**, *190* (4), 555–566.
107. Tafllin C, Favier B, Baudhuin J, et al. Human Endothelial Cells Generate Th17 and Regulatory T Cells under Inflammatory Conditions. *Proc. Natl. Acad. Sci. U. S. A.* **2011**, *108* (7), 2891–2896.
108. Luster AD, Unkeless JC, Ravetch J V. Gamma-Interferon Transcriptionally Regulates an Early-Response Gene Containing Homology to Platelet Proteins. *Nature* **1985**, *315* (6021), 672–676.
109. Doukas J, Pober JS. IFN-Gamma Enhances Endothelial Activation Induced by Tumor Necrosis Factor but Not IL-1. *J. Immunol.* **1990**, *145* (6), 1727–1733.
110. Austrup F, Vestweber D, Borges E, et al. P- and E-Selectin Mediate Recruitment of T-Helper-1 but Not T-Helper-2 Cells into Inflamed Tissues. *Nature* **1997**, *385* (6611), 81–83.
111. Chaplin DD. Cell Cooperation in Development of Eosinophil-Predominant Inflammation in Airways. *Immunol. Res.* **2002**, *26* (1–3), 55–62.
112. David R, Marelli-Berg FM. Regulation of T-Cell Migration by Co-Stimulatory Molecules. *Biochem. Soc. Trans.* **2007**, *35* (Pt 5), 1114–1118.
113. Brosens JJ, Pijnenborg R, Brosens IA. The Myometrial Junctional Zone Spiral Arteries in Normal and Abnormal Pregnancies: A Review of the Literature. *Am. J. Obstet. Gynecol.* **2002**, *187* (5), 1416–1423.
114. Powe CE, Levine RJ, Karumanchi SA. Preeclampsia, a Disease of the Maternal Endothelium: The Role of Antiangiogenic Factors and Implications for Later Cardiovascular Disease. *Circulation* **2011**, *123* (24), 2856–2869.
115. Lyall F, Robson SC, Bulmer JN. Spiral Artery Remodeling and Trophoblast Invasion in Preeclampsia and Fetal Growth Restriction: Relationship to Clinical Outcome. *Hypertens. (Dallas, Tex. 1979)* **2013**, *62* (6), 1046–1054.
116. Mor G, Aldo P, Alvero AB. The Unique Immunological and Microbial Aspects of Pregnancy. *Nat. Rev. Immunol.* **2017**, *17* (8), 469–482.
117. Szabo PA, Miron M, Farber DL. Location, Location, Location: Tissue Resident Memory T Cells in Mice and Humans. *Sci. Immunol.* **2019**, *4* (34).
118. Zhou H, Liu F. Regulation, Communication, and Functional Roles of Adipose Tissue-Resident CD4(+) T Cells in the Control of Metabolic Homeostasis. *Front. Immunol.* **2018**, *9*, 1961.

119. Sharma A, Rudra D. Emerging Functions of Regulatory T Cells in Tissue Homeostasis. *Front. Immunol.* **2018**, *9*, 883.
120. Gebhardt T, Palendira U, Tschärke DC, et al. Tissue-Resident Memory T Cells in Tissue Homeostasis, Persistent Infection, and Cancer Surveillance. *Immunol. Rev.* **2018**, *283* (1), 54–76.
121. Lutter L, Hoytema van Konijnenburg DP, Brand EC, et al. The Elusive Case of Human Intraepithelial T Cells in Gut Homeostasis and Inflammation. *Nat. Rev. Gastroenterol. Hepatol.* **2018**, *15* (10), 637–649.
122. Clark RA. Resident Memory T Cells in Human Health and Disease. *Sci. Transl. Med.* **2015**, *7* (269), 269rv1.
123. Cipolletta D, Feuerer M, Li A, et al. PPAR- γ Is a Major Driver of the Accumulation and Phenotype of Adipose Tissue Treg Cells. *Nature* **2012**, *486* (7404), 549–553.
124. Burzyn D, Kuswanto W, Kolodin D, et al. A Special Population of Regulatory T Cells Potentiates Muscle Repair. *Cell* **2013**, *155* (6), 1282–1295.
125. Niedzielska M, Israelsson E, Angermann B, et al. Differential Gene Expression in Human Tissue Resident Regulatory T Cells from Lung, Colon, and Blood. *Oncotarget* **2018**, *9* (90), 36166–36184.
126. Li J, Olshansky M, Carbone FR, et al. Transcriptional Analysis of T Cells Resident in Human Skin. *PLoS One* **2016**, *11* (1), e0148351.
127. Miragaia RJ, Gomes T, Chomka A, et al. Single-Cell Transcriptomics of Regulatory T Cells Reveals Trajectories of Tissue Adaptation. *Immunity* **2019**, *50* (2), 493–504.e7.
128. Delacher M, Imbusch CD, Weichenhan D, et al. Genome-Wide DNA-Methylation Landscape Defines Specialization of Regulatory T Cells in Tissues. *Nat. Immunol.* **2017**, *18* (10), 1160–1172.
129. Panduro M, Benoist C, Mathis D. Tissue Tregs. *Annu. Rev. Immunol.* **2016**, *34*, 609–633.
130. DiSpirito JR, Zemmour D, Ramanan D, et al. Molecular Diversification of Regulatory T Cells in Nonlymphoid Tissues. *Sci. Immunol.* **2018**, *3* (27).
131. Kumar B V, Ma W, Miron M, et al. Human Tissue-Resident Memory T Cells Are Defined by Core Transcriptional and Functional Signatures in Lymphoid and Mucosal Sites. *Cell Rep.* **2017**, *20* (12), 2921–2934.
132. Mackay LK, Minnich M, Kragten NAM, et al. Hobit and Blimp1 Instruct a Universal Transcriptional Program of Tissue Residency in Lymphocytes. *Science* **2016**, *352* (6284), 459–463.
133. Thome JJC, Yudanin N, Ohmura Y, et al. Spatial Map of Human T Cell Compartmentalization and Maintenance over Decades of Life. *Cell* **2014**, *159* (4), 814–828.
134. Mackay LK, Rahimpour A, Ma JZ, et al. The Developmental Pathway for CD103(+)CD8+ Tissue-Resident Memory T Cells of Skin. *Nat. Immunol.* **2013**, *14* (12), 1294–1301.
135. Mackay LK, Wynne-Jones E, Freestone D, et al. T-Box Transcription Factors Combine with the Cytokines TGF- β and IL-15 to Control Tissue-Resident Memory T Cell Fate. *Immunity* **2015**, *43* (6), 1101–1111.
136. Zhang N, Bevan MJ. Transforming Growth Factor- β Signaling Controls the Formation and Maintenance of Gut-Resident Memory T Cells by Regulating Migration and Retention. *Immunity* **2013**, *39* (4), 687–696.
137. Casey KA, Fraser KA, Schenkel JM, et al. Antigen-Independent Differentiation and Maintenance of Effector-like Resident Memory T Cells in Tissues. *J. Immunol.* **2012**, *188* (10), 4866–4875.

138. Nath AP, Braun A, Ritchie SC, et al. Comparative Analysis Reveals a Role for TGF-Beta in Shaping the Residency-Related Transcriptional Signature in Tissue-Resident Memory CD8+ T Cells. *PLoS One* **2019**, *14* (2), e0210495.
139. Strutt TM, Dhume K, Finn CM, et al. IL-15 Supports the Generation of Protective Lung-Resident Memory CD4 T Cells. *Mucosal Immunol.* **2018**, *11* (3), 668–680.
140. Hondowicz BD, Kim KS, Ruterbusch MJ, et al. IL-2 Is Required for the Generation of Viral-Specific CD4(+) Th1 Tissue-Resident Memory Cells and B Cells Are Essential for Maintenance in the Lung. *Eur. J. Immunol.* **2018**, *48* (1), 80–86.
141. Holz LE, Prier JE, Freestone D, et al. CD8(+) T Cell Activation Leads to Constitutive Formation of Liver Tissue-Resident Memory T Cells That Seed a Large and Flexible Niche in the Liver. *Cell Rep.* **2018**, *25* (1), 68–79.e4.
142. Laidlaw BJ, Zhang N, Marshall HD, et al. CD4+ T Cell Help Guides Formation of CD103+ Lung-Resident Memory CD8+ T Cells during Influenza Viral Infection. *Immunity* **2014**, *41* (4), 633–645.
143. Bergsbaken T, Bevan MJ. Proinflammatory Microenvironments within the Intestine Regulate the Differentiation of Tissue-Resident CD8(+) T Cells Responding to Infection. *Nat. Immunol.* **2015**, *16* (4), 406–414.
144. Zhou AC, Wagar LE, Wortzman ME, et al. Intrinsic 4-1BB Signals Are Indispensable for the Establishment of an Influenza-Specific Tissue-Resident Memory CD8 T-Cell Population in the Lung. *Mucosal Immunol.* **2017**, *10* (5), 1294–1309.
145. Mackay LK, Carbone FR. CD4 Helpers Put Tissue-Resident Memory Cells in Their Place. *Immunity* **2014**, *41* (4), 514–515.
146. Nakanishi Y, Lu B, Gerard C, et al. CD8(+) T Lymphocyte Mobilization to Virus-Infected Tissue Requires CD4(+) T-Cell Help. *Nature* **2009**, *462* (7272), 510–513.
147. Li C, DiSpirito JR, Zemmour D, et al. TCR Transgenic Mice Reveal Stepwise, Multi-Site Acquisition of the Distinctive Fat-Treg Phenotype. *Cell* **2018**, *174* (2), 285–299.e12.
148. Shioh LR, Rosen DB, Brdickova N, et al. CD69 Acts Downstream of Interferon-Alpha/beta to Inhibit S1P1 and Lymphocyte Egress from Lymphoid Organs. *Nature* **2006**, *440* (7083), 540–544.
149. Cibrian D, Sanchez-Madrid F. CD69: From Activation Marker to Metabolic Gatekeeper. *Eur. J. Immunol.* **2017**, *47* (6), 946–953.
150. Sullivan JM, Hollbacher B, Campbell DJ. Cutting Edge: Dynamic Expression of Id3 Defines the Stepwise Differentiation of Tissue-Resident Regulatory T Cells. *J. Immunol.* **2019**, *202* (1), 31–36.

Addendum



NEDERLANDSE SAMENVATTING

Dit proefschrift verkent lokale en systemische profielen van inflammatie, adaptatie en regulatie op het grensvlak tussen weefsels en immuniteit. In de samenvatting hieronder zullen deze begrippen toegelicht worden en de inhoud van het proefschrift in het kort besproken worden.

Ontsteking

Het afweersysteem is verantwoordelijk voor het beschermen van het lichaam tegen infectieziekten veroorzaakt door onder andere bacteriën en virussen. Wanneer een bacterie of virus het lichaam binnendringt, wordt het afweersysteem geactiveerd, wat resulteert in een ontsteking (*inflammatie*). Ontsteking is de natuurlijke reactie van het afweersysteem om een infectie te bestrijden. Tijdens een ontsteking komt er een scala aan signaalstoffen vrij (*cytokines en chemokines*). Deze signaalstoffen worden zowel door de cellen van het afweersysteem, als door de omliggende weefselcellen op de plek van de ontsteking gemaakt. De hoeveelheid en soort signaalstoffen die gemaakt wordt hangt af van het type ontsteking en de intensiteit ervan. Daarmee kan de concentratie en specifieke combinatie van signaalstoffen die wordt aangetroffen ter plaatse van de ontsteking of in het bloed, als informatiebron (*biomarker*) over de ontsteking dienen.

Een celtype dat een belangrijk onderdeel vormt van het afweersysteem zijn T cellen. T cellen hebben de capaciteit om lichaamsvreemde entiteiten, zoals bacteriën en virussen, te herkennen en te doden. T cellen komen zowel in het bloed als in weefsels voor. Zij zijn in staat hun gedrag en functie aan te passen aan de specifieke locatie waar ze zich bevinden (*adaptatie*). Om vanuit het bloed de weefsels te bereiken, moeten T cellen de wand van de bloedvaten passeren. Deze bloedvatwand, die het grensvlak markeert tussen het deel van het afweersysteem dat zich in het bloed bevindt (*systemisch*) en het deel dat zich in de weefsels bevindt (*lokaal*), bestaat uit een speciaal soort cellen genaamd endotheelcellen. Als grenswachters tussen bloed en weefsel vervullen endotheelcellen een belangrijke functie, vooral tijdens ontsteking, omdat ze de passage van T cellen van bloed naar weefsels actief reguleren. Bovendien zijn endotheelcellen, net als T cellen, in staat zich aan te passen aan hun omgeving.

Ontsteking is een nuttig, maar ook gevaarlijk proces. Het ontstekingsproces is erop gericht om een eventuele indringer schade te berokkenen. Tijdens een ontsteking kunnen daardoor echter ook omliggende lichaamseigen weefselcellen beschadigd worden. Om deze randschade zoveel mogelijk te beperken, maar tegelijkertijd een infectie effectief te bestrijden, wordt het ontstekingsproces nauw in balans gehouden door ontstekingsremmende signaalstoffen en cellen (*regulatie*). Op deze manier wordt ook

voorkomen dat ontsteking langdurig blijft bestaan (*chronische ontsteking*). Een voorbeeld van ontstekingsremmende cellen zijn regulatoire T cellen. Zij behoren tot de familie van de T cellen en hebben als belangrijkste taak om andere T cellen te remmen wanneer hun reactie disproportioneel is in verhouding tot de infectie, of voltooid is nadat de infectie is bestreden.

De strekking van dit proefschrift is om de twee compartimenten van het afweersysteem, te weten in het bloed (*systemisch*) en in de weefsels (*lokaal*), te verbinden. Hierin wordt ook de functie van de endotheelcellaag betrokken die het grensvlak vormt tussen bloed en weefsels. Deze verbinding wordt besproken binnen twee verschillende contextuele situaties van het menselijke lichaam: enerzijds tijdens chronische ontsteking zoals wordt gezien in auto-immuunziekten, en anderzijds tijdens de zwangerschap. Het doel van dit proefschrift is om nieuwe inzichten te creëren die kunnen bijdragen aan een vertaling van onderzoeksresultaten naar een klinische toepassing.

Biomarkers voor therapie op maat in auto-immuunziekten

Wanneer het afweersysteem niet goed gereguleerd is, ontsteking de overhand krijgt en chronisch wordt, kan er sprake zijn van een auto-immuunziekte. Bij een auto-immuunziekte ontstaat de ontsteking doordat het afweersysteem lichaamseigen weefsels aanvalt. Afhankelijk van de soort auto-immuunziekte kunnen er in verschillende weefsels ontstekingen ontstaan.

Bij juveniele dermatomyositis (JDM), een zeldzame auto-immuunziekte die optreedt op de kindereleeftijd, ontstaat er chronische ontsteking in de spieren en de huid, met ernstige gevolgen zoals spierzwakte en beschadiging van de huid. Naast ontsteking van de spieren en de huid, is een verstoorde functie van endotheelcellen (*endotheeldysfunctie*) een belangrijk kenmerk van JDM. Patiënten met JDM worden langdurig behandeld met zware afweer-onderdrukkende medicijnen, die in de meeste patiënten de ontsteking effectief dempen, maar ernstige bijwerkingen kunnen veroorzaken. De ziekte vertoont vaak een wispelturig beloop, met perioden van actieve ontsteking (*opvlamming*) afgewisseld door perioden van rustige ziekte (*remissie*). Een belangrijk probleem voor patiënten en behandelend artsen is dat er op dit moment geen objectieve meetinstrumenten bestaan om de activiteit van de ziekte betrouwbaar vast te stellen. Om een zo goed mogelijk beeld te krijgen van de ziekte-activiteit, wordt nu een aantal metingen gecombineerd – zoals spierkrachtmetingen en laboratoriumbepalingen van het bloed – echter geeft geen van deze metingen de activiteit altijd juist weer. Dit heeft tot gevolg dat het lastig is voor artsen om in te schatten hoeveel medicatie er precies nodig is. Patiënten lopen daardoor het risico op overbehandeling (met ernstige bijwerkingen) of onderbehandeling (met ziekte-opvlammingen). Een ander probleem is dat de huidige (standaard) behandeling niet bij alle patiënten even goed aanslaat. Er is op dit moment nog geen methode beschikbaar om te

voorspellen welke patiënten goed of minder goed op de behandeling zullen reageren. Er is er dus binnen verschillende aspecten van de behandeling van patiënten met JDM ruimte om de behandeling beter af te stemmen op de individuele behoeften van een patiënt (*therapie op maat*).

In **deel 1** van dit proefschrift onderzochten wij strategieën om therapie op maat te faciliteren voor patiënten met JDM. We maakten hierbij gebruik van biomarkers, signaalstoffen afkomstig van de ontsteking, die gemeten kunnen worden in het bloed van patiënten en zowel de aard als de intensiteit van de ontsteking kunnen weerspiegelen. **Hoofdstuk 2** geeft een overzicht van de huidige stand van de literatuur op het gebied van biomarker-geleide controles van ziekte-activiteit in JDM. De uitdagingen en kansen voor therapie op maat met behulp van biomarkermetingen worden besproken.

Onze groep heeft in een eerder onderzoeksproject twee biomarkers geïdentificeerd, genaamd CXCL10 en galectine-9, die de ziekte-activiteit in JDM kunnen weergeven: hoe hoger de waarden van de biomarkers in het bloed, des te actiever de ziekte (en des te meer medicatie patiënten nodig hebben). In **hoofdstuk 3** onderzochten we de betrouwbaarheid van deze twee biomarkers door ze te meten in twee nieuwe, onafhankelijke, grote, internationale patiëntengroepen (*validatie*). De validatie toonde aan dat beide biomarkers een betrouwbare maat vormen voor de ziekte-activiteit. Daarnaast onderzochten we of het mogelijk zou zijn om met deze biomarkers opvlamming van de ziekte te voorspellen vóórdat patiënten last kregen van spierzwakte of huidproblemen. Het doel hiervan was om in de toekomst te kunnen anticiperen op een dreigende opvlamming door de behandeling alvast te intensiveren. Op die manier zou de daadwerkelijke opvlamming voorkomen kunnen worden om de schade te beperken. We onderzochten de voorspellende waarde van de biomarkers in een groep van patiënten die over de tijd (jaren) werden gevolgd en lieten in een aantal patiënten veelbelovende resultaten zien. Tenslotte verkenden we een technische vernieuwing van de biomarkermetingen, middels via vingerprik verkregen bloeddruppels op een papieren kaartje (*dried blood spots*). We toonden aan dat de biomarkermetingen in de dried blood spots even goed werken als biomarkermetingen via de reguliere bloedafname. Het voordeel van de dried blood spots is dat de vingerprik weinig invasief is, en dat patiënten de kaartjes thuis kunnen maken en via de post kunnen opsturen naar het ziekenhuis. Bij een goede biomarkerwaarde (corresponderend met rustige ziekte) zou een controlebezoek uitgesteld kunnen worden. Bovendien zouden de dried blood spots ziektecontroles mogelijk kunnen maken in landen of gebieden waar patiënten op grote afstand van het ziekenhuis leven. De biomarkermetingen van CXCL10 en galectine-9 zijn in Utrecht inmiddels geïmplementeerd in de diagnostiek, en zijn daarmee als standaard zorg beschikbaar voor alle patiënten met JDM in Nederland.

In **hoofdstuk 4** onderzochten we of de combinatie van bepaalde biomarkers (*biomarkerprofiel*) voorspellend kan zijn voor het effect van de behandeling in individuele patiënten met JDM. Omdat naast ontsteking endotheeldysfunctie een belangrijk ziekte-aspect is van JDM, richtten we ons op biomarkers die in eerder onderzoek gerelateerd

waren aan ontsteking en/of endotheeldysfunctie. De biomarkerprofielen werden in twee onafhankelijke patiëntengroepen gemeten, voor aanvang van behandeling. We vonden dat hoge waarden van de twee bekende biomarkers CXCL10 en galectine-9, in combinatie met twee nieuwe biomarkers, TNFR2 en galectine-1, een groep van patiënten identificeerden die 1) voor aanvang van behandeling een ernstig ziektebeeld had (ernstige spierzwakte en huidverschijnselen), 2) vaker aanvullende medicatie benodigde naast de standaardbehandeling om de ontsteking succesvol te onderdrukken, 3) vaak een langere behandelduur nodig had (langere tijd van aanvang van behandeling tot stoppen van alle medicatie). Hiermee toonden we aan dat hoge waarden van deze vier biomarkers bij ziektebegin voorspellend zouden kunnen zijn voor een ernstiger ziektebeloop met minder goede effecten van de behandeling. Als deze resultaten bevestigd kunnen worden in een grotere patiëntengroep, zou dit in de toekomst kunnen helpen om deze 'risicopatiënten' bij ziektebegin te identificeren en het behandelingsbeleid voor hen aan te passen.

Verschillende auto-immuunziekten worden gekenmerkt door verschillende soorten ontsteking, en verschillende betrokken weefsels. Niet alleen in JDM, maar ook in sommige andere auto-immuunziekten speelt endotheeldysfunctie een belangrijke rol. Bij patiënten met auto-immuunziekten waarbij meerdere weefsels of organen betrokken zijn (*systemische auto-immuunziekten*) is de endotheeldysfunctie in de regel meer uitgesproken dan bij patiënten met auto-immuunziekten van een enkel weefsel of orgaan (*lokale auto-immuunziekten*). Uit eerder onderzoek is bekend dat langdurige endotheeldysfunctie een risicofactor is voor het ontwikkelen van hart- en vaatziekten. Vooral bij patiënten met systemische auto-immuunziekten is dit verhoogde risico op hart- en vaatziekten dan ook aangetoond.

In **hoofdstuk 5** onderzochten we biomarkerprofielen gerelateerd aan endotheel(dys)functie en ontsteking in patiënten met verschillende auto-immuunziekten. We lieten zien dat in het bloed van patiënten met auto-immuunziekten de balans tussen signaalstoffen verstoord is ten opzichte van gezonde personen: sommige signaalstoffen die belangrijk zijn voor een goede functie van het endotheel waren verminderd aanwezig, terwijl andere signaalstoffen waarvan een versturende functie op het endotheel bekend is, verhoogd aanwezig bleken. Daarnaast waren bij de meeste patiënten verhoogde waarden van biomarkers voor ontsteking aanwezig. We vonden dat verschillende auto-immuunziekten ziekte-specifieke biomarkerprofielen hebben. Deze profielen bleken onder andere afhankelijk van de locatie van de ontsteking (*lokaal versus systemisch*). De ziekte-specifieke biomarkerprofielen lieten ook een relatie zien met de activiteit van de ziekte: hoe actiever de ziekte, des te uitgesprokener het biomarkerprofiel. Bovendien bleken er in een aanzienlijk deel van de patiënten zonder symptomen of klachten (*klinisch inactieve ziekte*) nog steeds verhoogde biomarkerwaarden aanwezig, wat suggereert dat deze patiënten ondanks behandeling een niet zichtbare (*subklinische*) ontsteking en endotheeldysfunctie hadden. Deze suboptimale onderdrukking van ontsteking en endotheeldysfunctie zou het reeds verhoogde risico op hart- en vaatziekten nog verder kunnen vergroten.

De bevindingen in dit hoofdstuk zouden in de toekomst kunnen bijdragen aan een betere controle van ontsteking en endotheeldysfunctie bij patiënten met auto-immuunziekten, om zo het lange-termijn risico op hart- en vaatziekten te verkleinen.

Immunitet op het grensvlak tussen weefsels en bloed

In **deel 2** van dit proefschrift bestudeerden wij hoe afweercellen en endotheelcellen zich aanpassen aan hun directe weefselomgeving, onder andere tijdens de zwangerschap op het grensvlak tussen moeder en kind in de baarmoeder.

Een zwangerschap stelt een unieke uitdaging aan het lichaam van een vrouw. Om de groei van het kind te faciliteren, vinden er grote veranderingen plaats in baarmoeder. Een van de belangrijkste aanpassingen is een bijzondere vormverandering in de bloedvaten van de baarmoeder (*spiraalarteriën*), die ervoor zorgt dat grote hoeveelheden voedingsstoffen via het bloed kunnen worden uitgewisseld met het groeiende kind. Een ernstige complicatie die kan optreden tijdens de zwangerschap is zwangerschapsvergiftiging (*pre-eclampsie*). Hoewel het precieze mechanisme dat ten grondslag ligt aan pre-eclampsie nog niet is achterhaald, lijkt er een belangrijke rol te zijn voor een verstoorde functie van endotheelcellen (*endotheeldysfunctie*) in de bloedvaten van de baarmoeder. Een van de gevolgen is dat de vorming van de spiraalarteriën is verstoord bij pre-eclampsie, wat kan leiden tot ernstige gezondheidsproblemen bij zowel moeder als kind.

In **hoofdstuk 6** hebben wij de endotheeldysfunctie tijdens zwangerschapsvergiftiging onderzocht. Om dit te bestuderen werden tijdens de keizersnede stukjes weefsel uit de baarmoeder van vrouwen met pre-eclampsie en vrouwen met ongecompliceerde zwangerschappen afgenomen. Vervolgens werden de endotheelcellen uit deze weefselstukjes aan een diepgaande analyse onderworpen die alle facetten van hun functie en gedrag belichtte. We vonden dat de endotheelcellen zich gedroegen alsof ze belangrijke signaalstoffen tekort kwamen. Om dit te bevestigen onderzochten we de biomarkerprofielen van signaalstoffen gerelateerd aan endotheelfunctie en ontsteking in het bloed van vrouwen met pre-eclampsie. Dit bevestigde een tekort aan signaalstoffen die cruciaal zijn voor een goede functie van het endotheel. De bevindingen in dit hoofdstuk tonen aan dat in het bloed van vrouwen met pre-eclampsie signaalstoffen ontbreken die belangrijk zijn voor de functie van het endotheel. Bovendien 'voelen' de endotheelcellen in de baarmoeder dit tekort, wat deels zou kunnen verklaren waarom de vorming van de spiraalarteriën verstoord is tijdens pre-eclampsie.

Niet alleen endotheelcellen, maar ook het afweersysteem heeft een bijzondere rol tijdens de zwangerschap. Cellen van het afweersysteem, en specifiek T cellen, herkennen niet alleen virussen en bacteriën, maar in principe alle 'lichaamsvreemde' entiteiten. Tijdens de zwangerschap draagt de vrouw een kind dat voor de helft uit genetisch materiaal van de vader bestaat. In theorie zou het afweersysteem de cellen van het kind daardoor

als lichaamsvreemd kunnen herkennen (vergelijkbaar met de afstotingsreactie van een donororgaan na transplantatie). Gewoonlijk verloopt een zwangerschap echter zonder een dergelijke reactie. De zwangerschap is in dit opzicht dus een immunologisch mysterie.

In **hoofdstuk 7** onderzochten wij een van de mogelijke verklaringen hoe een afweerreactie tegen het kind tijdens de zwangerschap voorkomen kan worden. Een verklaring zou kunnen zijn dat het afweersysteem, en met name de functie van T cellen, tijdens de zwangerschap heel nauw gereguleerd is. Regulatorische T cellen vervullen een belangrijke rol in het remmen van T cellen en zouden daarom een cruciale rol kunnen spelen in het voorkomen van een afweerreactie tegen het kind. In dit hoofdstuk toonden wij aan dat regulatorische T cellen in de baarmoeder hun functie specifiek aanpassen aan hun weefselomgeving in de nabijheid van de moederkoek en het kind. Precies op het grensvlak tussen moeder en kind, daar waar de moederkoek is aangehecht, zijn regulatorische T cellen actiever dan op andere plekken in de zwangere baarmoeder, en veel actiever dan in het bloed. Regulatorische T cellen passen dus hun functie specifiek aan aan hun weefselomgeving en zijn bijzonder effectief in het remmen van T cellen op het grensvlak tussen moeder en kind, daar waar dit het meest noodzakelijk is. De bevindingen in dit hoofdstuk geven een mogelijke verklaring voor het ontbreken van een afweerreactie tegen het kind tijdens een gezonde zwangerschap. In de toekomst zou deze kennis gebruikt kunnen worden om te achterhalen of in gecompliceerde zwangerschappen, zoals zwangerschappen waarin het kind niet voldoende groeit, een verminderde functie van regulatorische T cellen een rol speelt.

Inmiddels is bekend is dat T cellen in diverse weefsels in het lichaam voorkomen. Niet alleen regulatorische T cellen, maar ook andere T cellen in weefsels laten een bijzonder uiterlijk en gedrag zien. Tot zover is het nog niet bekend hoe en op welk moment T cellen in weefsels deze eigenschappen gaan vertonen. Een van de mogelijkheden is dat T cellen deze eigenschappen verkrijgen op het moment dat ze de bloedbaan verlaten en de weefsels betreden. Op dat moment zijn ze in nauw contact met de bloedvatwand bestaande uit endotheelcellen, die ze moeten passeren om de weefsels te bereiken.

In **hoofdstuk 8** onderzochten wij of endotheelcellen een rol spelen in het aanzetten van de weefsel-specifieke eigenschappen van T cellen. Een van de typische eigenschappen die T cellen in weefsels onderscheidt van T cellen in de bloedbaan, is de aanwezigheid van het CD69 molecuul op hun oppervlakte. Wij vonden dat de interactie met endotheelcellen inderdaad presentatie van CD69 teweegbrengt. Naast het verkrijgen van CD69, vertoonden T cellen die in aanraking waren geweest met endotheelcellen ook een aantal andere uiterlijke en functionele kenmerken die geassocieerd zijn met T cellen in weefsels. Omdat deze experimenten buiten een levend lichaam zijn uitgevoerd, is het niet mogelijk om met zekerheid aan te tonen dat T cellen na interactie met endotheelcellen echte weefsel-T cellen worden. De bevindingen in dit hoofdstuk suggereren echt wel dat endotheelcellen het uiterlijk en gedrag van T cellen kunnen beïnvloeden, op een manier die lijkt op de kenmerken van T cellen in weefsels. Deze resultaten kunnen van waarde zijn voor onder andere auto-immuunziekten, waarbij kwaadaardige T cellen de weefsels betreden en daar

een ontsteking veroorzaken. Een beter begrip van de mechanismen die het gedrag van T cellen in weefsels bepalen kan in de toekomst aangrijpingspunten bieden voor nieuwe behandelingen van auto-immuunziekten.

CONCLUSIE

In dit proefschrift hebben we lokale en systemische profielen van inflammatie, adaptatie en regulatie op het grensvlak tussen weefsels en immuniteit verkend. Specifiek hebben wij verschillende aspecten van de wisselwerking tussen (T-cel afhankelijke) chronische inflammatie en endotheelcellen onderzocht. De belangrijkste bevindingen van dit proefschrift zijn:

- De validatie en implementatie van galectine-9 en CXCL10 als biomarkers voor de ziekte-activiteit van JDM
- De identificatie van biomarkerprofielen die:
 - o In JDM gerelateerd zijn aan ziekte-ernst en de respons op therapie kunnen voorspellen
 - o Specifiek zijn voor auto-immuunziekten en gerelateerd zijn aan ziekte-activiteit en het risico op hart- en vaatziekten
 - o In preeclampsie mogelijk bijdragen aan of een uiting zijn van endotheeldysfunctie in de baarmoeder
- Het inzicht dat regulatoire T cellen hun gedrag aanpassen aan hun specifieke weefselomgeving, en bijzonder actief zijn op het grensvlak tussen moeder en kind in de baarmoeder, hetgeen kan bijdragen aan de regulatie van de afweerreactie tijdens de zwangerschap
- Het inzicht dat T cellen in weefsels hun bijzondere uiterlijk en gedrag (deels) zouden kunnen verkrijgen door nauwe interactie met endotheelcellen tijdens het uittreden uit de bloedbaan naar weefsels.

DANKWOORD

De betrokkenheid van velen om mij heen, zowel op het werk als daarbuiten, heeft de totstandkoming van dit proefschrift mogelijk gemaakt. Daarom hier een woord van dank aan iedereen die er in de afgelopen jaren voor me is geweest en heeft bijgedragen!

Femke en Annet, ik had me geen betere begeleiding kunnen wensen. Heel erg bedankt voor al het vertrouwen dat jullie in me hebben gehad en de enorme vrijheid die jullie me hebben gegeven om mijn eigen pad te ontdekken. Ik heb me altijd door jullie gehoord, gesteund en gewaardeerd gevoeld, inhoudelijk maar ook persoonlijk. Femke, met het plezier, de gedrevenheid maar ook ontspannenheid waarmee je de uitdagingen van de wetenschap lijkt te trotseren ben je een inspiratie voor me. Als ik even door de bomen het bos niet meer zag wist jij weer overzicht te creëren. Je vooruitstrevende blik en passie voor het doorgronden van nieuwe concepten zijn aanstekelijk. Ik bewonder je kracht waarmee je je inzet voor de positie van vrouwen in de wetenschap. Dankjewel voor je persoonlijke en geduldige begeleiding. Annet, jouw toewijding en visie op patiëntenzorg zijn een belangrijke drijfveer voor me geweest. Ik bewonder de tomeloze energie, gedrevenheid en het plezier waarmee je patiëntenzorg, onderwijs, onderzoek (en een leven buiten werk!) combineert. Het vertrouwen dat ouders en patiënten in jou hebben, is onmisbaar geweest voor het JDM onderzoek. Bedankt voor je toewijding en betrokkenheid bij onze projecten, maar vooral ook bij mij en mijn persoonlijke ontwikkeling. Je warme aanwezigheid heeft veel voor me betekend.

Berent, dankjewel voor de kans die je me geboden hebt om eerst in jouw lab, en later onder supervisie van Femke en Annet, in aanraking te komen met translationeel onderzoek en mijn passie ervoor te ontdekken. Ik waardeer het dat je me niet alleen als onderzoeker, maar ook als mens hebt geprobeerd iets mee te geven. Dank voor je vertrouwen en steun op afstand.

Sytze, zonder jou als begeleider van mijn masterstage was ik niet geweest waar ik nu ben. Ook al hebben onze paden elkaar in de afgelopen jaren wat minder gekruist dan voorheen, ik ben je nog steeds dankbaar dat je me de kans hebt gegeven om deel uit te maken van deze groep en me de vrijheid hebt geboden om mijn eigen richting te kiezen.

Marianne en Ruth, dankjulliewel voor jullie enthousiasme en betrokkenheid in de afgelopen jaren als mijn AIO-begeleidingscommissie. Met jullie open maar kritische blik heb ik altijd het gevoel gehad een veilig vangnet te hebben in het geval dat nodig zou zijn.

Bas, Dr. van Rijn, dankjewel voor het fantastische idee waarmee je bij ons kwam aankloppen, en het vertrouwen in ons en onze gezamenlijke projecten! Het is een mooie achtbaanrit geweest, waarin ik jouw visie en gedrevenheid altijd enorm heb gewaardeerd. Ik ben blij dat we de sprong in de diepten van de reproductieve immunologie hebben gewaagd!

Beste **Stefan**, dankjewel voor je persoonlijke betrokkenheid bij mijn beslommingen over carrièrepaden, en al je hulp en inzet om de implementatie van onze biomarkers in de diagnostiek te realiseren. Beste diagnostiek-team, **Henny, Karin, Lisette, Loes, Omar**, en anderen, dankjulliewel voor jullie geduld en doorzettingsvermogen om de biomarkermetingen te optimaliseren voor gebruik in de klinische praktijk!

Jeroen en Pien, heel veel dank voor jullie eindeloze geduld en zowel morele als technische steun in de wispelturige uurtjes van de Aria's. **Wilco, Mariska, Mariëlle, Ben, Zorica, Stephanie**, dank voor jullie hulp bij de luminex en biobank!

Kristin, dankjewel voor je steun in het onderwijs en voor de kansen die je me hebt geboden.

Beste kinderreumatologen binnen en buiten het WKZ, **Bas, Ellen, Esther, Joost, Marc, Merlijn, Nico, Petra, Sylvia** en **Wineke**, beste **Annette**, dankjulliewel voor jullie enorme ad-hoc inzet om ondanks de drukte van de kliniek tijd te maken om patiënten in onze biomarkerstudie te includeren, en ze te vervolgen. Dankjulliewel dat ik altijd weer bij jullie mocht aankloppen met vragen. Zonder jullie was de JDM biomarkerstudie niet mogelijk geweest!

Beste leden van het Myositis Netwerk Nederland, in het bijzonder **Anneke, Anke, Christiaan, Ger, Johan, Joost, Marianne, Saskia**, dank voor de vele gezellige uren tijdens congressen in Washington en Berlijn en onze inspirerende etentjes (Johan, volgende keer Koreaans bij jou toch?), voor de mooie samenwerkingen die daaruit zijn voortgevloeid en voor jullie enorme enthousiasme en inzet om een verschil te maken voor patiënten met myositis.

Dear co-authors and collaborators, thank you for your contributions and efforts to make our projects into a success!

De **Bas Stichting**, en in het bijzonder Annita en Rob, dank voor jullie vertrouwen in ons JDM team. Zonder jullie tomeloze energie en morele en financiële steun hadden we nooit zo ver kunnen komen. Dankzij jullie hulp is ons JDM biomarker project uitgegroeid tot een langlopende onderzoekslijn, die hopelijk in de toekomst nog veel prachtige resultaten gaat brengen en de zorg voor patiënten met JDM blijft verbeteren.

Marco en **Kiki**, dankjulliewel voor de mooie samenwerking, jullie bevoegenheid om ook vermoeidheid en vermoeibaarheid als onderwerpen onder de aandacht te brengen in JDM, en voor jullie rol in het “JDM team” in het WKZ.

Dear (ex-)roomies, **Ale, Feli, Genoveva, Nienke**, (part 1), **Andrea, Doron, Ellen, Jorre, José, Jingwen, Lotte, Weiyang**, (part 2 and 4) and **Janneke** and **Lucas** (part 3), thank you all for sharing the highs and lows of my PhD with me, the spontaneous moments of relief or frustration, always accompanied by lots of coffee and tea (**Nienke**, your green thermos is still going strong!). **Ale**, thank you for being such an inspiring example as a strong woman in science, and for the unforgettable experience of joining a true Italian wedding! **Feli**, danke für deine Freundschaft, die superschönen Wochenenden in Lausanne, und die tolle Zusammenarbeit über diese ganzen Jahre. Ohne dich hätte es das JDM Biomarkerprojekt nicht gegeben! **Jorre**, voor de fijne samenwerking, je heerlijke sarcasme en de gedeelde smart over ethische commissies en monitors. **Nienke**, roomie en congresmattie! Dankjewel voor alle mooie herinneringen in de afgelopen jaren, inclusief de nodige feestjes (op congressen en daarbuiten), stadstour in Belgrado, sneeuwbalgevecht in Lausanne, badhuischillen in Boedapest en nog veel meer! ☺ **Lotte**, buurvrouw, voor al je gezelligheid en alle besommeringen over artsen in de wetenschap en het (on)nut van ethische bureaucratie. **Lucas** en **Janneke**, dank voor jullie gezelligheid, gedeelde voogdij over de droppot en (door mij verwaarloosde) plant, en de nodige deur-dicht-bijpraatmomenten.

Dear present and past Van Wijk group members, **Ale, Arjan, Barbara, Eelco, Eveline, Feli, Gerdien, José, Laura, Lek, Lisanne, Marlot, Roos, Theo, Yvonne**, thank you for all the great times and all your help and moral as well as practical support during these years. You have taught me that Femke’s group is like Hotel California (you can check out, but you can never leave), in the best possible way. I think it says a lot that all of you/us are still connected and dedicated to helping each other out where possible even after starting new jobs all over the world, and I certainly hope we can keep that spirit alive in the future. Lieve **Marlot**, dankjewel dat je het nooit hebt opgegeven! Ik waardeer het enorm dat je – ondanks alles – altijd rond lunchtijd je hoofd om de deur bent blijven steken. Dankjewel voor alle keren dat je me in het lab uit de brand hebt geholpen, voor je aanstekelijke lach en voor je onmisbare aanwezigheid die de Femke-groep tot een groep maakt. Lieve **Lisanne**, wat heb ik een enorme bewondering voor jouw motivatie, volharding en scherpe analytische blik. Dankjewel voor de fijne spontane momenten waarin we even ons hart konden luchten. Lieve **Eelco**, Mr. Brand, ik ben onder de indruk van je gedrevenheid en hoe je moeiteloos work and play lijkt te combineren, met altijd tijd en oog voor anderen. Ik vind het een eer dat ik op de valreep nog jouw tweede thuis in het AZU heb mogen leren kennen, inclusief de beruchte rode bank! **José**, dankjewel voor de gezellige gesprekken en voor je enorme hulp bij de iDisco. Dear **Lek**, thank you for having my back in the JDM project! I really appreciate your enthusiasm and admire your dedication. I hope you will keep enjoying your time here in the lab and in the Netherlands. **Gerdien**, dankjewel voor alle Treg tips

en de nodige koffiemomenten. **Yvonne**, dankjewel voor de leuke koffiemomenten en dat je altijd bereid bent tot een helpende gedachte of hand! **Theo**, dankjewel voor je goede carrière-adviezen, en dat ik een poosje op jouw fijne thuis mag passen. Lieve **Arjan**, ik heb je stralende aanwezigheid het afgelopen jaar gemist in het WKZ en in Sterk! Dankjewel voor alle heerlijke biermomenten (op SF-avonden, in de klimhal, tijdens het bakken voor de cake-om-de-week, op whatsapp), en dat je er voor me was tijdens het klim-akkefietje in Münster. Gelukkig heeft Kerstin ons onder haar hoede genomen met de Bloemstraat-BBQs en blijven de bier- en koffiemomenten gewoon bestaan ☺

Lieve **Lau**, wat een mooie turbulente jaartjes hebben we gedeeld in ons prachtige iSPAR project, met 'hours of boredom, minutes of thrill, and seconds of terror' achter de sorter. Dankjewel dat ik altijd op je kon rekenen als mijn partner in crime, voor de fantastische samenwerking en de fijne gesprekken. Ik bewonder je enorme daadkracht en doorzettingsvermogen, en je motiverende woorden als ik er doorheen zat. Ik had me geen betere uterusbuddy kunnen wensen, op naar die volgende fles bubbels!

Beste **Fjodor, Eva** en **Leone**, dankjulliewel voor al jullie enthousiasme, bijdragen en inzet tijdens jullie stages bij mij! Ik heb er enorm van genoten om met jullie samen te werken en ben heel trots dat ik een stukje van jullie opleiding heb mogen meemaken. Ieder van jullie heeft een unieke stempel gedrukt op de projecten met jullie eigen ideeën en kwaliteiten. Zonder jullie inbreng waren de projecten nooit geworden tot wat ze nu zijn, waarvoor mijn grote dank!

Dear Prakken/Loosdregt/Vastert/Boes/Gin-Tonic/other LTI group members, **Bas, Jenny, Jorg, Fran, Janneke, Kamil, Lot, Lucas, Luuk, Noor, Rianne, Samu, Willie**, thank you for all the good times! Lieve **Fran**, van chillen (euhh hard studeren) op het dek van de Van Kinsbergen boot tot zeilklaar maken van jullie eigen boot, wat een ontwikkelingen! Dankjewel voor vele mooie momenten door de jaren heen. Lieve **Noor**, congresroomie! De gezellige snapshots van je bruiloft zijn nog steeds trotse versiering boven mijn bureau en zullen ook op mijn volgende werkplek weer een ereplaatsje krijgen. Dankjewel voor de fijne en waardevolle bijkletsmomenten waarin ik het gevoel had dat ik alles met je kon delen, de beste tour naar de leukste inside-plekjes in Liverpool, inclusief de onvergetelijke karaokebar, en natuurlijk de murder mystery! **Luuk** and **Samu**, thank you for the nice collaboration! **Rianne**, ik zal nooit ons Londen-avontuur vergeten, wat een 'belevenis' was dat! Dankjewel voor alle mooie avonden met sing-stars, gin-tonics, bridgen en andere borrels, en al je hulp in de afgelopen jaren! **Willie**, dankjewel voor de mooie op-de-valreep gesprekken op random avonden als we eigenlijk allebei allang op het punten stonden om naar huis te gaan.

Lieve **Lot**, van werkgroepbuddies tot WKZ-buddies, en over een paar jaar het Spel-Wienke lab! Volgens mij zijn we goed on track, de Goldstrike was gewoon een voorbode van wat er nog komen gaat ;) Dankjewel voor de mooie vriendschap door de jaren heen. Je bent een inspiratie voor me met de manier waarop jij met volle overtuiging en heel veel plezier nieuwe uitdagingen en avonturen aangaat. Dankjewel voor het introduceren van gin-tonic avonden, de bridge club, wandelweekenden en nog zoveel meer!

Lieve I&I band, Erik en de Hakkers, McTBCL of band met de wijzigende naam, **Dani, Do, Erik, Kevin, Michiel, Pieter-Jan, Shamir** en **Tjomme**, dankjulliewel voor de heerlijke uurtjes in DB's en de mooie optredens!

Lieve salsamaatjes, door de fijne dansavonden en gesprekken met jullie ga ik me vanzelf altijd weer blij voelen, ook als de dag of de week wat minder was. Dankjulliewel voor alle soepele en gekke dansjes door de jaren heen, afgetopt met speciaalbiertjes! **Jasper**, dank voor de open bier- en fietsgesprekken en de pretentieloze gitaarsessies die we precies vaak genoeg plannen. Lieve **Auke**, onze semi-autistische bieb/café-werkdagen waren de hoogtepunten van mijn werkweken het afgelopen half jaar, en dat kwam zeker niet alleen door de hoeveelheid taartjes die we hebben getest! Zowel op als naast de dansvloer ben je een fantastisch maatje, dankjewel dat ik altijd over alles met je kan praten!

Lieve Murmelvrienden, **Hedwig, Jort, Mirjam, Remco**, ik vind het heel bijzonder dat we na al die jaren nog steeds betrokken zijn in elkaars levens en hoop dat dat nog heel lang zo blijft. Dankjulliewel voor jullie langdurige vriendschap!

Lieve eetclub-vriendinnen, **Ellen, Esther, Jarka** en **Merel**, wat hebben we door de jaren heen veel gedeeld met elkaar: fantastische cocktails, maaltijden, witte-chocolade-kardamom-dadel-cheesecake en bergen lief en leed. Dankjulliewel voor de mooie (maal) tijden, en op naar de volgende ronde!

Lieve SSL-buddies, **Bé, Björn, Fre, GJ, Jules, Makoto, Lars, Rob, Stéphanie**, dankjulliewel voor alle culinaire hoogstandjes, inzichten in het leven binnen en buiten de wetenschap en vooral de gesprekken over heeeeeeel andere zaken tijdens onze fantastische avonden en weekenden samen. Ik vind het enorm bijzonder dat we ondanks de wisselende, en tegenwoordig toenemende fysieke afstanden (Jules, zucht...), elkaar toch zo regelmatig blijven zien, en dat het zo dichtbij blijft voelen. Ik hoop dat we ondanks het verzuimen van de Canada-editie de SSL Down Under kunnen realiseren, en dat onze jaarlijkse spontane weekenden een langdurige traditie worden.

Lieve **Fre**, van de Ardennen tot Nicaragua, Zeeland tot Indonesië en Mexico tot Patagonië, onze prachtige reizen waren altijd de hoogtepunten van mijn jaar waar ik naartoe kon

leven. Niet alleen vanwege al het moois dat we samen hebben gezien en meegemaakt, maar ook om de tijd die we samen konden doorbrengen om onze levens te overdenken en weer met fris zelfinzicht, relativiseringsvermogen, moed en plezier aan de slag te gaan.

Lieve **Lieke** en **Astrid**, wat had ik zonder jullie ontmoeten! In al die jaren zijn jullie er geweest om thuis de blije momenten te delen, maar ook om me door de moeilijke uurtjes en frustraties heen te slepen, met altijd een luisterend oor paraat. Ik had me geen betere huisgenootjes kunnen wensen!

Lieve **Harrie** (voor buitenstaanders Henriette), van Aegee-band tot tweelingzussen in Guatemala en Portugal (en nu zelfs in Nederland). Onze fijne wandeldagen waarin we onze levens op de mooiste plekken buiten weer even op een rijtje zetten voelen altijd als een mini-vakantie. Dankjewel voor je luisterend oor en mooie vriendschap, dat Pieterpad komt nog wel aan de beurt!

Lieve **Kerstin**, ik vind het ontzettend fijn dat we elkaar in de afgelopen jaren zoveel beter hebben leren kennen, je bent een fantastische vrouw en vriendin. Ik bewonder jouw plezier, innerlijke rust, kracht en goed gedoseerde onafhankelijkheid waarmee je de uitdagingen van het leven en de wetenschap aangaat. Dankjewel voor alle heerlijke ontspannen uren binnen en buiten de klimhal, onze mooie gesprekken betekenen veel voor me.

Lieve **Merel**, lief vriendinnetje. Dankjewel voor je onmisbare en onvoorwaardelijke vriendschap door de jaren heen; altijd heb je aan mijn zijde gestaan, nu ook letterlijk bij mijn verdediging. Je inspireert me met je energie, passie voor het leven, veerkracht en liefdevolle luisterend oor. Ik kan niet in woorden vatten hoeveel je voor me betekent, dankjewel dat je er altijd voor me bent!

Lieber **Papa**, auch wenn wir uns nicht immer einig waren über meinen Lebenspfad, bin ich froh daß du dich jetzt auch freust über was ich erreicht habe. Ich bewundere deine Lebensfreude und Energie und ich hoffe daß du auch weiterhin hinter meinen Entscheidungen stehen kannst. Liebe **Petra**, danke für deine warme Anwesenheit in all diesen Jahren und alle schönen Momente die du und Papa mit eurer Unternehmungslust verwirklicht.

Lieve **Marc**, dankjewel dat je er altijd, onvoorwaardelijk voor me bent geweest. Jouw liefdevolle steun in de keuzes die ik heb gemaakt betekent heel veel voor me. Dankjewel dat je in me gelooft en dat je me hebt geleerd mijn zegeningen te tellen, maar ook op de eerste rang staat om mij aan te moedigen als ik daaraan voorbij wil streven. Samen met Mama ben jij mijn thuis.

Liebe **Mama**, ohne dich wäre ich nicht wer ich jetzt bin. Du warst schon immer mein großes Vorbild, und wirst das auch immer bleiben. Du inspirierst mich mit der Art wie du im Leben stehst und der grenzenlosen Energie mit der du jede neue Herausforderung angehst. Danke dass du immer an mich glaubst und mir die Kraft und Freiheit gibst genau das zu tun was mich glücklich macht. Hab dich ganz doll lieb!

CURRICULUM VITAE

Judith Wienke was born on January 17th 1988 in Jena, Germany. She and her parents moved to the Netherlands when she was 3 years old. In 2006 she completed secondary education Cum Laude at the Mummelliusgymnasium in Alkmaar. The same year she started her study Biomedical Sciences at Utrecht University where she received her Bachelor's degree Cum Laude in 2009 and discovered her interest in immunology. In these years she also completed a minor in Cognition (neuropsychological research) at the faculty of Psychology. She subsequently enrolled in the 4-year competitive Master's program



Selective Utrecht Medical Master (SUMMA) to become a clinician-scientist, combining a medical degree with research training. While studying the immunomodulatory effects of mesenchymal stem cells on T cells of patients with Juvenile Idiopathic Arthritis during her research internship at the laboratory of Prof. dr. Berent Prakken, she discovered and developed her fascination for translational research in immunology. She received her MD & MSc in 2013 and decided to continue working in immunology research. After travelling to Latin-America for several months to learn Spanish, she started her PhD under supervision of Dr. Femke van Wijk, Dr. Annet van Royen-Kerkhof and Prof. dr. Berent Prakken (Laboratory of Translational Immunology, UMC Utrecht) in 2014, of which the results are presented in this thesis. During her PhD, she completed the University Teaching Qualification (Basiskwalificatie onderwijs) and received the Erik Hack publication award at the UMC Utrecht, the abstract and presentation award at the Global Conference on Myositis and twice the Young Investigator's presentation award at the annual conference of the Pediatric Rheumatology European Society. She is now pursuing a career in human translational immunology research.

LIST OF PUBLICATIONS

Galectin-9 and CXCL10 as biomarkers for disease activity in juvenile dermatomyositis: a longitudinal cohort study and multi-cohort validation. Wienke J, Bellutti Enders F, Lim J, Mertens JS, van den Hoogen LL, Wijngaarde CA, Yeo JG, Meyer A, Otten HG, Fritsch-Stork RDE, Kamphuis SSM, Hoppenreijns EPAH, Armbrust W, van den Berg JM, Hissink Muller PCE, Tekstra J, Hoogendijk JE, Deakin CT, de Jager W, van Roon JAG, van der Pol WL, Nistala K, Pilkington C, de Visser M, Arkachaisri T, Radstake TRDJ, van der Kooi AJ, Nierkens S, Wedderburn LR, van Royen-Kerkhof A, van Wijk F. *Arthritis Rheumatol*. 2019 Aug;71(8):1377-1390

Systemic and Tissue Inflammation in Juvenile Dermatomyositis: From Pathogenesis to the Quest for Monitoring Tools. Wienke J, Deakin CT, Wedderburn LR, van Wijk F, van Royen-Kerkhof A. *Front Immunol*. 2018 Dec 18;9:2951. Review.

The identification of CCL18 as biomarker of disease activity in localized scleroderma. Mertens JS, de Jong EMGJ, van den Hoogen LL, Wienke J, Thurlings RM, Seyger MMB, Hoppenreijns EPAH, Wijngaarde CA, van Vlijmen-Willems IMJJ, van den Bogaard E, Giovannone B, van Wijk F, van Royen-Kerkhof A, Marut W, Radstake TRD. *J Autoimmun*. 2019 Jul;101:86-93

Galectin-9 is an easy to measure biomarker for the interferon signature in systemic lupus erythematosus and antiphospholipid syndrome. van den Hoogen LL, van Roon JAG, Mertens JS, Wienke J, Lopes AP, de Jager W, Rossato M, Pandit A, Wichers CGK, van Wijk F, Fritsch-Stork RDE, Radstake TRDJ. *Ann Rheum Dis*. 2018 Dec;77(12):1810-1814.

Regarding "Transcriptional and Cytokine Profiles Identify CXCL9 as a Biomarker of Disease Activity in Morphea". Mertens JS, de Jong EMGJ, Pandit A, Seyger MMB, Hoppenreijns EPAH, Thurlings RM, Vonk MC, Wienke J, van Wijk F, van Royen-Kerkhof A, Marut W, Radstake TRD. *J Invest Dermatol*. 2018 May;138(5):1212-1215.

Trajectories of cardiorespiratory fitness in patients with juvenile dermatomyositis. Blom KJ, Takken T, Huijgen BCH, Wienke J, van Royen-Kerkhof A, van Brussel M. *Rheumatology (Oxford)*. 2017 Dec 1;56(12):2204-2211.

A novel human STAT3 mutation presents with autoimmunity involving Th17 hyperactivation. Wienke J,* Janssen W,* Scholman R, Spits H, van Gijn M, Boes M, van Montfrans J, Moes N, de Roock S. *Oncotarget*. 2015 Aug 21;6(24):20037-42.

